AD NUMBER
AD091877
LIMITATION CHANGES
TO: **Approved for public release; distribution is unlimited. Document partially illegible.**
FROM: **Distribution authorized to U.S. Gov't. agencies and their contractors; Administrative/Operational Use; FEB 1956. Other requests shall be referred to Wright Air Development Center, Wright-Patterson AFB, OH 45433. Document partially illegible.**
AUTHORITY
AFWAL ltr, 17 Apr 1980

UNCLASSIFIED

WADC TECHNICAL REPORT 55-104

STUDY OF THE EFFECT OF TWIST IN YARNS ON PARACHUTE FABRICS

CHAUNCEY C. CHU

CHARLES A. LERMOND

AND

MILTON M. PLATT

FABRIC RESEARCH LABORATORIES, INC.

FEBRUARY 1956

WRIGHT AIR DEVELOPMENT CENTER

WADC TECHNICAL REPORT 55-104

STUDY OF THE EFFECT OF TWIST IN YARNS ON PARACHUTE FABRICS

CHAUNCEY C. CHU

CHARLES A. LERMOND

AND

MILTON M. PLATT

FABRIC RESEARCH LABORATORIES, INC.

FEBRUARY 1956

MATERIALS LABORATORY

CONTRACT No. AF 33(616)-387

PROJECT No. 7320

TASK No. 73201

WRIGHT AIR DEVELOPMENT CENTER

AIR RESEARCH AND DEVELOPMENT COMMAND

UNITED STATES AIR FORCE

WRIGHT-PATTERSON AIR FORCE BASE, OHIO

Carpenter Litho & Prtg. Co., Springfield, O.
500 - April 1956

FOREWORD

This report was prepared by Fabric Research Laboratories, Inc., under USAF Contract AF 33(616)-387. The contract was initiated under Project No. 7320, "Air Force Textile Materials", Task No. 73201, "Textile Materials for Parachutes", formerly RDO No. 612-12, "Textiles for High Speed Parachutes", and was administered under the direction of Materials Laboratory, Directorate of Research, Wright Air Development Center, with Mr. W. O. Perry acting as project engineer.

The authors gratefully acknowledge the following individuals for their many contributions to the work covered in this report: Dr. Walter J. Hamburger for his guidance both in the initial phases and at various stages in the progress of the research; Mr. Eric Singer who contributed to the early research effort; Mr. Newton Teixeira for his suggestions on light penetrability measurements; and Mrs. Yvonne Arbuckle for her painstaking efforts in the laboratory. Finally, a special acknowledgment is due to Mr. William G. Klein for his efforts in biaxial testing and in the writing of that section of this report.

On several occasions, this report identifies data by Specification Mil-7020. This is in error and should read Mil-C-7020.

This report covers work conducted from January 1952 to January 1955.

ABSTRACT

This is the final report on the "Study of the Effect of Twist in Yarns on Parachute Fabrics". Analytical developments on the mechanics of air flow through textile structures were made by adopting classical flow equations with due consideration to the visco-elastic behavior of textile materials. Experimental results on a large number of fabric samples (MIL-C-7020, Types I and II) with yarn twists varying from 0.5 to 35 turns per inch are given to demonstrate the various changes in the performance characteristics affected by changes in yarn geometry.

From the work accomplished, it is concluded that:

1. The flow of air through the open areas of a fabric obeys the general rules of fluid mechanics namely: flow at any given pressure differential varies with the amount of open area; and the rate of flow at varying pressure differentials follows the square root of the pressure differential with suitable modifying constants to allow for those changes in the open area which occur when the fabric is subjected to biaxial extensions exerted by the air pressure.

2. The free area available for air flow varies as a function of fabric and yarn geometry. The ellipticity of the yarn cross section is functional with the yarn twist; flatter the yarn, the less is the open space between adjacent yarns. Hence, for a given texture (threads per inch) the free area varies inversely with the yarn width.

3. The open areas change when the fabric under test is subjected to increased pressure differentials. The yarn systems in the fabric structure, when so stressed, result in biaxial extensions which widen the spaces between yarns. The rate at which the open areas vary with pressure differential may be determined by studying the fabrics' biaxial stress-strain behavior. At the present writing only limited studies have been made.

4. The magnitude of open areas in any given fabric may be calculated from the yarn widths determined microscopically and the fabric texture. However, a more precise method has been developed by measuring light penetrability through the use of a Beckman Spectrophotometer.

5. In general, the following trends have been shown to be evident: with the increase of yarn twist

Fabric thickness	increased
Denier of yarn removed from fabric	increased
Horizontal yarn diameter	decreased
Vertical yarn diameter	increased
Free area: area between yarns	increased
Light penetrability	increased

Air permeability	increased
Freedom of yarn slippage	increased
Yarn tensile strength	increased
Yarn elongation	increased
Energy to rupture yarn	increased
Strip tensile strength	no visible change
Fabric elongation	no visible change
Secondary creep	increased
Tear strength	decreased
Tear energy	decreased

PUBLICATION REVIEW

This report has been reviewed and is approved.

FOR THE COMMANDER:

M.R.WHITMORE
Technical Director
Materials Laboratory
Directorate of Research

TABLE OF CONTENTS

Table of Contents (Contd.)

APPENDICES

LIST OF TABLES

LIST OF TABLES (Continued)

LIST OF TABLES (Continued)

LIST OF FIGURES

LIST OF FIGURES (Continued)

LIST OF FIGURES (Continued)

LIST OF FIGURES (Continued)

LIST OF FIGURES (Continued)

LIST OF FIGURES (Continued)

LIST OF FIGURES (Continued)

LIST OF FIGURES (Continued)

LIST OF FIGURES (Continued)

LIST OF FIGURES (Continued)

LIST OF FIGURES (Continued)

LIST OF FIGURES (Continued)

LIST OF FIGURES (Continued)

LIST OF FIGURES (Continued)

LIST OF FIGURES (Continued)

LIST OF FIGURES (Continued)

LIST OF FIGURES (Continued)

LIST OF PHOTOMICROGRAPHS

LIST OF PHOTOMICROGRAPHS (Continued)

NOMENCLATURE

A = Area of the orifice.

C = Calendered finish.

D = Yarn diameter (horizontal unless otherwise specified), inches.

d = Yarn denier.

E = Energy required to rupture a yarn, in-lb/in/denier.

e = Fabric extension due to biaxial loading.

(ED) = Effective yarn diameter of rip-stop fabrics.

FA = Projected free area: fraction of total fabric surface which the open pores occupy, dimensionless.

g = Acceleration due to gravity, 32.18 ft/sec/sec.

G.P.D. = Grams per denier.

h = Pressure differential, ft. of air.

k = Discharge coefficient or any constant.

LP = Light penetrability, dimensionless.

N = Non-calendered finish

n = Number of orifices

n = Exponential constant.

P = Load, pressure, or tear strength.

$\overline{P}$ = Average tear strength, lbs.

P_u = Maximum tear load, lbs.

ΔP = Pressure differential, inches of water.

Q = Air permeability, $ft^3/min/ft^2$

q = Air permeability, $ft^3/sec/ft^2$

R = Rip-stop weave.

T = Yarns per inch of fabric (texture)

t = Yarn twist, turns per inch.

(TE) = Tear energy, inch pounds per inch of fabric.

V = Velocity of flow, ft/sec.

α = Constants.

β = Constants.

γ = Constants.

ε = Elongation.

μ = Microns.

δ = Poisson's Ratio.

ρ = Density of air, lbs/ft^3

Subscripts

o = Initial condition, at rest.

$1, 2$ = Other conditions.

w = Warp direction.

f = Filling direction.

I. INTRODUCTION

I-1 In order for a parachute to function properly its canopy requires certain air permeability characteristics. In most textile laboratories air permeability is still commonly measured at a pressure differential across the fabric equal to one-half inch of water. Under actual flight conditions air flow and accompanying pressure differentials may be enormously higher. In this research program, measurements of air flow were made with pressure differentials of up to fifty inches of water.

Generally speaking, empiricism has been employed in determining the air permeability characteristics of fabrics. This technique has precluded investigators from designing textile fabrics with requisite air flow properties at requisite pressure drops as may be demanded by the Air Force. One of the objectives of this research, therefore, was a rational engineering study of those fiber, yarn, and fabric factors which influence fabric air permeability.

It should be recognized that any attempt to quantitize the mechanism of air flow through a textile structure is an extremely complicated activity. This is due, in part, to the fact that textile fabrics are visco-elastic. Their properties are not constant but vary with the force which may result from the application of a pressure differential. Yarn and fabric geometry principles developed at Fabric Research Laboratories, Inc. and elsewhere have been most helpful in the understanding and development of the mechanisms of air flow through parachute fabrics.

I-2 This report is divided into three sections. First, a discussion of the effect of varying yarn twist on the geometrical and mechanical properties of parachute fabrics. Second, a study of the mechanics of air flow through fabric structures wherein preliminary developments in the analytical phases of the research are presented. Third, a compilation of all accumulated data and findings together with test procedures, techniques, graphical representations and photomicrographs.

I-3 The fabric samples used throughout this project came from two sources. At the onset of the program, twenty eight twill (MIL-C-7020, Type II) and six rip-stop (MII-C-7020, Type I) fabrics were woven and made available by Cheney Brothers, Manchester, Connecticut. Half the number of fabrics within each type were calendered while the other half were not. These fabrics proved to be of extreme value; much of the preliminary information on the effects of yarn twist on parachute fabric performance was obtained on them. However, certain shortcomings existed in the series. First, the range of yarn twists, while quite adequate in the filling direction of the Type II fabrics was grossly insufficient in the warp direction of both Type I and Type II fabrics. Second, the total amount of each fabric made available to Fabric Research Lab 'ories, Inc. was approximately two yards. In view of the numerous experiments necessary for a rational research program as well as those tests called for in Exhibit A of the contract, it was obvious that the samples available were entirely insufficient.

Particularly lacking were fabrics of Type I construction. It was decided, therefore, to design an additional series of forty essentially different fabrics of basic Specification MIL-C-7020; i.e., of rip-stop construction, having four different warp and five filling twists. These fabrics were woven by Warwick Mills. Again, as in the Cheney series, the fabrics were finished both calendered and uncalendered.

I-4 . With the thirty-four Cheney fabrics and the forty Warwick fabrics, it was both impossible (lack of sufficient materials in the Cheney series) as well as impractical (time and money involved) to subject all seventy-four fabrics to the same number of tests. Hence a judicious selection of samples was made for each experiment conducted to minimize the number of tests and yet produce the maximum amount of information.

I-5 Despite the voluminous data collected and conclusions arrived at, the work reported herein still indicates that this is only the initial step in the understanding of the mechanics of air flow through fabric structures, and the application of engineering methods to the design of parachute fabrics.

II. EFFECTS OF YARN TWIST ON FABRIC PROPERTIES

According to the basic concepts of fabric geometry, as pioneered by F. T. Peirce*, in the plain weave alone, ideally, there may be as many as eleven constructional variables. Variations in any one or more of these will affect the geometry and the mechanical behavior of the fabric. Fortunately, the fabrics studied in this program have been confined to the two types of Specification MIL-C-7020, wherein within each type all variables were nominally held constant with the exception of yarn twist.

The principal, or the primary effect of varying the yarn twist is the alteration of the yarn cross section. In the range of yarn twists investigated (from 0.5 to 35 turns per inch), the cross sectional shapes undergo a considerable amount of change. From a nearly flat ribbon at low twist the section becomes an ellipse, and finally circular at high twist. The secondary effects of yarn twist variation are manifold, and all are consequences of the change in cross sectional shape.

II-1 Effects of Yarn Twist on the Geometrical Properties of Yarn and Fabric.

1.1 The changes in the cross sectional shape of the yarn with increasing twist are best shown in the photomicrographs given in **Appendix V. It** is seen that between 0.5 and 5.0 turns per inch, the change in the cross sectional shape is small since the yarn is very much flattened by the lack of twist. The big change occurs between twist of 5.0 and 20 turns per inch, where the transition from a flat ribbon to an ellipse takes place. Beyond this point, where the yarn is already nearly circular, further addition of twist may only serve to make the yarn diameter somewhat smaller by tightening the structure. The extent of yarn flattening may be characterized by such terms as the circularity coefficient or the flattening coefficient, usually defined by the ratio of the vertical and the horizontal yarn diameters.

Tables 16 through 19 give yarn diameters as measured by the microscope. Plots of yarn twist versus yarn diameter are shown in Figures 2 - 4. In the case of rip-stop fabrics, effective yarn diameters were calculated since four out of every eighteen yarns are woven as two rip-stop yarns. Thus:

$$\text{Eff. Diam.} = \frac{14}{18}\,\text{Diam.}_{\text{single yarn}} + \frac{2}{18}\,\text{Diam.}_{\text{rip-stop yarn}} \quad \text{----(2.1)}$$

1.2 In studies of air permeability performance of parachute fabrics, one is primarily concerned with the horizontal diameter which, together with the number of yarns per inch of fabric, determine the amount of open area available for air flow. The open area, otherwise called the projected free area, is defined as the fraction of the total fabric surface not occupied by yarns, hence open to flow of air:

* F. T. Peirce - "The Geometry of Cloth Structure", Journal of the Textile Institute, March 1937.

$$FA = (1 - D_w T_w)\ (1 - D_f T_f) \text{ ------------------------ } (2.2)$$

(All terms are defined in the "Nomenclature.")

Free areas of the various fabric samples are given in Tables 20 through 22. Results show, as expected, that free area increases with increase in yarn twist.

II-2 Effects of Yarn Twist on the Mechanical Properties of the Fabric

II-2.1 Effects of Yarn Twist on Air Permeability

The flow of air through any given fabric generally takes place between adjacent yarns and, to a lesser degree, between fibers within a yarn. The effects of yarn twist on air permeability are twofold. As yarn twist increases, from (say) a zero twist yarn, both the circularity and the packing density of the yarn are increased. As the yarns become more circular, the pore space between yarns is enlarged; hence an increase in air flow results. The addition of twist bunches the fibers closer together, which restricts the flow of air between the fibers. However, as has already been stated, this latter effect is small. The gross effect is that as the yarn twist increases, so does the permeability. This is evident in Figures 10 to 27. These figures show curves of permeability versus pressure differential. The curves of fabrics woven from yarns of higher twist exhibit a higher rate of air flow.

Figures 5 to 9 plot air permeability versus yarn twist at given levels of pressure differential. It is seen that as yarn twist increases, the air flow increases with it. However, beyond twenty turns per inch, where the yarn is already circular in cross section, further addition of twist may only serve to make the yarn diameter somewhat smaller by increasing the packing factor. Hence the air permeability still increases with increasing yarn twist but at a slower rate. These observations may be readily confirmed by examining the photomicrographs.

Data for Figures 5 to 27 are tabulated in Tables 23 to 25. The Frazier Permeometer, at Fabric Research Laboratories, supplied data on the low pressure permeability tests (up to 10 inches of water for certain fabrics.) The high pressure tests were conducted at the Georgia Institute of Technology Experimental Station under the supervision of a representative from Fabric Research Laboratories. The equipment at Georgia Institute of Technology has a capacity of up to 50 inches of water.

Half of the fabrics under study were calendered. Calendering causes yarn flattening. Flattened yarns exhibit decreased vertical diameters and increased horizontal diameters. This tends to diminish the free space between yarns which naturally will reduce air flow. Q_c/Q_n is a ratio of air permeabilities of calendered over uncalendered fabrics. The effect of calendering is depicted by the magnitude of this ratio. Figure 197 plots this effect with varying yarn twist. Twists of 15 turns per inch or under are most affected by calendering. Figure 198 plots the effect of calendering at various pressure differentials which shows that the ratio of Q_c/Q_n becomes a constant at pressure differentials of 20 inches of water or more.

In general, the control of air permeability, by varying the yarn twist is a more desirable method than calendering. As mentioned above, the effect of calendering is not a constant until the pressure differential exceeds 20 inches of water. This adds to the difficulties of properly engineering parachute fabrics as will be further discussed in Section III.

II-2.2 Yarn Stability Tests

As required by Exhibit A of the research contract, yarn stability tests were performed on the Cheney fabrics. In these tests, a row of pins arranged in the shape of a comb was used to measure the amount of fabric distortion under a given applied load.

Samples two inches wide by five inches long were used. The longer dimension of the sample was in the filling direction in order that the displacement of the warp yarns sliding over the filling yarns might be measured. Tests in the other direction; i.e., filling yarns being displaced over warp yarns, were omitted since there was insufficient material for the performance of tests in both directions. It was believed that filling twist variation which existed over a broader range than did warp twist variations would influence warp yarn mobility more than filling yarn mobility. A metal bar two inches long with a row of 23 pins (approximately 0.04 inches in diameter) equally spaced was attached to one of the jaws of the Instron Tensile Tester. The row of pins was made to pierce through the fabric sample at a distance of about one inch from the end. The other end of the sample was clamped in the opposite jaw such that the gauge length between the row of pins and the other jaw was exactly three inches (see Figure 28 for test arrangement.) As the load was applied to the sample (the jaw began to move away from the pins) the displacement of the yarns caused by the clawing action of the pins was continuously measured as the load increased. The recorder on the test instrument registered the total elongation of the sample; i.e., the elongation of the sample due to the applied load plus the extension provided by the displaced yarns. Hence in order to measure the actual yarn displacement under the particular applied load, the natural elongation of the fabric must be subtracted from the load-elongation curve provided by the recorder. Figure 29 shows a typical illustration: Curve A is the total extension curve, obtained directly from the recorder. Curve B is the average strip tensile load-elongation curve of the fabric sample (3 inch gage length.) Curve C was plotted by taking the difference between Curves A and B.

In all these tests, the displacement measurements were taken at a load of 1.5 pounds, for the two-inch wide sample. For most of the fabrics tested, the displacement curve became almost asymptotic to the load axis; any further increase in load did not cause much additional yarn displacement. This occurs when the slopes of curves A and B in Figure 29 became parallel. The results of these tests are tabulated in Table 26 and are plotted in Figure 30. The data seem to show an upward trend with increase in yarn twist (see dotted "average" line in Figure 30), which might be explained with the aid of the photomicrographs of the cross sections. Assuming that the coefficient of friction remains unchanged with increase in twist, as the yarns become more circular in cross section, the less the areas of contact between the warp and filling yarns become, hence the increase in mobility. No careful lengthy analysis has been made of the cause of the observed results, since this work was not intended to constitute a major portion of the research.

II-2.3 Tensile Properties of Yarns Removed from Fabrics

Tensile tests of yarns removed from the Cheney fabrics have been conducted to evaluate the effect of yarn twist. Tables 27 and 28 list the breaking strengths, elongations to rupture, and the energies calculated from the load-elongation curves of each fabric. The load-elongation curves are plotted in Figures 31 to 64. The effects of yarn twist on yarn tensile properties are very apparent: both the rupture load and rupture elongation are increased with increased twist. Consequently, the rupture energy is greatly increased.

II-2.4 Repeated Stress Tests

All parachutes, other than those which are designed for one-time use only, may be subjected to repeated stressing at each use. In the laboratory, repeated stressing may be accomplished by subjecting a test specimen to either a selected load or selected elongation, followed by release of the load, with subsequent cyclical repetitions of the process. In parachutes, it is probable that the maximum load rather than extension, is more or less constant on each occasion that it is used. Thus, it was decided to conduct tests by imposing a predetermined stress level.

In planning the experiments, in order to cover as wide a range as possible, three different load levels were selected; namely, 25%, 50% and 75% of the fabrics' ultimate breaking strength. The average breaking strength of the Type I fabrics was about 43 pounds per inch, while the Type II fabrics broke at approximately 57 pounds per inch. Hence it was convenient to take load levels of 10, 20 and 30 pounds for Type I fabrics and 15, 30 and 45 pounds for Type II fabrics.

Samples one inch wide by six inches long were tested in the Instron Tensile Tester at a 3 inch initial gage length and at a pulling jaw speed of two inches per minute. Upon reaching the preset maximum load level, the lower pulling jaw returned at the same rate to the no-load position, and then the load was reapplied. After the fifth cycle, the test paused for one minute to enable primary creep recovery to occur, and then the load was reapplied for a sixth time to rupture the sample.

Figure 75 illustrates diagrammatically the various phases of a repeated stress test:

First cycle, loading from 0 to A, reaching a load level of A.

First cycle, unloading from A to B, from load A to zero load.

Fifth cycle, loading from C to A, reaching a load level of A. Point C is determined following a 1 minute wait after the 4th unloading reaches 0 load.

Fifth cycle, unloading from A to D, from load A to 0 load, with 0 load maintained for 1 minute, the sample length stabilizing at point D'

Sixth cycle, loading from D' the recovered length at 0 load after 1 minute wait, to ultimate rupture point E.

Of particular interest with respect to parachute fabrics is the secondary creep (or permanent set) after cyclical loading. In Figure 75, the distance OC is the secondary creep for the fifth cycle and the distance OD' the secondary creep for the sixth cycle. Tables 32 and 33 give the tabulated results as well as other pertinent data, among which are the corrected residual elongation and the energy to rupture. The corrected residual elongation is defined as follows:

$$\% \text{ C.R.E.} = \frac{D'F}{\text{Original Gage Length} + OD'} \times 100 \quad \text{--------------}(2.3)$$

and thus represents the elongation to rupture, following the repeated stressing, based on the new gage length.

The energy to rupture is the area under the rupture curve D'EF, expressed in inch-pounds per inch of the new gage length.

The relationship of the filling secondary creep versus filling yarn twist, is plotted in Figure 76. At the 15 pound load level, a definite trend of increasing secondary creep with increasing filling yarn twist may be seen. A similar trend exists at the 30 pound level. At 45 pounds, the trend is less well defined due to the scattering of individual points. There is also a trend for the lower warp twist to result in lower permanent set for a given filling twist. The dependence of warp permanent set on warp or filling twist is too scattered and inconsistent to permit any conclusions at this time.

In terms of practical application, the major effect of secondary creep or permanent set results in a reduction of the fabric's cover factor; i.e., the amount of the open area available for air flow is increased. Other studies in this research have shown that the amount of air flow at a given pressure differential is proportional to the amount of free area. Thus, after repeated use, the air permeability of a parachute may increase because of secondary creep's "opening up" the fabric and thereby increasing the free area. However, the data presented in Tables 32 and 33 are not directly applicable in the prediction of this increase in permeability. The tests performed were uniaxial while the forces involved in a parachute opening are biaxial. An intelligent estimate can still be made, pending future biaxial investigations, if it is assumed that the secondary creep in biaxial tests is approximately one half of the uniaxial ones.

The effect of secondary creep on Equation (2.2) deals primarily with the change in the yarns per inch of fabric. The portion of secondary creep resulting from crimp removal will alter yarn spacings without any appreciable effect on yarn diameters. That portion of fabric elongation attributable to yarn extension; i.e., fabric elongation in excess of the crimp removal point, may slightly reduce yarn diameters. This reduction in diameter can be accomplished by either or both of the following:

1. Increase in the circularity of the yarn cross section due to tension.

2. Slenderizing through lateral contraction consistent with Poisson's ratio; i.e., the elongation of a cylinder at constant volume causes lateral contraction.

These effects will be studied in conjunction with the biaxial tests. For the time being, there does not appear to be a sufficient basis for quantitative analyses of lateral yarn dimension changes. Thus, ignoring any changes in yarn diameter, the free area of a fabric sample following secondary creep removal becomes:

$$FA' = \left(1 - \frac{D_w T_w}{1 + SC_f}\right)\left(1 - \frac{D_f T_f}{1 + SC_w}\right) \qquad \text{-------------------------}(2.4)$$

where FA' = The fraction of the fabric area available for air flow after the sample has been subjected to repeated stressing.

SC_w = Secondary creep in the warp direction.

SC_f = Secondary creep in the filling direction.

Taking fabrics 10N 1/2 and 10N35 as examples, the changes in the free areas due to secondary creep at the various load levels were calculated from Equation (2.4) and are tabulated in Table 34. The predicted values of air permeability are based on the fact that the flow is proportional to the free area:

$$Q' = Q\,\frac{FA'}{FA} \qquad \text{---}(2.5)$$

where Q = Air permeability through a given fabric sample before repeated stressing.

Q' = Air permeability through the same fabric after it has been subjected to repeated stressing.

Considering the above assumptions, Table 34 shows that at the first load level (approximately 25% of the breaking strength) the increase in free area, and thereby the increase in air permeability, ranges from 5.4% for the high twist fabric 10N35, to as much as 10.9% for the low twist fabric 10N10. At the 75% repeated stress level the increases for these same fabrics are 15.6% and 60.2% respectively. Needless to say, this phenomenon is of great significance in parachute performance. To understand fully the effect of secondary creep on air flow, work in future projects will be directed to a study of biaxial repeated stress experiments.

Typical load-elongation curves of these repeated stress tests are plotted in Figures 77 to 196.

II-2.5 Effect of Yarn Twist on Fabrics' Tear Resistance

The tongue tear test was used to evaluate the effect of yarn twist on the tear resistance of these experimental parachute fabrics. Figure 199 depicts a warp test sample. The various lines on the diagram are made with a rubber stamp. The specimen is three inches wide and eight inches long. The dotted horizontal lines are spaced one inch apart. A slit OC, 2 3/4 inches long, is cut along the center of the sample. The ends, A and B are clamped in the upper and lower jaws of the Instron tester. As the jaws separate, a line of tear propagates from C toward D and thence to E. An autographic record of the tear force is plotted.

Figure 200 shows a typical tear diagram as obtained from the recorder of the Instron. As the path of tear proceeds from the end of the slit, C, load is built up from the cross yarns (perpendicular to line OCDE) thereby resisting the tearing action. The tear path may progress without rupturing any yarns because the yarns are being bunched together at the point of tear. As soon as the load is built up sufficiently high to tear across the bunched yarns, rupture occurs, and instantly the load drops. With the jaws moving apart from each other continuously, the cycle is repeated, hence the saw-tooth shaped curve.

The number of ruptures (or peaks in the diagram) per inch of sample torn is usually much less than the number of yarns in that inch of fabric. The exact number depends upon the ease with which the fabric can be distorted; i.e., a tight fabric, with the same number of yarns per inch as a loose fabric, will tear with a higher number of peaks than the looser one, but at a lower peak load. The number of yarns ruptured per peak is inversely proportional to the number of peaks. If there are two fabrics, one tight (say a plain weave), the other loose (say a 3/1 twill), even with the same number of yarns per inch from the same yarns, the plain weave will tear with more peaks, and fewer yarns per peak. This will result in a lower tear strength than for the 3/1 twill.

Based upon previous research on the mechanics of tear*, the following parameters were chosen as criteria of evaluation. These are the average peak load, P_a; the mean tear strength, $\bar{F}$, equal to $\frac{P_a + P_m}{2}$; and the energy, E, (defined as the area under the saw-tooth curve between the limits of D and E in Figure 200) required to tear across one inch of sample. Tables 35 and 36 list these parameters for the Cheney and Warwick fabrics.

The effect of filling yarn twist on tear performance of the Cheney fabrics can be seen graphically in Figure 201 which plots tear energy and average tear strength against filling yarn twist. Very little difference, if any, can be observed in the filling tear characteristics with varying filling yarn twist. However, the resulting effects on warp tear properties are quite pronounced. As has been mentioned before, the yarns to be torn may slide along the cross yarns and become bunched prior to their rupture. At 0.5 turns per inch, the filling yarn is practically a flat ribbon without any obstructions to deter the sliding of the warp yarns. This allows a greater number of warp yarns to be bunched together for each peak. As the twist is increased in the filling yarns, the configuration is changed: the helical paths formed by the individual filaments permit "nesting" action to take place with the counter parts of the warp yarns. Thus the freedom of warp yarn motion is greatly reduced which results in a fewer number of yarns being ruptured at each peak, and hence a lower tear strength.

Similarly, a change of from 7 to 10 turns per inch in the warp yarn twist results in a loss of filling tear strength and energy.

Samples from the Warwick series were tested and their results were divided into three groups as shown in Table 36. The first group had constant filling twist with varying warp twist. The second group varied the filling twist while the warp twist was held constant. In the final group, both the warp and filling twists were varied.

The data again show that loss of tear performance results from increase in yarn twist. In each of the three groups, substantial decreases in tear strength and energy are evident when either the warp or filling yarn twist increases beyond 5 turns per inch. Both the warp and filling properties are changed when the yarn twist in only one direction is varied. This phenomenon is different from the behavior of the Cheney fabrics wherein the warp tear properties are only functional with filling yarn twist. The explanation

* Quartermaster Reports: Fabric Research Laboratories, Inc. Case Number C48861.

might be that the Cheney fabrics are of twill construction (Type II), whereas the Warwick fabrics are of rip-stop construction (Type I). The latter is a much more stable structure, and therefore any distortion or displacement occurring in one direction might easily cause a similar disturbance in the other direction.

An additional check was made by testing three groups of calendered fabrics with virtually the same results. The calendering process did not produce any noticeable effect on the tear properties of these parachute fabrics.

II-2.6 Biaxial Testing

Introduction

In biaxial testing, the testing machine and methods of which are discussed more fully in Appendix (I), a material is subjected to simultaneous stresses in two directions. For all cases considered here the two directions will be those of the warp and filling yarns. The machine axes will be designated as X and Y. It is easy to see that the stress-strain curves so derived will in general be steeper than those obtained from uniaxial or strip tensile tests due the interaction of the warp and filling yarn systems. This results in a sort of Poisson effect and is analogous to the well known relationships for homogeneous, isotropic media which follow Hook's Law:

$$e_x = \frac{1}{E} (\sigma_x - \sigma_y) \quad \text{------------------------} (2.6)$$

$$e_y = \frac{1}{E} (\sigma_y - \nu\sigma_x) \quad \text{------------------------} (2.7)$$

where

e_x = strain in the X direction

e_y = strain in the Y direction

E = Young's Modulus

σ_x = stress in the X direction

σ_y = stress in the Y direction

ν = Poisson's Ratio

Unfortunately, the biaxial problem in textile structures is neither linear nor can the principles of superposition be applied, both of which are necessary for a direct application of the above equations. However, they will be of value later for indicating in a qualitative way, the effect of biaxial tensioning.

With respect to air permeability, a uniaxial test is particularly inadequate since the air pressure creates simultaneous tensions in warp and filling yarn systems. The biaxial extension of either under such conditions will in general be less for any given load than the corresponding uniaxial extensions. Since one of the important factors governing air permeability is the increase in free area under a given pressure and this is closely related to the increased dimensions under a biaxial load, the latter-type of stress application seems the more logical here.

It is important to note that since the problem is not soluble by means of superposition there may be an infinity of strain states with given X and Y loads and thus it becomes necessary to specify the mode by which the given loads were reached. Clearly, for the case of uniform surface pressure over a spherical section the X and Y loads must at all times be equal. This is probably the configuration of greatest interest at the moment and thus the tests which will be discussed were conducted at a warp to filling load ratio of unity, so that for the symmetrically shaped samples used $\sigma_x = \sigma_y$.

Qualitative Analysis of Biaxial Test

On tensioning a sample biaxially the first effect is a crimp interchange which occurs at essentially zero load. That is, the more highly crimped direction will lose crimp while the less crimped direction will contract and become more highly crimped.

From considerations of the static equilibrium of the surface of the fabric it can be shown that:

$$\frac{P_x}{P_y} = \frac{\tan \theta_y}{\tan \theta_x} \qquad \text{------------------------------------(2.8)}$$

where P_x and P_y are the loads per yarn in the X and Y direction and θ_x and θ_y are the angles of the warp and filling yarns with respect to the fabric surface. Thus for a symmetrically loaded square fabric $\theta_1 = \theta_2$ and crimp interchange will take place until this condition results.

This and the subsequent biaxial deformation can be illustrated in a qualitative way by means of an adaptation of the foregoing biaxial formulas (Equations 2.6 and 2.7) as follows:

$$e_x = \frac{\sigma_x}{E_x}\left(1 - \frac{\int_{yx}}{K}\right) \qquad \text{----------------------------(2.9)}$$

$$e_y = \frac{\sigma_y}{E_y}\left(1 - K \int_{xy}\right) \qquad \text{----------------------------(2.10)}$$

where

$\int_{yx}$ = dimensionless factor indicating the influence of y stress on x strain

$\int_{xy}$ = dimensionless factor indicating the influence of x stress on y strain

E_x = the instantaneous X modulus

E_y = the instantaneous Y modulus

$K = \dfrac{\sigma_y}{\sigma_y}$

E_x and E_y are primarily determined by the tensile properties of the X and Y yarns while the values of $\int_{yx}$ and $\int_{xy}$ are largely dependent on the angle of inclination of the y and x yarns respectively. That is, a change in tension on a yarn which is highly crimped will produce more change in its orthogonal counterpart than will one which is fairly straight.

The previous expressions are more nearly correct if written in incremental form as:

$$\delta e_x = \frac{\delta \sigma_x}{E_x}\left(1 - \frac{\int_{yx}}{K}\right) \quad \text{------------------}(2.11)$$

$$\delta e_y = \frac{\delta \sigma_y}{E_y}\left(1 - K \int_{xy}\right) \quad \text{------------------}(2.12)$$

which are analogous to the Levy Mises formulas for plastic deformation. These equations state that the changes in extensions may be predicted for small changes in stresses but do not indicate the total extensions. which are complicated functions of the various non-linear components.

By writing the load-extension equations in the following manner an interpretation can be made which indicates the approximate values of the E's and $\int$'s.

$$de_x = \left(\frac{\partial e_x}{\partial \sigma_x}\right)_{\sigma_y} d\sigma_x + \left(\frac{\partial e_x}{\partial \sigma_y}\right)_{\sigma_x} d\sigma_y$$

$$de_y = \left(\frac{\partial e_y}{\partial \sigma_y}\right)_{\sigma_x} d\sigma_y + \left(\frac{\partial e_y}{\partial \sigma_x}\right)_{\sigma_y} d\sigma_x$$

$$\frac{d\sigma_x}{d\sigma_y} = K \quad \text{as before}$$

$$de_x = d\sigma_x \left[\left(\frac{\partial e_x}{\partial \sigma_x}\right)_{\sigma_y} + \left(\frac{\partial e_x}{\partial \sigma_y}\right)_{\sigma_x} \left(\frac{1}{K}\right)\right]$$

$$\left(\frac{\partial e_x}{\partial \sigma_x}\right)_{\sigma_y} = \frac{1}{E_y} \qquad \text{(Definition)}$$

$$de_x = \frac{d\sigma_x}{E_x}\left[1 + \left(\frac{\partial \sigma_x}{\partial e_x}\right)_{\sigma_y}\left(\frac{\partial e_x}{\partial \sigma_y}\right)_{\sigma_y}\left(\frac{1}{K}\right)\right] \qquad (2.13)$$

Comparing this expression with Equation (2.11) above it can be seen that

$$\nu_{yx} = -\left(\frac{\partial \sigma_x}{\partial e_x}\right)_{\sigma_y}\left(\frac{\partial e_x}{\partial \sigma_y}\right)_{\sigma_x}$$

$$\nu_{yx} = -\frac{\left(\frac{\partial e_x}{\partial \sigma_y}\right)_{\sigma_x}}{\left(\frac{\partial e_x}{\partial \sigma_x}\right)_{\sigma_y}} = -\frac{\left(\frac{\partial e_x}{\partial \sigma_y}\right)_{\sigma_x}}{\frac{1}{E_y}} \qquad \text{---------}(2.14)$$

and by analogy

$$\nu_{xy} = -\frac{\left(\frac{\partial e_y}{\partial \sigma_x}\right)_{\sigma_y}}{\left(\frac{\partial e_y}{\partial \sigma_y}\right)_{\sigma_x}} = -\frac{\left(\frac{\partial e_y}{\partial \sigma_x}\right)_{\sigma_x}}{\frac{1}{E_y}} \qquad \text{----------}(2.15)$$

It is clear that for any fabric neither the numerator nor the denominator can vanish and the numerator must always be negative. Thus the ν's are always positive numbers. The upper limit of the ν's is not so easily estimated because their value near the beginning of a test is determined by the initial crimp unbalance.

Whenever a large crimp unbalance exists such that Equation (2.8) is not satisfied, one of the ν's takes on a high value such that the δ e corresponding to the direction with the angle which is too low becomes negative. This, however, is a transient phenomenon and occurs at loads just sufficient to perform crimp interchange. Once an equilibrium has been established it is not likely that any negative extensions will occur, at least with stress ratio's near unity. For higher values of K it is of course possible to obtain a negative extension. For K = 1, the condition for the test to be described later,

$$\left(\frac{\partial e_y}{\partial y}\right)_{\sigma_y} \text{ and } \left(\frac{\partial e_x}{\partial \sigma_x}\right)_{\sigma_y}$$

will be considerably greater than either of

$$\left(\frac{\partial e_x}{\partial \sigma_y}\right)_{\sigma_x} \text{ and } \left(\frac{\partial e_y}{\partial \sigma_x}\right)_{\sigma_y}$$

and then the $\sqrt{}$'s will be much less than one for the equilibrium portion of the test, probably on the order of 0.2 to 0.5.

It should be emphasized here that E_x and E_y are not the moduli of the X and Y yarns but are partial fabric moduli defined by $E_x = \left(\frac{\partial \sigma_x}{\partial \sigma_y}\right)_{\sigma_y}$ and $E_y = \left(\frac{\partial \sigma_y}{\partial e_y}\right)_{\sigma_y}$ At very low crimps these will approach the yarn moduli and the $\sqrt{}$'s will of course become very small. Thus a fabric with a very low crimp would not be expected to exhibit radically different biaxial and uniaxial stress-strain response.

Experimental Results

All fabrics to be discussed here are nominally square, that is, have nominally the same warp and filling count and same original yarns. On this basis it would seem possible to compare these fabrics on the basis of yarn twist differences from one to the other. Unfortunately, such is not the case, because the nominal squareness of these fabrics was achieved by a process of stretching and heat setting and the properties of the warp and filling yarns are by no means identical. This is clear even from the uniaxial tests (Figures 65-74) where it can be seen that the warp direction is much stiffer in every case. Since this treatment varied from fabric to fabric and was fairly important in determining fabric properties, a good quantitative comparison on the basis of twist is not possible. Nevertheless, the biaxial behavior can be compared with the theoretical on the basis of the experimental uniaxial results.

From the analysis of the foregoing section it would be concluded that the biaxial stress-strain curves of these low crimp materials should show initially a lower elongation than their uniaxial counterparts and subsequently follow a path quite similar to the latter. This is what occurs in every case as can be seen by inspection of Figures 202-205. The very early portion of the curves near zero load, are not accurate due to the inability of the testing machine to compensate quickly enough at very slight load errors, and thus the crimp interchange portions of the test results were not consistent. The extensions here can be theoretically calculated purely on the basis of fabric geometry*.

The fact that the biaxial test rupture load is always much less than that for the uniaxial tests is due to the stress concentration in the corners of the sample outside the uniformly strained region. The true biaxial rupture load would be slightly lower than the uniaxial due to yarn inclination.

With respect to effects due to yarn twist, Figures 206 and 207 show the comparison of filling and warp characteristics respectively for the same series of fabrics considered in Figures 202-205, plus two calendered fabrics. With the exception of R30N30, which is stiffer than would be expected on the basis of twist, all fabrics fall into the proper order, that is, the fabrics comprised of more highly twisted yarns are more extensible. As mentioned before, due to processing the relative magnitude cannot be considered indicative of solely twist effects. The reason for the deviation of R30N30 from the anticipated is not clear, but it is small anyway.

At first examination it might seem that the differences from uniaxial behavior are not of sufficient magnitude to warrant a large amount of attention, but this is not true, particularly with respect to air permeability. To illustrate this, Table 40 has been made which shows the change in extension of these fabrics under symmetrical biaxial loads of five pounds and twenty pounds per inch and the corresponding uniaxial data. At the bottom of this table the per cent increase of area calculated from uniaxial and biaxial data are compared. Since the increase in total area is closely related to the increase in free area it is clear that the biaxial correction is not a small one, particularly at low loads.

These figures do not lend themselves to comparison with permeometer readings since:

a. The fabric loads in the permeometer are unknown.
b. The highly restricted boundary condition during a permeometer test make uniform biaxial tension impossible.

Conclusions

An analysis of the biaxial behavior of fabrics shows that experimental work is necessary in order to obtain quantitative performance information. A preliminary experimental program involving a few fabrics has shown that the information to be obtained from biaxial tensile testing is of value. Considerably more work should be done on these and other fabrics in order to investigate the effect of other loading conditions and constructions and if possible relate these results to the data obtained from an improved type of laboratory permeability test.

*Painter, E. V., "Mechanics of Elastic Performance of Textile Materials" , Part VIII T.R.J. Vol. XXII, No. 3, March, 1952.

III. MECHANICS OF AIR FLOW THROUGH PARACHUTE FABRICS

III-1 In any woven fabric structure, there are two sets of yarns, the warp and filling, running orthogonal to each other. With the exception of a jammed fabric, there exists a finite space between any two adjacent yarns. Upon superpositioning the two sets of yarns, the two sets of "space-between-yarns" form a series of rectangular openings, or pores, through which air flow may take place. Although it is theoretically possible for flow to occur between the individual fibers within a yarn, the existance of yarn twist which, in varying degrees, binds the fibers together, inhibits the flow of air. All evidence tends to indicate that if any air flows through the yarns, the quantity is usually negligible; thus only flow between yarns, need by considered.

III-2 In view of the foregoing, a fabric sample may be idealized as a plate with a large number of orifices. Consider a plate having n holes, each of area A_1; the velocity of air flowing through the holes is V_1 at a pressure of P_1. On the upstream side, the area is A_o; the velocity, V_o; and the pressure, P_o. Thus writing Bernoulli's equation and the equation of continuity, assuming air density changes between points o and 1 to be negligible, gives:

$$\frac{V_o^2}{2g} + \frac{P_o}{\rho_o} = \frac{V_1^2}{2g} + \frac{P_1}{\rho_1} \quad \text{------------------------------------(3.1)}$$

and

$$A_o V_o = nA_1 V_1 \quad \text{--(3.2)}$$

where

V_o = Velocity of upstream air, ft/sec.

V_1 = Velocity of air flow through holes, ft/sec.

g = Acceleration due to gravity, ft/sec.^{2}

P_o = Pressure of upstream air, lbs/ft.^{2}

P_1 = Pressure of air through holes, lbs/ft.^{2}

ρ_o = Density of upstream air, lbs/ft.^{3}

ρ_1 = Density of air through holes, lbs/ft.^{3}

A_o = Area of upstream duct, ft.^{2}

A_1 = Area of each hole, ft.^{2}

n = Number of holes over area A_o, dimensionless.

Equation (3.2) may be rewritten as:

$$V_o = \frac{n A_1}{A_o} V_1 \text{ ------------------- } (3.3)$$

Since, by definition, nA_1/A_o = FA = Free area, or that fraction of total fabric surface which the open pores occupy and which is available for air flow, then

$$V_o = (FA) V_1 \text{ ------------------- } (3.4)$$

Substituting (4.4) into Equation (.‥1):

$$\frac{(FA)^2 V_1^2}{2g} + \frac{P_o}{\rho_o} = \frac{V_1^2}{2g} + \frac{P_1}{\rho_1}$$

$$\frac{V_1^2}{2g} (1-FA^2) = \frac{P_o}{\rho_o} - \frac{P_1}{\rho_1} \text{ ------------------- } (3.5)$$

Since the pressure differential, h, in feet of air, is $\frac{P_o}{\rho_o} - \frac{P_1}{\rho_1}$ then Equation (3.5) becomes:

$$V_1 = \sqrt{\frac{2gh}{1-FA^2}} \text{ ------------------- } (3.6)$$

By definition:

$$q = V_1 (FA) \text{ ------------------- } (3.7)$$

where

q = Air permeability, ft^3/sec. per ft^2 of sample

However, Equation (3.7) applies to a perfect orifice with a discharge coefficient, K, of unity. All other types of orifices usually have a discharge coefficient of less than one; thus:

$$q = K \frac{FA}{\sqrt{1 - FA^2}} \sqrt{2gh} \qquad (3.8)$$

Again, by definition, the free area may be written as:

$$FA = (1 - D_W T_W)(1 - D_F T_F) \qquad (3.9)$$

where

D_W = Horizontal diameter of the warp yarns, inches.

D_F = Horizontal diameter of the filling yarns, inches.

T_W = Threads per inch in the warp direction.

T_F = Threads per inch in the filling direction.

In practice, the pressure differential term in Equation (3.8) should be in inches of water rather than feet of air, thus the expression becomes, neglecting small changes in air density over the pressure ranges involved,

$$Q = 4007K \frac{FA}{\sqrt{1 - (FA)^2}} \sqrt{\Delta P} \qquad (3.10)$$

where

Q = Air permeability, cubic feet per minute per square foot of fabric sample - 60 q.

4007 — Numerical constant, combination of 2g, the ratio of densities between air and water and a factor of 60 seconds per minute.

ΔP = Pressure differential, inches of water.

According to Equation (3.10), if the discharge coefficient, K, and the free area, FA, remain constant with pressure changes, then the flow, Q, should be proportional to the square root of the pressure differential, P. However, this is not so. While the discharge coefficient might change, perhaps by a small amount, with increasing pressure differential, the free area definitely does increase as a result of biaxial extensions. This behavior is very evident in Figures 12 through 19 wherein the slopes of the lines are all greater than one-half. The slopes would have been equal to one-half had the fabrics followed the square root relationship. The curves in these figures all are expressible in the following form:

$$Q = 4007K \frac{FA_o}{\sqrt{1 - (FA_o)^2}} (\Delta P)^n \text{ ----------------------------------(3.11)}$$

where

FA_o = The free area determined while the sample is at rest (under zero pressure with zero biaxial extension).

$$FA_o = (1 - D_{Wo} T_{Wo}) (1 - D_{Fo} T_{Fo}) \text{ ----------------------------(3.12)}$$

n = The exponent of the pressure differential if it is assumed that the free area does not change with pressure.

The numerical values of n have been calculated from the experimental data and are given in Column 4 of Table 37 . In Column 2 of the same table are given the values of light penetrability, LP, which in light of the experimental evidence is equal to the free area at rest (See Appendix IV):

$$LP = FA_o \text{ ---(3.13)}$$

The magnitude of n appears to be inversely functional with LP as seen in Figure 211. The departure from the square root relationship becomes less as the free area gets larger.

Equation (3.11) with the exponent n greater than one-half has an ambiguous physical meaning. To make the data fit Equation (3.10), or to conform with the square root relationship, the free area must be analyzed in terms of the pressure differential:

$$FA = f (FA_o, \Delta P) \text{ ---(3.14)}$$

More precisely, the free area changes under biaxial tension as a result of (1) Decrease in yarn diameter from slenderizing and (2) Reduction in the threads per inch through yarn stretching (the more complex case of fabric stretch with no yarn stretch; i.e., crimp interchange, will be analyzed following the experimental determination of biaxial stress-strain effects):

$$D_W = \frac{D_{Wo}}{1 + \int_W \mathcal{E}_W}; \quad D_F = \frac{D_{Fo}}{1 + \int_F \mathcal{E}_F} \qquad (3.15)$$

$$T_W = \frac{T_{Wo}}{1 + \mathcal{E}_F}; \quad T_F = \frac{T_{Fo}}{1 + \mathcal{E}_W} \qquad (3.16)$$

where

$\mathcal{E}_W$, $\mathcal{E}_F$ = Elongation in the warp and filling directions

$\int_W$, $\int_F$ = Poisson's ratios of the two directions

Then

$$FA = \left(1 - \frac{D_{Wo}}{1 + \int_W \mathcal{E}_W} \times \frac{T_{Wo}}{1 + \mathcal{E}_F}\right)\left(1 - \frac{D_{Fo}}{1 + \int_F \mathcal{E}_F} \times \frac{T_{Fo}}{1 + \mathcal{E}_W}\right) \qquad (3.17)$$

In the case of a square fabric, symmetrically strained,

$$FA = \left(1 - \frac{D_O}{1 + \int \mathcal{E}} \times \frac{T_O}{1 + \mathcal{E}}\right)^2 \qquad (3.18)$$

The elongation $\mathcal{E}$ is functional with ΔP, wherein a linear relationship will be assumed. Equation (3.18) may then be written as:

$$FA = \left(1 - \frac{D_O}{1 + \alpha \Delta P} \times \frac{T_O}{1 + \beta \Delta P}\right)^2 \qquad (3.19)$$

or

$$FA = \left(1 - \frac{1 - \overline{FA_O}}{1 + \gamma \Delta P + \delta \Delta P^2}\right)^2 \qquad (3.20)$$

Assuming that the biaxial strains are small and thus that the term $\delta \Delta P^2$ is very small compared to $\gamma \Delta P$ and may be neglected, Equation (3.20) becomes:

$$FA = \left(1 - \frac{1 - \sqrt{FA_O}}{1 + \gamma \Delta P}\right)^2 = \left(1 - \frac{1 - \sqrt{LP}}{1 + \gamma \Delta P}\right)^2 \qquad (3.21)$$

Substituting Equation (3.21) into Equation (3.10):

$$Q = 4007K \frac{\left(1 - \frac{1 - \sqrt{LP}}{1 + \gamma \Delta P}\right)^2}{\sqrt{1 - \left(1 - \frac{1 - \sqrt{LP}}{1 + \gamma \Delta P}\right)^4}} \sqrt{\Delta P} \qquad (3.22)$$

Among the fabrics listed in Table 24, eight are nominally square in construction. As a first order approximation, assuming that the discharge coefficient for any fabric is a constant, it is possible to determine the values of γ, for each experimental value of ΔP (from the measured values of air permeabilities and light penetrabilities). Performing the necessary calculations, on only one fabric; namely, R 1/2 N 1/2, γ was found to be 0.011 units of strain per inch of water. The actual values of the discharge coefficients for all fabrics, assuming γ to be a constant among all fabrics for all values of ΔP, may now be obtained (Table 38). Actually, γ varies considerably with ΔP, and somewhat with fabric construction. Figure 212 plots values of K computed on the basis of $\gamma = 0.011$ versus LP on semi-log paper. The curve in this plot seems to conform to the following equation:

$$K = 1.0467 + 0.4315 \log LP \text{ ------------------------------(3.23)}$$

Substituting Equation (3.23) into Equation (3.22):

$$Q = 4007(1.0467 + 0.4315 \log LP) \frac{\left(1 - \frac{1 - \sqrt{LP}}{1 + 0.0115\Delta P}\right)^2}{\sqrt{1 - \left(1 - \frac{1 - \sqrt{LP}}{1 + 0.0115\Delta P}\right)^4}} \sqrt{\Delta P} \text{ --(3.24)}$$

The calculated values of air permeabilities at pressure differentials of 0.5 and 10.0 inches of water of the available square fabrics are given in Table 39. The agreement between the calculated and the experimental data is shown in the plot of Figure 213. It is seen that the agreements for the non-calendered fabrics are somewhat better than the calendered ones. Despite the fact that Equation (3.24) was derived for square fabrics, and that only approximate values of γ were used, it checks remarkably well for fabric R 1/2 C30 which is non-square. To make Equation (3.24) generally acceptable for design use, additional refinements will be necessary. It is anticipated that in any future program this will be pursued more rigorously.

APPENDIX I

EXPERIMENTAL PROCEDURES

TEST PROCEDURES

The following test procedures cover methods of testing employed but not discussed elsewhere in the text.

1. Fabric Thickness

Thickness was measured using a dial gage equipped with a 3/8" diameter presser foot and a six ounce headweight (A.S.T.M. D-76-49) and D-39-49.

2. Texture (Picks and Ends Per Inch)

Picks or ends per inch were counted in at least five different areas of the fabric and the average reported (A.S.T.M. D-39).

3. Yarn Twist

Warp and filling yarn twist was determined on a ten inch length of yarn using a standard twist tester. The yarn to be tested was attached to both jaws of the tester while still in the fabric, raveled from the fabric, tensioned to remove loom crimp, and was then untwisted. The average number of turns per inch of yarn was reported from ten such tests.

4. Denier

Yarn denier was determined by weighing 10 inch lengths (crimp removed) of yarn to the nearest 0.01 mg. Five such measurements were made and the denier calculated from the following equation.

$$3543.3 \times \text{grams}/100 \text{ inches} = \text{denier} \qquad (1)$$

Denier by definition is the number of grams of yarn per 9,000 meters.

5. Yarn Diameter (Measured Microscopically)

The fabrics were first imbedded in a suitable mixture of two parts iso-butyl methacrylate polymer, 1 part xylol and 1 part toluol. The mixture was heated at a low temperature until solution was effected and there was no longer any sign of bubbles. It was then allowed to cool and poured onto a glass plate. The fabric was then placed carefully on the plastic layer. The next day a second layer of methacrylate was poured over the fabric. The whole mass was then allowed to harden until it was impossible to make a finger print in the surface.

Specimens approximately 1/2" x 3/4" were cut from each sample. From these, cross-sections 20 microns thick were cut using a sliding microtome. The cross-sections were mounted in mineral oil on a conventional microscope slide.

Using a conventional filar micrometer, the yarn diameters were measured. Each measurement reported is an average of 20 determinations. In the case of rip-stop yarns, pairs were measured as a single yarn since it was extremely difficult to define the yarn boundary.

6. Load-Elongation

Load-elongation diagrams of yarns were determined on an Instron Tensile Tester.

Per cent elongation to rupture was calculated as follows:

$$\% \text{ Elongation} = \frac{\text{inches of chart}_{(\text{no load to rupture})} \times 100}{\text{gage length} \times \frac{\text{chart speed}}{\text{jaw speed}}} \quad \text{---}(2)$$

From typical curves (average of ten tests), it is possible to calculate the energy to rupture. This energy is represented by the area under the curve from no load to rupture.

$$\text{Energy Per Denier} = \frac{0.007341 \times \text{Area under curve}}{\text{denier}} \quad \text{---------}(3)$$

$$0.007341 = \frac{\text{full scale load (gms)}}{454 \times \text{chart length}} \times \frac{1}{\text{gage length}} \times \frac{\text{jaw speed}}{\text{chart speed}} \quad \text{---}(4)$$

The areas for the above calculation are determined by a planimeter. For all values reported the constants in (3) were the following:

full scale load	400 grams
chart length	9.6 inches
gage length	5 inches
jaw speed	2 inches per minute
chart speed	5 inches per minute
energy units	gm. cm/cm/denier

7. Biaxial Tension

General Description

There are two orthogonal sets of jaws. (See Figures 209 and 210). Opposing jaws move with equal speed but the motion of one set is controlled by the load experienced by the other. The independent motion will be designated as being along the X-axis; and the dependent motion along the Y-axis. X-axis motion is controlled by a lightly loaded induction motor suitably geared to give extension rates of 0.05"/min. to 0.20"/min. Thus, the rate of jaw separation in the X-direction is essentially constant, but due to the fact that the tails of the sample are under uniaxial tension, the X-extension of the biaxial region will not be a known function of jaw separation (or time), so this biaxial extension is measured and recorded directly. Similarly, the Y extension must be found directly. Y extension is controlled by a servo system operating such that the load in the Y direction will always bear the same relation to the load in the X direction; that is $\frac{P_y}{P_x} = K$ where P_y is the Y load, Px is the X load and K is a constant which can be chosen at will for a given test. Both loads and extensions are recorded on the same chart in a broken line fashion.

Figure 208 shows all main components in block form. The contents of the block are as follows:

Load cells X_1, X_2, Y_1 and Y_2 are identical Wheatstone bridges composed of four SR-4 resistance gages each. All four are bonded to a thin walled dural cylinder with two gages active and two providing temperature compensation. The load cells X_1 and Y_1 are the servo sensing elements and are connected in series. The load cell X_1 sensitivity control is simply a variable resistance connected across the bridge of load cell X_1. Load cell X_2 and load cell Y_2 are used to measure the X and Y loads respectively.

The X-extension and Y-extension gages are Schaevitz Linear Differential Transformers whose motion is controlled by small pins pushed through the fabric near the center where there is no boundary effect of jaw attachment and initially set at a separation of one half inch. Thus, as the fabric extends, the pins move apart and the moving slug in the Linear Differential Transformer is displaced.

Amplifiers 1 and 2 are both Sanborn Strain Gage Amplifiers. No. 1 is used as a servo-amplifier and feeds an amplidyne whose output controls the speed and direction of the Y-axis drive motor. No. 2 is used as a source voltage and amplifier for the measurement gages. The automatic switching causes traces of X loads, X extensions, Y load and Y extension to be recorded cyclically for periods of one second each.

The A.C. induction motor runs the X-axis drive, and since it is running at only a very small fraction of full load, its speed is essentially constant.

Operation

A cross-shaped sample* is loaded in the jaws as shown in Figure 209 with just enough tension applied to straighten it. The extension gages are placed in position, and all four traces zeroed on the recorder. The X-drive is then turned on.

*The sample has tails 2 inches in width, which provides an area two inches square to be subjected to biaxial tension. The cross shaped sample is used in preference over a square sample (for biaxial grab tests), because it is difficult to ascertain the exact stress conditions within the area under biaxial tension in a grab test.

As the material extends in the X direction a load is of course built up along this direction and a signal arises in load cell X_1. This signal is in excess of that at load cell Y_1, and the difference is in a direction to cause the servo motor to extend the sample in the Y direction. The motion of the Y-jaws will always be in such a direction as to make the signal from load cell Y_1 equal to that from load cell X_1. If the sensitivity (output/unit load) of load cells X_1 and Y_1 is equal, the X and Y load will be equal, but if, for example, the X axis sensitivity were one-half that of the Y, the Y load would be one-half of the X load. Although any X to Y sensitivity ratio from 1 to 0 is possible, there is the practical limitation that there is always a load error in the following system, and this error increases directly as the ratio.

As previously stated, X load, X extension, Y load and Y extension are plotted cyclically during this extension process. From these traces it is possible to plot load-elongation diagrams for each axis for any stress ratio between the axes.

APPENDIX II

TABULATION OF DATA

TABLE 1

ROSTER OF FABRICS USED IN THIS INVESTIGATION

Specification MIL-C-7020 Type I*		Specification MIL-C-7020 Type II**	
Not Calendered	Calendered	Not Calendered	Calendered
R 1/2 N 1/2	R 1/2 C 1/2	7N 1/2	7C 1/2
R 1/2 N5	R 1/2 C5	7N2 1/2	7C2 1/2
R 1/2 N10	R 1/2 C10	7N5	7C5
R 1/2 N20	R 1/2 C20	7N7	7C7
R 1/2 N30	R 1/2 C30	7N15	7C15
		7N20	7C20
R5N 1/2	R5C 1/2	7N35	7C35
R5N5	R5C5		
R5N10	R5C10	10N 1/2	10C 1/2
R5N20	R5C20	10N2 1/2	10C2 1/2
R5N30	R5C30	10N5	10C5
		10N7	10C7
R7N 1/2	R7C 1/2	10N15	10C15
R7N7	R7C7	10N20	10C20
R7N30	R7C30	10N35	10C35
R20N 1/2	R20C 1/2		
R20N5	R20C5		
R20N10	R20C10		
R20N20	R20C20		
R20N30	R20C30		
R30N 1/2	R30C 1/2		
R30N5	R30C5		
R30N10	R30C10		
R30N20	R30C20		
R30N30	R30C30		

NOTE: Code for the notations in the above table:-

R - Rip-stop or Type I construction.
N - Not calendered.
C - Calendered.

First Number - Nominal warp twist, turns per inch.
Last Number - Nominal filling twist, turns per inch.

* All Type I fabrics (except R7 Series) were woven by Warwick.

** All Type II fabrics and the R7 Series of Type I were woven by Cheney.

TABLE 2

Summary of Cheney Brothers' Experimental Fabrics

	Specification MIL-C-7020	
	Type I	Type II
Warp twists, t.p.i.	7	7 and 10
Filling twists, t.p.i.	1/2, 7, and 30	1/2,2-1/2,5,7,15,20 & 35
Types of finish	Calendered and not calendered	Calendered and not calendered
Number of fabrics	6	28
Yardage of each made available to F.R.L.(approx.)	2 yds.	2 yds.

TABLE 3

SPECIFICATIONS OF ADDITIONAL NYLON PARACHUTE FABRICS

Based on Specification MIL-C-7020

1. Yarns: 30 denier (10 filament) Type 200 nylon
2. Weave: Modified Type I - Ripstop (See Figure 1)
3. Threads per inch: 120 x 120
4. Yarn twists:-

   a. Warp: 1/2, 5, 20 and 30 t.p.i.
   b. Filling: 1/2, 5, 10, 20 and 30 t.p.i.

5. Finish:-

   a. One-half of the yardage calendered.
   b. One-half of the yardage not calendered.

TABLE 4

SELECTION OF RIP-STOP FABRICS TO REPRESENT THE COMPLETE RANGE OF YARN TWIST COMBINATIONS

(Warwick)

Warp Yarn Twists	Filling Yarn Twists 0.5	5	10	20	30
0.5	x	-	-	-	-
5	x	x	-	-	-
20	x	-	-	x	-
30	x	x	x	x	x

The twenty fabrics (ten calendered and ten non-calendered) listed in Table 4 may be logically classified into three series:

Series A - The twist in one set of yarns is being held constant at 0.5 turns per inch while the twist in the other set of yarns varied from 0.5 to 30 turns per inch:

R 1/2 N 1/2	and	R 1/2 C 1/2
R5N 1/2	and	R5C 1/2
R20N 1/2	and	R20C 1/2
R30N 1/2	and	R30C 1/2

Series B - The same as in Series A except the twist that is being held constant is 30 turns per inch:

R30N 1/2	and	R30C 1/2
R30N5	and	R30C5
R30N10	and	R30C10
R30N20	and	R30C20
R30N30	and	R30C30

Series C - The twists in the two sets of yarns vary simultaneously from 0.5 to 30 turns per inch:

R 1/2 N 1/2	and	R 1/2 C 1/2
R5N5	and	R5C5
R20N20	and	R20C20
R30N30	and	R30C30

TABLE 5

THICKNESS OF TYPE I FABRICS
(Cheney)

Fabric Code	Fabric Thickness In Inches
R7N 1/2	0.0035
R7N7	0.003[illegible]
R7N30	0.004[illegible]
R7C 1/2	0.0034
R7C7	0.0031
R7C30	0.0033

TABLE 6

THICKNESS OF TYPE II FABRICS
(Cheney)

Fabric Code	Fabric Thickness In Inches
7N 1,2	0.004[illegible]
7N2 1,2	[illegible]
7N5	0.0044
7N7	[illegible]
7N15	[illegible]
7N20	0.005[illegible]
7N35	0.005[illegible]
10N 1,2	0.0035
10N2 1,2	0.0036
10N5	0.0037
10N7	0.0038
10N15	0.0042
10N20	0.0045
10N35	0.004[illegible]
7C 1,2	0.004[illegible]
7C2 1,2	0.0044
7C5	0.0045
7C7	0.0048
7C15	0.0051
7C20	0.0055
7C35	0.0062
10C 1,2	0.0035
10C2 1,2	0.0036
10C5	0.0037
10C7	0.0038
10C15	0.0043
10C20	0.0047
10C35	0.0053

TABLE 7

FABRIC TEXTURE FOR TYPE I FABRICS
(Cheney)

Fabric Code	Ends Per Inch	Picks Per Inch
R7N 1/2	126	120
R7N7	124	119
R7N30	121	120
R7C 1/2	126	119
R7C7	124	120
R7C30	124	117

TABLE 8

FABRIC TEXTURE FOR TYPE I FABRICS
(Warwick)

Fabric Number	Texture (Threads/Inch) Warp	Filling
R 1/2 N 1/2	120.0	124.4
R 1/2 N5	118.6	122.2
R 1/2 N10	119.0	123.8
R 1/2 N20	120.2	123.2
R 1/2 N30	120.4	121.8
R5N 1/2	120.8	123.8
R5N5	121.2	124.2
R5N10	121.4	123.0
R5N20	120.0	121.8
R5N30	120.6	121.8
R20N 1/2	121.4	120.0
R20N5	120.6	119.6
R20N10	121.2	118.6
R20N20	120.4	116.8
R20N30	121.0	119.8
R30N 1/2	121.0	119.4
R30N5	120.6	119.0
R30N10	120.4	116.2
R30N20	120.6	116.8
R30N30	120.0	115.8
R 1/2 C 1/2	121.4	126.8
R 1/2 C5	120.2	122.2
R 1/2 C10	121.0	123.8
R 1/2 C20	120.0	122.8
R 1/2 C30	120.6	124.2
R5C 1/2	120.6	125.6
R5C5	121.0	125.2
R5C10	120.6	123.4
R5C20	121.0	122.0
R5C30	120.8	122.6
R20C 1/2	121.6	122.4
R20C5	121.0	121.4
R20C10	121.0	119.4
R20C20	121.4	119.2
R20C30	121.6	121.6
R30C 1/2	121.6	121.4
R30C5	121.2	121.2
R30C10	121.0	117.8
R30C20	121.0	118.4
R30C30	120.8	117.4

TABLE 9

FABRIC TEXTURE FOR TYPE II FABRICS
(Cheney)

Fabric Code	Ends Per Inch	Picks Per Inch
7N 1/2	131	77
7N2 1/2	128	79
7N5	130	78
7N7	128	78
7N15	125	78
7N20	126	80
7N35	126	76
7C 1/2	130	79
7C2 1/2	130	78
7C5	129	77
7C7	129	77
7C15	128	78
7C20	131	80
7C35	130	78
10N 1/2	130	77
10N2 1/2	131	75
10N5	128	75
10N7	130	77
10N15	124	76
10N20	125	77
10N35	124	78
10C 1/2	130	77
10C2 1/2	129	77
10C5	128	76
10C7	131	77
10C15	129	77
10C20	128	78
10C35	132	77

TABLE 10

YARN TWIST OF TYPE I FABRICS
(Cheney)

Fabric Code		Twist Per Inch Warp	Twist Per Inch Filling
R7N 1/2	Regular Yarn*	7.5	1.2
	Ripstop Yarn*	7.9	1.2
R7N7	Regular Yarn	7.6	8.6
	Ripstop Yarn	7.7	8.6
R7N30	Regular Yarn	8.2	33.0
	Ripstop Yarn	7.7	32.7
R7C 1/2	Regular Yarn	7.5	1.0
	Ripstop Yarn	7.5	1.2
R7C7	Regular Yarn	7.6	8.6
	Ripstop Yarn	7.6	8.8
R7C30	Regular Yarn	7.6	31.4
	Ripstop Yarn	7.4	31.4

* 16 regular yarns followed by a ripstop yarn (2 regular yarns woven as one); or a repeat every 18 yarns.

TABLE 11

YARN TWIST FOR TYPE I FABRICS
(Warwick)

Fabric Code	Yarn Twist (t.p.i.) Warp	Yarn Twist (t.p.i.) Filling
R 1/2 N 1/2	1.5	1.7
R 1/2 N5	1.6	6.8
R 1/2 N10	1.5	11.6
R 1/2 N20	1.4	23.4
R 1/2 N30	1.3	34.4
R5N 1/2	6.7	1.0
R5N5	6.3	7.1
R5N10	6.2	12.0
R5N20	6.7	22.9
R5N30	6.6	33.1
R20N 1/2	22.4	1.2
R20N5	22.5	6.6
R20N10	22.4	11.7
R20N20	22.4	22.9
R20N30	22.2	33.8
R30N 1/2	32.1	1.5
R30N5	32.1	6.8
R30N10	32.8	11.2
R30N20	31.4	23.4
R30N30	32.0	34.2
R 1/2 C 1/2	1.5	1.4
R 1/2 C5	1.4	6.2
R 1/2 C10	1.5	11.8
R 1/2 C20	1.4	23.5
R 1/2 C30	1.5	33.8
R5C 1/2	6.6	1.1
R5C5	6.1	6.7
R5C10	6.8	11.4
R5C20	7.0	23.6
R5C30	6.1	33.8
R20C 1/2	23.2	1.0
R20C5	22.5	6.6
R20C10	22.4	11.4
R20C20	22.8	23.4
R20C30	22.5	34.1
R30C 1/2	33.0	1.5
R30C5	33.1	6.7
R30C10	33.6	11.3
R30C20	33.0	23.9
R30C30	32.7	33.9

TABLE 12

YARN TWIST FOR TYPE II FABRICS
(Cheney)

Fabric Code	Twist Per Inch Warp	Twist Per Inch Filling
7N 1/2	7.9	1.2
7N2 1/2	7.8	3.3
7N5	7.8	6.2
7N7	8.0	7.8
7N15	8.0	16.8
7N20	7.7	23.2
7N35	7.7	39.3
7C 1/2	7.7	1.0
7C2 1/2	7.7	3.0
7C5	7.9	6.3
7C7	8.0	7.9
7C15	8.0	16.4
7C20	8.6	23.6
7C35	7.8	39.6
10N 1/2	10.9	1.0
10N2 1/2	10.7	3.3
10N5	10.8	6.2
10N7	10.6	7.4
10N15	10.8	16.2
10N20	10.5	22.9
10N35	10.3	38.6
10C 1/2	10.9	1.0
10C2 1/2	10.3	3.2
10C5	11.1	6.3
10C7	10.8	7.8
10C15	10.7	16.6
10C20	10.6	23.1
10C35	10.9	40.3

TABLE 13

YARN DENIER FOR TYPE I FABRICS
(Cheney)

Fabric Code		Yarn Denier	
		Warp	Filling
R7N 1,2	Regular Yarn	30.[illegible]	32.4
	Ripstop Yarn	2[illegible].8	31.4
R7N7	Regular Yarn	31.[illegible]	32.[illegible]
	Ripstop Yarn	31.6	31.7
R7N30	Regular Yarn	32.0	33.0
	Ripstop Yarn	32.2	33.2
R7C 1/2	Regular Yarn	31.2	33.0
	Ripstop Yarn	31.8	32.9
R7C7	Regular Yarn	32.1	32.5
	Ripstop Yarn	31.6	32.7
R7C30	Regular Yarn	31.8	33.5
	Ripstop Yarn	32.0	33.4

TABLE 14

YARN DENIERS FOR TYPE I FABRICS
(Warwick)

Fabric Code	Yarn Denier Warp	Yarn Denier Filling	Fabric Code	Yarn Denier Warp	Yarn Denier Filling
R 1/2 N 1/2	31.0	31.6	R 1/2 C 1/2	30.7	33.3
R 1/2 N5	31.0	30.9	R 1/2 C5	31.4	31.6
R 1/2 N10	30.7	32.2	R 1/2 C10	31.0	32.8
R 1/2 N20	31.0	31.9	R 1/2 C20	30.8	32.1
R 1/2 N30	31.3	31.9	R 1/2 C30	31.3	32.9
R5N 1/2	30.8	32.7	R5C 1/2	30.9	32.4
R5N5	30.8	32.1	R5C5	31.1	32.7
R5N10	30.9	31.8	R5C10	30.6	32.3
R5N20	30.9	32.1	R5C20	30.6	32.8
R5N30	29.9	32.7	R5C30	30.9	32.6
R20N 1/2	30.9	31.5	R20C 1/2	30.8	32.0
R20N5	31.2	32.0	R20C5	31.5	32.7
R20N10	31.1	31.5	R20C10	31.5	31.8
R20N20	30.6	30.7	R20C20	31.4	31.9
R20N30	30.8	32.1	R20C30	31.8	32.2
R30N 1/2	30.9	31.7	R30C 1/2	30.6	32.1
R30N5	31.3	32.0	R30C5	31.8	31.8
R30N10	30.6	31.0	R30C10	30.8	31.6
R30N20	31.2	31.7	R30C20	31.6	32.8
R30N30	30.6	32.1	R30C30	31.9	32.6

TABLE 15

YARN DENIER FOR TYPE II FABRICS
(Cheney)

Fabric Code	Yarn Denier Warp	Yarn Denier Filling
7N 1/2	42.5	77.2
7N2 1/2	42.2	75.8
7N5	41.5	77.6
7N7	41.5	74.4
7N15	41.8	74.0
7N20	41.5	74.8
7N35	41.1	77.9
10N 1/2	41.5	74.4
10N2 1/2	42.2	75.1
10N5	41.8	75.8
10N7	41.8	76.9
10N15	41.8	74.4
10N20	41.1	76.9
10N35	41.5	78.3
7C 1/2	42.5	75.8
7C2 1/2	42.2	77.2
7C5	42.5	77.6
7C7	42.5	77.2
7C15	42.2	76.5
7C20	42.5	76.9
7C35	42.2	79.4
10C 1/2	42.2	77.2
10C2 1/2	43.2	76.5
10C5	42.9	76.5
10C7	42.5	77.2
10C15	42.9	77.9
10C20	42.9	77.2
10C35	42.5	76.2

TABLE 16

YARN DIAMETERS FOR TYPE I FABRICS
(Cheney)

Yarn Diameters Measured In The Fabric Using A Microscope, (In Inches)

	Warp		Filling	
Fabric	Horizontal Diameter	Vertical Diameter	Horizontal Diameter	Vertical Diameter
R7N 1/2	.0045[illegible]	.00176	.00779	.00088
R7N7	.00442	.00134	.006[illegible]2	.00168
R7N30	.00467	.00184	.00467	.00236
R7C 1/2	.00474	.00168	.00[illegible]06	.000[illegible]
R7C7	.00543	.00168	.00845	.00145
R7C30	.00482	.00184	.00622	.00134

TABLE 17

HORIZONTAL YARN DIAMETERS OF FABRICS
(Warwick)

Fabric Code	Yarn Diameters (Inches)			
	Single Yarns		Rip-Stop Yarns	
	Warp	Filling	Warp	Filling
Series A				
R 1/2 N 1/2	0.005003	0.007204	0.007285	0.010183
R5N 1/2	0.004815	0.007349	0.007486	0.010063
R20N 1/2	0.003370	0.007466	0.006464	0.009882
R30N 1/2	0.003110	0.005825	0.005521	0.009120
R 1/2 C 1/2	0.006205	0.007323	0.008631	0.011604
R5C 1/2	0.005499	0.007506	0.008262	0.011500
R20C 1/2	0.003945	0.007430	0.007266	0.010726
R30C 1/2	0.003810	0.007104	0.007542	0.010995
Series B				
R30N 1/2	0.003110	0.005825	0.005521	0.009120
R30N5	0.002979	0.005418	0.005559	0.008720
R30N10	0.003148	0.005159	0.005723	0.009252
R30N20	0.003163	0.003772	0.005825	0.007870
R30N30	0.003023	0.003719	0.005863	0.006560
R30C 1/2	0.003810	0.007104	0.007542	0.010995
R30C5	0.003676	0.006885	0.007332	0.010814
R30C10	0.003813	0.005988	0.007173	0.009645
R30C20	0.004006	0.005180	0.006910	0.008823
R30C30	0.003834	0.004279	0.006733	0.008350
Series C				
R 1/2 N 1/2	0.005003	0.007204	0.007285	0.010183
R5N5	0.004514	0.005598	0.006548	0.009468
R20N20	0.003218	0.004256	0.006292	0.008430
R30N30	0.003023	0.003719	0.005863	0.006560
R 1/2 C 1/2	0.006205	0.007323	0.008631	0.011604
R5C5	0.005145	0.006940	0.007079	0.010598
R20C20	0.004258	0.005059	0.007476	0.009136
R30C30	0.003834	0.004279	0.006733	0.008350

NOTE: Values were averaged from 20 readings.

TABLE 18

YARN DIAMETERS FOR TYPE II FABRICS
(Cheney)

Yarn Diameters Measured In The Fabric Using A Microscope, (In Inches)

Fabric	Warp Horizontal Diameter	Warp Vertical Diameter	Filling Horizontal Diameter	Filling Vertical Diameter
7N 1/2	.00561	.00252	.01273	.00215
7N2 1/2	.00513	.00248	.01173	.00197
7N5	.00546	.00264	.01106	.00215
7N7	.00565	.00224	.01087	.00236
7N15	.00564	.00244	.00850	.00264
7N20	.00548	.00260	.00754	.00362
7N35	.00574	.00272	.00604	.00410
10N 1/2	.00486	.00256	.01171	.00207
10N2 1/2	.00520	.00288	.01190	.00244
10N5	.00485	.00232	.01018	.00260
10N7	.00538	.00240	.01050	.00276
10N15	.00541	.00256	.00892	.00305
10N20	.00536	.00256	.00733	.00367
10N35	.00533	.00268	.00557	.00461
7C 1/2	.00585	.00256	.01333	.00166
7C2 1/2	.00526	.00288	.01274	.00170
7C5	.00582	.00260	.01279	.00172
7C7	.00572	.00256	.01299	.00178
7C15	.00565	.00256	.01055	.00252
7C20	.00543	.00268	.00890	.00287
7C35	.00565	.00272	.00614	.00403
10C 1/2	.00563	.00248	.01342	.00170
10C2 1/2	.00535	.00216	.01339	.00209
10C5	.00485	.00256	.01253	.00213
10C7	.00547	.00232	.01228	.00213
10C15	.00559	.00232	.00937	.00240
10C20	.00548	.00232	.00850	.00307
10C35	.00567	.00240	.00683	.00399

TABLE 19

EFFECTIVE HORIZONTAL YARN DIAMETERS OF TYPE I FABRICS
(Warwick)

Fabric Code	Effective Diameter* Warp	Effective Diameter* Filling
Series A		
R 1/2 N 1/2	0.004696	0.006728
R5N 1/2	0.004572	0.006827
R20N 1/2	0.003336	0.006898
R30N 1/2	0.003029	0.005538
R 1/2 C 1/2	0.005779	0.006978
R5C 1/2	0.005190	0.007109
R20C 1/2	0.003814	0.006964
R30C 1/2	0.003797	0.006740
Series B		
R30N 1/2	0.003029	0.005538
R30N5	0.002932	0.005178
R30N10	0.003081	0.005036
R30N20	0.003104	0.003804
R30N30	0.003000	0.003618
R30C 1/2	0.003797	0.006740
R30C5	0.003670	0.006480
R30C10	0.003759	0.005723
R30C20	0.003880	0.005004
R30C30	0.003726	0.004252
Series C		
R 1/2 N 1/2	0.004696	0.006728
R5N5	0.004234	0.005412
R20N20	0.003199	0.004243
R30N30	0.003000	0.003618
R 1/2 C 1/2	0.005779	0.006978
R5C5	0.004783	0.006569
R20C20	0.004138	0.004945
R30C30	0.003726	0.004252

* Effective diameter, inches.

TABLE 20

FREE AREA AND LIGHT PENETRABILITY FOR TYPE I FABRICS
(Cheney)

Fabric	(%) Light Penetrability	(%) Free Area*
R7N 1/2	8.9[illegible]	2.[illegible]0
R7N7	18.4	7.[illegible]8
R7N30	27.1	1[illegible].2
R7C 1/2	4.75	**
R7C7	8.64	**
R7C30	15.8	10.[illegible]5

* Free areas calculated from measurements made on samples not imbedded in medium.

** Data not available: adjacent yarns overlap each other.

TABLE 21

FREE AREA AND LIGHT PENETRABILITY FOR TYPE I FABRICS
(Warwick)

Fabric Code	(%) Free Area*	(%) Light Penetrability	Fabric Code	(%) Free Area*	(%) Light Penetrability
R 1/2 N 1/2	7.2	6.8	R 1/2 C 1/2	3.4	3.0
R 1/2 N5	----	13.2	R 1/2 C5	----	7.2
R 1/2 N10	----	16.2	R 1/2 C10	----	9.0
R 1/2 N20	----	22.4	R 1/2 C20	----	13.6
R 1/2 N30	----	26.3	R 1/2 C30	----	15.8
R5N 1/2	6.9	7.2	R5C 1/2	3.9	4.0
R5N5	16.0	14.4	R5C5	7.5	7.5
R5N10	----	17.2	R5C10	----	10.1
R5N20	----	24.8	R5C20	----	15.6
R5N30	----	28.3	R5C30	----	18.7
R20N 1/2	10.3	11.8	R20C 1/2	8.0	6.7
R20N5	----	18.7	R20C5	----	10.2
R20N10	----	23.5	R20C10	----	13.5
R20N20	31.0	30.4	R20C20	20.5	18.6
R20N30	----	34.7	R20C30	----	20.8
R30N 1/2	21.6	15.1	R30C 1/2	9.9	7.6
R30N5	24.8	21.3	R30C5	12.0	11.7
R30N10	26.2	26.5	R30C10	17.7	15.5
R30N20	34.6	33.6	R30C20	21.7	21.6
R30N30	37.1	37.0	R30C30	27.6	25.4

* Free areas were calculated on selected fabrics as listed in Table 4.

TABLE 22

FREE AREA AND LIGHT PENETRABILITY FOR TYPE II FABRICS
(Cheney)

Fabric Code	(%) Free Area	(%) Light Penetrability
7N 1/2	0.5	4.2
7N2 1/2	2.5	4.9
7N5	4.0	6.9
7N7	4.2	7.4
7N15	9.9	13.2
7N20	12.3	15.8
7N35	15.0	19.8
10N 1/2	2.7	3.9
10N2 1/2	3.4	5.4
10N5	6.7	6.9
10N7	6.5	10.2
10N15	10.6	14.7
10N20	14.4	17.7
10N35	19.2	21.2

TABLE 23

AIR PERMEABILITY CHARACTERISTICS OF TYPE I, RIP-STOP FABRICS (CHENEY) TESTED ON THE FRAZIER PERMEOMETER AT F.R.L., INC.

Static Pressure, Inches of Water	Air Permeability, CFM Per Sq. Ft.					
	R7N 1/2	R7N7	R7N30	R7C 1/2	R7C7	R7C30
0.5	161	352	684	116	152	362
1.0	256	540	---	188	246	540
2.5	444	---	---	201	462	---
5.0	---	---	---	307	---	---
10.0	---	---	---	---	---	---

AIR PERMEABILITY CHARACTERISTICS OF TYPE I, RIP-STOP FABRICS (CHENEY) TESTED ON THE GEORGIA INSTITUTE HIGH PRESSURE PERMEOMETER.

Static Pressure, Inches of Water	R7N 1/2	R7N7	R7N30	R7C 1/2	R7C7	R7C30
0.5	---	---	714	---	---	---
1.0	---	594	1069	---	---	625
2.0	---	881	1538	---	---	958
3.0	525	1107	1924	---	565	---
3.5	---	---	---	---	---	1268
4.0	---	---	2266	---	---	---
5.0	702	1439	2567	349	765	1511
6.0	---	---	2830	---	---	---
7.5	---	1783	---	---	989	1897
8.0	---	---	3318	---	---	---
10.0	1057	2114	3721	542	1195	2255
11.0	---	---	3943	---	---	---
12.5	---	2432	---	---	---	2557
15.0	1332	2679	---	716	1511	2842
17.5	---	---	---	---	---	3128
20.0	1558	3142	---	850	1819	3337
25.0	1799	3556	---	976	2090	---
30.0	1996	---	---	1112	2354	---
35.0	2188	---	---	1219	2604	---
40.0	2374	---	---	1408	2804	---
45.0	2531	---	---	1462	---	---

TABLE 24

AIR PERMEABILITY AT VARIOUS PRESSURE DIFFERENTIALS FOR TYPE I FABRICS USING THE FRAZIER PERMEOMETER.
(Warwick)

Fabric Code	Pressure Differentials, ΔP, Inches of Water 0.5	1.0	2.5	5.0	7.5	10.0	Others
R 1/2 N 1/2	104	169	314	502	641	769	----
R 1/2 N5	236	362	659	998	*	*	----
R 1/2 N10	312	479	831	*	*	*	----
R 1/2 N20	517	746	1288	*	*	*	----
R 1/2 N30	591	884	*	*	*	*	1333(1)
R5N 1/2	121	193	356	559	707	847	----
R5N5	285	435	772	1187	*	*	----
R5N10	356	550	957	*	*	*	----
R5N20	576	862	*	*	*	*	1298(1)
R5N30	691	1039	*	*	*	*	1307(2)
R20N 1/2	221	344	620	*	*	*	----
R20N5	387	595	1032	*	*	*	----
R20N10	536	782	1365	*	*	*	----
R20N20	732	1109	*	*	*	*	1402(2)
R20N30	884	1320	*	*	*	*	650(3)
R30N 1/2	304	469	623	*	*	*	----
R30N5	466	701	1242	*	*	*	----
R30N10	603	915	*	*	*	*	1161(2)
R30N20	838	1257	*	*	*	*	620(3)
R30N30	977	*	*	*	*	720(3)	1376(4)

(Continued)

* (See end of table)

TABLE 24 (CONTINUED)

AIR PERMEABILITY AT VARIOUS PRESSURE DIFFERENTIALS FOR TYPE I FABRICS USING THE FRAZIER PERMEOMETER
(Warwick)

Fabric Code	Pressure Differentials, ΔP, Inches of Water						
	0.5	1.0	2.5	5.0	7.5	10.0	Others
R 1/2 C 1/2	31	53	100	181	246	302	[illegible](5)
R 1/2 C5	103	166	313	506	655	[illegible]	----
R 1/2 C10	151	237	422	658	840	*	----
R 1/2 C20	270	403	694	1050	*	*	----
R 1/2 C30	329	496	832	1266	*	*	----
R5C 1/2	50	85	164	269	351	428	----
R5C5	113	185	354	577	744	909	----
R5C10	177	279	504	778	1017	*	----
R5C20	319	487	826	*	*	*	----
R5C30	399	603	1014	*	*	*	----
R20C 1/2	100	161	306	499	648	785	----
R20C5	166	274	517	819	1086	*	----
R20C10	251	395	705	1120	*	*	----
R20C20	403	613	1041	*	*	*	----
R20C30	492	718	1248	*	*	*	----
R30C 1/2	112	183	353	578	746	913	----
R30C5	203	324	609	952	*	*	----
R30C10	303	472	830	*	*	*	----
R30C20	498	730	1280	*	*	*	----
R30C30	597	904	*	*	*	*	1344(1)

* Data not available.

(1) Data taken at 2.0 inches of water
(2) Data taken at 1.5 inches of water
(3) Data taken at 0.3 inches of water
(4) Data taken at 0.9 inches of water
(5) Data taken at 12.5 inches of water

All values were averaged from five tests. The air permeability data are expressed in cubic feet of air per minute per square foot of sample.

TABLE 25

AIR PERMEABILITY CHARACTERISTICS OF TYPE II, 2/1 TWILL FABRICS (CHENEY) TESTED ON THE FRAZIER PERMEOMETER AT F.R.L., INC., CALENDERED AND UNCALENDERED.

Static Pressure, Inches of Water	Air Permeability, CFM Per Sq. Ft.						
	7N 1/2	7N2 1/2	7N5	7N7	7N15	7N20	7N35
0.5	105	136	190	201	352	455	597
1.0	156	200	276	316	527	600	---
2.5	296	343	533	561	---	---	---
5.0	451	597	---	---	---	---	---
10.0	---	---	---	---	---	---	---

	10N 1/2	10N2 1/2	10N5	10N7	10N15	10N20	10N35
0.5	98	158	201	223	371	507	646
1.0	162	239	303	338	569	---	---
2.5	320	440	507	635	---	---	---
5.0	477	---	---	---	---	---	---
10.0	---	---	---	---	---	---	---

	7C 1/2	7C2 1/2	7C5	7C7	7C15	7C20	7C35
0.5	25	30	51	62	174	262	393
1.0	43	58	88	98	283	384	540
2.5	89	104	182	217	480	---	---
5.0	149	178	264	307	---	---	---
10.0	236	279	451	483	---	---	---

	10C 1/2	10C2 1/2	10C5	10C7	10C15	10C20	10C35
0.5	26	33	57	75	223	278	421
1.0	48	54	94	115	338	425	654
2.5	94	121	184	230	581	---	---
5.0	156	200	211	266	---	---	---
10.0	252	307	462	---	---	---	---

(Continued)

TABLE 25 (CONTINUED)

AIR PERMEABILITY CHARACTERISTICS OF TYPE II, 2/1 TWILL FABRICS (CHENEY) TESTED ON THE GEORGIA INSTITUTE HIGH PRESSURE INSTRUMENT, CALENDERED AND UNCALENDERED.

Static Pressure, Inches of Water	7N 1/2	7N5	7N15	7N35	7C 1/2	7C5	7C15	7C35
0.5	---	---	---	596	---	---	---	---
1.0	---	---	---	900	---	---	---	576
2.0	---	---	915	1288	---	---	---	---
2.5	---	---	---	---	---	---	546	---
3.0	---	---	---	1586	---	---	---	1080
4.0	---	705	1315	---	---	---	---	---
5.0	416	---	---	2080	---	---	797	1384
6.0	---	---	1610	---	---	---	---	---
7.0	487	---	---	---	---	---	---	---
7.5	---	---	---	---	---	401	1011	1708
8.0	---	1008	1866	2691	172	---	---	---
10.0	615	---	2099	---	---	477	1179	2008
12.0	---	1257	2324	3318	250	---	---	---
13.0	---	---	---	---	---	---	---	2321
15.0	784	---	---	3702	---	614	1485	---
16.0	---	1453	2727	3792	311	---	---	2617
17.0	---	---	---	3985	---	---	---	---
19.0	---	---	---	---	---	---	---	2880
20.0	930	1673	3080	---	374	737	1737	---
22.0	---	---	3235	---	402	---	---	3104
24.0	---	1847	3393	---	---	---	---	---
25.0	1058	---	---	---	444	854	1985	---
26.0	---	---	---	---	---	---	---	3381
28.0	---	2026	---	---	---	---	---	---
30.0	1173	---	---	---	496	959	2197	---
32.0	---	2181	---	---	---	---	---	---
35.0	1286	---	---	---	---	1066	2407	---
36.0	---	2335	---	---	---	---	---	---
40.0	1393	2489	---	---	608	1158	2592	---
44.0	---	2560	---	---	---	---	---	---
45.0	1496	---	---	---	662	1248	---	---
50.0	1581	---	---	---	712	1331	---	---

(Continued)

TABLE 25 (CONTINUED)

AIR PERMEABILITY CHARACTERISTICS OF TYPE II, 2/1 TWILL FABRICS (CHENEY) TESTED ON THE GEORGIA INSTITUTE HIGH PRESSURE INSTRUMENT, CALENDERED AND UNCALENDERED

Static Pressure, Inches of Water	10N 1/2	10N5	10N15	10N35	10C 1/2	10C5	10C15	10C35
0.5	---	---	---	695	---	---	---	---
1.0	---	---	671	---	---	---	---	686
2.0	---	---	969	1462	---	---	591	992
3.0	---	659	---	1806	---	---	---	---
4.0	---	---	1371	2106	---	---	---	1429
5.0	---	873	---	---	161	359	981	---
6.0	---	---	1699	2624	---	---	---	1784
7.0	---	1027	---	---	---	430	1176	---
8.0	563	---	1969	3068	---	---	---	2081
9.0	---	---	---	3291	---	---	---	---
10.0	---	1246	2222	3494	253	538	1439	2356
12.0	703	---	2448	3902	---	---	---	2617
13.0	---	---	---	4067	---	---	---	---
14.0	---	---	2668	---	---	---	---	---
15.0	---	1546	---	---	331	714	1777	2950
16.0	834	---	2863	---	---	---	---	---
18.0	---	---	3065	---	---	---	---	3255
20.0	958	1807	3250	---	411	822	2091	---
21.0	---	---	---	---	---	---	---	3527
24.0	1102	---	---	---	---	---	---	---
25.0	---	---	---	---	473	941	2371	---
28.0	1265	---	---	---	---	---	---	---
30.0	---	2262	---	---	538	1066	2613	---
32.0	1307	---	---	---	---	---	---	---
35.0	---	---	---	---	592	1158	2863	---
36.0	1426	---	---	---	---	---	---	---
40.0	1537	2678	---	---	658	1261	3085	---
44.0	1613	---	---	---	---	---	---	---
45.0	---	2875	---	---	707	1358	---	---
48.0	1726	---	---	---	---	---	---	---
50.0	---	3066	---	---	757	1532	---	---
55.0	---	---	---	---	817	---	---	---

TABLE 26

YARN STABILITY TESTS FOR TYPES I AND II FABRICS
(Cheney)

Filling Yarn Twist, t.p.i.	Displacement*, Inches 7C Series	7N Series	10C Series	10N Series	R7C Series	R7N Series	Average
1/2	0.046	0.056	0.044	0.059	0.053	0.046	0.051
2 1/2	0.045	0.051	0.047	0.057	-----	-----	0.050
5	0.057	0.059	0.053	0.051	-----	-----	0.055
7	0.051	0.067	0.056	0.041	0.057	0.050	0.054
15	0.055	0.060	0.045	0.062	-----	-----	0.056
20	0.067	0.066	0.047	0.065	-----	-----	0.061
30	-----	-----	-----	-----	0.046	0.048	-----
35	0.072	0.062	0.072	0.056	-----	-----	0.066

* Under 1.5 lb. load for 2" samples. Results shown are averages of 5 tests.

TABLE 27

TENSILE TEST DATA OF YARNS REMOVED FROM TYPE I FABRICS
(Cheney)

Fabric Code		Warp Load, Grams	Warp Elongation, Per Cent	Warp Energy*	Filling Load, Grams	Filling Elongation, Per Cent	Filling Energy*
R7N 1/2	Regular Yarn	155.2	25.5	144	146.4	33.3	146
	Ripstop Yarn	159.6	27.2	182	147.9	34.3	150
R7N7	Regular Yarn	160.0	29.5	198	152.2	38.4	194
	Ripstop Yarn	159.1	27.6	182	153.0	38.2	200
R7N30	Regular Yarn	162.2	32.0	204	159.0	36.3	190
	Ripstop Yarn	154.5	35.4	240	161.2	37.5	162
R7C 1/2	Regular Yarn	153.8	25.7	150	150.3	39.1	190
	Ripstop Yarn	152.2	25.1	136	148.3	38.0	170
R7C7	Regular Yarn	152.6	27.8	166	168.3	38.1	200
	Ripstop Yarn	157.2	26.2	150	168.3	38.6	178
R7C30	Regular Yarn	149.2	26.6	142	153.3	39.9	184
	Ripstop Yarn	153.9	27.8	150	154.7	40.5	196

* Energy expressed in inch-pounds/inch/denier x 10^{-5}

TABLE 28

TENSILE TEST DATA OF YARNS REMOVED FROM TYPE II FABRICS
(Cheney)

Fabric Code	Warp			Filling		
	Load, Grams	Elongation, Per Cent	Energy*	Load, Grams	Elongation, Per Cent	Energy*
7N 1/2	198.0	32.0	202	334.1	39.0	218
7N2 1/2	185.8	30.8	182	342.8	41.2	204
7N5	200.3	31.8	212	364.3	45.5	254
7N7	201.0	31.3	208	343.4	40.7	224
7N15	199.5	33.0	218	342.9	46.9	292
7N20	197.4	32.5	198	352.2	44.4	254
7N35	198.4	30.1	176	347.8	43.0	230
7C 1/2	195.1	32.2	206	297.9	31.1	124
7C2 1/2	198.9	32.3	196	296.0	35.9	150
7C5	197.6	31.5	196	318.4	32.5	134
7C7	194.7	31.6	210	334.9	36.4	156
7C15	195.6	31.8	184	341.3	37.1	168
7C20	193.4	31.8	176	330.2	42.8	200
7C35	196.6	33.4	198	350.5	47.3	226
10N 1/2	196.6	32.4	218	323.2	35.8	166
10N2 1/2	195.9	33.3	210	346.3	41.2	200
10N5	204.3	31.8	214	343.9	39.3	192
10N7	204.3	33.7	216	356.4	41.1	208
10N15	205.8	30.4	192	343.9	42.2	228
10N20	204.7	30.5	190	342.5	44.5	260
10N35	202.7	31.4	198	351.6	44.3	238
10C 1/2	201.5	33.0	200	328.7	35.4	162
10C2 1/2	193.5	28.9	156	325.8	36.9	180
10C5	194.6	29.6	172	331.1	35.9	144
10C7	194.5	30.1	162	340.1	35.4	156
10C15	202.6	34.2	222	356.6	39.8	186
10C20	195.4	28.7	148	336.5	40.3	178
10C35	196.2	30.2	172	352.5	45.4	236

* Energy expressed in inch-pounds/inch/denier x 10^{-5}

TABLE 29

STRIP TENSILE DATA FOR TYPE I FABRICS
(Cheney)

Fabric Code	Warp Load lbs.	Warp Elongation %	Filling Load lbs.	Filling Elongation %
R7N 1/2	40.6	24.0	40.1	35.2
R7N7	44.0	29.7	42.5	43.6
R7N30	44.4	32.1	43.3	38.2
R7C 1/2	40.9	24.6	42.0	43.0
R7C7	43.1	29.4	45.7	41.6
R7C30	43.1	30.4	41.0	42.5

TABLE 30

STRIP TENSILE DATA FOR TYPE II FABRICS
(Cheney)

Fabric Code	Warp Load lbs.	Warp Elongation %	Filling Load lbs.	Filling Elongation %
7N 1/2	56.8	33.5	56.6	45.7
7N2 1/2	57.2	35.3	58.2	47.3
7N5	57.9	32.7	61.5	41.6
7N7	53.8	25.5	59.5	43.7
7N15	52.7	26.4	58.1	44.5
7N20	55.9	35.7	59.3	46.6
7N35	55.2	35.1	56.6	43.1
10N 1/2	57.3	30.3	57.4	41.7
10N2 1/2	57.3	31.7	60.8	43.8
10N5	58.1	32.7	59.7	44.3
10N7	57.3	32.2	60.6	43.9
10N15	56.2	33.7	58.8	46.5
10N20	54.7	33.1	57.4	46.2
10N35	55.3	34.7	58.4	45.3
7C 1/2	58.1	33.4	52.9	37.4
7C2 1/2	56.0	32.4	52.5	39.7
7C5	56.6	32.5	57.5	38.0
7C7	57.4	33.8	57.8	40.3
7C15	55.3	34.5	58.0	41.1
7C20	55.8	34.7	56.5	44.6
7C35	54.8	33.6	55.9	47.5
10C 1/2	56.7	32.4	55.9	40.2
10C2 1/2	56.3	32.8	56.4	43.2
10C5	56.6	32.2	57.7	41.2
10C7	56.7	32.0	57.8	39.4
10C15	55.3	33.2	58.4	45.4
10C20	54.2	32.9	53.9	46.0
10C35	53.8	30.5	54.5	44.3

TABLE 31

STRIP TENSILE DATA FOR TYPE I FABRICS
(Warwick)

Fabric Code	Warp Load, lbs.	Warp Elongation %	Filling Load, lbs.	Filling Elongation %
R 1/2 N 1/2	39.5	23.5	39.7	30.4
R5N 1/2	42.5	26.2	43.3	34.5
R20N 1/2	42.7	25.3	39.8	33.4
R30N 1/2	41.6	25.0	41.7	38.4
R30N 1/2	41.6	25.0	41.7	38.4
R30N5	42.0	29.1	40.2	38.2
R30N10	42.6	29.3	38.4	31.8
R30N20	41.4	28.1	40.8	40.4
R30N30	41.8	28.6	40.5	41.4
R 1/2 N 1/2	39.5	23.5	39.7	30.4
R5N5	42.7	27.2	42.7	37.5
R20N20	41.9	25.6	41.9	35.8
R30N30	41.8	28.6	40.5	41.4

TABLE 32

REPEATED STRESS TEST ON TYPE I FABRICS
(Cheney)

I. Repeated Stress Level - 10 Pounds (Approximately 25% of Average Breaking Strength)

Fabric Code	Warp: Ultimate Breaking Strength lbs.	Warp: Corrected Residual Elongation %	Warp: Secondary Creep % 5th Cycle	Warp: Secondary Creep % 6th Cycle	Warp: Energy Rupt. Cycle in-lbs/in.	Filling: Ultimate Breaking Strength lbs.	Filling: Corrected Residual Elongation %	Filling: Secondary Creep % 5th Cycle	Filling: Secondary Creep % 6th Cycle	Filling: Energy Rupt. Cycle in-lbs/in.
R7N 1/2	41.7	24.8	0.69	0.72	5.40	43.6	42.1	2.94	3.02	9.77
R7N7	43.2	29.6	0.84	0.88	7.54	41.6	42.5	4.29	4.33	9.76
R7N30	41.7	29.5	0.78	0.83	6.83	41.8	32.4	4.53	4.62	6.00
R7C 1/2	41.2	27.0	0.73	0.77	5.19	40.7	40.0	3.21	3.33	7.41
R7C7	41.6	27.8	0.70	0.76	6.00	40.6	37.9	5.05	5.17	6.82
R7C30	42.3	31.2	0.83	0.92	6.78	41.5	36.2	6.35	6.44	6.28

II. Repeated Stress Level - 20 Pounds (Approximately 50% of Average Breaking Strength)

Fabric Code	Warp: Ultimate Breaking Strength lbs.	Warp: Corrected Residual Elongation %	Warp: Secondary Creep % 5th Cycle	Warp: Secondary Creep % 6th Cycle	Warp: Energy Rupt. Cycle in.-lbs/in.	Filling: Ultimate Breaking Strength lbs.	Filling: Corrected Residual Elongation %	Filling: Secondary Creep % 5th Cycle	Filling: Secondary Creep % 6th Cycle	Filling: Energy Rupt. Cycle in.-lbs/in.
R7N 1/2	40.3	19.7	2.07	2.15	4.39	43.6	37.5	7.27	7.49	8.99
R7N7	42.0	25.6	1.95	3.52	5.82	42.0	35.9	7.24	7.67	8.32
R7N30	41.9	26.3	2.28	2.40	5.84	43.4	29.6	7.14	7.32	6.00
R7C 1/2	41.2	25.0	1.93	1.95	4.65	40.1	30.8	7.31	7.58	5.45
R7C7	42.3	27.1	2.00	2.09	5.55	40.2	28.3	9.93	10.20	5.38
R7C30	42.4	23.0	2.47	2.62	5.73	42.6	31.5	11.74	11.97	5.92

TABLE 32 (CONTINUED)

REPEATED STRESS TESTS ON TYPE I FABRICS
(Cheney)

III. Repeated Stress Level - 30 Pounds (Approximately 75% of Average Breaking Strength)

Fabric Code	Warp: Ultimate Breaking Strength lbs.	Warp: Corrected Residual Elongation %	Warp: Secondary Creep % 5th Cycle	Warp: Secondary Creep % 6th Cycle	Warp: Energy Rupt. Cycle in.-lbs/in.	Filling: Ultimate Breaking Strength lbs.	Filling: Corrected Residual Elongation %	Filling: Secondary Creep % 5th Cycle	Filling: Secondary Creep % 6th Cycle	Filling: Energy Rupt. Cycle in.-lbs/in.
R7N 1/2	41.2	21.0	3.55	3.71	4.07	43.9	30.5	9.80	9.72	7.06
R7N7	44.0	22.0	3.05	3.17	4.85	43.0	29.9	10.66	10.90	6.53
R7N30	42.9	22.6	3.69	3.79	4.70	43.0	26.3	9.11	9.36	5.23
R7C 1/2	42.2	24.3	3.51	3.71	5.79	41.1	27.5	10.24	10.51	5.73
R7C7	42.2	24.1	3.96	4.15	5.65	45.5	25.0	11.20	11.37	5.18
R7C30	42.7	24.4	4.22	4.41	5.78	41.3	26.2	13.67	14.06	5.28

TABLE 33

REPEATED STRESS TESTS ON TYPE II FABRICS
(Cheney)

I. Repeated Stress Level - 15 Pounds (Approximately 25% of Average Breaking Strength)

Fabric Code	Warp: Ultimate Breaking Strength lbs.	Warp: Corrected Residual Elongation %	Warp: Secondary Creep % 5th Cycle	Warp: Secondary Creep % 6th Cycle	Warp: Energy Rupt. Cycle in.-lbs/in.	Filling: Ultimate Breaking Strength lbs.	Filling: Corrected Residual Elongation %	Filling: Secondary Creep % 5th Cycle	Filling: Secondary Creep % 6th Cycle	Filling: Energy Rupt. Cycle in.-lbs/in.
7N 1/2	57.9	33.6	1.12	1.05	11.60	56.7	40.2	3.86	4.12	13.54
7N2 1/2	57.2	31.9	1.27	1.30	11.06	60.7	41.3	3.44	3.51	15.04
7N5	55.4	31.7	1.07	1.14	11.05	61.0	39.6	3.73	3.75	13.41
7N7	56.5	31.2	1.16	2.03	10.39	60.1	37.4	4.23	4.38	11.92
7N15	53.6	32.0	1.27	1.29	10.02	56.5	39.8	4.78	4.98	13.18
7N20	53.6	32.9	1.14	1.15	10.50	58.5	36.6	4.82	4.86	12.16
7N35	54.4	35.4	1.43	1.58	10.75	56.1	38.2	5.05	5.29	11.78
10N 1/2	54.1	28.5	1.15	1.22	8.90	55.7	38.4	3.74	3.81	11.92
10N2 1/2	57.1	29.5	1.17	1.26	9.66	56.4	35.1	3.87	4.02	10.43
10N5	54.0	29.1	1.05	1.13	9.28	57.9	39.8	4.22	4.40	12.79
10N7	57.4	29.0	1.06	1.18	9.41	61.0	35.9	4.00	4.13	11.36
10N15	53.9	31.2	1.17	1.21	9.87	55.9	40.0	4.81	4.92	13.42
10N20	53.4	29.2	1.27	1.28	8.64	55.2	39.1	4.84	4.87	12.46
10N35	53.2	33.1	1.32	1.37	10.11	56.5	37.3	4.89	5.11	11.90

TABLE 33 (CONTINUED)

REPEATED STRESS TESTS ON TYPE II FABRICS
(Cheney)

II. Repeated Stress Level - 30 pounds (Approximately 50% of Average Breaking Strength)

Fabric Code	Warp: Ultimate Breaking Strength lbs.	Warp: Corrected Residual Elongation %	Warp: Secondary Creep % 5th Cycle	Warp: Secondary Creep % 6th Cycle	Warp: Energy Rupt. Cycle in.-lbs/in.	Filling: Ultimate Breaking Strength lbs.	Filling: Corrected Residual Elongation %	Filling: Secondary Creep % 5th Cycle	Filling: Secondary Creep % 6th Cycle	Filling: Energy Rupt. Cycle in.-lbs/in.
7N 1/2	56.7	29.5	3.15	3.33	10.07	55.7	34.4	7.84	8.18	11.31
7N2 1/2	56.3	28.3	3.33	3.50	9.65	57.8	35.2	7.79	7.85	12.47
7N5	56.3	31.2	3.04	3.12	10.69	60.2	35.2	7.87	8.13	12.42
7N7	53.9	26.8	3.06	3.13	8.51	57.9	29.0	8.61	8.94	9.06
7N15	52.9	30.8	3.21	3.36	9.73	55.4	32.3	9.01	9.28	10.42
7N20	49.8	30.4	3.52	3.65	9.10	53.6	35.9	10.27	10.61	11.53
7N35	50.8	31.1	4.04	4.14	8.79	58.9	33.8	8.62	8.89	11.52
10N 1/2	59.5	27.2	2.82	2.91	9.21	58.4	31.8	8.40	8.59	10.21
10N2 1/2	56.5	25.1	3.26	3.36	8.16	55.0	29.4	8.00	8.33	9.07
10N5	59.6	29.7	2.90	3.02	10.53	62.0	34.2	8.99	9.19	12.13
10N7	55.9	25.5	3.02	3.12	8.21	59.4	29.1	8.83	9.08	9.78
10N15	53.8	28.2	3.67	3.82	8.63	55.8	34.5	8.86	9.22	11.58
10N20	53.1	29.8	3.61	3.73	9.14	57.6	32.9	8.91	9.18	11.06
10N35	54.3	30.2	3.76	4.01	9.45	58.0	33.4	9.11	9.28	11.32

TABLE 33 (CONTINUED)

REPEATED STRESS TESTS ON TYPE II FABRICS
(Cheney)

III. Repeated Stress Level - 45 Pounds (Approximately 75% of Average Breaking Strength)

Fabric Number	Warp: Ultimate Breaking Strength lbs.	Warp: Corrected Residual Elongation %	Warp: Secondary Creep % 5th Cycle	Warp: Secondary Creep % 6th Cycle	Warp: Energy Rupt. Cycle in.-lbs/in.	Filling: Ultimate Breaking Strength lbs.	Filling: Corrected Residual Elongation %	Filling: Secondary Creep % 5th Cycle	Filling: Secondary Creep % 6th Cycle	Filling: Energy Rupt. Cycle in.-lbs/in.
7N 1/2	57.7	26.3	5.71	6.00	9.03	57.4	29.0	12.29	12.71	9.61
7N2 1/2	56.9	24.7	5.52	5.71	8.21	61.3	30.7	11.60	11.80	11.44
7N5	55.4	27.2	2.91	3.10	8.76	57.0	30.1	14.52	15.33	9.92
7N7	56.9	25.2	5.56	5.76	8.45	59.4	26.7	12.79	13.13	8.87
7N15	54.9	24.8	5.97	6.27	7.36	57.2	28.2	12.78	13.20	9.30
7N20	54.1	24.8	6.17	6.43	7.17	60.3	27.4	13.79	14.13	10.30
7N35	52.5	22.6	6.56	6.90	5.76	56.7	27.5	13.81	14.07	8.90
10N 1/2	56.4	23.6	7.20	7.38	7.52	58.0	28.3	13.32	13.64	9.39
10N2 1/2	57.2	23.3	5.67	5.93	7.63	57.9	25.0	12.17	12.45	7.99
10N5	56.2	24.8	7.36	7.61	7.96	57.8	25.6	15.76	16.15	7.96
10N7	57.6	23.9	5.52	5.68	7.88	61.2	25.2	12.31	12.58	8.19
10N15	54.5	21.1	7.61	7.99	6.57	56.4	26.7	15.22	15.66	8.53
10N20	54.7	25.2	7.07	7.34	7.66	56.3	26.7	13.78	14.14	8.59
10N35	54.9	27.7	6.72	6.98	8.29	57.2	29.3	13.62	13.97	9.75

TABLE 34.

EFFECT OF SECONDARY CREEP ON AIR PERMEABILITY

	Unstressed Sample	Repeated Stress Level, 15 lbs.	Repeated Stress Level, 30 lbs.	Repeated Stress Level, 45 lbs.
Fabric 10N 1/2				
Secondary Creep*, warp	---	0.0061	0.0146	0.0369
Secondary Creep*, filling	---	0.0191	0.0430	0.0682
Free Area, %	2.74	3.04	3.46	4.39
% Increase in FA	---	10.9	26.3	60.2
Air Permeability**, cfm/sq.ft.	98	109	124	157
Fabric 10N35				
Secondary Creep*, warp	---	0.0069	0.0201	0.0349
Secondary Creep*, filling	---	0.0256	0.0464	0.0699
Free Area, %	19.18	20.22	21.15	22.18
% Increase in FA	---	5.4	10.3	15.6
Air Permeability**, cfm/sq.ft.	646	681	712	747

*This is assumed to be 1/2 of the value obtained from uniaxial tests (6th cycle).
**At 0.5 inches water pressure differential.

TABLE 35

TONGUE TEAR TEST DATA FOR TYPE I FABRICS

(Warwick)

Fabric Number	Tear Energy in.-lbs./in. fabric		Ave. Tear Load $\bar{P}$, lbs.		Max. Tear Load P_u, lbs.	
	Warp	Filling	Warp	Filling	Warp	Filling
R 1/2 N 1/2	14.22	12.19	6.11	5.38	6.67	5.78
R5N 1/2	16.23	13.67	6.72	6.23	7.18	6.72
R20N 1/2	6.86	6.76	3.02	3.35	3.62	3.89
R30N 1/2	8.30	6.06	3.79	2.94	4.37	3.60
R30N 1/2	8.30	6.06	3.79	2.94	4.37	3.60
R30N5	5.07	4.88	2.27	2.34	2.84	2.79
R30N10	5.53	5.18	2.41	2.56	2.92	3.07
R30N20	4.88	5.22	2.22	2.40	2.68	2.85
R30N30	4.83	7.03	2.20	3.30	2.71	3.78
R 1/2 N 1/2	14.22	12.19	6.11	5.38	6.67	5.78
R5N5	5.11	7.02	2.46	3.20	3.10	3.69
R20N20	5.16	4.97	2.22	2.32	2.77	2.72
R30N30	4.83	7.03	2.20	3.30	2.71	3.78
R 1/2 C 1/2	10.95	12.17	4.93	5.56	5.40	6.13
R5C 1/2	18.40	16.80	7.46	6.94	7.99	7.71
R20C 1/2	13.59	9.08	5.53	4.25	6.26	4.83
R30C 1/2	6.50	4.61	2.90	2.23	3.57	2.70
R30C 1/2	10.95	12.17	2.90	2.23	3.57	2.70
R30C5	5.26	5.36	2.44	2.52	2.94	2.94
R30C10	5.60	5.17	2.55	2.45	2.93	2.87
R30C20	4.89	5.49	2.13	2.57	2.60	2.99
R30C30	4.73	4.35	2.09	2.08	2.54	2.45
R 1/2 C 1/2	10.95	12.17	4.93	5.56	5.40	6.13
R5C5	12.92	12.53	5.38	5.36	5.80	5.80
R20C20	5.12	4.94	2.29	2.30	2.68	2.58
R30C30	4.73	4.35	2.09	2.08	2.54	2.45

TABLE 36

TONGUE TEAR TEST DATA FOR TYPE II FABRICS
(Cheney)

Fabric Code	Tear Energy in.-lbs./in. fabric		Ave. Tear Load, P, lbs.		Max. Tear Load, P_u, lbs.	
	Warp	Filling	Warp	Filling	Warp	Filling
7N 1/2	11.12	9.31	4.84	4.41	5.61	5.07
7N2 1/2	9.08	10.94	4.29	4.88	5.08	5.77
7N5	9.98	9.69	4.42	4.49	5.18	5.23
7N7	9.68	10.56	4.38	4.68	4.98	5.71
7N15	8.42	10.93	3.82	4.94	4.30	5.73
7N20	7.93	9.29	3.51	4.34	4.04	5.24
7N35	7.71	10.59	3.61	5.03	4.44	5.78
10N 1/2	9.92	9.68	4.44	4.46	5.08	5.11
10N2 1/2	8.59	9.00	3.78	4.26	4.35	4.82
10N5	9.20	8.65	4.13	4.41	4.83	4.93
10N7	9.29	9.25	4.17	4.33	4.74	4.90
10N15	8.56	9.17	3.86	4.23	4.38	4.97
10N20	6.88	8.91	3.07	4.13	3.52	4.99
10N35	6.55	10.48	2.99	4.81	3.53	5.66

TABLE 37

PERMEABILITY PERFORMANCE FACTORS
(Warwick)

Fabric Code	(1) Q_1	(2) LB %	(3) Q_1/LP	(4) n
R 1/2 N 1/2	168.6	6.8	24.69	0.664
R 1/2 N5	361.9	13.2	27.42	0.626
R 1/2 N10	479.2	16.2	29.58	0.607
R 1/2 N20	746.2	22.4	33.31	0.566
R 1/2 N30	883.9	26.3	33.61	0.584
R5N 1/2	192.5	7.2	26.85	0.643
R5N5	435.3	14.4	30.23	0.618
R5N10	550.0	17.2	31.98	0.614
R5N20	862.3	24.8	34.77	0.584
R5N30	1038.6	28.3	36.69	0.579
R20N 1/2	343.8	11.8	29.14	0.631
R20N5	595.0	18.7	31.82	0.607
R20N10	782.4	23.5	33.29	0.579
R20N20	1108.9	30.4	36.48	0.588
R20N30	1320.3	34.7	38.05	0.575
R30N 1/2	469.3	15.1	31.08	0.619
R30N5	700.5	21.3	32.89	0.607
R30N10	914.9	26.5	35.12	0.593
R30N20	1257.3	33.6	37.42	0.584
R30N30	1470*	37.0	39.73	0.573

* Extrapolated.

(Continued)

TABLE 37 (CONTINUED)

PERMEABILITY PERFORMANCE FACTORS
(Warwick)

Fabric Code	(1) Q_1	(2) LP, %	(3) Q_1/LP	(4) n
R 1/2 C 1/2	53.2	3.0	17.85	0.754
R 1/2 C5	166.0	7.2	23.15	0.680
R 1/2 C10	237.0	9.0	26.33	0.639
R 1/2 C20	402.0	13.6	29.63	0.595
R 1/2 C30	496.0	15.8	31.39	0.586
R5C 1/2	85.0	5.0	21.41	0.702
R5C5	184.5	7.5	24.63	0.693
R5C10	278.5	10.1	27.57	0.643
R5C20	486.5	15.6	31.18	0.591
R5C30	603.2	18.7	32.25	0.579
R20C 1/2	161.2	6.7	24.24	0.687
R20C5	273.5	10.2	26.84	0.693
R20C10	394.9	13.5	29.25	0.649
R20C20	612.7	18.6	32.94	0.589
R20C30	717.8	20.8	34.50	0.578
R30C 1/2	183.2	7.6	24.04	0.698
R30C5	324.4	11.7	27.72	0.672
R30C10	471.7	15.5	30.42	0.626
R30C20	730.0	21.6	33.79	0.586
R30C30	903.5	25.4	35.57	0.586

NOTES:

(1) Q_1 = Air permeability at a pressure differential of one inch of water, cfm/sq. ft.

(2) LP = Light penetrability at a wave length of 230 mu, per cent.

(4) n = Exponent in the classical flow equation:

$$\frac{Q_1}{Q_2} = \left(\frac{\Delta P_1}{\Delta P_2}\right)^n$$

where Q_1 and Q_2 are values of permeability at pressure differentials of ΔP_1 and ΔP_2.

TABLE 38

DISCHARGE COEFFICIENTS FOR SQUARE FABRICS
(Warwick)

Fabric Code	LP, Per Cent	Discharge Coefficient
R 1/2 N 1/2	6.8	0.548
R5N5	14.4	0.687
R30N20	30.4	0.837
R30N30	37.0	0.857
R 1/2 C 1/2	3.0	0.381
R5C5	7.5	0.550
R20C20	18.6	0.745
R30C30	25.4	0.799

TABLE 39

CALCULATED VALUES OF AIR PERMEABILITY**

Fabric Code	At P = 0.5" Calculated	Measured	% Error	At P = 10.0" Calculated	Measured	% Error
Square Fabrics: (Warwick)						
R 1/2 N 1/2	108	104	3.9	787	769	2.6
R5N5	267	285	0.7	1738	1800*	3.6
R20N20	752	732	2.7	3992	3940*	1.3
R30N30	979	977	0.2	5058	5600*	10.7
R 1/2 C 1/2	35	31	12.8	332	302	9.9
R5C5	123	113	8.9	872	909	4.2
R20C20	399	403	1.0	2293	2330*	1.6
R30C30	595	597	0.3	3243	3500*	7.9
Square Fabrics: (Cheney)						
R7N7	392	352	11.3	2260	2114	6.9
R7C7	149	152	2.0	1011	1195	18.2
Non-Square Fabric: (Warwick)						
R 1/2 C30	323	329	1.9	1920	1850*	3.8

** Calculations were made from Equation (3.24) for Rip-Stop fabrics of square construction.

* Extrapolated from Figures 13, 14, 15, 18, and 19.

TABLE 40

EFFECT OF BIAXIAL LOADING ON EXTENSIBILITY AND AREA

Stress Conditions	Extensions, %			
	R 1/2 N 1/2	R5N5	R20N20	R30N30
Uniaxial Loads				
5 lbs./in., Warp	3.2	3.9	4.1	5.9
20 lbs./in., Warp	12.8	12.2	12.3	13.9
5 lbs./in., Filling	5.3	8.3	9.7	11.2
20 lbs./in., Filling	17.7	19.2	20.4	22.7
Biaxial Loads				
5 lbs./in., Warp	1.3	2.5	2.8	1.3
20 lbs./in., Warp	9.2	10.7	13.2	9.0
5 lbs./in., Filling	4.3	5.4	7.7	5.0
20 lbs./in., Filling	14.5	17.7	17.5	19.7

	Increases in Areas, %			
	R 1/2 N 1/2	R5N5	R20N20	R30N30
Uniaxial Load, 5 lbs./in.	8.7	12.5	14.2	17.8
Biaxial Load, 5 lbs./in.	5.7	8.0	10.7	6.4
Uniaxial Load, 20 lbs./in.	32.8	33.7	35.2	39.8
Biaxial Load, 20 lbs./in.	25.0	30.3	33.0	30.5

TABLE 41

FREE AREA AND LIGHT PENETRABILITY OF ALUMINIUM PLATES

Plate No. (Drill Size)	Free Area, FA, %	Light Pen. LP*, %	LP / FA
59	4.1	3.8	0.93
58	4.4	4.3	0.98
53	9.1	9.3	1.02
51	10.8	10.4	0.96
47	14.4	13.8	0.96
43	19.4	19.7	1.02
40	21.2	21.3	1.00
38	24.2	24.8	1.02
36	26.8	27.4	1.02
34	30.4	31.2	1.03
37	33.5	34.2	1.02
32	34.4	35.8	1.04
30	39.1	39.8	1.02
29	46.0	46.8	1.02
			$\bar{x}$ = 1.00

* LP measured at wave length of 230 mμ.

TABLE 42

WIRE SCREEN DATA

Screen No.	Thread Count	Wire Diam. Inches x 10^{-3}	Free Area, FA, %	Light Pen. LP*, %	$\frac{LP}{FA}$
30A	33 x 31	11.6 x 11.6	39.6	40.2	1.02
50A	40 x 50	9.0 x 8.7	36.2	36.5	1.01
80A	76 x 81	5.6 x 5.4	32.4	33.5	1.03
100A	105 x 101	4.5 x 4.2	30.4	31.9	1.05
120A	128 x 121	4.0 x 3.3	31.4	32.2	1.03
30B	31 x 33	11.6 x 12.2	38.2	38.8	1.02
50B	51 x 41	8.6 x 8.0	35.7	36.2	1.01
80B	82 x 72	5.2 x 5.2	36.7	34.9	0.95
100B	103 x 93	4.0 x 4.1	37.3	36.2	0.97
120B	129 x 129	3.1 x 3.8	33.3	31.8	0.95
					$\bar{x}$ = 1.00

* LP measured at 230 $m\mu$.

TABLE 43

PROJECTED FREE AREA AND LIGHT PENETRABILITY
DATA OF TYPE I FABRICS
(Warwick)

Fabric Code	Per Cent FA	Per Cent LP	FA/LP
Series A			
R 1/2 N 1/2	7.2	6.8	1.06
R5N 1/2	6.9	7.2	0.95
R20N 1/2	10.3	11.8	0.87
R30N 1/2	21.6	15.1	1.43
R 1/2 C 1/2	3.4	3.0	1.13
R5C 1/2	3.9	4.0	0.97
R20C 1/2	8.0	6.7	1.19
R30C 1/2	9.9	7.6	1.30
Series B			
R30N 1/2	21.6	15.1	1.43
R30N5	24.8	21.3	1.16
R30N10	26.2	26.5	0.98
R30N20	34.6	34.6	1.00
R30N30	37.1	37.0	1.00
R30C 1/2	9.9	7.6	1.30
R30C5	12.0	11.7	1.02
R30C10	17.7	15.5	1.14
R30C20	21.7	21.6	1.00
R30C30	27.6	25.4	1.08
Series C			
R 1/2 N 1/2	7.2	6.8	1.06
R5N5	16.0	14.4	1.11
R20N20	31.0	30.4	1.01
R30N30	37.1	37.0	1.00
R 1/2 C 1/2	3.4	3.0	1.13
R5C5	7.5	7.5	1.00
R20C20	20.5	18.6	1.10
R30C30	27.6	25.4	1.08

APPENDIX III

DIAGRAMS AND GRAPHS

FIGURE I

WEAVE PATTERN OF ADDITIONAL PARACHUTE FABRICS (MODIFIED TYPE I RIPSTOP, WARWICK)

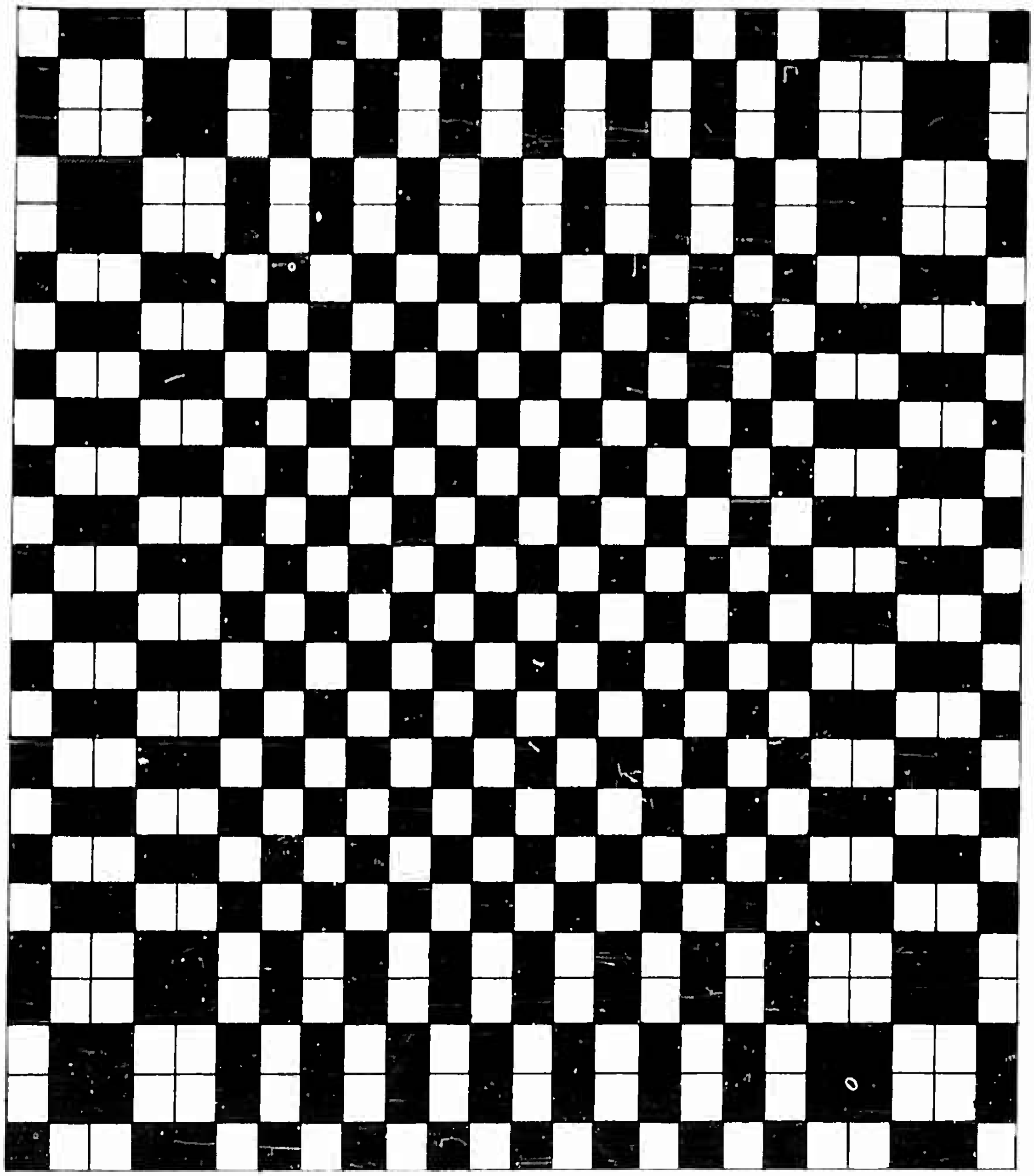

FIGURE 2

WARWICK FABRICS

HORIZONTAL YARN DIAMETER VS. YARN TWIST

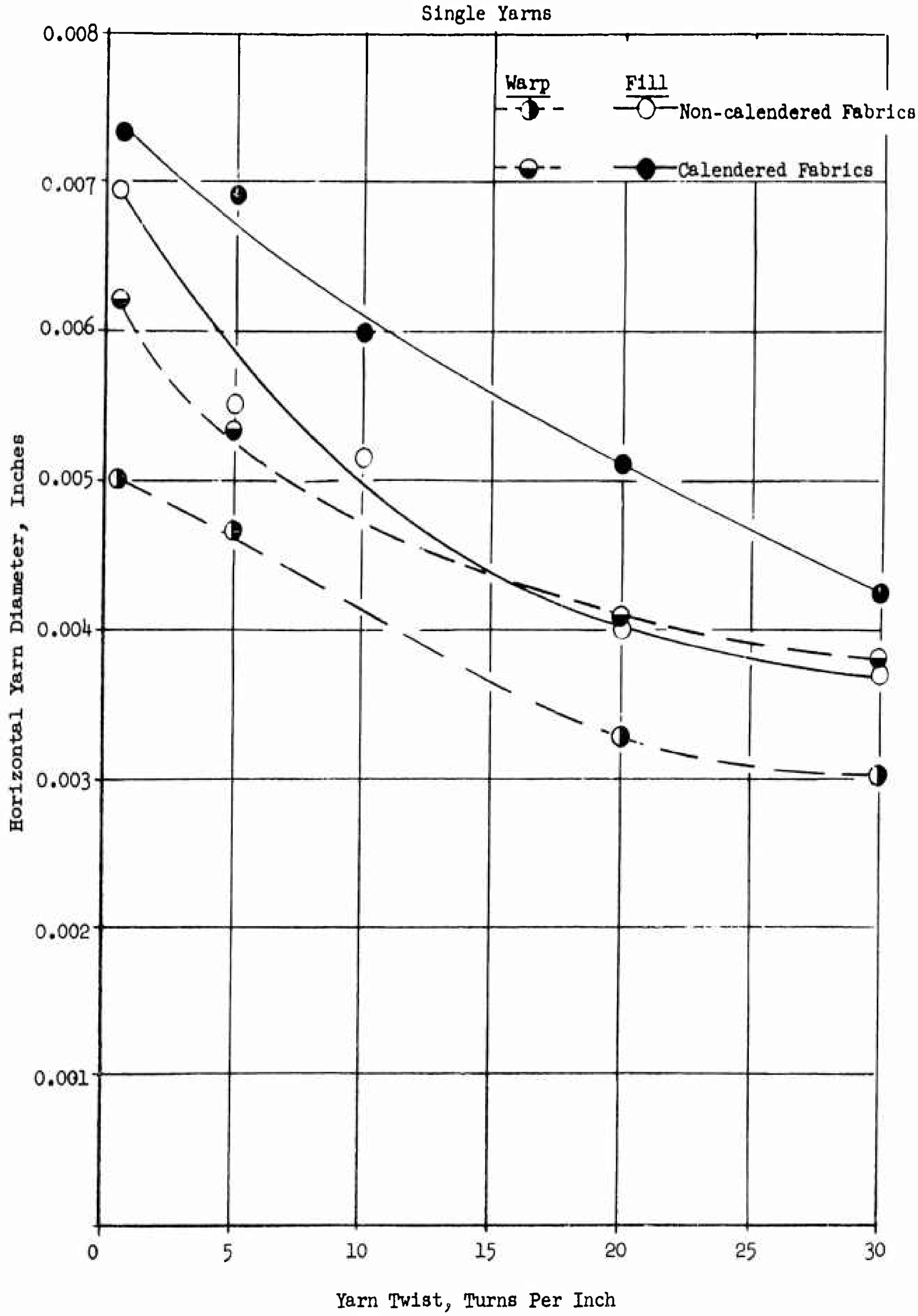

FIGURE 3

WARWICK FABRICS

HORIZONTAL YARN DIAMETER VS. YARN TWIST

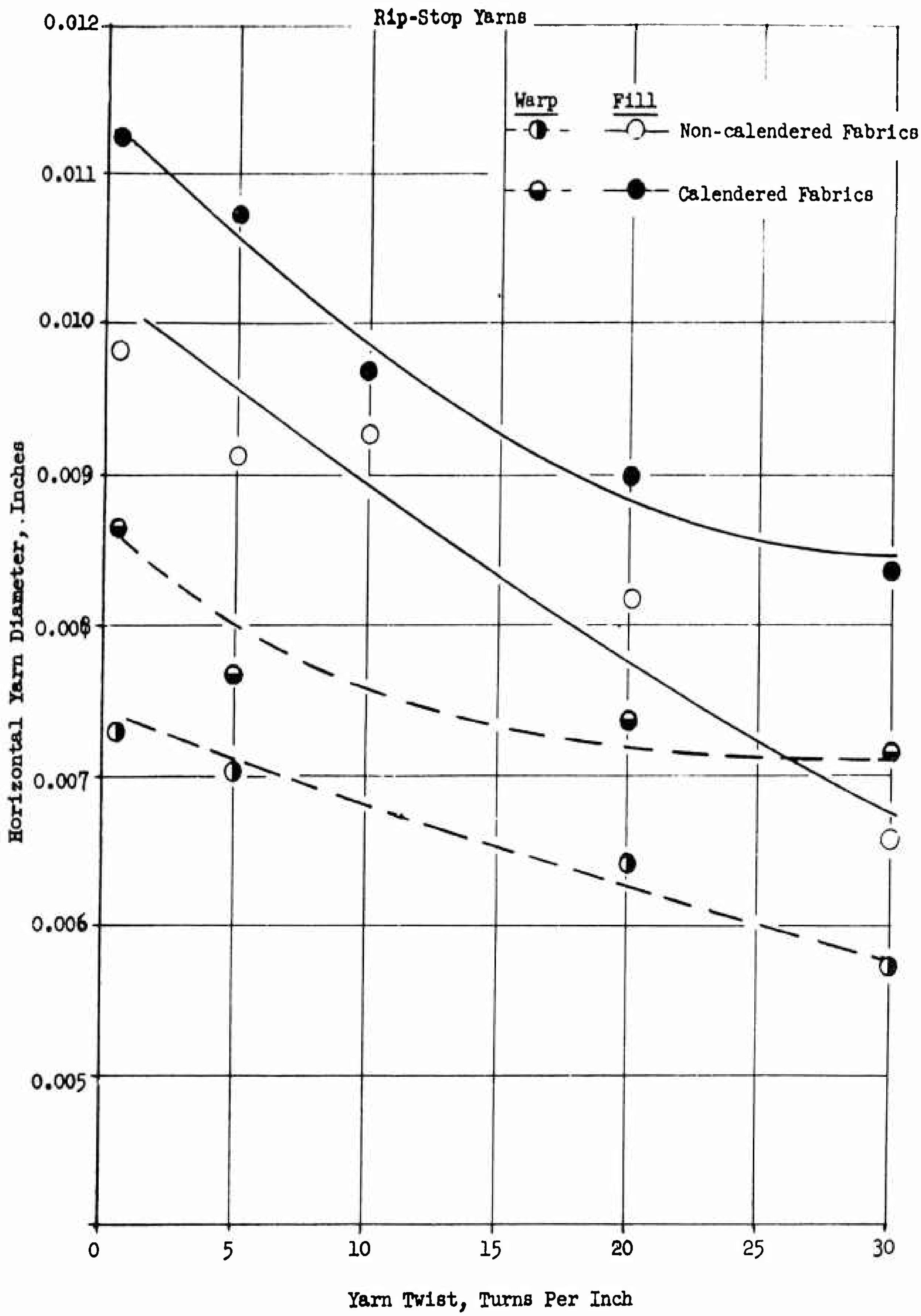

FIGURE 4

WARWICK FABRICS

EFFECTIVE HORIZONTAL YARN DIAMETER VS. YARN TWIST

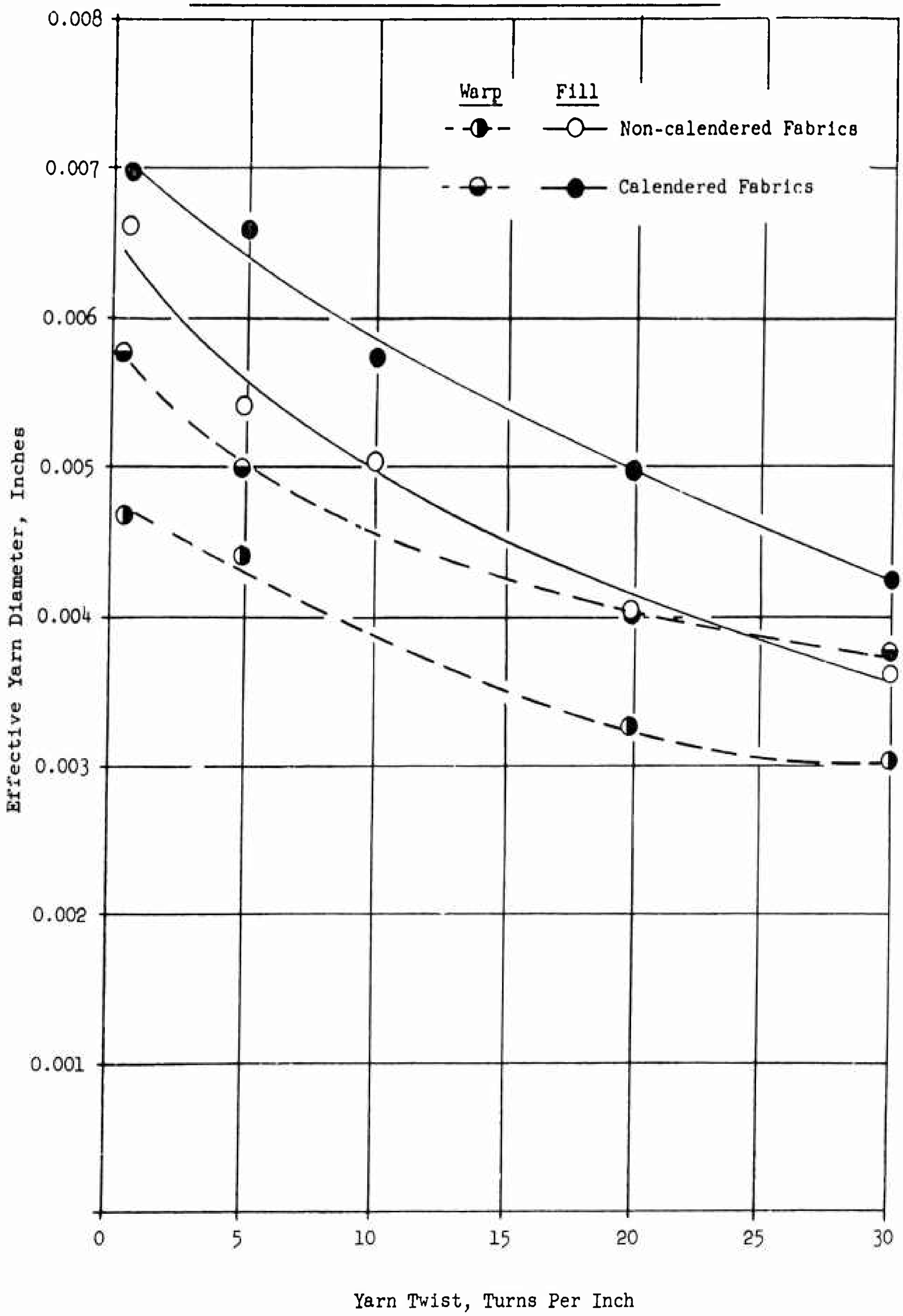

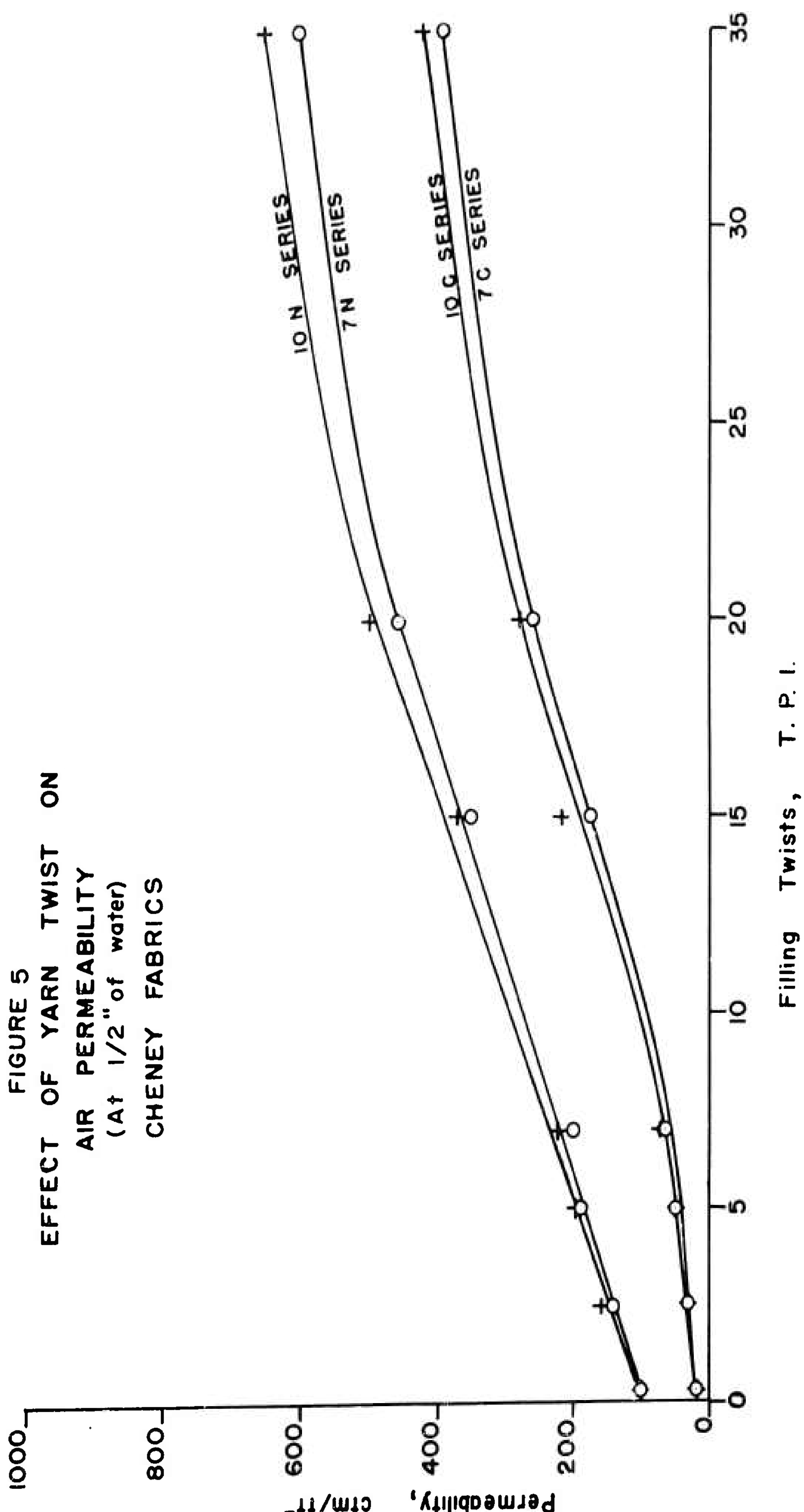

FIGURE 5
EFFECT OF YARN TWIST ON AIR PERMEABILITY
(At 1/2" of water)
CHENEY FABRICS

FIGURE 6
EFFECT OF YARN TWIST ON AIR PERMEABILITY
(At 10" of water)
CHENEY FABRICS

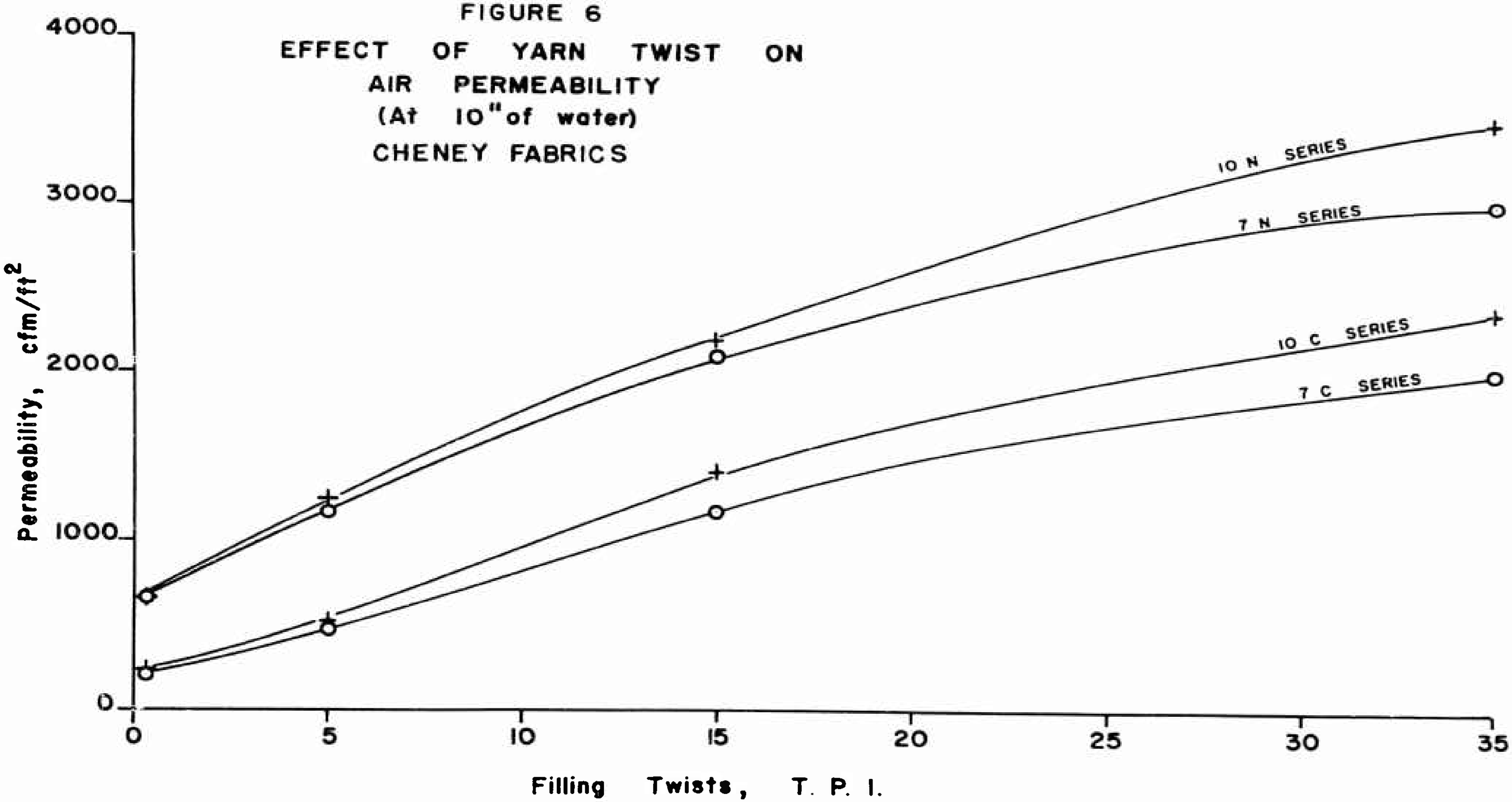

FIGURE 7

AIR PERMEABILITY AT 0.5 INCHES OF WATER

NON-CALENDERED FABRICS (WARWICK)

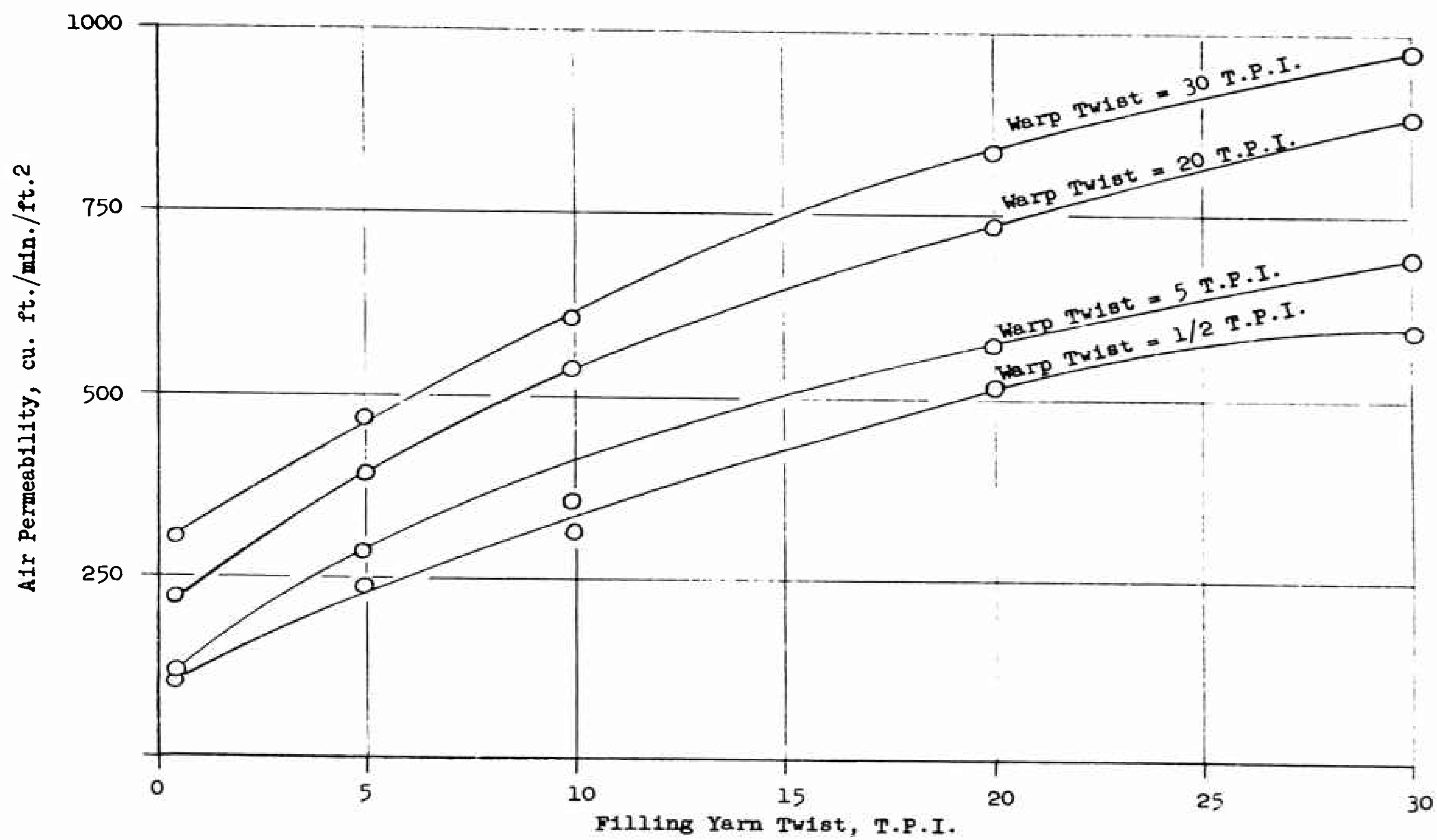

FIGURE 8
AIR PERMEABILITY AT 0.5 INCHES OF WATER
CALENDERED FABRICS (WARWICK)

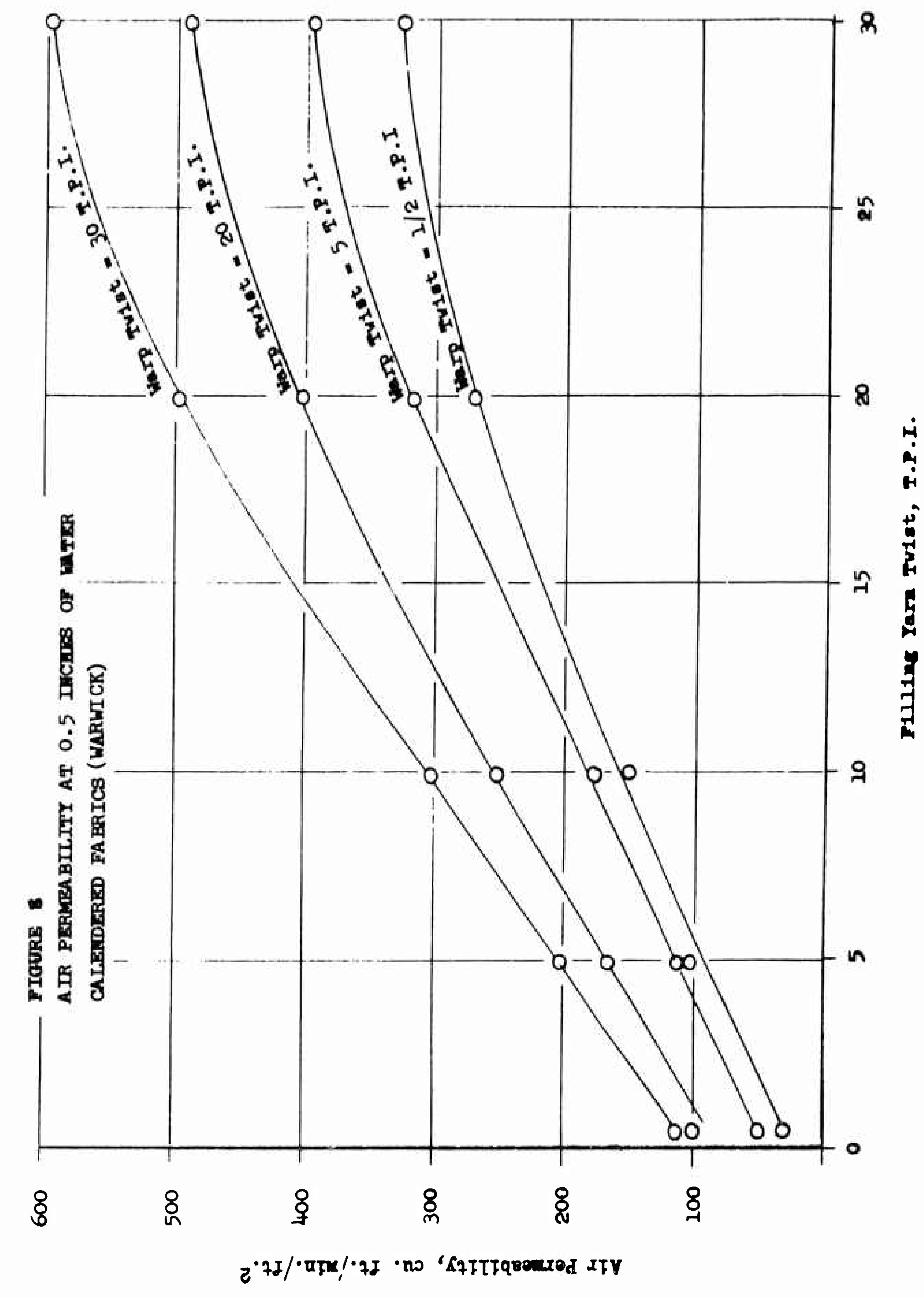

FIGURE 9

AIR PERMEABILITY AT 1/2 INCH OF WATER

Fabrics with equal warp and filling yarn twists
(WARWICK)

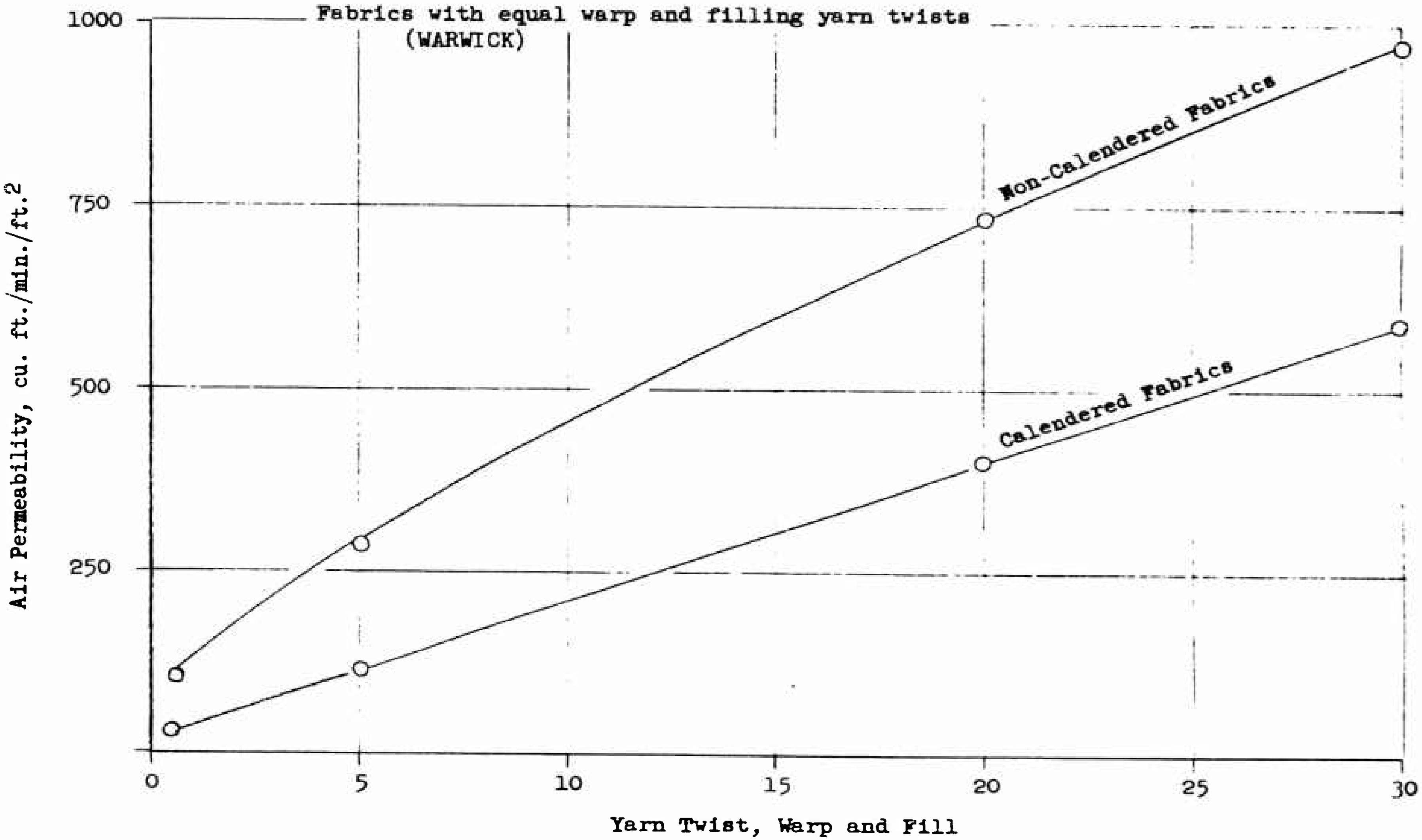

FIGURE 10

AIR FLOW VS PRESSURE DIFFERENTIAL CURVES

CHENEY BROTHERS' FABRICS

7 T.P.I RIPSTOP SERIES

UNCALENDERED SERIES

TYPE I

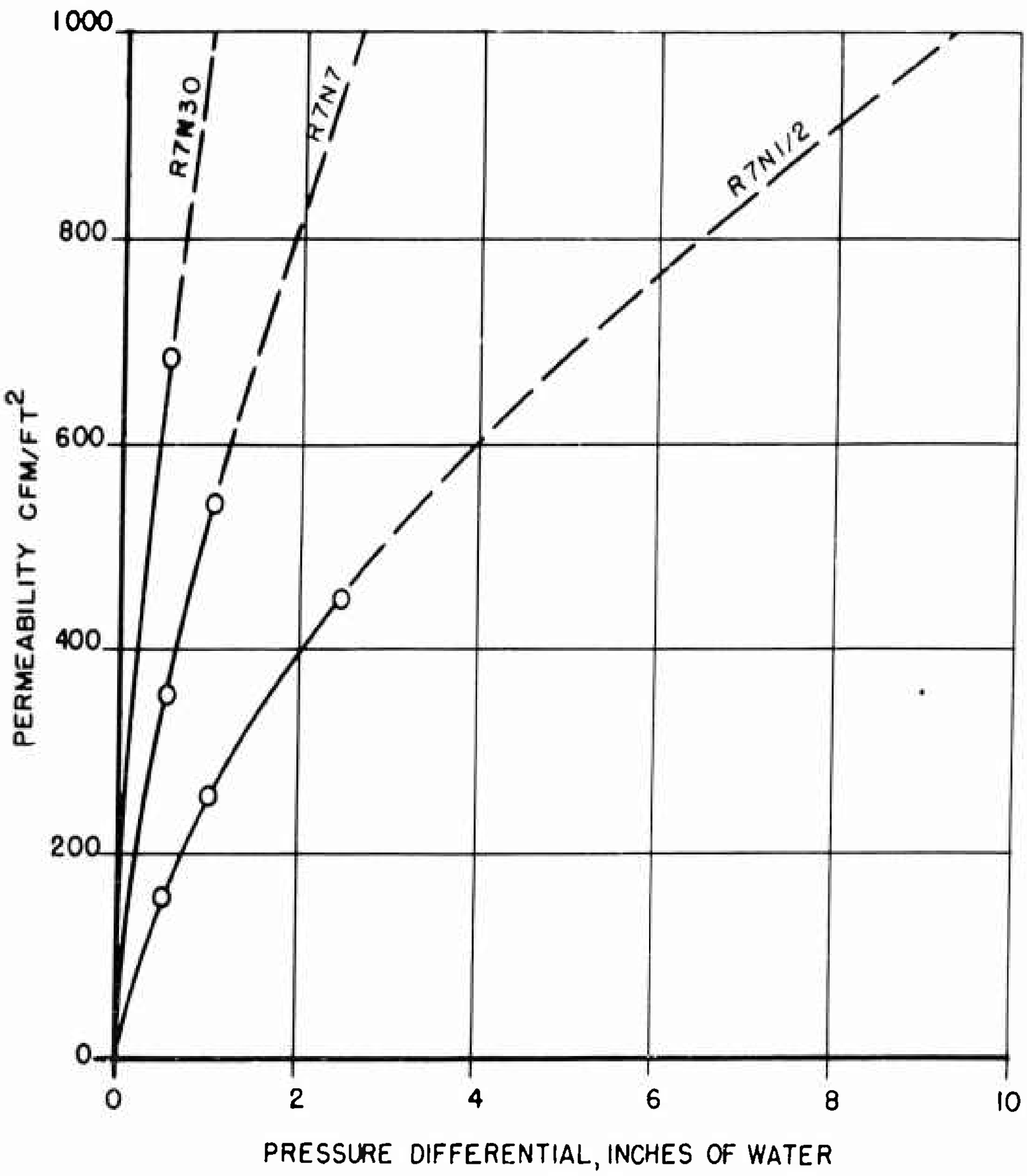

FIGURE 11

AIR FLOW VS PRESSURE DIFFERENTIAL CURVES

CHENEY BROTHERS' FABRICS

7 TPI RIPSTOP SERIES

CALENDERED FABRICS

TYPE I

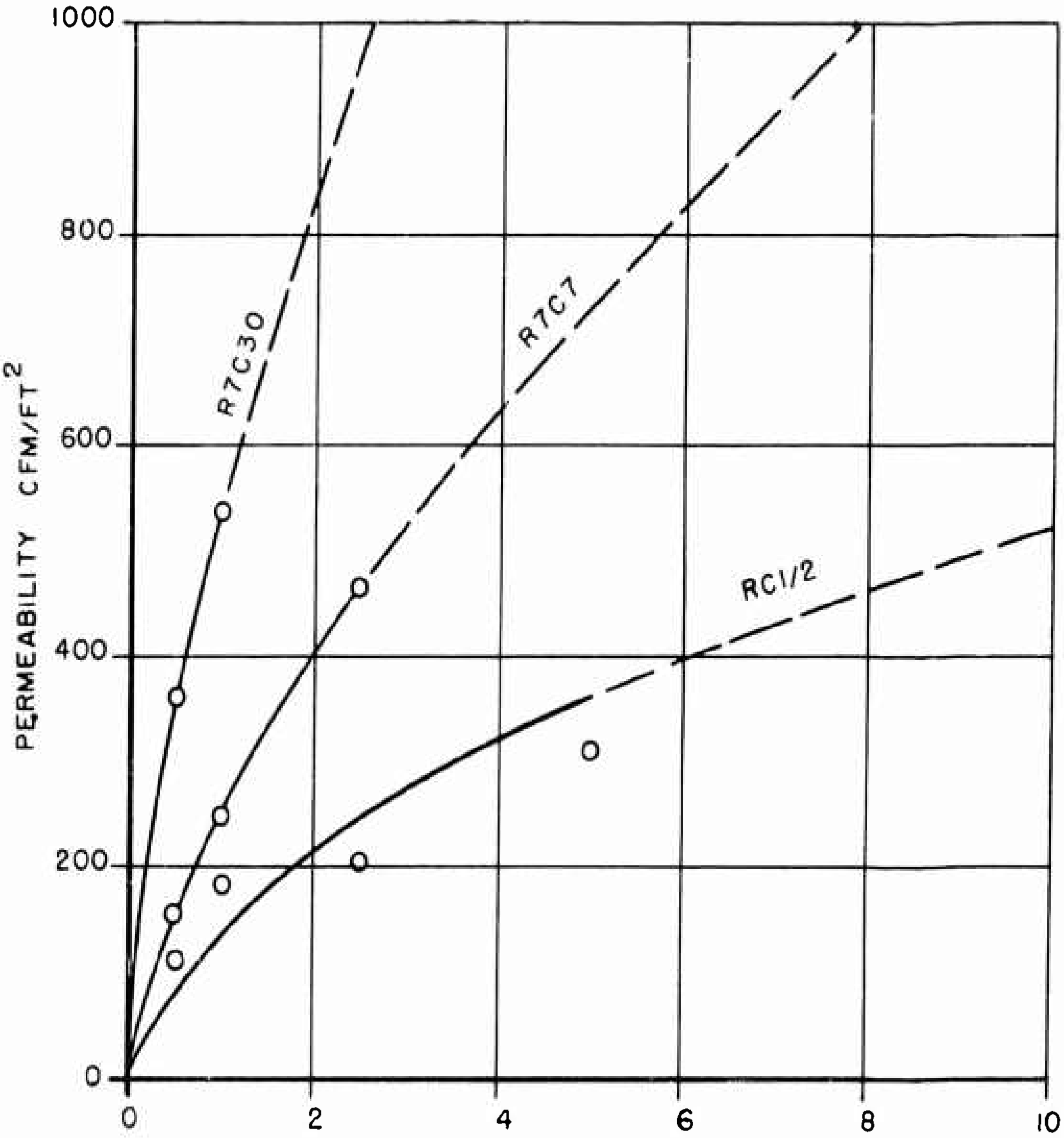

FIGURE 12

AIR PERMEABILITY AT VARIOUS PRESSURE DIFFERENTIALS

Non-Calendered Fabrics

(Plotted on 3 cycle x 3 cycle log-log paper)

R½N Series, Type I Warwick Fabrics

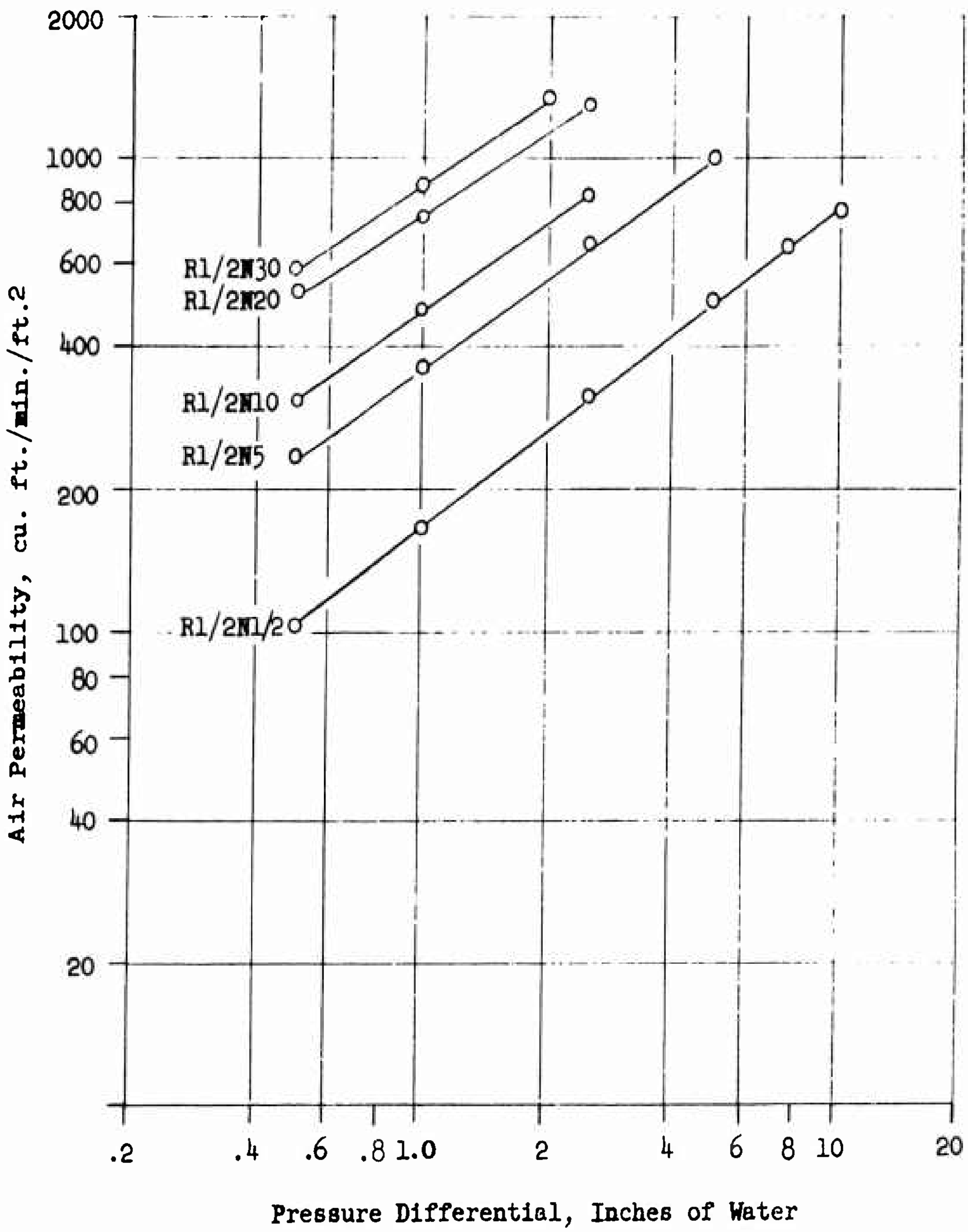

FIGURE 13

AIR PERMEABILITY AT VARIOUS PRESSURE DIFFERENTIALS

Non-Calendered Fabrics

(Plotted on 3 cycle x 3 cycle log-log paper)

R5N Series, Type I Warwick Fabrics

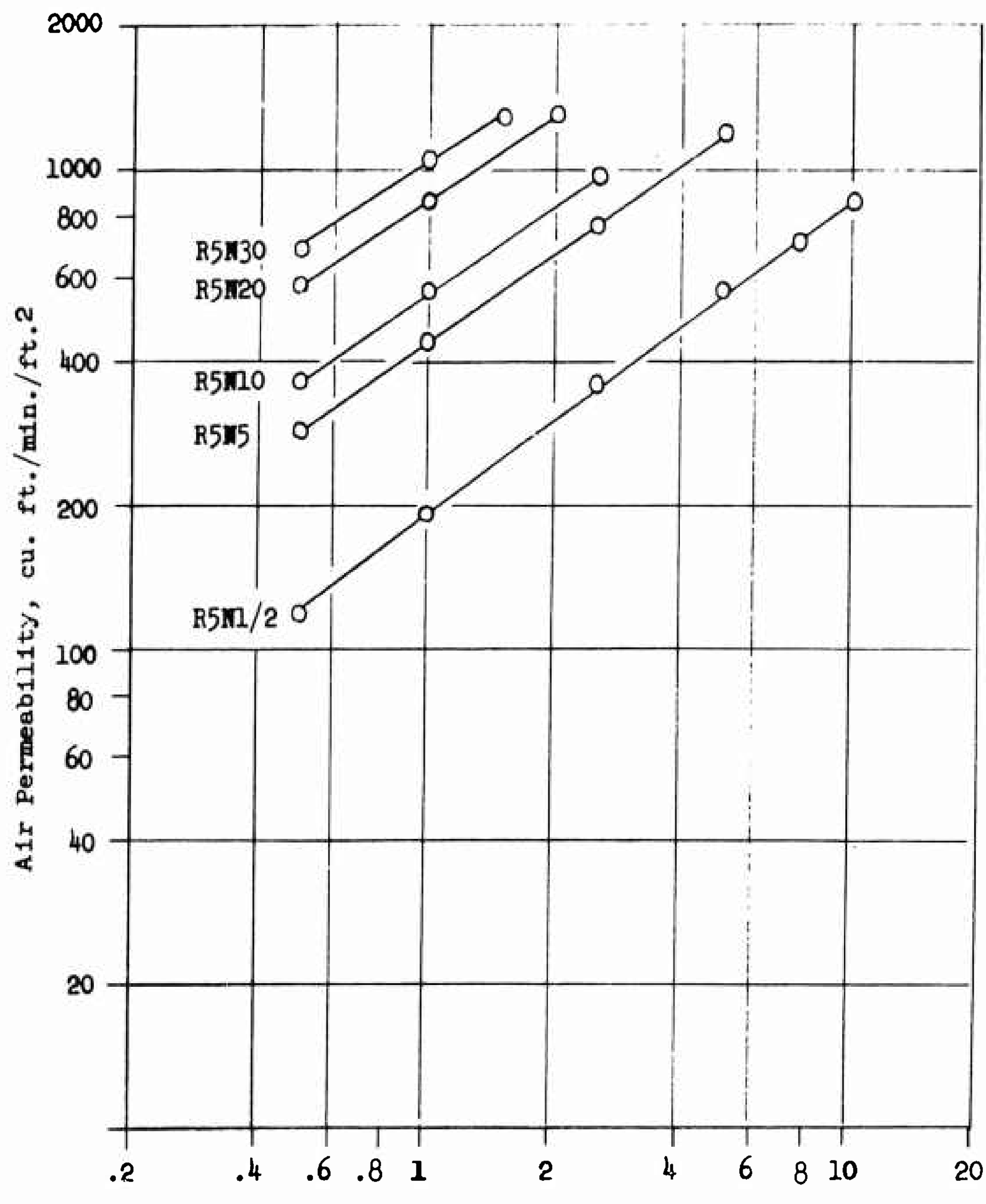

FIGURE 14

AIR PERMEABILITY AT VARIOUS PRESSURE DIFFERENTIALS

Non-Calendered Fabrics

(Plotted on 3 cycle x 3 cycle log-log paper)

R20N Series, Type I Warwick Fabrics

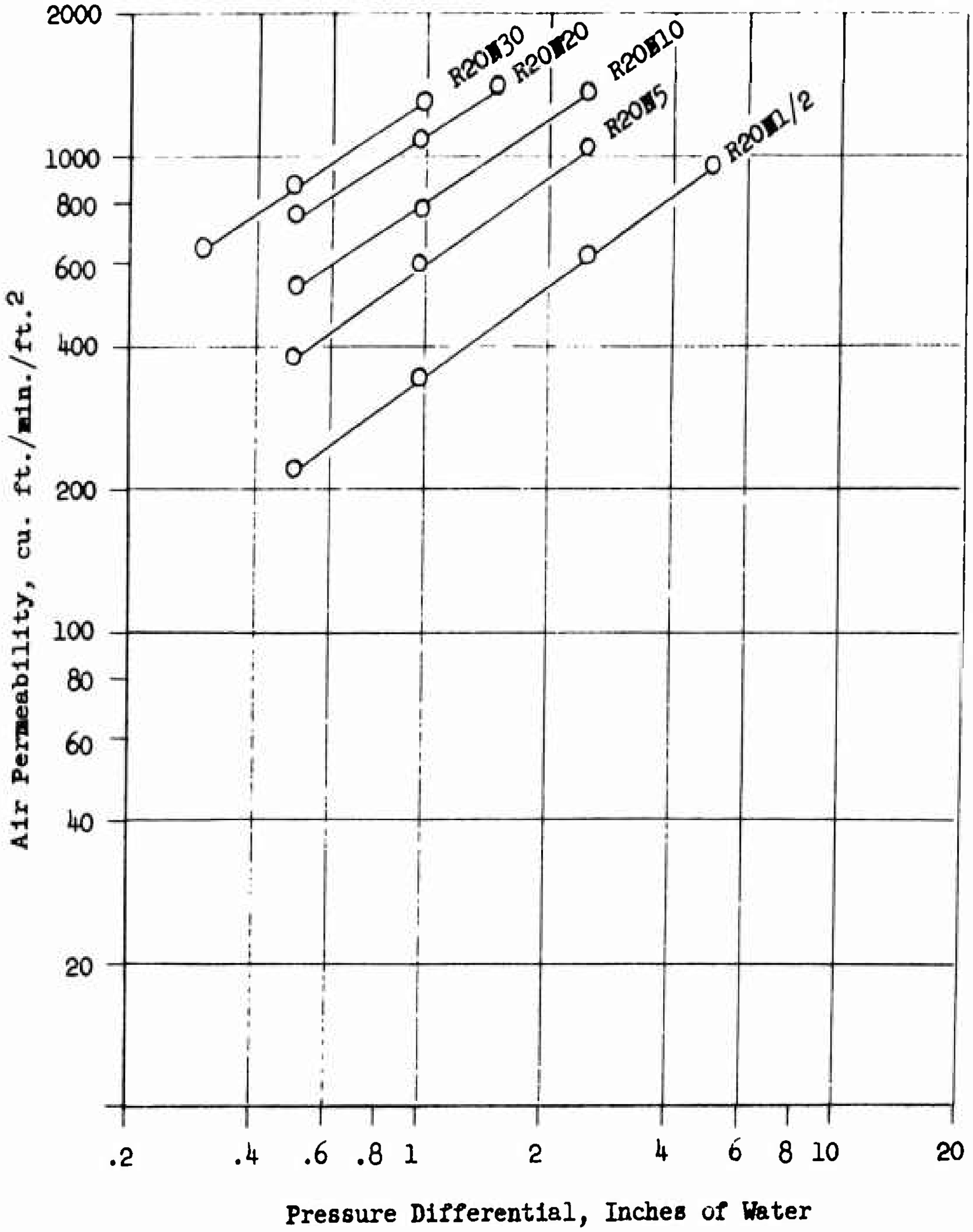

FIGURE 15

AIR PERMEABILITY AT VARIOUS PRESSURE DIFFERENTIALS

Non-Calendered Fabrics

(Plotted on 3 cycle x 3 cycle log-log paper)

R30N Series, Type I Warwick Fabrics

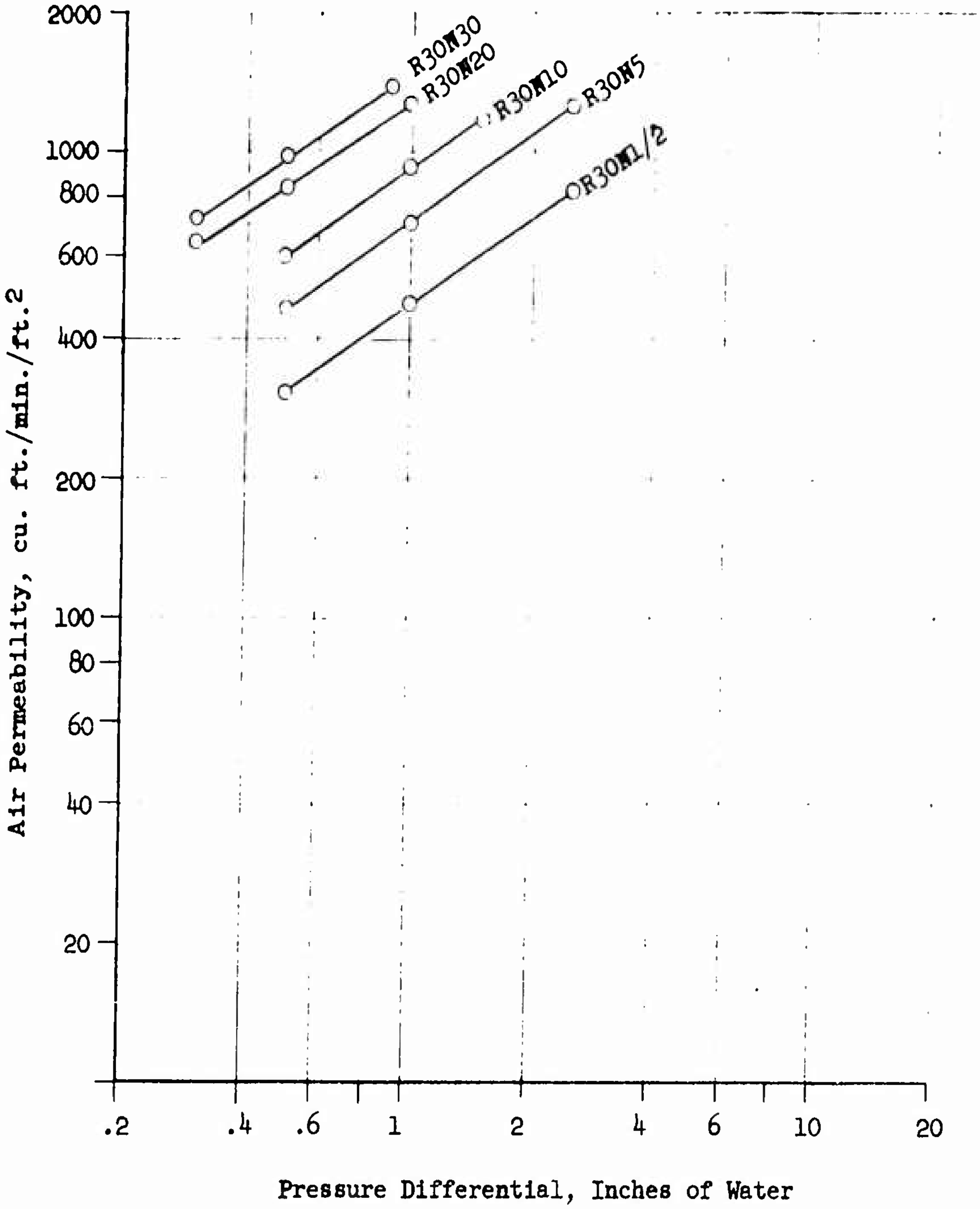

FIGURE 16

AIR PERMEABILITY AT VARIOUS PRESSURE DIFFERENTIALS

Calendered Fabrics

(Plotted on 3 cycle x 3 cycle log-log paper)

R½C Series, Type I Warwick Fabrics

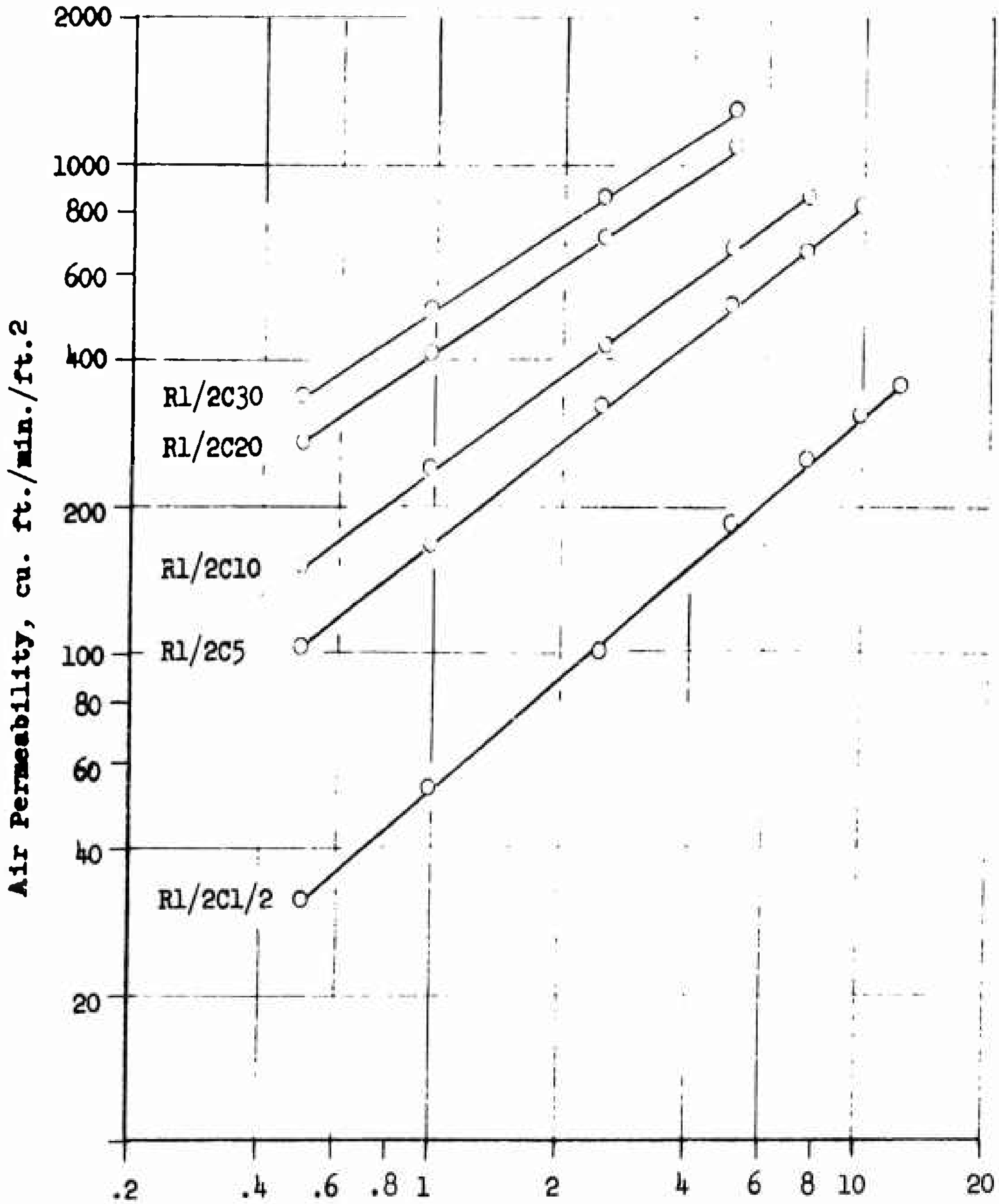

FIGURE 17

AIR PERMEABILITY AT VARIOUS PRESSURE DIFFERENTIALS

Calendered Fabrics

(Plotted on 3 cycle x 3 cycle log-log paper)

R5C Series, Type I Warwick Fabrics

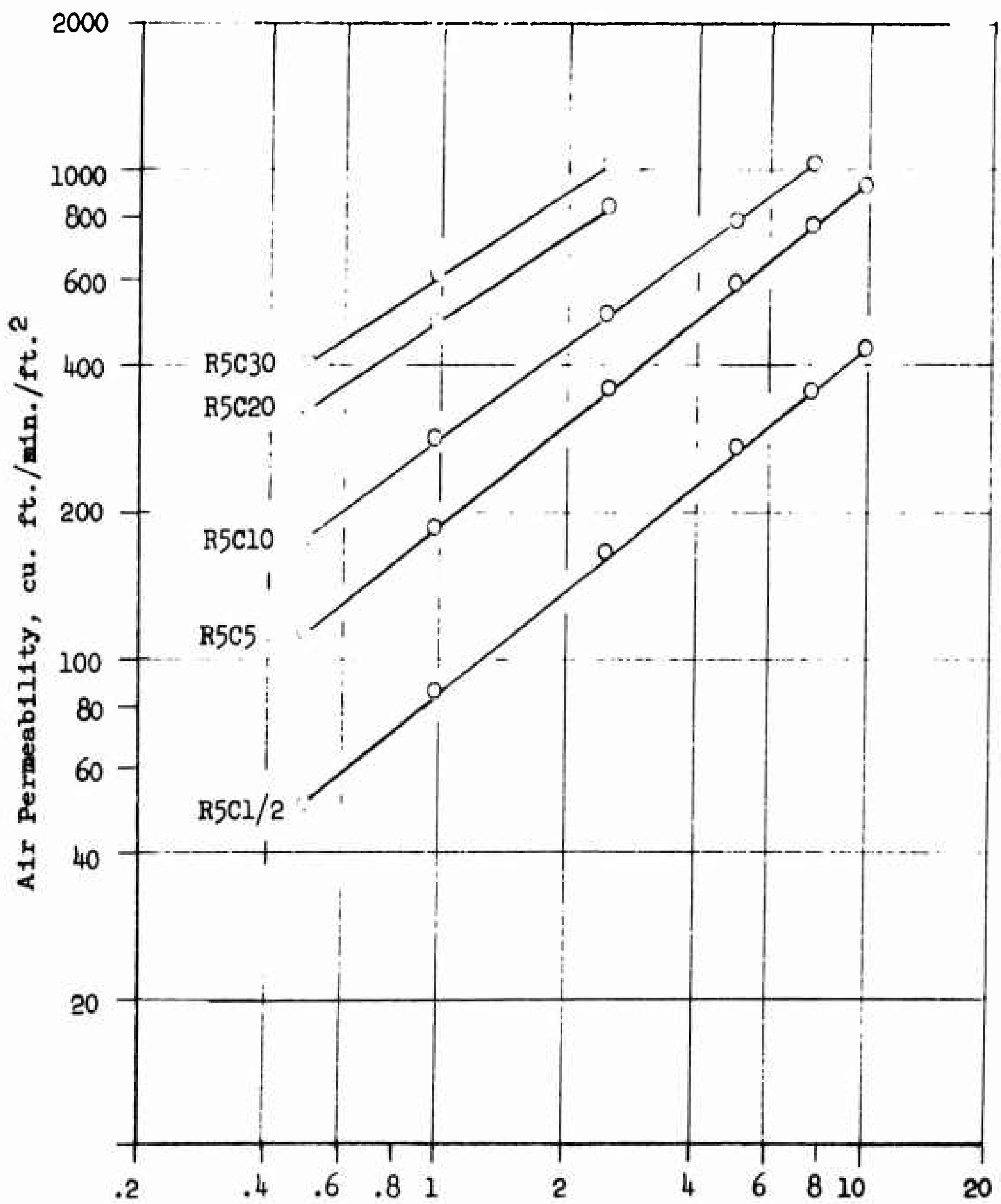

Pressure Differential, Inches of Water

FIGURE 18

AIR PERMEABILITY AT VARIOUS PRESSURE DIFFERENTIALS

Calendered Fabrics

(Plotted on 3 cycle x 3 cycle log-log paper)

R20C Series, Type I Warwick Fabrics

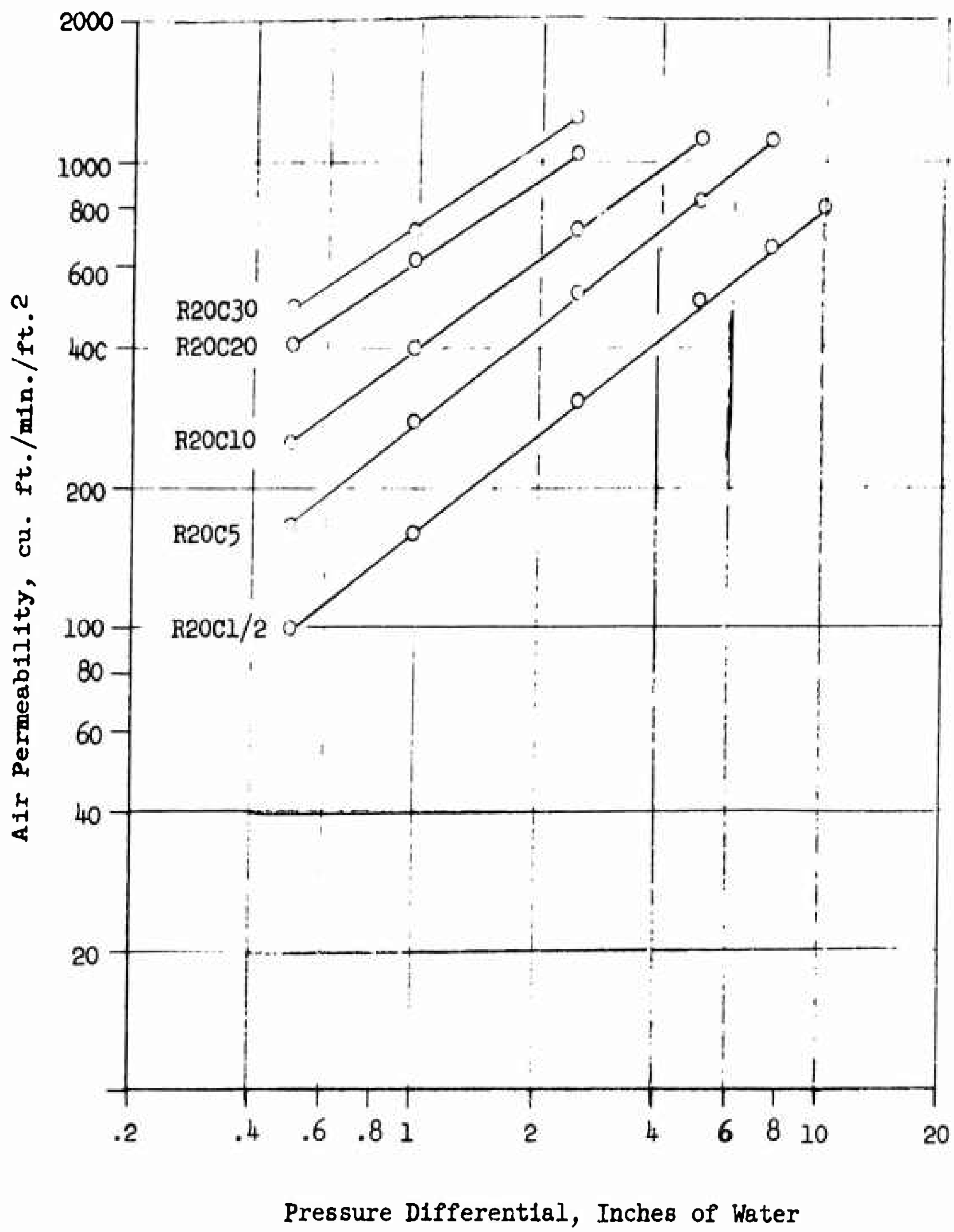

FIGURE 19

AIR PERMEABILITY AT VARIOUS PRESSURE DIFFERENTIALS

Calendered Fabrics

(Plotted on 3 cycle x 3 cycle log-log paper)

R30C Series, Type I Warwick Fabrics

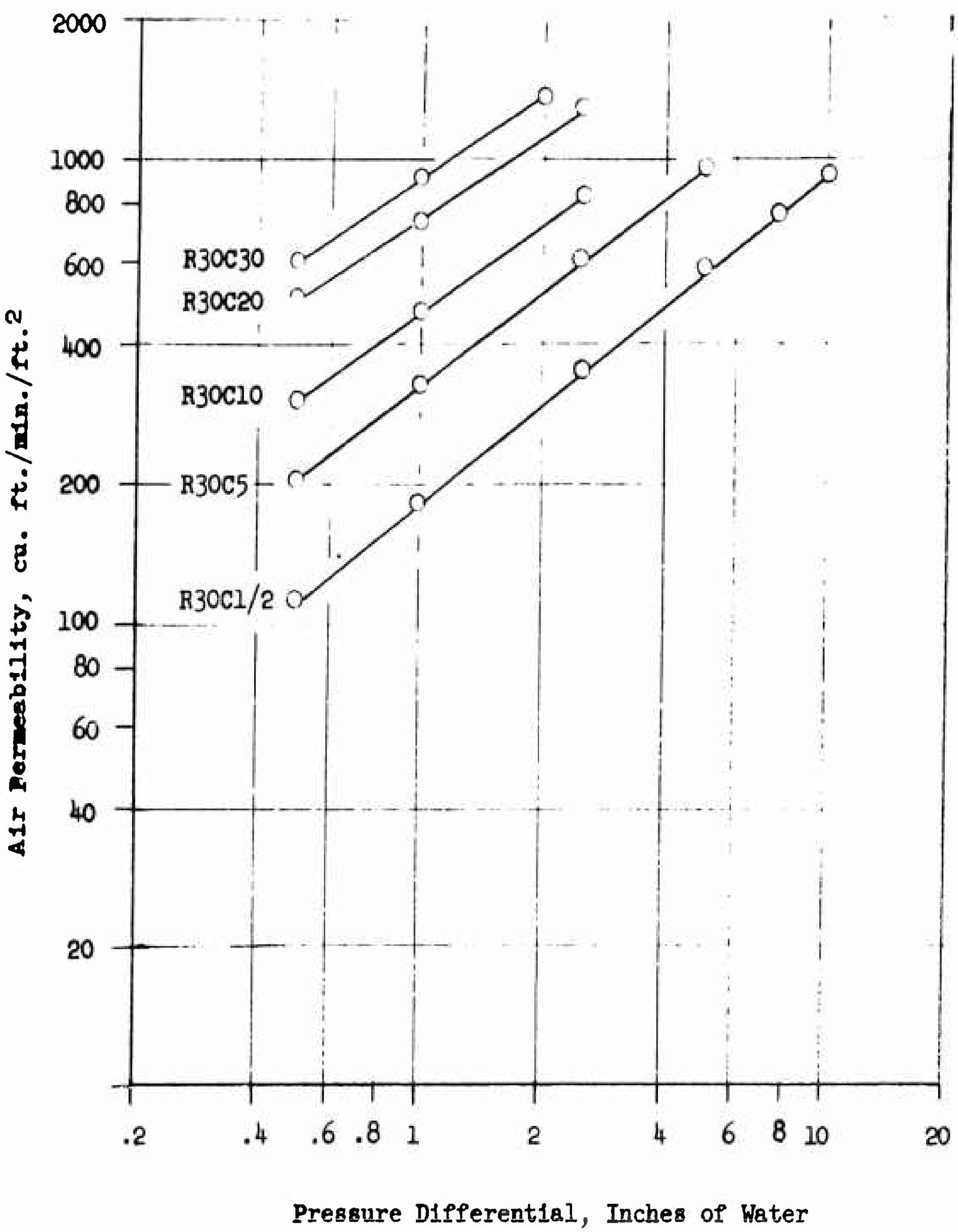

FIGURE 20

AIR FLOW VS PRESSURE DIFFERENTIAL CURVES

CHENEY BROTHERS' FABRICS

7 T.P.I. TWILL SERIES

UNCALENDERED FABRICS

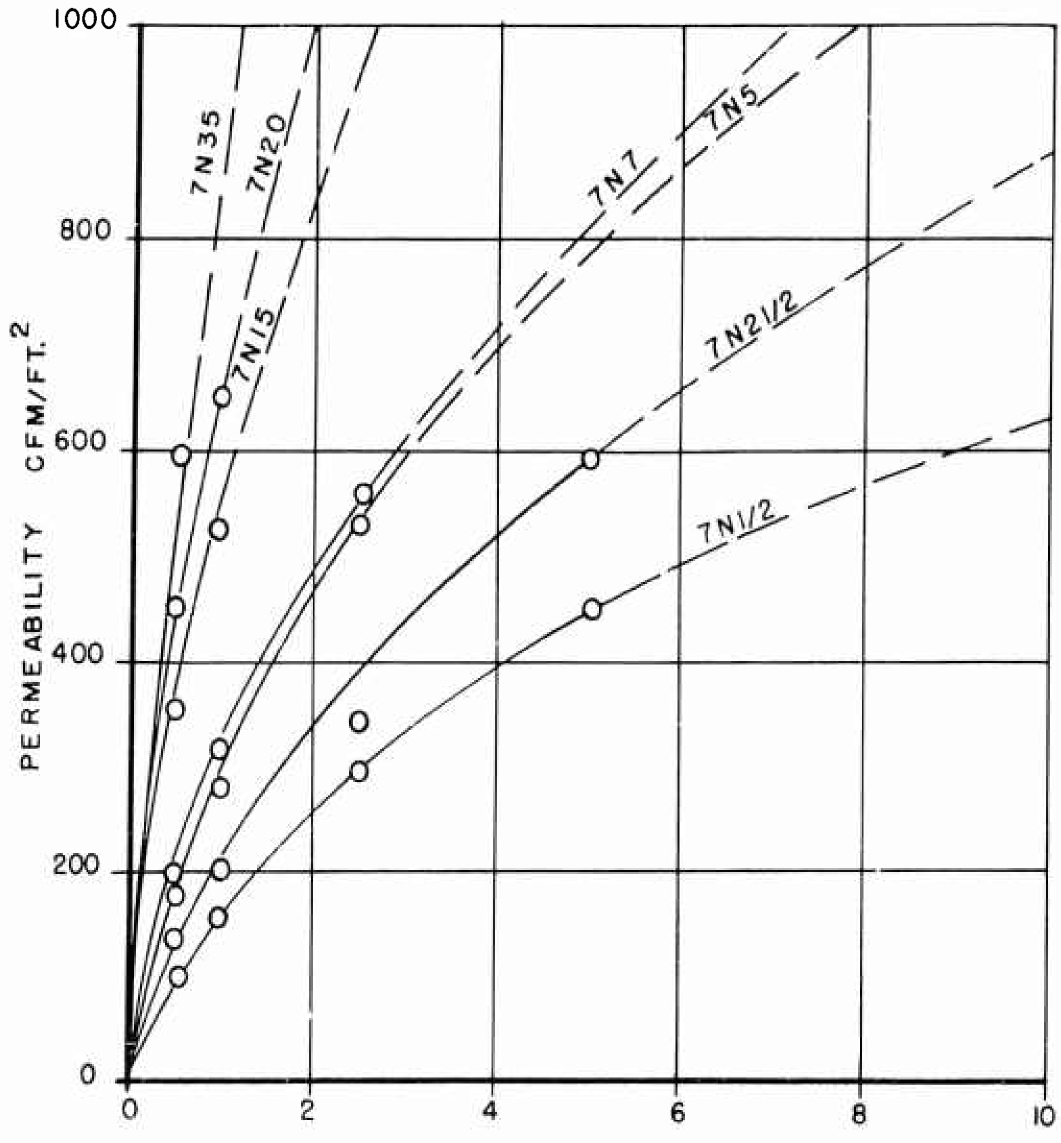

FIGURE 21

AIR FLOW VS PRESSURE DIFFERENTIAL CURVES

CHENEY BROTHERS' FABRICS

7 T.P.I. TWILL SERIES

CALENDERED FABRICS

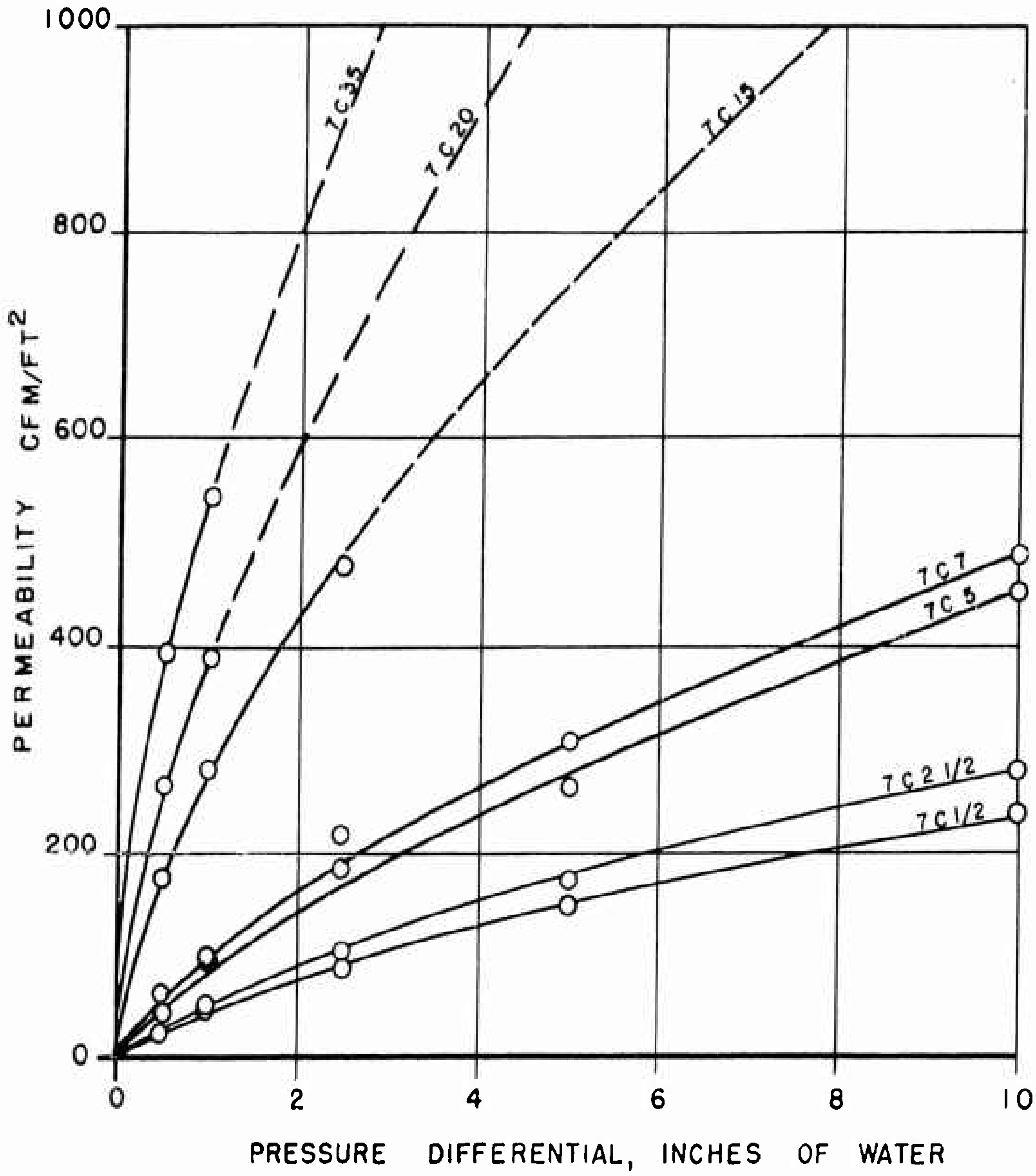

FIGURE 22

AIR FLOW VS PRESSURE DIFFERENTIAL CURVES

CHENEY BROTHERS' FABRICS

10 T.P.I TWILL SERIES

UNCALENDERED FABRICS

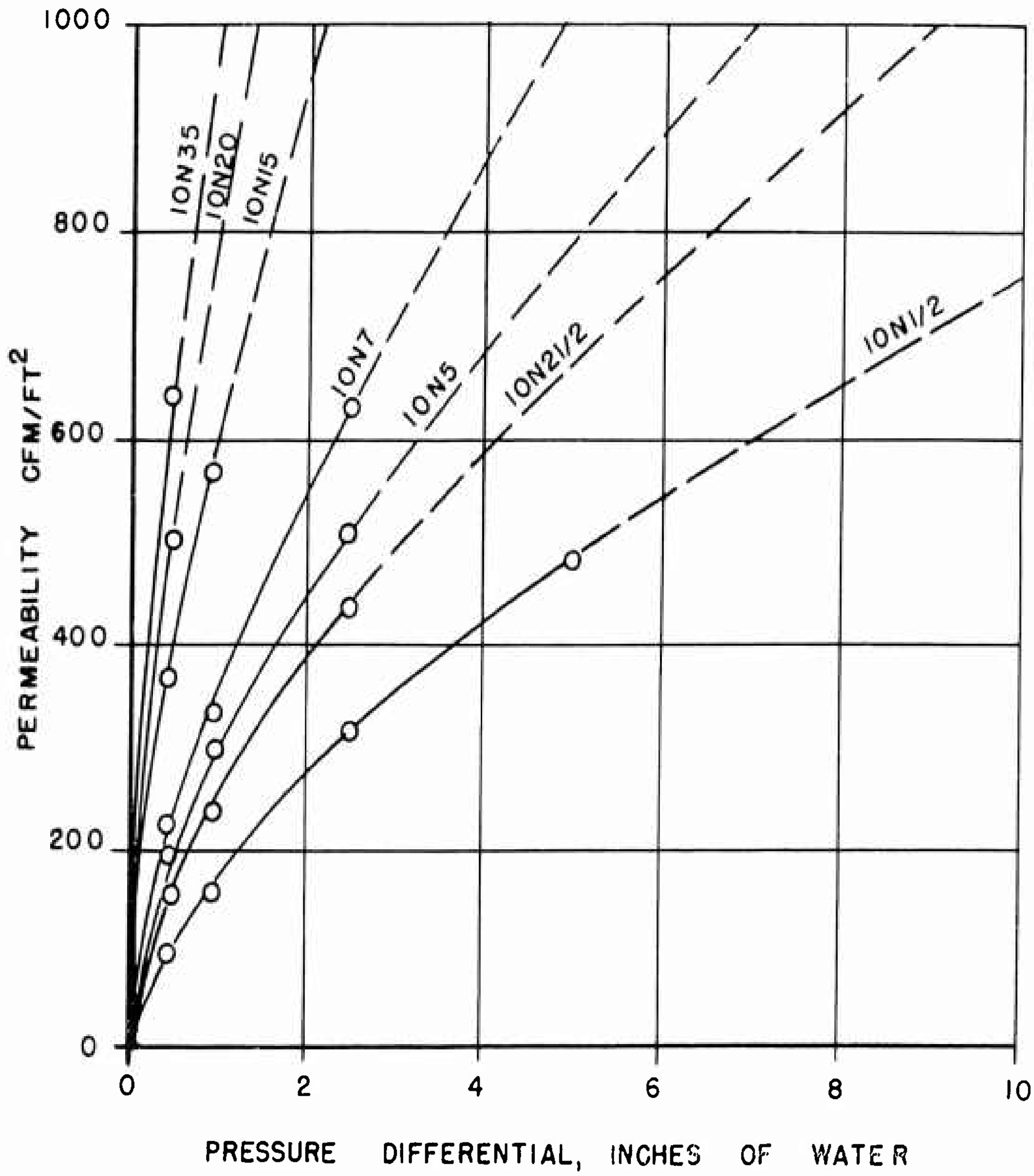

FIGURE 23

AIR FLOW VS PRESSURE DIFFERENTIAL CURVES

CHENEY BROTHERS' FABRICS

10 T.P.I. TWILL SERIES

CALENDERED FABRICS

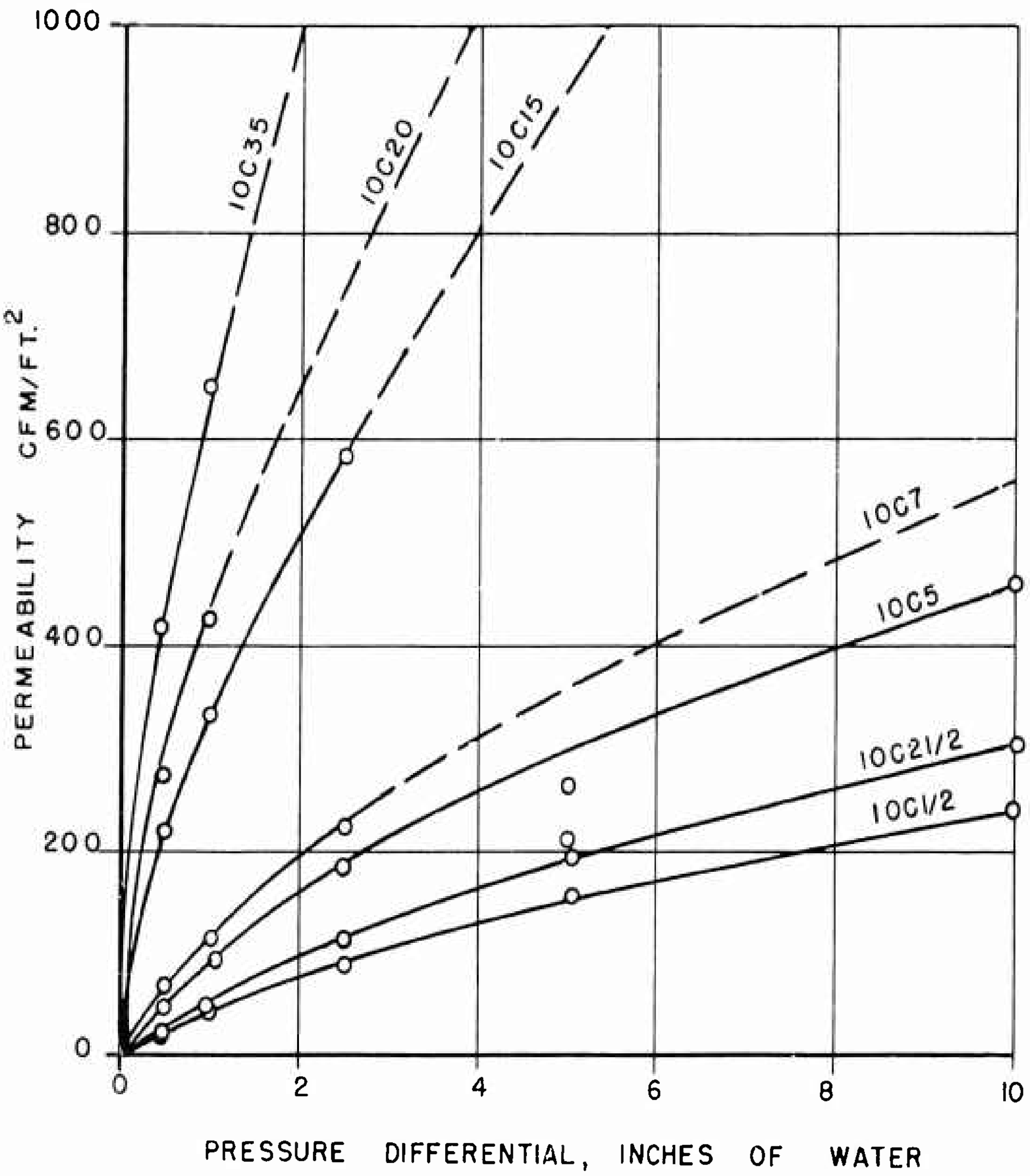

FIGURE 24

AIR FLOW VS PRESSURE DIFFERENTIAL CURVES

CHENEY BROTHERS' FABRICS

7 t.p.i. RIPSTOP SERIES

UNCALENDERERED FABRICS

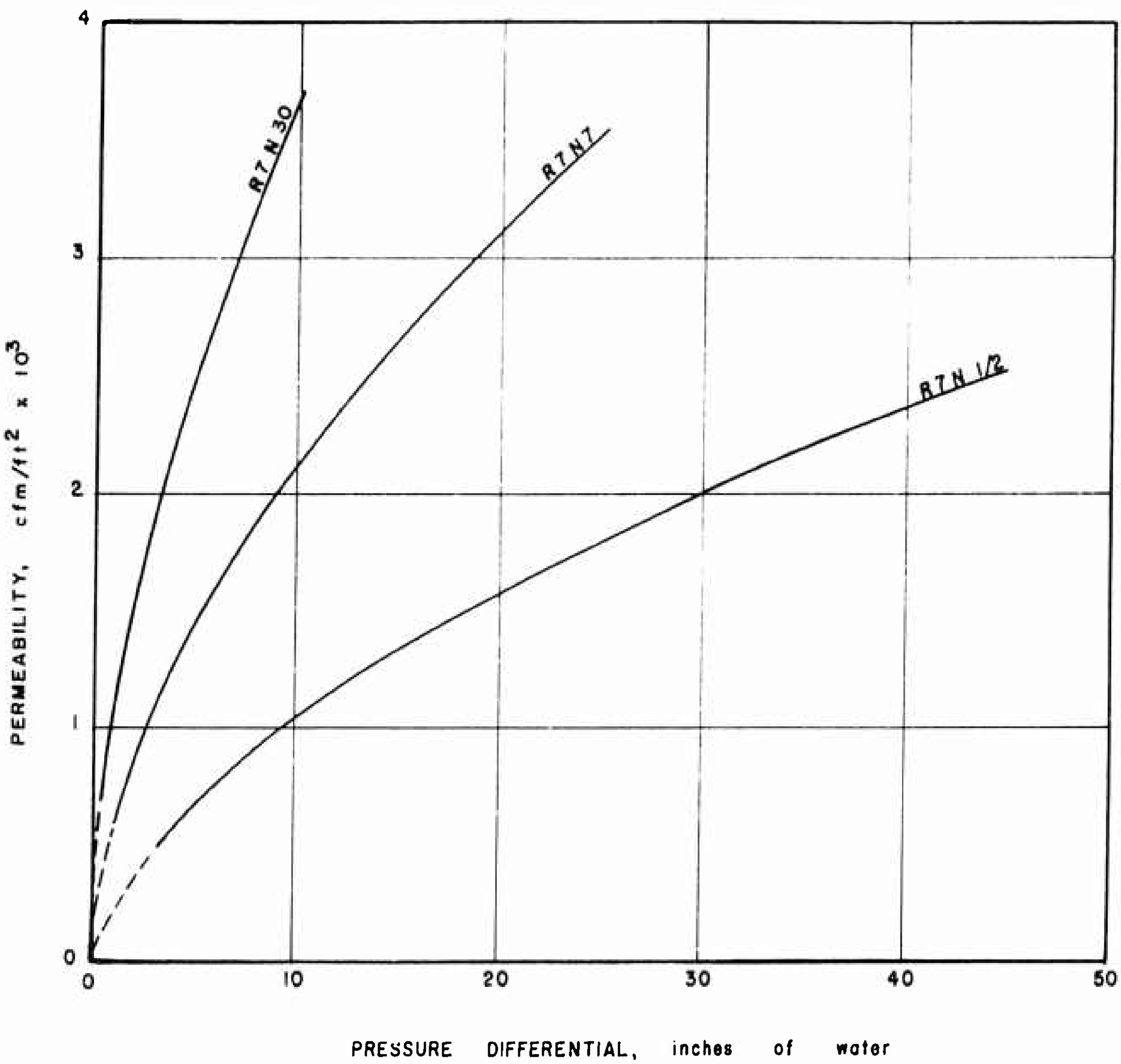

FIGURE 25

AIR FLOW VS PRESSURE DIFFERENTIAL CURVES

CHENEY BROTHERS' FABRICS

7 tpi. RIPSTOP SERIES

CALENDERED FABRICS

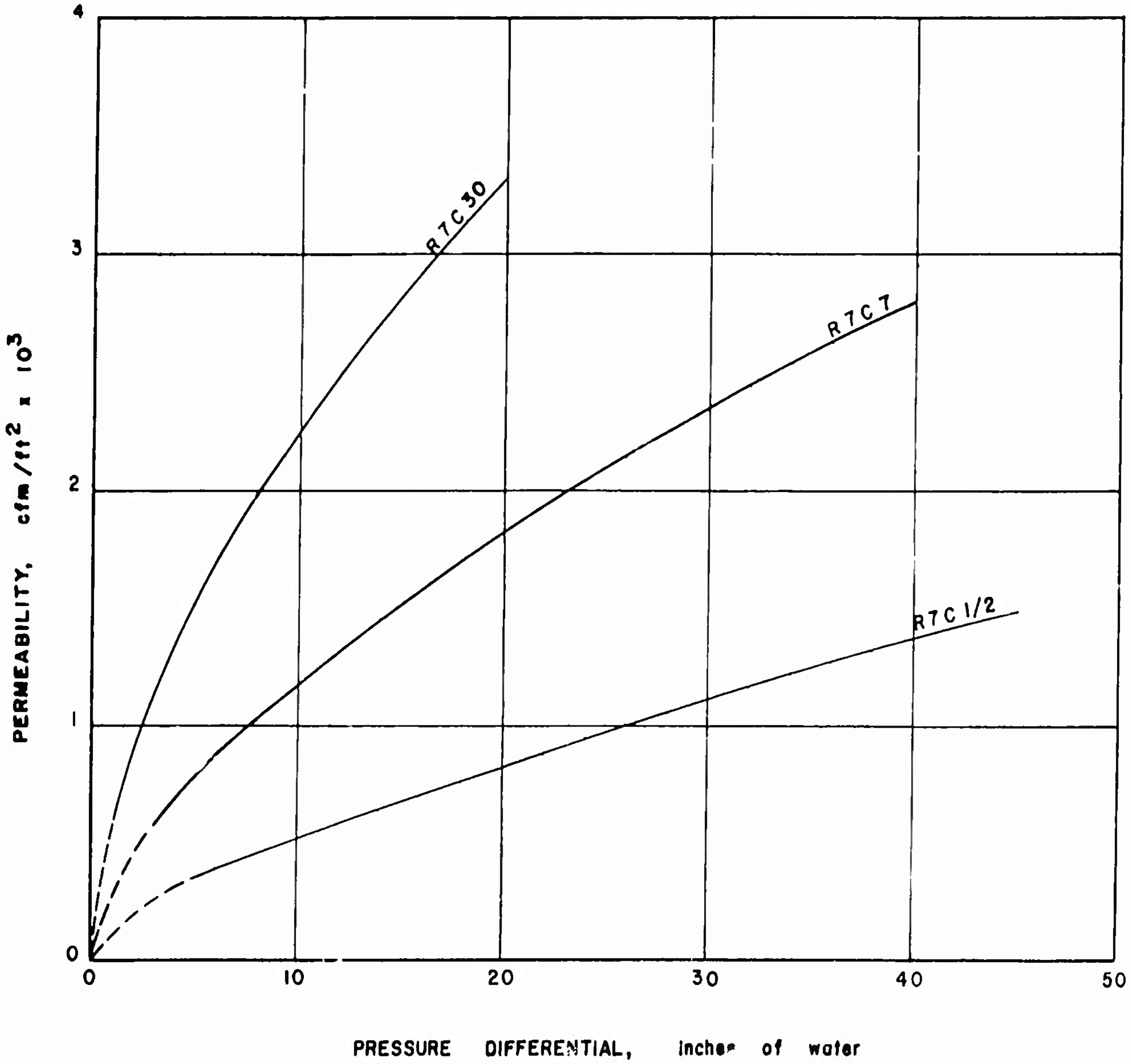

FIGURE 26

AIR FLOW vs PRESSURE DIFFERENTIAL CURVES

CHENEY BROTHERS' FABRICS

7 & 10 t.p.i TWILL SERIES

UNCALENDERED FABRICS

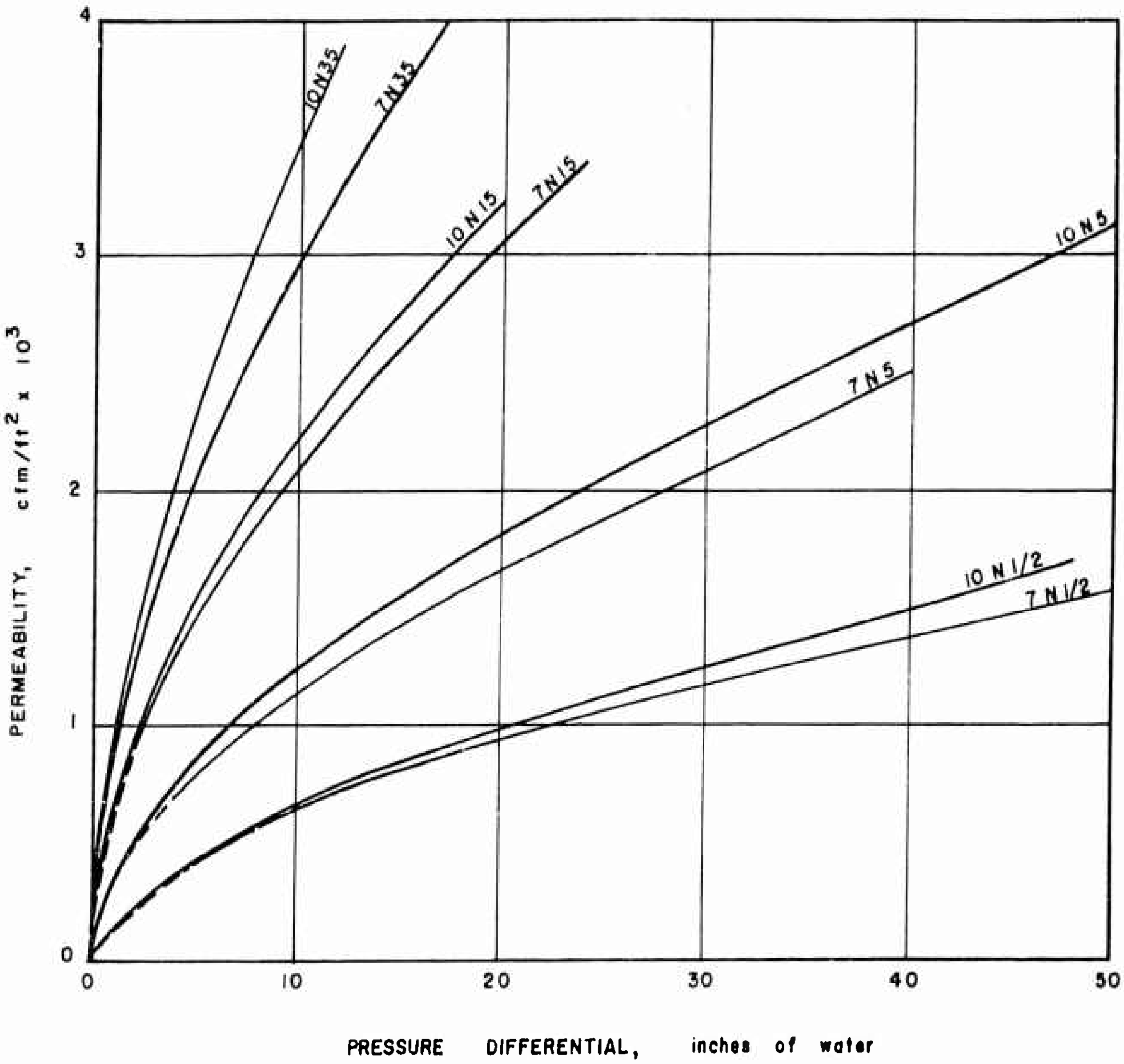

FIGURE 27

AIR FLOW VS PRESSURE DIFFERENTIAL CURVES

CHENEY BROTHERS' FABRICS

7 & 10 t p i TWILL SERIES

CALENDERED FABRICS

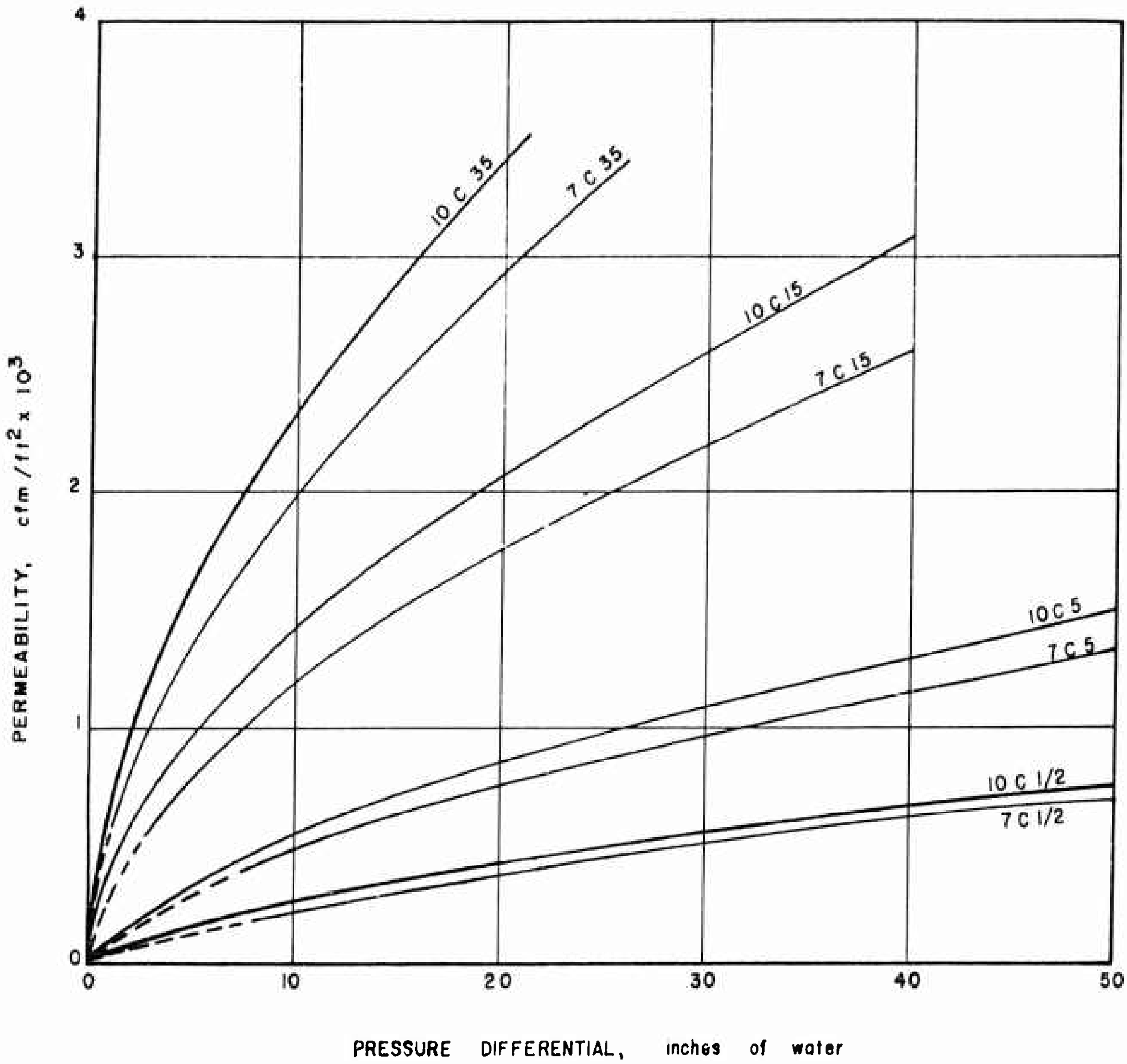

FIGURE 28

DIAGRAM OF YARN SLIPPAGE TEST

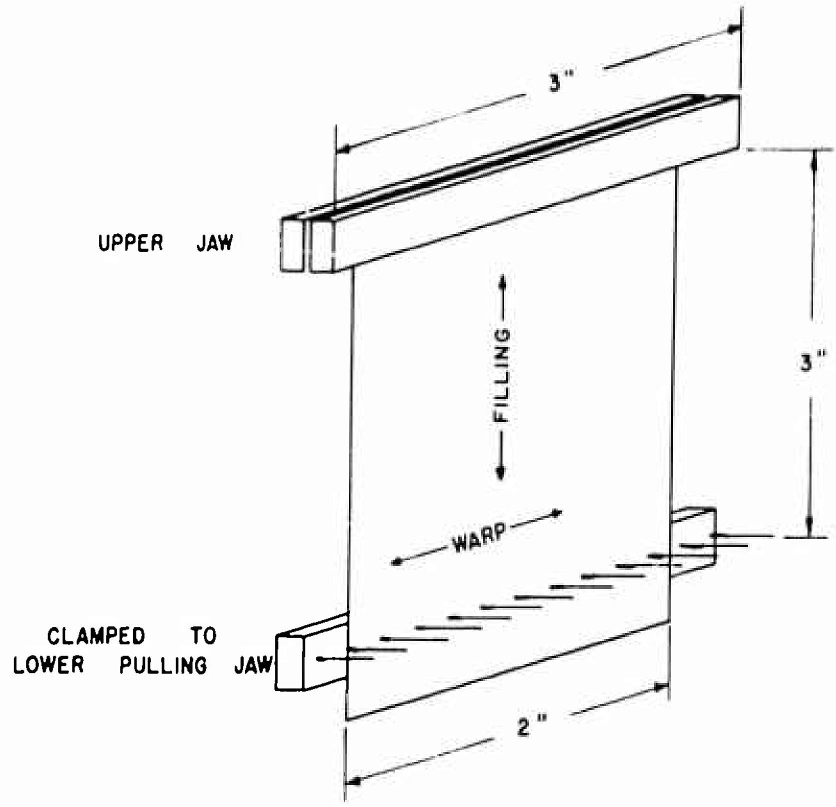

Diagram shows a warp sample under test;
i.e. warp yarns are being displaced.

FIGURE 29

TYPICAL LOAD-DISPLACEMENT CURVE OF YARN STABILITY TESTS

(Specimen no. I R7C7)

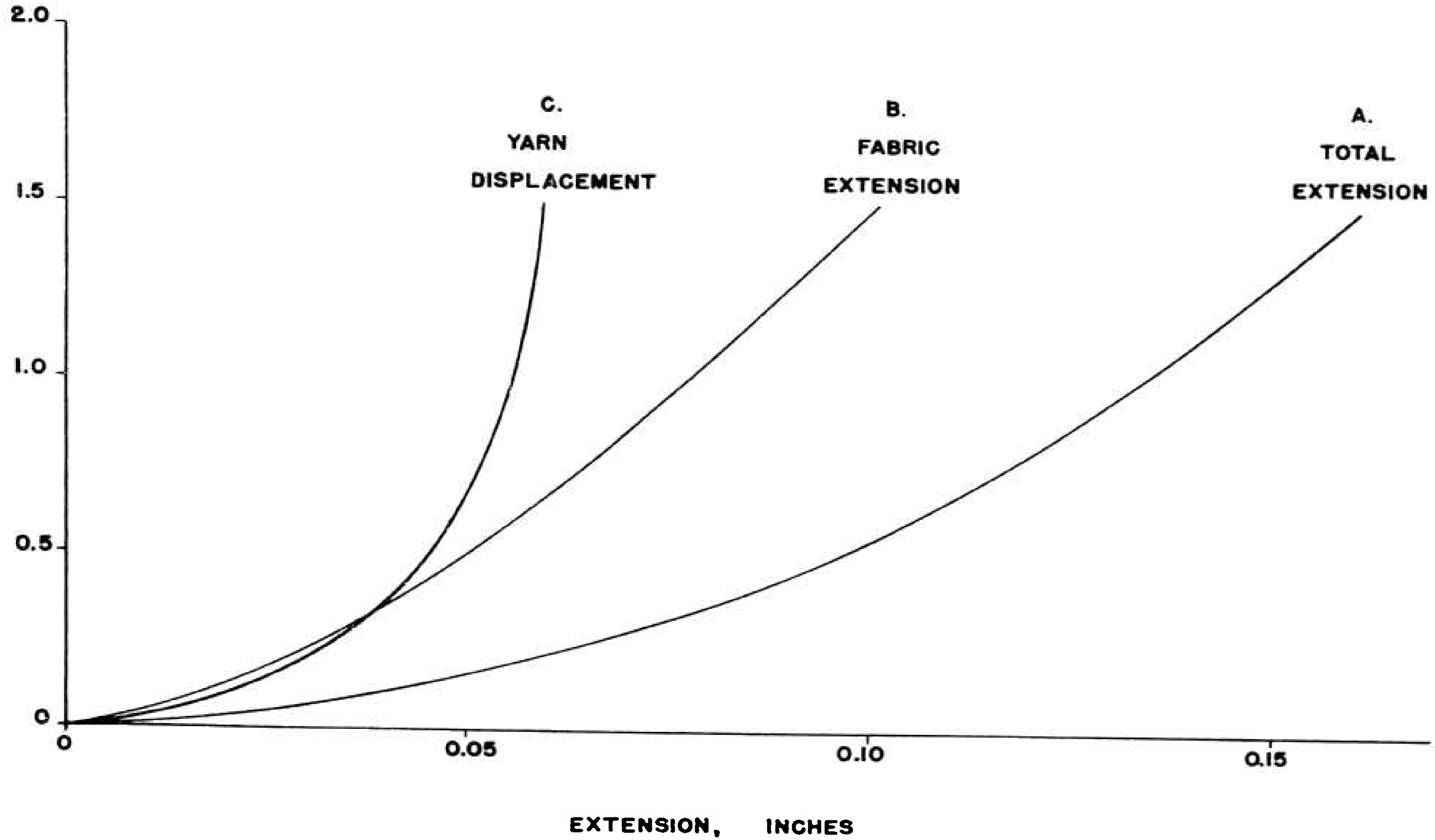

FIGURE 30

EFFECT OF YARN TWIST ON STABILITY

CHENEY FABRICS

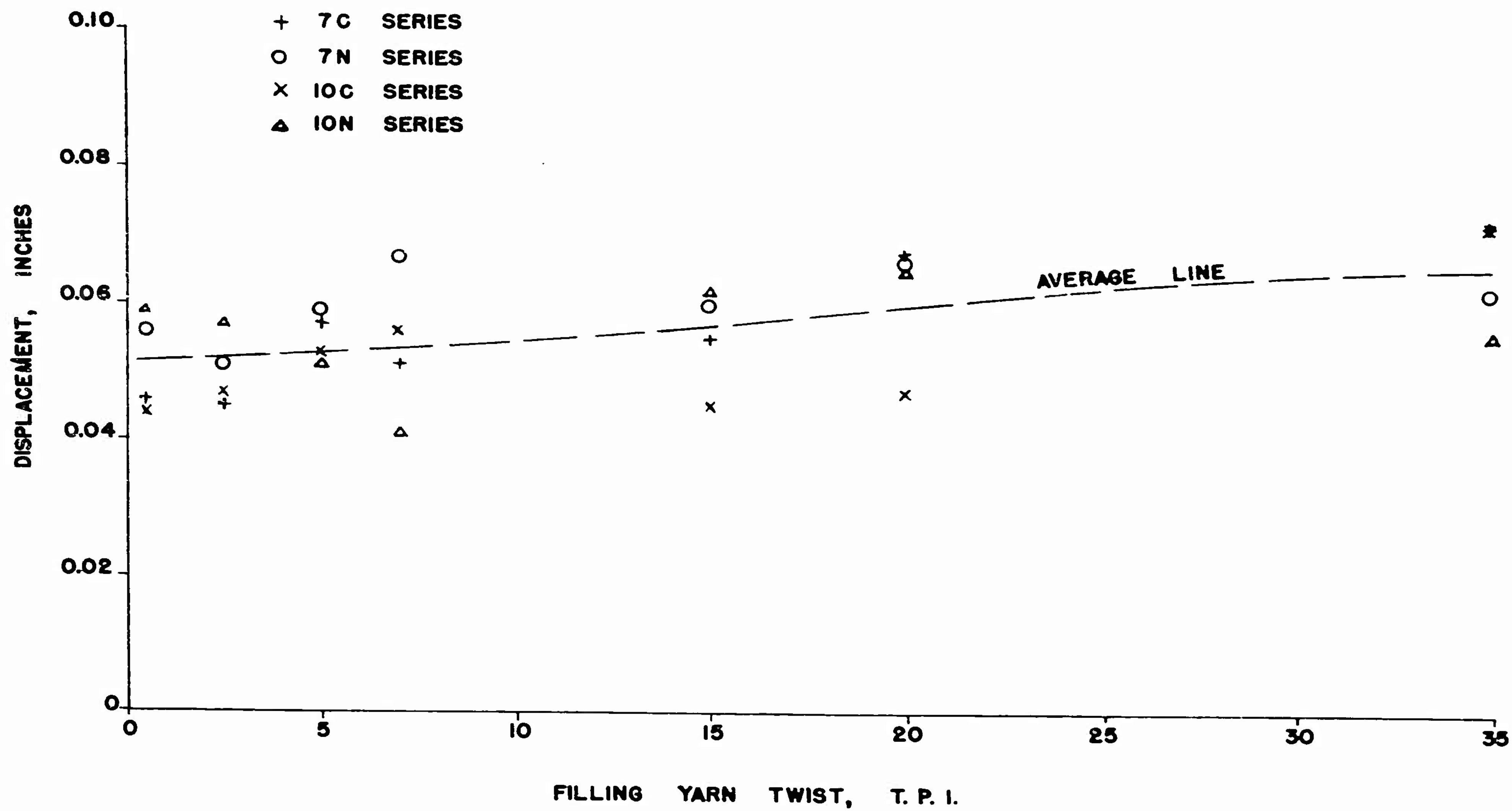

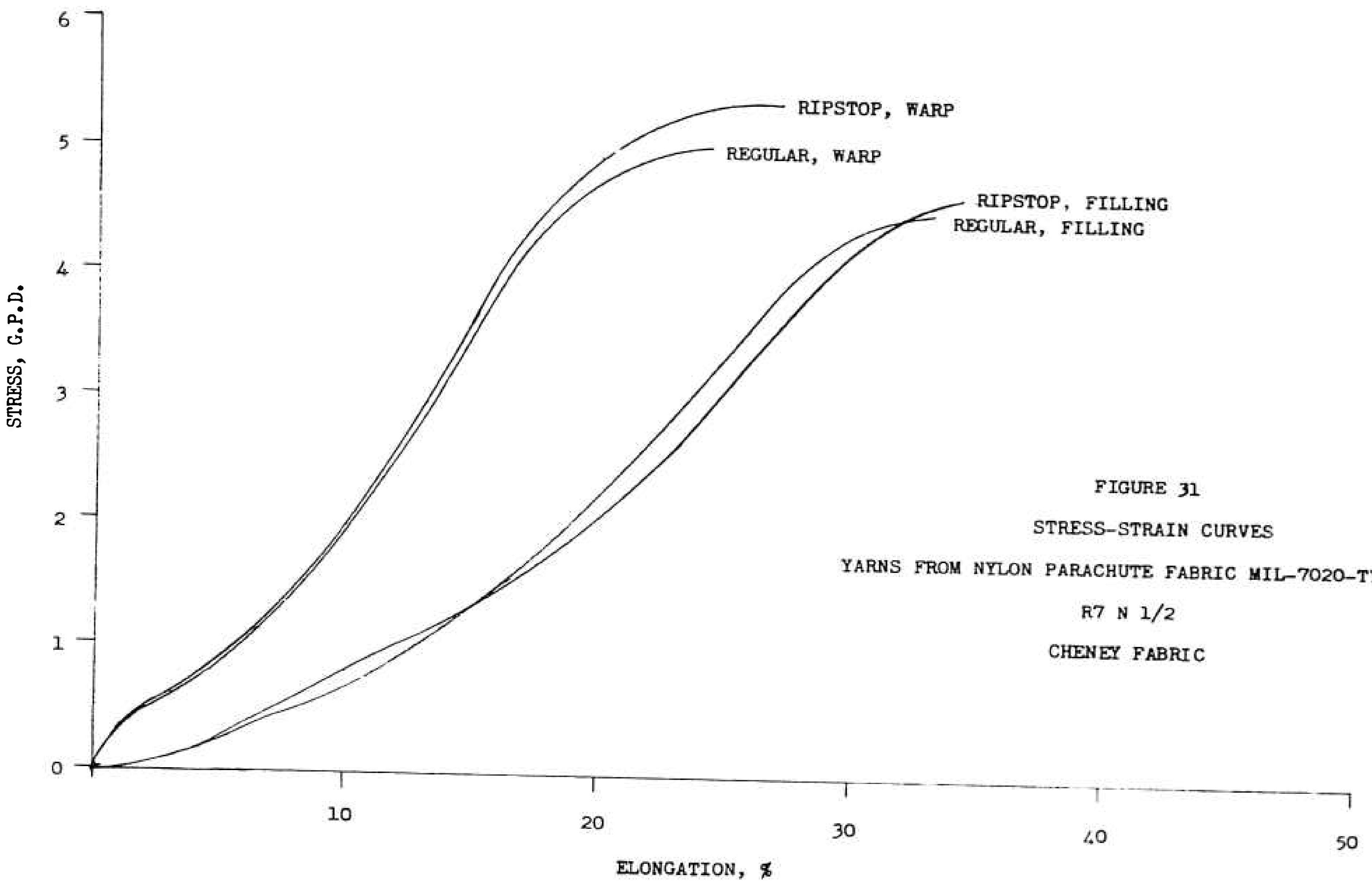

FIGURE 31

STRESS-STRAIN CURVES

YARNS FROM NYLON PARACHUTE FABRIC MIL-7020-TYPE I

R7 N 1/2

CHENEY FABRIC

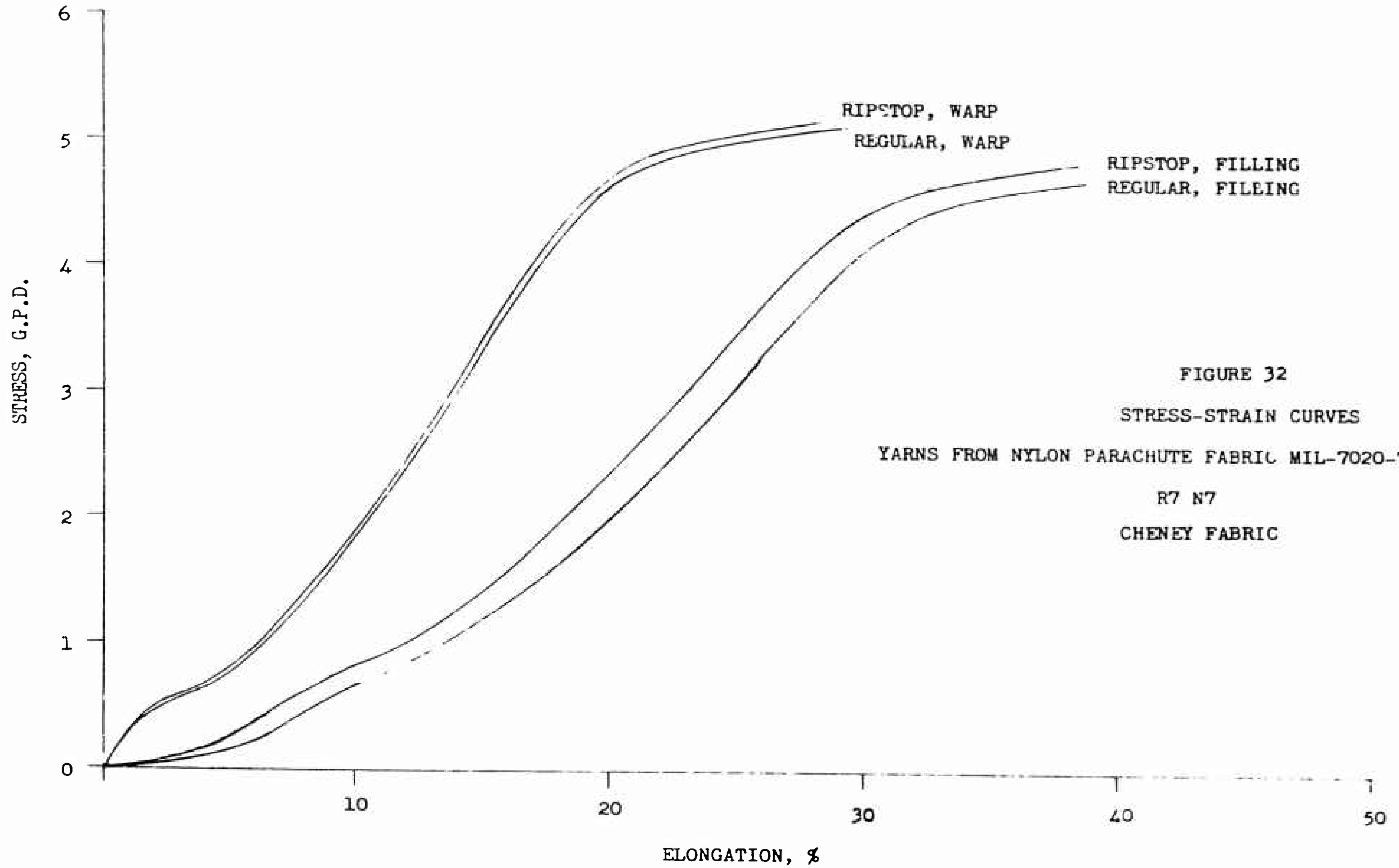

FIGURE 32

STRESS-STRAIN CURVES

YARNS FROM NYLON PARACHUTE FABRIC MIL-7020-TYPE I

R7 N7

CHENEY FABRIC

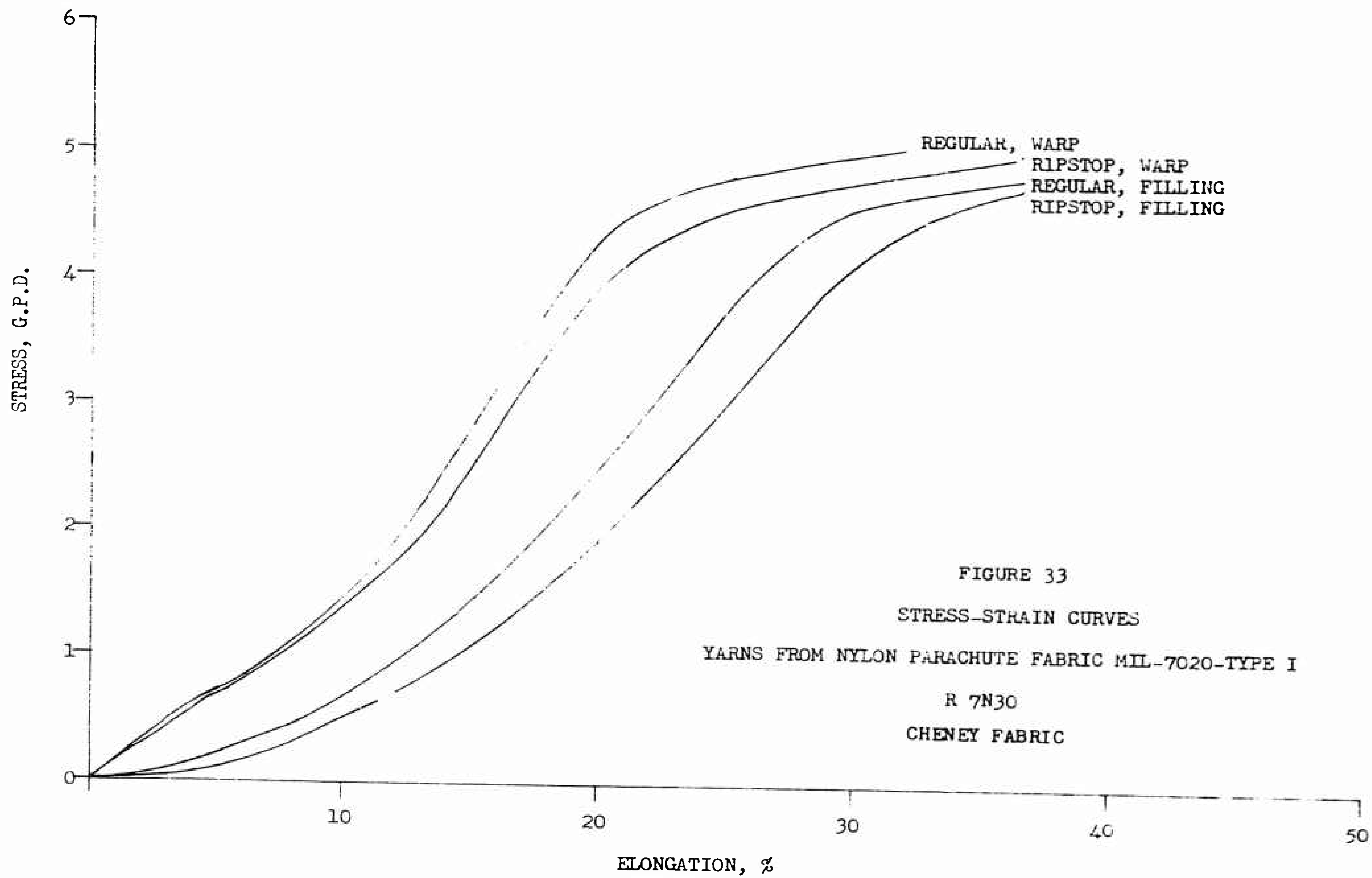

FIGURE 33

STRESS-STRAIN CURVES

YARNS FROM NYLON PARACHUTE FABRIC MIL-7020-TYPE I

R 7N30

CHENEY FABRIC

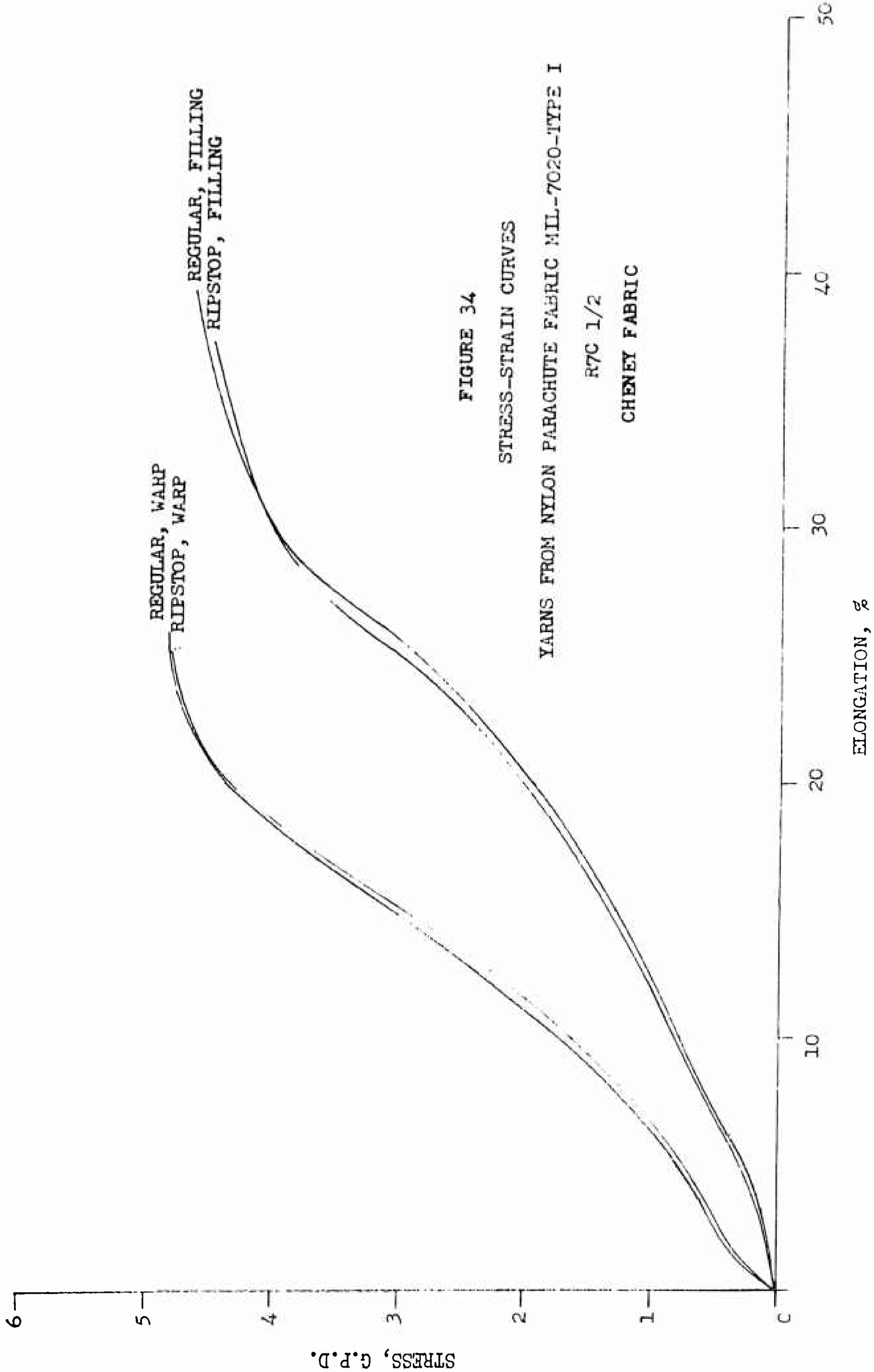

FIGURE 34

STRESS-STRAIN CURVES

YARNS FROM NYLON PARACHUTE FABRIC MIL-7020-TYPE I

R7C 1/2

CHENEY FABRIC

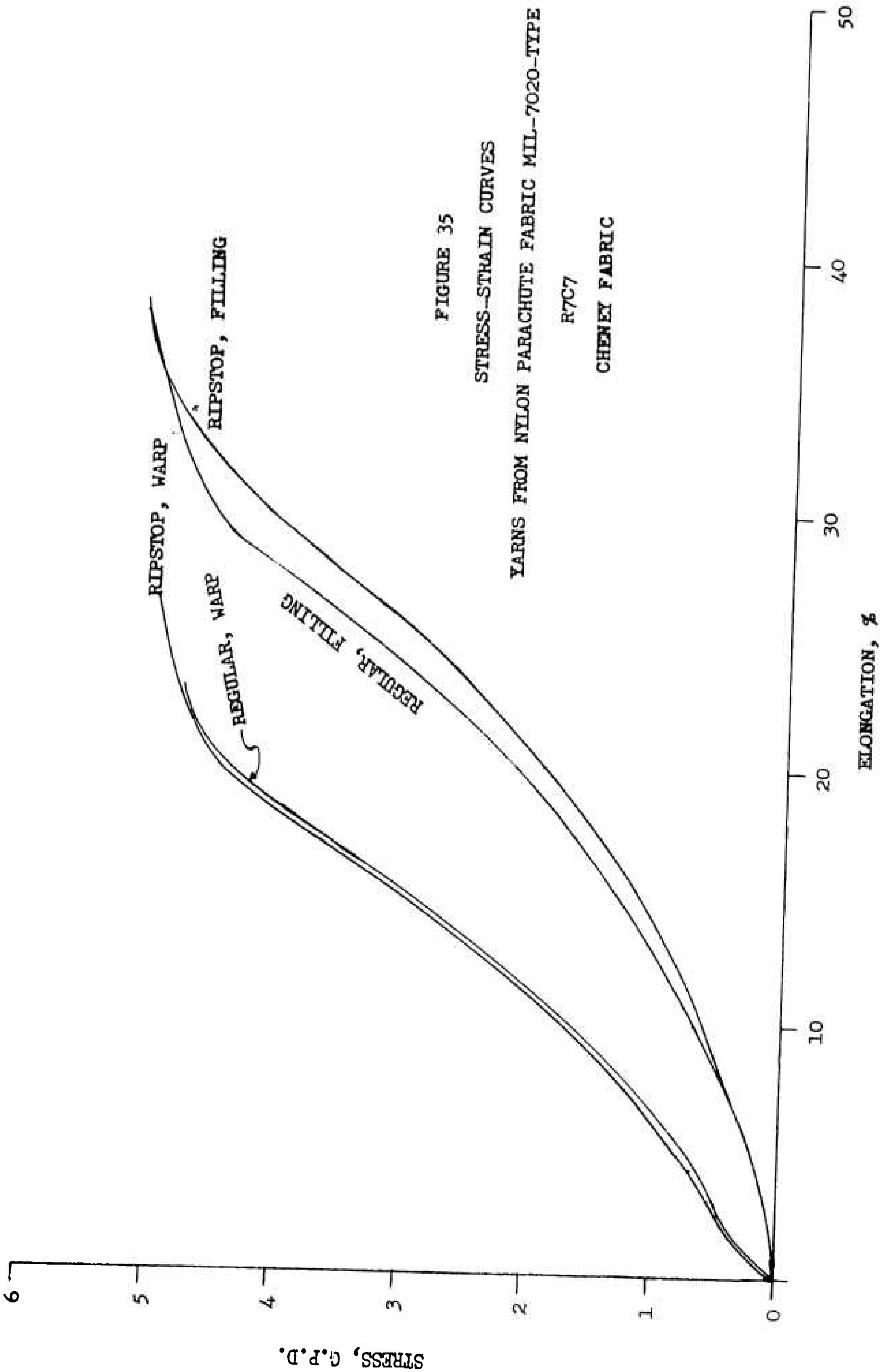

FIGURE 35

STRESS-STRAIN CURVES

YARNS FROM NYLON PARACHUTE FABRIC MIL-7020-TYPE I

R7C7

CHENEY FABRIC

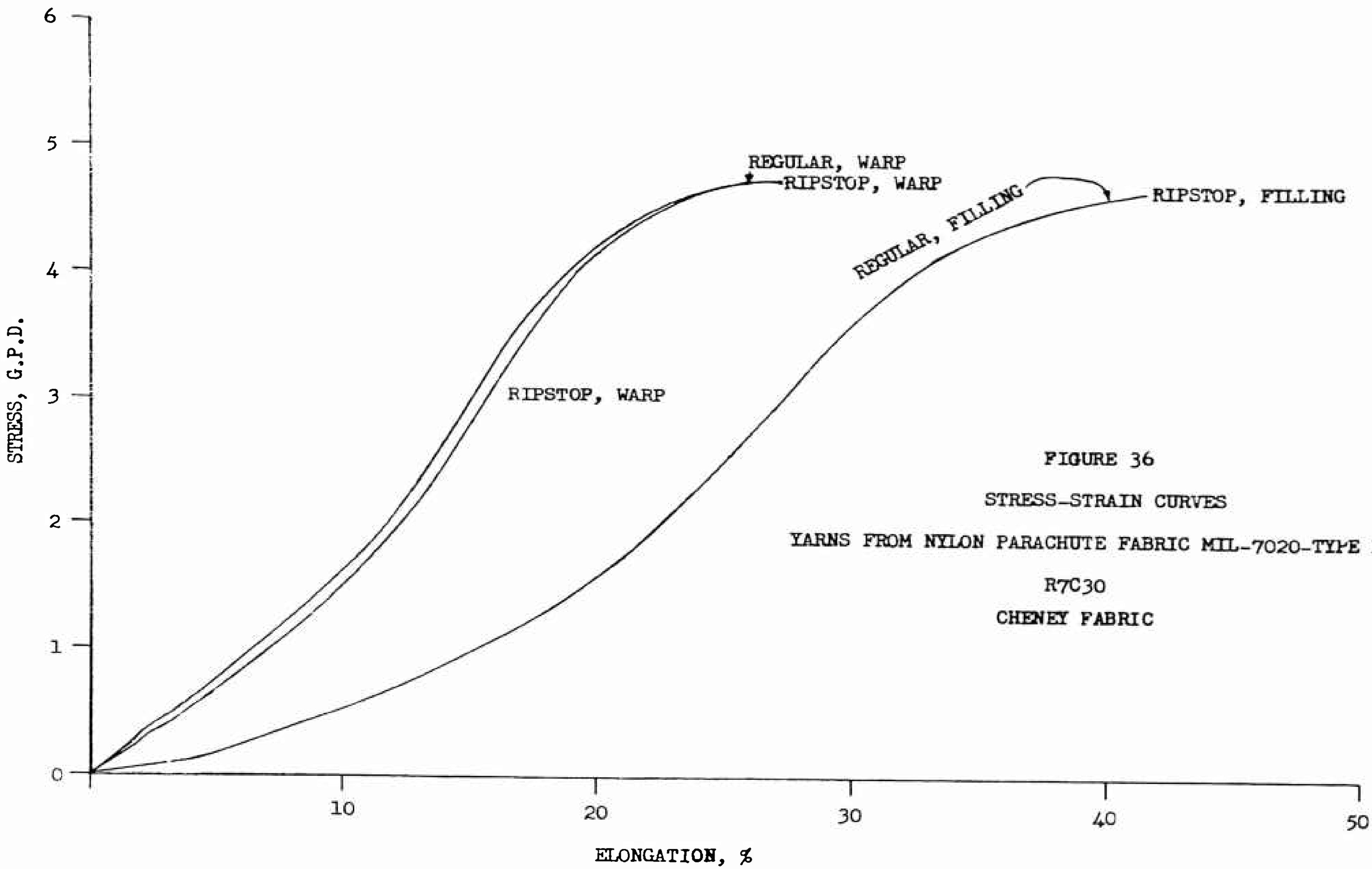

FIGURE 36

STRESS-STRAIN CURVES

YARNS FROM NYLON PARACHUTE FABRIC MIL-7020-TYPE I

R7C30

CHENEY FABRIC

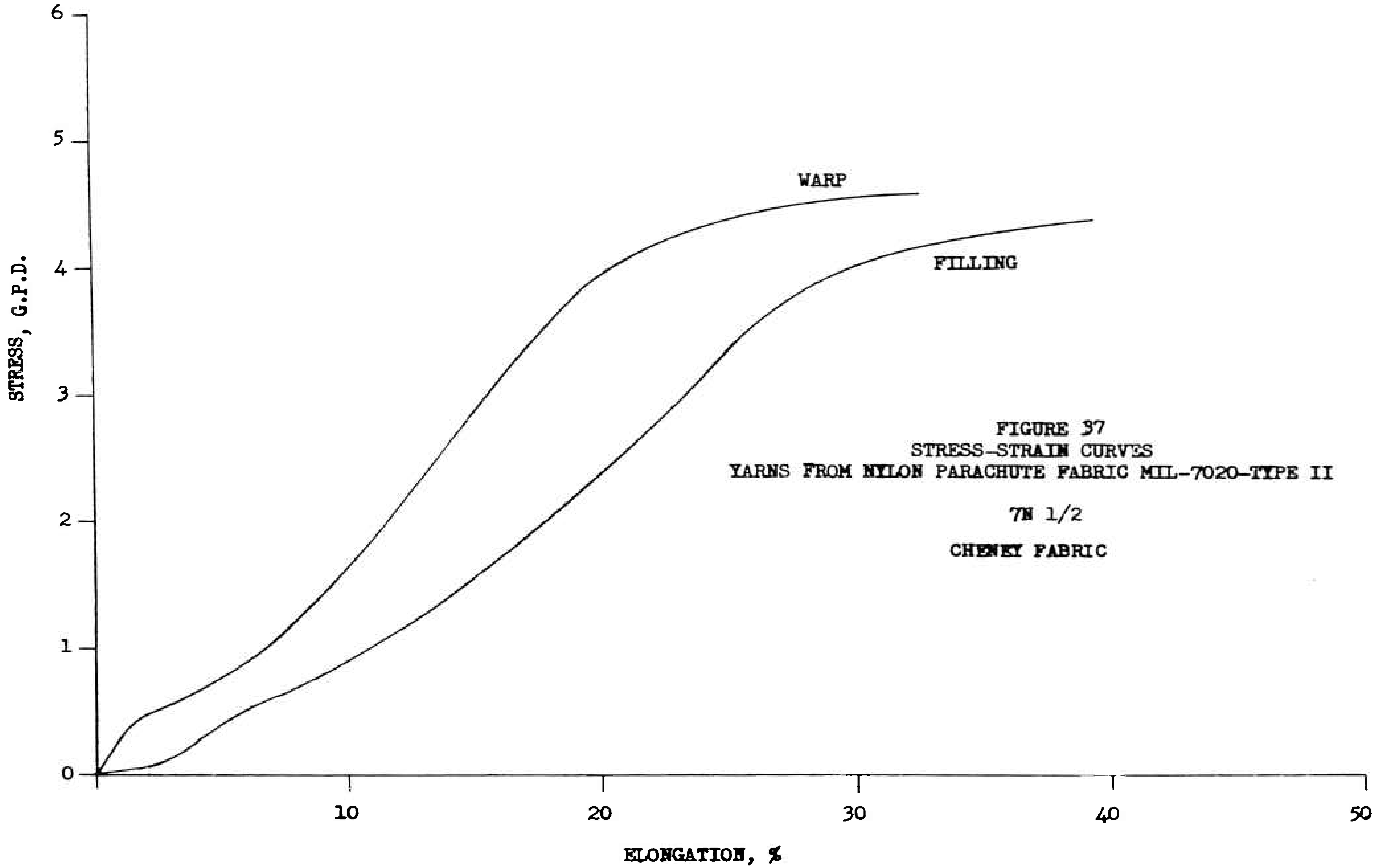

FIGURE 37
STRESS-STRAIN CURVES
YARNS FROM NYLON PARACHUTE FABRIC MIL-7020-TYPE II

7N 1/2

CHENEY FABRIC

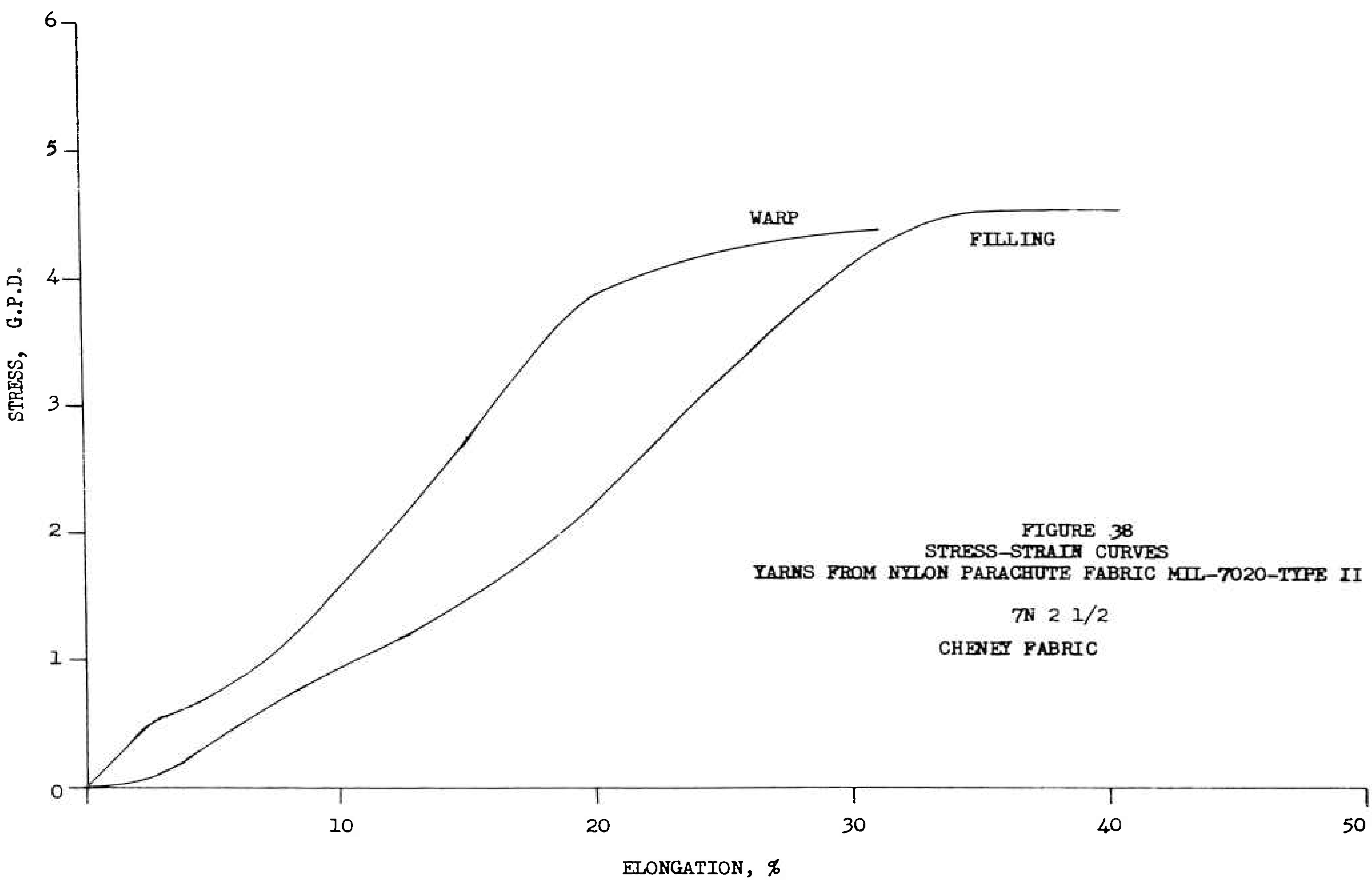

FIGURE 38
STRESS-STRAIN CURVES
YARNS FROM NYLON PARACHUTE FABRIC MIL-7020-TYPE II

7N 2 1/2

CHENEY FABRIC

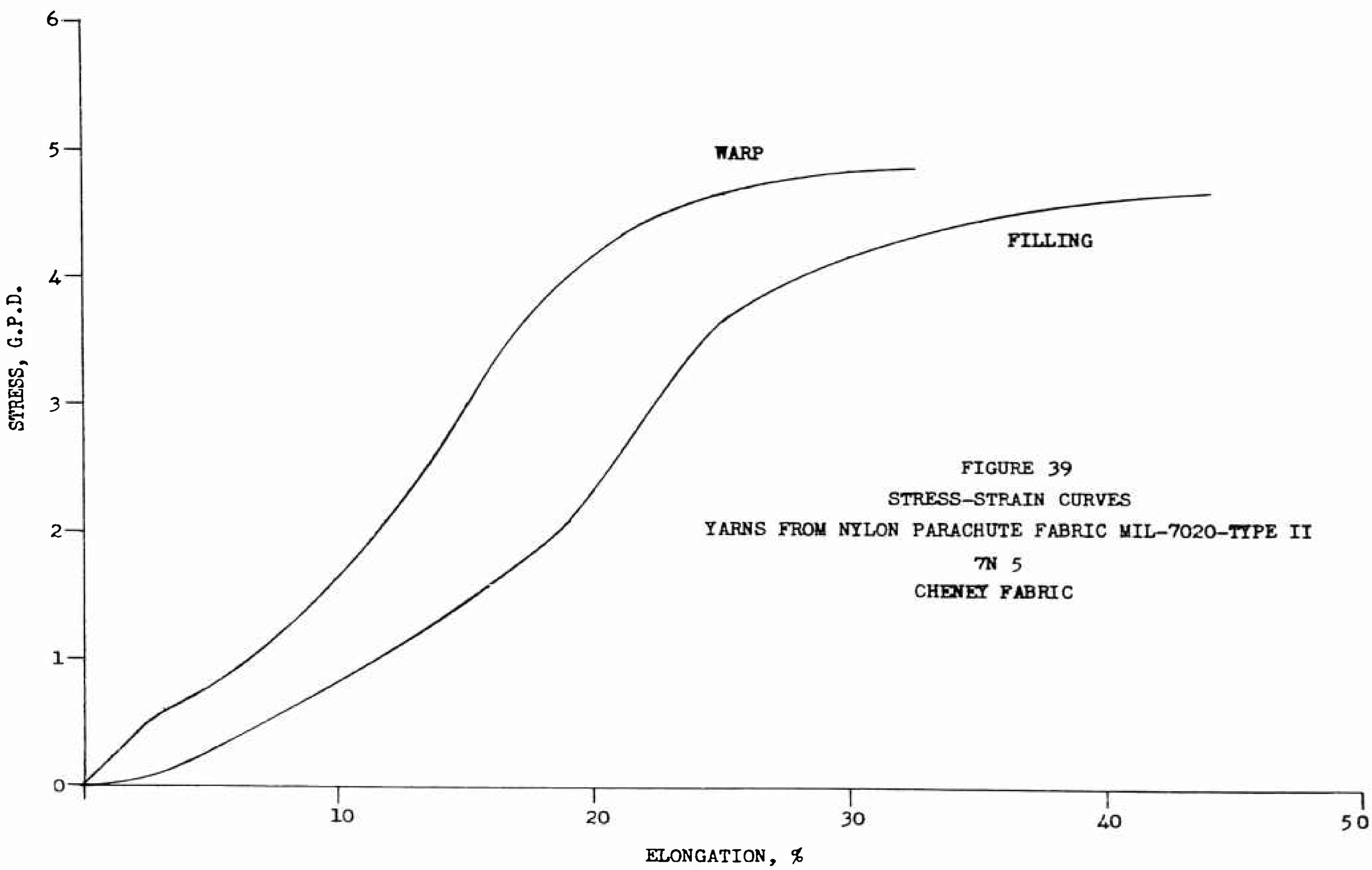

FIGURE 39
STRESS-STRAIN CURVES
YARNS FROM NYLON PARACHUTE FABRIC MIL-7020-TYPE II
7N 5
CHENEY FABRIC

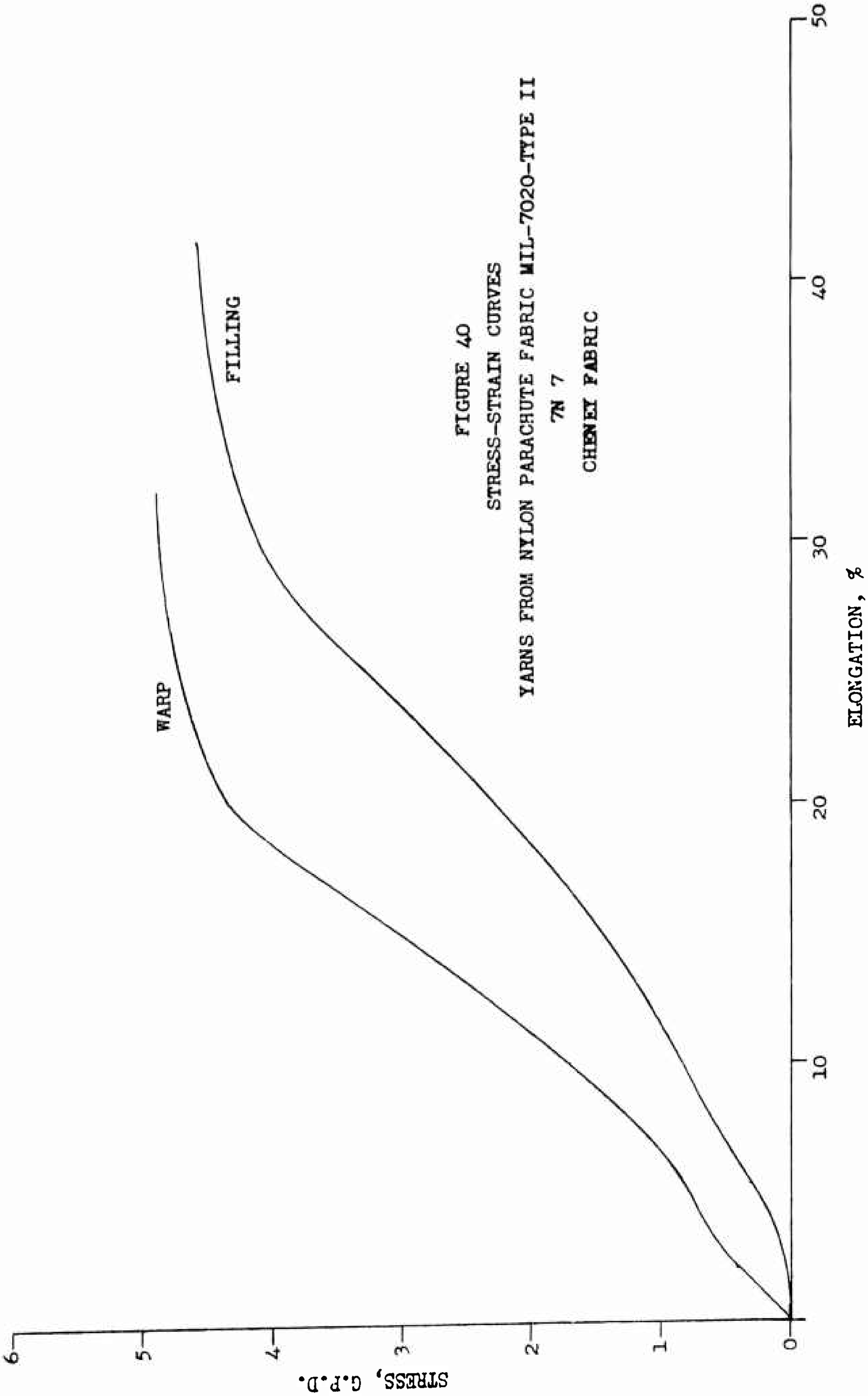

FIGURE 40
STRESS-STRAIN CURVES
YARNS FROM NYLON PARACHUTE FABRIC MIL-7020-TYPE II
7N 7
CHENEY FABRIC

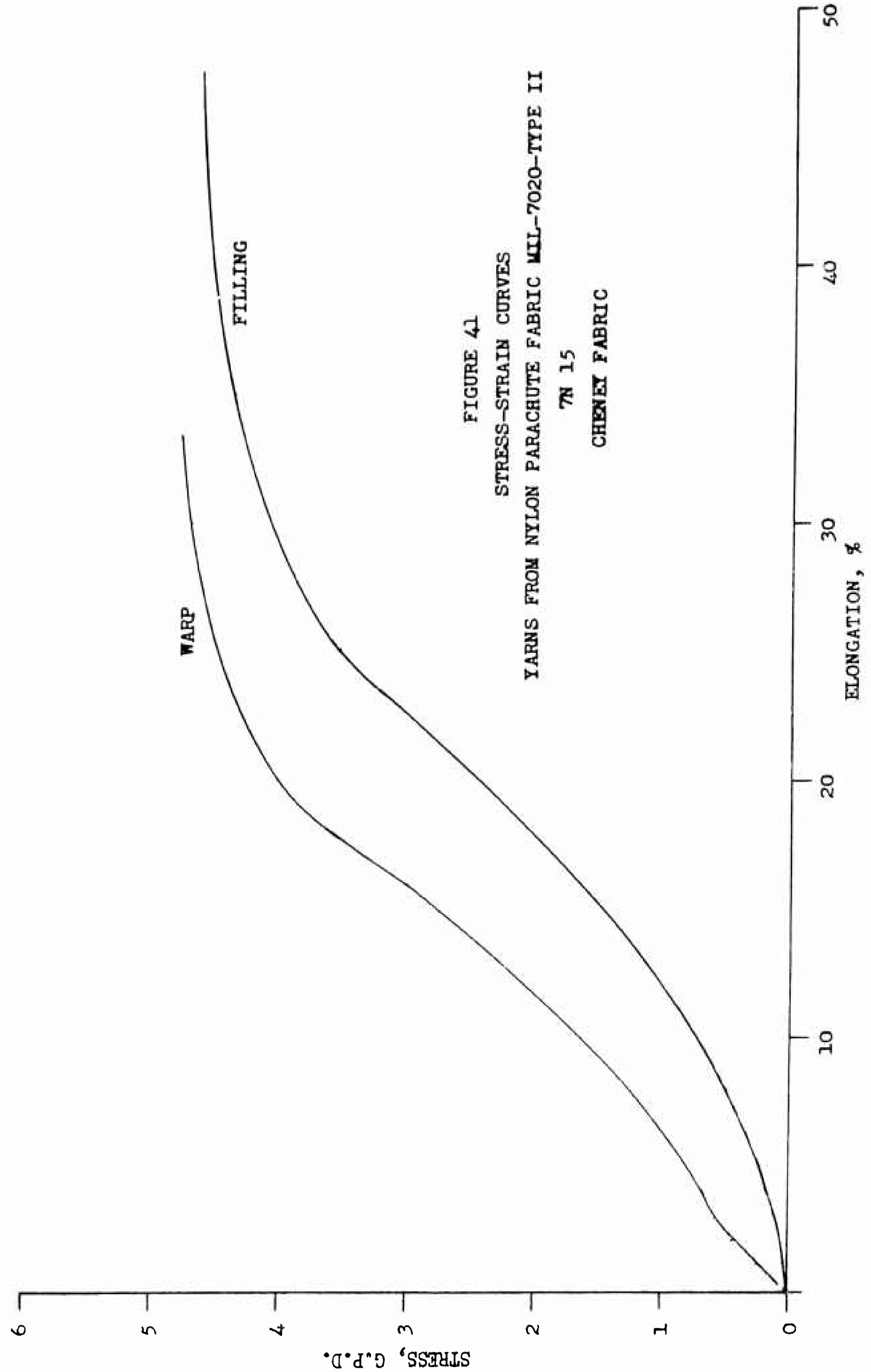

FIGURE 41
STRESS-STRAIN CURVES
YARNS FROM NYLON PARACHUTE FABRIC MIL-7020-TYPE II
7N 15
CHENEY FABRIC

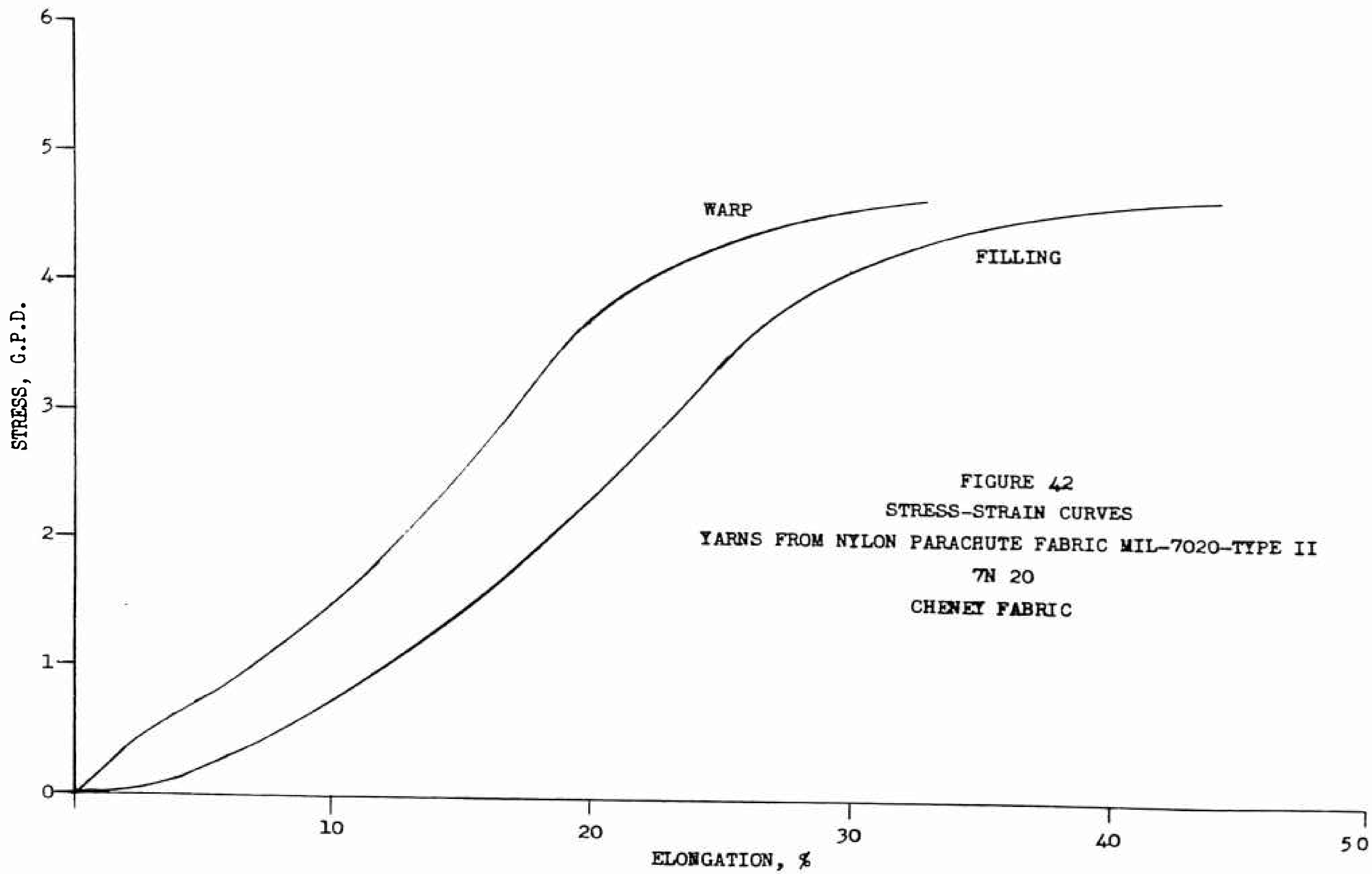

FIGURE 42
STRESS-STRAIN CURVES
YARNS FROM NYLON PARACHUTE FABRIC MIL-7020-TYPE II
7N 20
CHENEY FABRIC

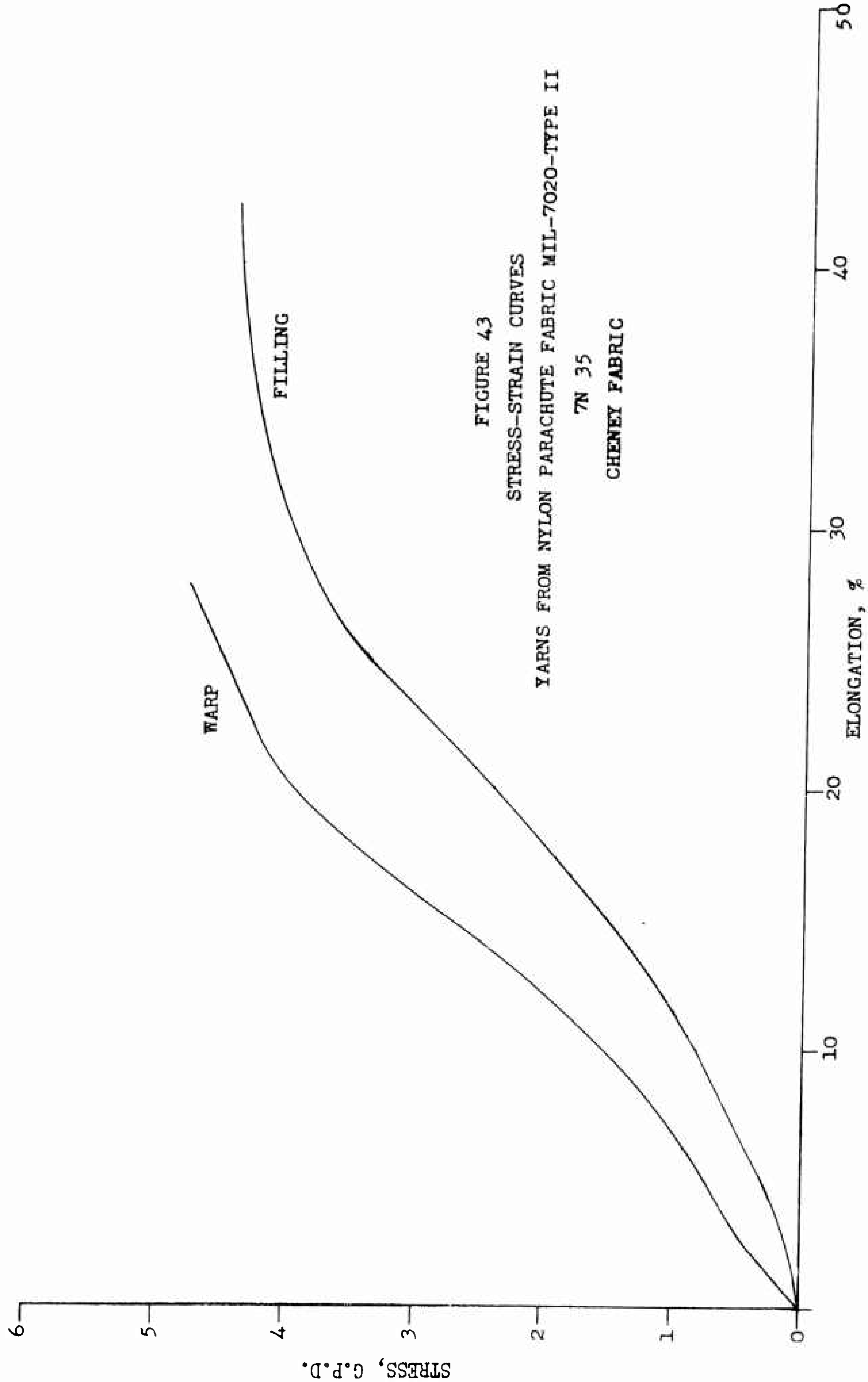

FIGURE 43
STRESS-STRAIN CURVES
YARNS FROM NYLON PARACHUTE FABRIC MIL-7020-TYPE II
7N 35
CHENEY FABRIC

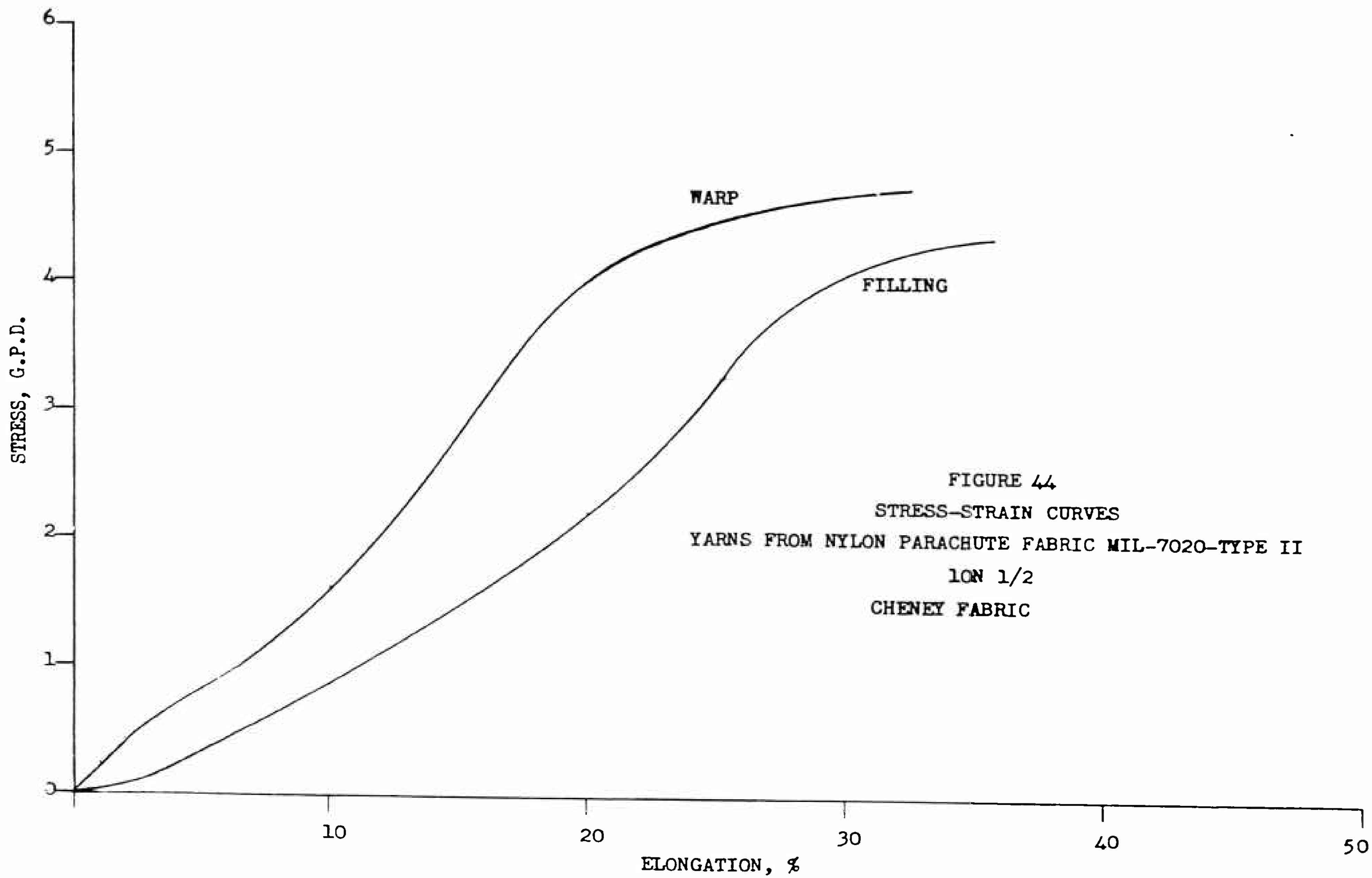

FIGURE 44
STRESS-STRAIN CURVES
YARNS FROM NYLON PARACHUTE FABRIC MIL-7020-TYPE II
10N 1/2
CHENEY FABRIC

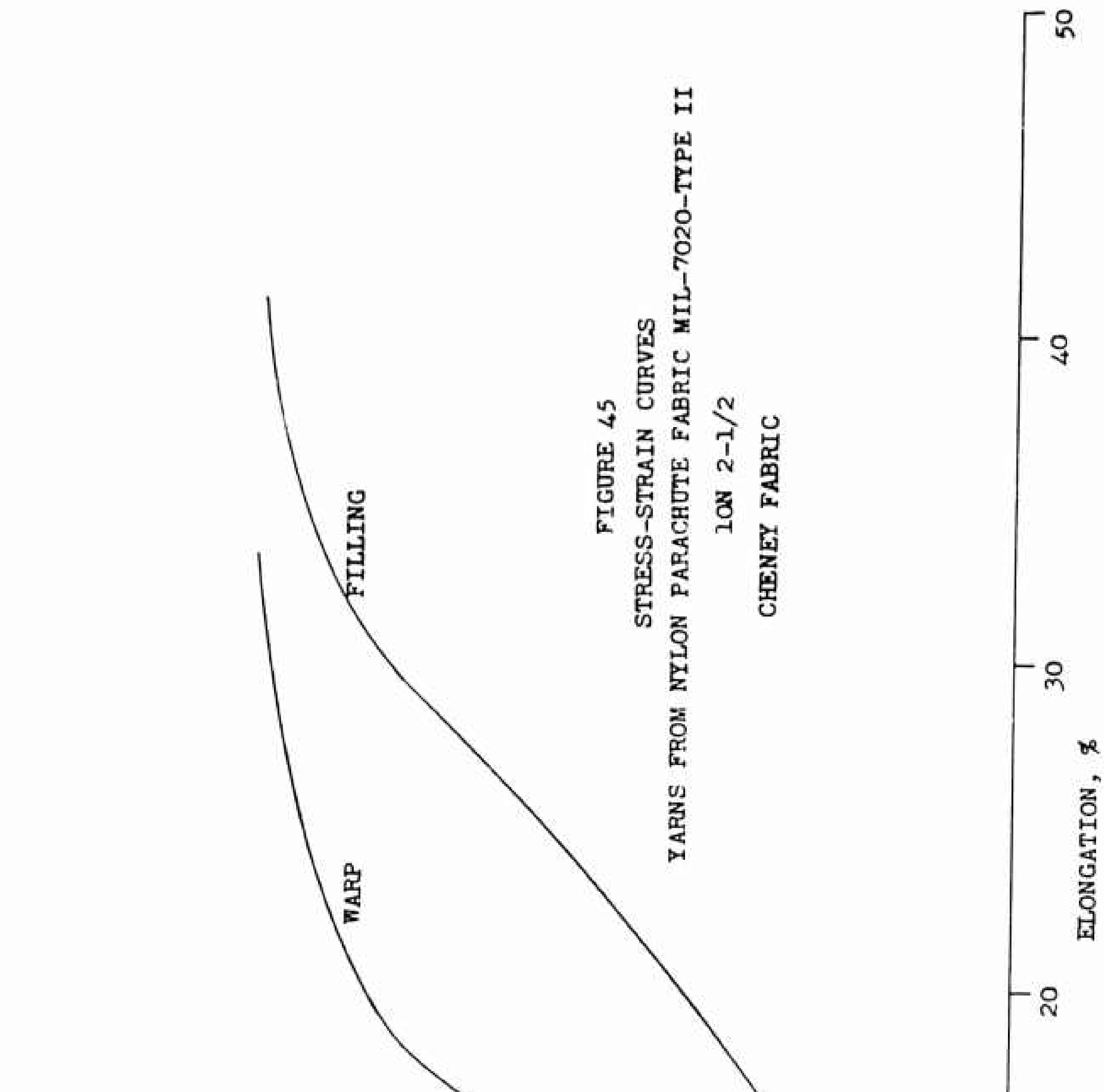

FIGURE 45
STRESS-STRAIN CURVES
YARNS FROM NYLON PARACHUTE FABRIC MIL-7020-TYPE II
1OW 2-1/2
CHENEY FABRIC

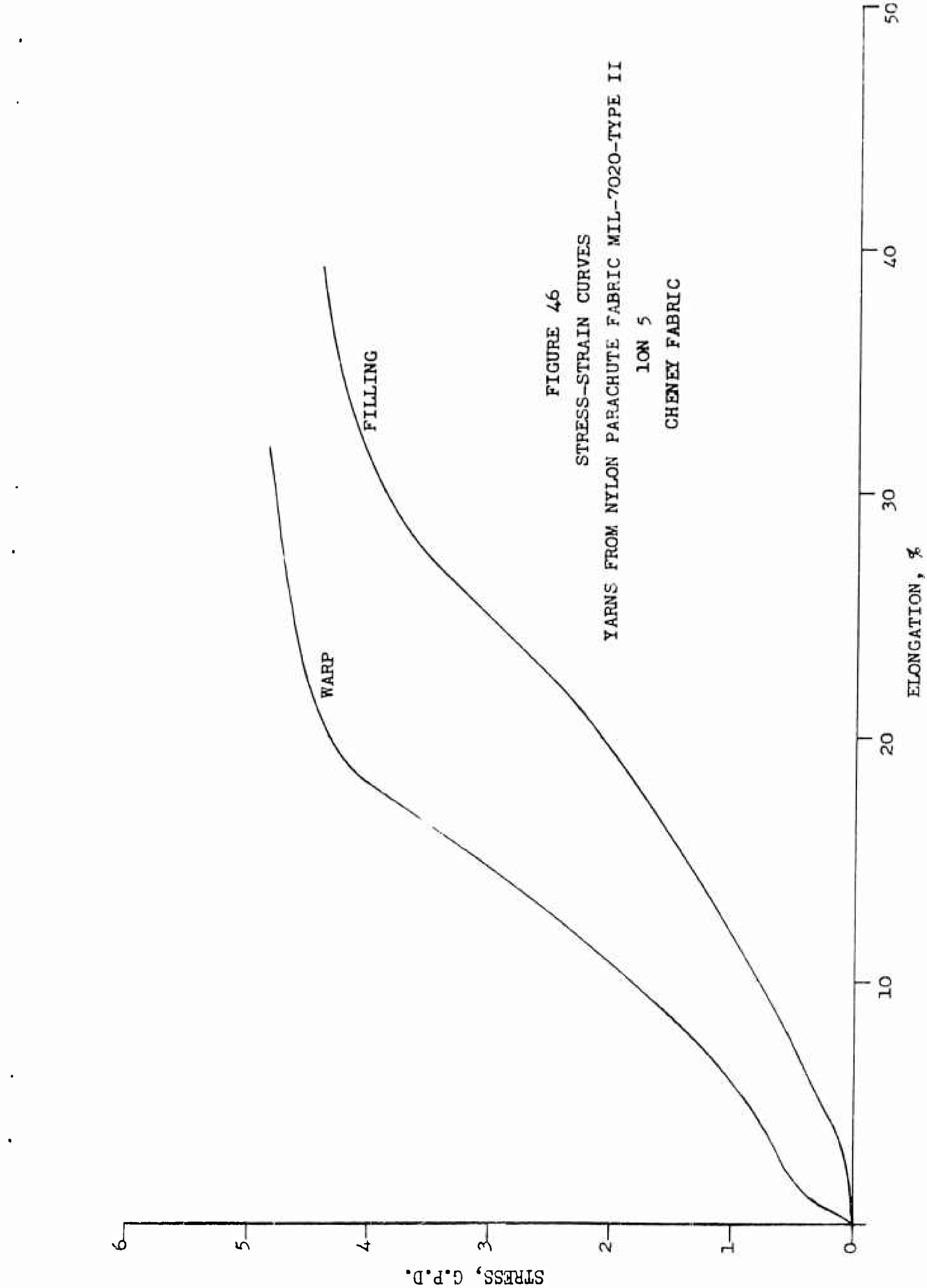

FIGURE 46
STRESS-STRAIN CURVES
YARNS FROM NYLON PARACHUTE FABRIC MIL-7020-TYPE II
1ON 5
CHENEY FABRIC

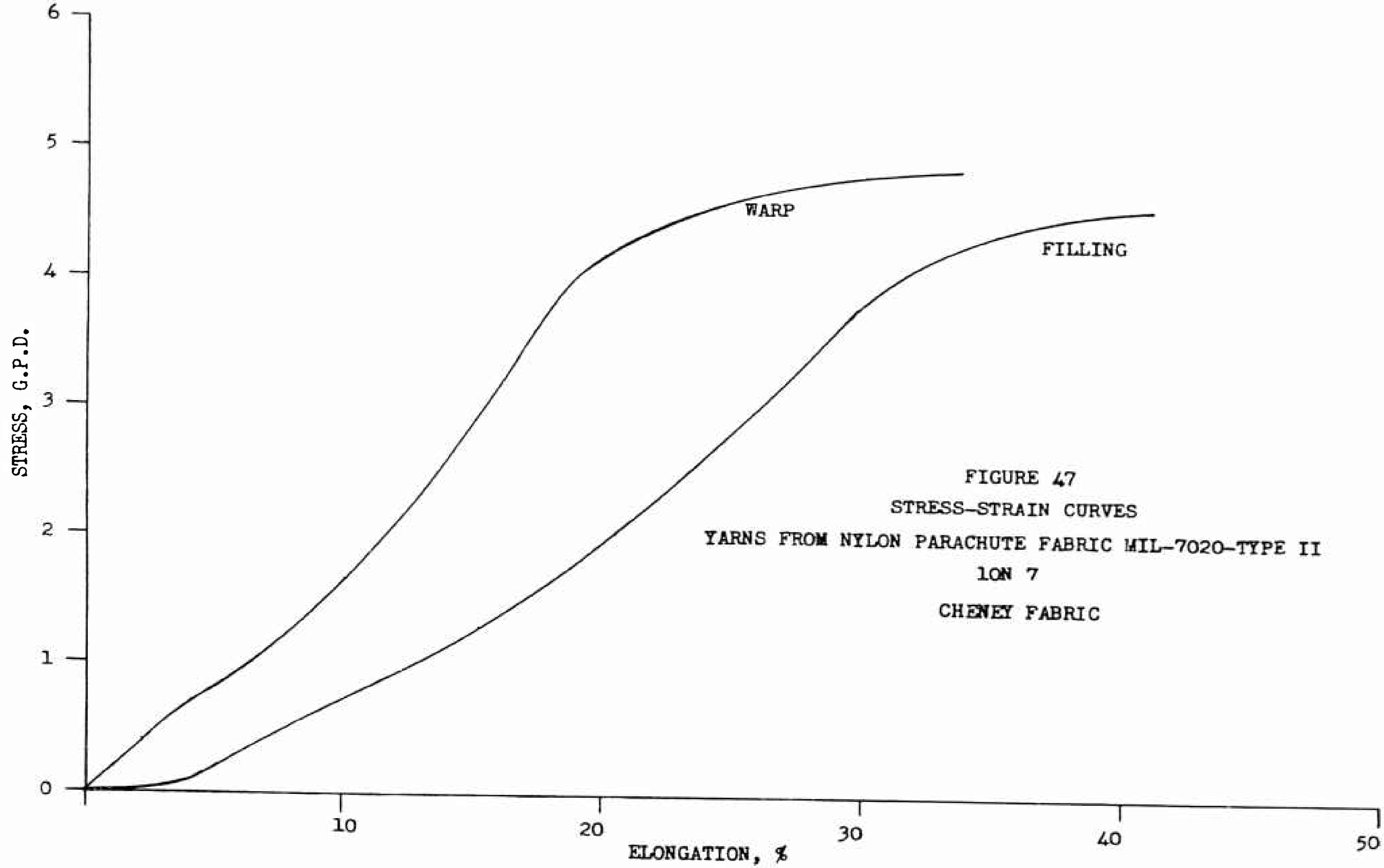

FIGURE 47
STRESS-STRAIN CURVES
YARNS FROM NYLON PARACHUTE FABRIC MIL-7020-TYPE II
1ON 7
CHENEY FABRIC

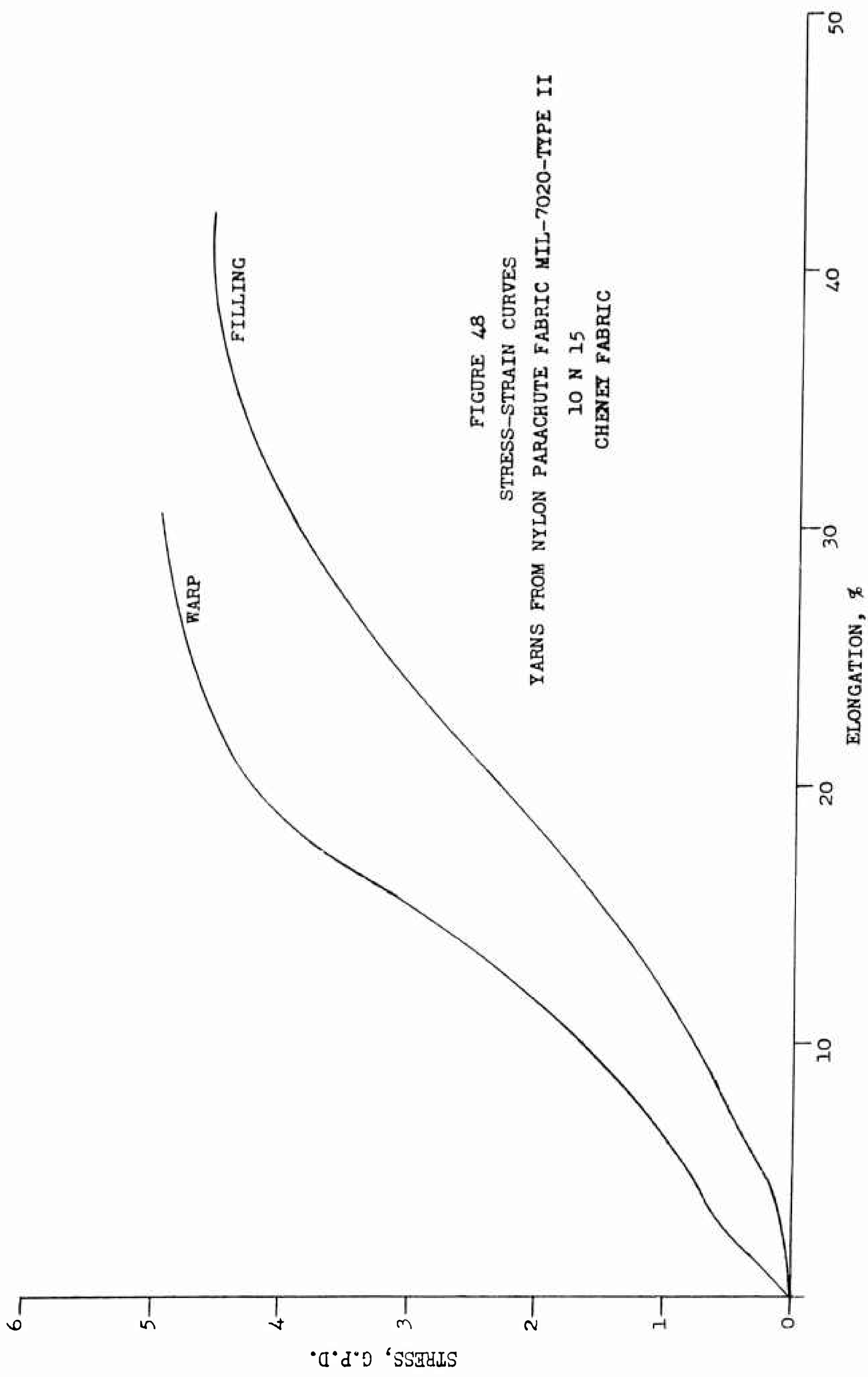

FIGURE 48
STRESS-STRAIN CURVES
YARNS FROM NYLON PARACHUTE FABRIC MIL-7020-TYPE II
10 N 15
CHENEY FABRIC

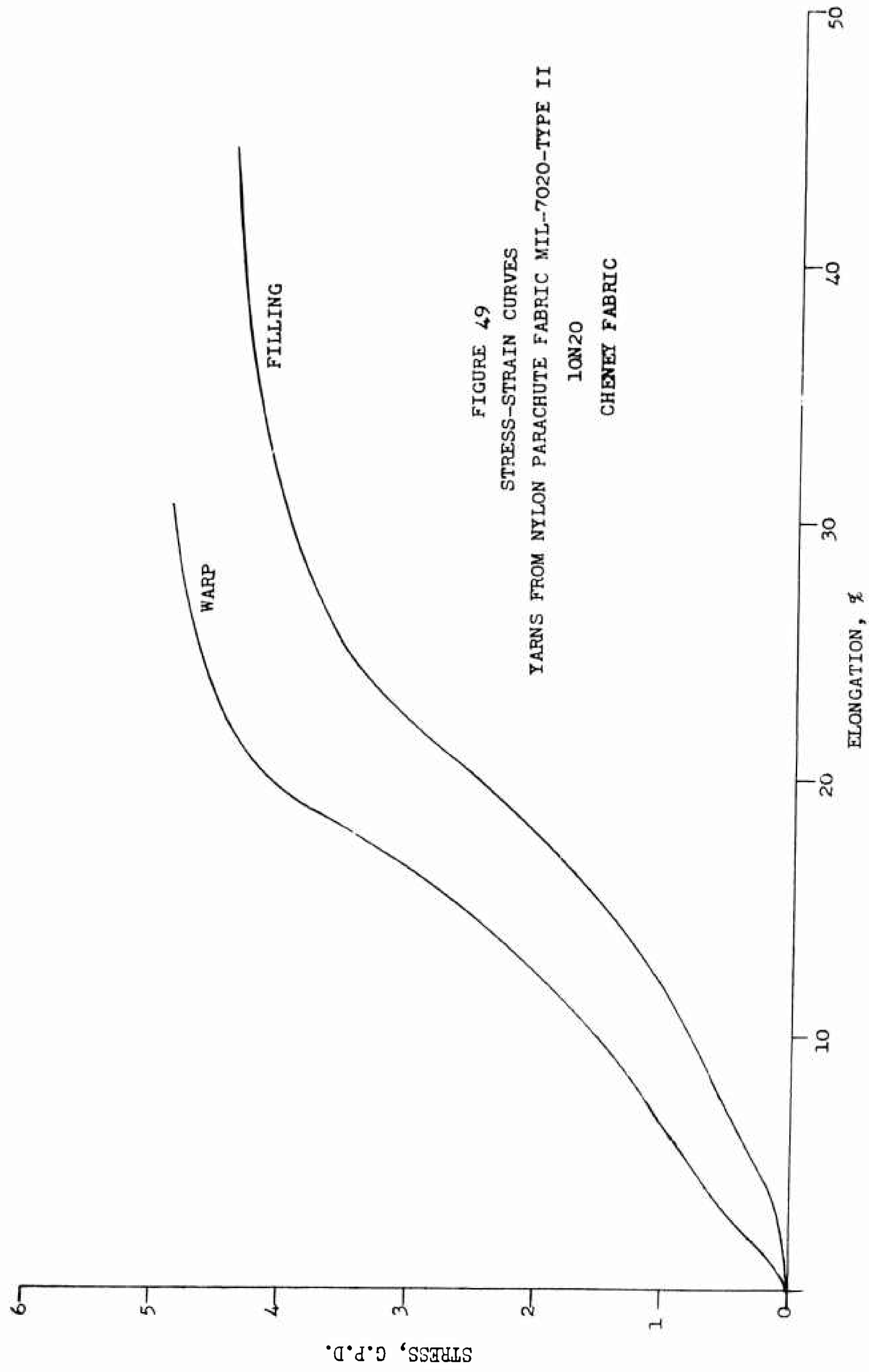

FIGURE 49
STRESS-STRAIN CURVES
YARNS FROM NYLON PARACHUTE FABRIC MIL-7020-TYPE II
10N20
CHENEY FABRIC

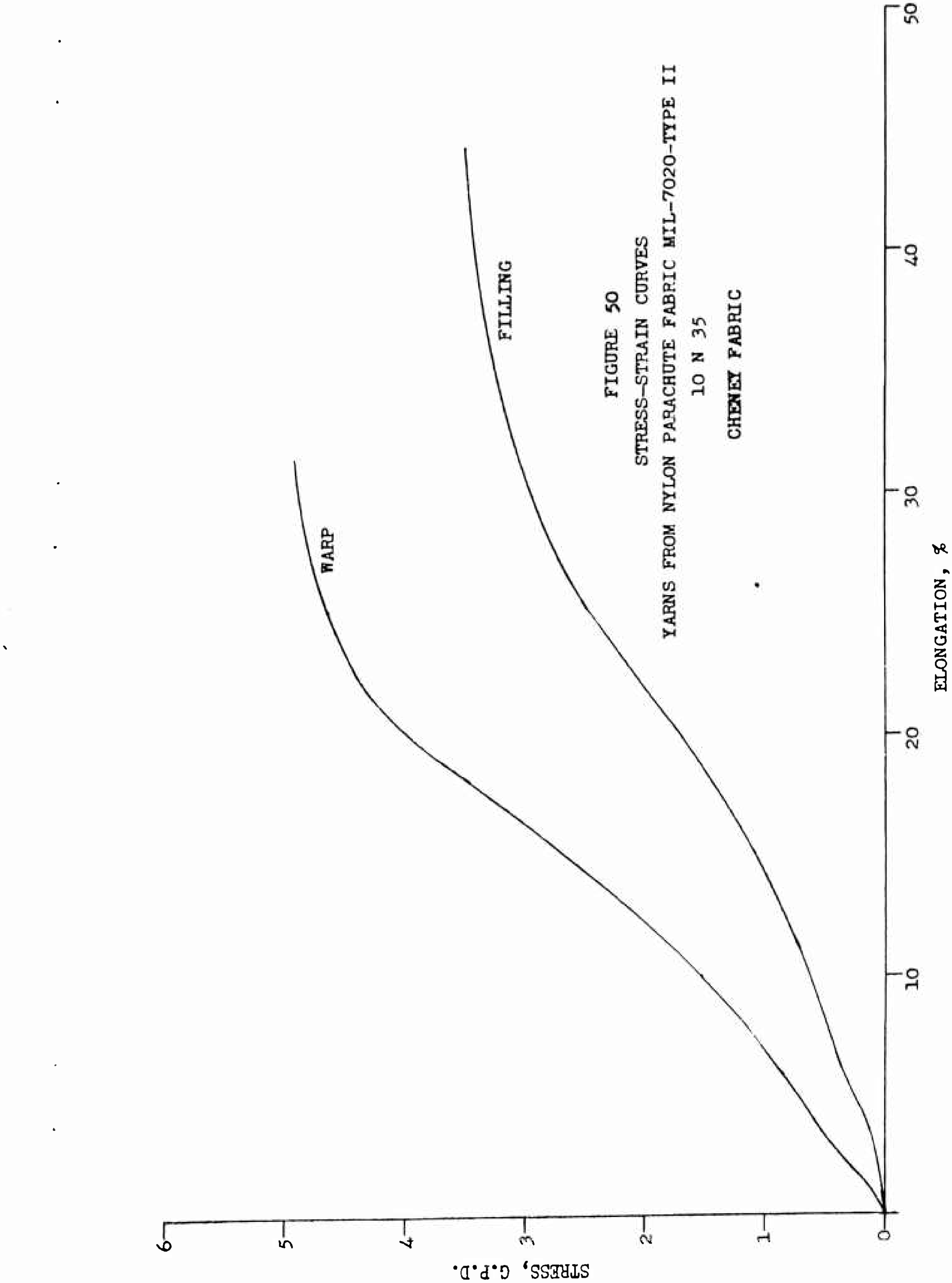

FIGURE 50
STRESS-STRAIN CURVES
YARNS FROM NYLON PARACHUTE FABRIC MIL-7020-TYPE II
10 N 35
CHENEY FABRIC

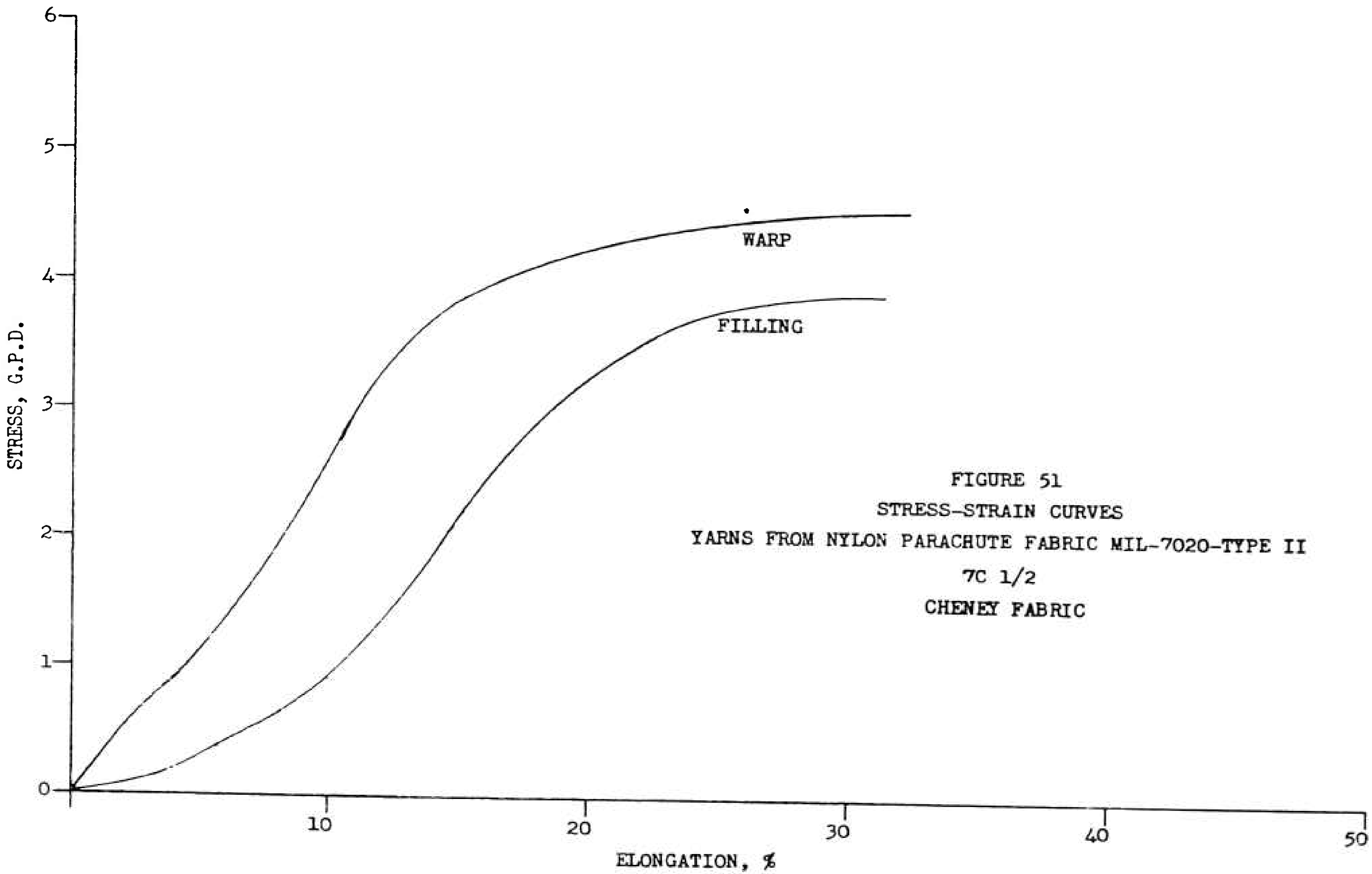

FIGURE 51
STRESS-STRAIN CURVES
YARNS FROM NYLON PARACHUTE FABRIC MIL-7020-TYPE II
7C 1/2
CHENEY FABRIC

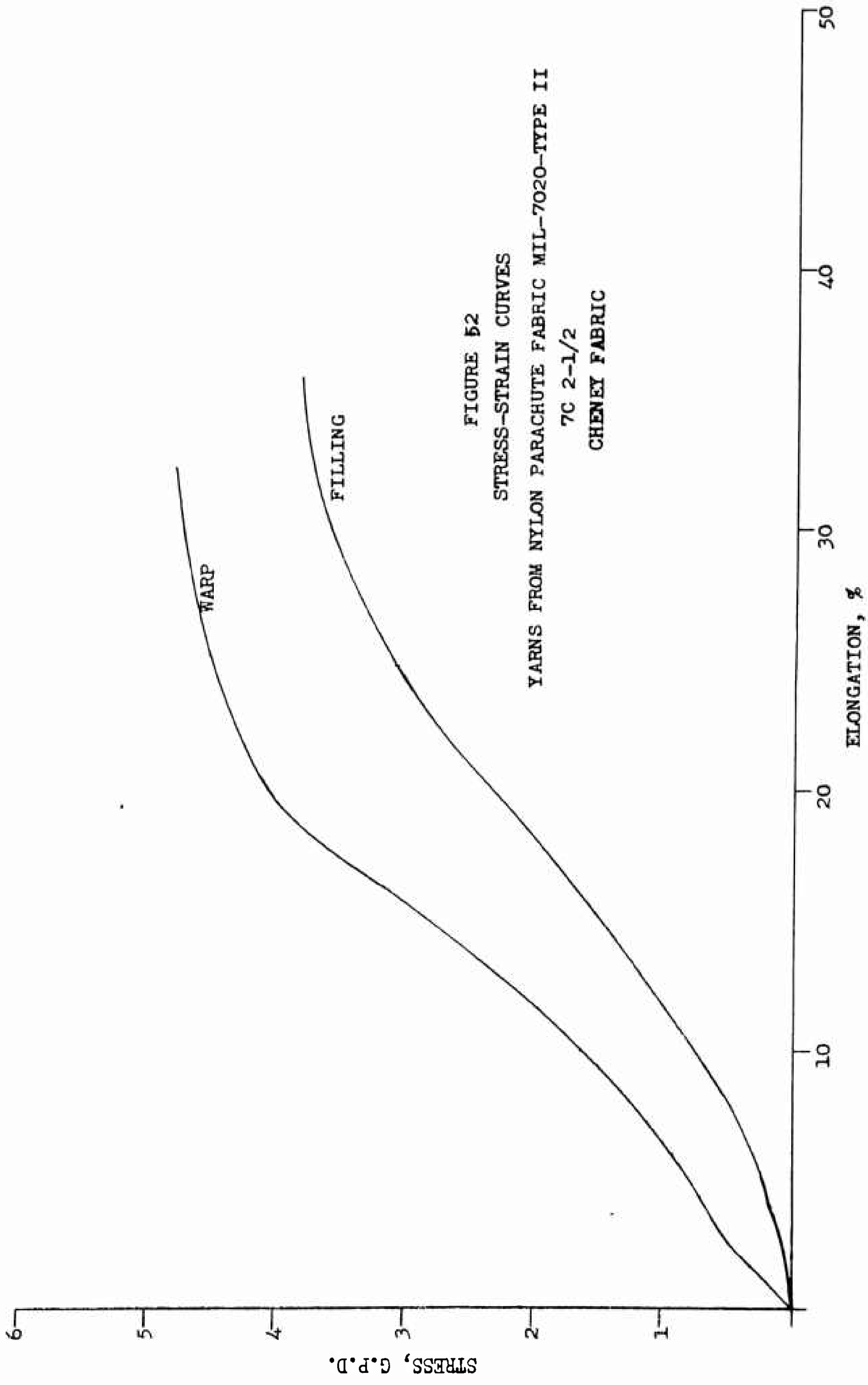

FIGURE 52
STRESS-STRAIN CURVES
YARNS FROM NYLON PARACHUTE FABRIC MIL-7020-TYPE II
7C 2-1/2
CHENEY FABRIC

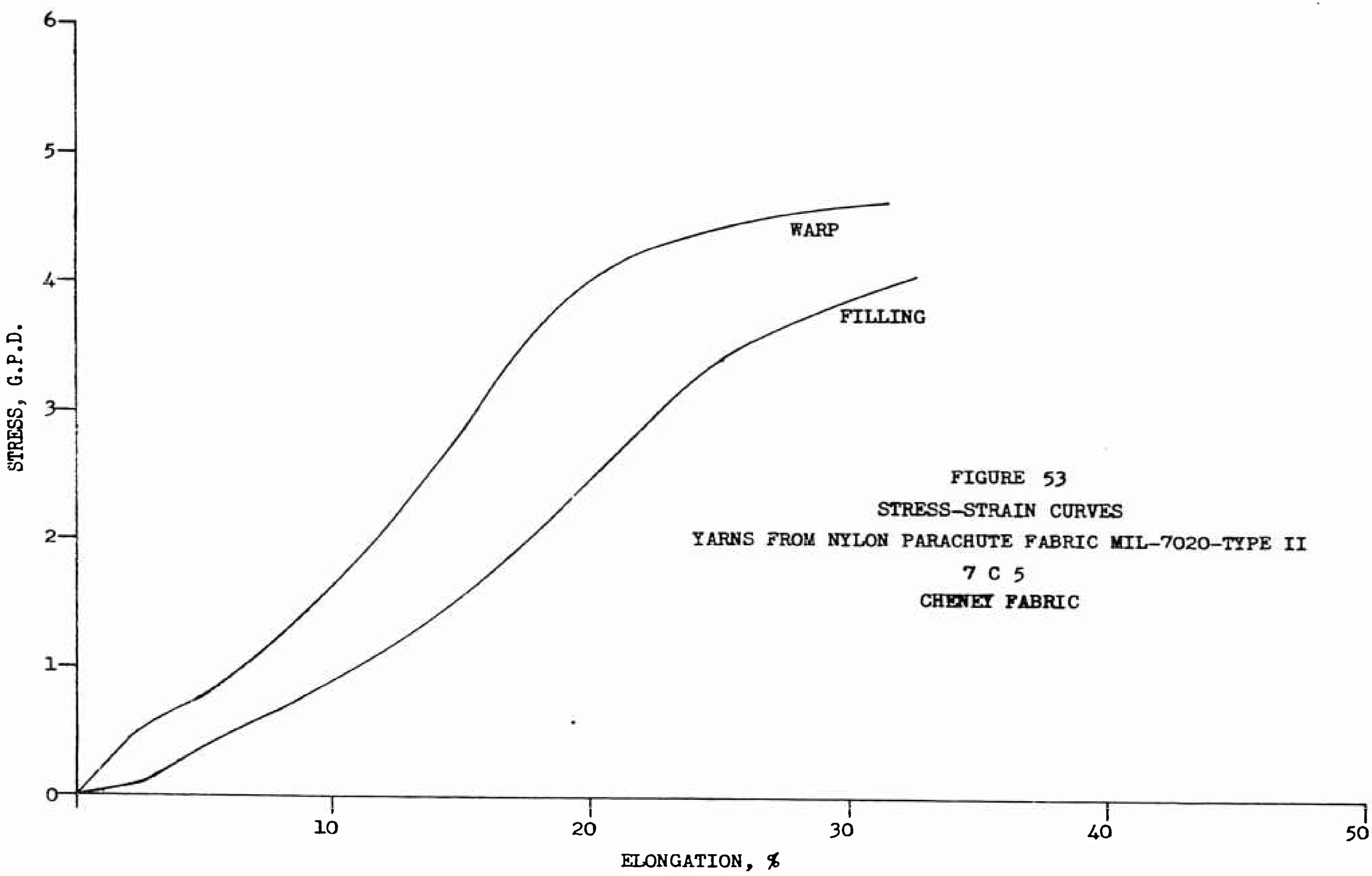

FIGURE 53
STRESS-STRAIN CURVES
YARNS FROM NYLON PARACHUTE FABRIC MIL-7020-TYPE II
7 C 5
CHENEY FABRIC

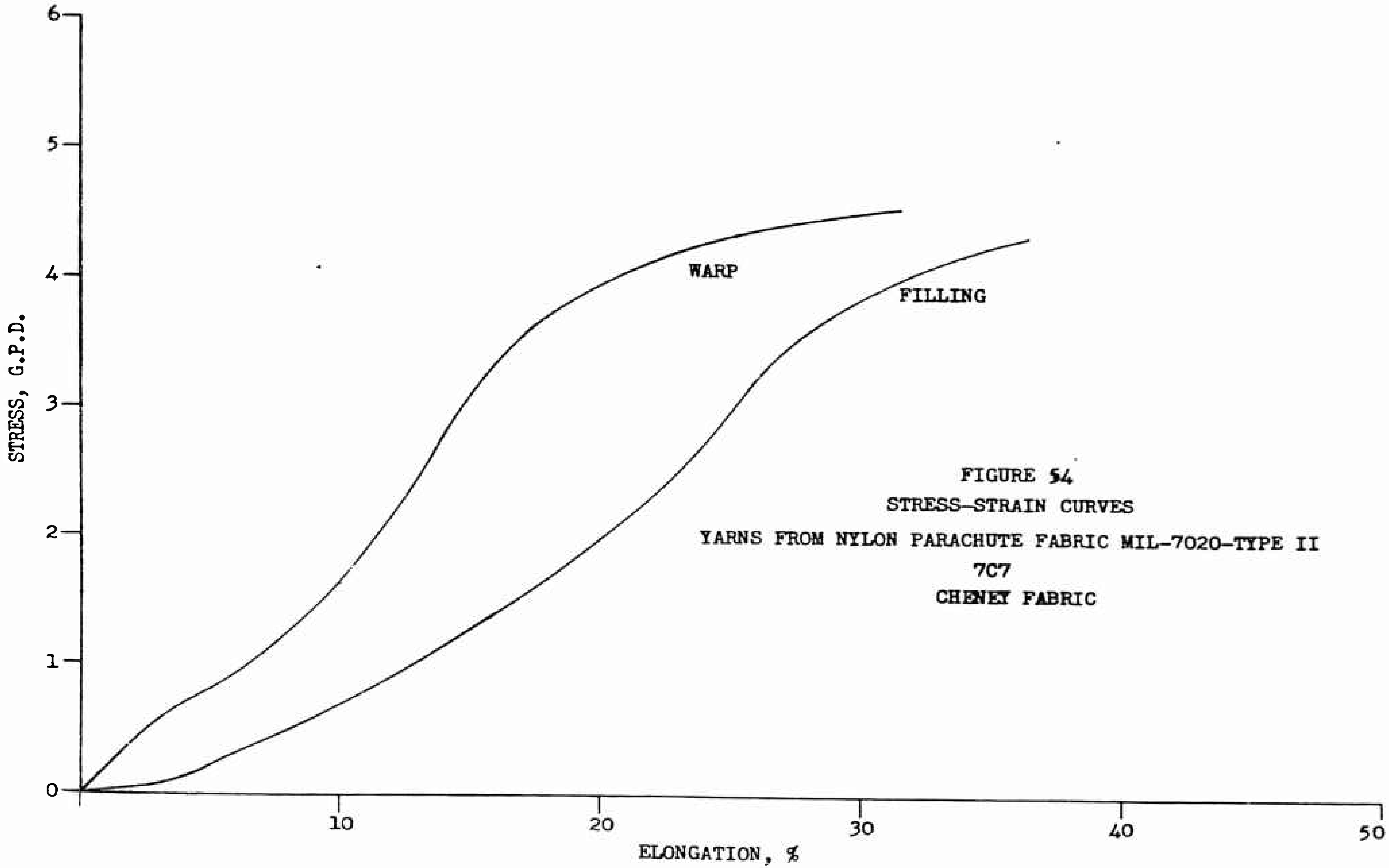

FIGURE 54
STRESS-STRAIN CURVES
YARNS FROM NYLON PARACHUTE FABRIC MIL-7020-TYPE II
7C7
CHENEY FABRIC

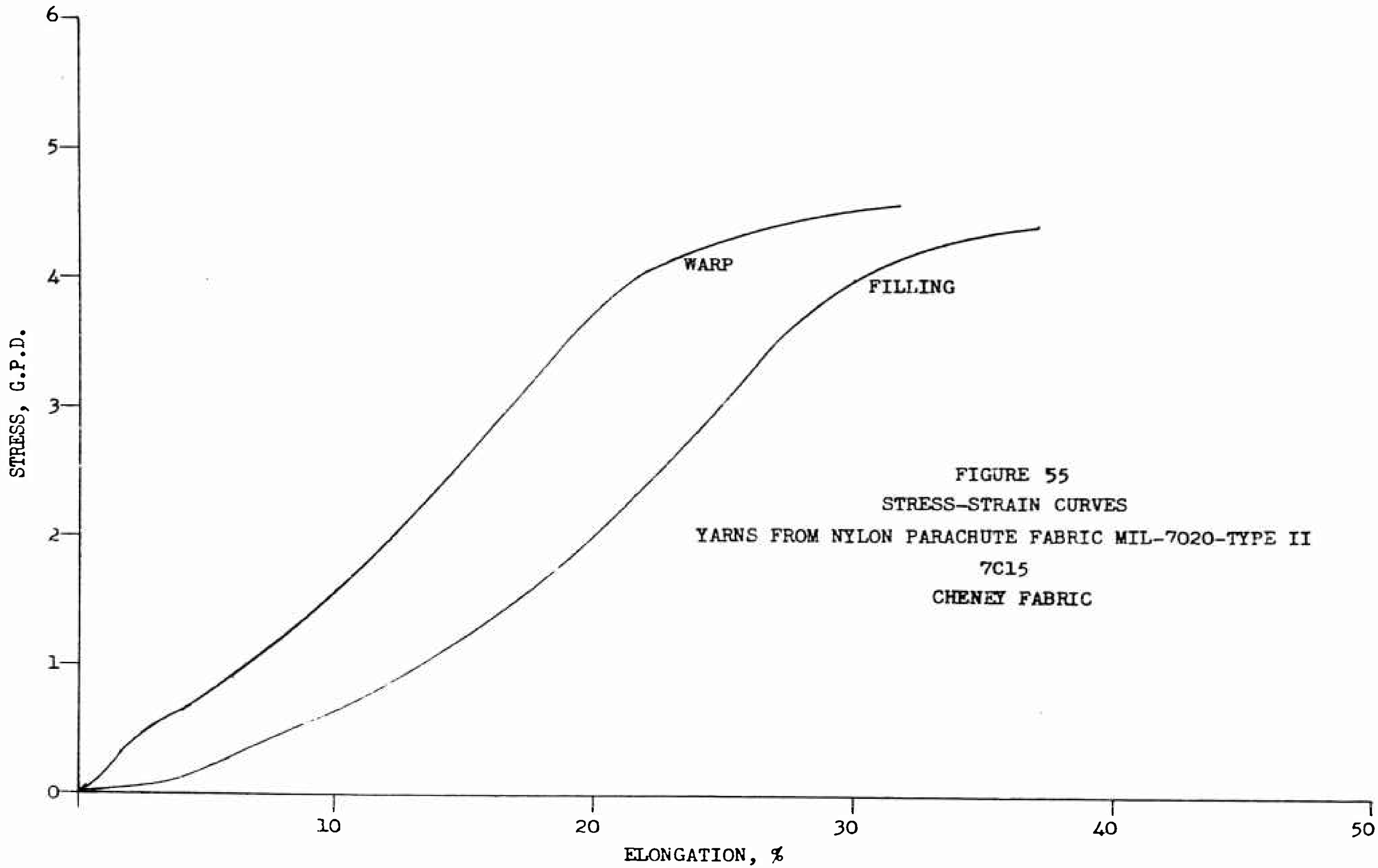

FIGURE 55
STRESS-STRAIN CURVES
YARNS FROM NYLON PARACHUTE FABRIC MIL-7020-TYPE II
7C15
CHENEY FABRIC

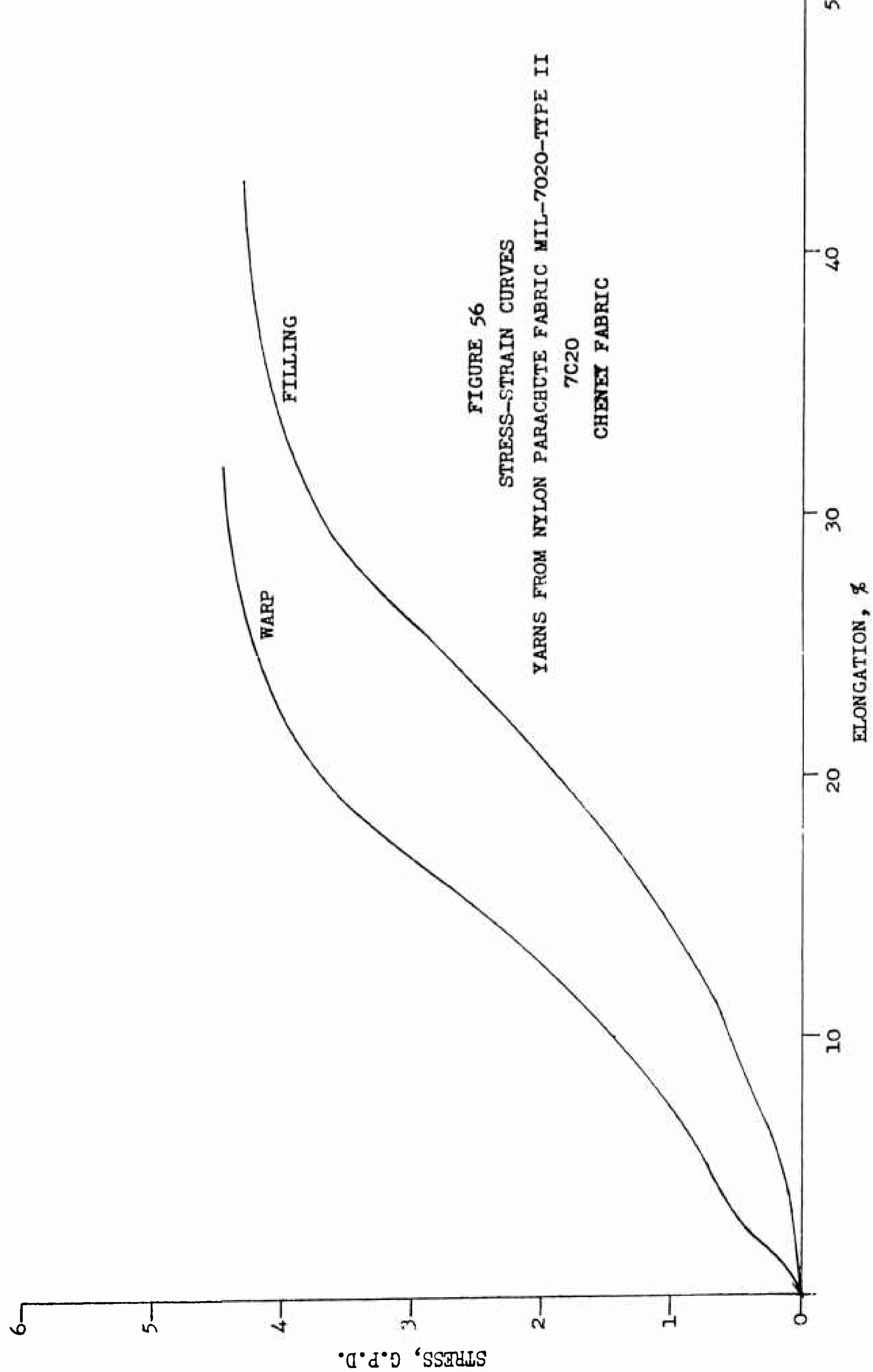

FIGURE 56
STRESS-STRAIN CURVES
YARNS FROM NYLON PARACHUTE FABRIC MIL-7020-TYPE II
7C20
CHENEY FABRIC

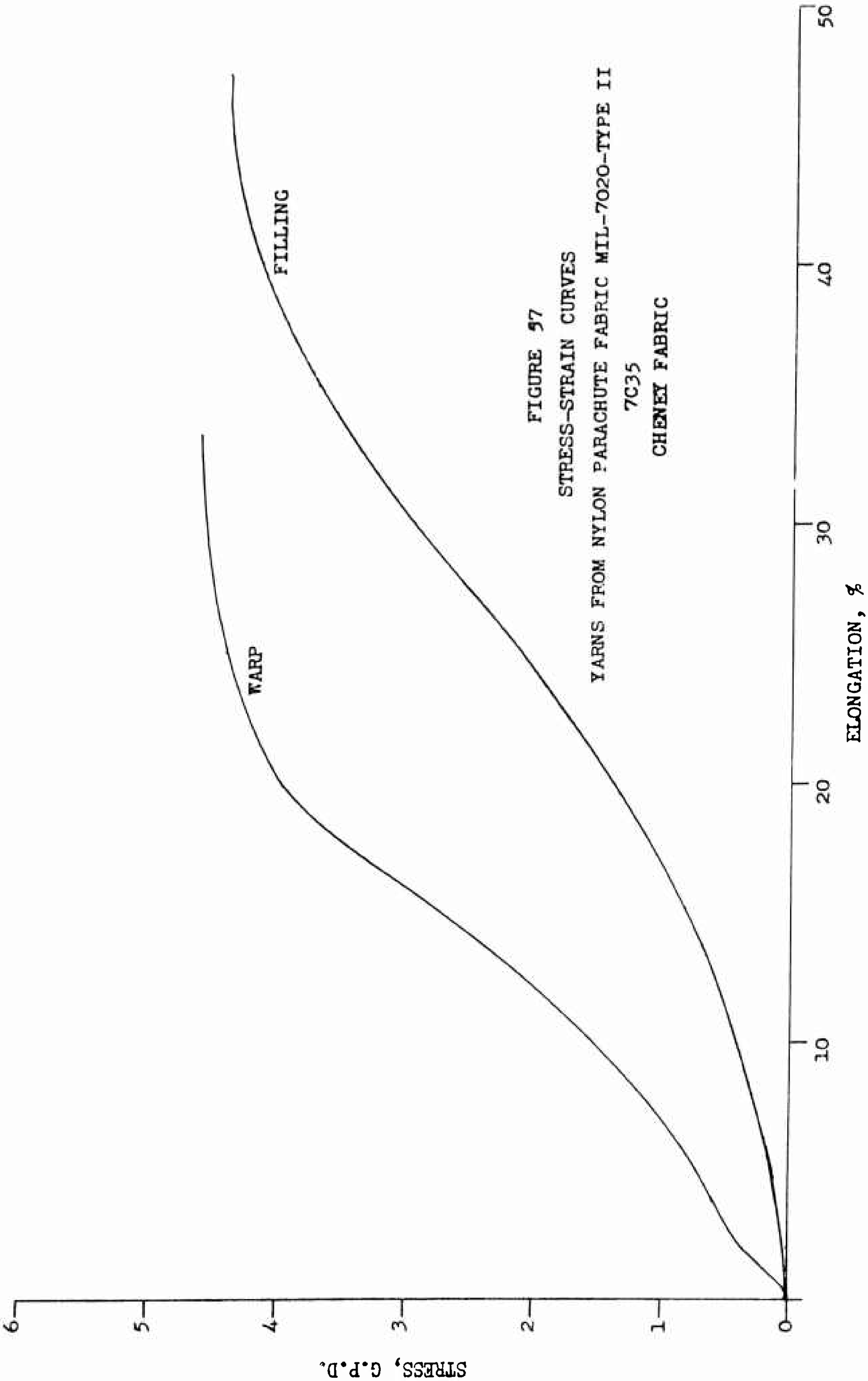

FIGURE 57
STRESS-STRAIN CURVES
YARNS FROM NYLON PARACHUTE FABRIC MIL-7020-TYPE II
7C35
CHENEY FABRIC

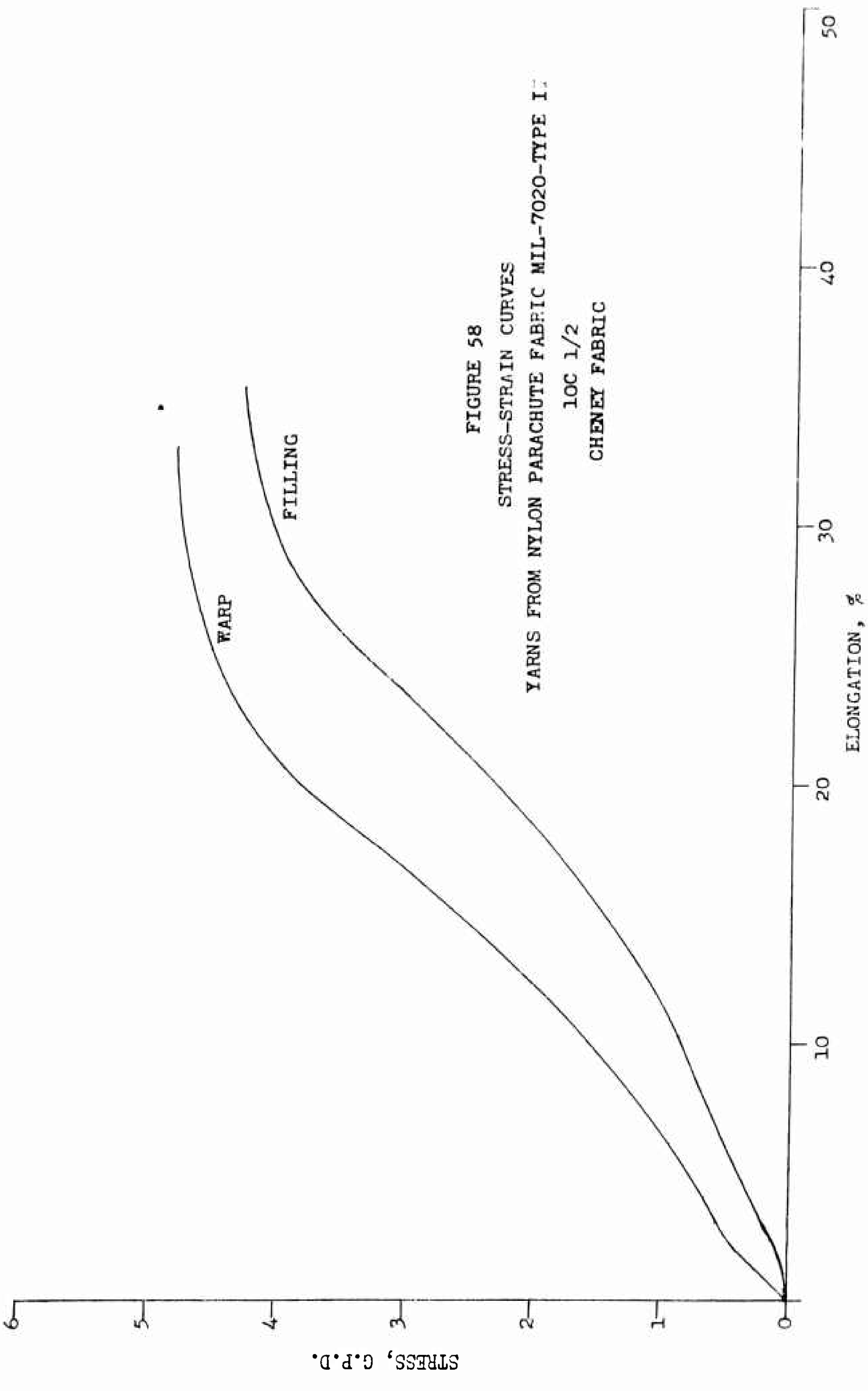

FIGURE 58
STRESS-STRAIN CURVES
YARNS FROM NYLON PARACHUTE FABRIC MIL-7020-TYPE I
10C 1/2
CHENEY FABRIC

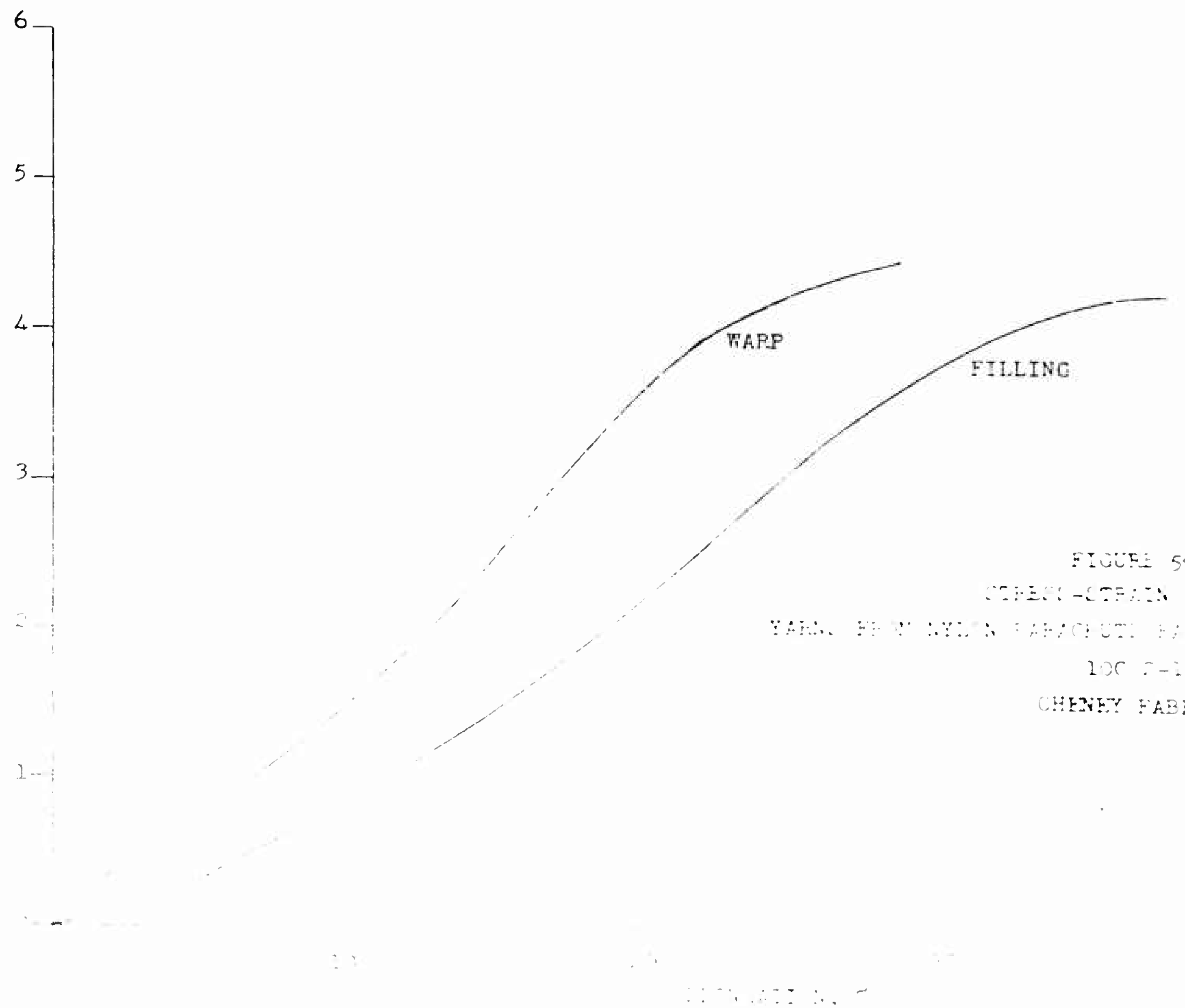

FIGURE 59
STRESS-STRAIN [illegible]
YARN FROM NYLON PARACHUTE FABRIC [illegible]
100 [illegible]
CHENEY FABRIC

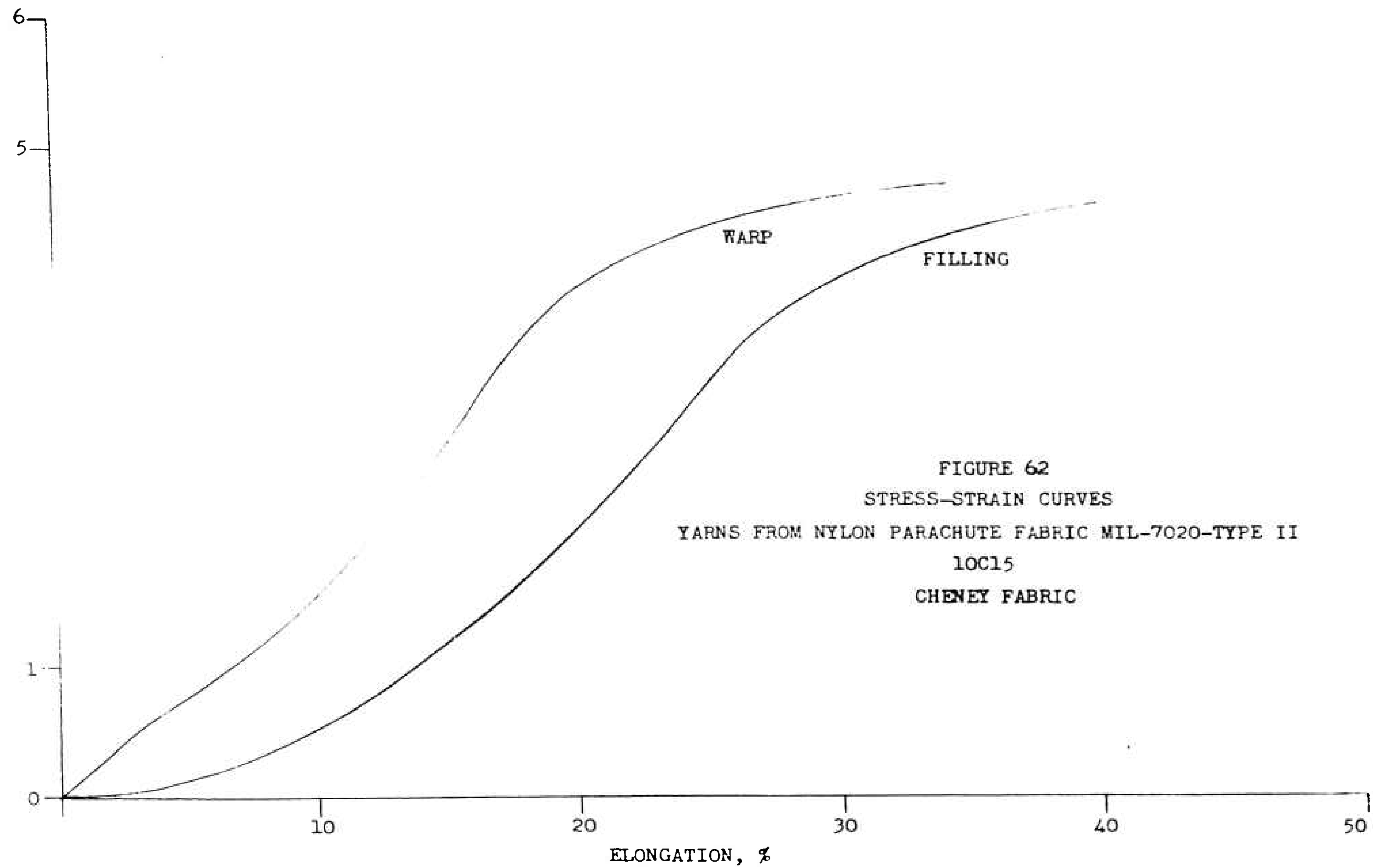

FIGURE 62

STRESS-STRAIN CURVES

YARNS FROM NYLON PARACHUTE FABRIC MIL-7020-TYPE II

10C15

CHENEY FABRIC

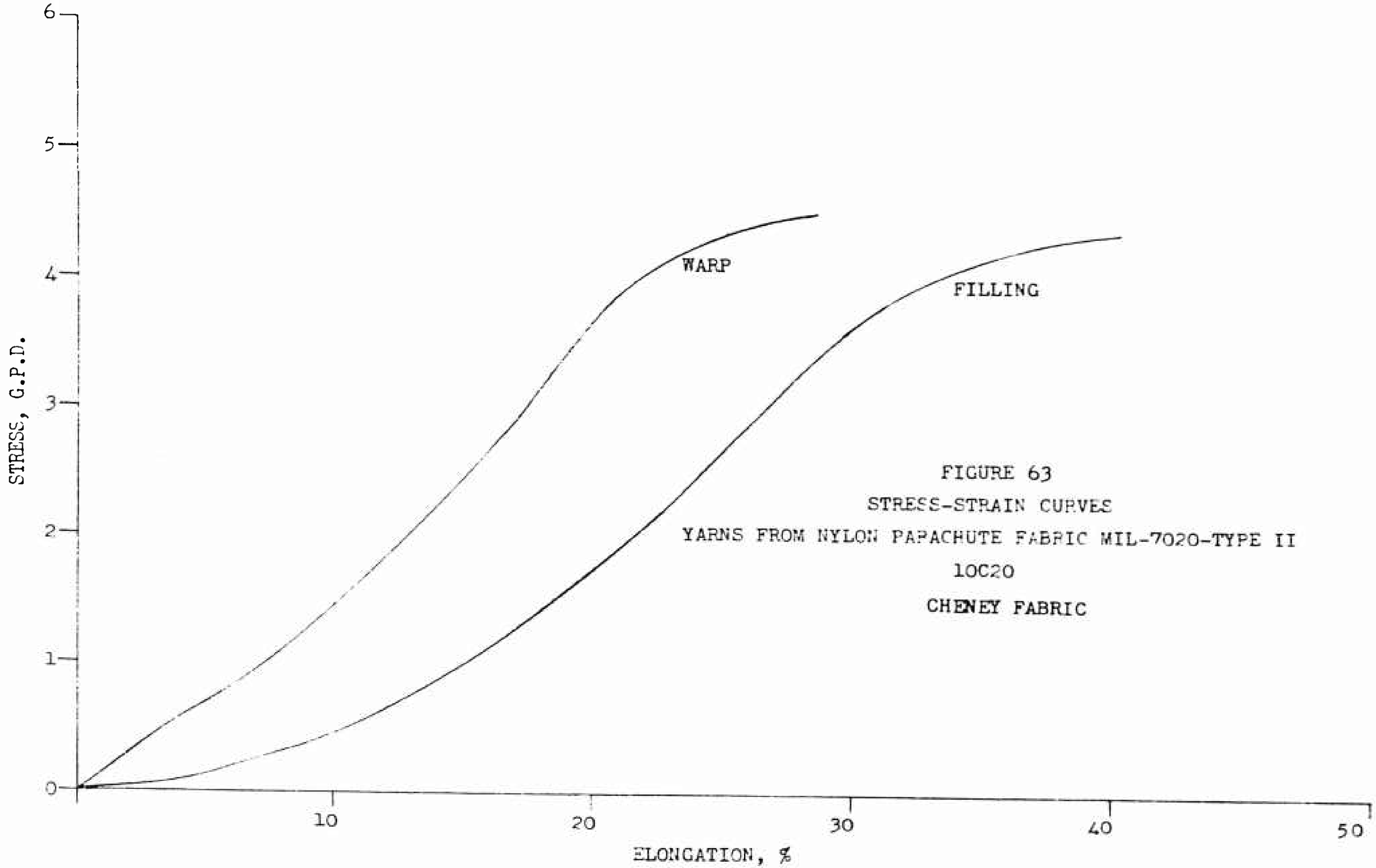

FIGURE 63
STRESS-STRAIN CURVES
YARNS FROM NYLON PARACHUTE FABRIC MIL-7020-TYPE II
10C20
CHENEY FABRIC

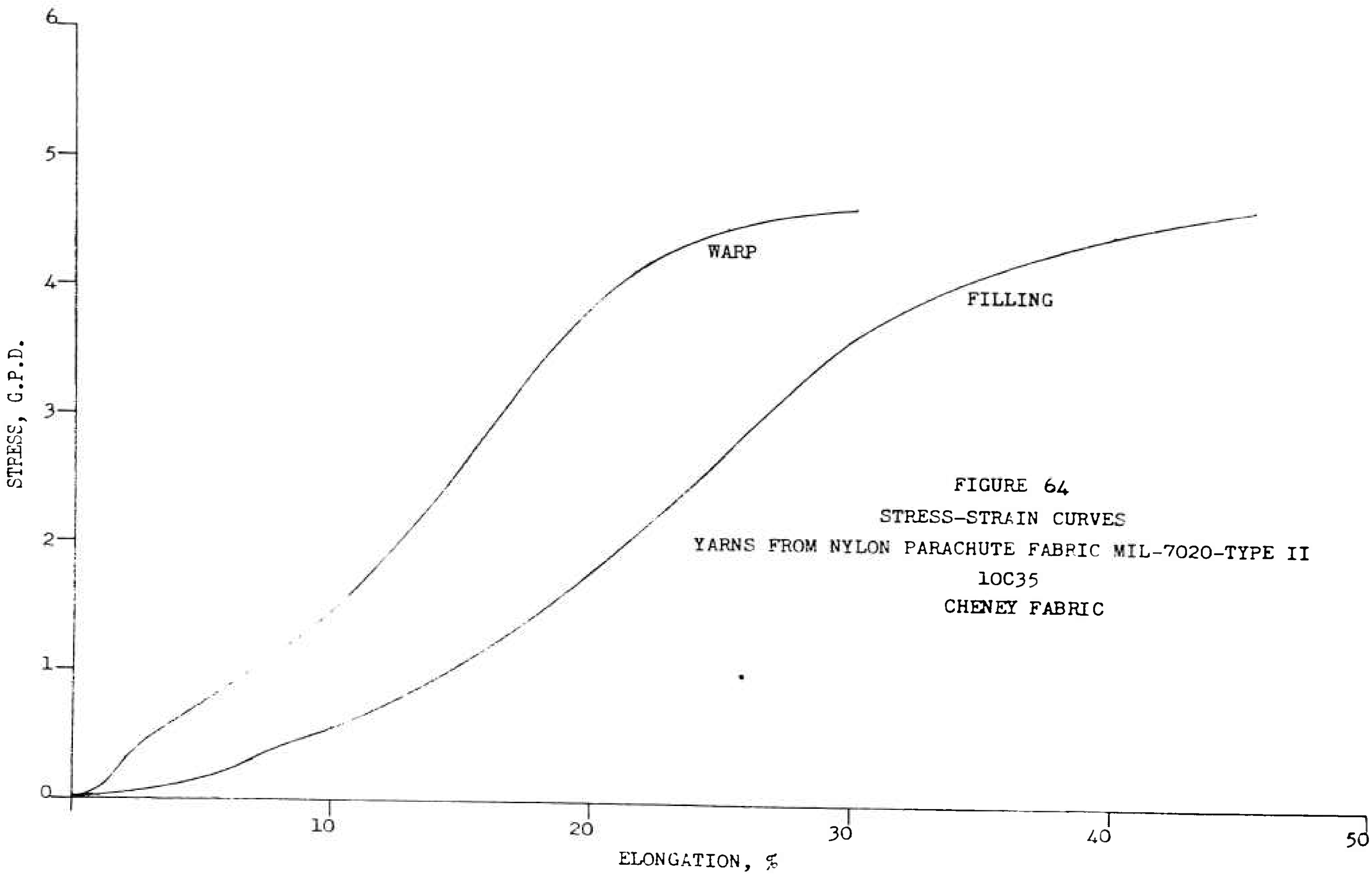

FIGURE 64
STRESS-STRAIN CURVES
YARNS FROM NYLON PARACHUTE FABRIC MIL-7020-TYPE II
10C35
CHENEY FABRIC

FIGURE 65

LOAD-ELONGATION CURVES OF TYPE I WARWICK FABRIC R 1/2 N 1/2

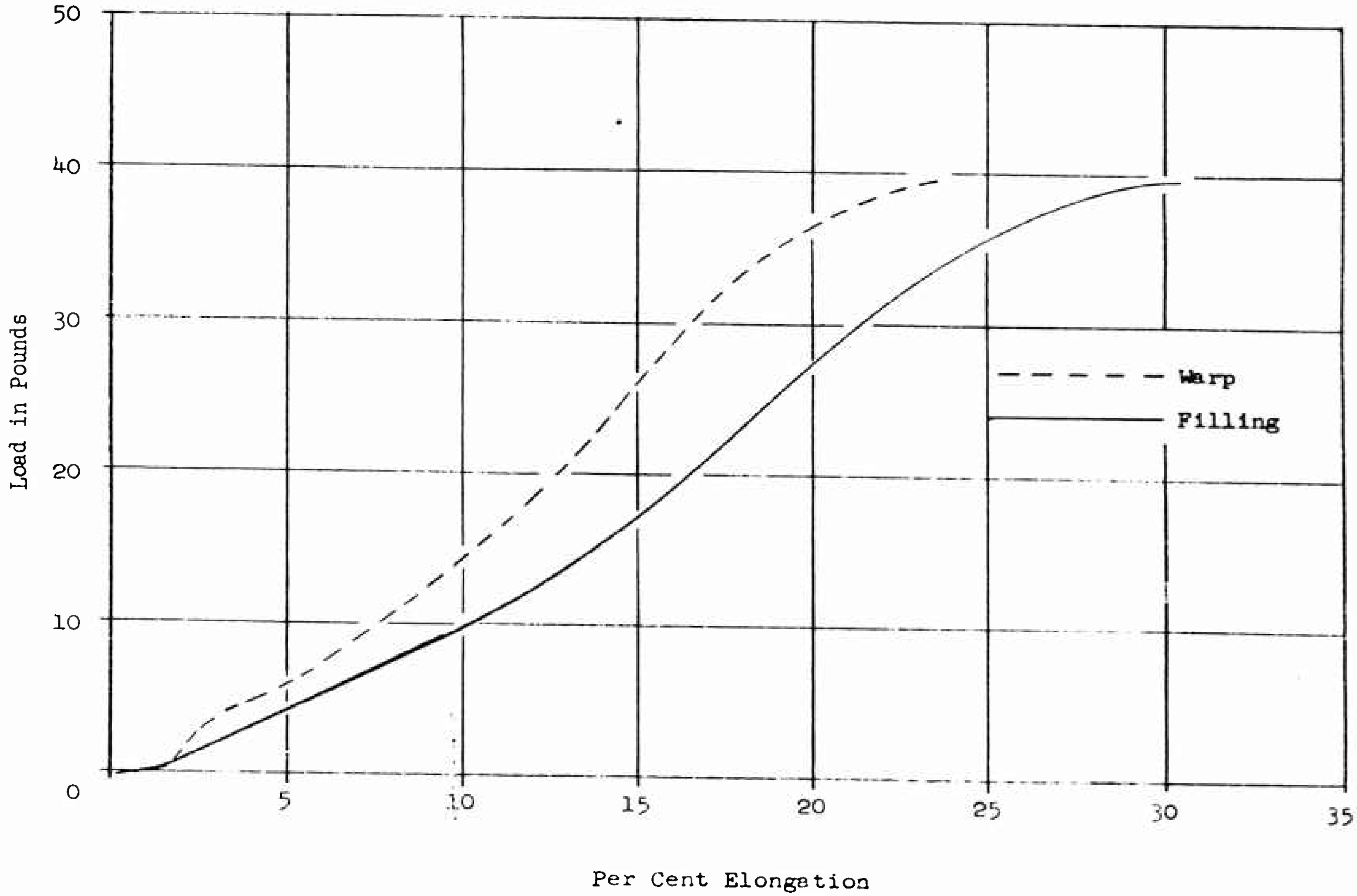

FIGURE 66

LOAD-ELONGATION CURVES OF TYPE I WARWICK FABRIC R5N 1/2

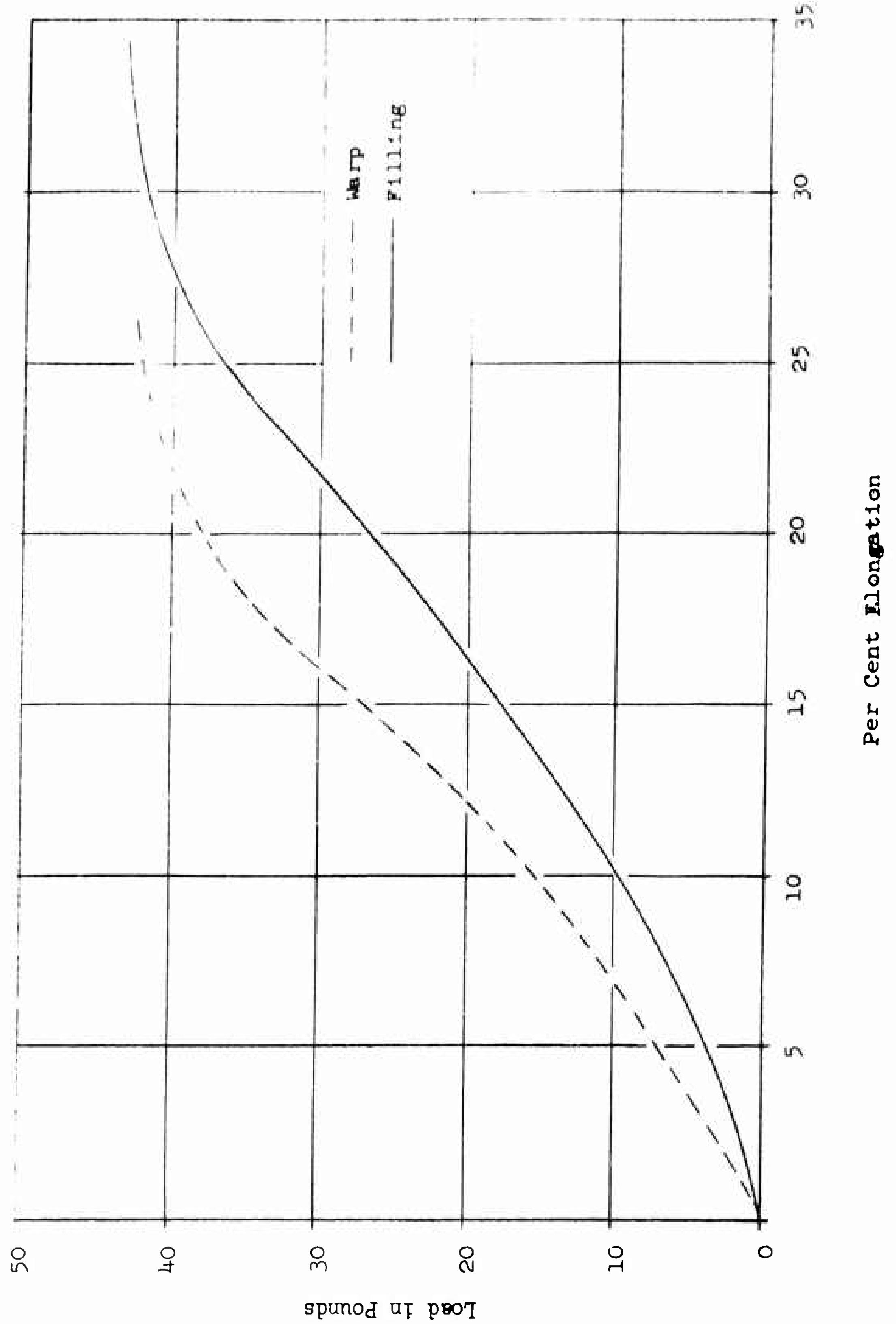

FIGURE 67

LOAD-ELONGATION CURVES OF TYPE I WARWICK FABRIC R5N5

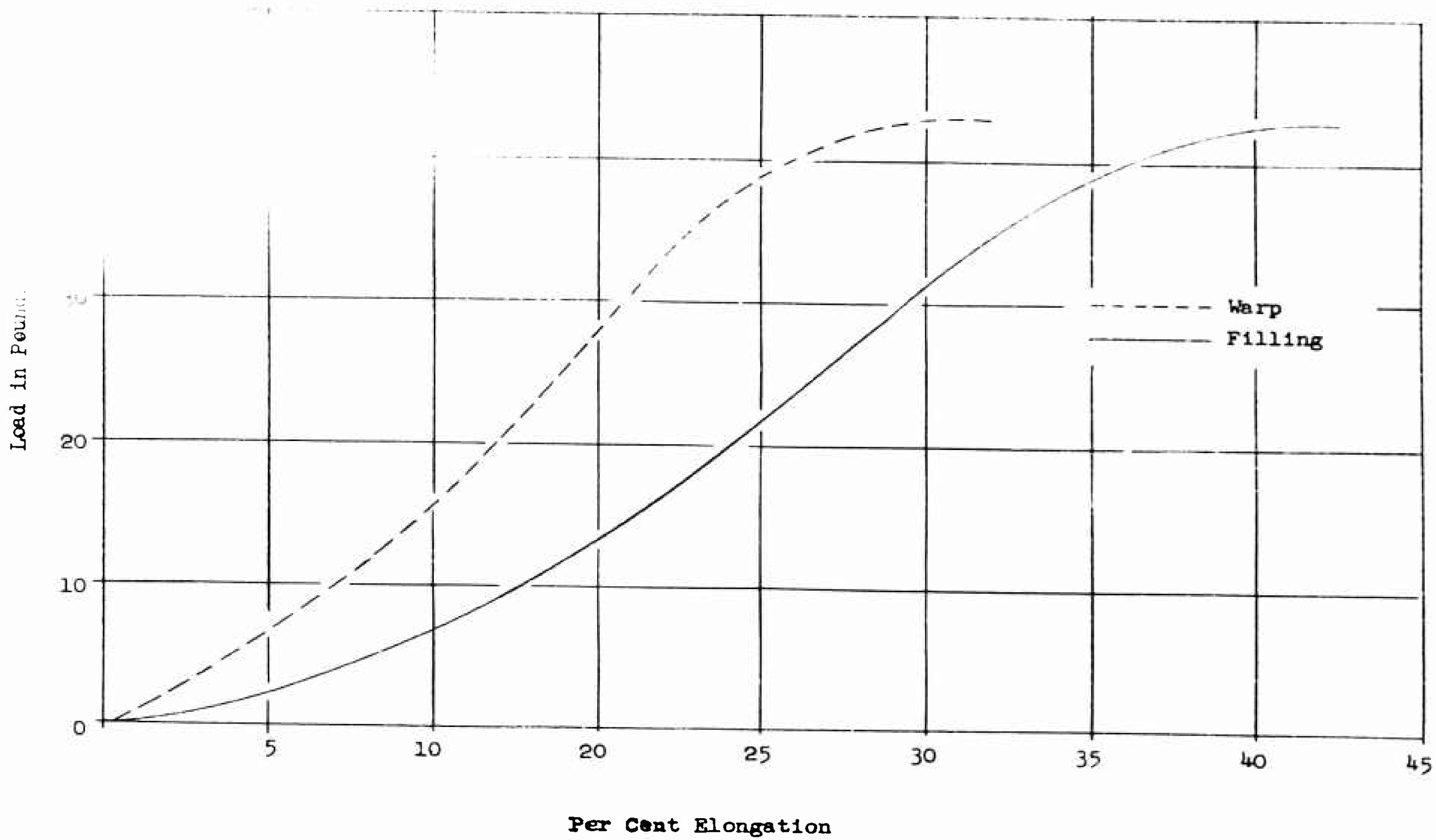

FIGURE 68

LOAD-ELONGATION CURVES OF TYPE I WARWICK FABRIC R20N 1/2

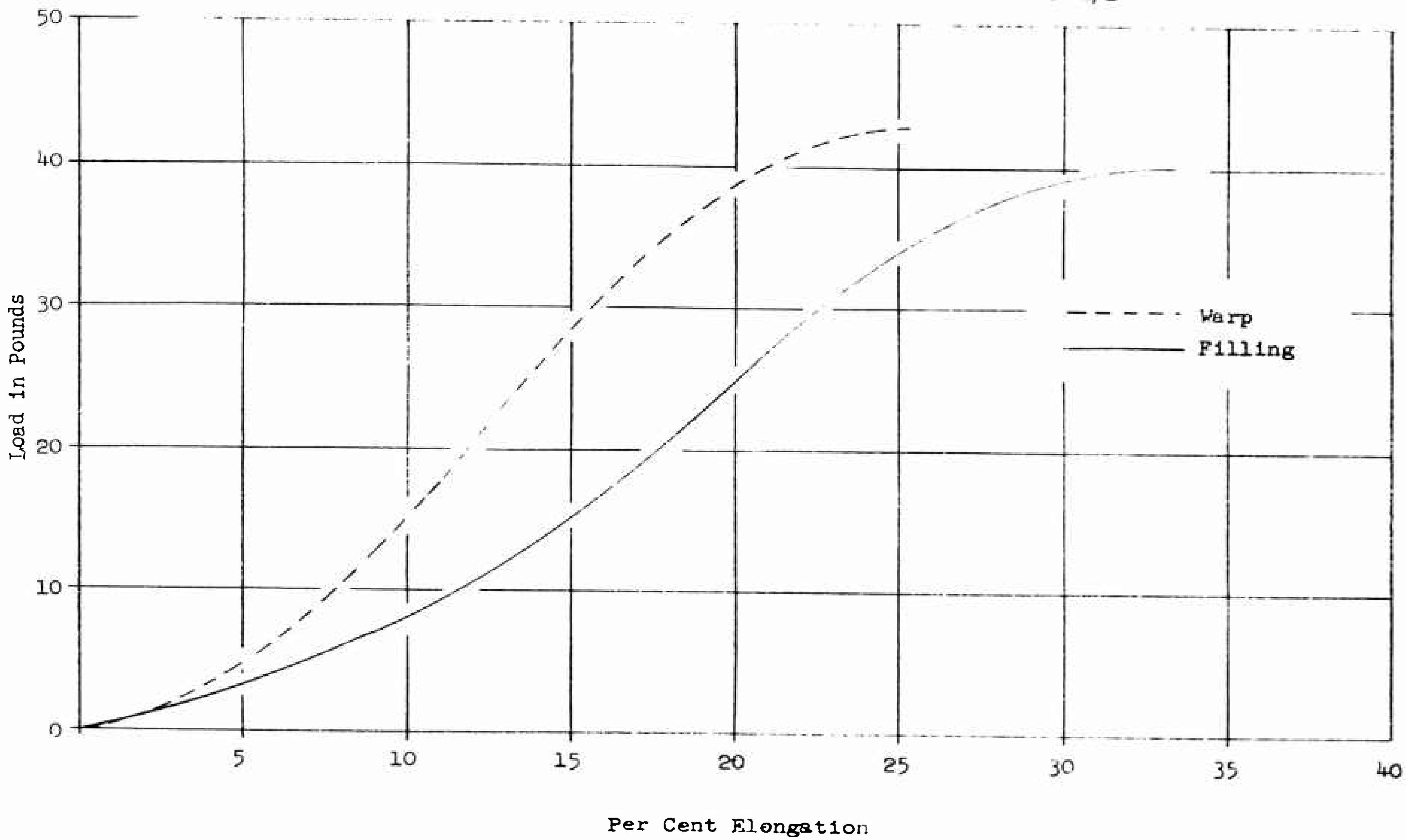

FIGURE 69

LOAD-ELONGATION CURVES OF TYPE I WARWICK FABRIC R20W20

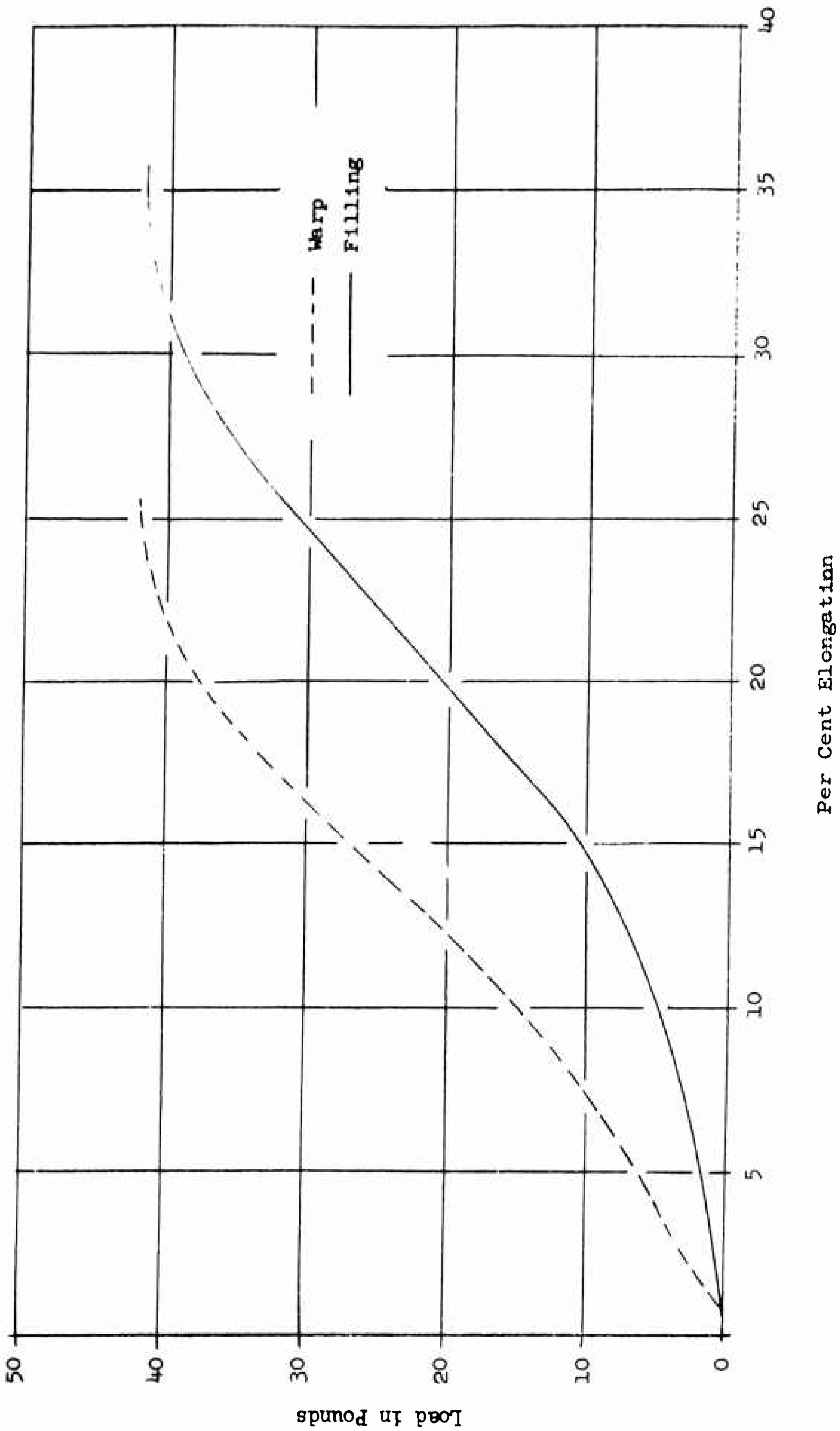

FIGURE 70

LOAD-ELONGATION CURVES OF TYPE I WARWICK FABRIC R30N 1/2

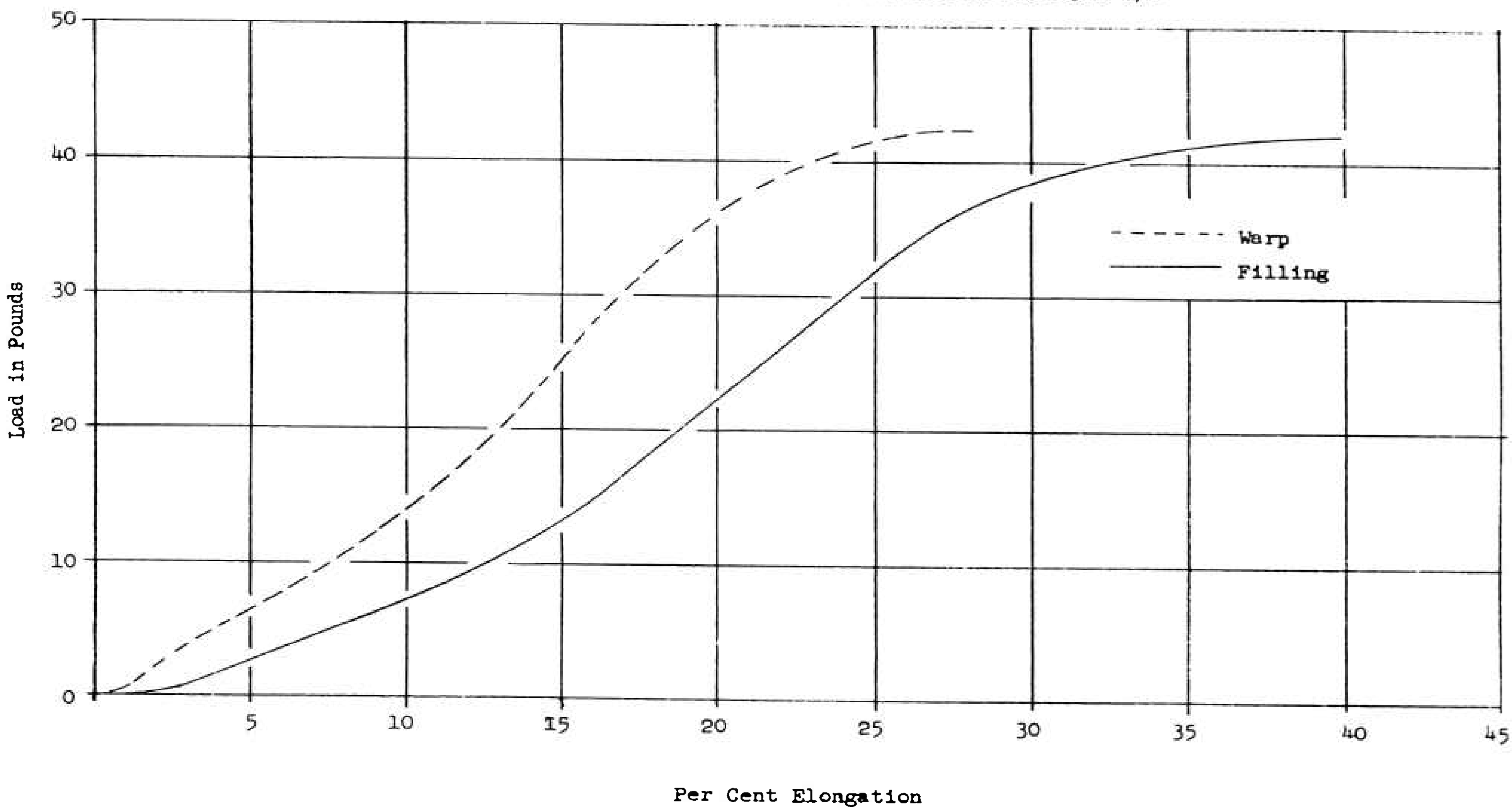

FIGURE 71

LOAD-ELONGATION CURVES OF TYPE I WARWICK FABRIC R30N5

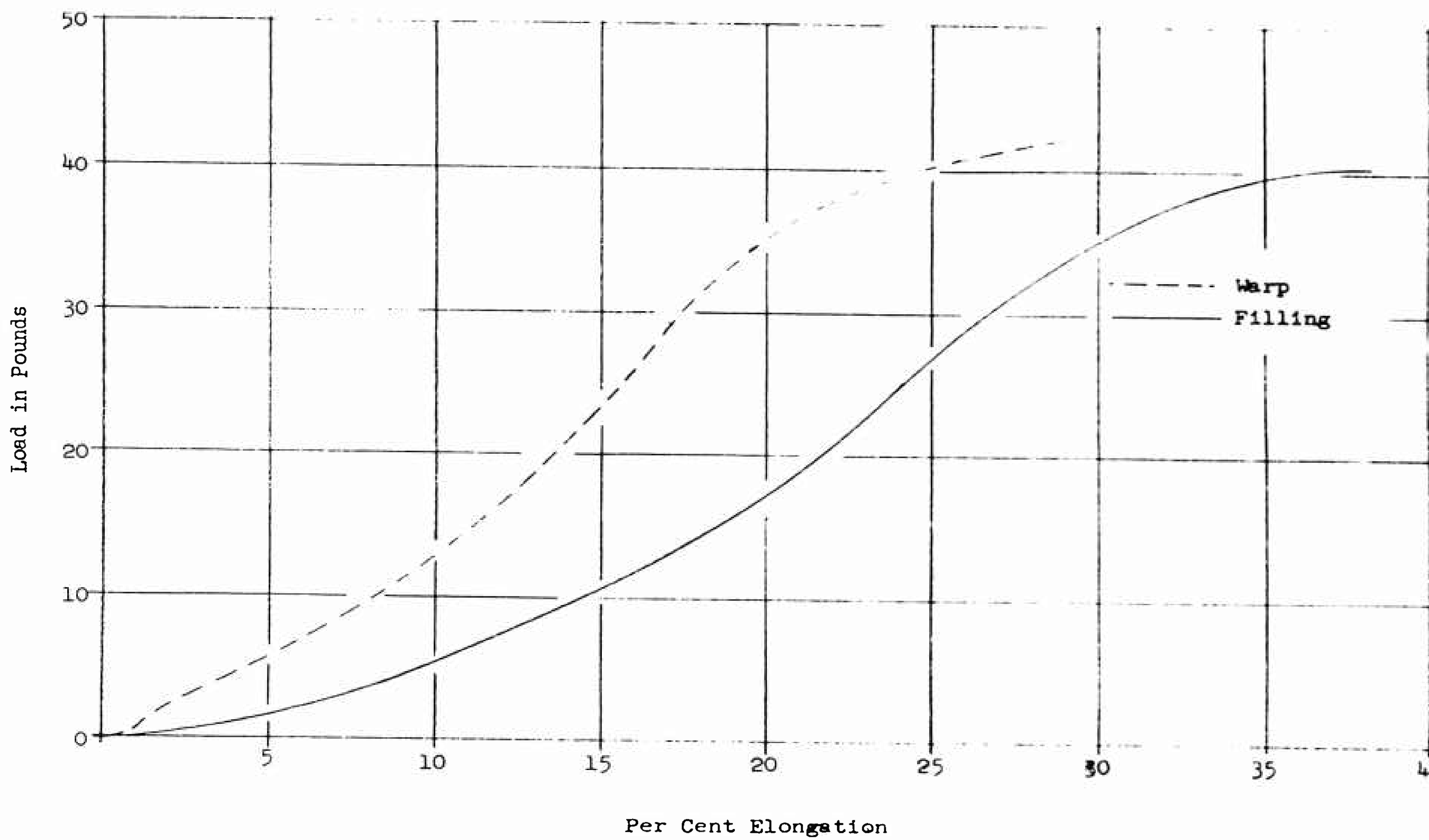

FIGURE 72

LOAD-ELONGATION CURVES OF TYPE I WARWICK FABRIC R30N10

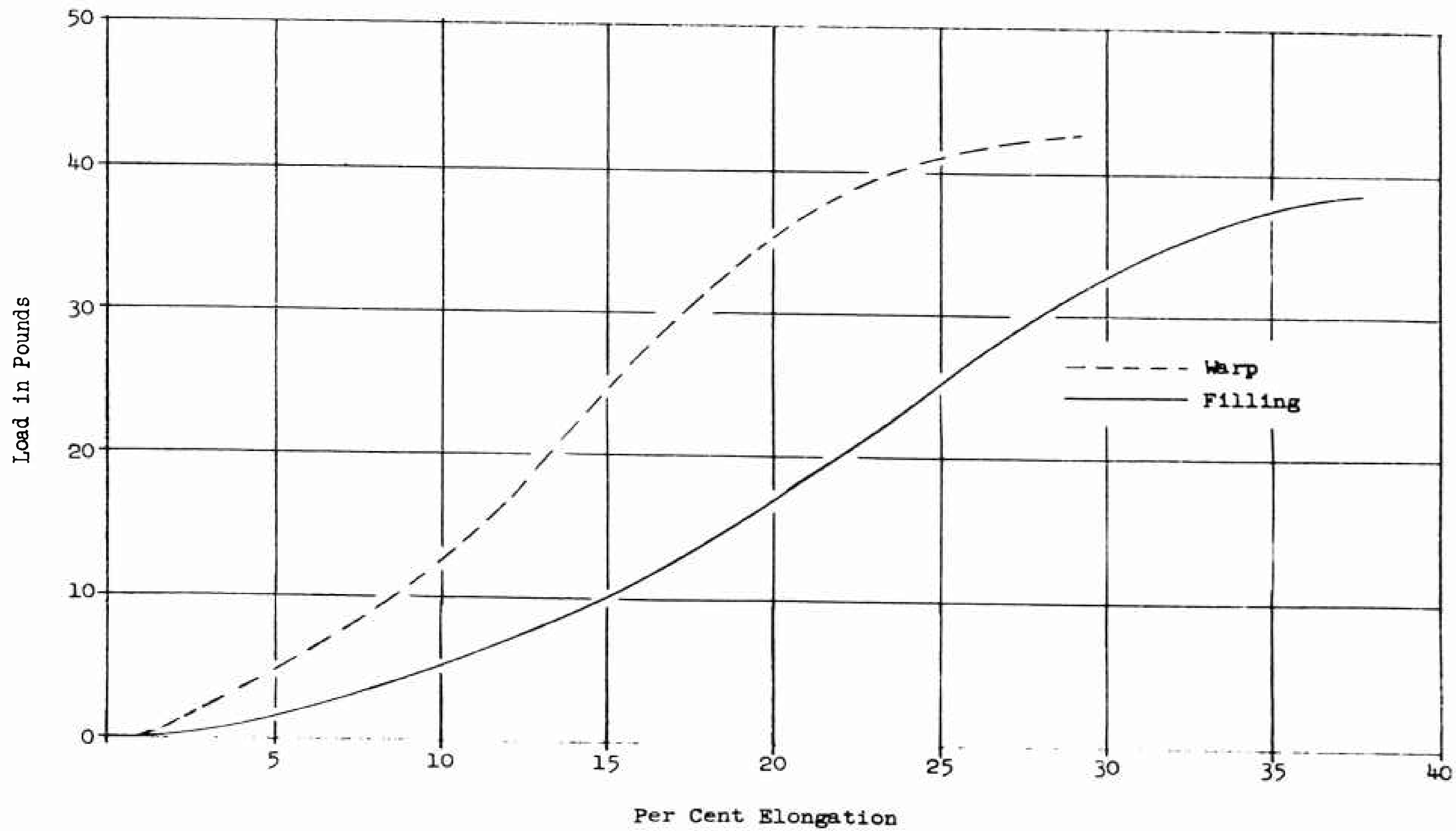

FIGURE 73

LOAD-ELONGATION CURVES OF TYPE I WARWICK FABRIC R30N20

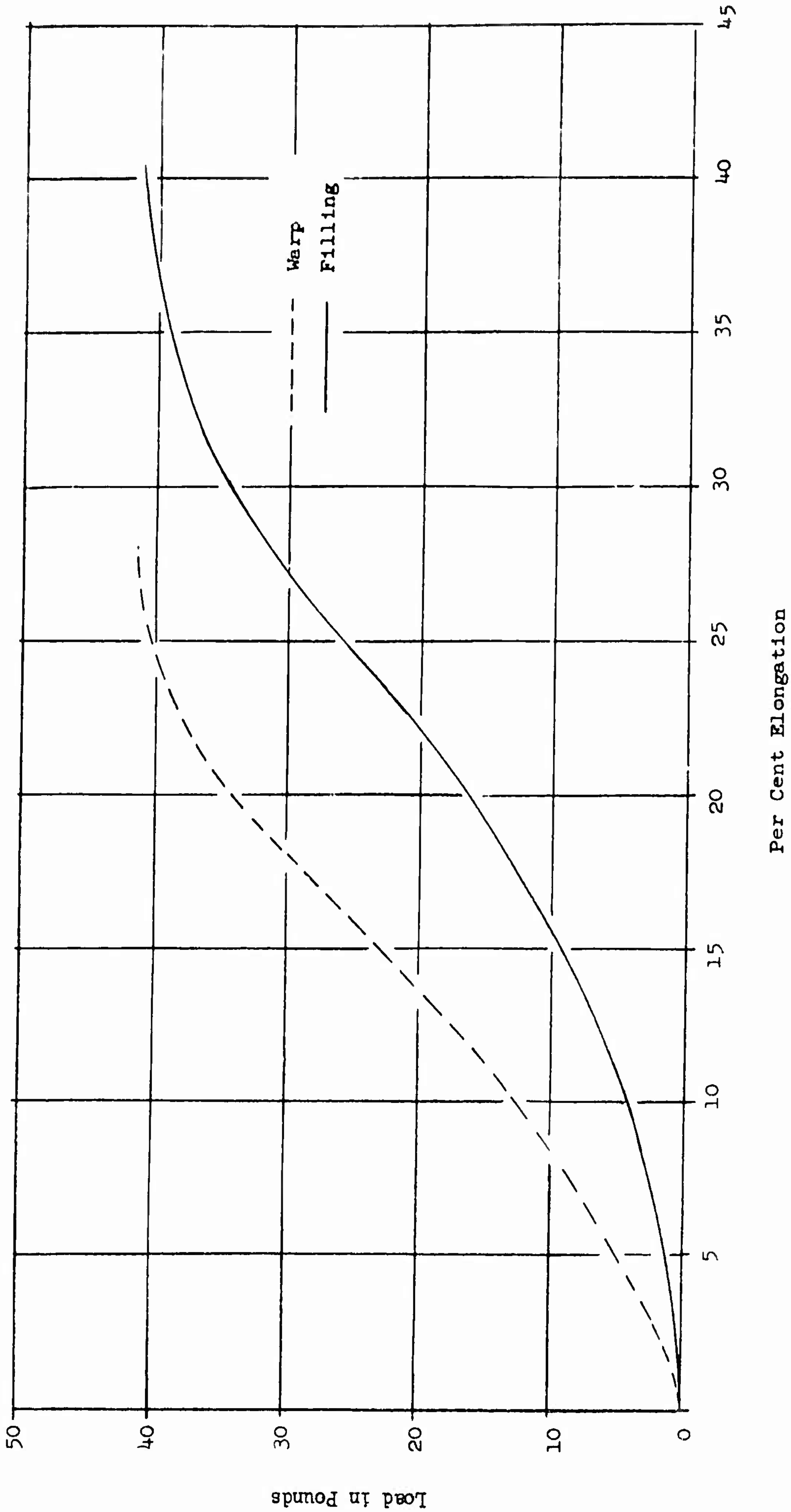

FIGURE 74

LOAD-ELONGATION CURVES OF TYPE I WARWICK FABRIC R30N30

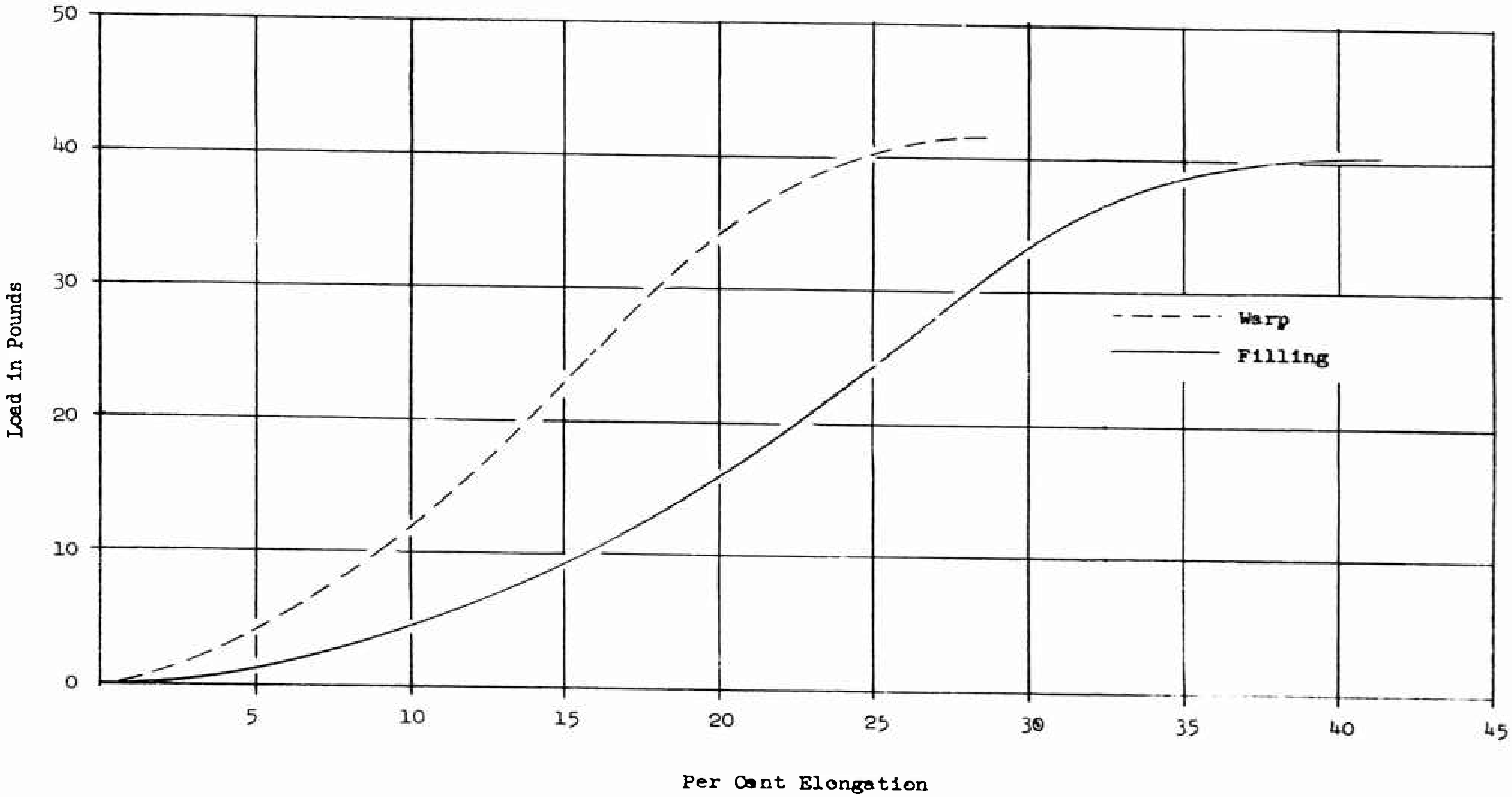

FIGURE 75

DIAGRAMMATIC DEPICTION OF REPEATED STRESS CURVES

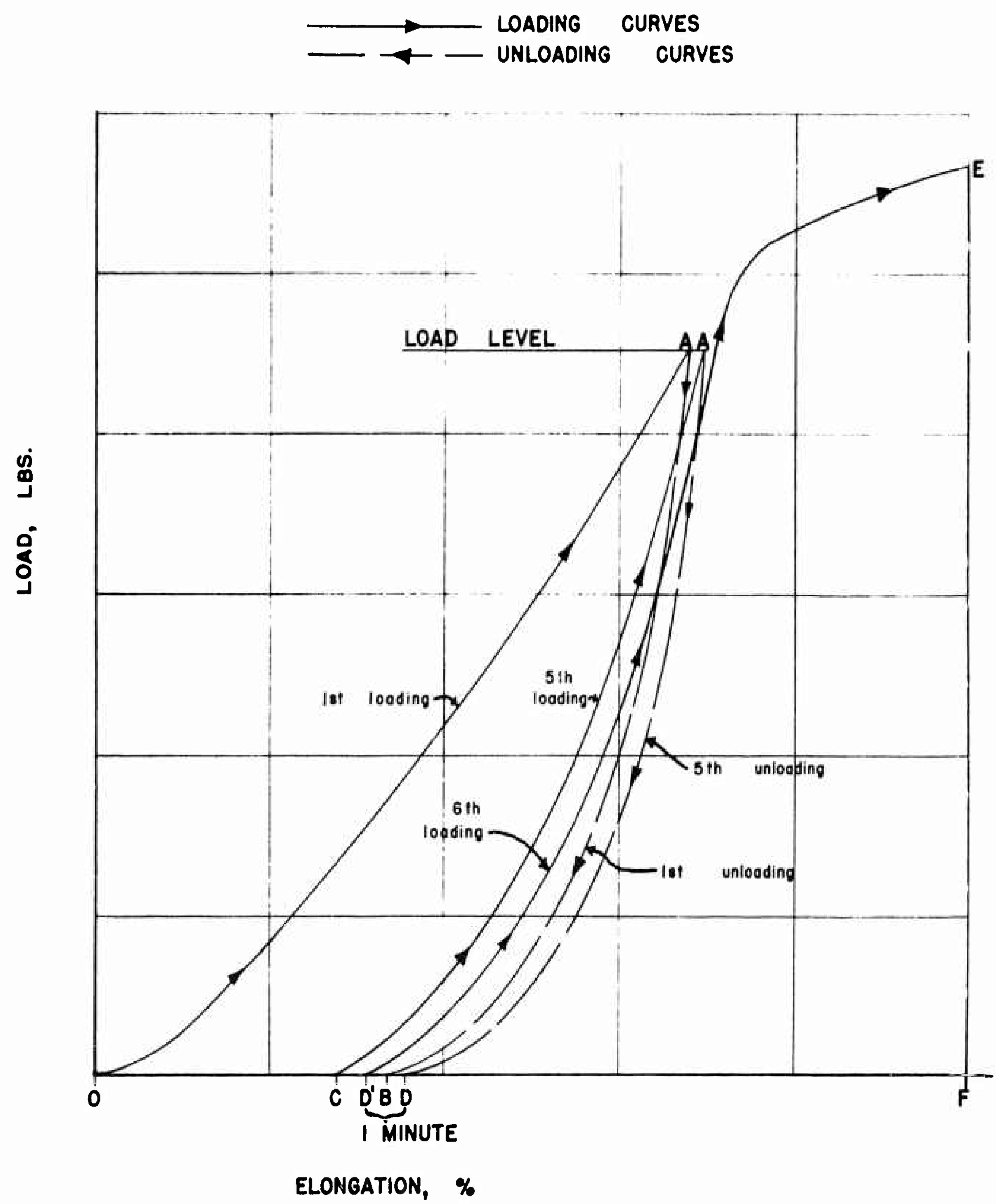

FIGURE 76

SECONDARY CREEP (FILLING) VS FILLING YARN TWIST

TYPE II, CHENEY FABRICS

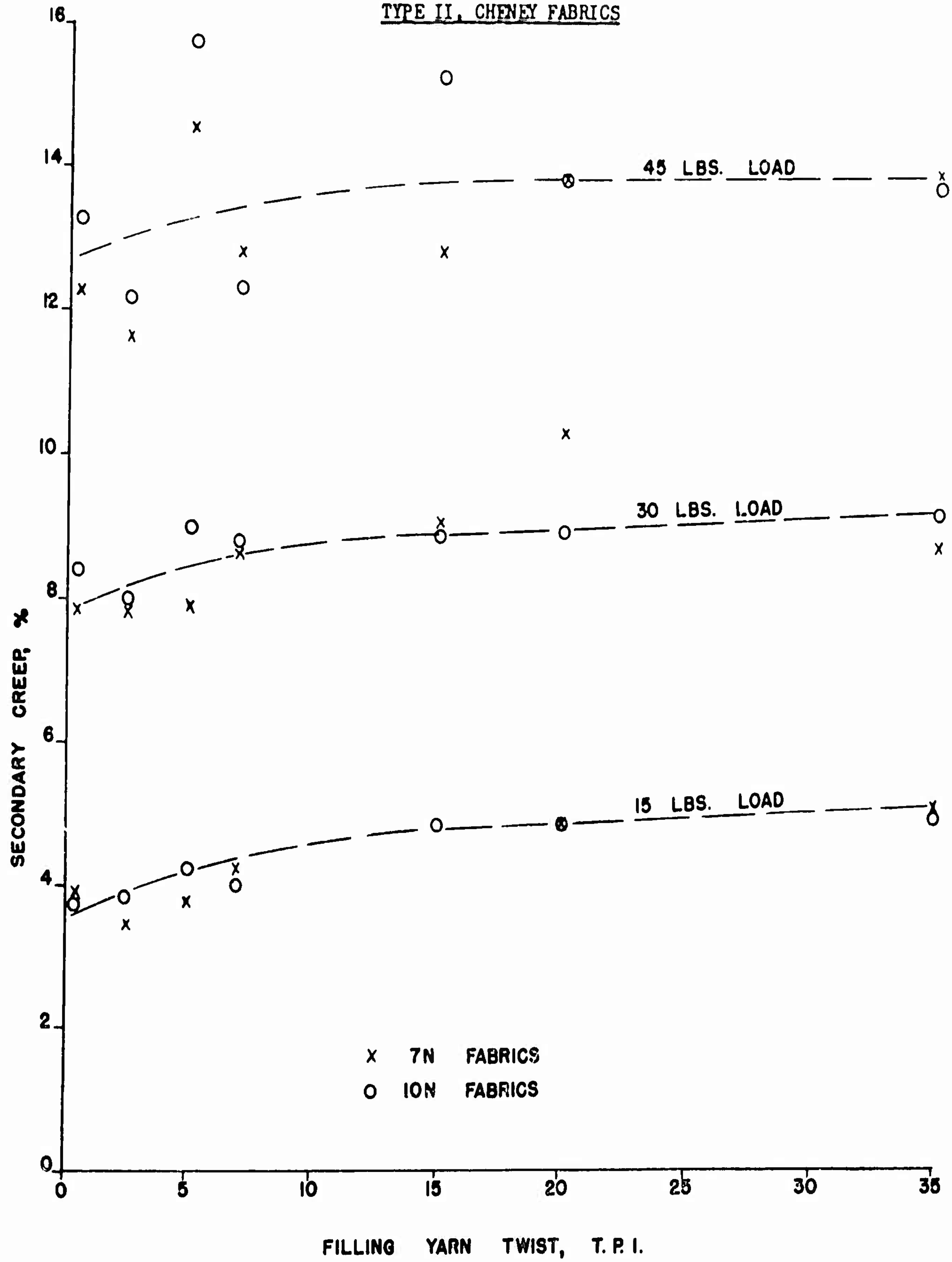

FIGURE 77

TYPICAL REPEATED STRESS-STRAIN CURVES SHOWING 1st & 5th CYCLES TO 1st LOAD LEVEL AND FINAL RUPTURE CYCLE

CHENEY

FABRIC 7N 1/2, WARP

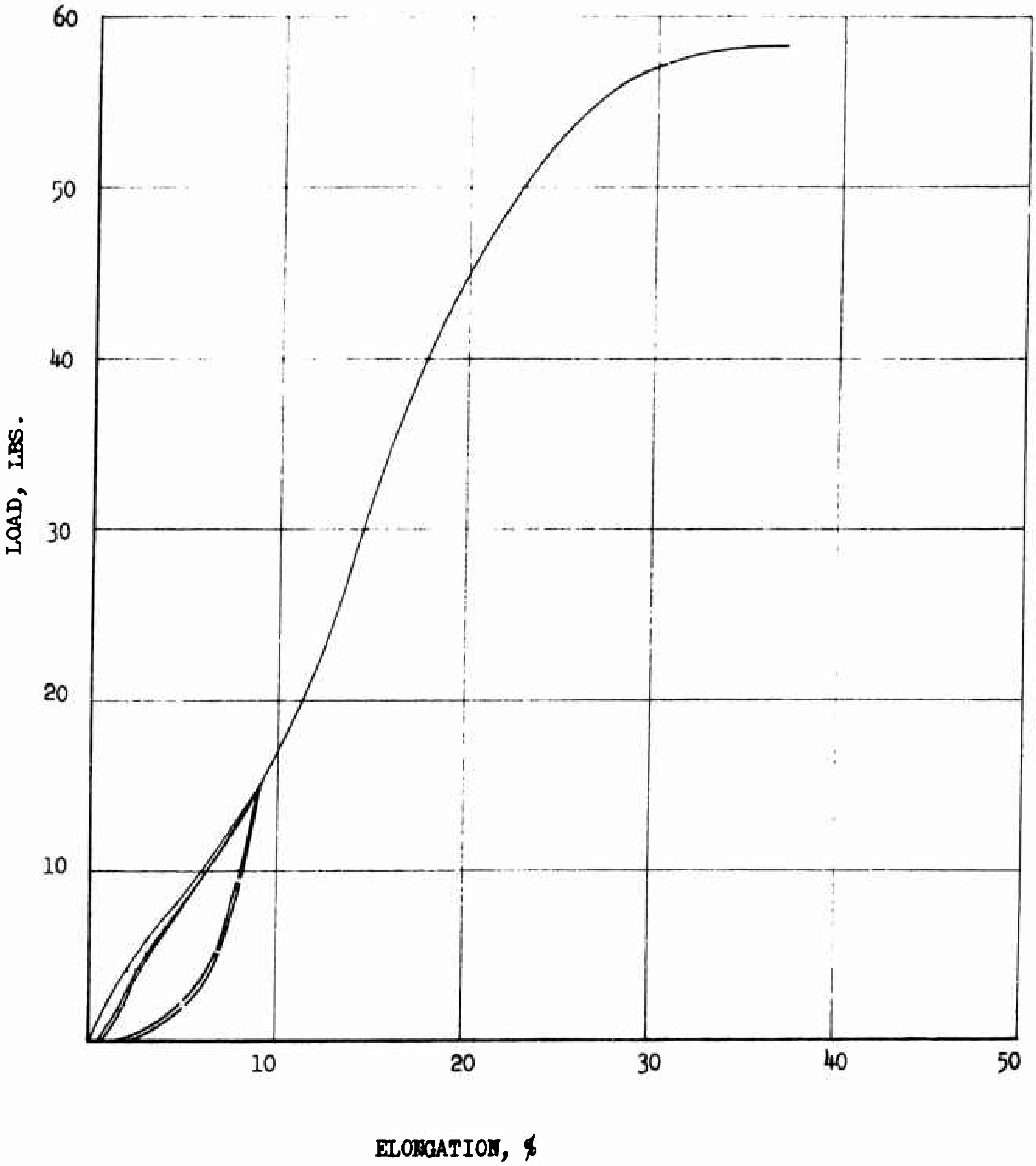

FIGURE 78

TYPICAL REPEATED STRESS-STRAIN CURVES SHOWING 1st & 5th CYCLES TO 1st LOAD LEVEL AND FINAL RUPTURE CYCLE

CHENEY

FABRIC 7N 1/2, FILLING

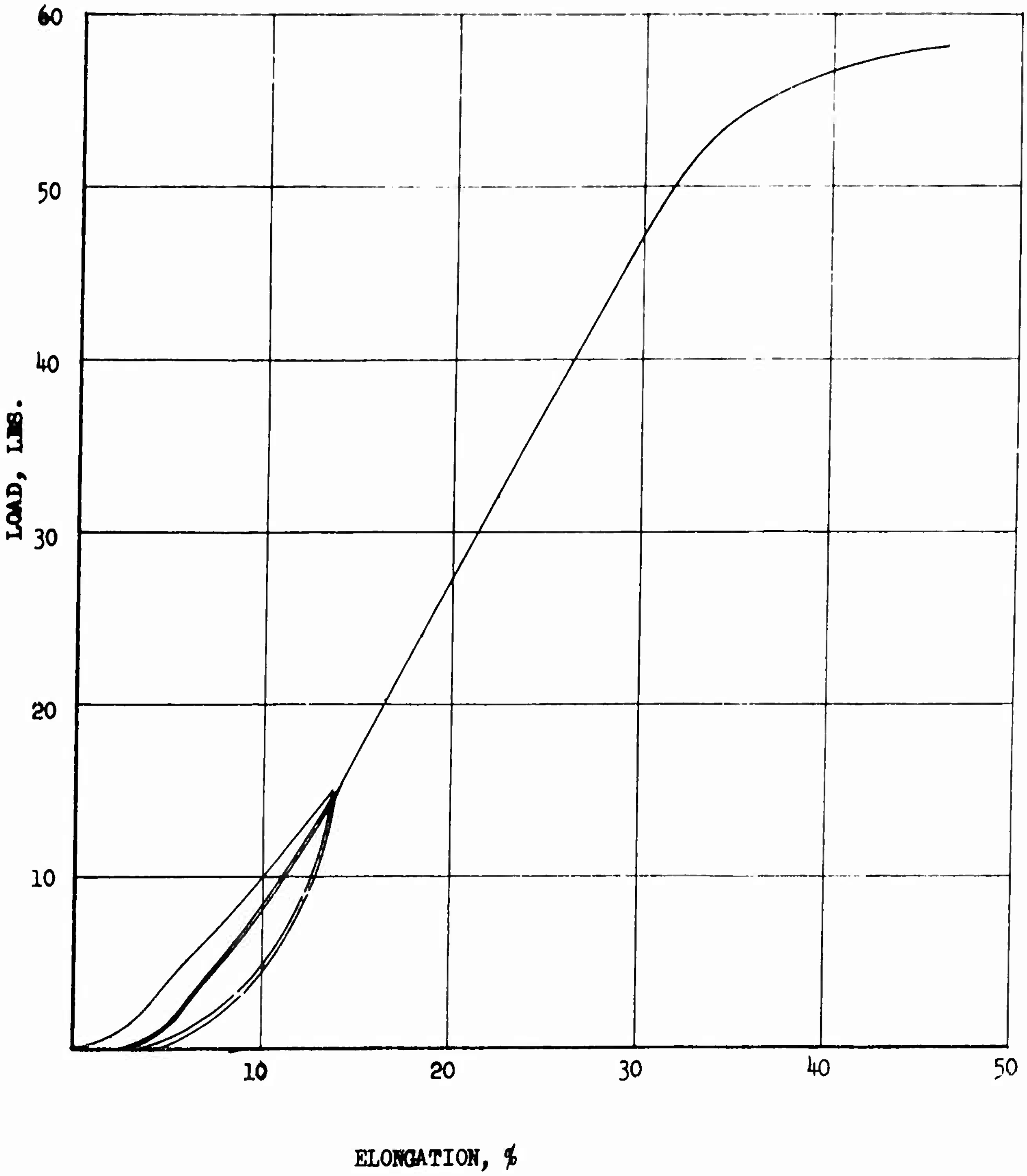

FIGURE 79

TYPICAL REPEATED STRESS-STRAIN CURVES SHOWING 1st & 5th CYCLES TO 2nd LOAD LEVEL AND FINAL RUPTURE CYCLE

CHENEY

FABRIC 7N 1/2, WARP

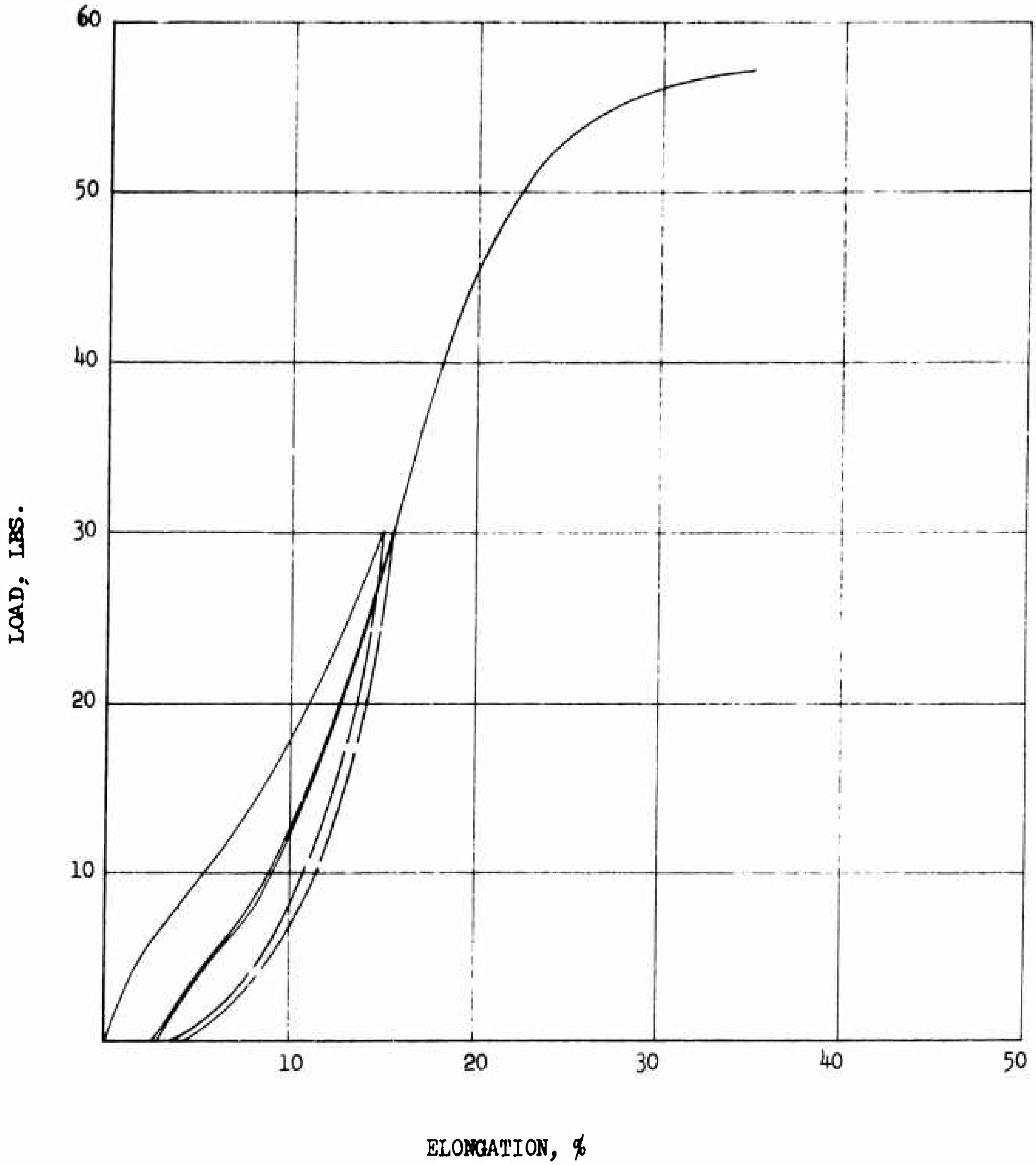

FIGURE 80

TYPICAL REPEATED STRESS-STRAIN CURVES SHOWING 1st & 5th CYCLES TO 2nd LOAD LEVEL AND FINAL RUPTURE CYCLE

CHENEY

FABRIC 7N 1/2, FILLING

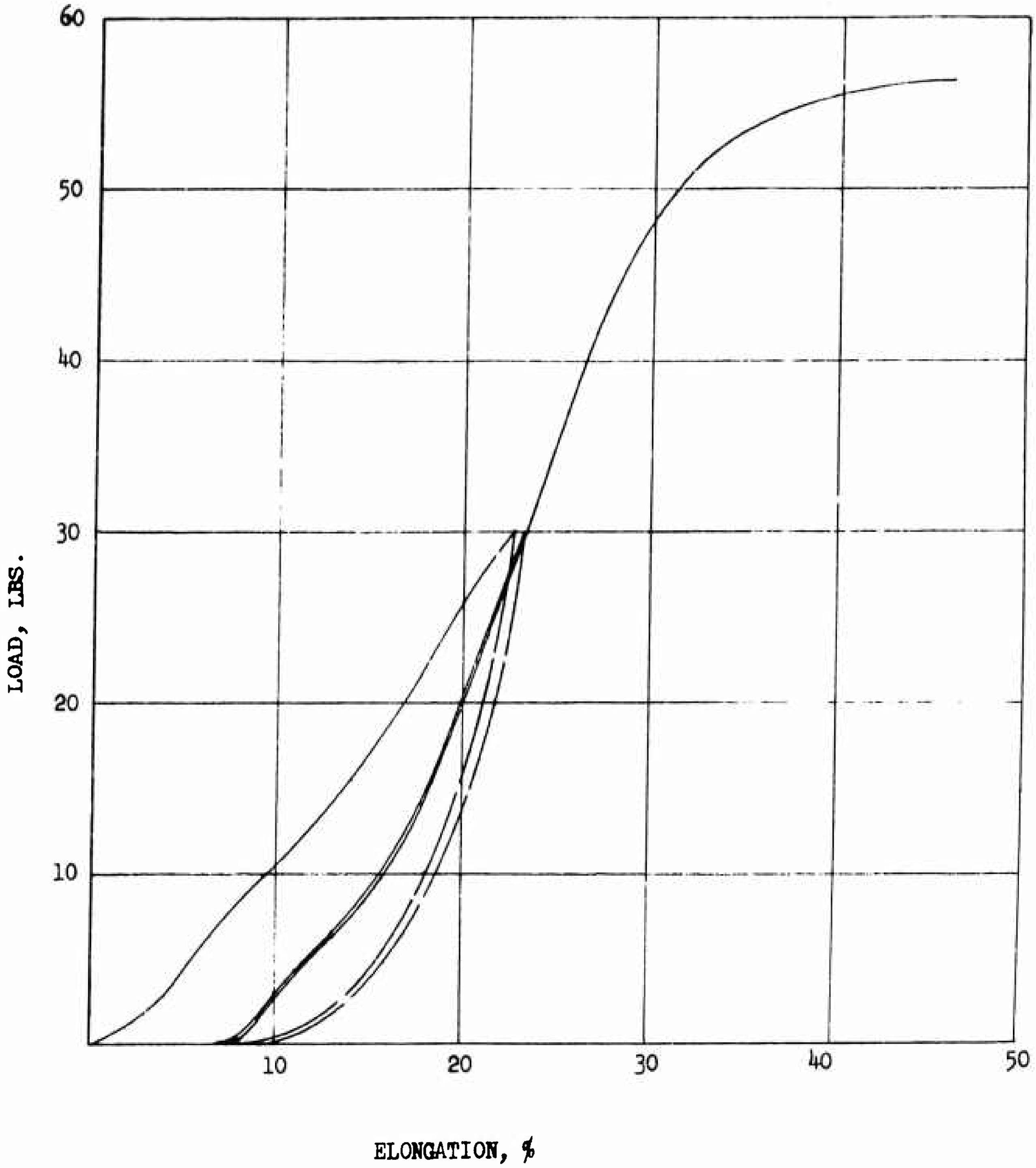

FIGURE 81

TYPICAL REPEATED STRESS-STRAIN CURVES SHOWING 1st & 5th CYCLES TO 3rd LOAD LEVEL AND FINAL RUPTURE CYCLE

CHENEY

FABRIC 7N 1/2, WARP

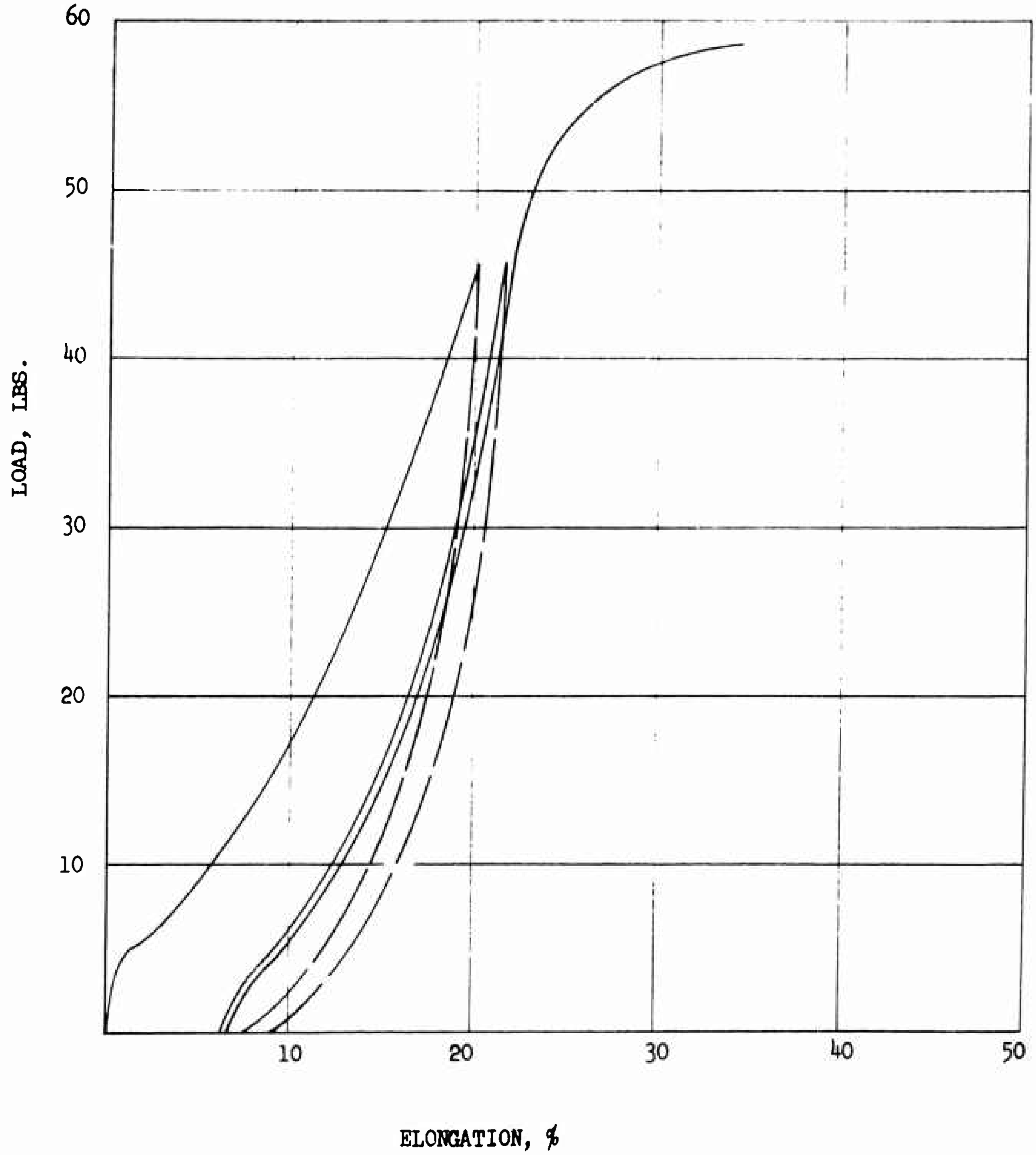

FIGURE 82

TYPICAL REPEATED STRESS-STRAIN CURVES SHOWING 1st & 5th CYCLES TO
3rd LOAD LEVEL AND FINAL RUPTURE CYCLE
CHENEY

FABRIC 7N 1/2, FILLING

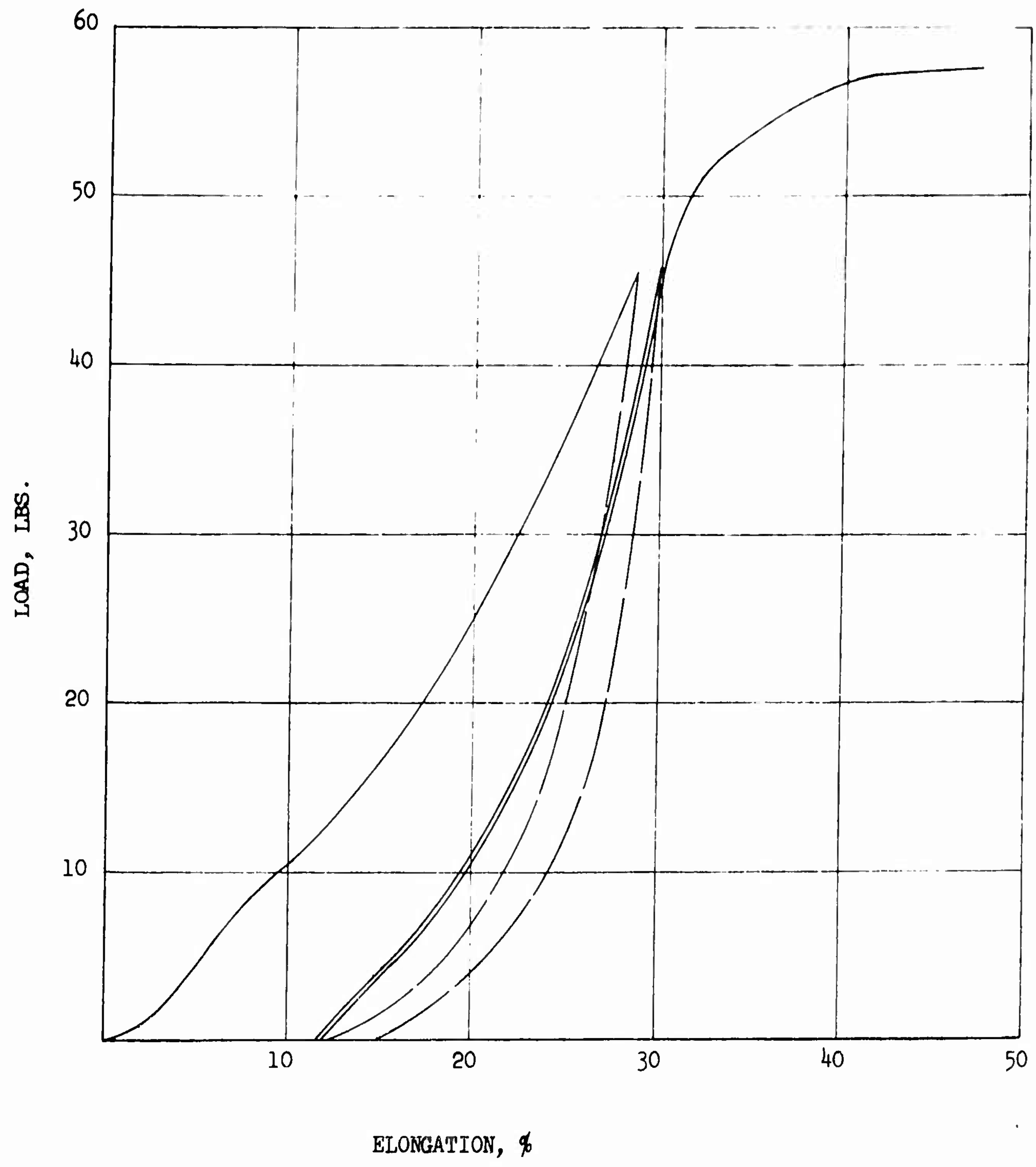

FIGURE 83

TYPICAL REPEATED STRESS-STRAIN CURVES SHOWING 1st & 5th CYCLES TO 1st LOAD LEVEL AND FINAL RUPTURE CYCLE

CHENEY

FABRIC 7N 2 1/2, WARP

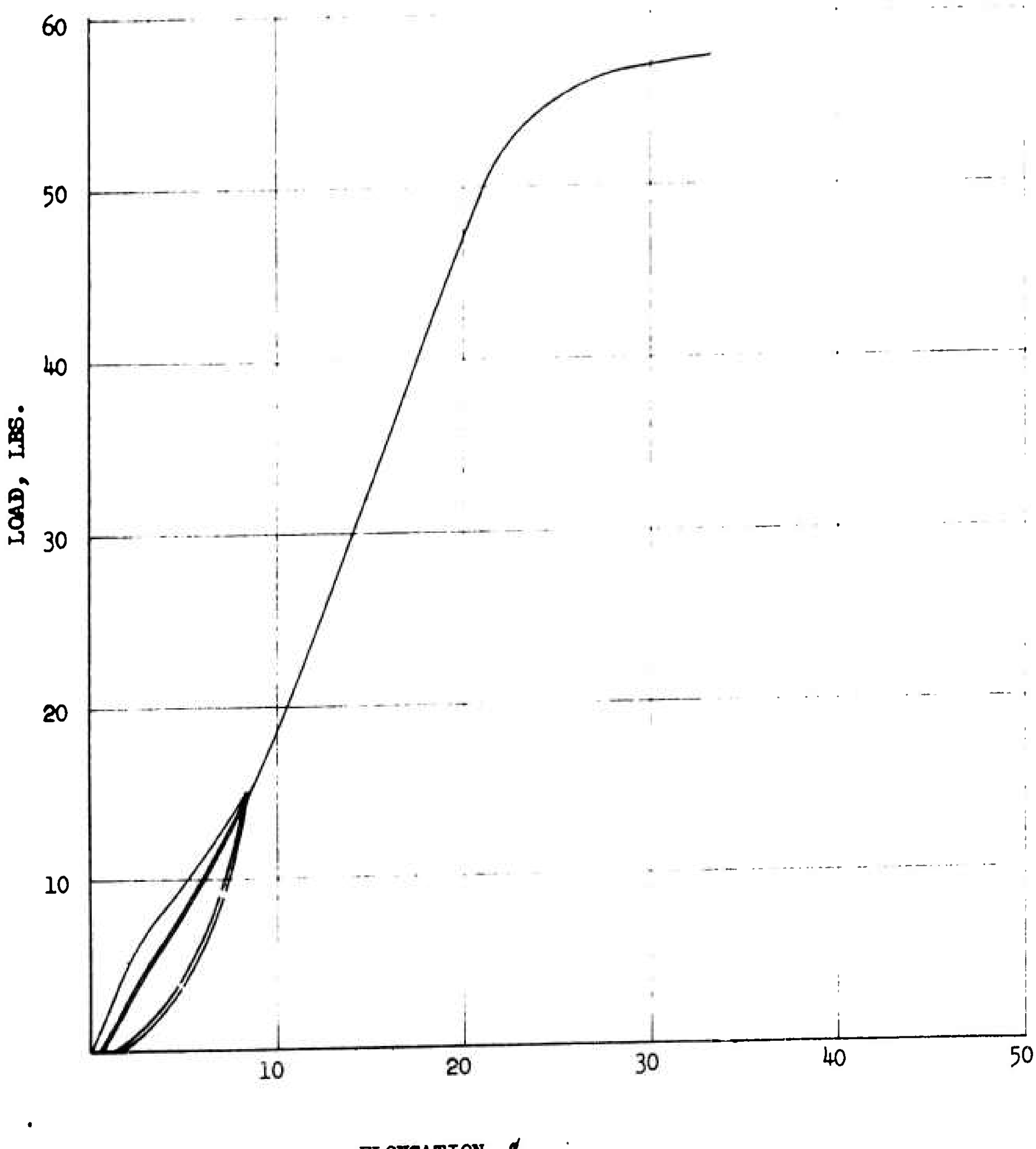

FIGURE 84

TYPICAL REPEATED STRESS-STRAIN CURVES SHOWING 1st & 5th CYCLES TO 1st LOAD LEVEL AND FINAL RUPTURE CYCLE

CHENEY
FABRIC 7N 2 1/2, FILLING

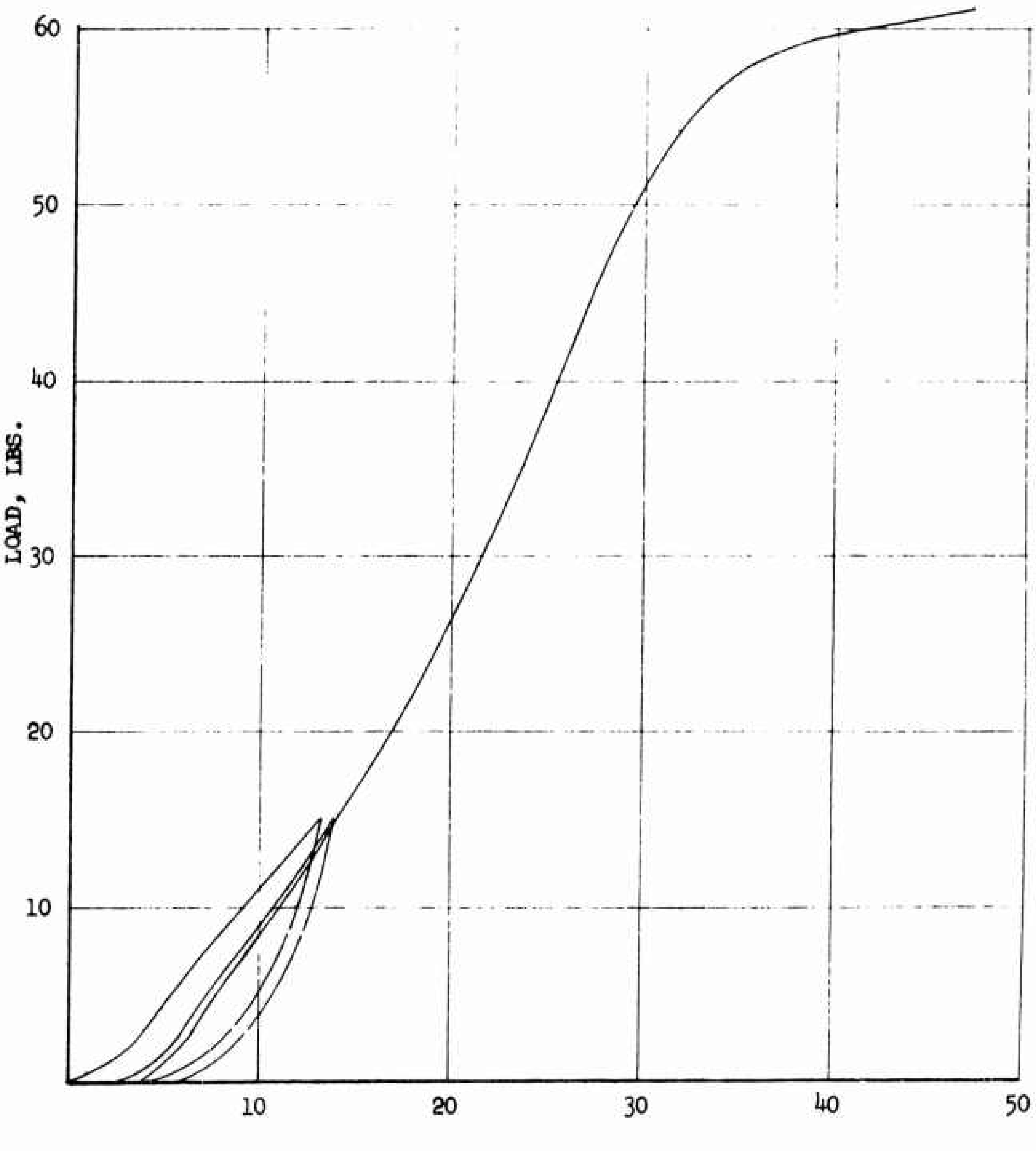

FIGURE 85

TYPICAL REPEATED STRESS-STRAIN CURVES SHOWING 1st & 5th CYCLES TO 2nd LOAD LEVEL AND FINAL RUPTURE CYCLE

CHENEY

FABRIC 7N 2 1/2, WARP

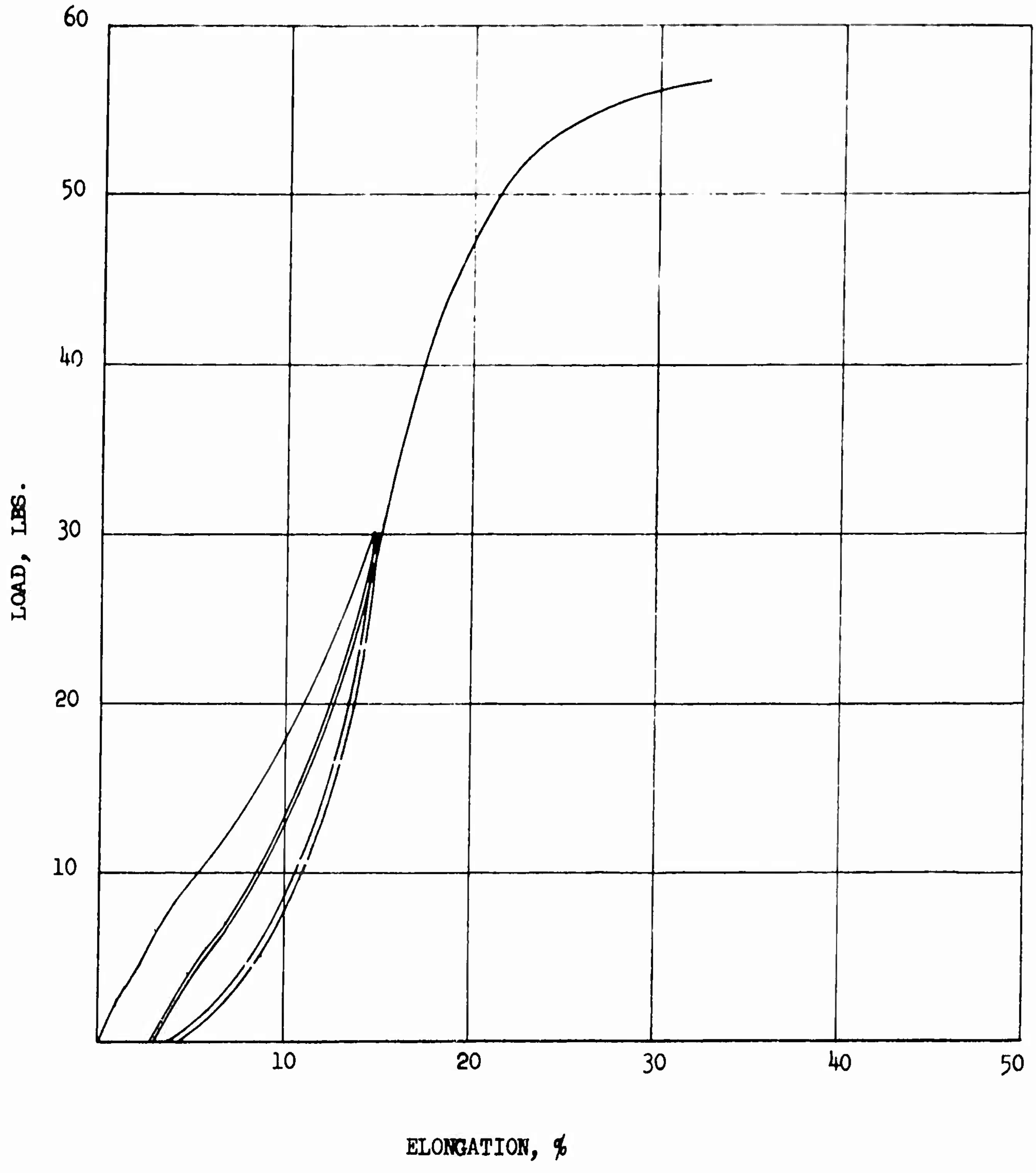

FIGURE 86

TYPICAL REPEATED STRESS-STRAIN CURVES SHOWING 1st & 5th CYCLES TO
2nd LOAD LEVEL AND FINAL RUPTURE CYCLE

CHENEY

FABRIC 7N 2 1/2, FILLING

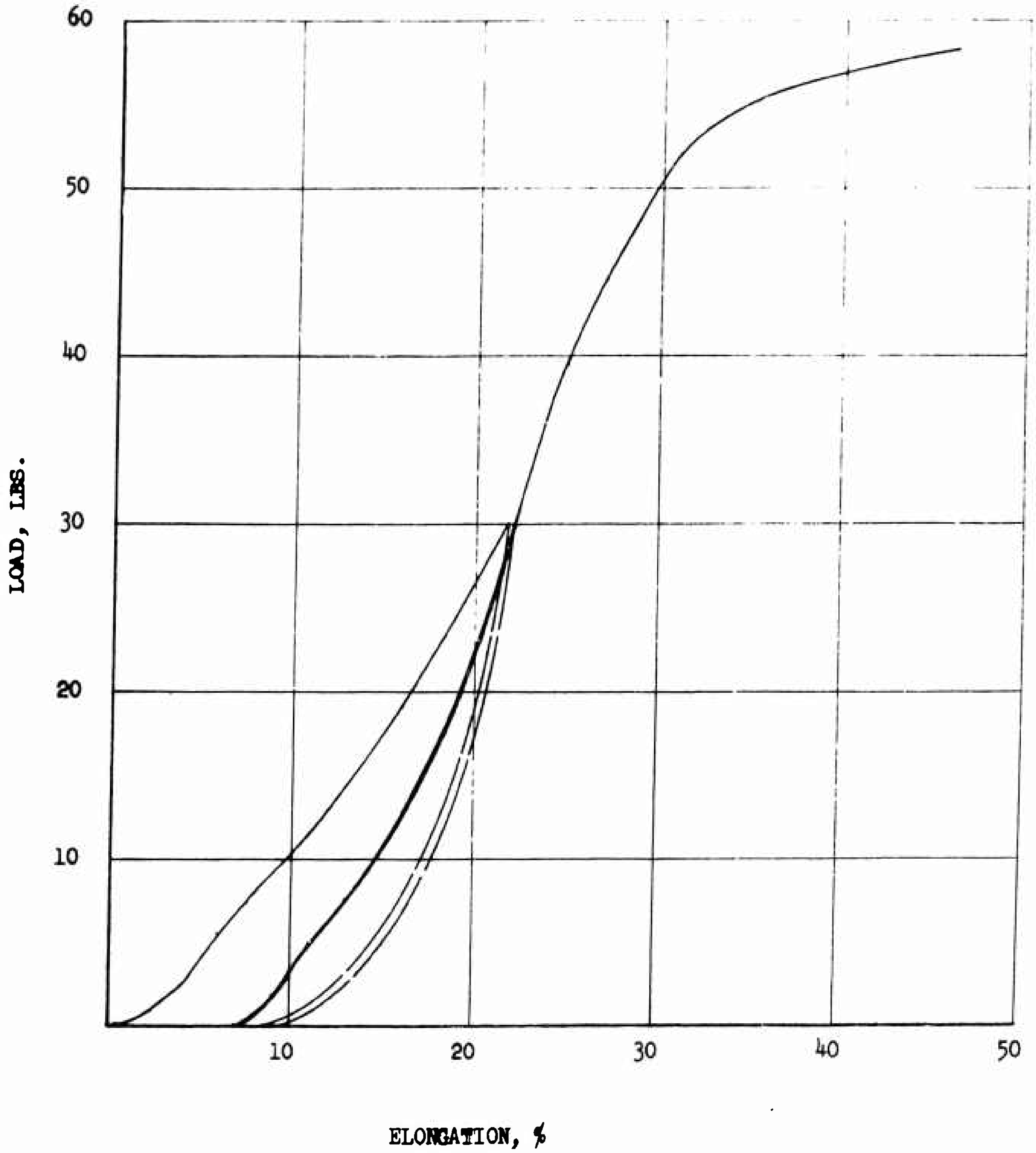

FIGURE 87

TYPICAL REPEATED STRESS-STRAIN CURVES SHOWING 1st & 5th CYCLES TO 3rd LOAD LEVEL AND FINAL RUPTURE CYCLE

CHENEY

FABRIC 7N2 1/2, WARP

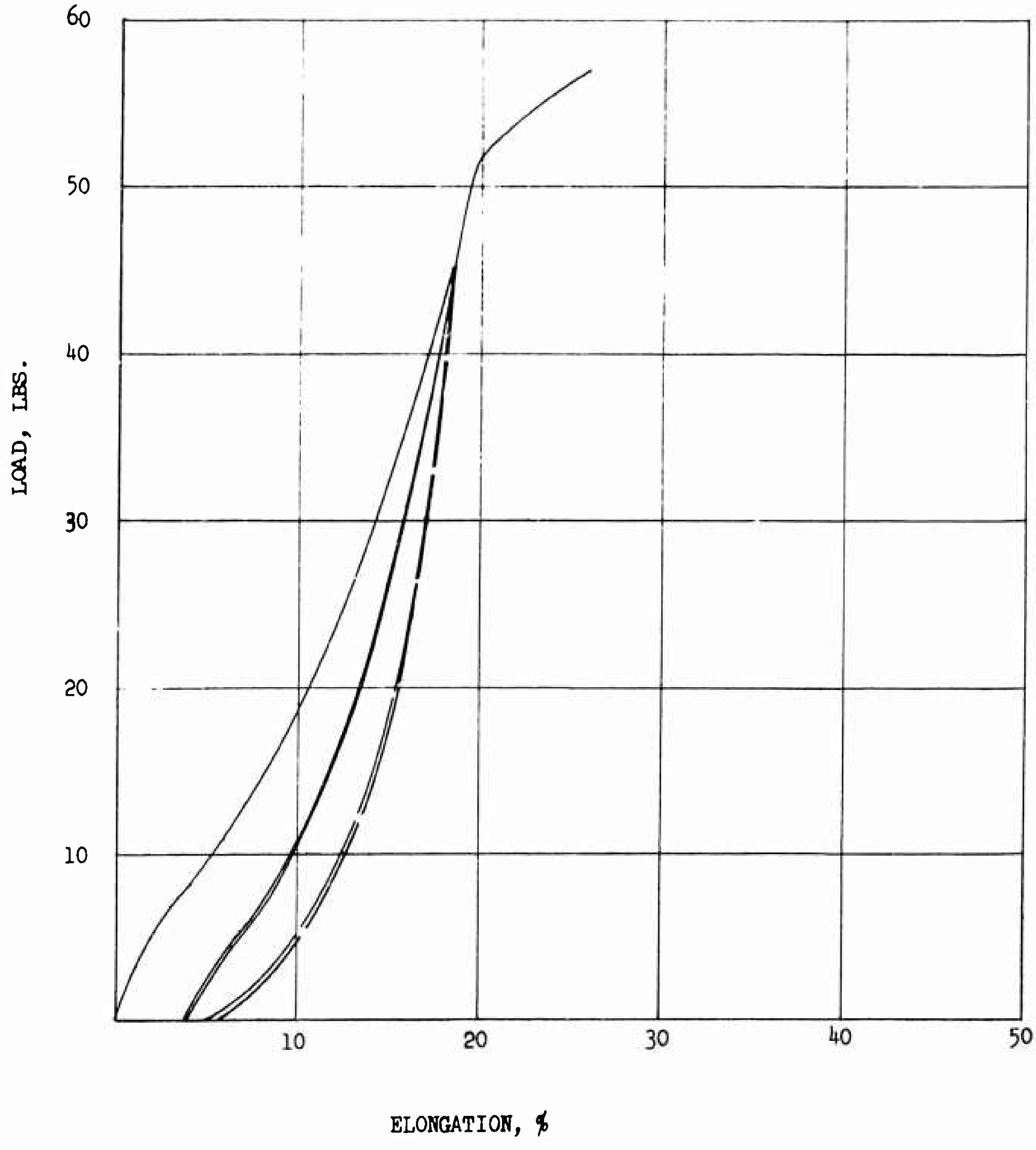

FIGURE 88

TYPICAL REPEATED STRESS-STRAIN CURVES SHOWING 1st & 5th CYCLES TO 3rd LOAD LEVEL AND FINAL RUPTURE CYCLE

CHENEY

FABRIC 7N2 1/2, FILLING

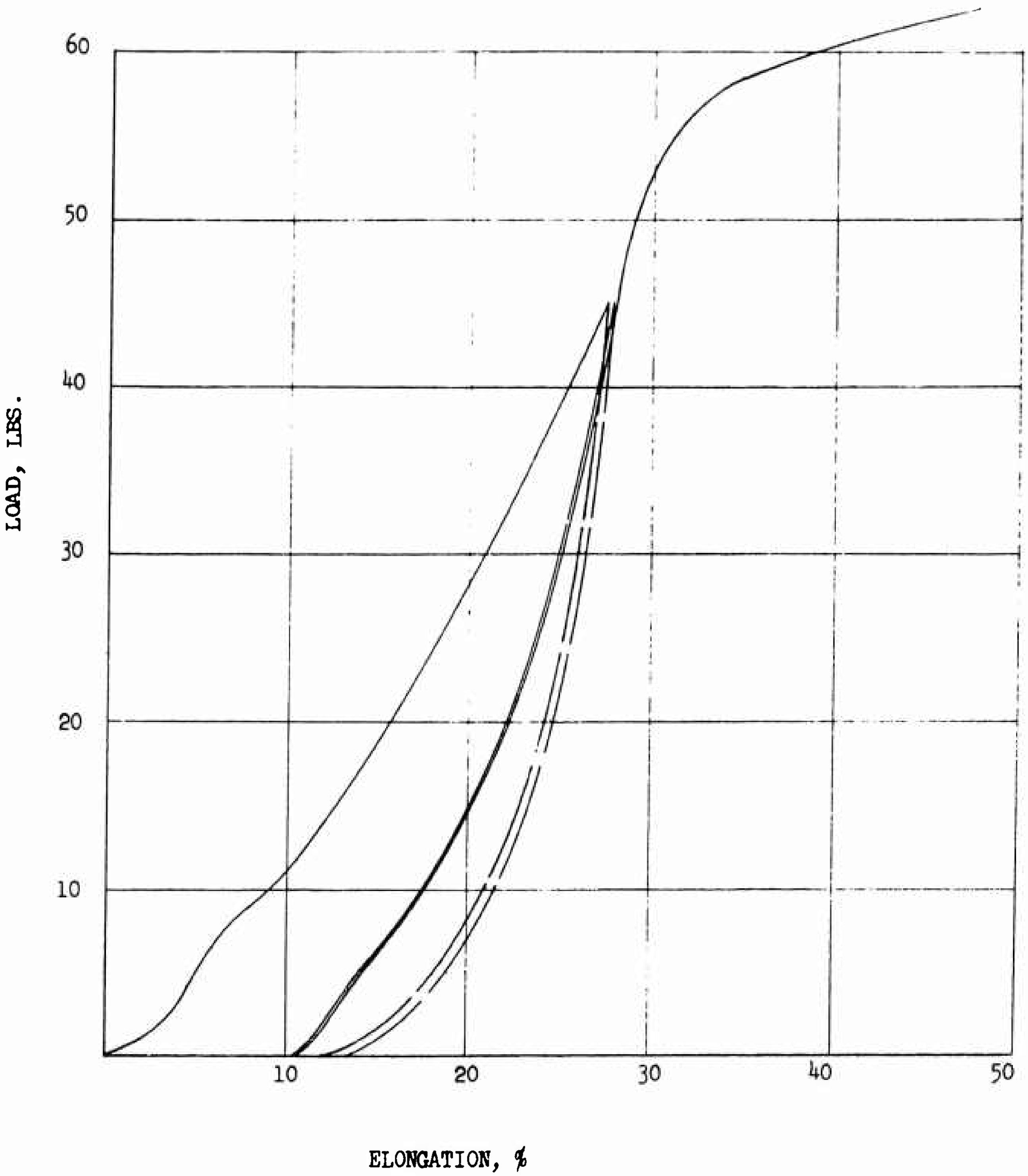

FIGURE 89

TYPICAL REPEATED STRESS-STRAIN CURVES SHOWING 1st & 5th CYCLES TO 1st LOAD LEVEL AND FINAL RUPTURE CYCLE

CHENEY

FABRIC 7N 5, WARP

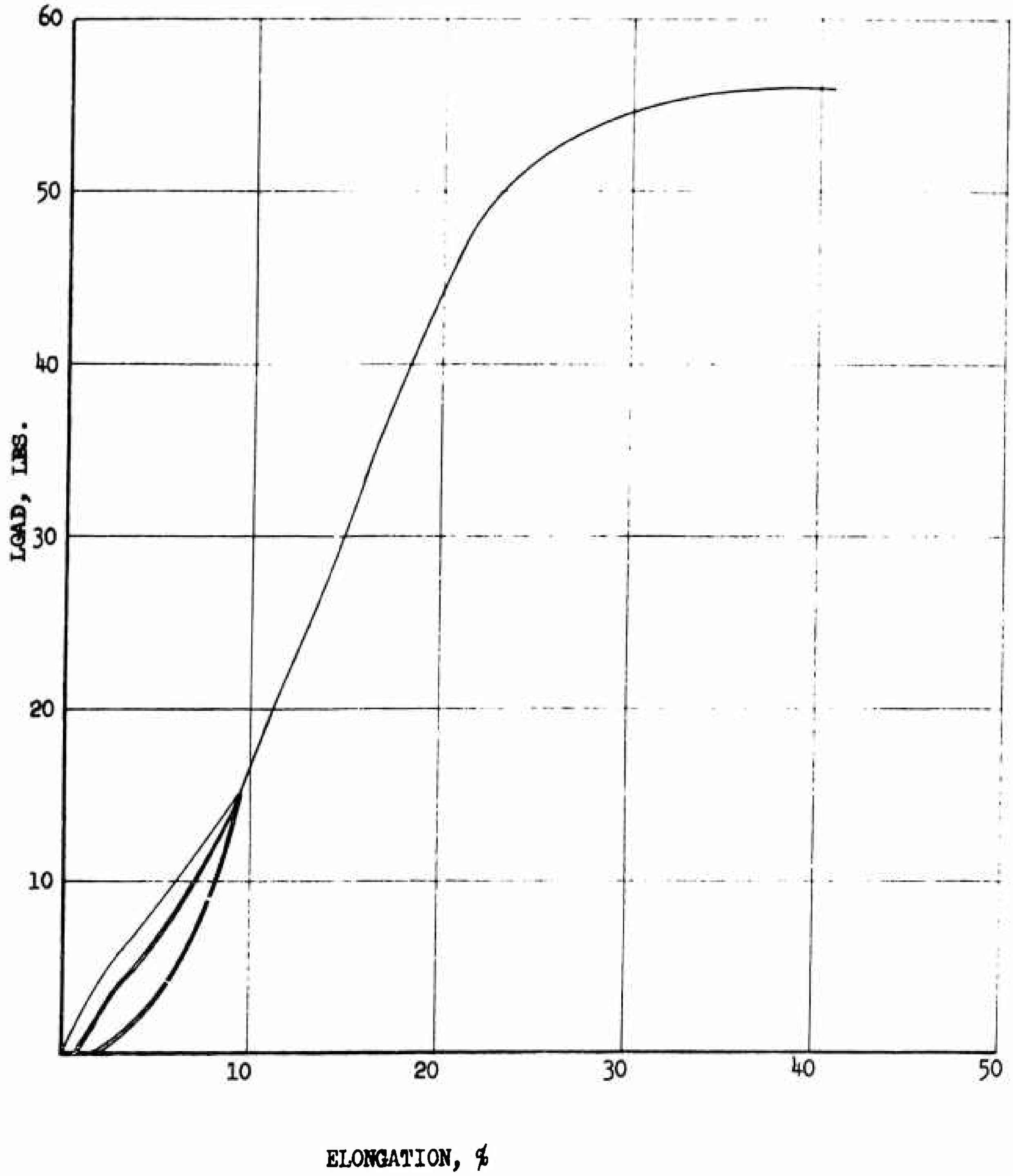

FIGURE 90

TYPICAL REPEATED STRESS-STRAIN CURVES SHOWING 1st & 5th CYCLES TO 1st LOAD LEVEL AND FINAL RUPTURE CYCLE

CHENEY

FABRIC 7N 5, FILLING

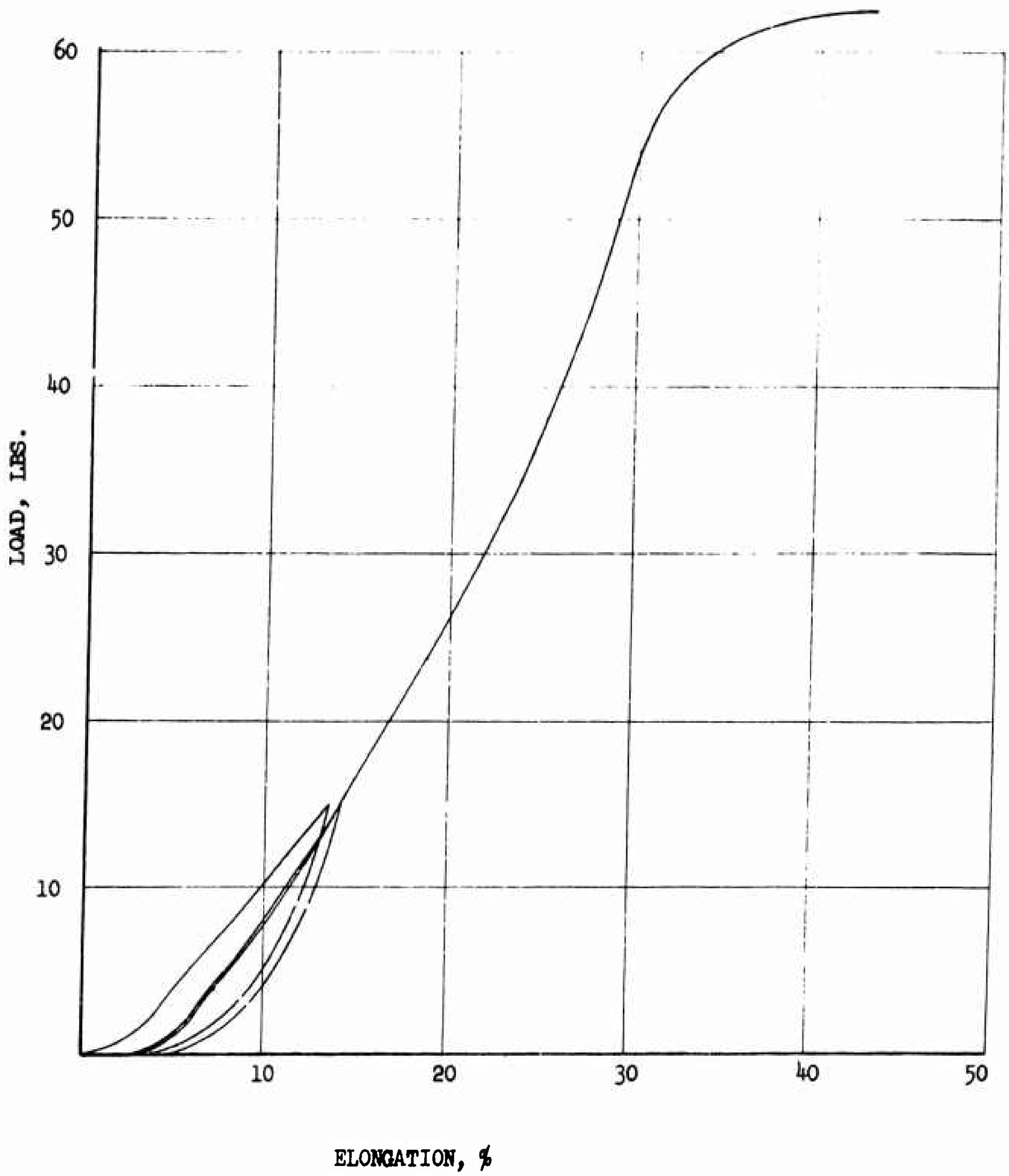

FIGURE 91

TYPICAL REPEATED STRESS-STRAIN CURVES SHOWING 1st & 5th CYCLES TO 2nd LOAD LEVEL AND FINAL RUPTURE CYCLE

CHENEY

FABRIC 7N5, WARP

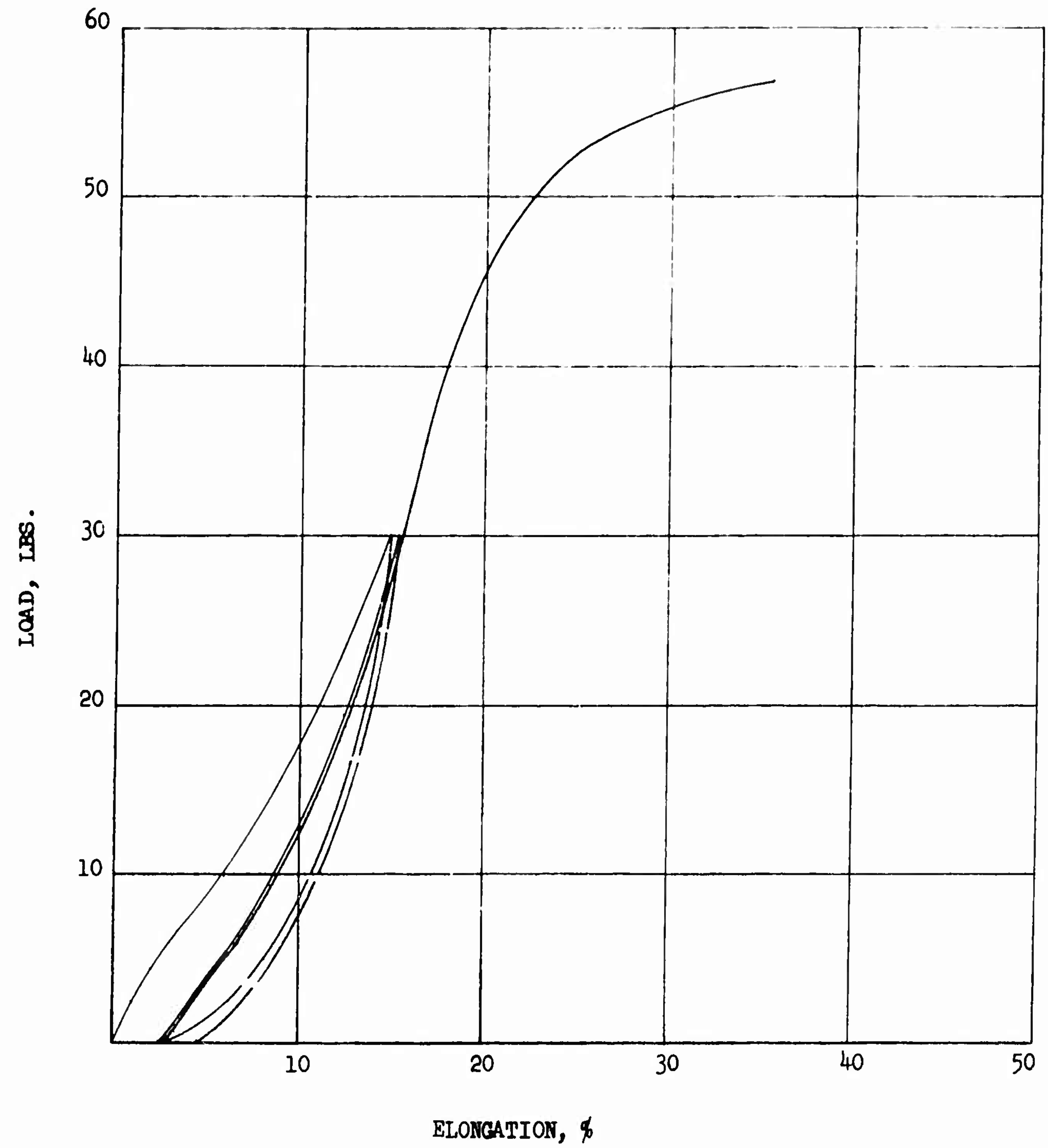

FIGURE 92

TYPICAL REPEATED STRESS-STRAIN CURVES SHOWING 1st & 5th CYCLES TO 2nd LOAD LEVEL AND FINAL RUPTURE CYCLE

CHENEY

FABRIC 7N5, FILLING

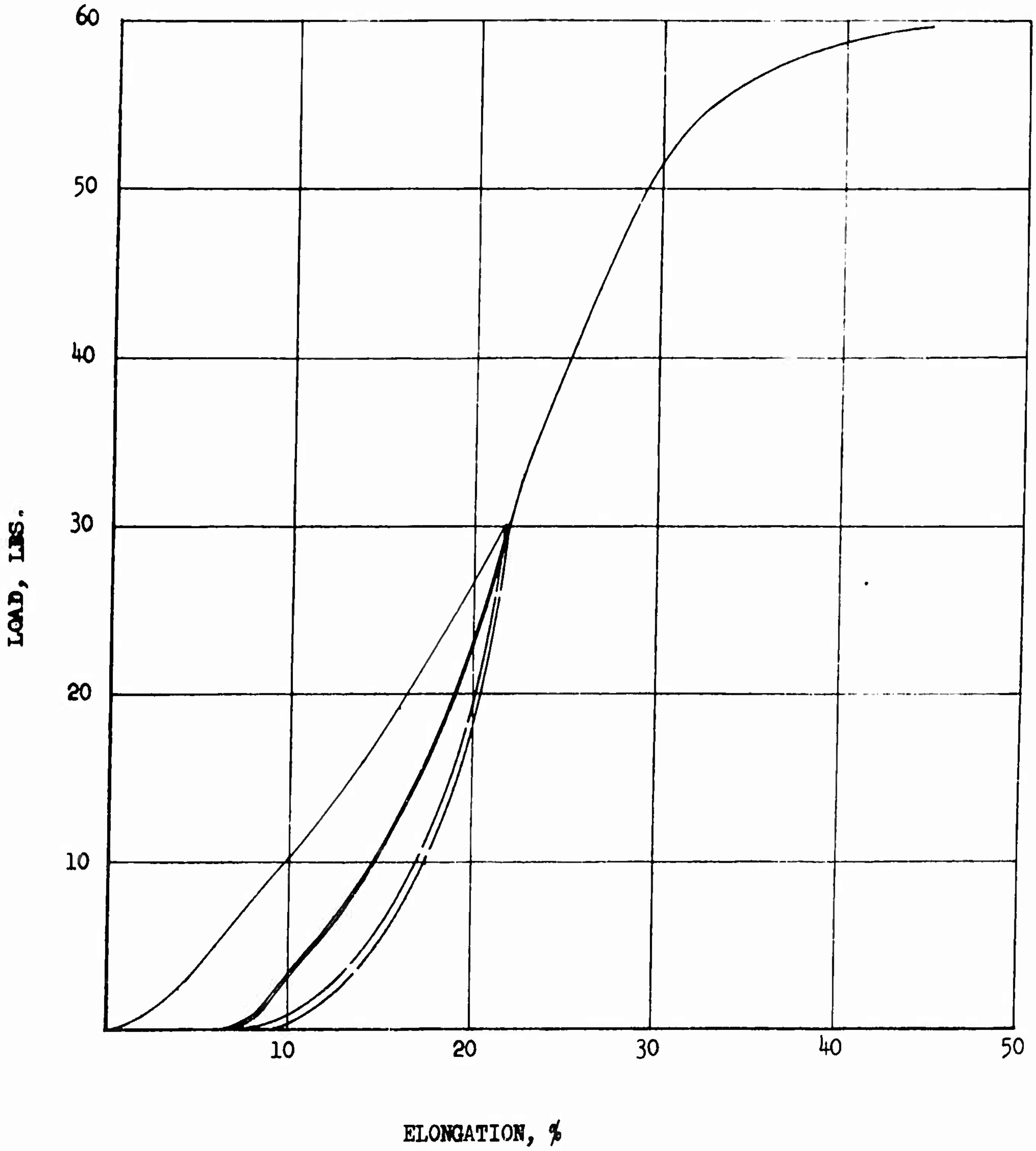

FIGURE 93

TYPICAL REPEATED STRESS-STRAIN CURVES SHOWING 1st & 5th CYCLES TO 3rd LOAD LEVEL AND FINAL RUPTURE CYCLE

CHENEY

FABRIC 7N5, WARP

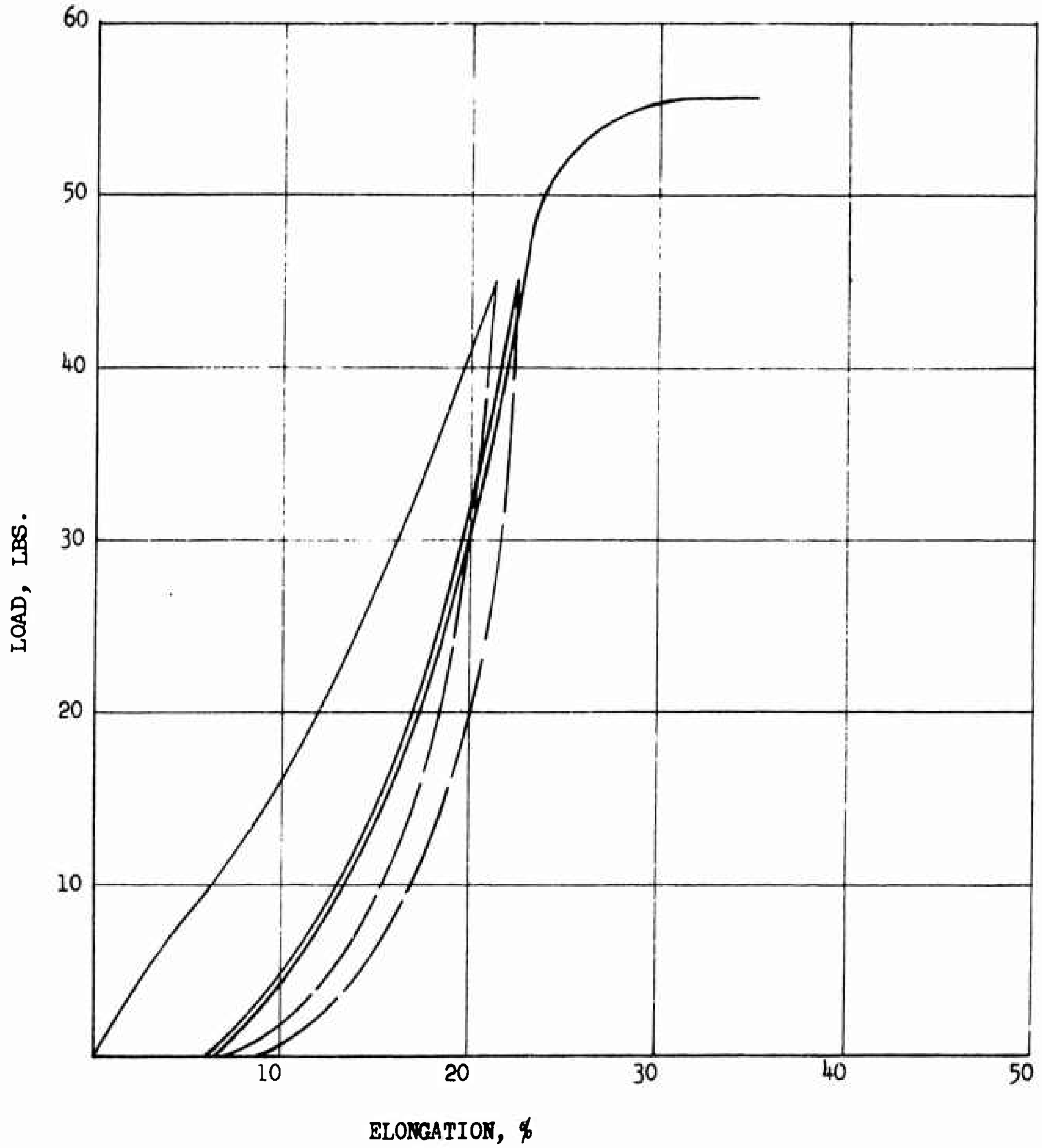

FIGURE 94

TYPICAL REPEATED STRESS-STRAIN CURVES SHOWING 1st & 5th CYCLES TO 3rd LOAD LEVEL AND FINAL RUPTURE CYCLE

CHENEY

FABRIC 7N5, FILLING

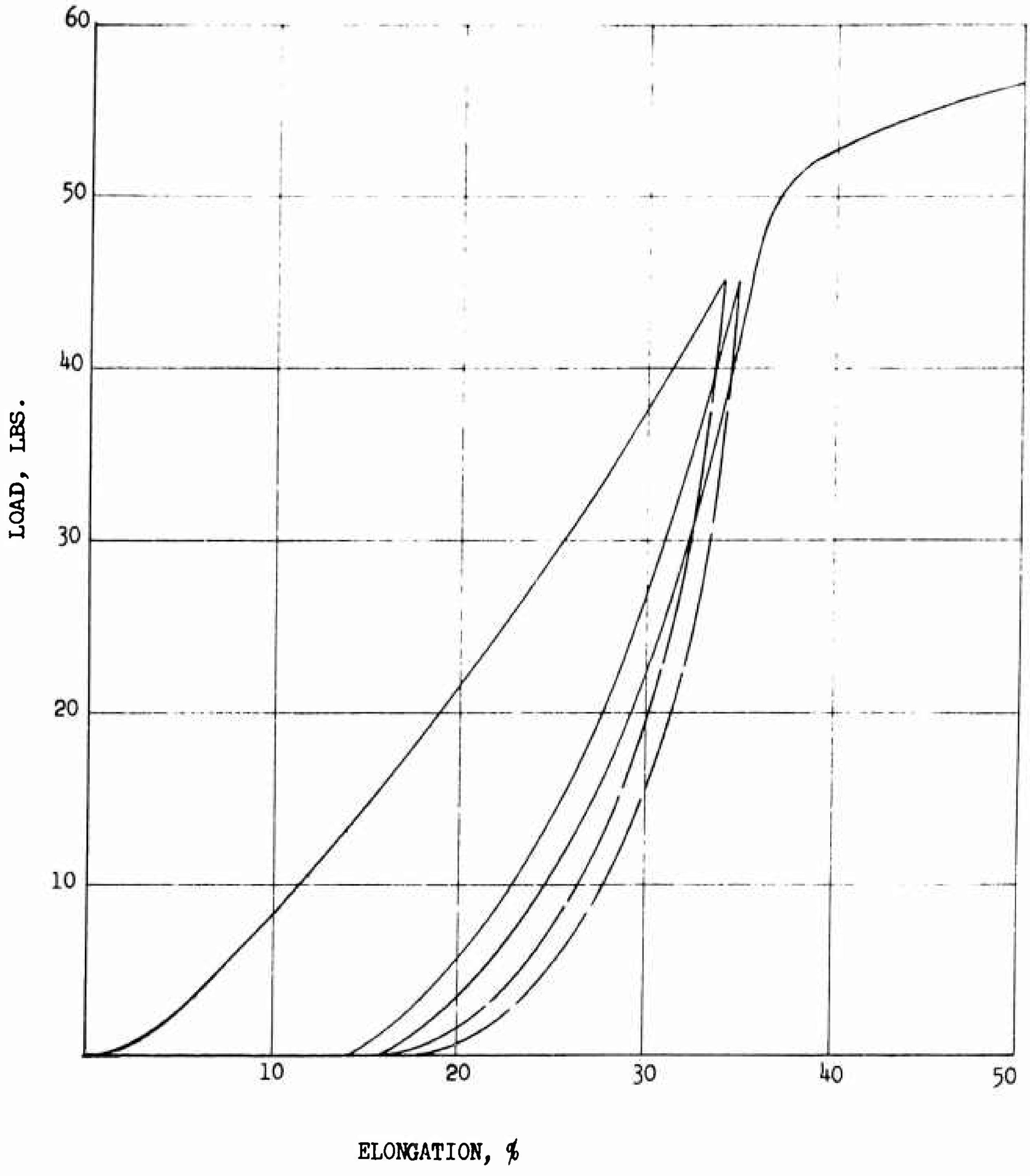

FIGURE 95

TYPICAL REPEATED STRESS-STRAIN CURVES SHOWING 1st & 5th CYCLES TO
1st LOAD LEVEL AND FINAL RUPTURE CYCLE

CHENEY

FABRIC 7N 7, WARP

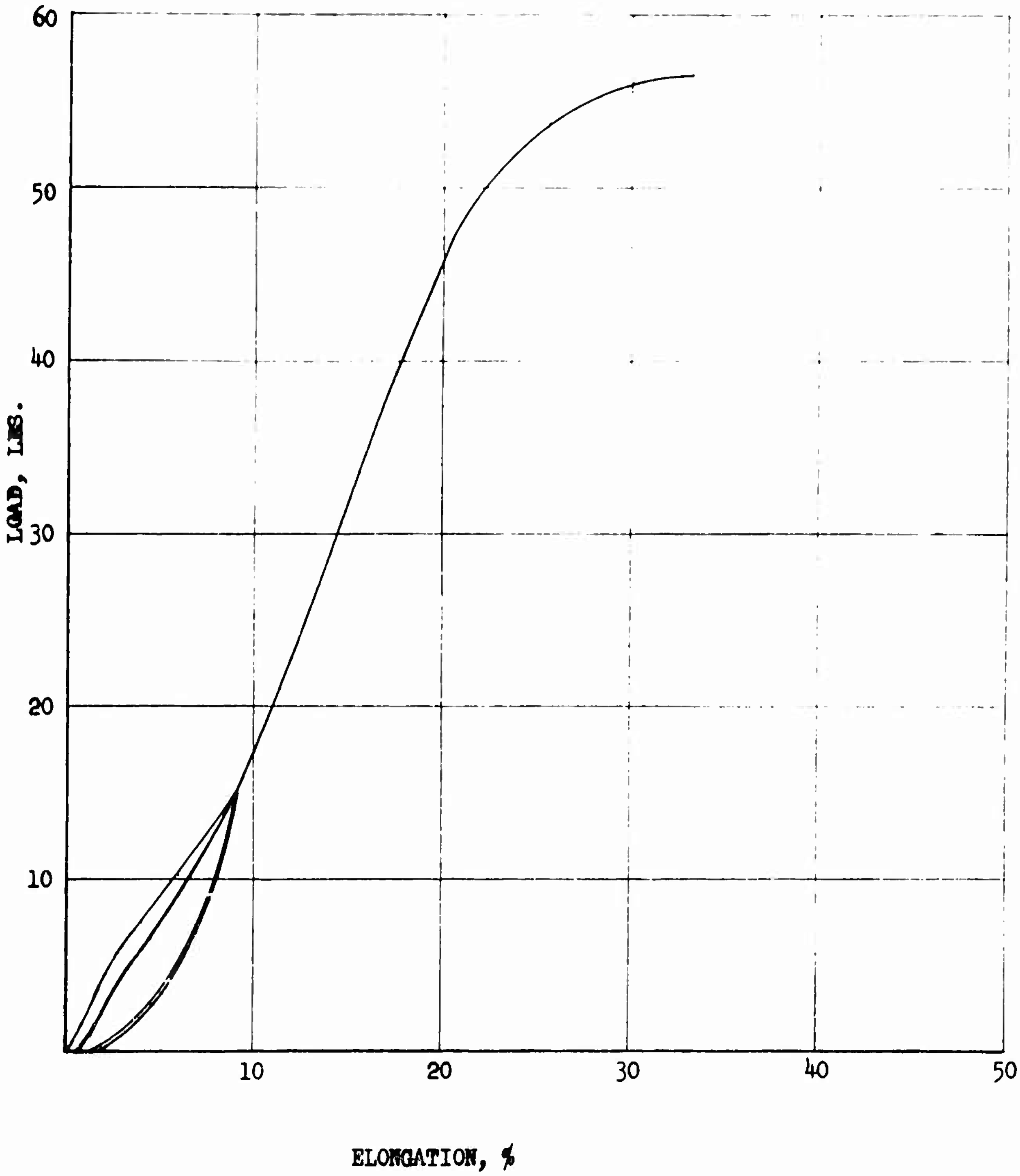

FIGURE 96

TYPICAL REPEATED STRESS-STRAIN CURVES SHOWING 1st & 5th CYCLES TO
1st LOAD LEVEL AND FINAL RUPTURE CYCLE

CHENEY

FABRIC 7N 7, FILLING

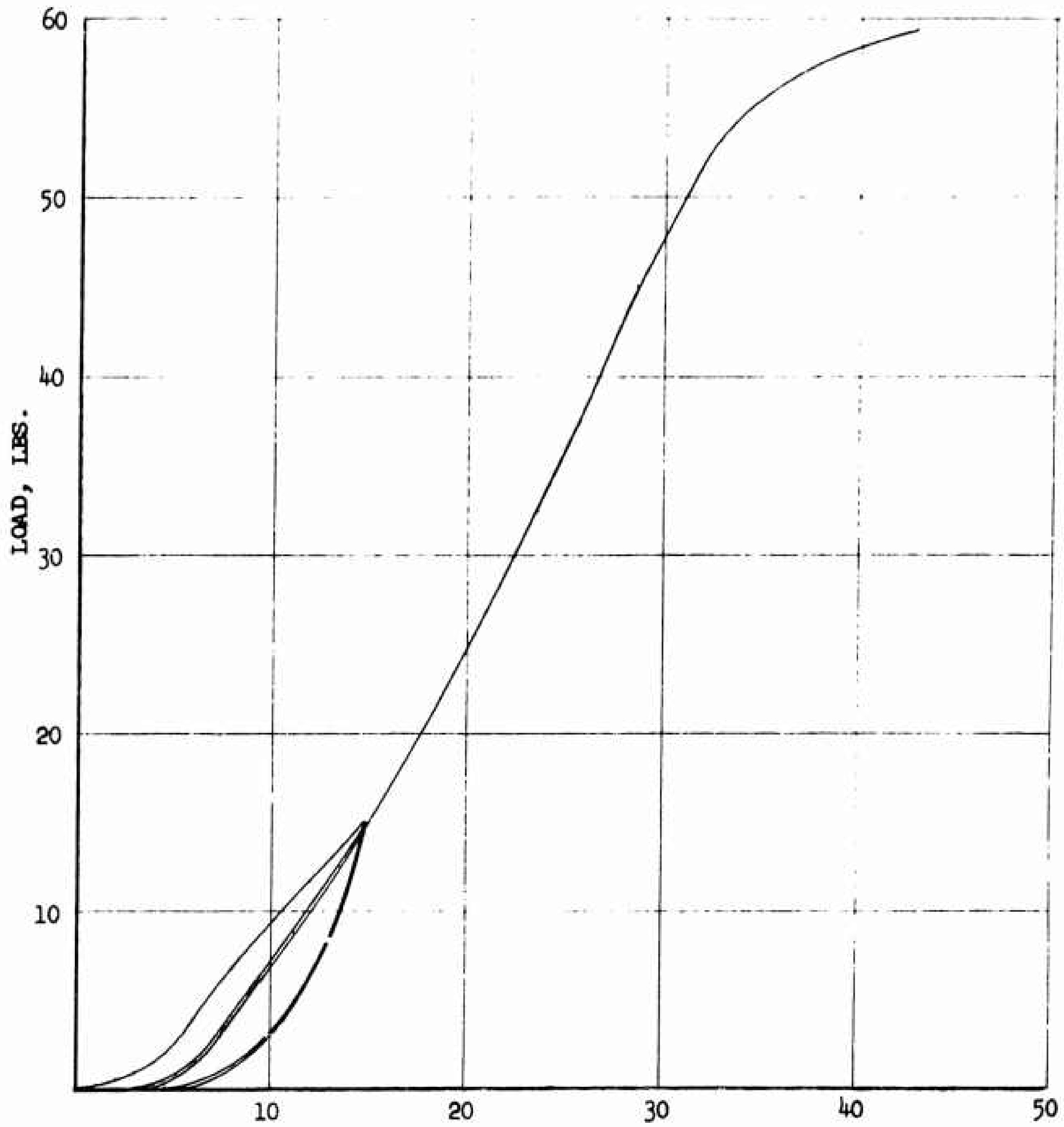

ELONGATION, %

FIGURE 96

TYPICAL REPEATED STRESS-STRAIN CURVES SHOWING 1st & 5th CYCLES TO
1st LOAD LEVEL AND FINAL RUPTURE CYCLE

CHENEY

FABRIC 7N 7, FILLING

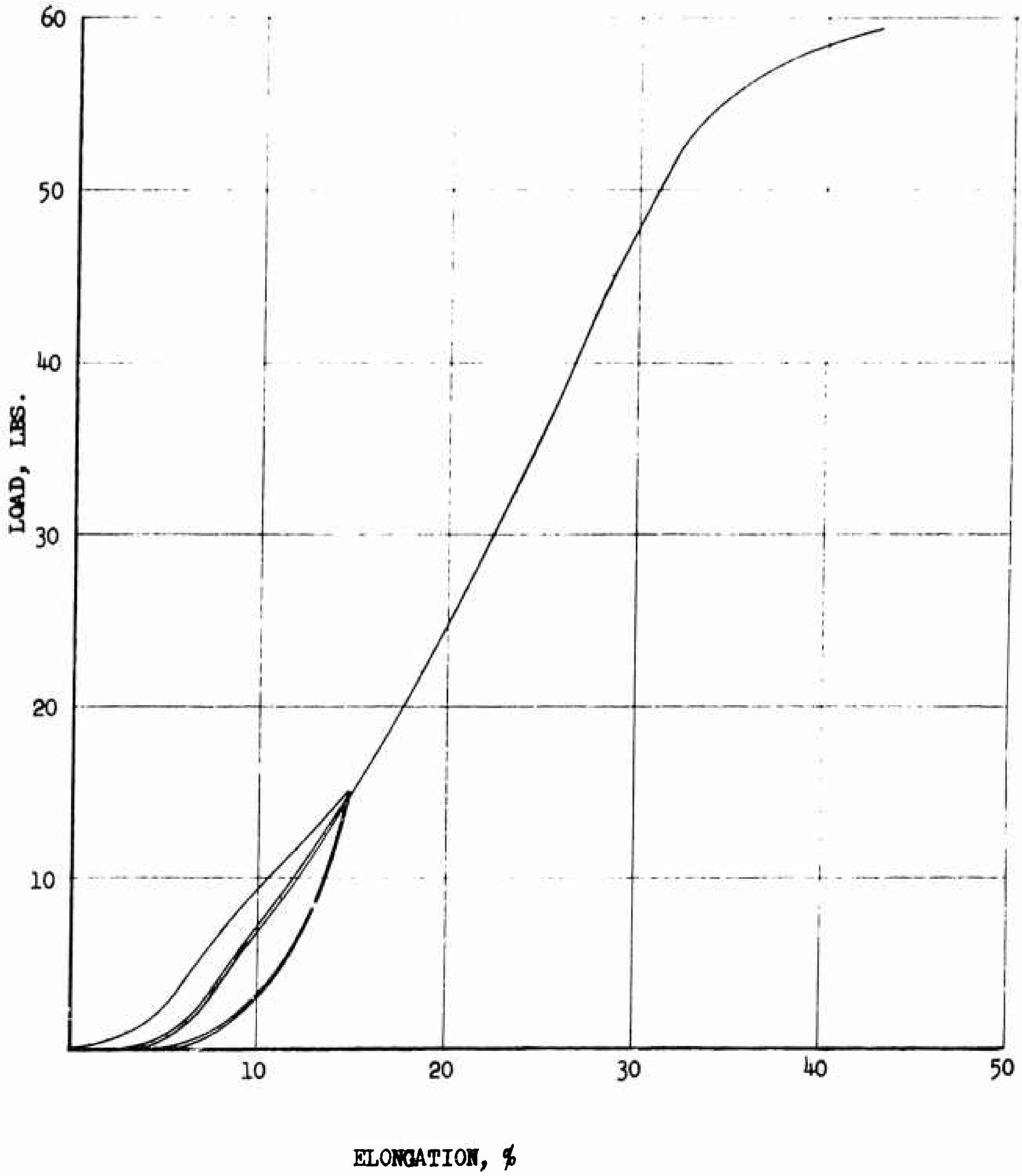

FIGURE 97

TYPICAL REPEATED STRESS-STRAIN CURVES SHOWING 1st & 5th CYCLES TO 2nd LOAD LEVEL AND FINAL RUPTURE CYCLE

FABRIC 7N7, WARP

CHENEY

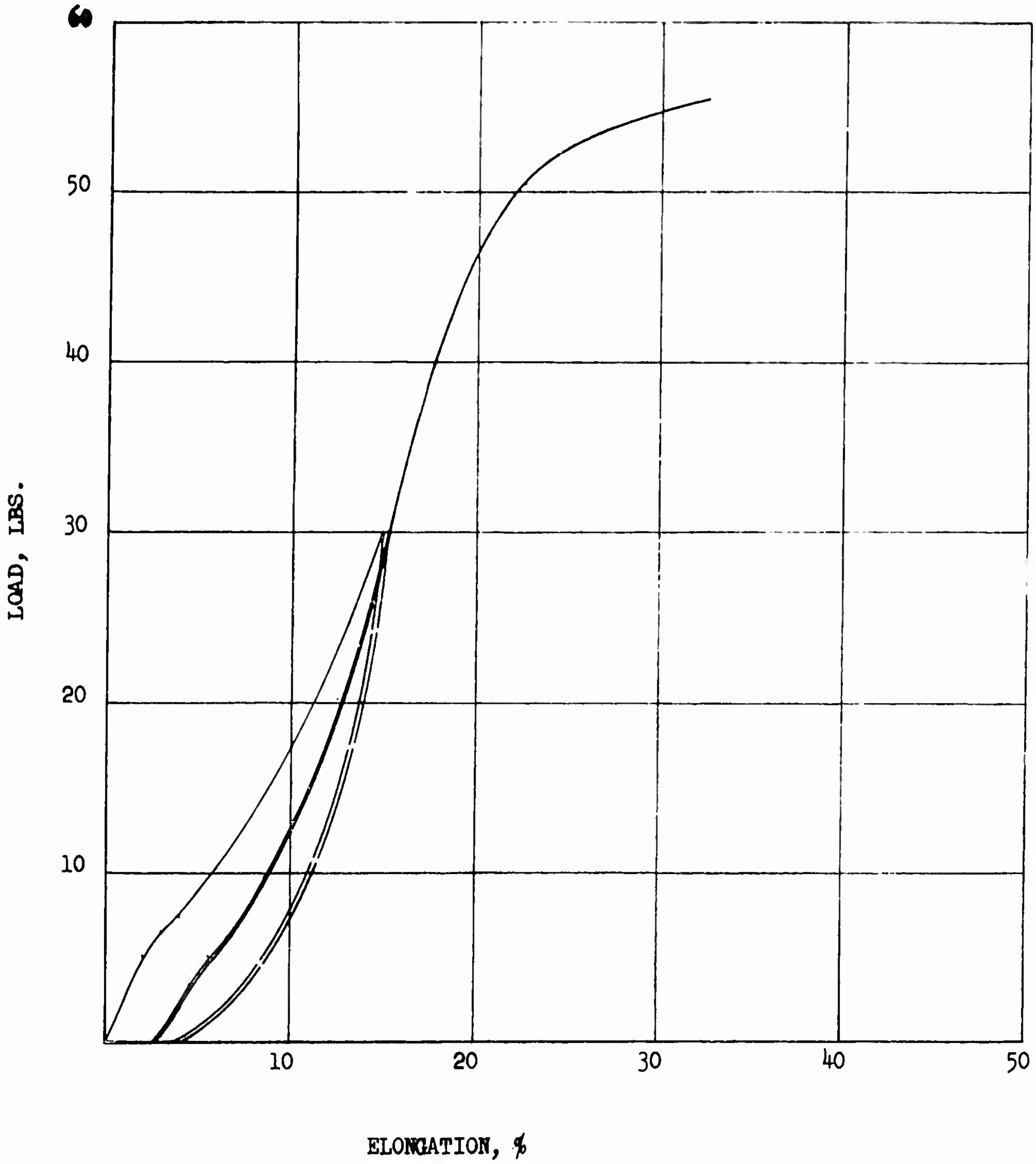

FIGURE 98

TYPICAL REPEATED STRESS-STRAIN CURVES SHOWING 1st & 5th CYCLES TO
2nd LOAD LEVEL AND FINAL RUPTURE CYCLE
CHENEY

FABRIC 7N7, FILLING

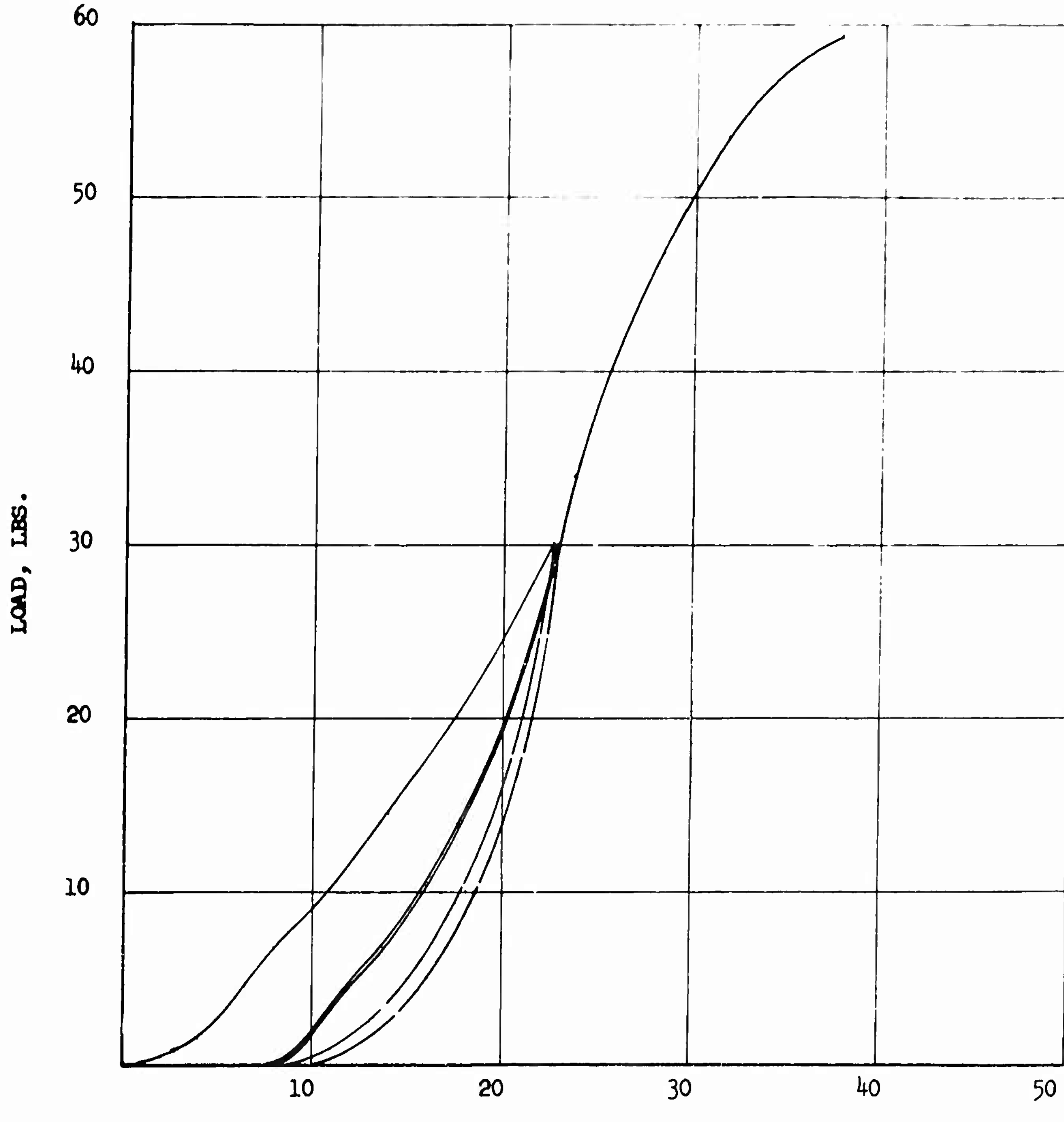

FIGURE 99

TYPICAL REPEATED STRESS-STRAIN CURVES SHOWING 1st & 5th CYCLES TO 3rd LOAD LEVEL AND FINAL RUPTURE CYCLE

CHENEY

FABRIC 7N7, WARP

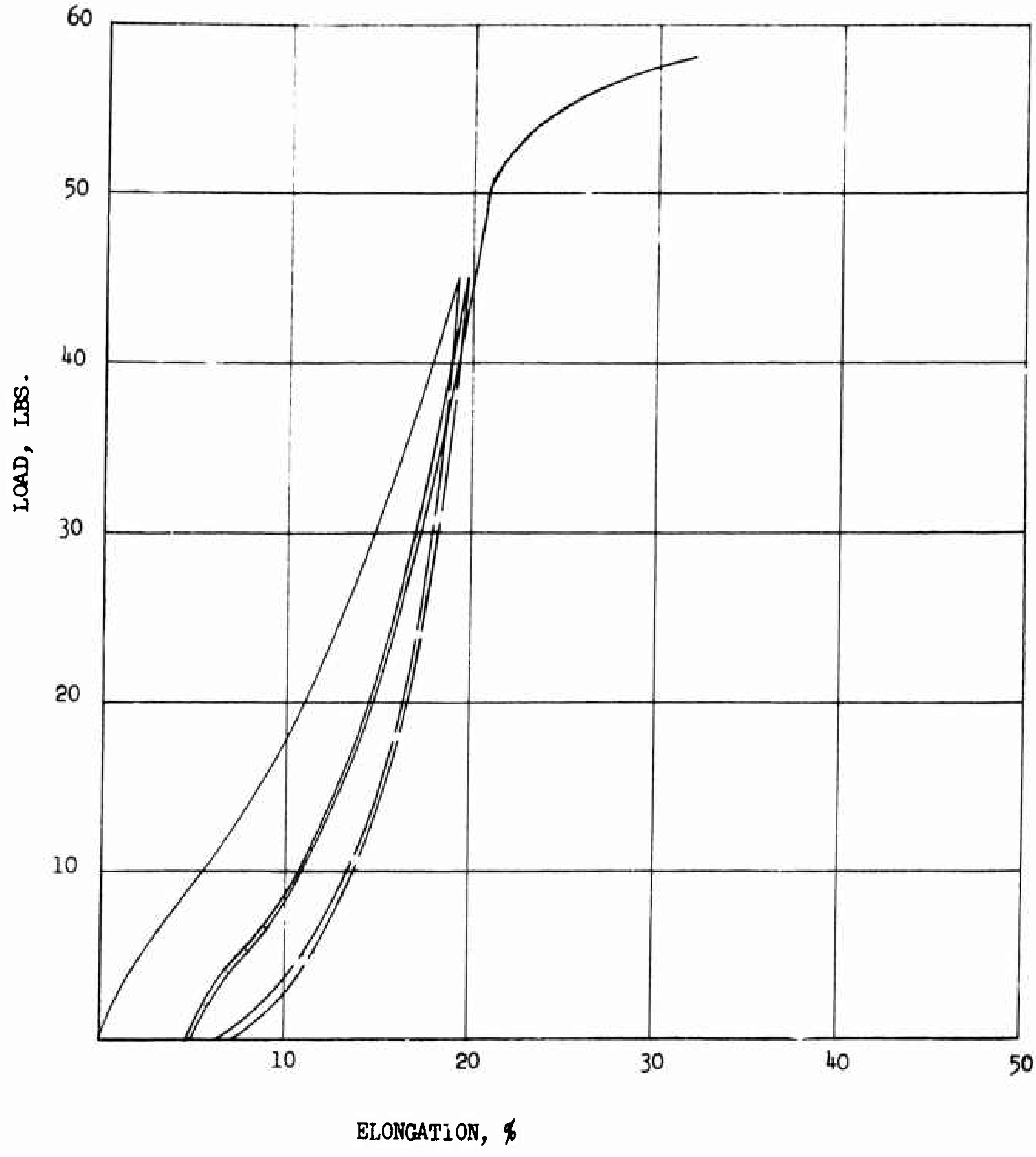

FIGURE 100

TYPICAL REPEATED STRESS-STRAIN CURVES SHOWING 1st & 5th CYCLES TO
3rd LOAD LEVEL AND FINAL RUPTURE CYCLE

CHENEY

FABRIC 7N7, FILLING

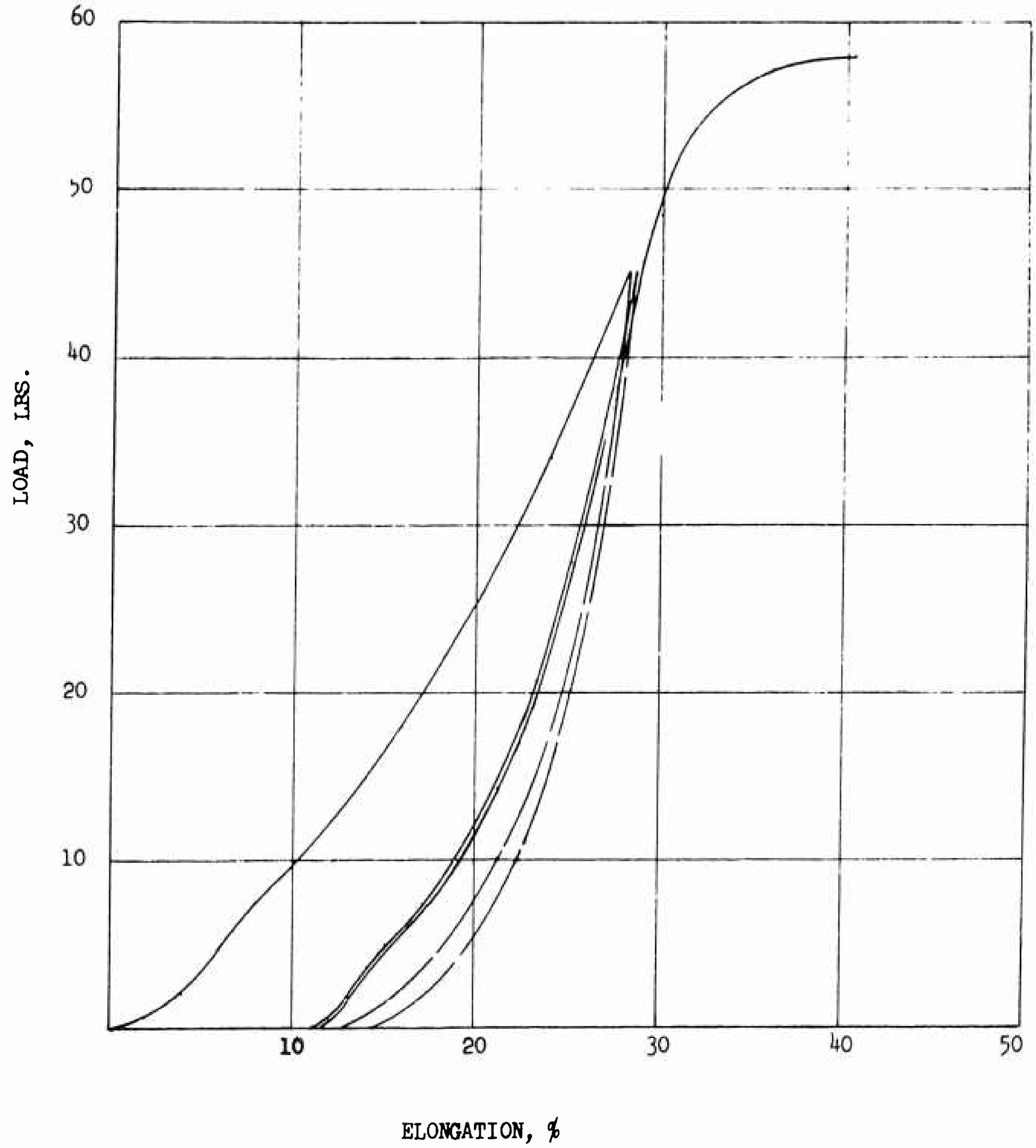

FIGURE 101

TYPICAL REPEATED STRESS-STRAIN CURVES SHOWING 1st & 5th CYCLES TO
1st LOAD LEVEL AND FINAL RUPTURE CYCLE
CHENEY

FABRIC 7N 15, WARP

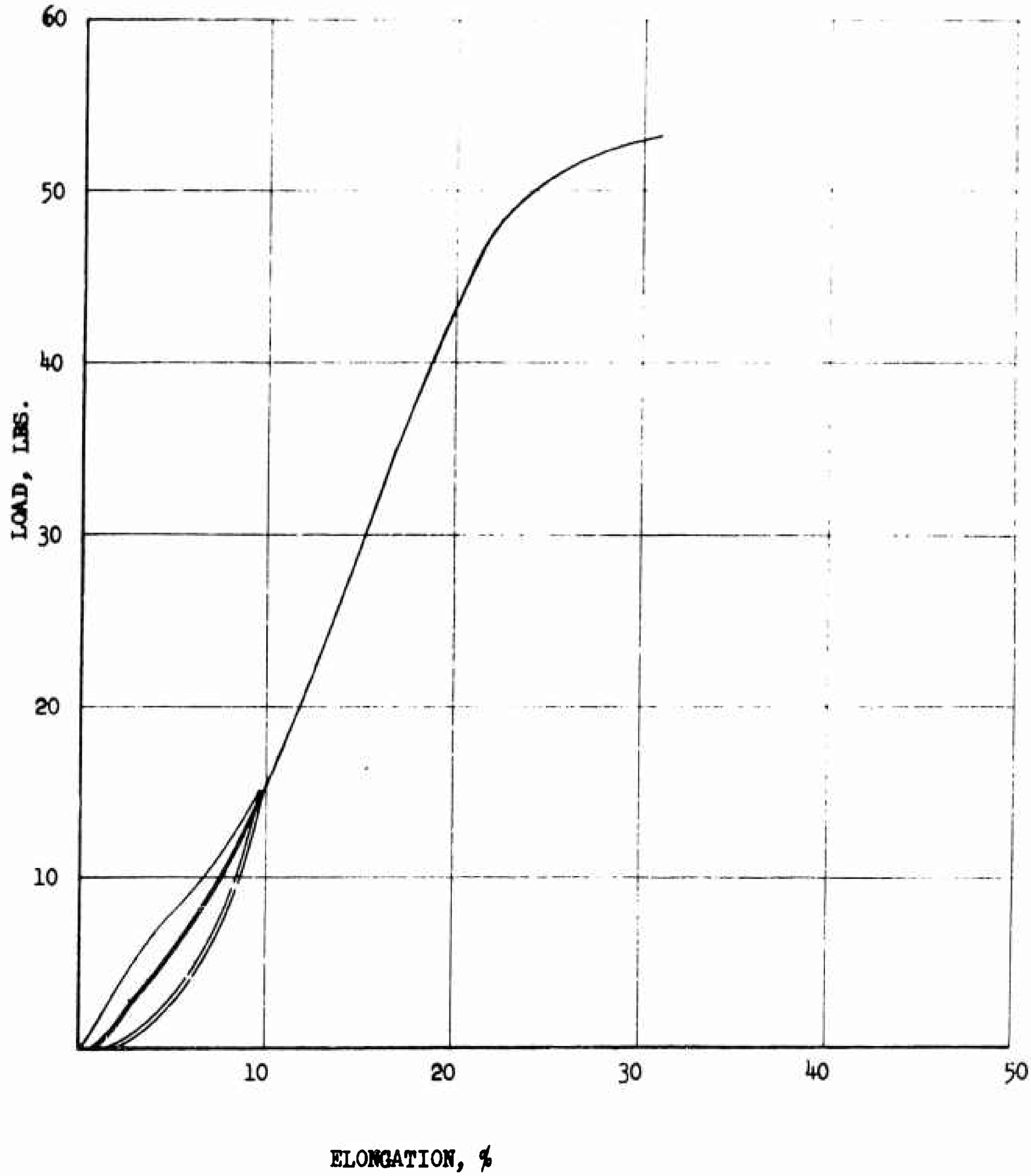

FIGURE 102

TYPICAL REPEATED STRESS-STRAIN CURVES SHOWING 1st & 5th CYCLES TO 1st LOAD LEVEL AND FINAL RUPTURE CYCLE

CHENEY

FABRIC 7N 15, FILLING

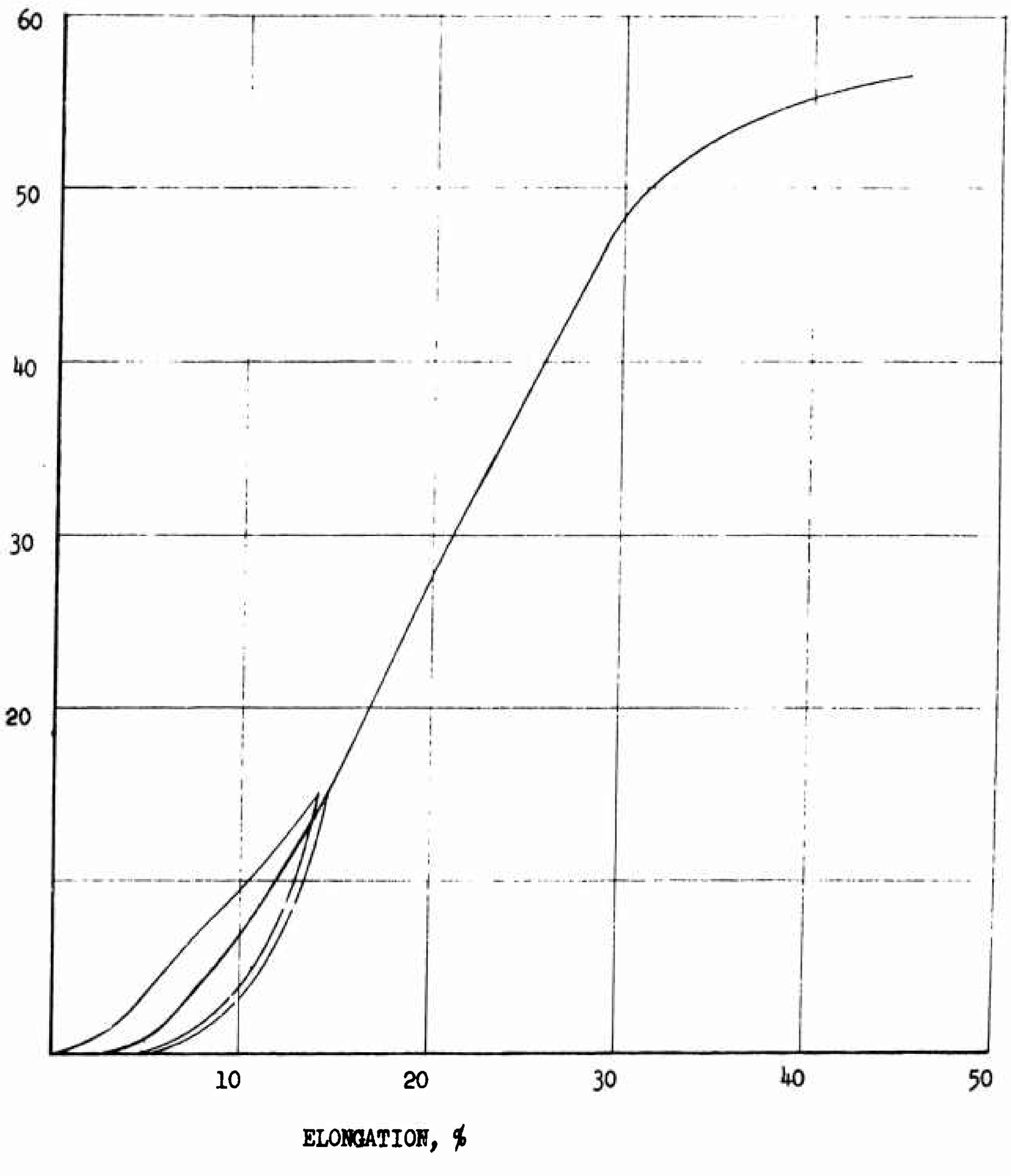

FIGURE 103

TYPICAL REPEATED STRESS-STRAIN CURVES SHOWING 1st & 5th CYCLES TO 2nd LOAD LEVEL AND FINAL RUPTURE CYCLE

CHENEY

FABRIC 7N15, WARP

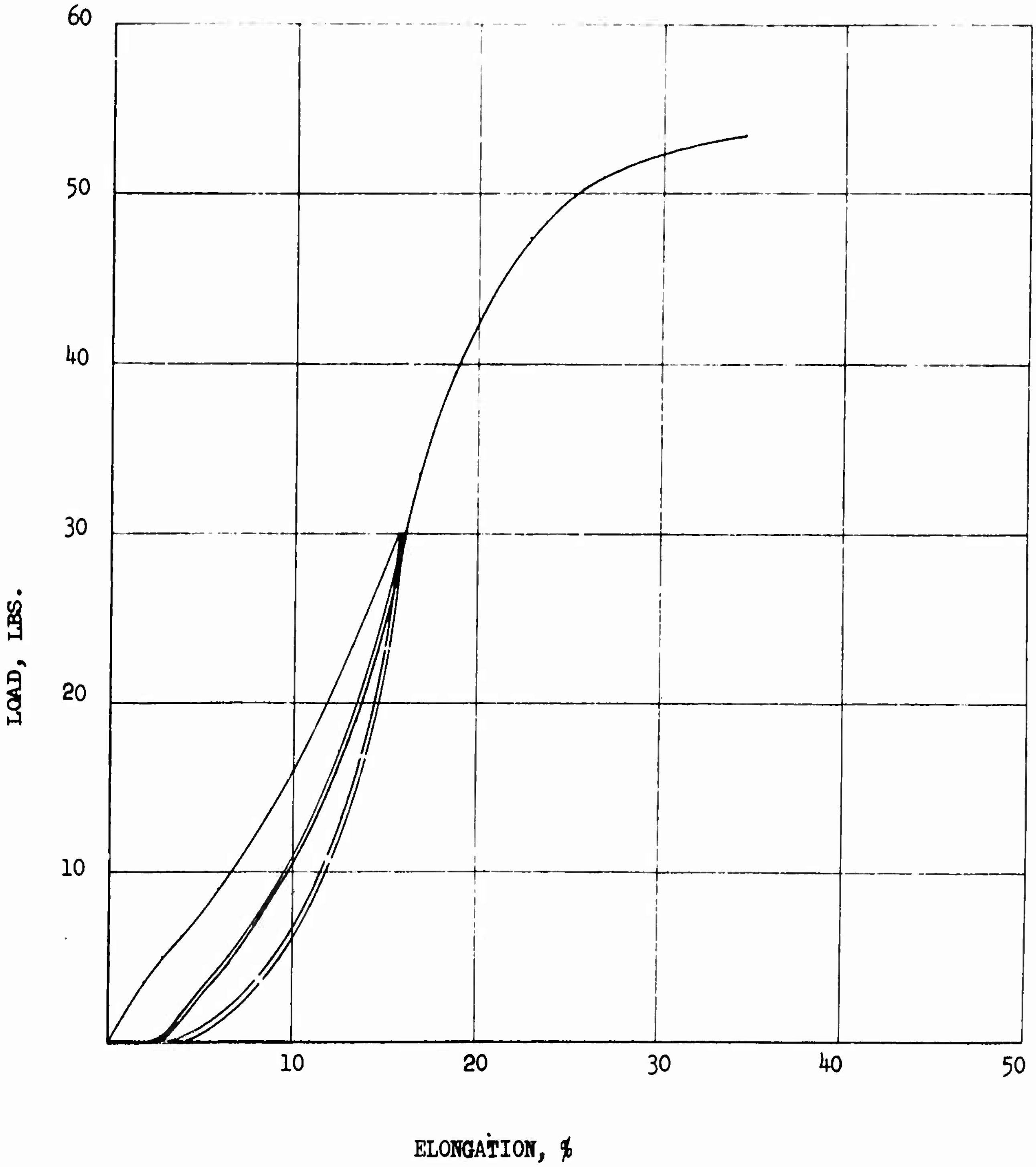

FIGURE 104

TYPICAL REPEATED STRESS-STRAIN CURVES SHOWING 1st & 5th CYCLES TO 2nd LOAD LEVEL AND FINAL RUPTURE CYCLE

CHENEY

FABRIC 7N15, FILLING

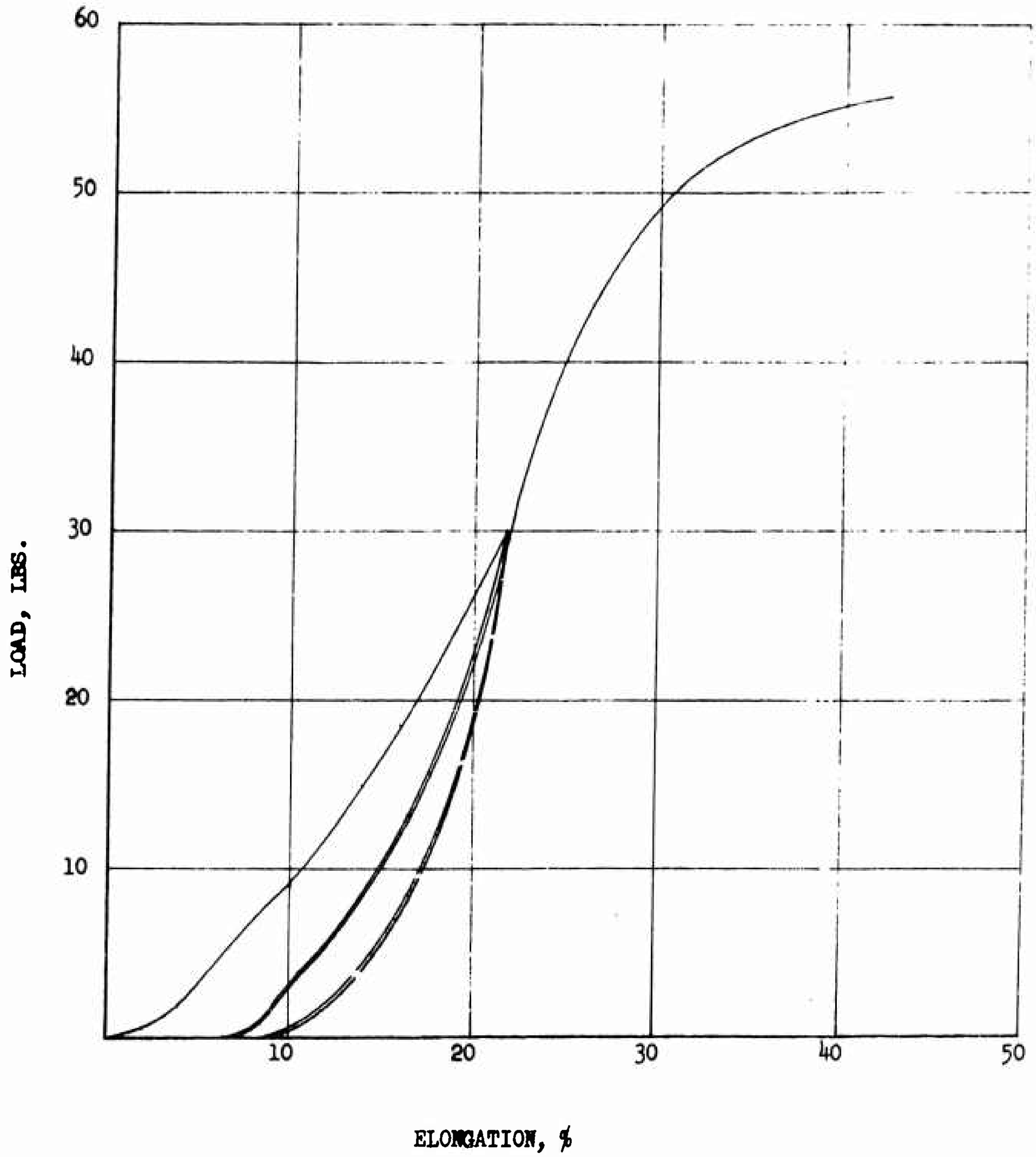

FIGURE 105

TYPICAL REPEATED STRESS-STRAIN CURVES SHOWING 1st & 5th CYCLES TO
3rd LOAD LEVEL AND FINAL RUPTURE CYCLE

CHENEY

FABRIC 7N 15, WARP

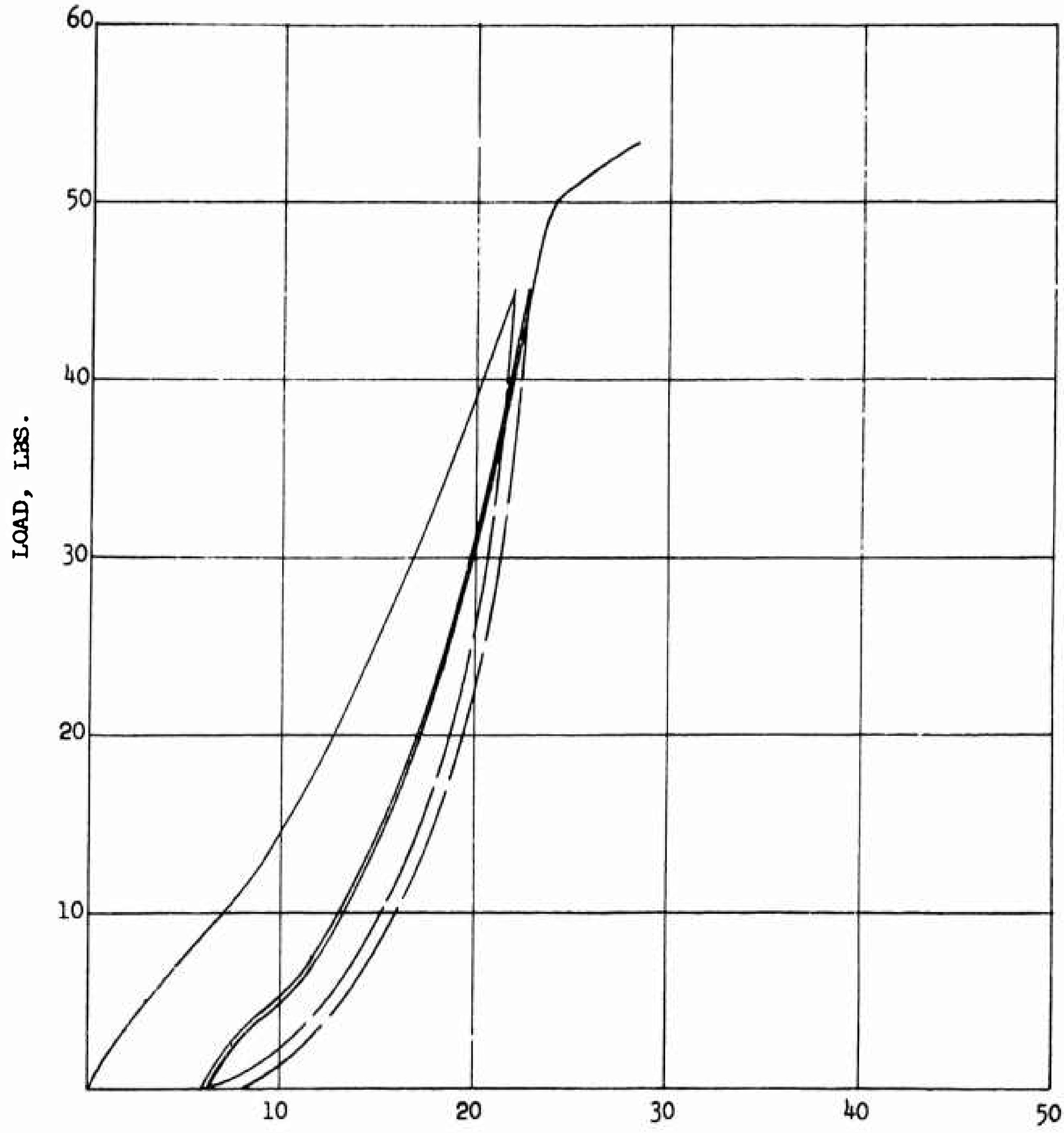

ELONGATION, %

FIGURE 106

TYPICAL REPEATED STRESS-STRAIN CURVES SHOWING 1st & 5th CYCLES TO 3rd LOAD LEVEL AND FINAL RUPTURE CYCLE

CHENEY

FABRIC 7N 15, FILLING

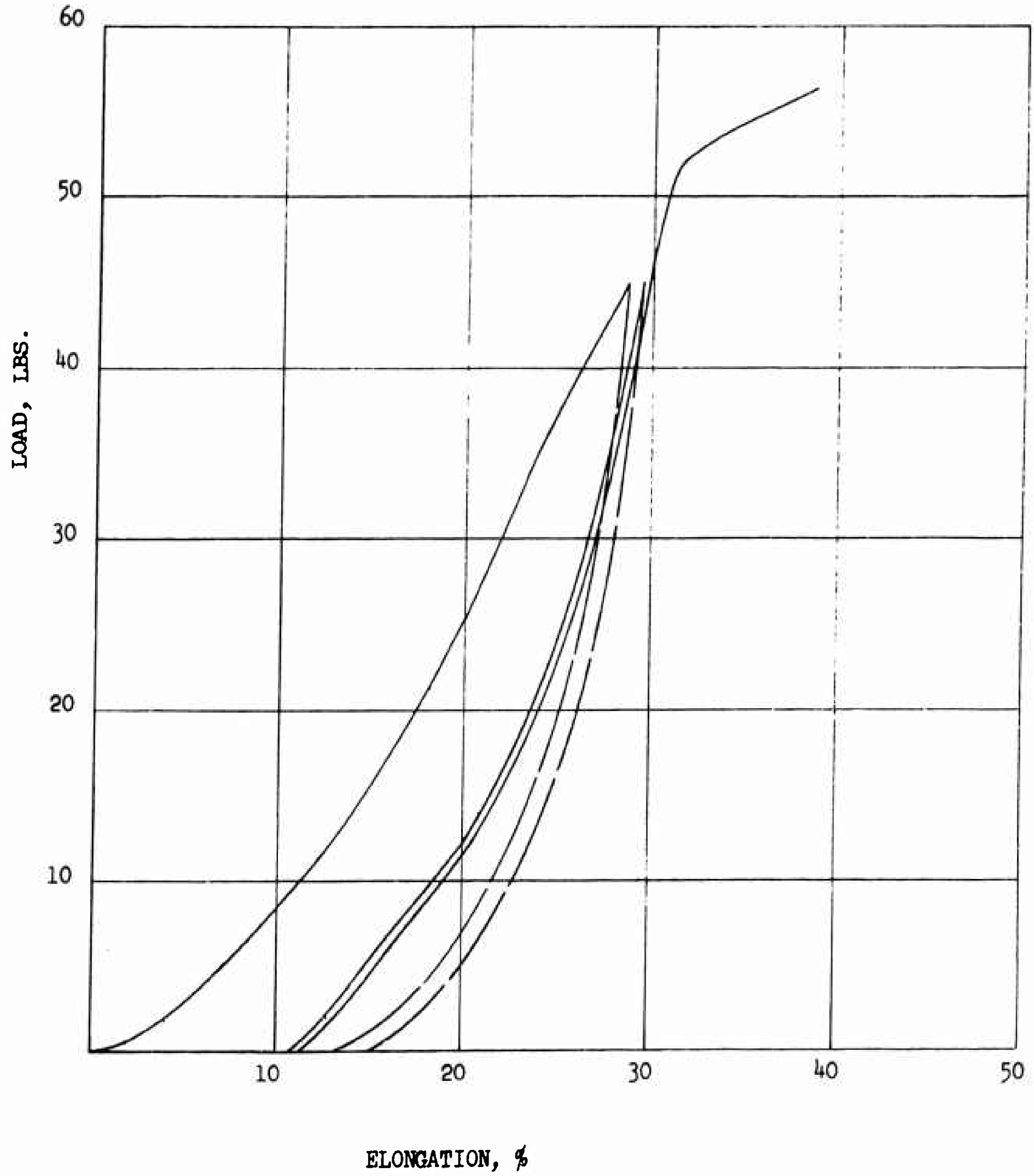

FIGURE 107

TYPICAL REPEATED STRESS-STRAIN CURVES SHOWING 1st & 5th CYCLES TO
1st LOAD LEVEL AND FINAL RUPTURE CYCLE

CHENEY

FABRIC 7N 20, WARP

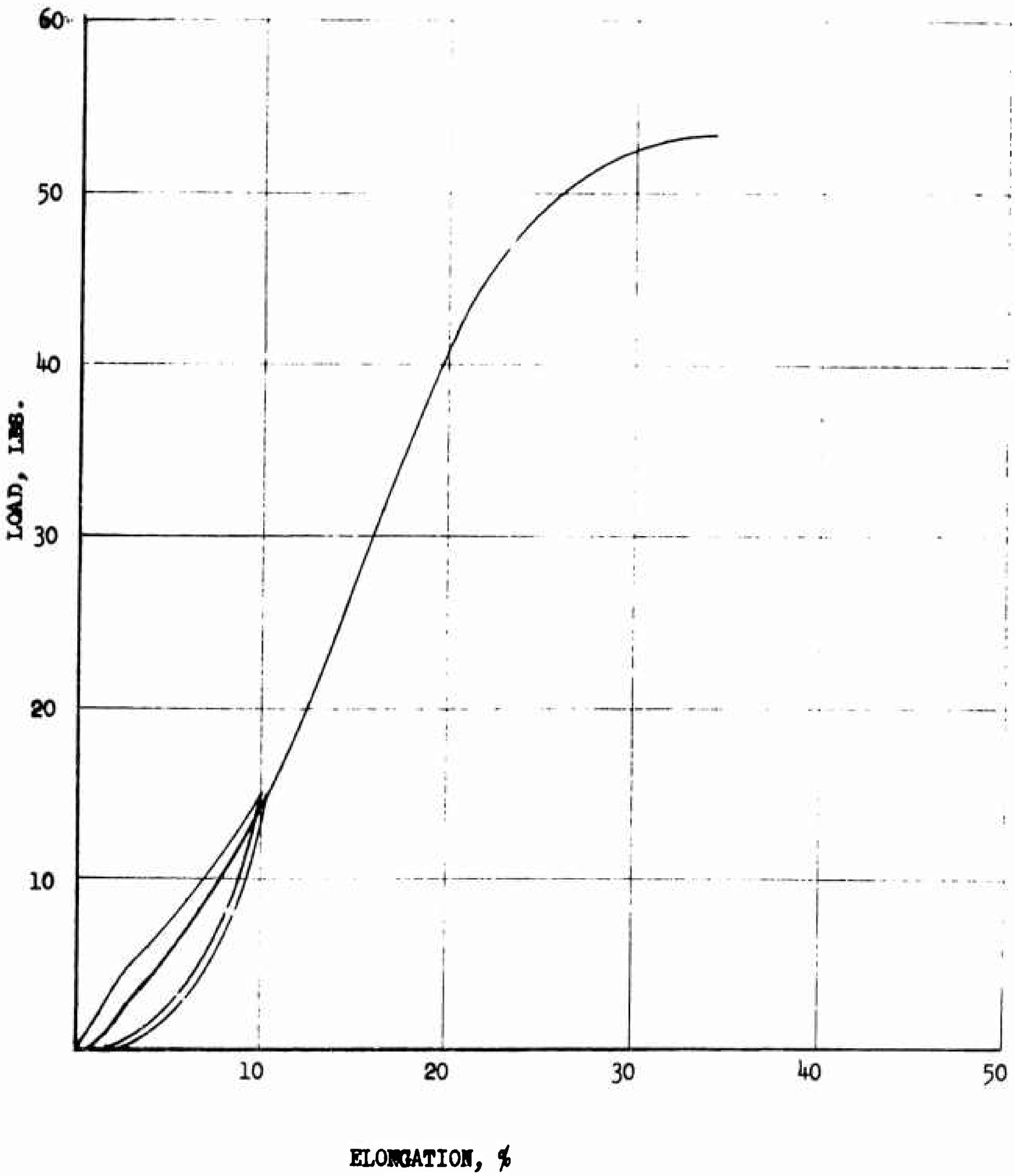

FIGURE 108

TYPICAL REPEATED STRESS-STRAIN CURVES SHOWING 1st & 5th CYCLES TO
1st LOAD LEVEL AND FINAL RUPTURE CYCLE
CHENEY

FABRIC 7N 20, FILLING

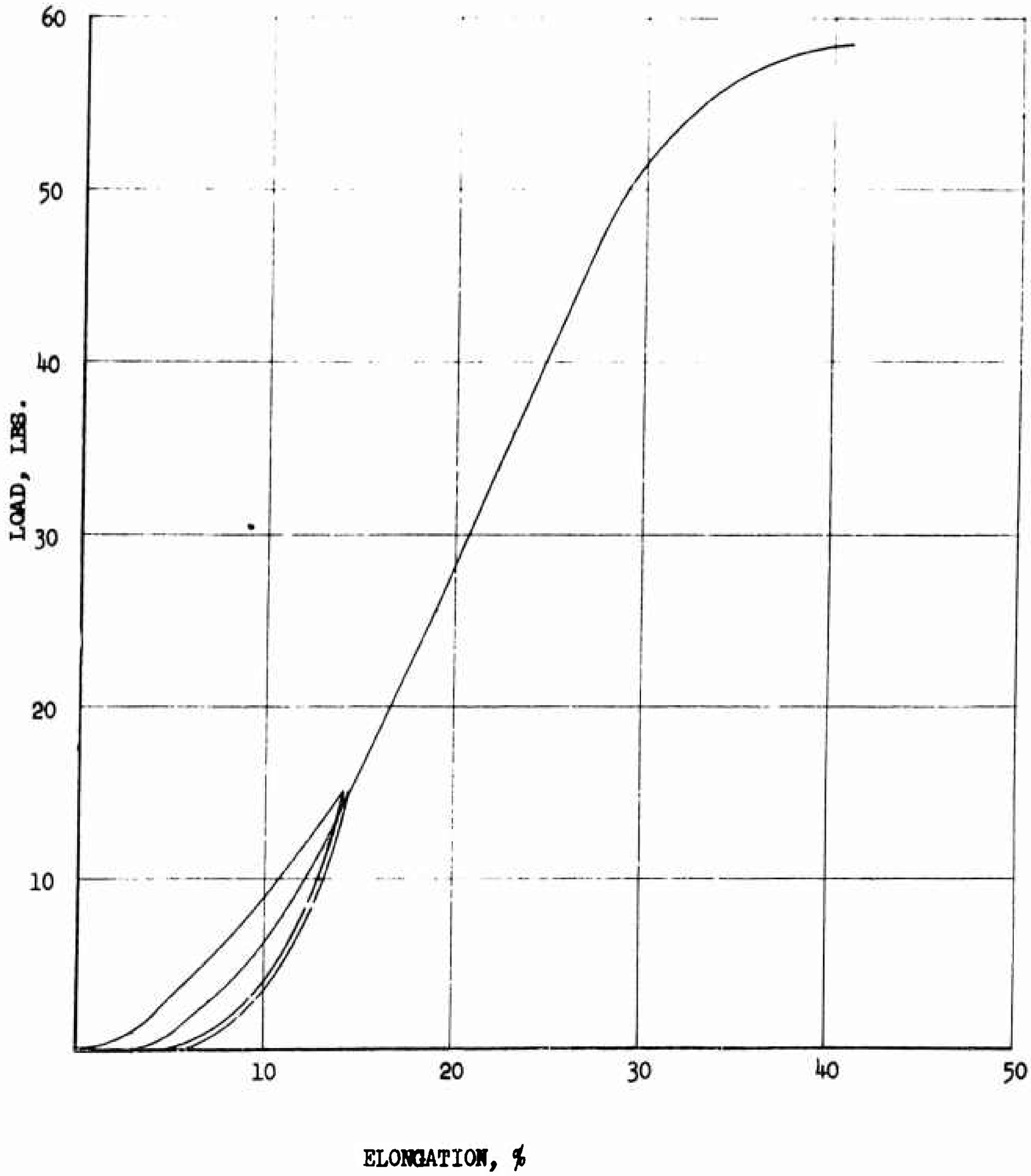

FIGURE 109

TYPICAL REPEATED STRESS-STRAIN CURVES SHOWING 1st & 5th CYCLES TO
2nd LOAD LEVEL AND FINAL RUPTURE CYCLE

CHENEY

FABRIC 7N20, WARP

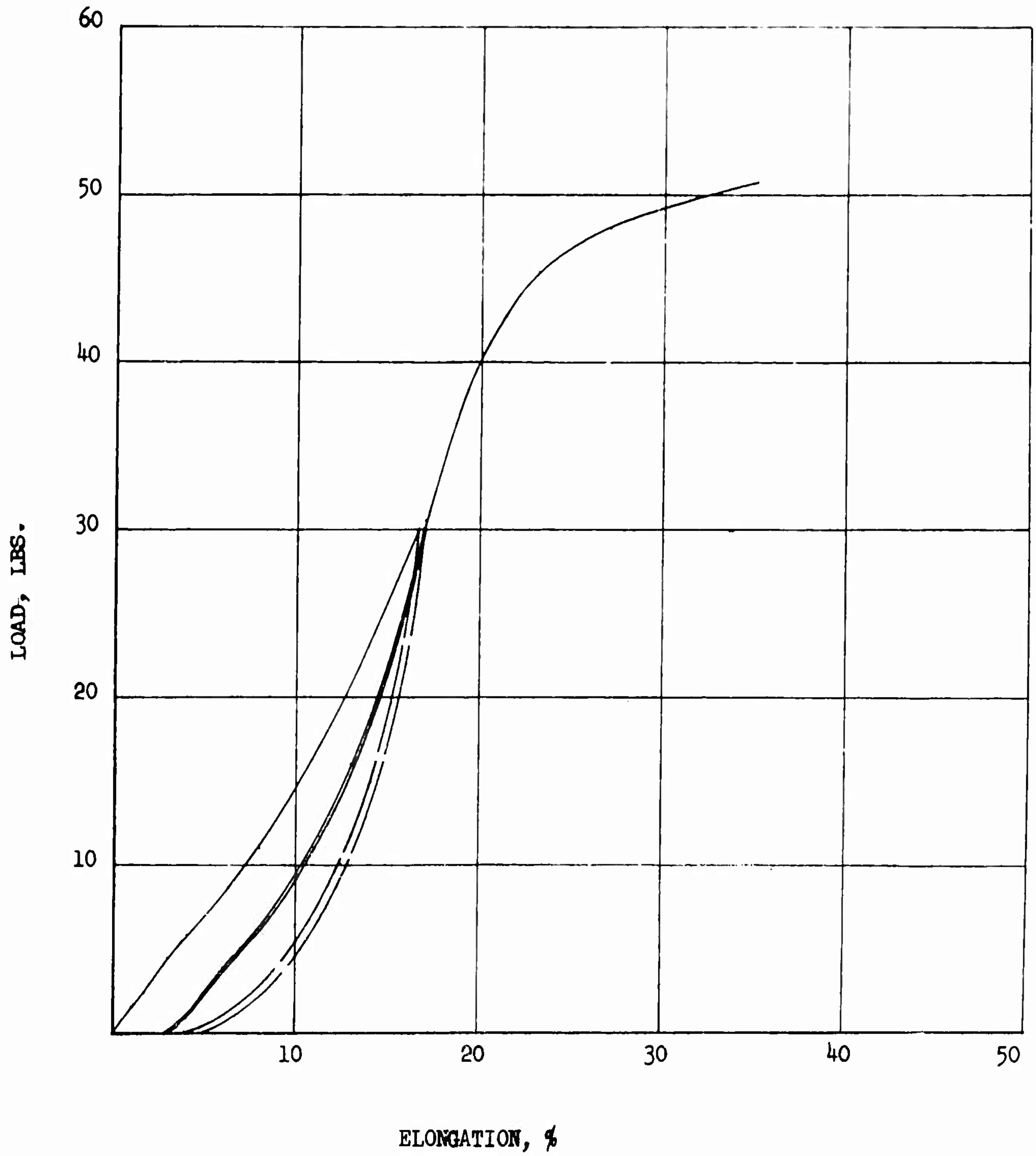

FIGURE 110

TYPICAL REPEATED STRESS-STRAIN CURVES SHOWING 1st & 5th CYCLES TO 2nd LOAD LEVEL AND FINAL RUPTURE CYCLE

CHENEY

FABRIC 7N20, FILLING

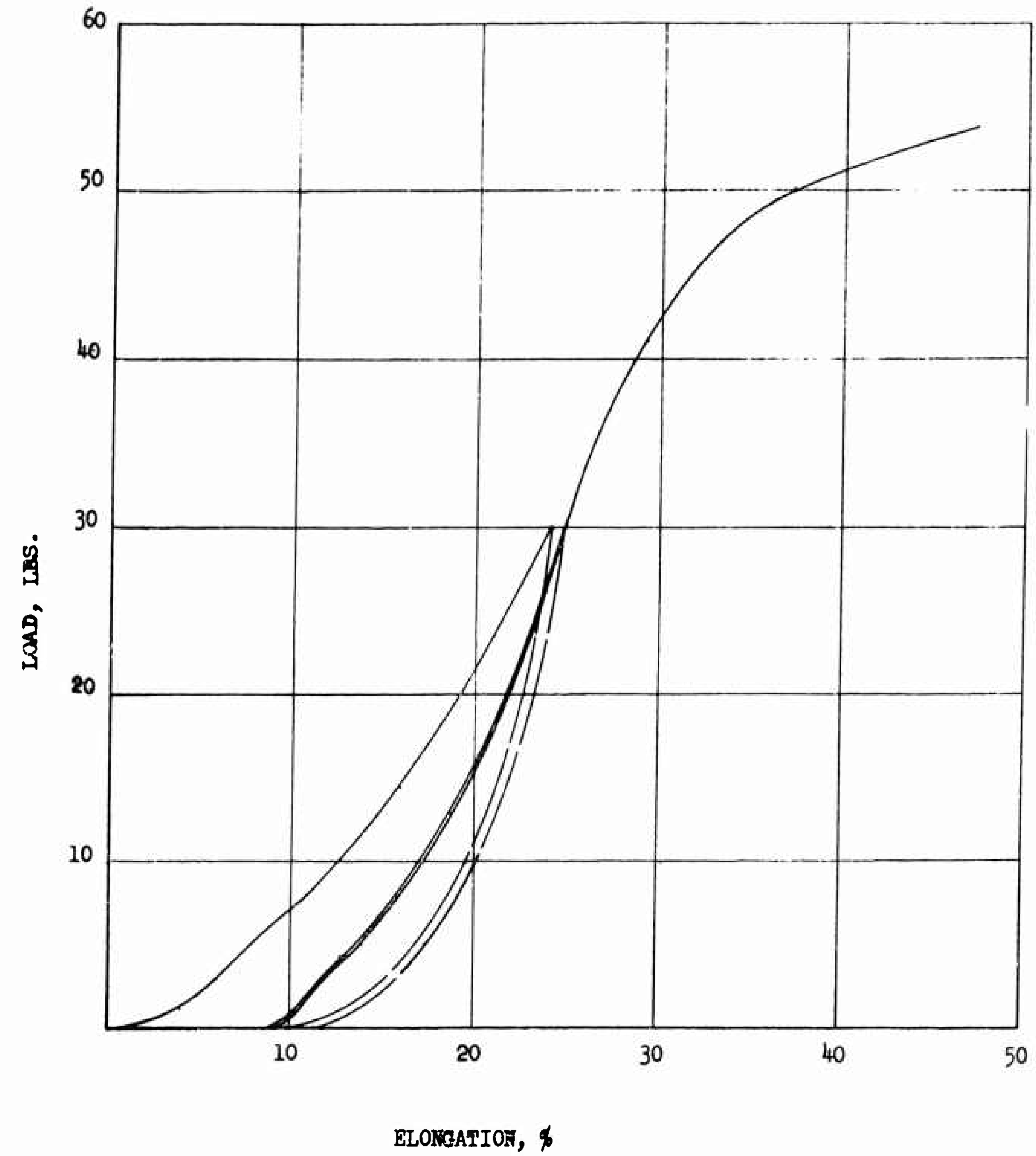

FIGURE 111

TYPICAL REPEATED STRESS-STRAIN CURVES SHOWING 1st & 5th CYCLES TO 3rd LOAD LEVEL AND FINAL RUPTURE CYCLE

CHENEY

FABRIC 7N 20, WARP

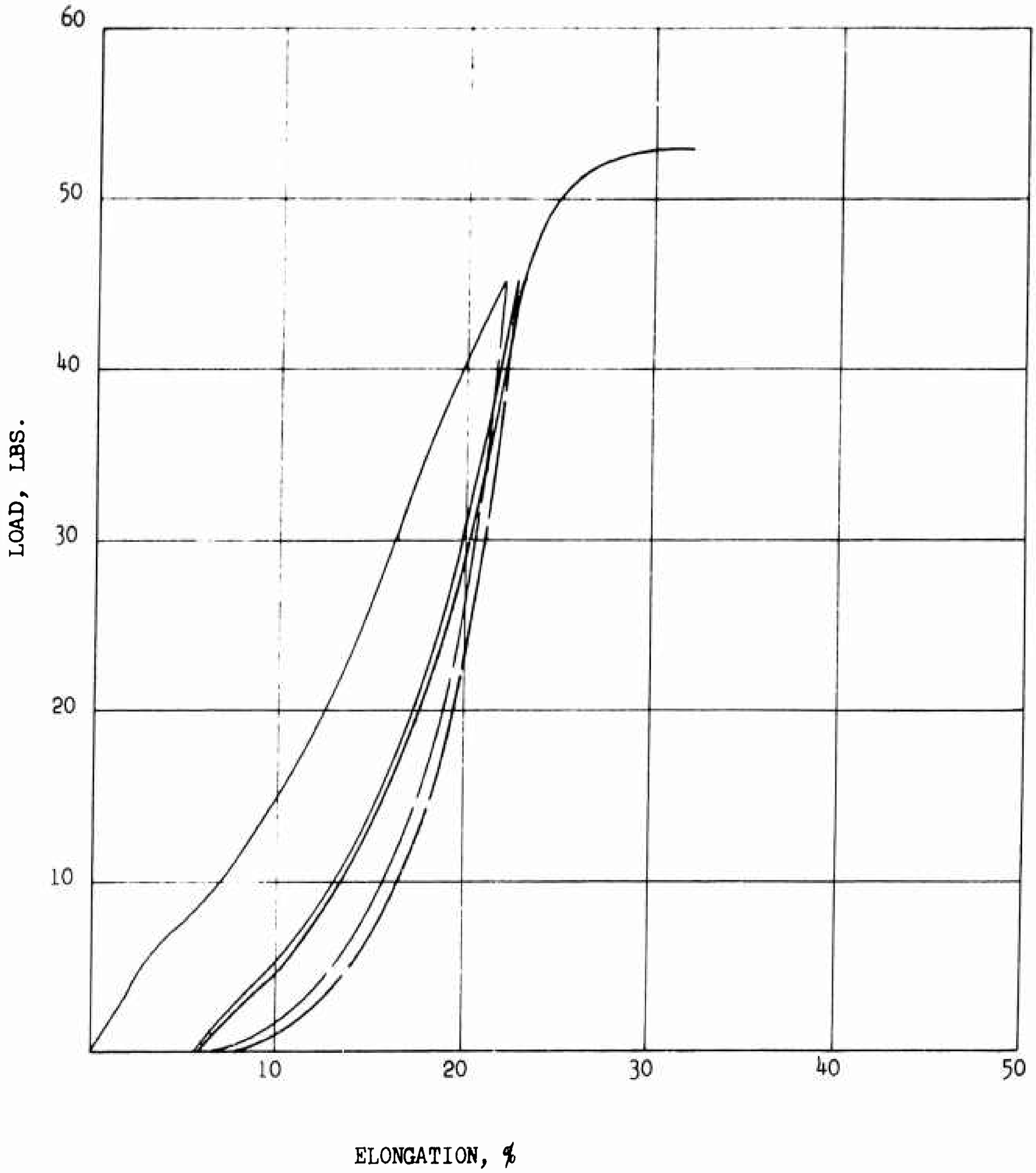

FIGURE 112

TYPICAL REPEATED STRESS-STRAIN CURVES SHOWING 1st & 5th CYCLES TO
3rd LOAD LEVEL AND FINAL RUPTURE CYCLE

CHENEY

FABRIC 7N 20, FILLING

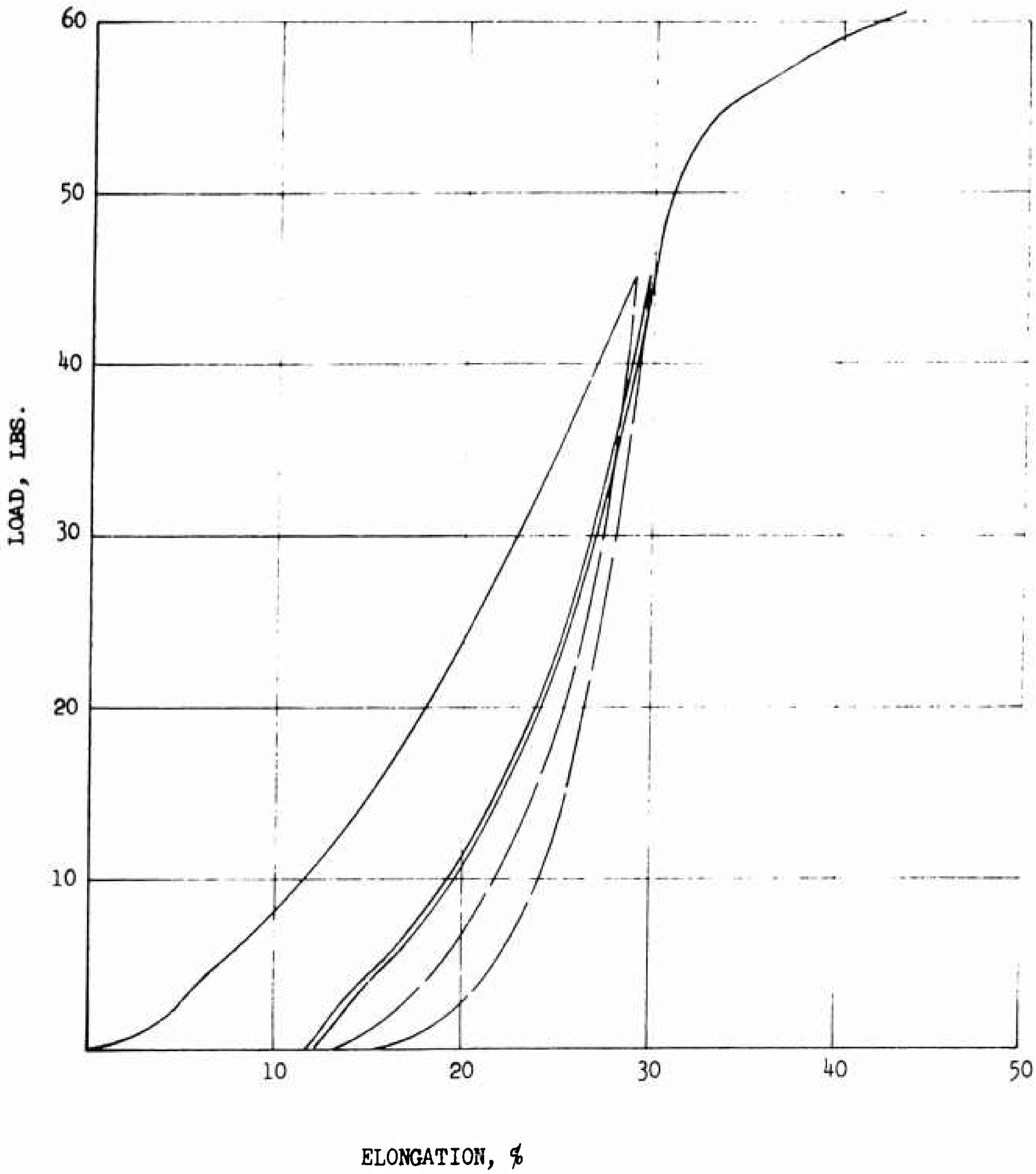

FIGURE 113

TYPICAL REPEATED STRESS-STRAIN CURVES SHOWING 1st & 5th CYCLES TO 1st LOAD LEVEL AND FINAL RUPTURE CYCLE

CHENEY

FABRIC 7N 35, WARP

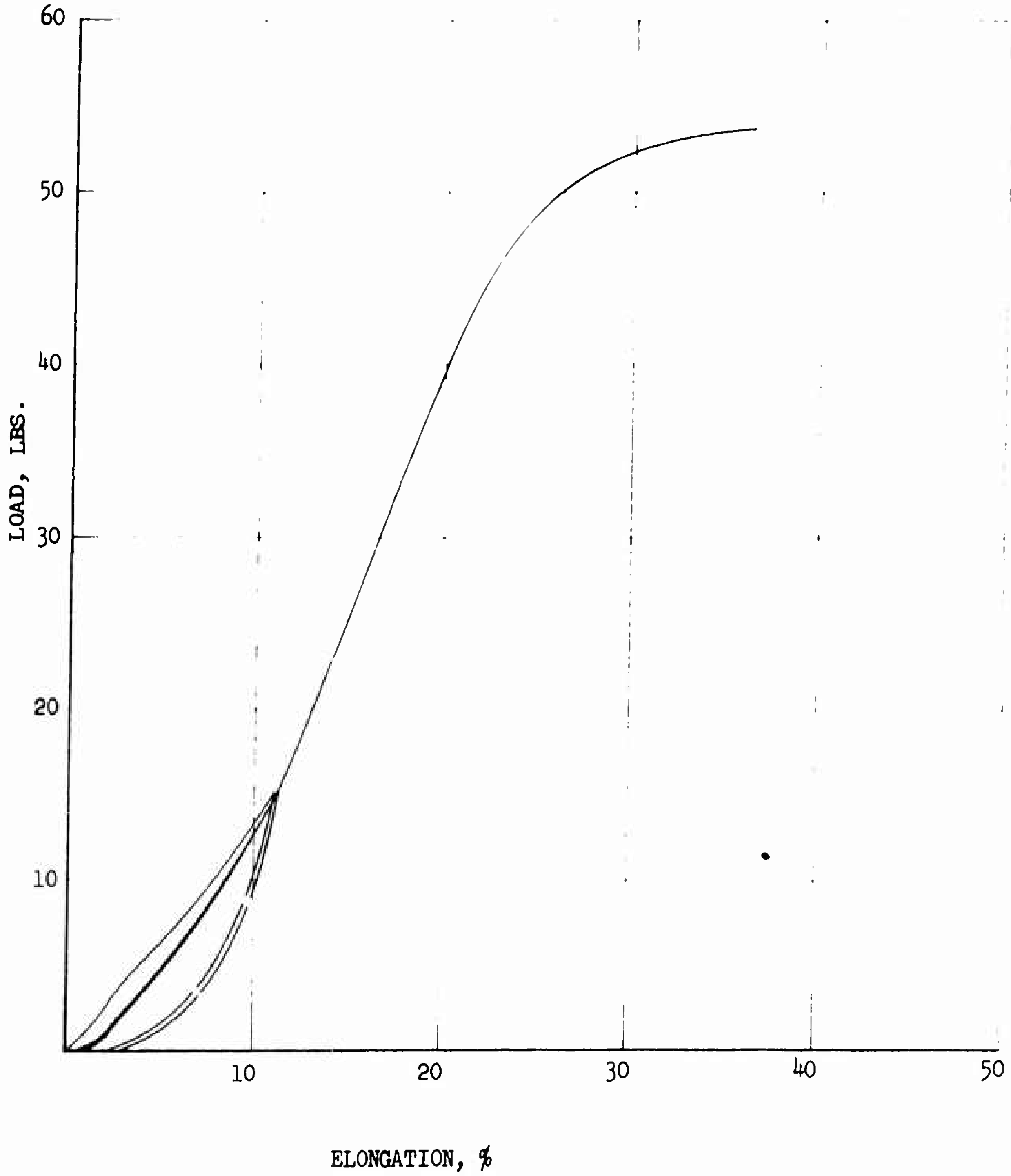

FIGURE 114

TYPICAL REPEATED STRESS-STRAIN CURVES SHOWING 1st & 5th CYCLES TO 1st LOAD LEVEL AND FINAL RUPTURE CYCLE

CHENEY

FABRIC 7N 35, FILLING

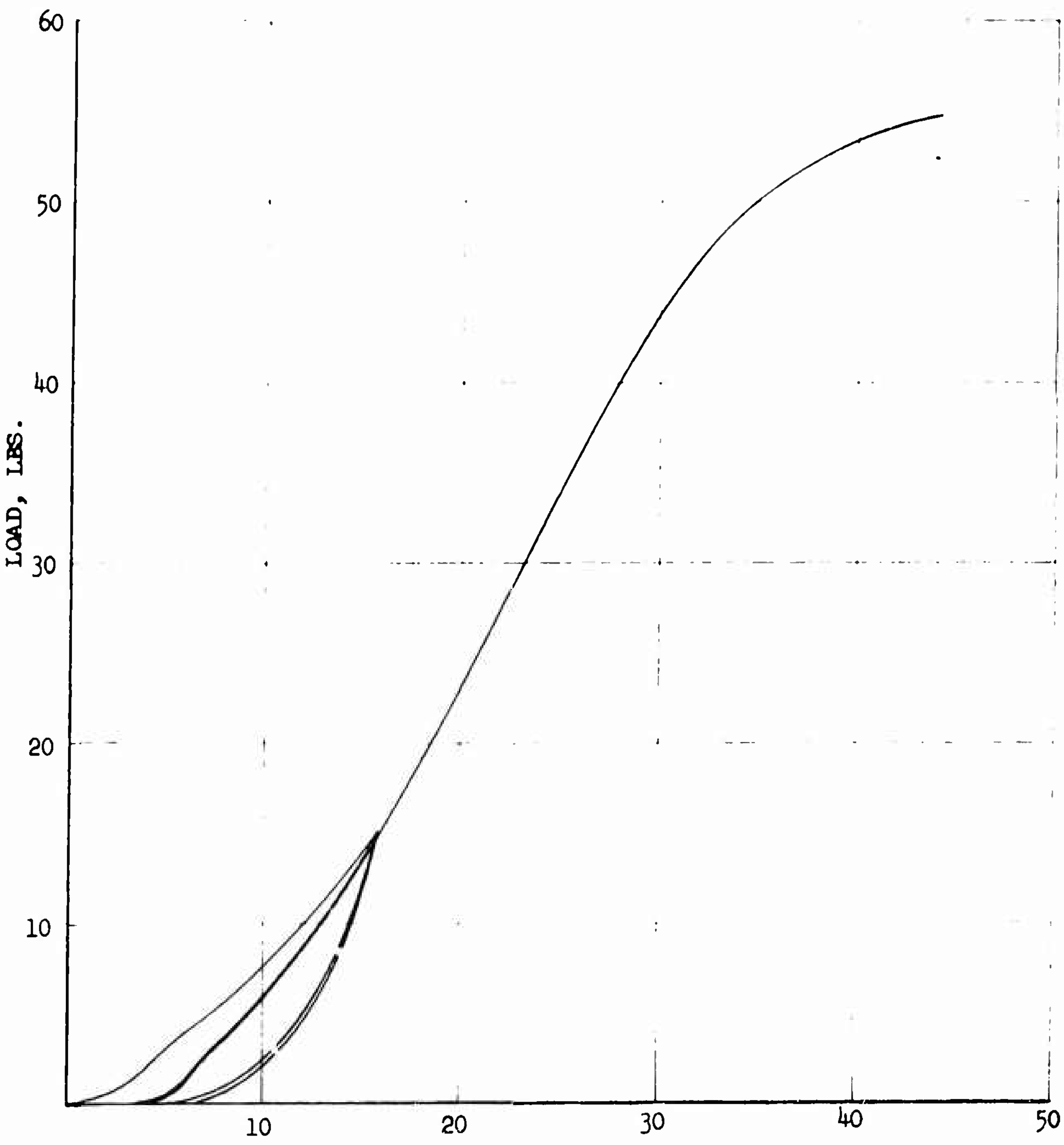

FIGURE 115

TYPICAL REPEATED STRESS-STRAIN CURVES SHOWING 1st & 5th CYCLES TO
2nd LOAD LEVEL AND FINAL RUPTURE CYCLE

CHENEY

FABRIC 7N35, WARP

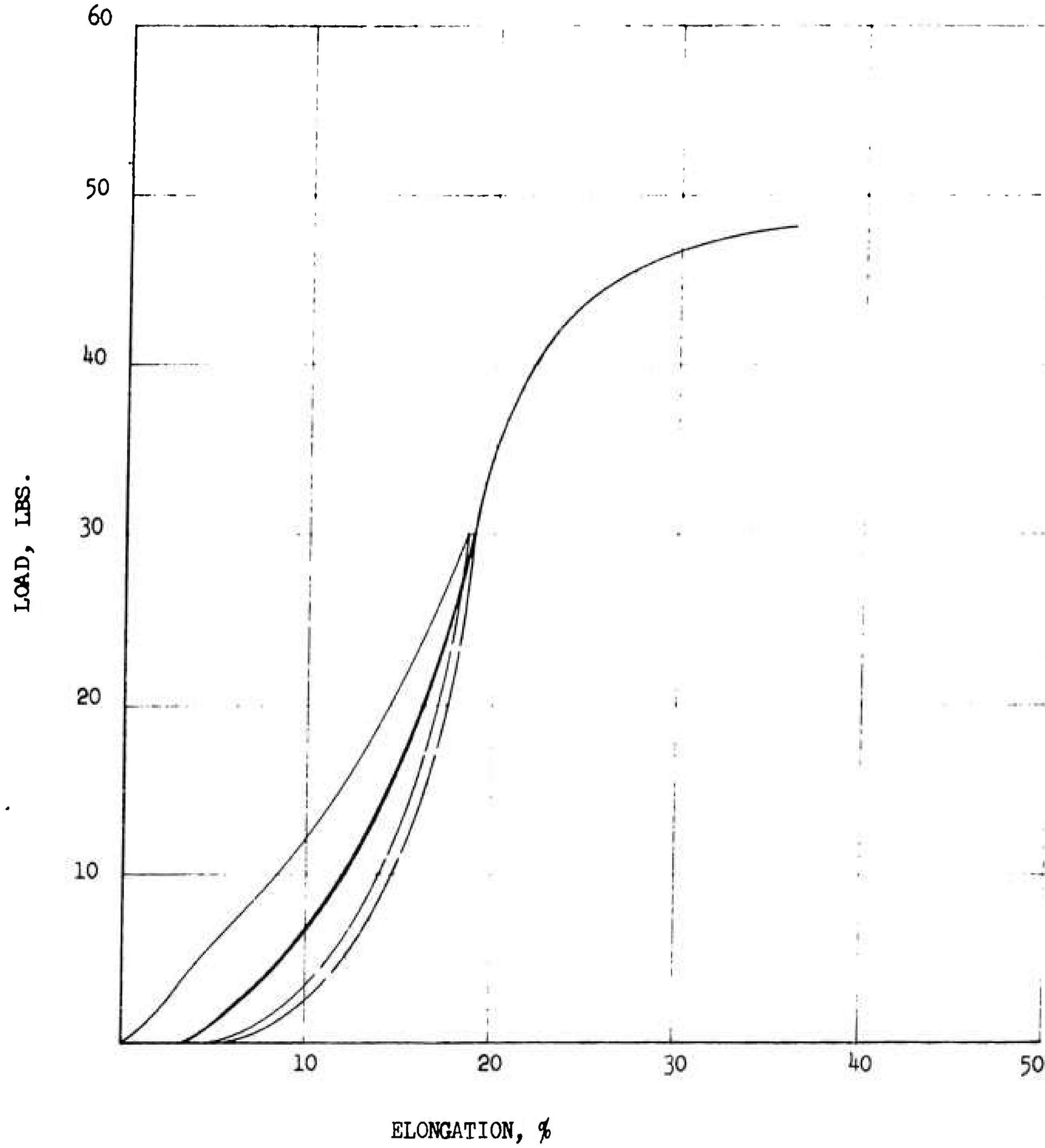

FIGURE 116

TYPICAL REPEATED STRESS-STRAIN CURVES SHOWING 1st & 5th CYCLES TO 2nd LOAD LEVEL AND FINAL RUPTURE CYCLE

CHENEY

FABRIC 7N35, FILLING

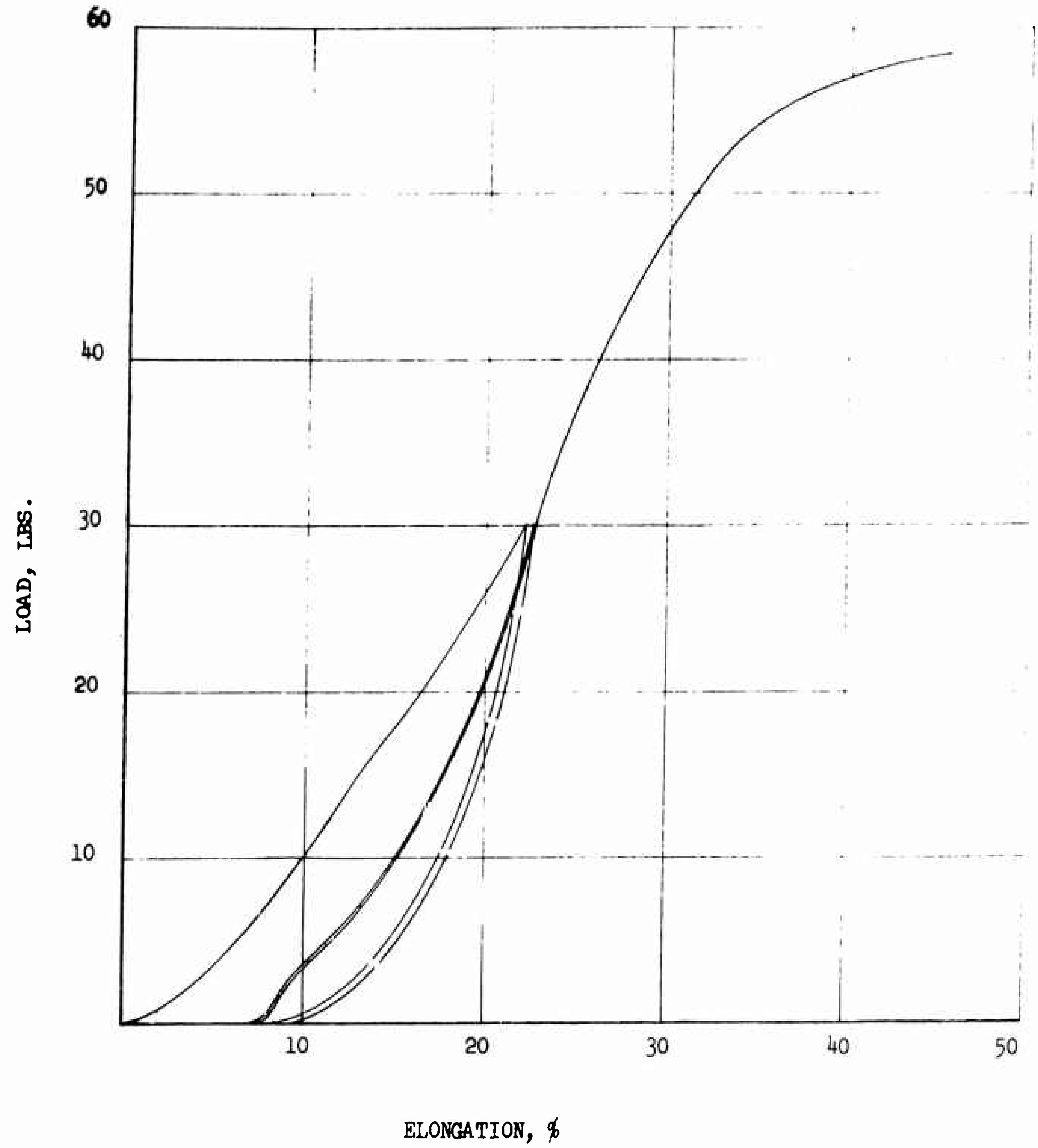

FIGURE 117

TYPICAL REPEATED STRESS-STRAIN CURVES SHOWING 1st & 5th CYCLES TO
3rd LOAD LEVEL AND FINAL RUPTURE CYCLE

CHENEY

FABRIC 7N 35, WARP

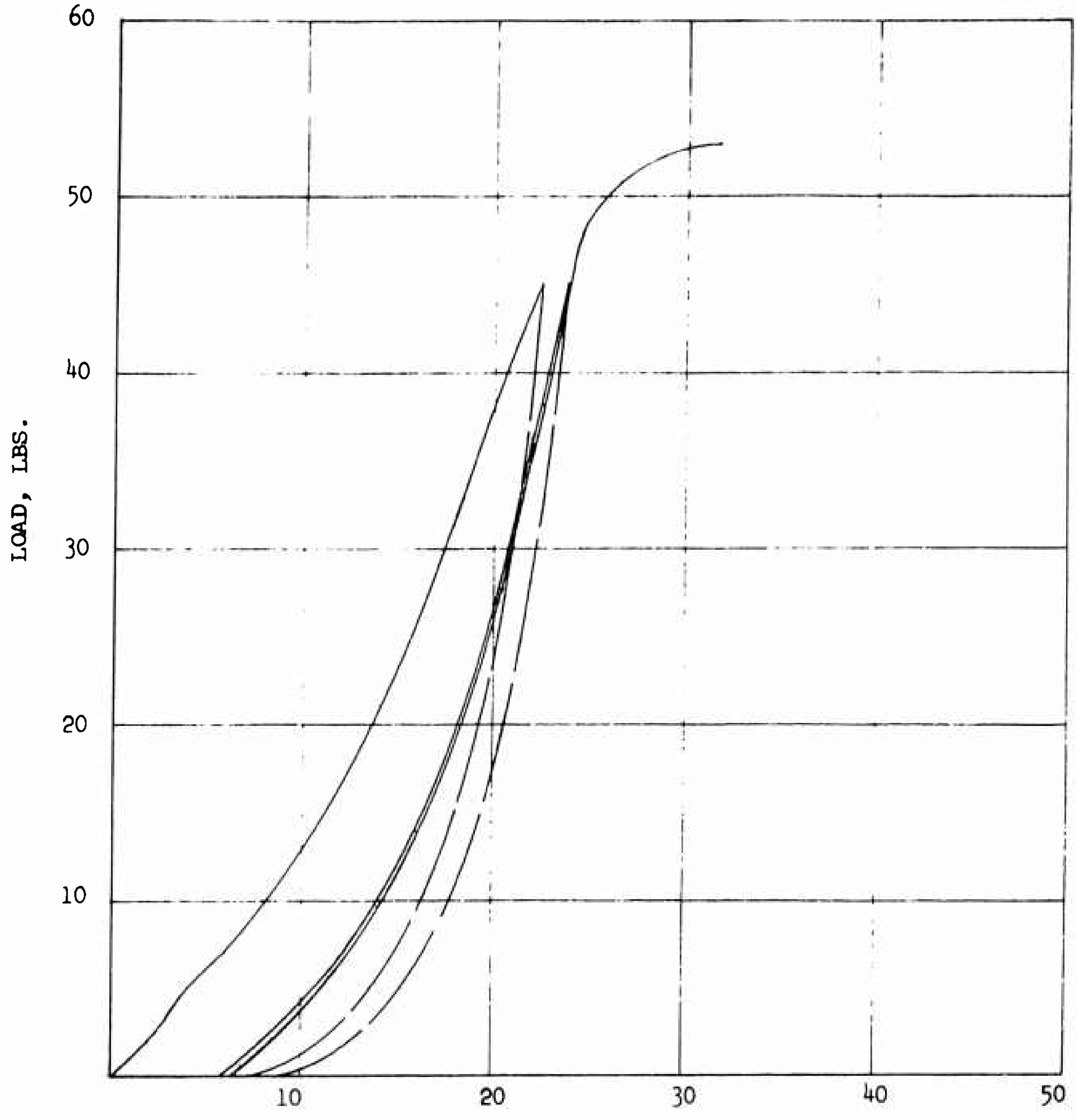

ELONGATION, %

FIGURE 118

TYPICAL REPEATED STRESS-STRAIN CURVES SHOWING 1st & 5th CYCLES TO 3rd LOAD LEVEL AND FINAL RUPTURE CYCLE

CHENEY

FABRIC 7N 35, FILLING

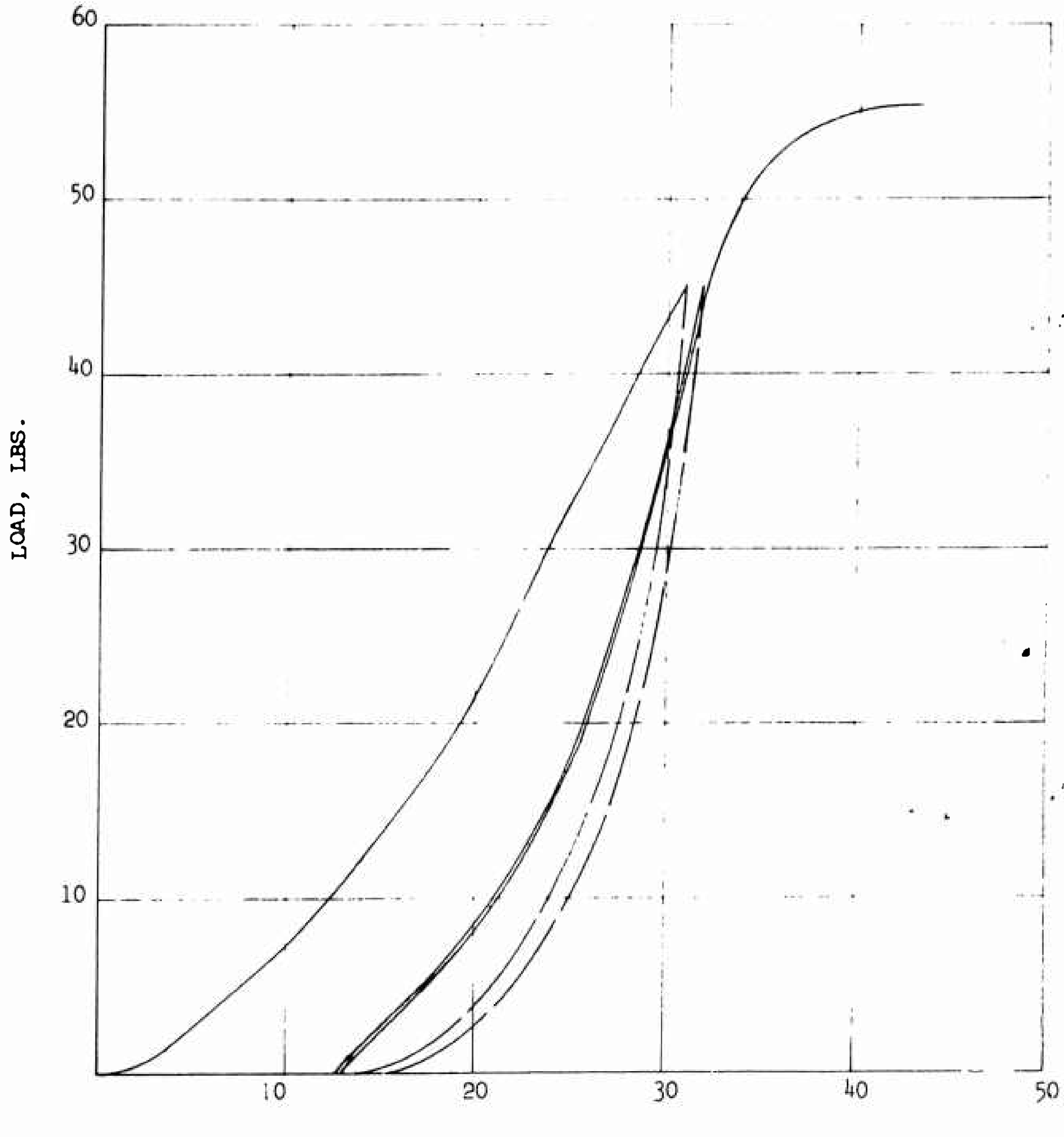

FIGURE 119

TYPICAL REPEATED STRESS-STRAIN CURVES SHOWING 1st & 5th CYCLES TO 1st LOAD LEVEL AND FINAL RUPTURE CYCLE

CHENEY

FABRIC 10N 1/2, WARP

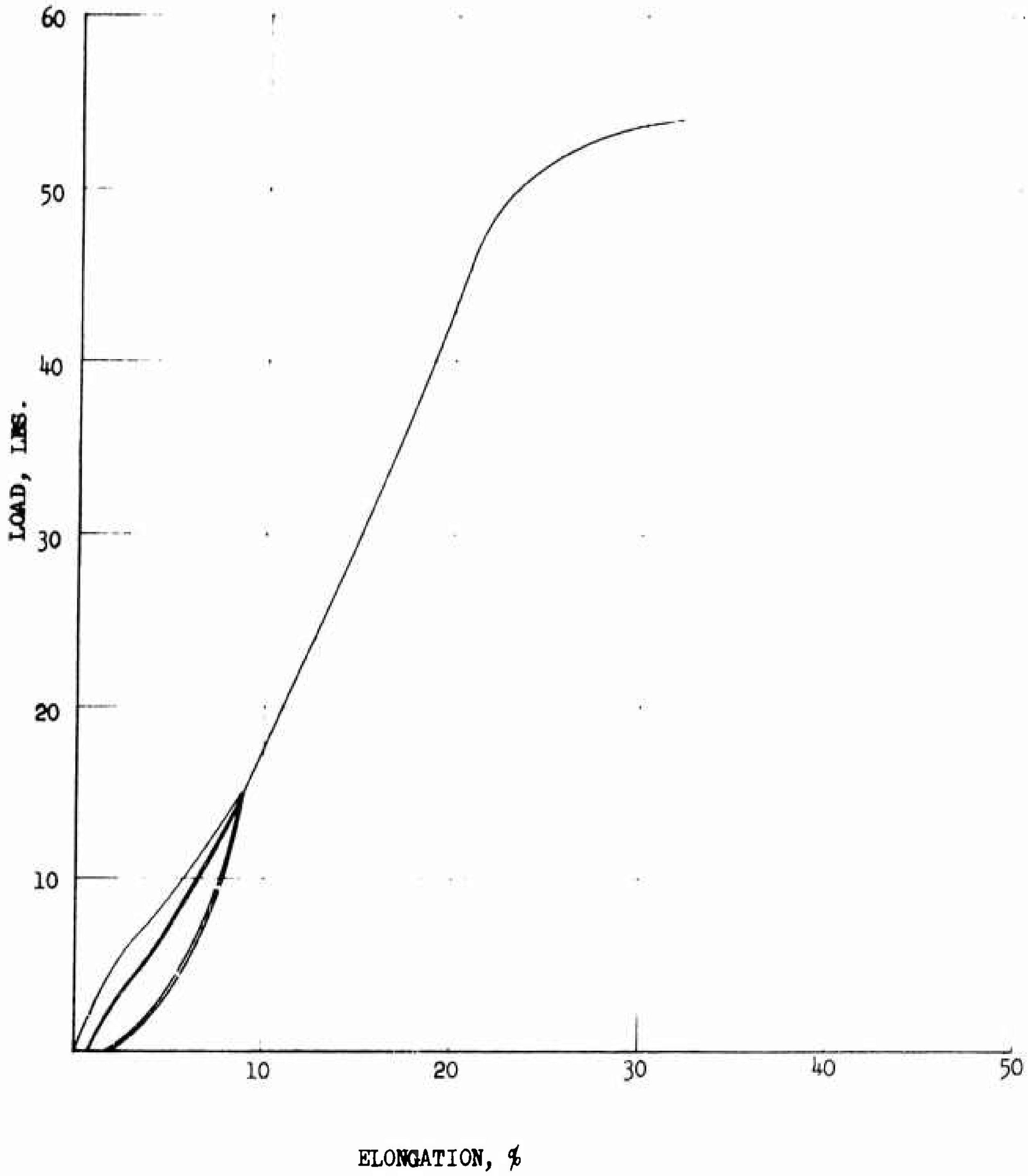

FIGURE 120

TYPICAL REPEATED STRESS-STRAIN CURVES SHOWING 1st & 5th CYCLES TO 1st LOAD LEVEL AND FINAL RUPTURE CYCLE

CHENEY

FABRIC 10N 1/2, FILLING

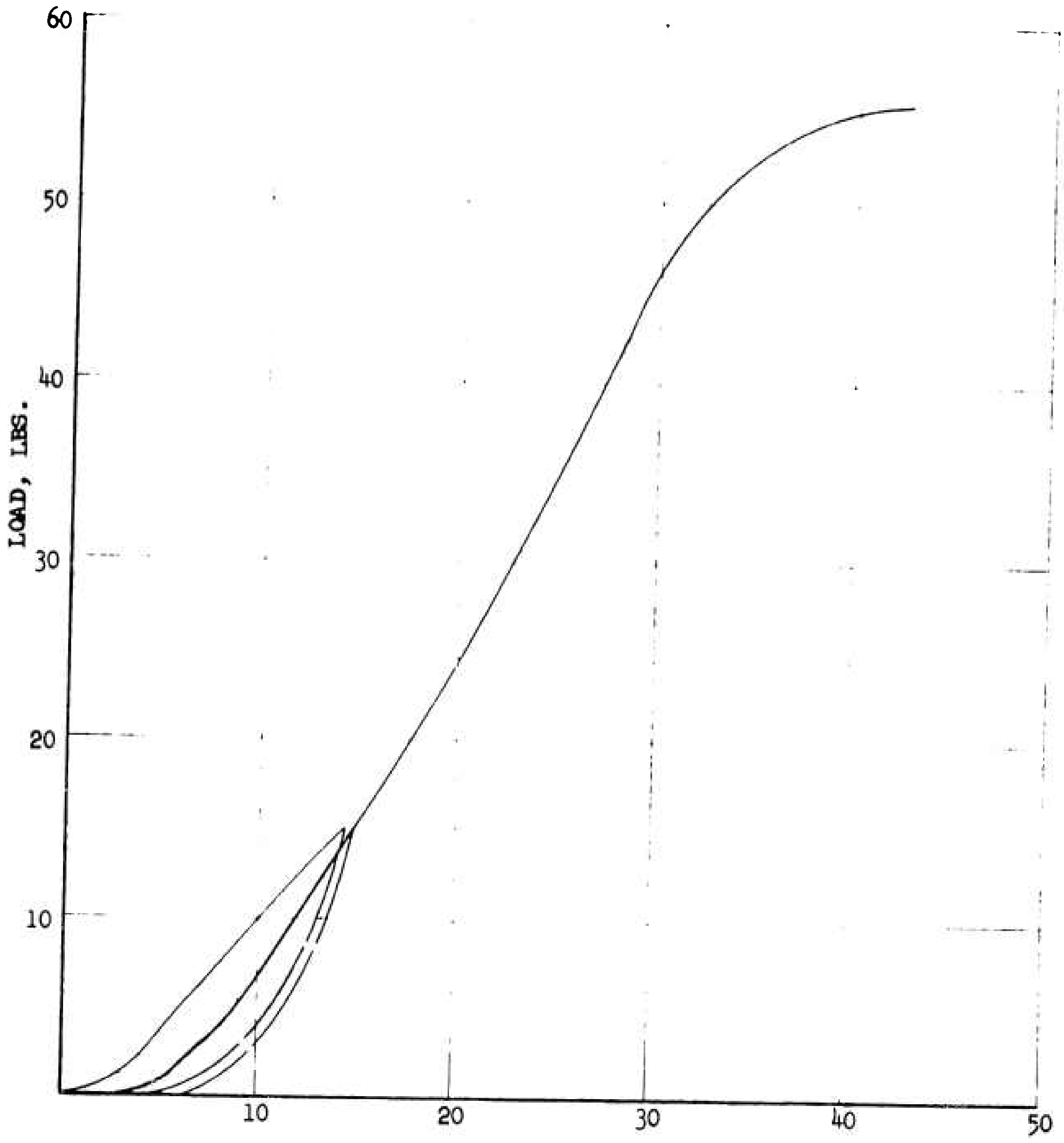

FIGURE 121

TYPICAL REPEATED STRESS-STRAIN CURVES SHOWING 1st & 5th CYCLES TO 2nd LOAD LEVEL AND FINAL RUPTURE CYCLE

CHENEY

FABRIC 10N 1/2, WARP

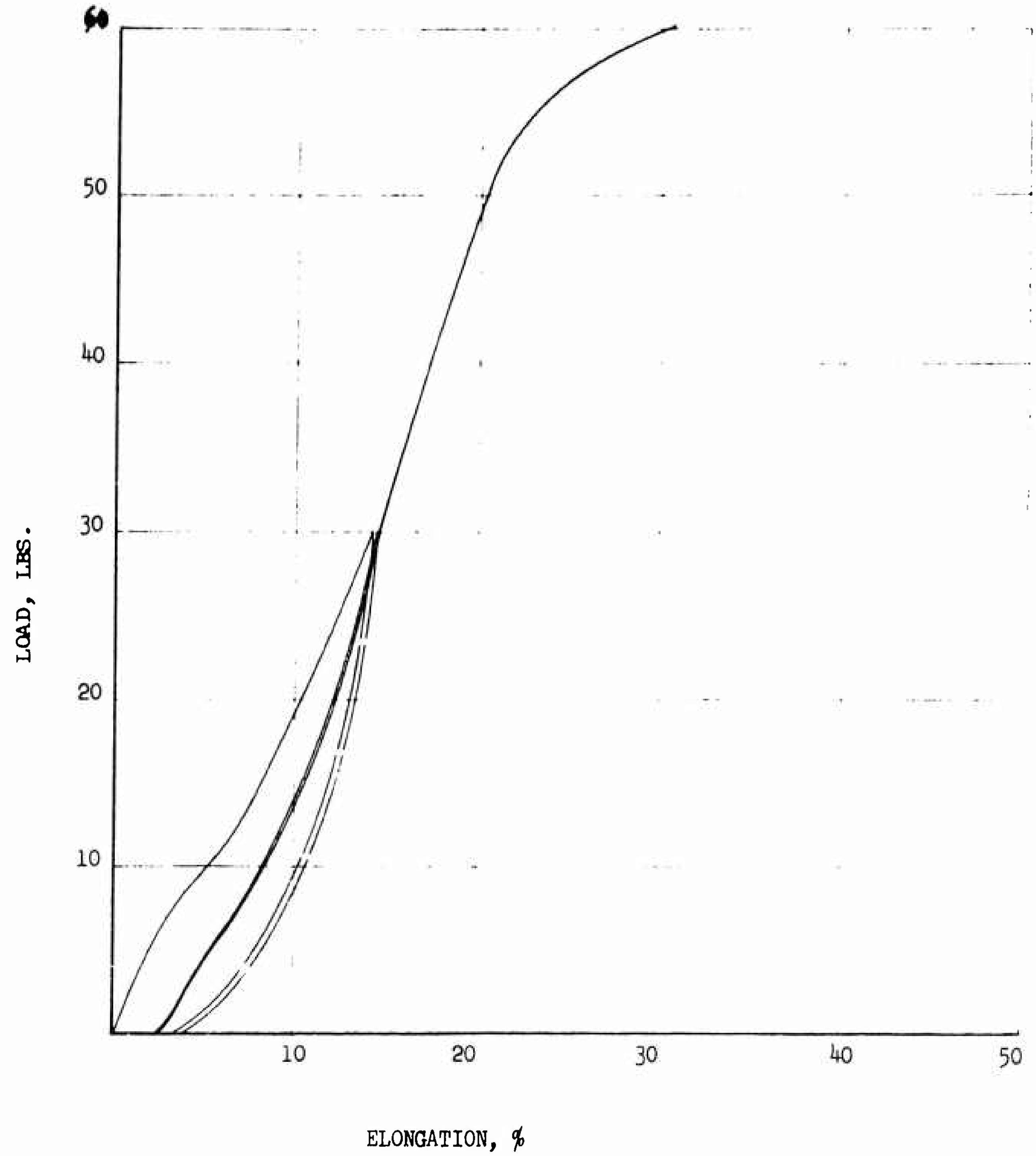

FIGURE 122

TYPICAL REPEATED STRESS-STRAIN CURVES SHOWING 1st & 5th CYCLES TO
2nd LOAD LEVEL AND FINAL RUPTURE CYCLE

CHENEY

FABRIC 10N 1/2, FILLING

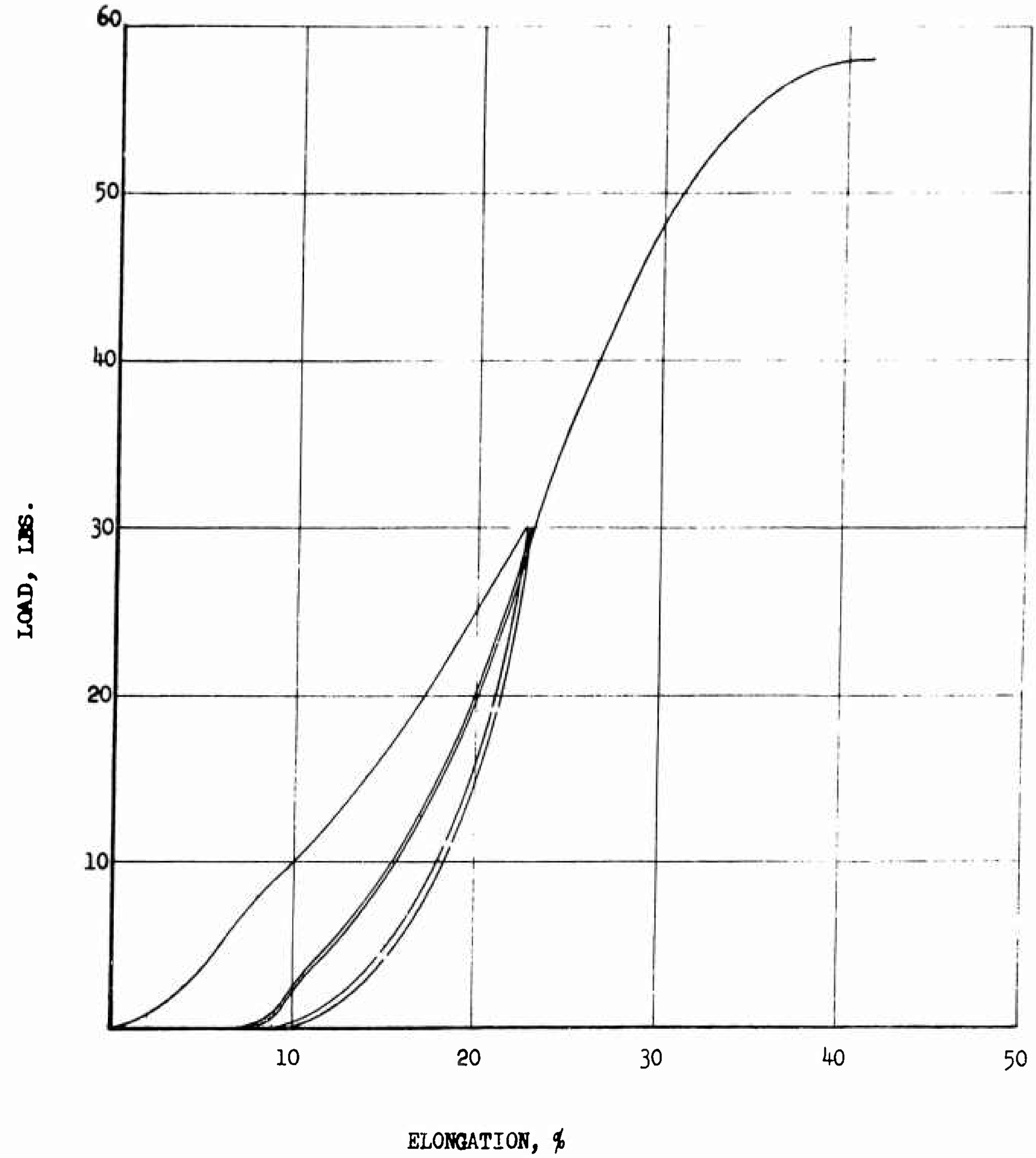

FIGURE 123

TYPICAL REPEATED STRESS-STRAIN CURVES SHOWING 1st & 5th CYCLES TO 3rd LOAD LEVEL AND FINAL RUPTURE CYCLE

CHENEY

FABRIC 10N 1/2, WARP

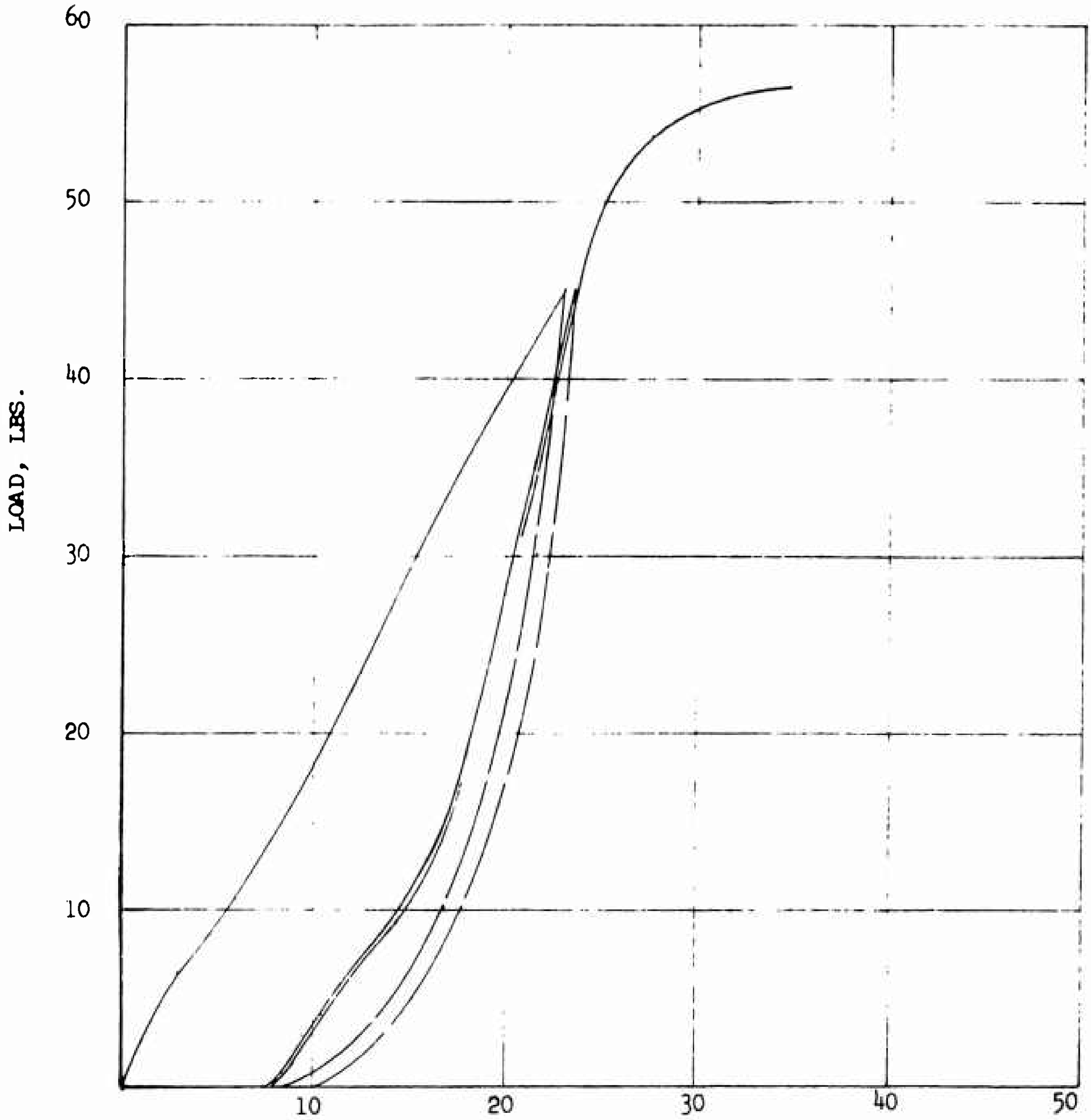

ELONGATION, %

FIGURE 124

TYPICAL REPEATED STRESS-STRAIN CURVES SHOWING 1st & 5th CYCLES TO 3rd LOAD LEVEL AND FINAL RUPTURE CYCLE

CHENEY

FABRIC 10N 1/2, FILLING

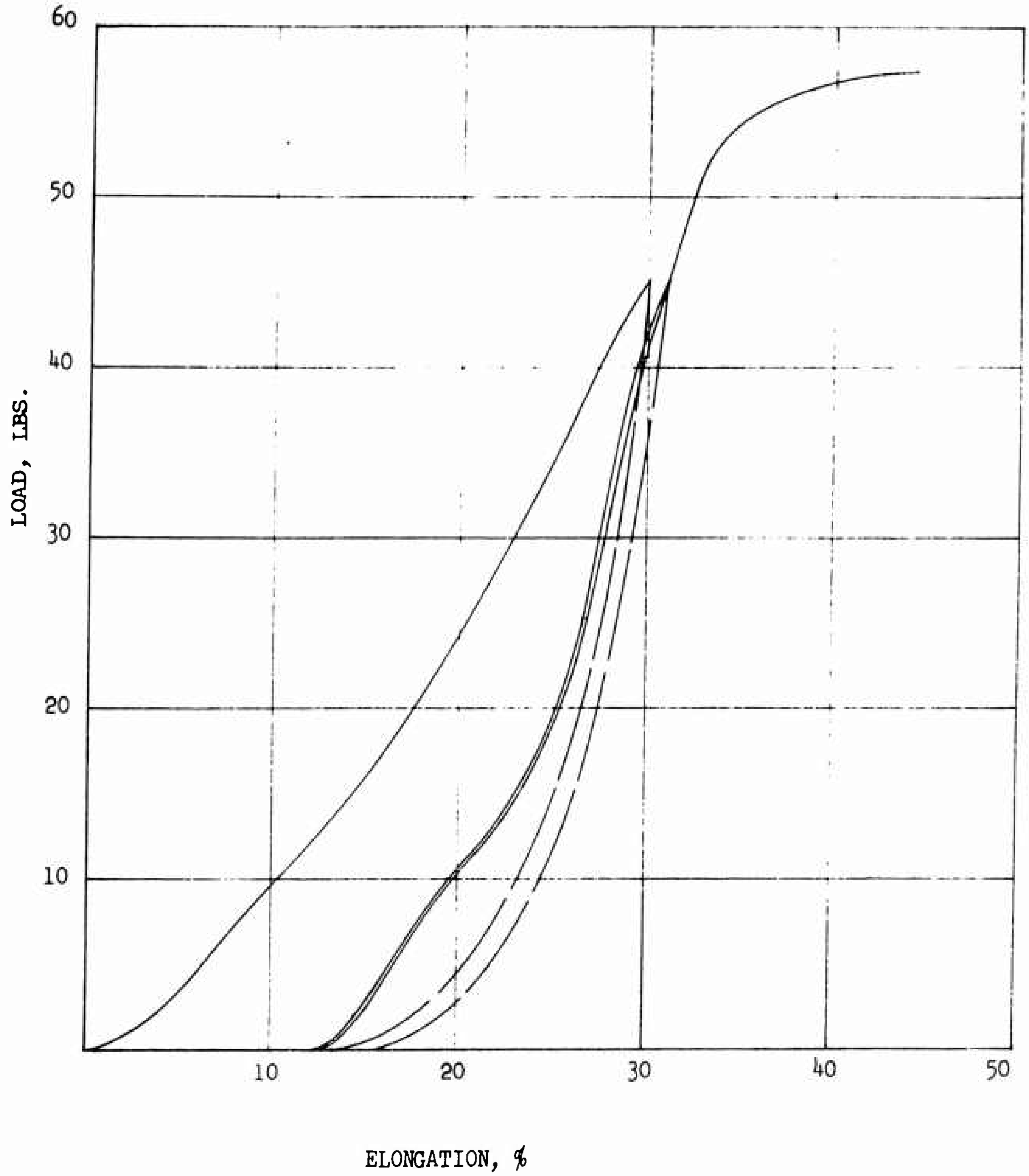

FIGURE 125

TYPICAL REPEATED STRESS-STRAIN CURVES SHOWING 1st & 5th CYCLES TO 1st LOAD LEVEL AND FINAL RUPTURE CYCLE

CHENEY

FABRIC 10N 2 1/2, WARP

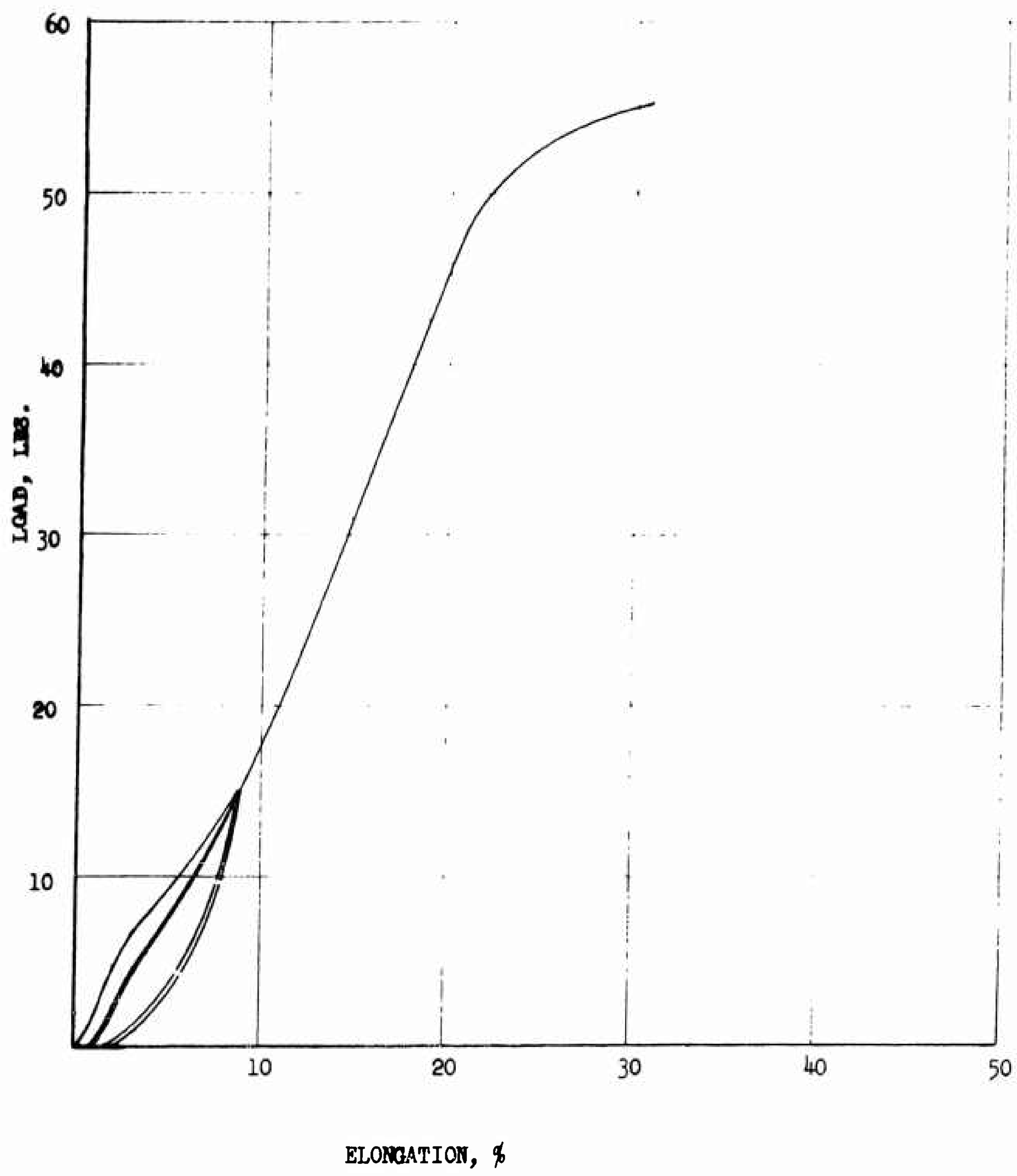

FIGURE 126

TYPICAL REPEATED STRESS-STRAIN CURVES SHOWING 1st & 5th CYCLES TO 1st LOAD LEVEL AND FINAL RUPTURE CYCLE

CHENEY

FABRIC 10N 2 1/2, FILLING

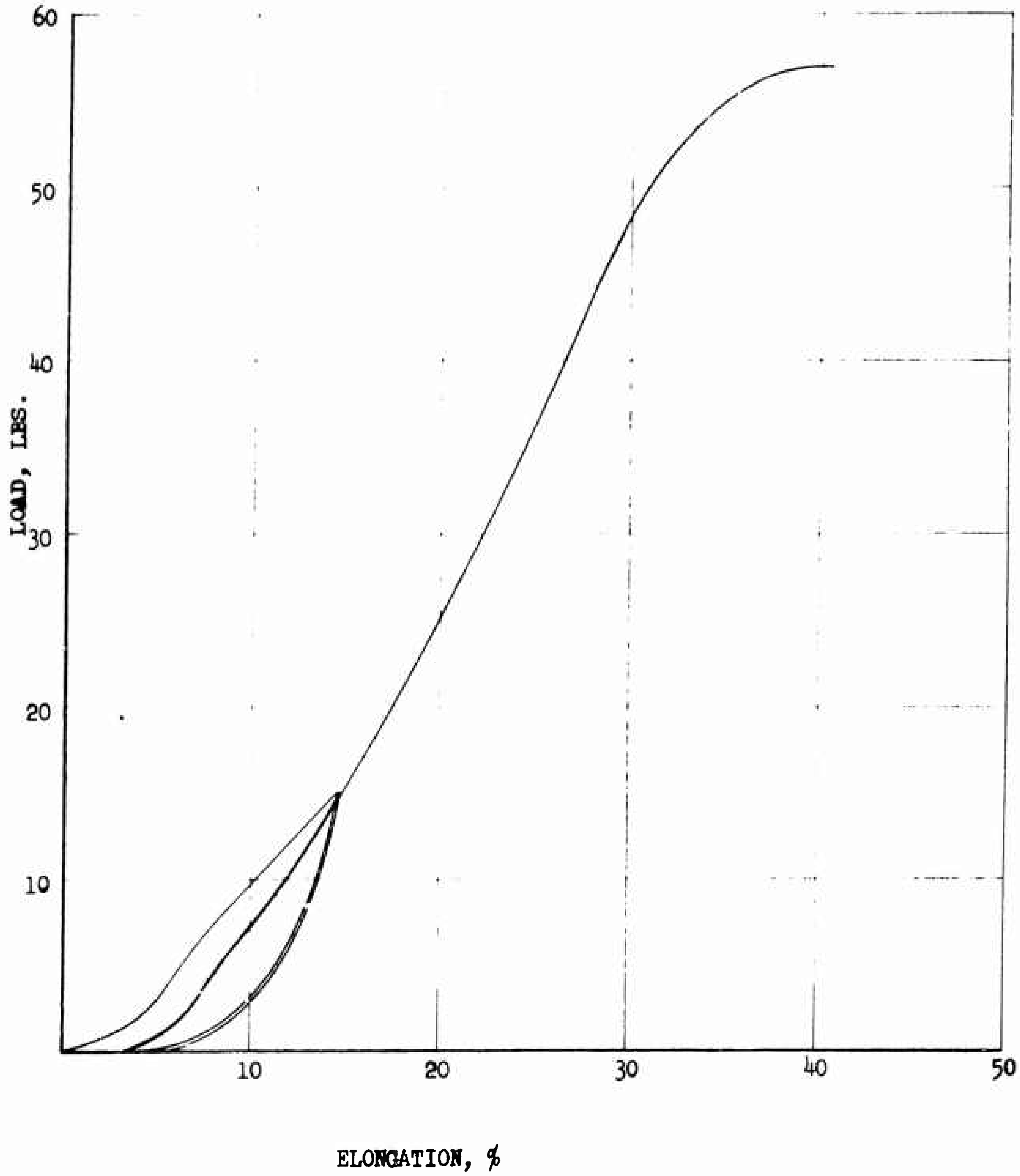

FIGURE 127

TYPICAL REPEATED STRESS-STRAIN CURVES SHOWING 1st & 5th CYCLES TO
2nd LOAD LEVEL AND FINAL RUPTURE CYCLE

CHENEY

FABRIC 10N 2 1/2, WARP

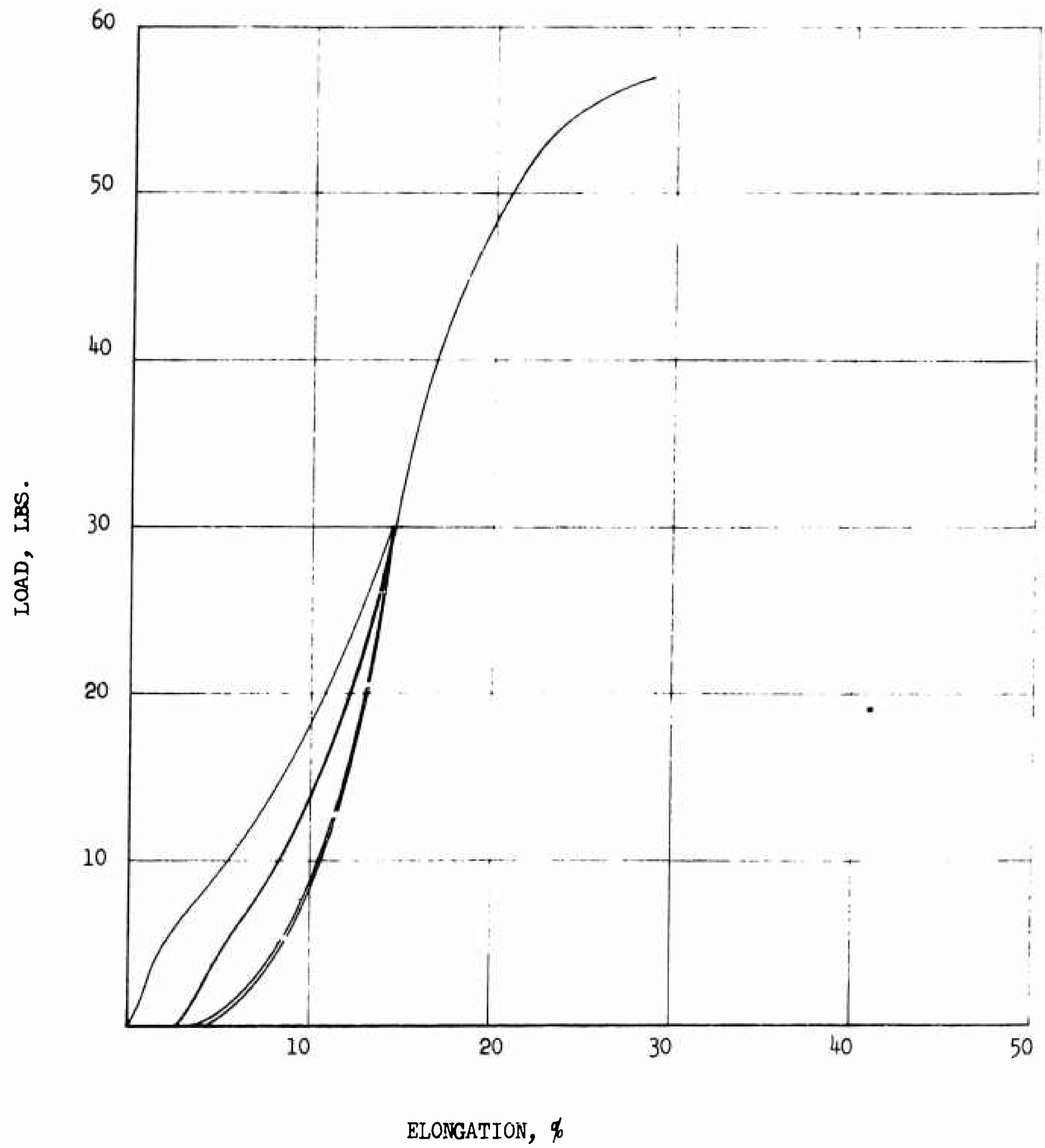

FIGURE 128

TYPICAL REPEATED STRESS-STRAIN CURVES SHOWING 1st & 5th CYCLES TO
2nd LOAD LEVEL AND FINAL RUPTURE CYCLE

CHENEY
FABRIC 10N 2 1/2, FILLING

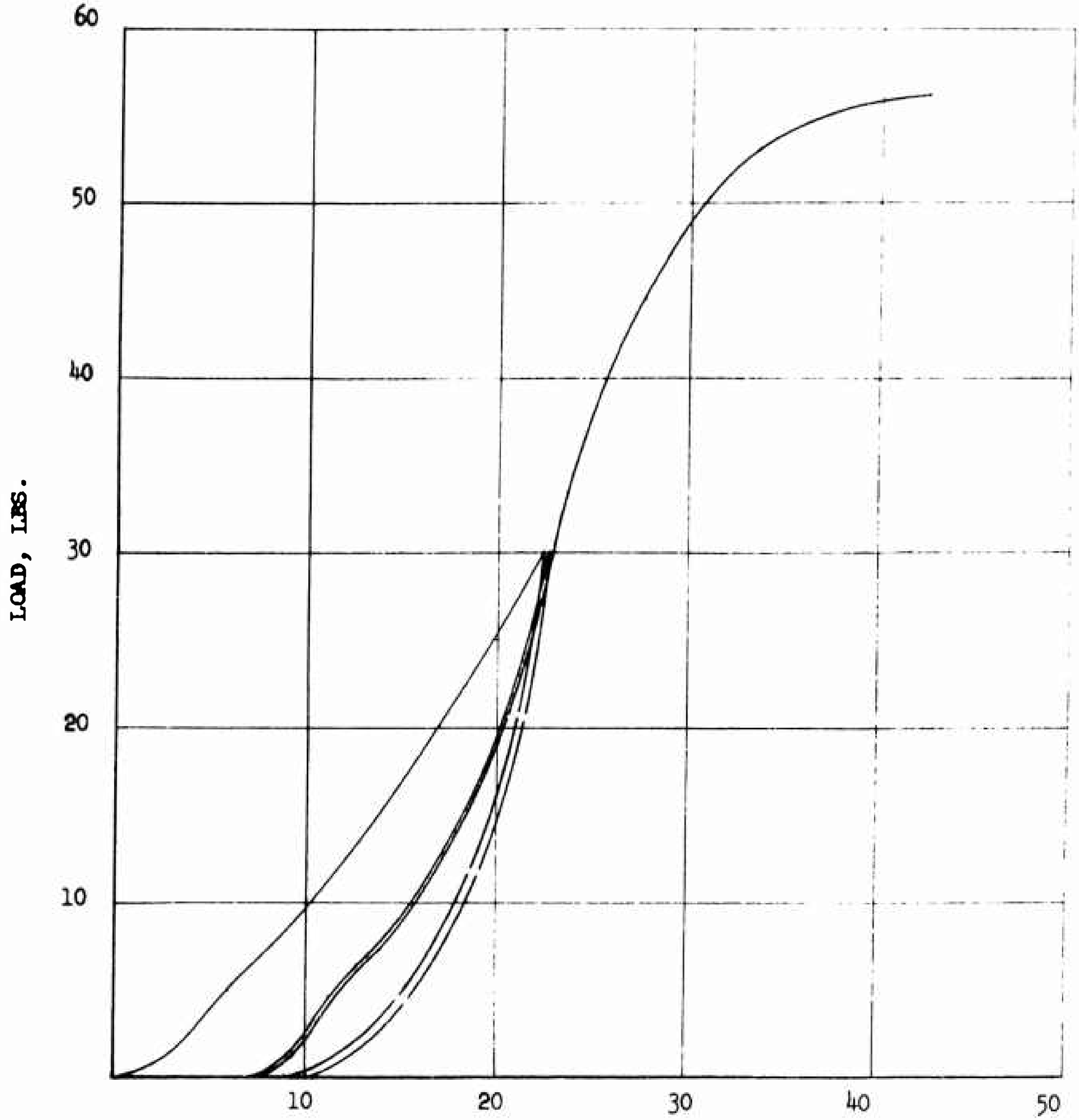

ELONGATION, %

FIGURE 129

TYPICAL REPEATED STRESS-STRAIN CURVES SHOWING 1st & 5th CYCLES TO 3rd LOAD LEVEL AND FINAL RUPTURE CYCLE

CHENEY

FABRIC 10N 2 1/2, WARP

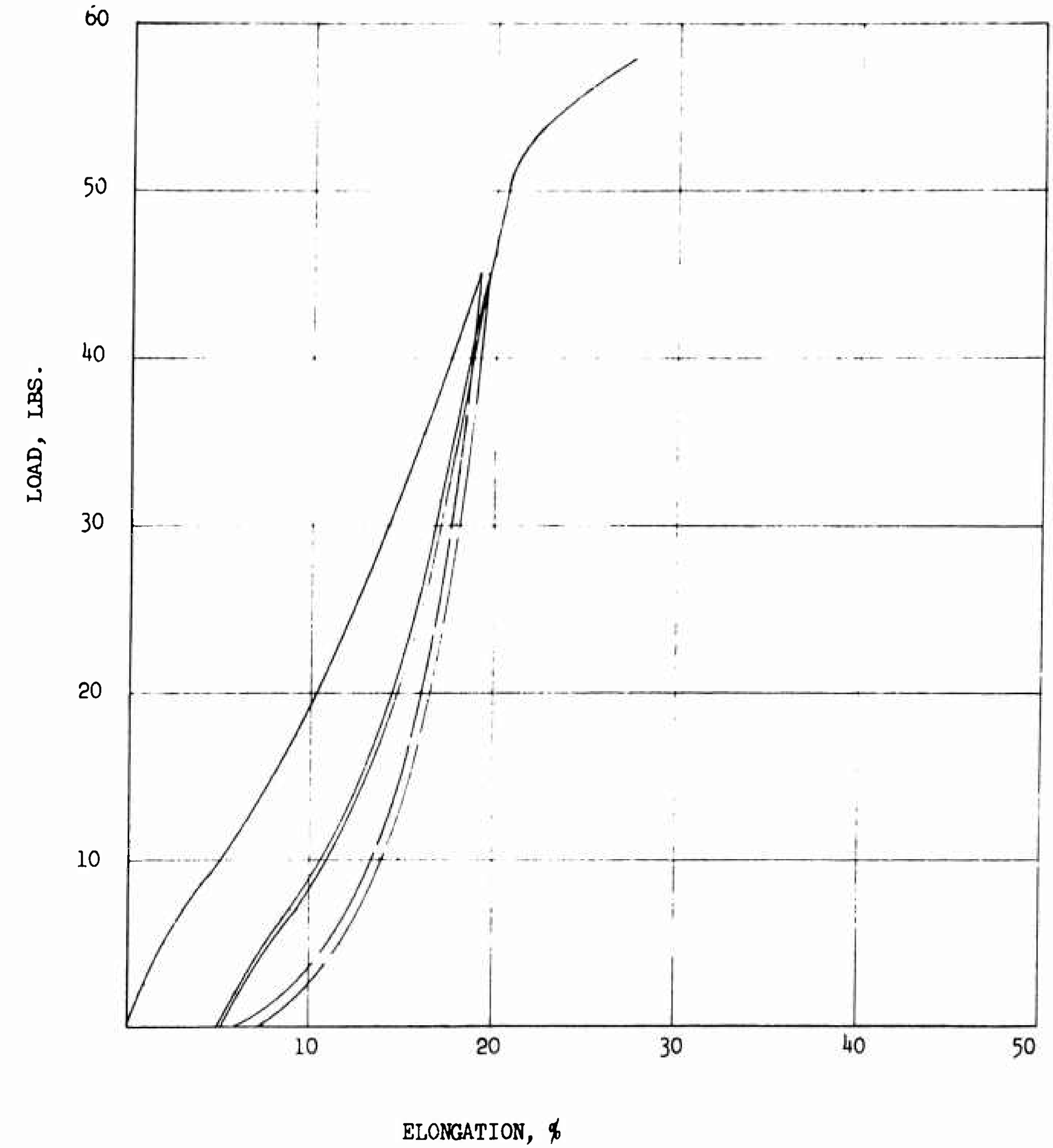

FIGURE 130

TYPICAL REPEATED STRESS-STRAIN CURVES SHOWING 1st & 5th CYCLES TO 3rd LOAD LEVEL AND FINAL RUPTURE CYCLE

CHENEY

FABRIC 10N 2 1/2, FILLING

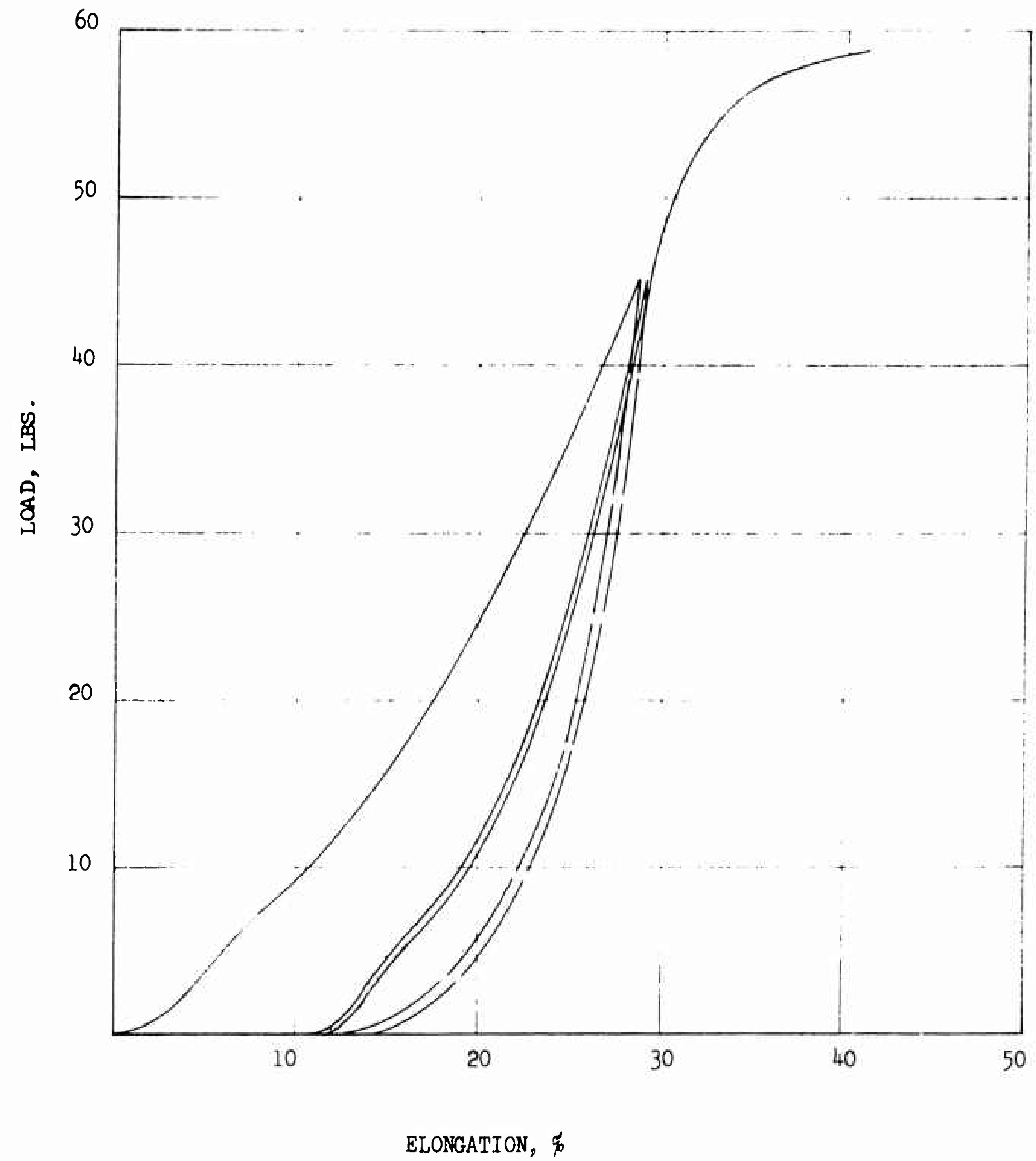

FIGURE 131

TYPICAL REPEATED STRESS-STRAIN CURVES SHOWING 1st & 5th CYCLES TO
1st LOAD LEVEL AND FINAL RUPTURE CYCLE

CHENEY

FABRIC 10N 5, WARP

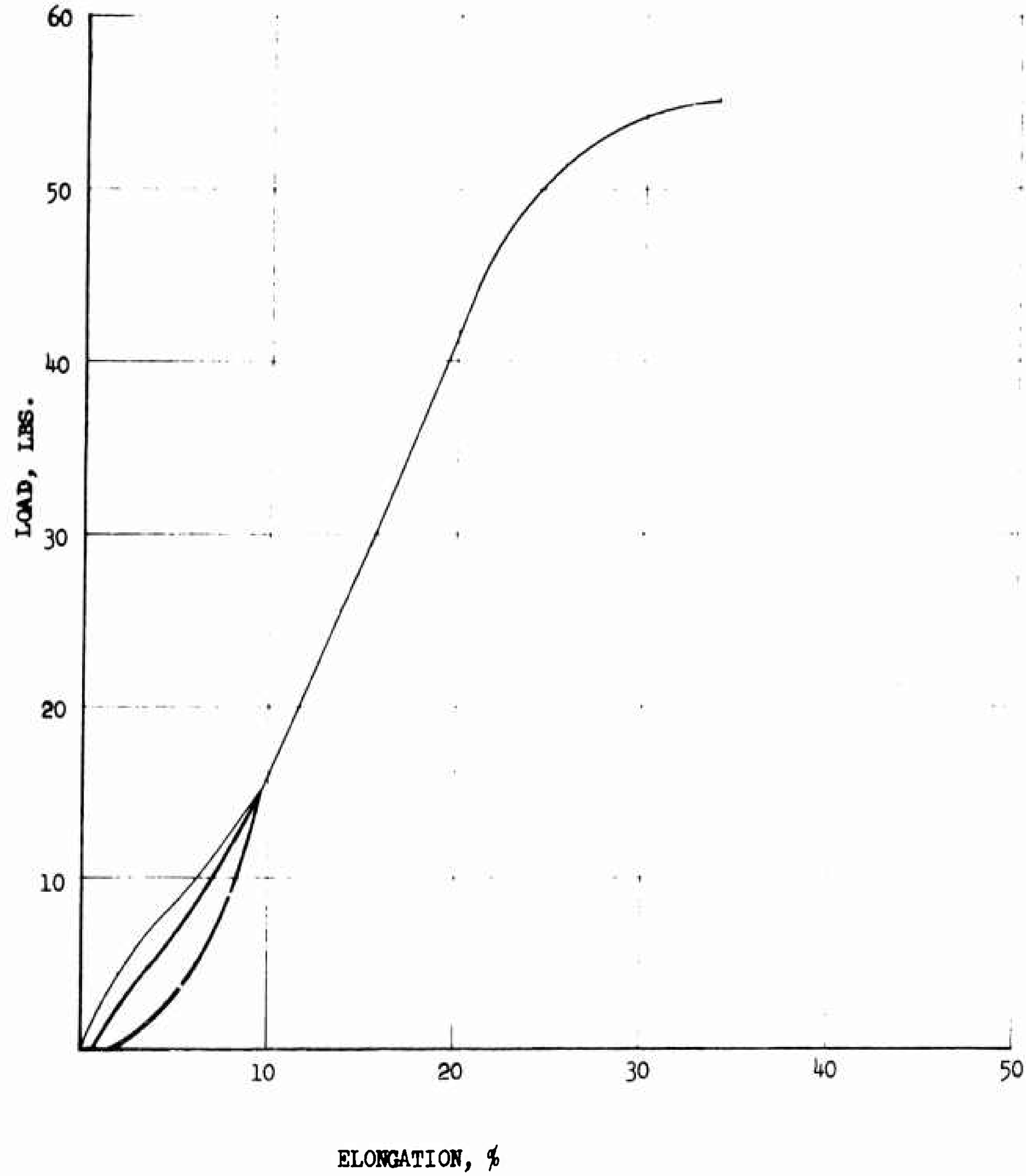

FIGURE 132

TYPICAL REPEATED STRESS-STRAIN CURVES SHOWING 1st & 5th CYCLES TO 1st LOAD LEVEL AND FINAL RUPTURE CYCLE

CHENEY

FABRIC 10N 5, FILLING

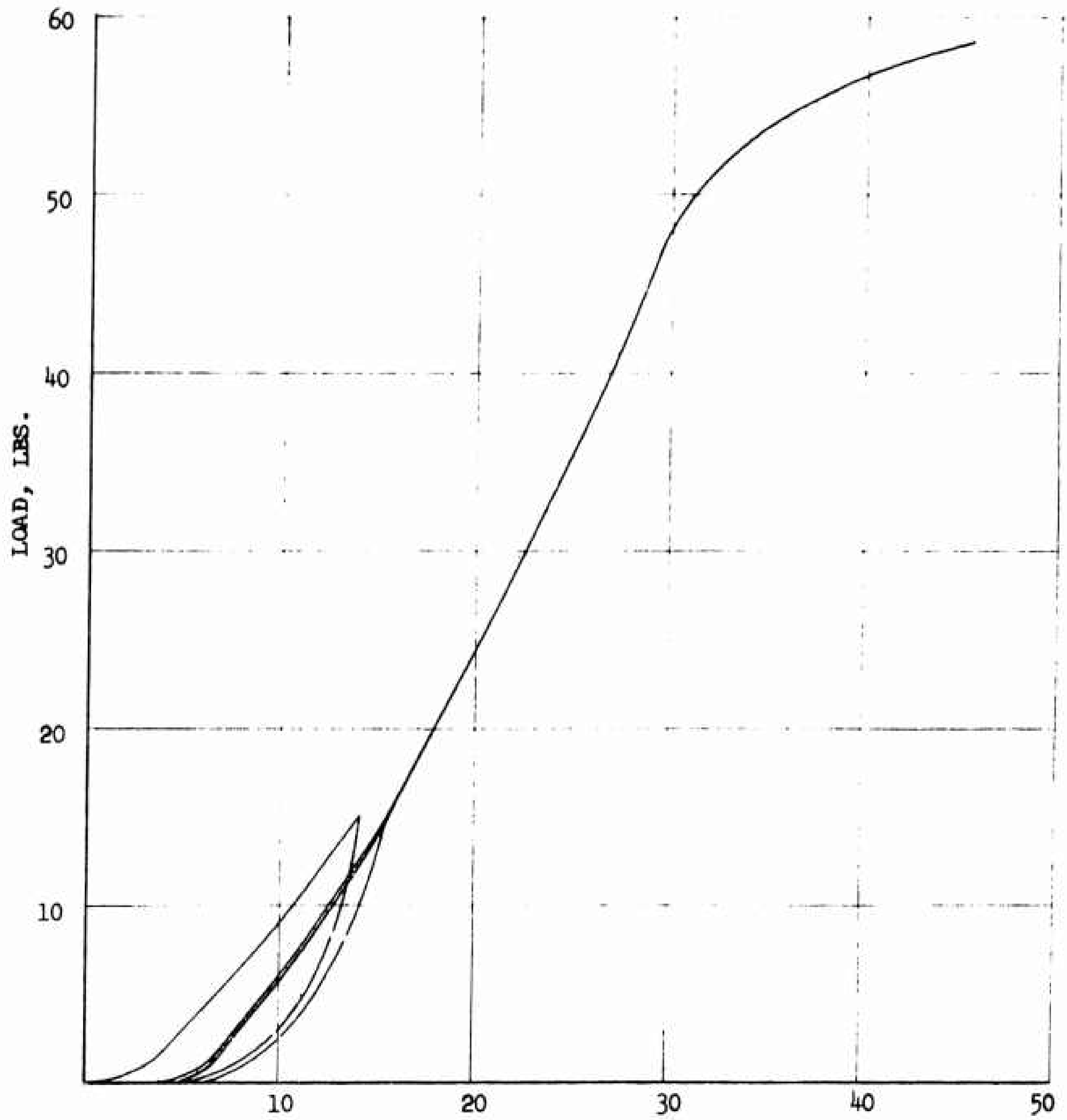

ELONGATION, %

FIGURE 133

TYPICAL REPEATED STRESS-STRAIN CURVES SHOWING 1st & 5th CYCLES TO 2nd LOAD LEVEL AND FINAL RUPTURE CYCLE

CHENEY

FABRIC 10N5, WARP

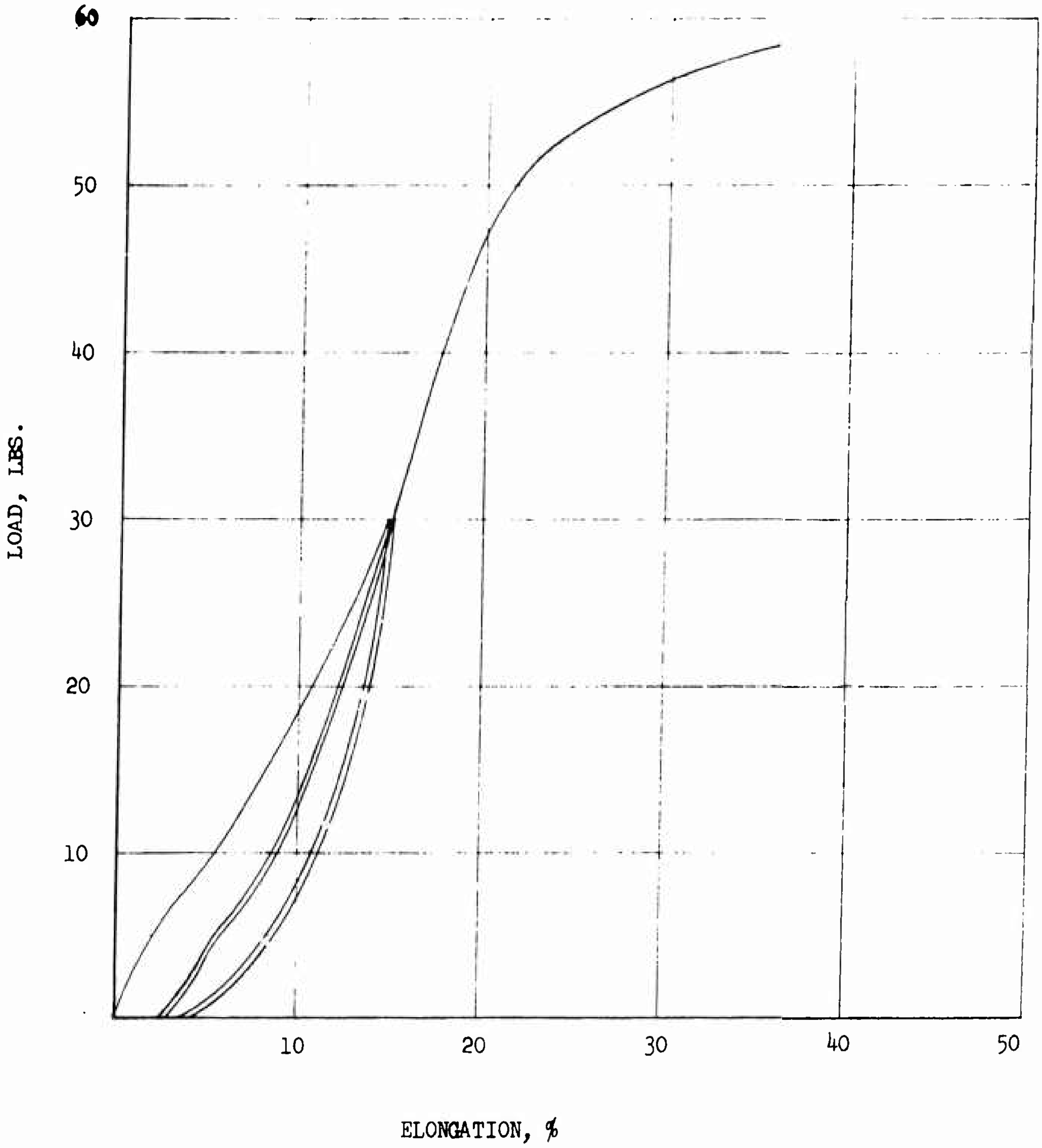

FIGURE 134

TYPICAL REPEATED STRESS-STRAIN CURVES SHOWING 1st & 5th CYCLES TO 2nd LOAD LEVEL AND FINAL RUPTURE CYCLE

CHENEY

FABRIC 10N5, FILLING

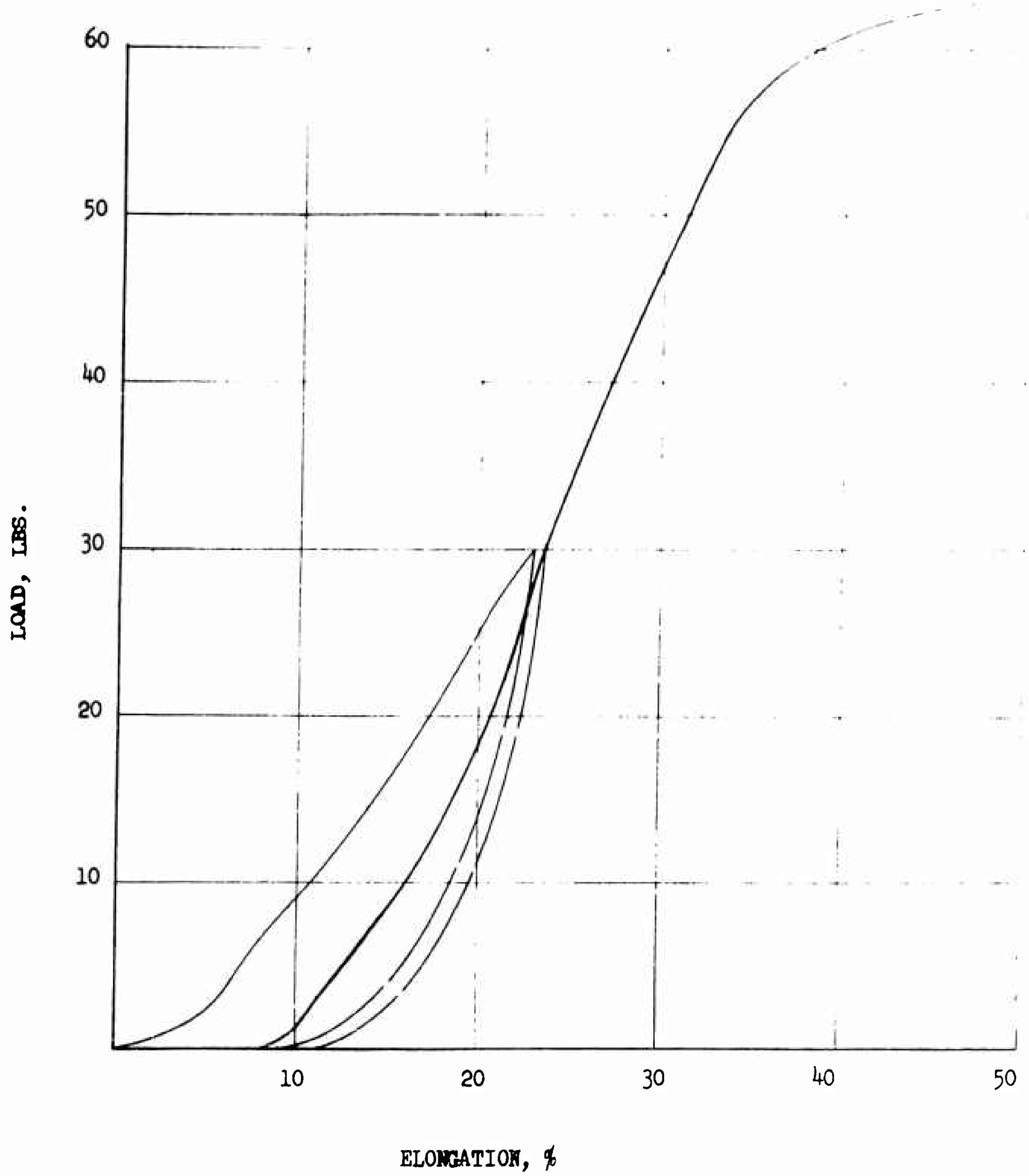

FIGURE 135

TYPICAL REPEATED STRESS-STRAIN CURVES SHOWING 1st & 5th CYCLES TO 3rd LOAD LEVEL AND FINAL RUPTURE CYCLE

CHENEY

FABRIC 10N 5, WARP

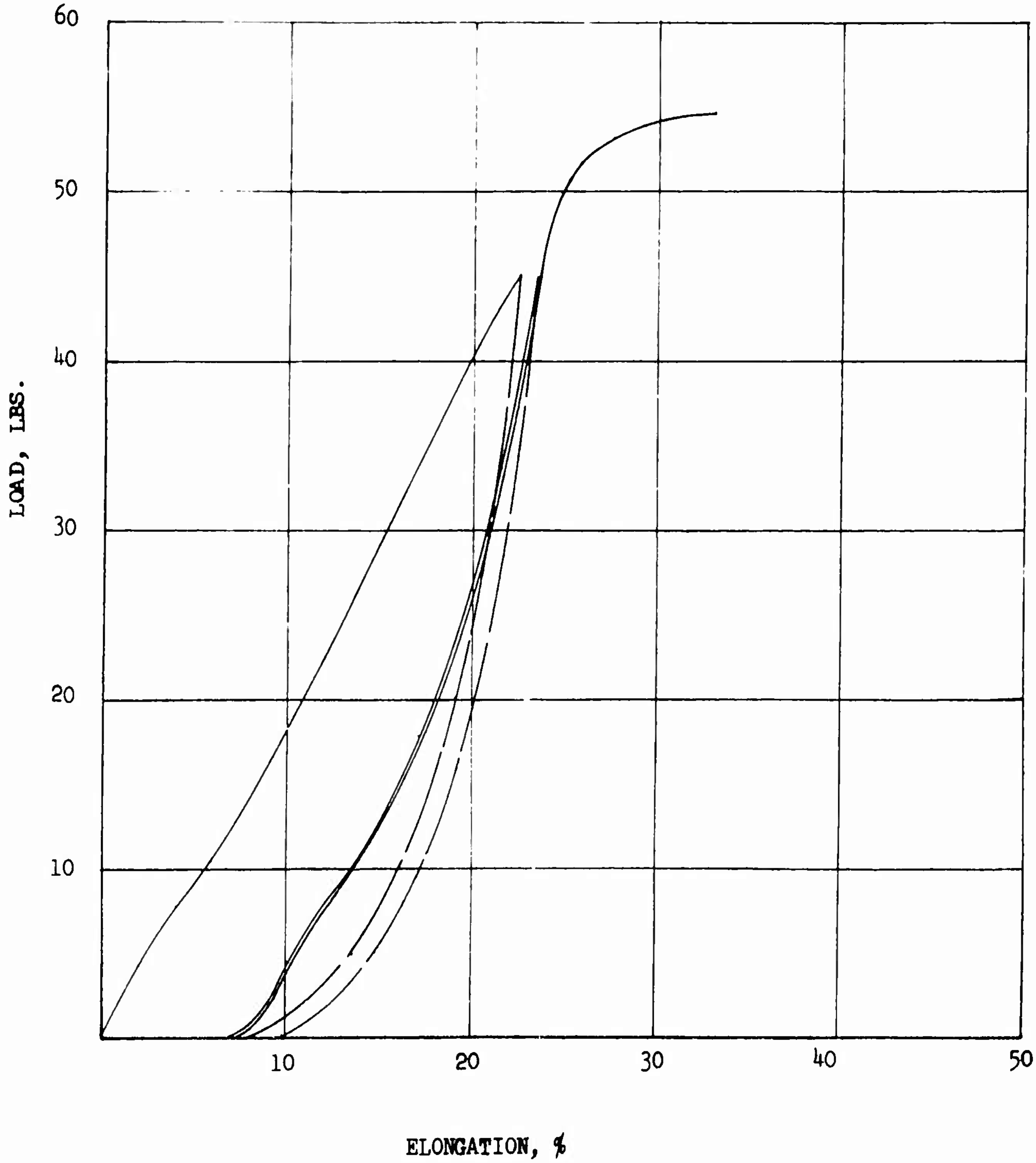

FIGURE 136

TYPICAL REPEATED STRESS-STRAIN CURVES SHOWING 1st & 5th CYCLES TO 3rd LOAD LEVEL AND FINAL RUPTURE CYCLE

CHENEY

FABRIC 10N 5, FILLING

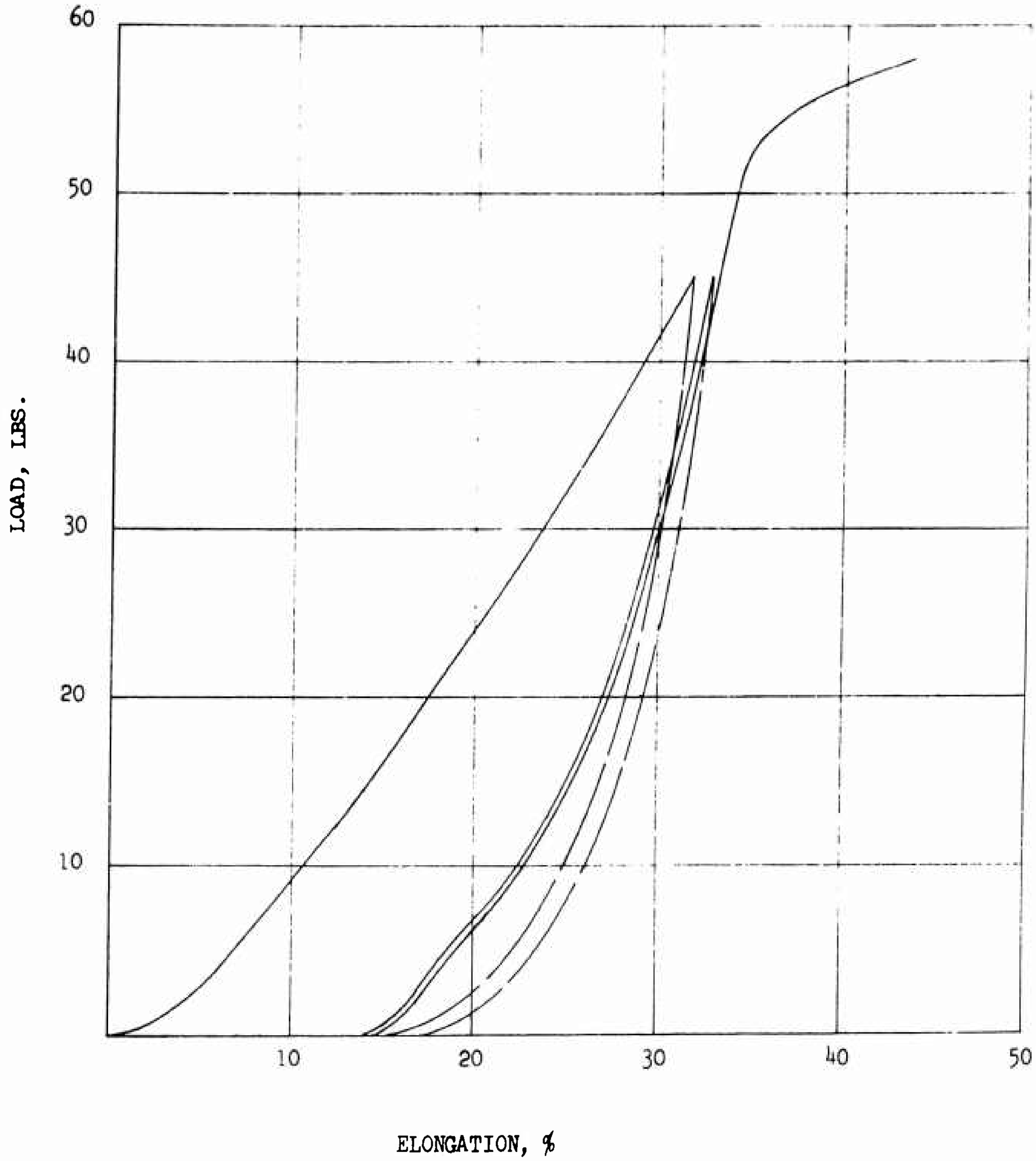

FIGURE 137

TYPICAL REPEATED STRESS-STRAIN CURVES SHOWING 1st & 5th CYCLES TO
1st LOAD LEVEL AND FINAL RUPTURE CYCLE

CHENEY

FABRIC 10N 7, WARP

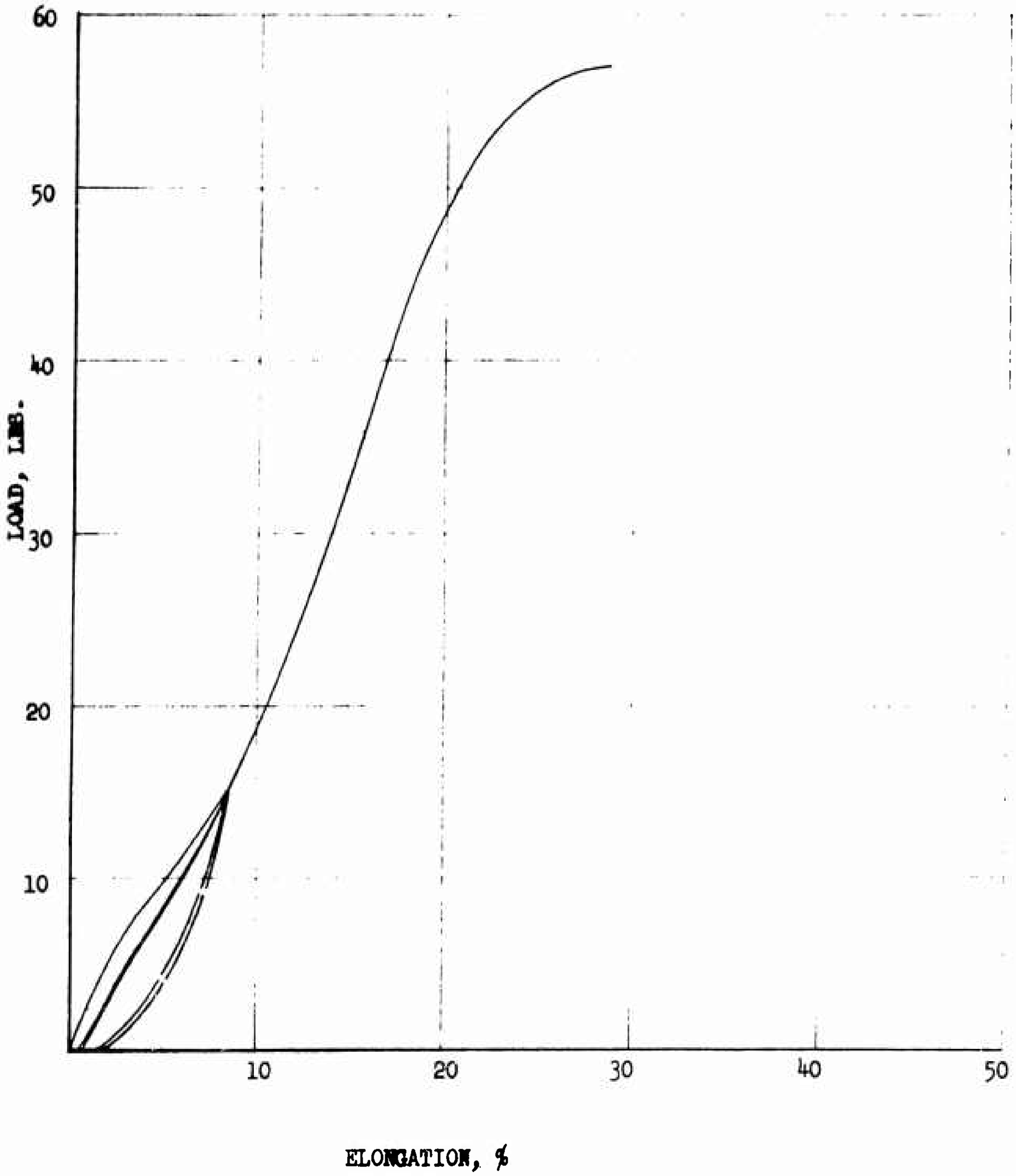

FIGURE 138

TYPICAL REPEATED STRESS-STRAIN CURVES SHOWING 1st & 5th CYCLES TO 1st LOAD LEVEL AND FINAL RUPTURE CYCLE

CHENEY

FABRIC 10N 7, FILLING

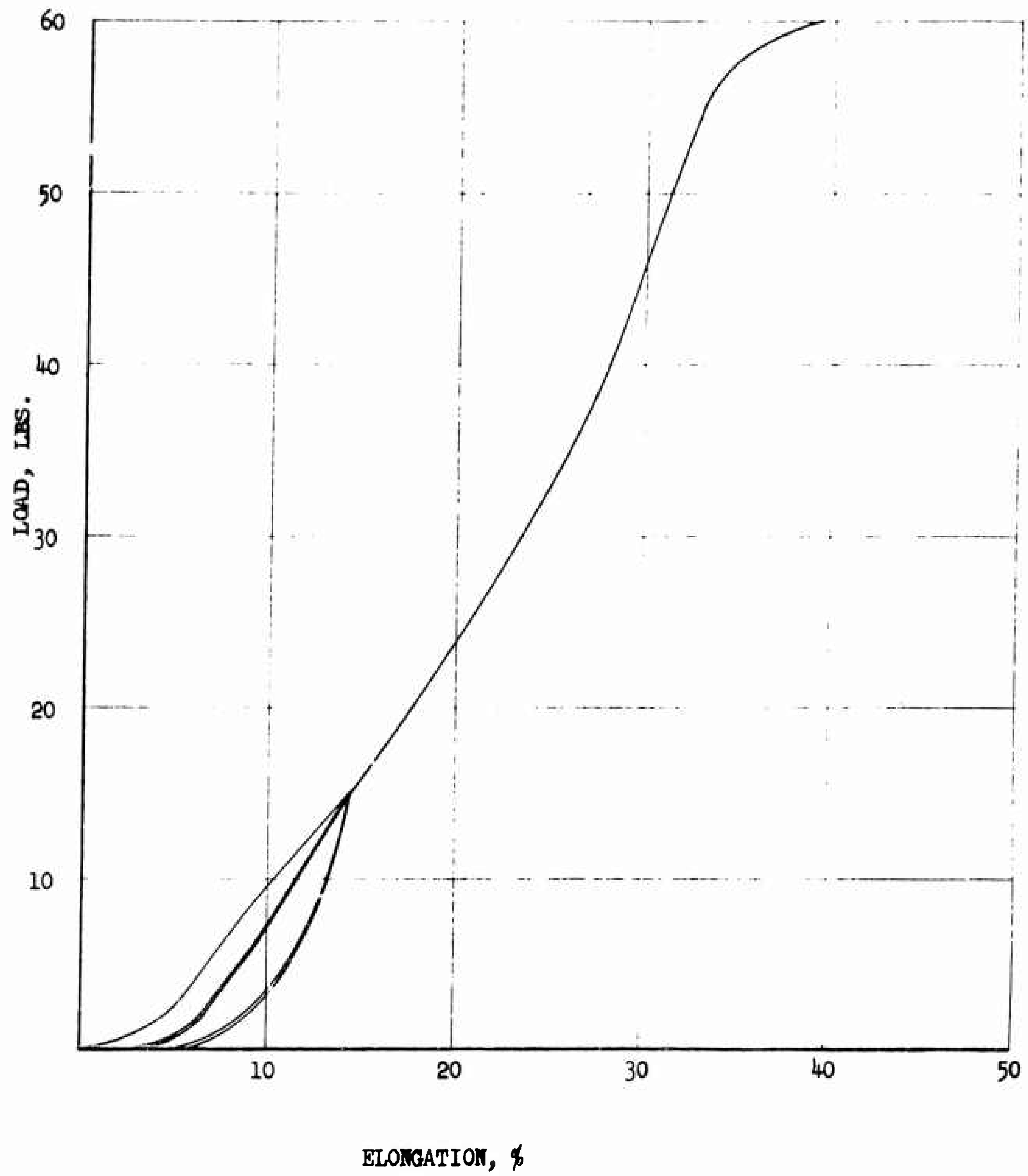

FIGURE 139

TYPICAL REPEATED STRESS-STRAIN CURVES SHOWING 1st & 5th CYCLES TO 2nd LOAD LEVEL AND FINAL RUPTURE CYCLE

CHENEY

FABRIC 10N7, WARP

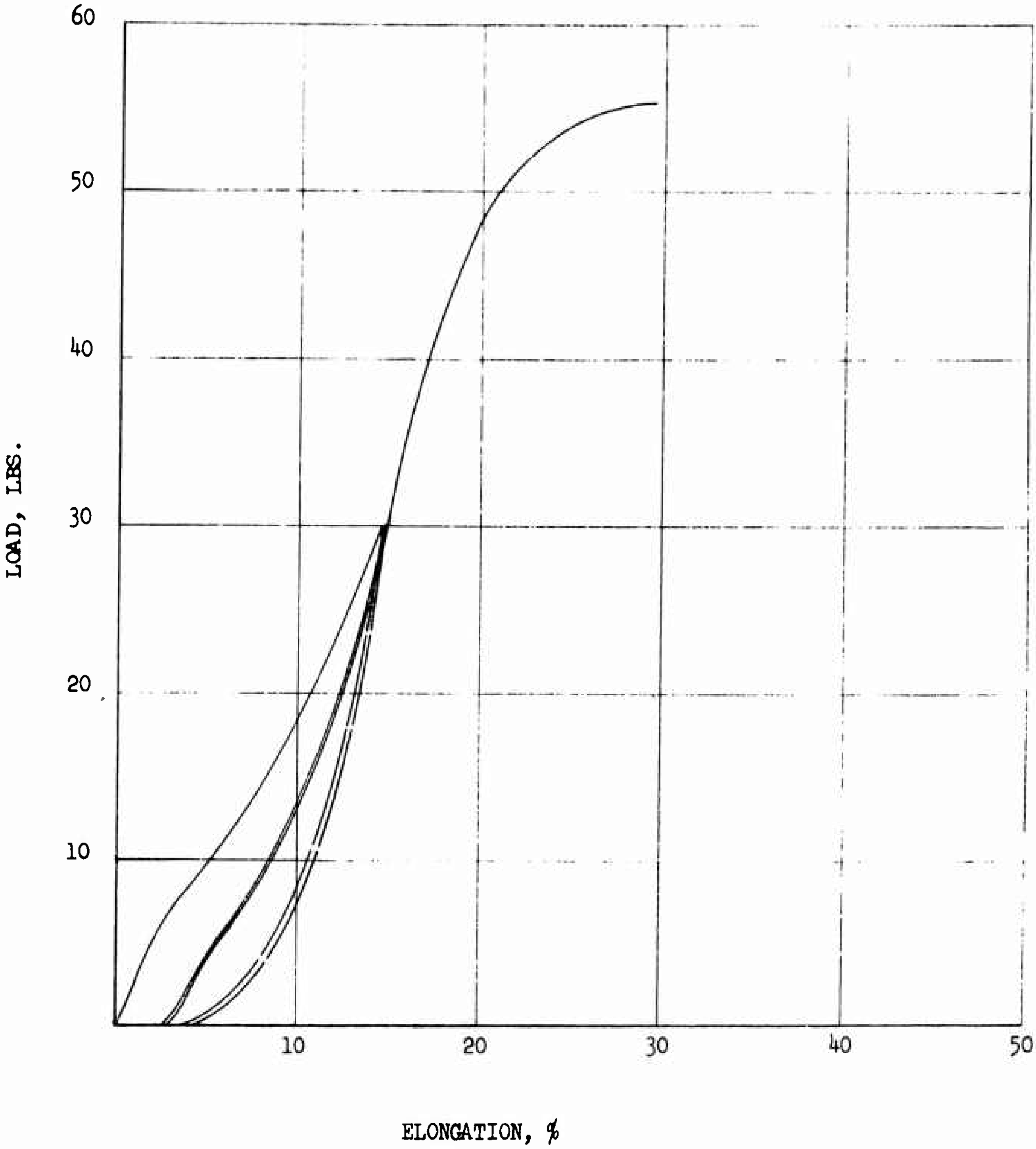

FIGURE 140

TYPICAL REPEATED STRESS-STRAIN CURVES SHOWING 1st & 5th CYCLES TO 2nd LOAD LEVEL AND FINAL RUPTURE CYCLE

CHENEY

FABRIC 10N7, FILLING

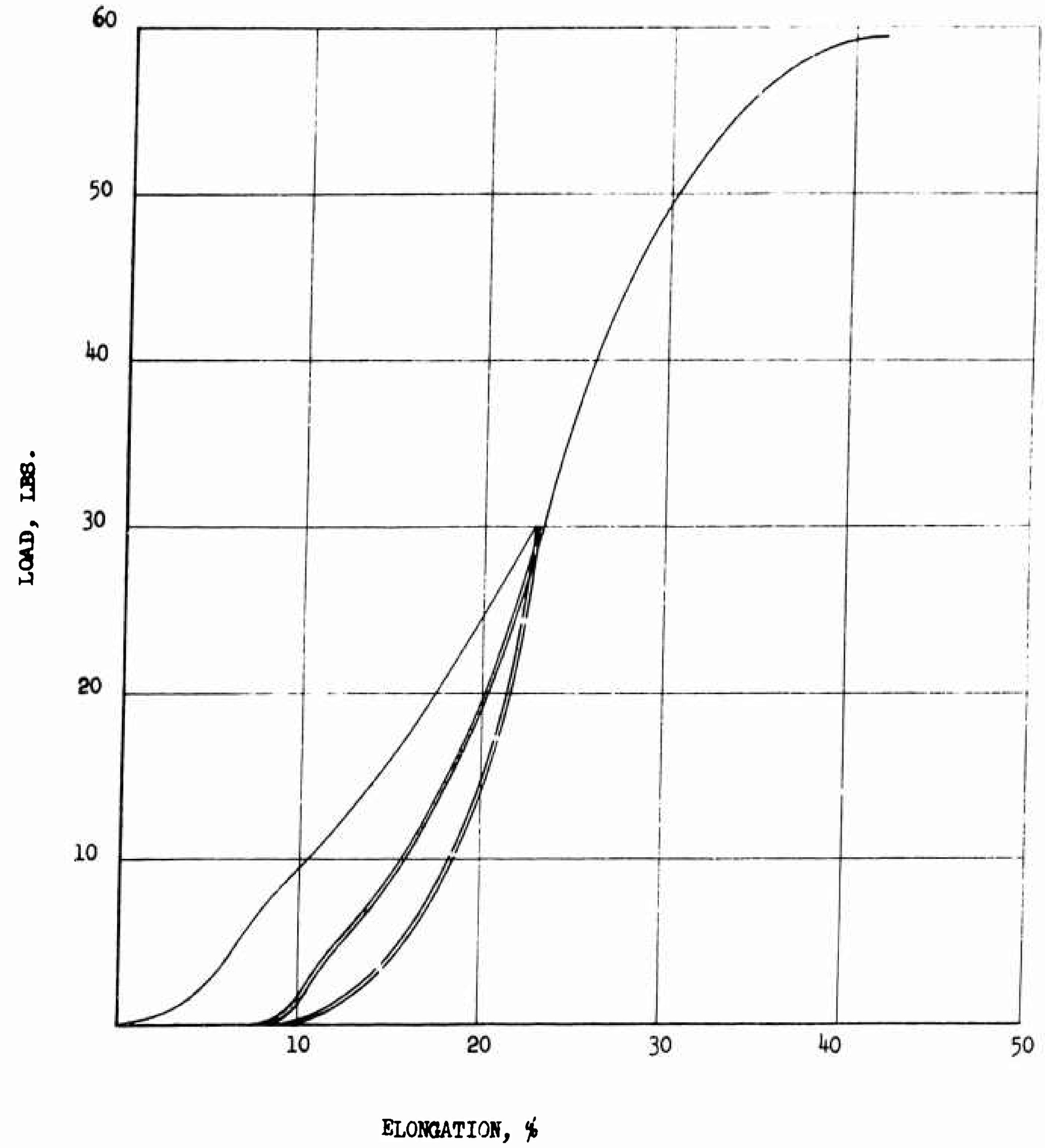

FIGURE 141

TYPICAL REPEATED STRESS-STRAIN CURVES SHOWING 1st & 5th CYCLES TO 3rd LOAD LEVEL AND FINAL RUPTURE CYCLE

CHENEY

FABRIC 10N 7, WARP

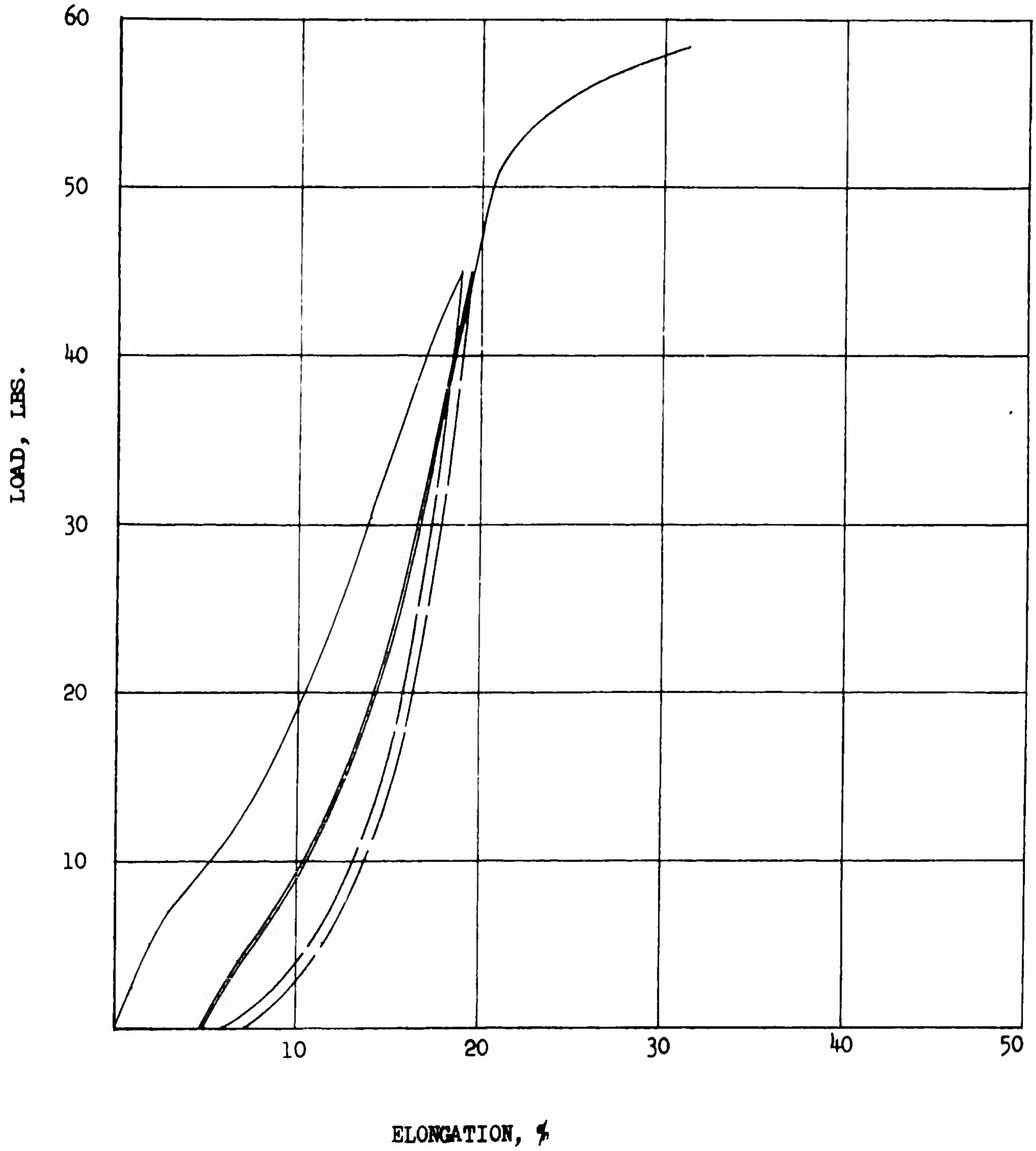

FIGURE 142

TYPICAL REPEATED STRESS-STRAIN CURVES SHOWING 1st & 5th CYCLES TO
3rd LOAD LEVEL AND FINAL RUPTURE CYCLE

CHENEY

FABRIC 10N 7, FILLING

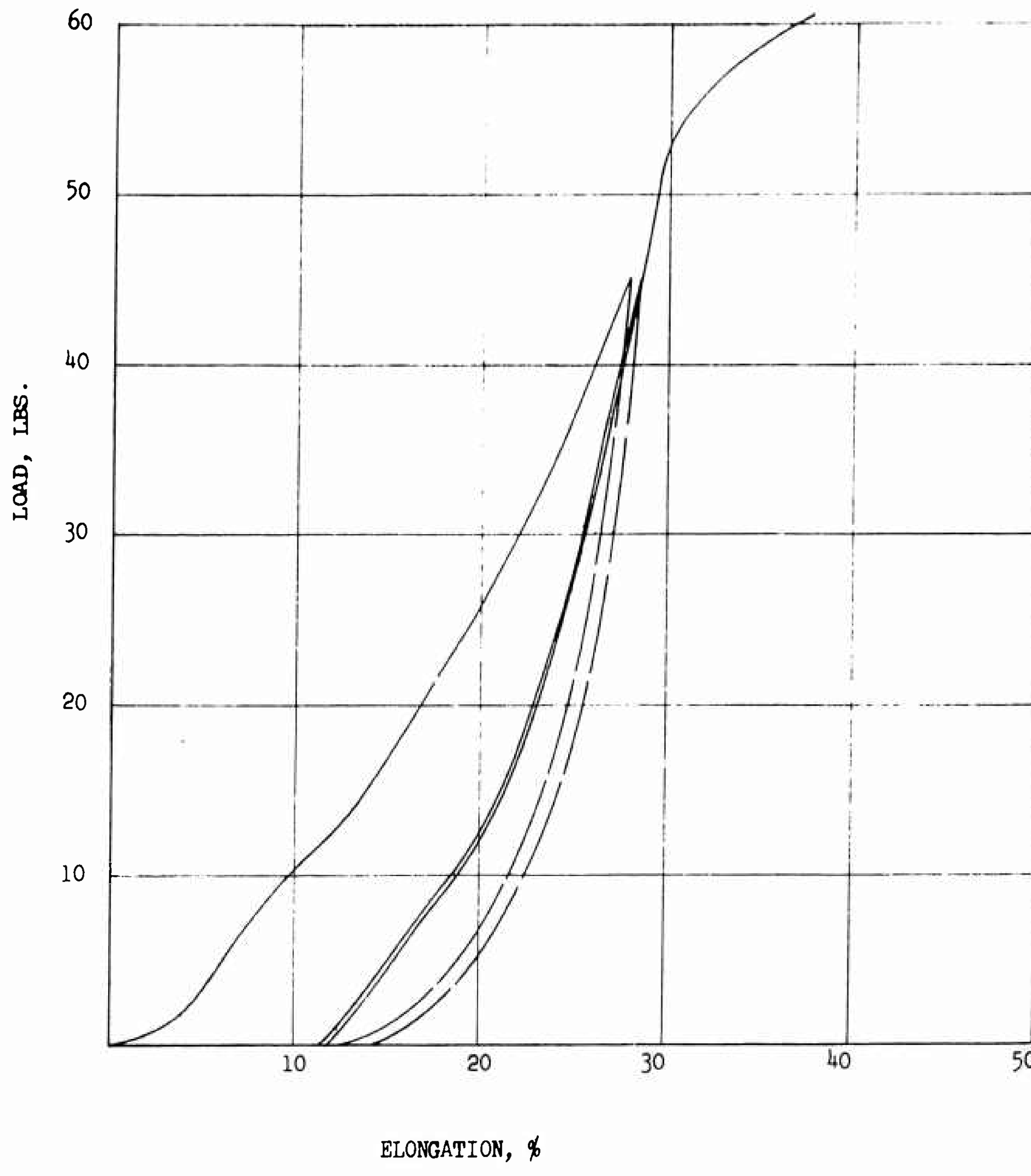

FIGURE 142

TYPICAL REPEATED STRESS-STRAIN CURVES SHOWING 1st & 5th CYCLES TO
3rd LOAD LEVEL AND FINAL RUPTURE CYCLE

CHENEY

FABRIC 10N 7, FILLING

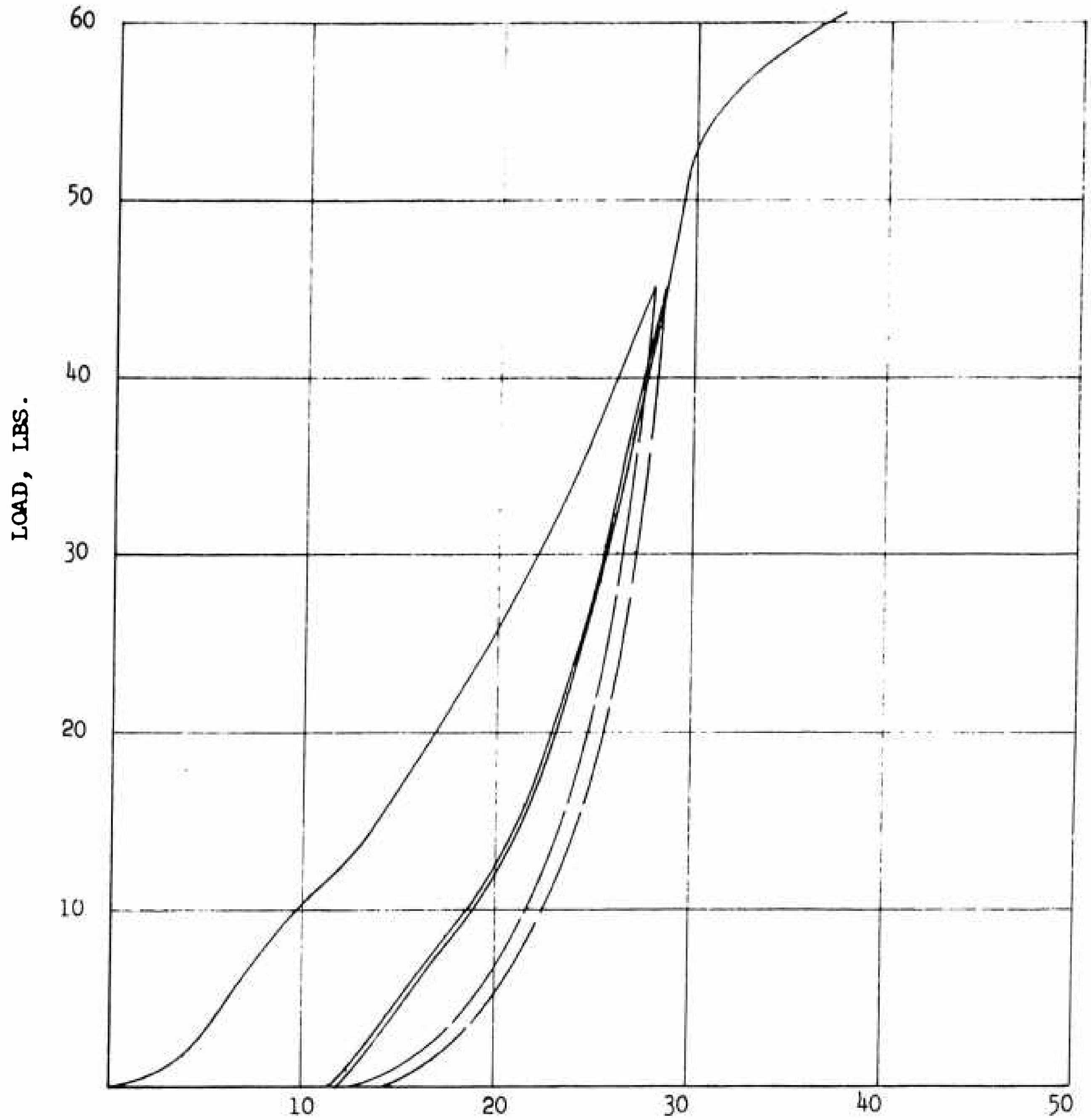

ELONGATION, %

FIGURE 143

TYPICAL REPEATED STRESS-STRAIN CURVES SHOWING 1st & 5th CYCLES TO 1st LOAD LEVEL AND FINAL RUPTURE CYCLE

CHENEY

FABRIC 10N 15, WARP

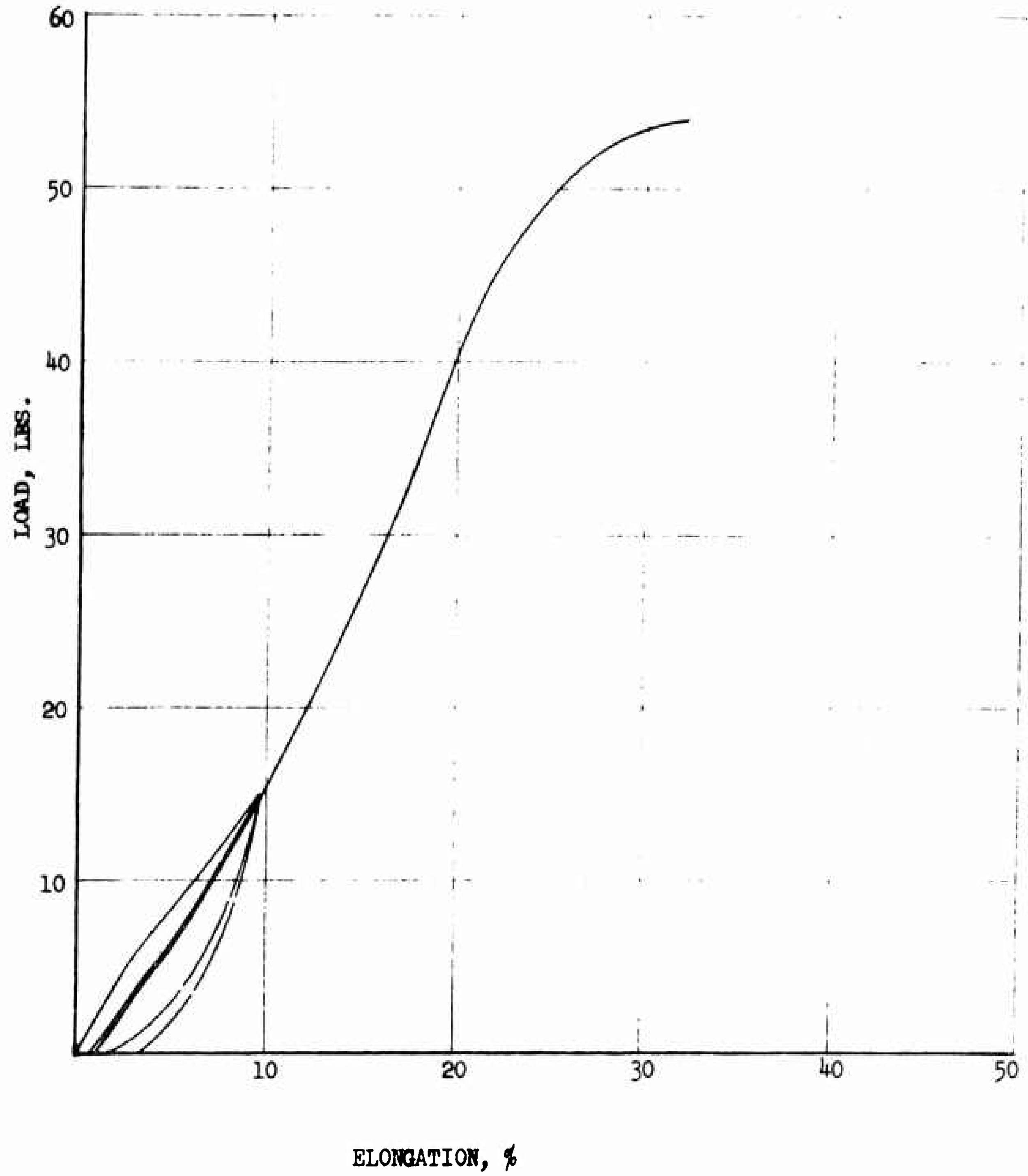

FIGURE 144

TYPICAL REPEATED STRESS-STRAIN CURVES SHOWING 1st & 5th CYCLES TO
1st LOAD LEVEL AND FINAL RUPTURE CYCLE

CHENEY

FABRIC 10N 15, FILLING

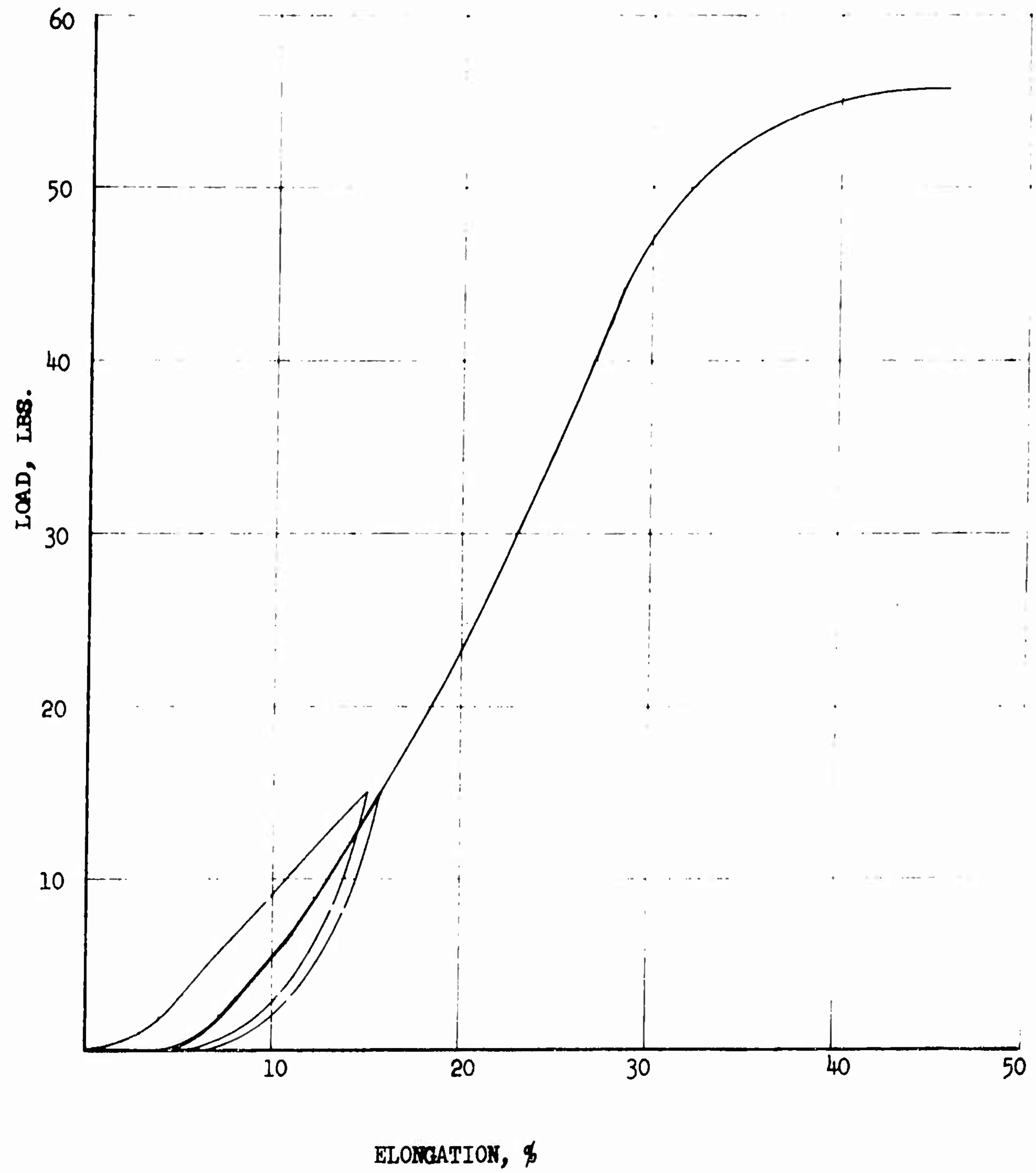

FIGURE 145

TYPICAL REPEATED STRESS-STRAIN CURVES SHOWING 1st & 5th CYCLES TO
2nd LOAD LEVEL AND FINAL RUPTURE CYCLE

CHENEY

FABRIC 10N15, WARP

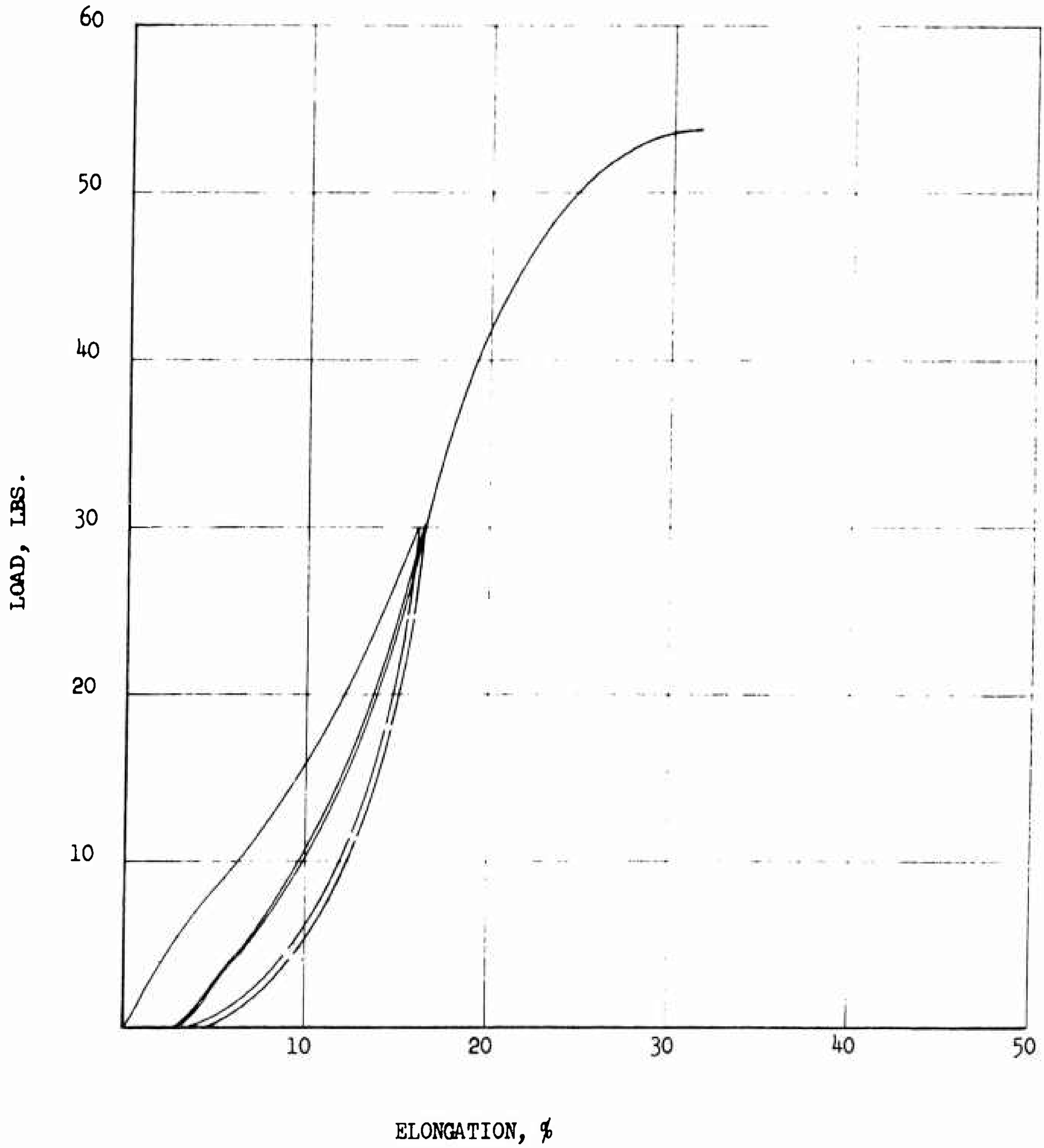

FIGURE 146

TYPICAL REPEATED STRESS-STRAIN CURVES SHOWING 1st & 5th CYCLES TO
2nd LOAD LEVEL AND FINAL RUPTURE CYCLE

CHENEY

FABRIC 10N15, FILLING

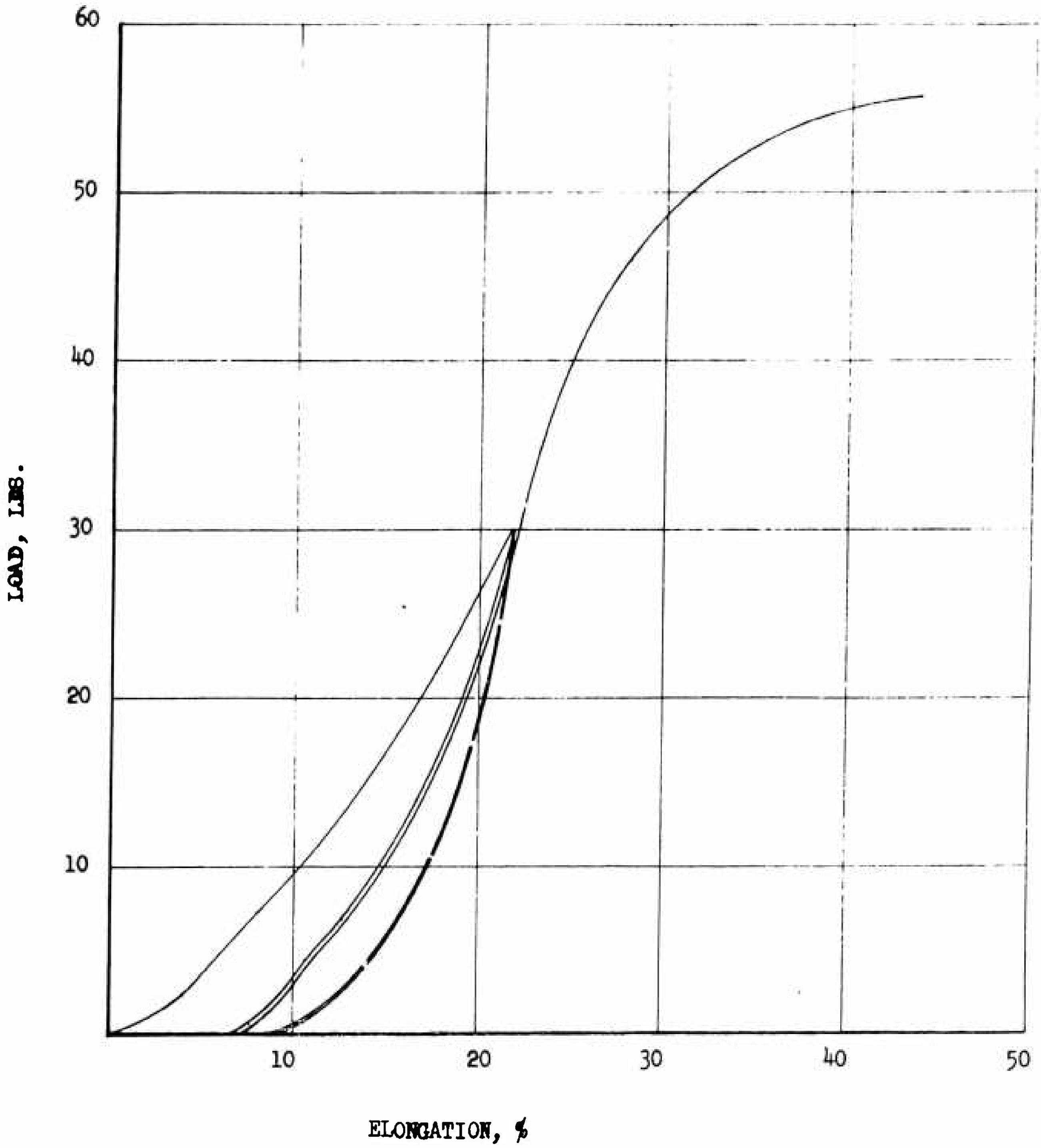

FIGURE 147

TYPICAL REPEATED STRESS-STRAIN CURVES SHOWING 1st & 5th CYCLES TO 3rd LOAD LEVEL AND FINAL RUPTURE CYCLE

CHENEY

FABRIC 10N 15, WARP

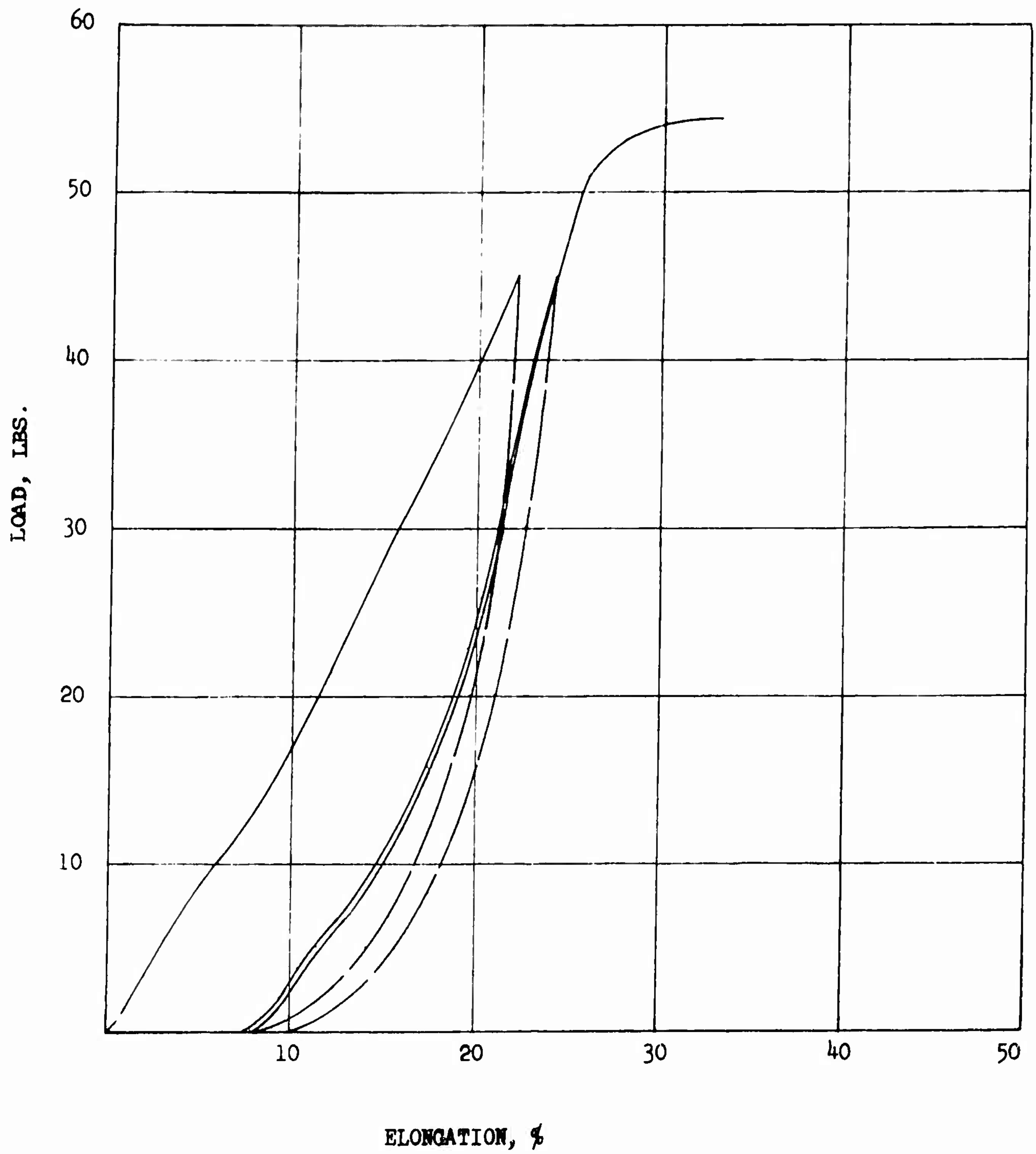

FIGURE 148

TYPICAL REPEATED STRESS-STRAIN CURVES SHOWING 1st & 5th CYCLES TO 3rd LOAD LEVEL AND FINAL RUPTURE CYCLE

CHENEY

FABRIC 10N 15, FILLING

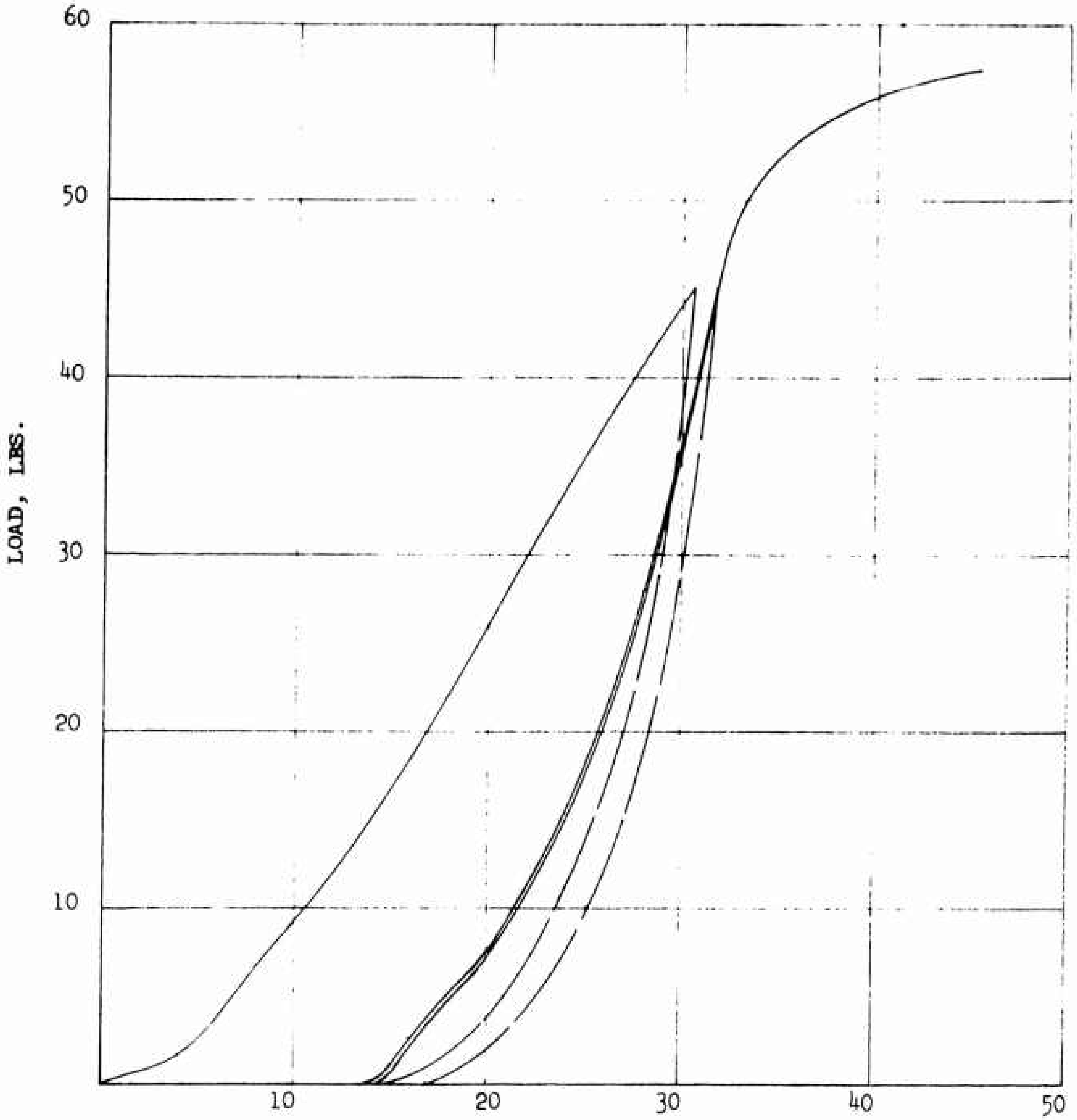

ELONGATION, %

FIGURE 149

TYPICAL REPEATED STRESS-STRAIN CURVES SHOWING 1st & 5th CYCLES TO 1st LOAD LEVEL AND FINAL RUPTURE CYCLE

CHENEY

FABRIC 10N 29 WARP

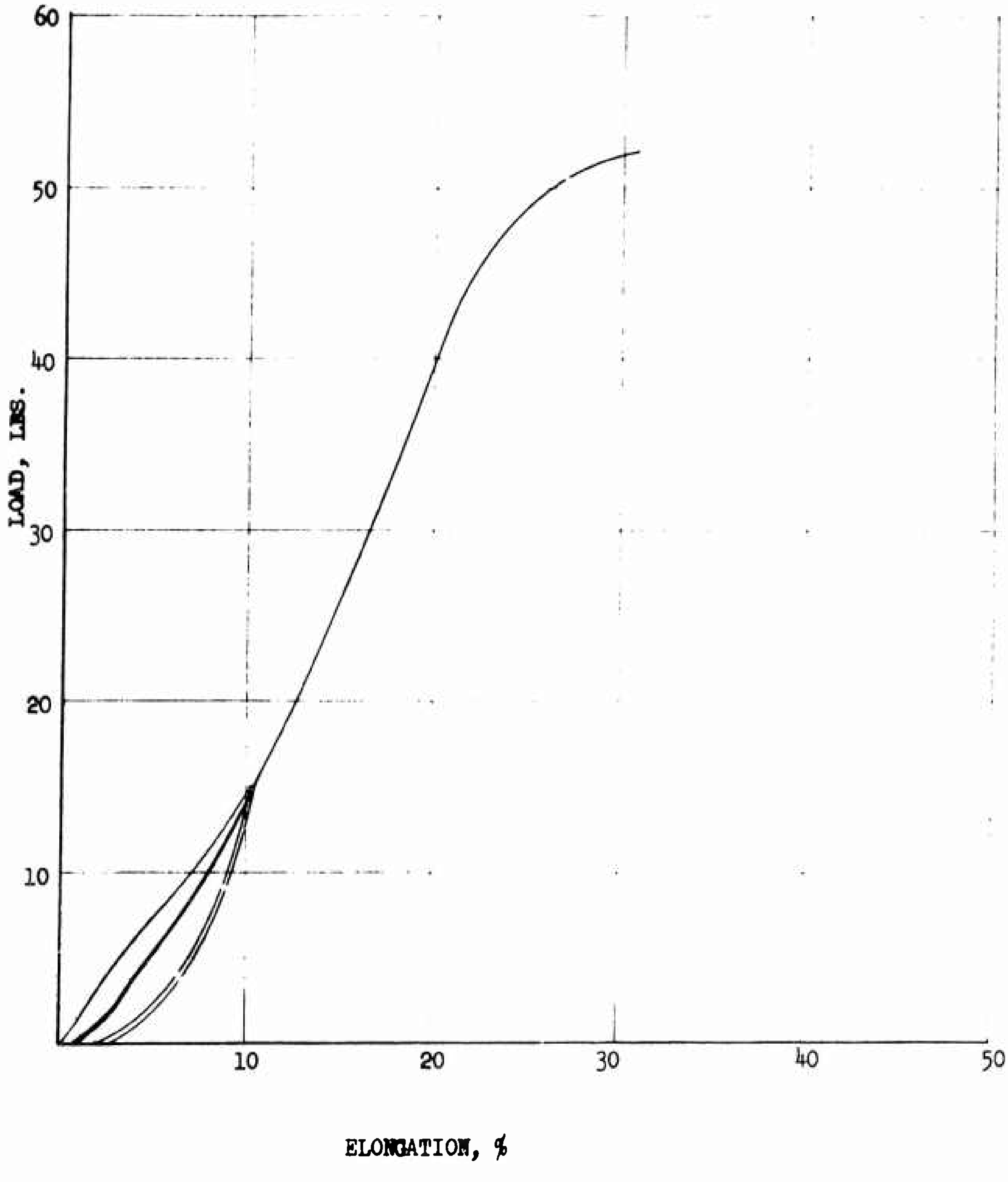

FIGURE 150

TYPICAL REPEATED STRESS-STRAIN CURVES SHOWING 1st & 5th CYCLES TO 1st LOAD LEVEL AND FINAL RUPTURE CYCLE

CHENEY

FABRIC 10N 20, FILLING

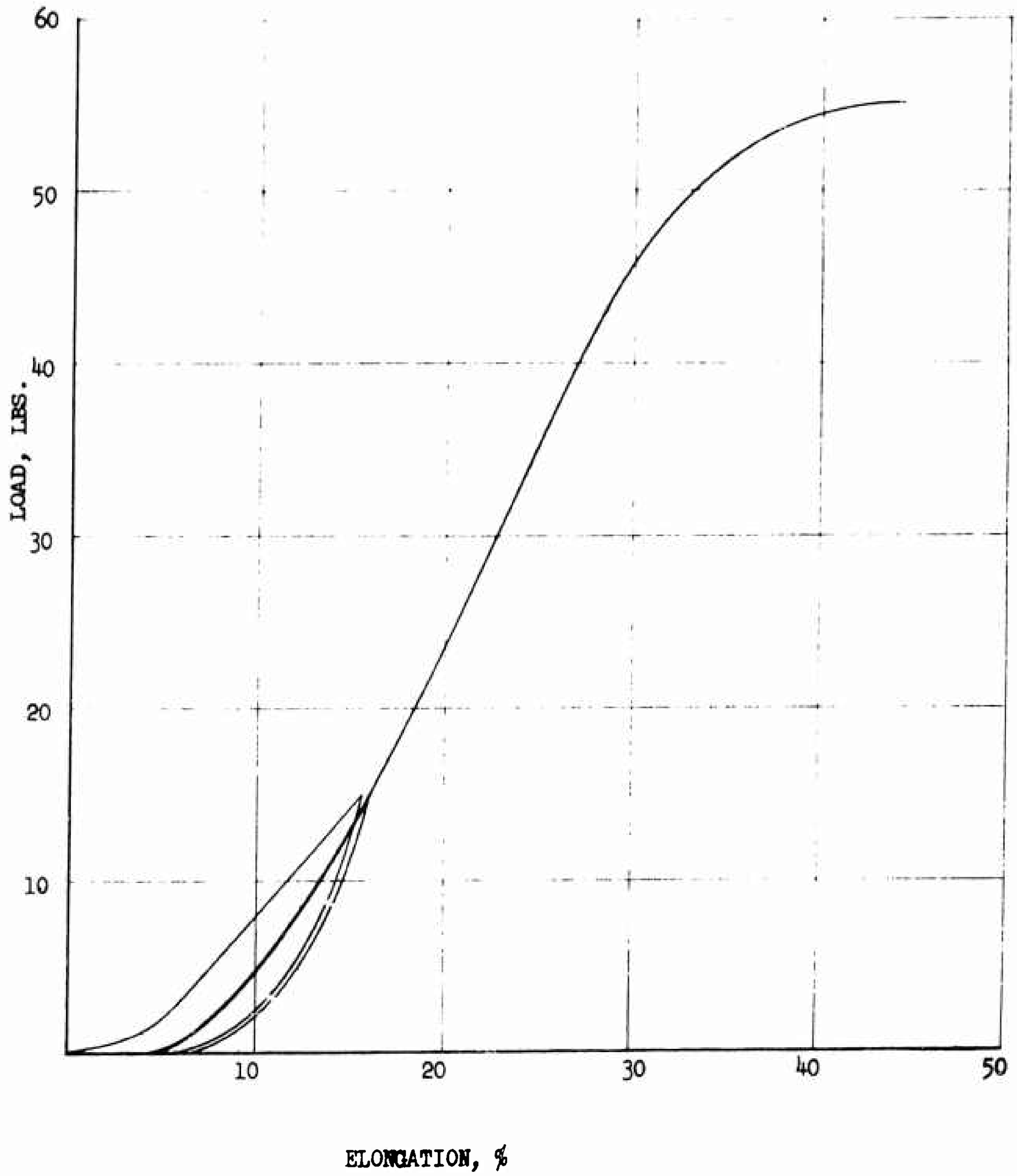

FIGURE 151

TYPICAL REPEATED STRESS-STRAIN CURVES SHOWING 1st & 5th CYCLES TO 2nd LOAD LEVEL AND FINAL RUPTURE CYCLE

CHENEY

FABRIC 10N20, WARP

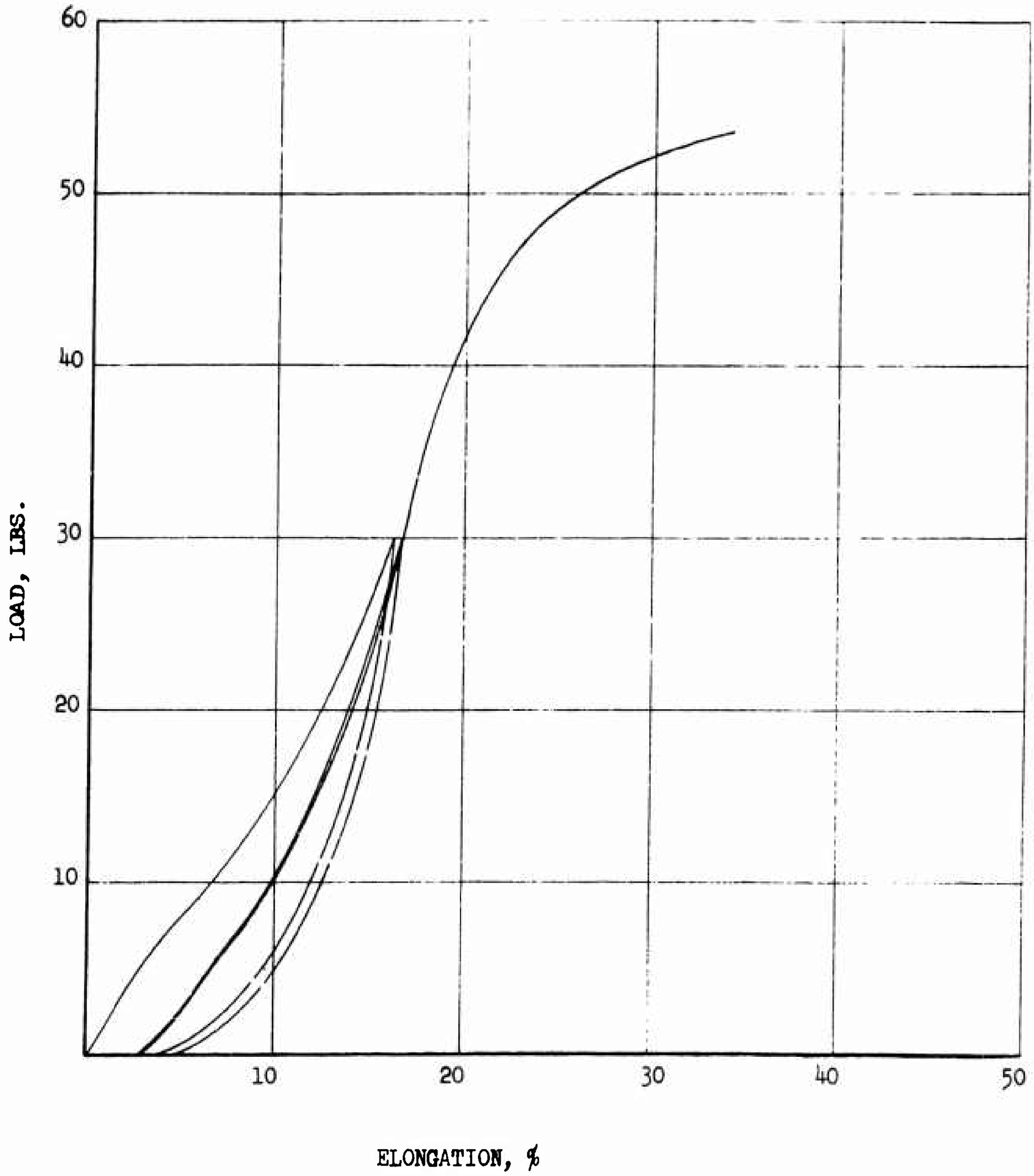

FIGURE 152

TYPICAL REPEATED STRESS-STRAIN CURVES SHOWING 1st & 5th CYCLES TO
2nd LOAD LEVEL AND FINAL RUPTURE CYCLE

CHENEY

FABRIC 10N20, FILLING

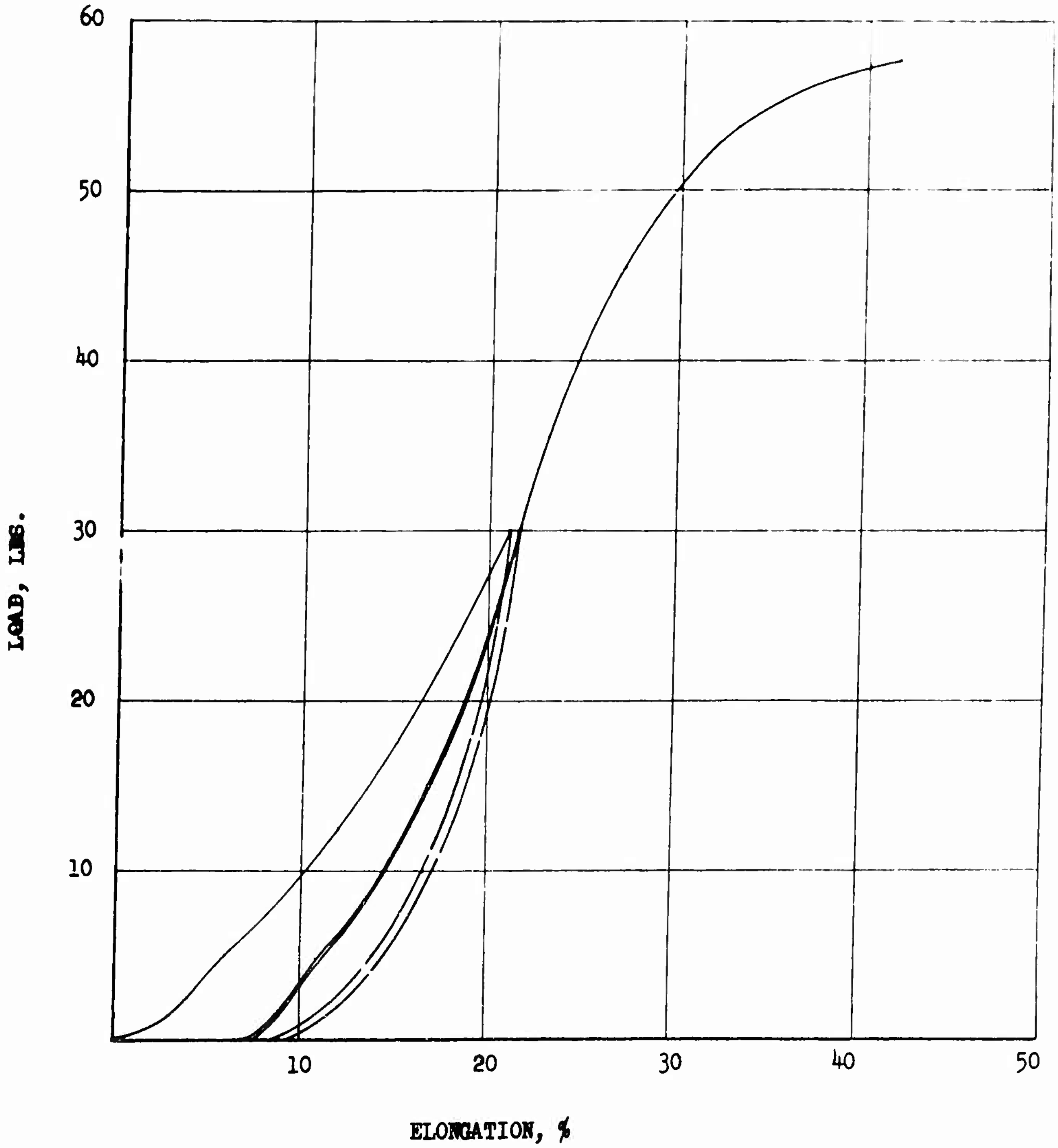

FIGURE 153

TYPICAL REPEATED STRESS-STRAIN CURVES SHOWING 1st & 5th CYCLES TO 3rd LOAD LEVEL AND FINAL RUPTURE CYCLE

CHENEY

FABRIC 10N 20, WARP

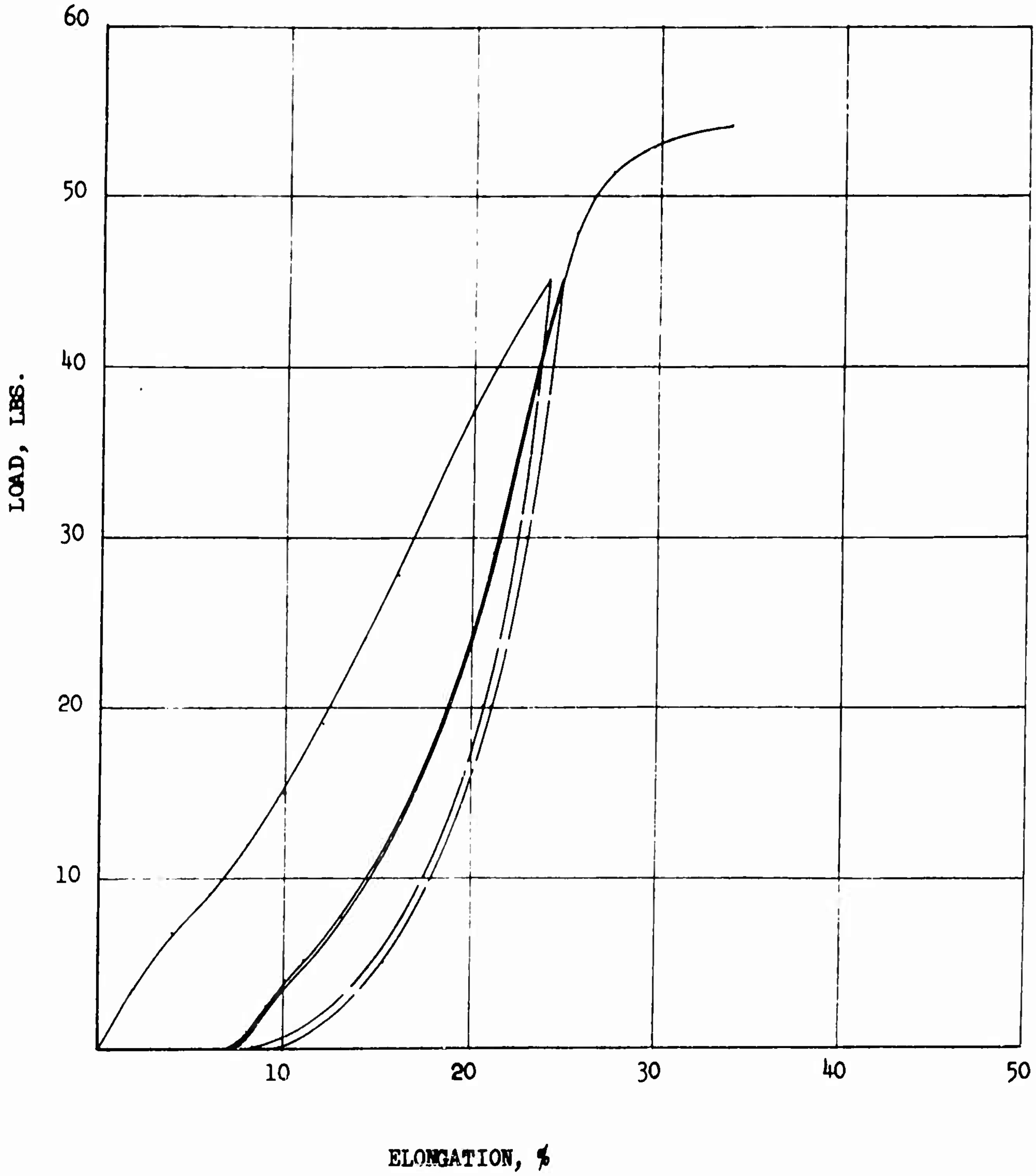

FIGURE 154

TYPICAL REPEATED STRESS-STRAIN CURVES SHOWING 1st & 5th CYCLES TO 3rd LOAD LEVEL AND FINAL RUPTURE CYCLE

CHENEY

FABRIC 10N 20, FILLING

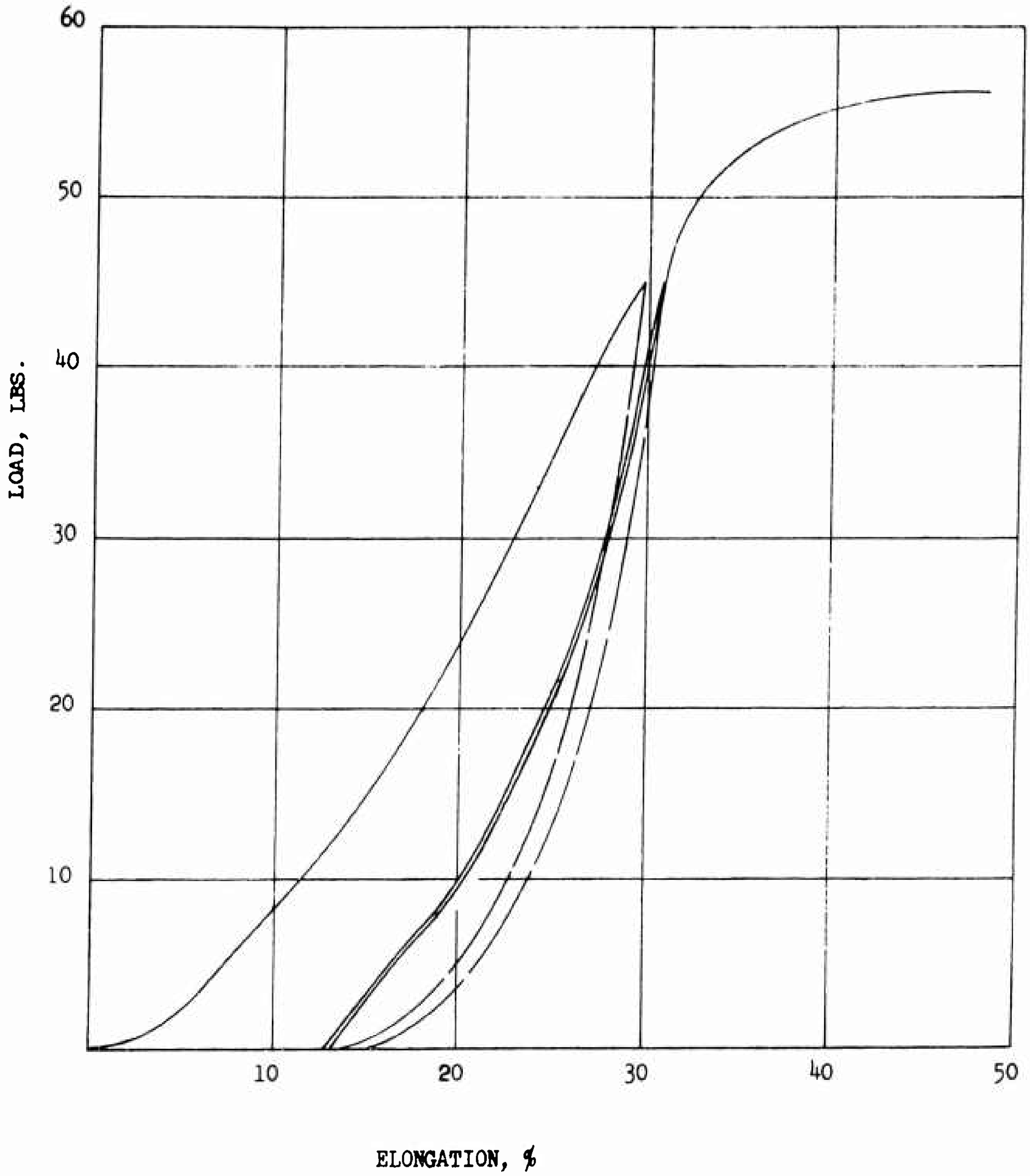

FIGURE 155

TYPICAL REPEATED STRESS-STRAIN CURVES SHOWING 1st & 5th CYCLES TO
1st LOAD LEVEL AND FINAL RUPTURE CYCLE

CHENEY

FABRIC 10N 35, WARP

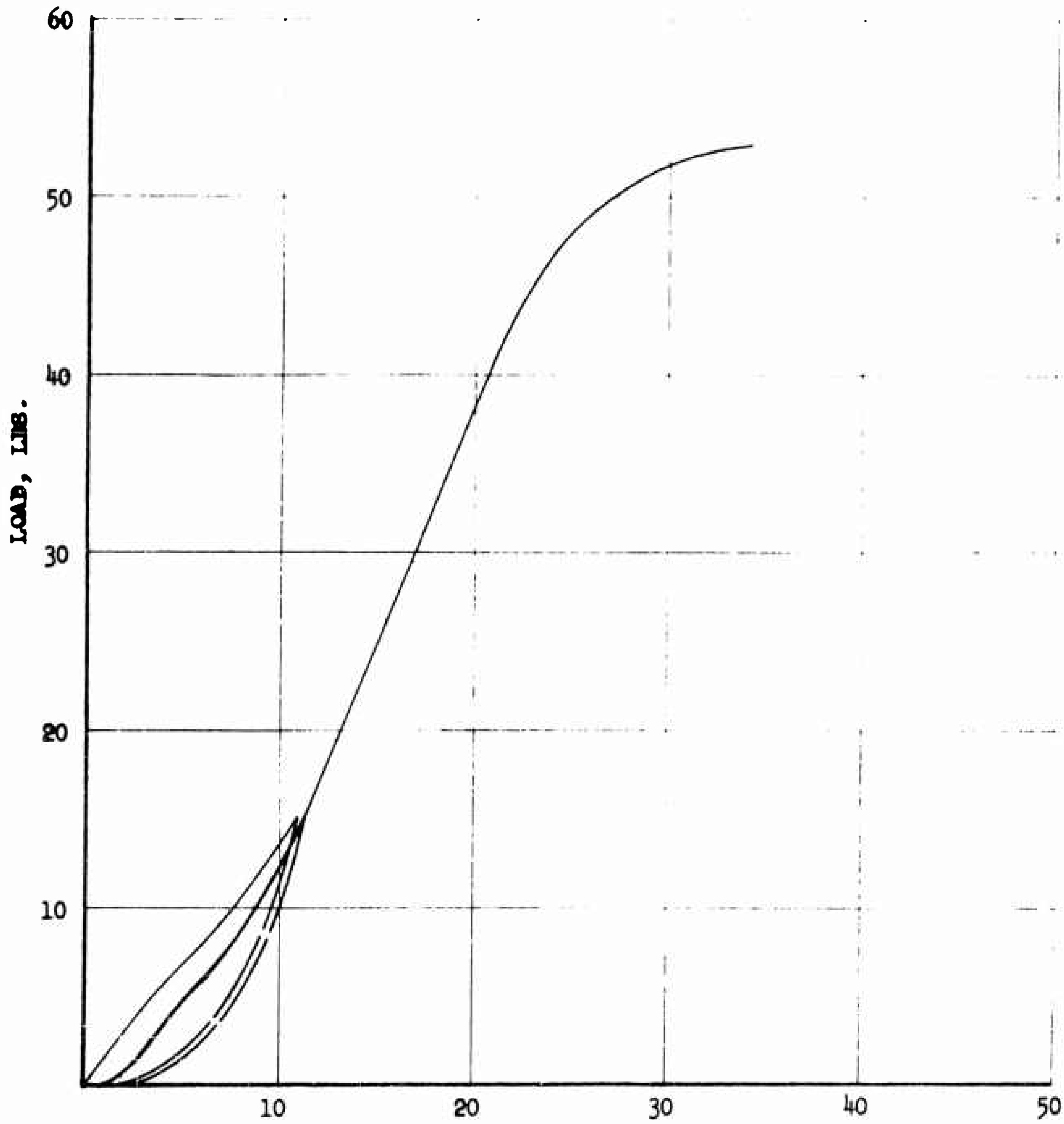

FIGURE 156

TYPICAL REPEATED STRESS-STRAIN CURVES SHOWING 1st & 5th CYCLES TO
1st LOAD LEVEL AND FINAL RUPTURE CYCLE

CHENEY

FABRIC 10N 35, FILLING

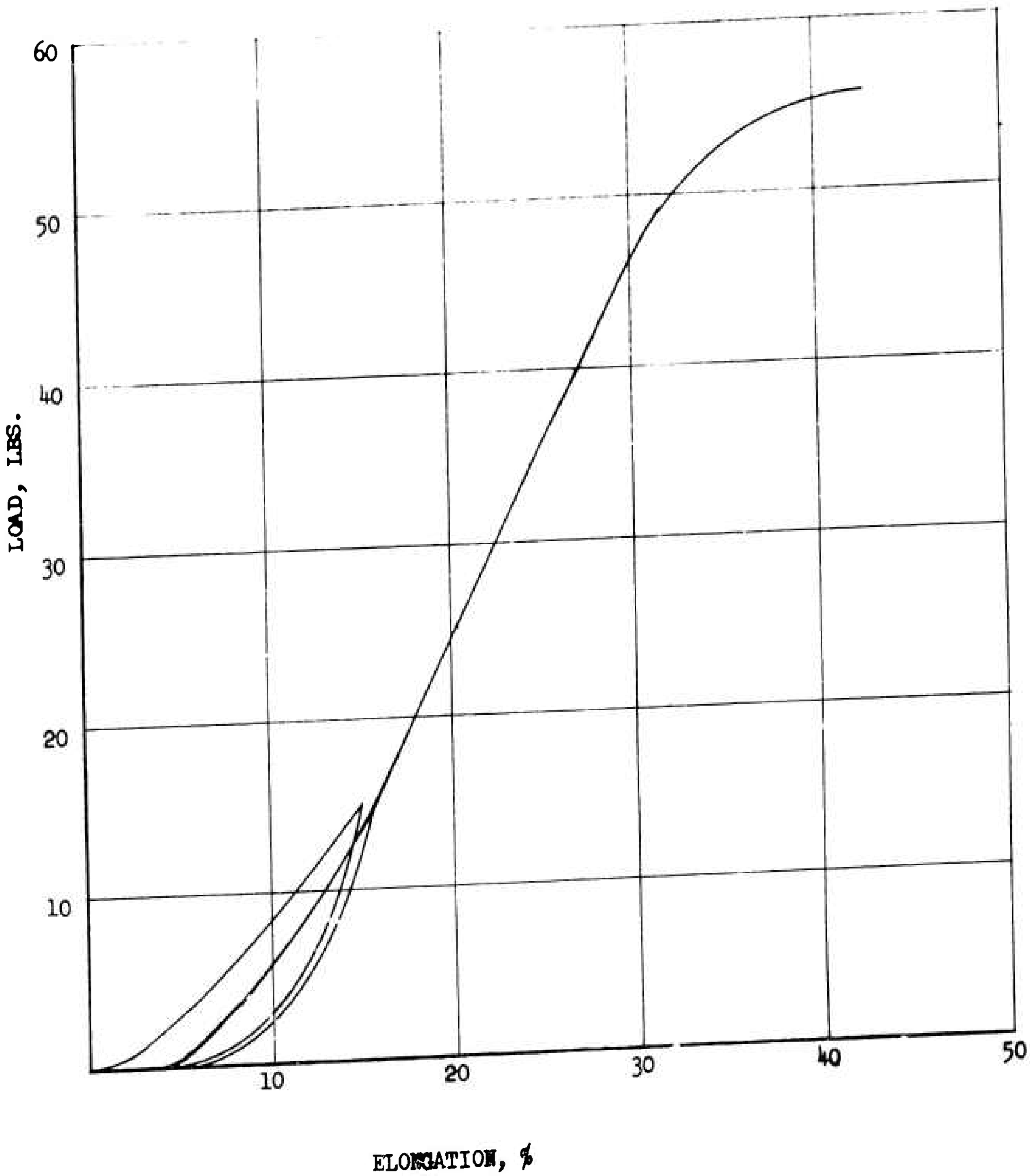

FIGURE 157

TYPICAL REPEATED STRESS-STRAIN CURVES SHOWING 1st & 5th CYCLES TO 2nd LOAD LEVEL AND FINAL RUPTURE CYCLE

CHENEY

FABRIC 10N35, WARP

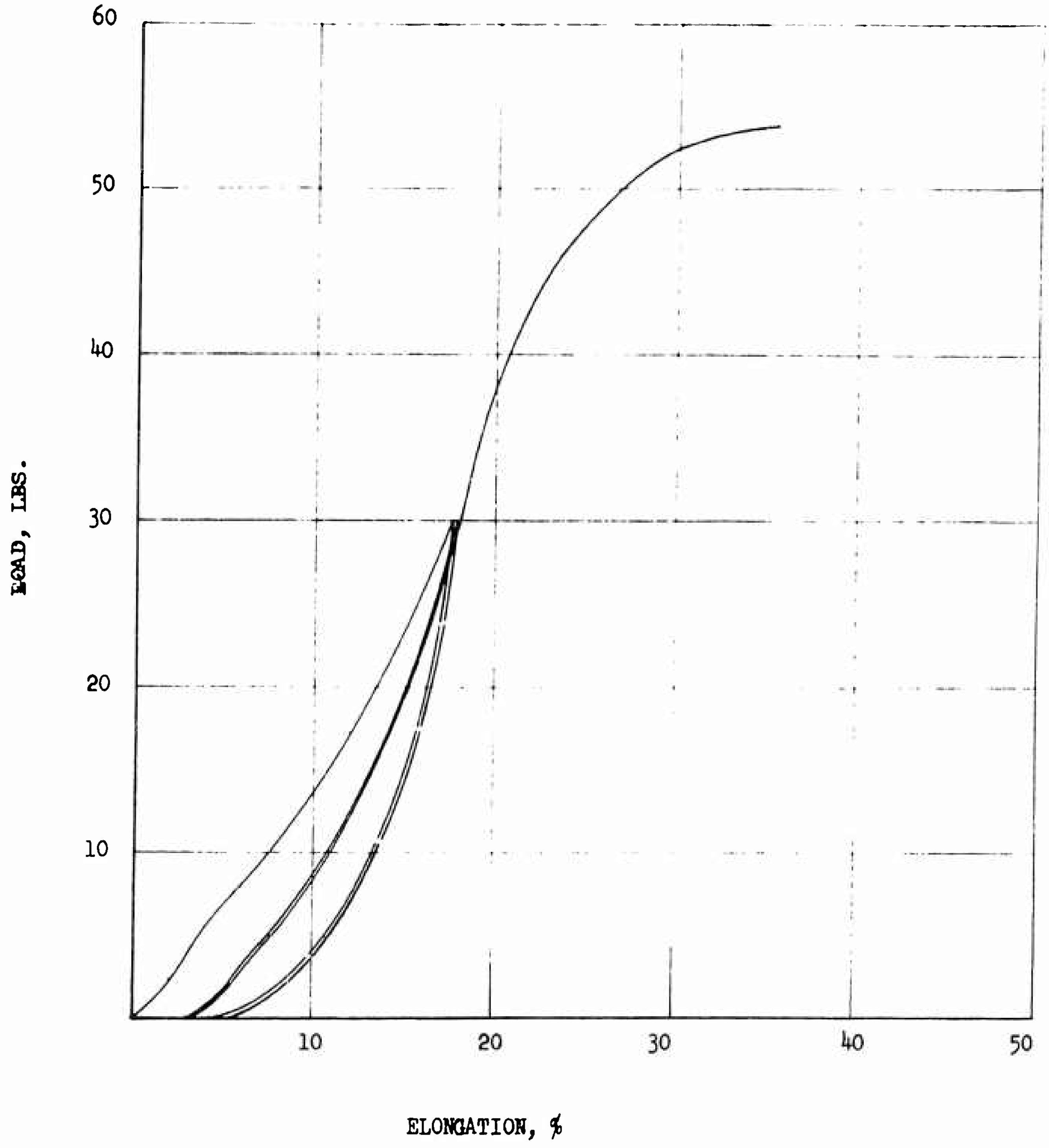

FIGURE 158

TYPICAL REPEATED STRESS-STRAIN CURVES SHOWING 1st & 5th CYCLES TO 2nd LOAD LEVEL AND FINAL RUPTURE CYCLE

CHENEY

FABRIC 10N35, FILLING

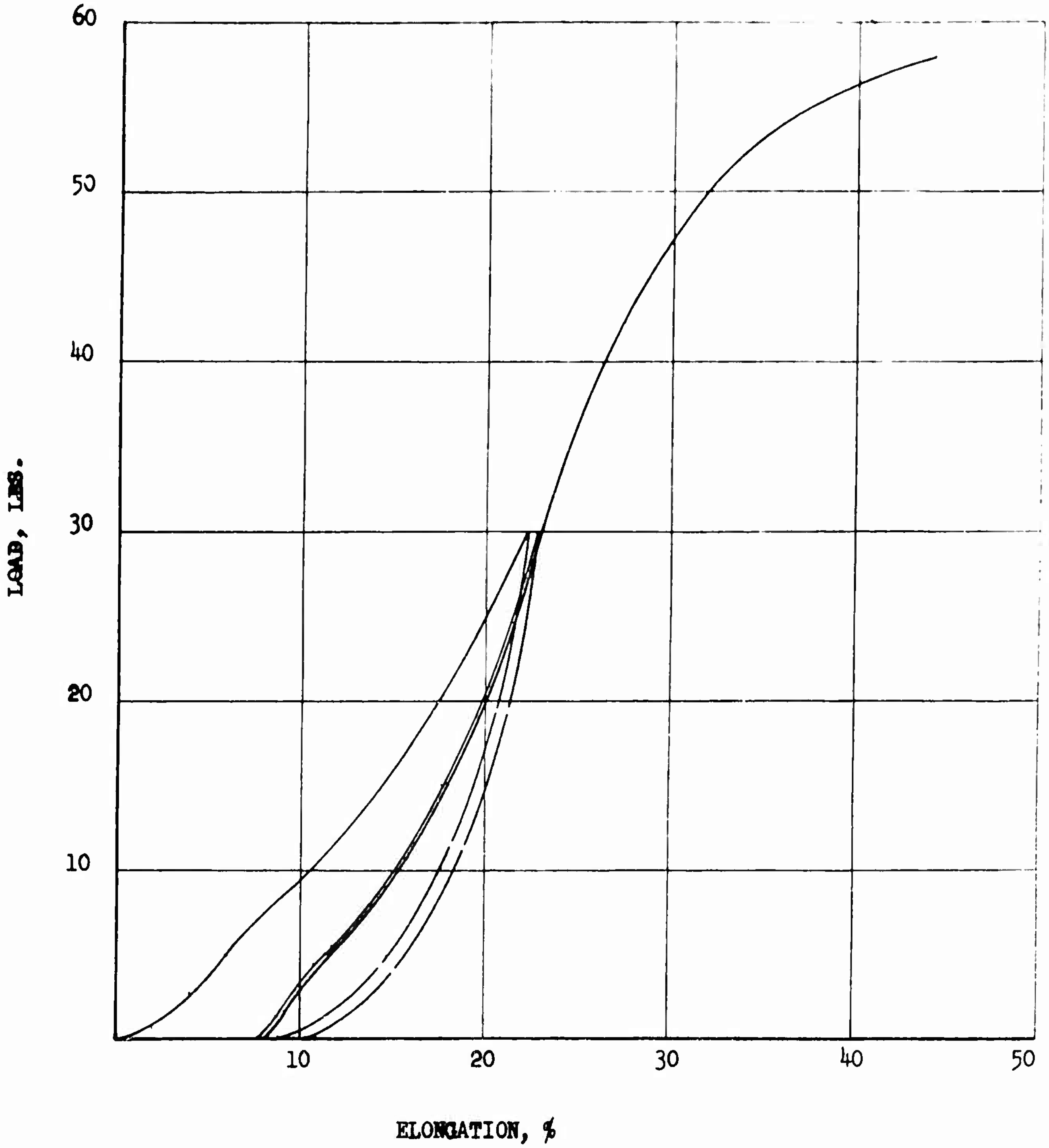

FIGURE 159

TYPICAL REPEATED STRESS-STRAIN CURVES SHOWING 1st & 5th CYCLES TO 3rd LOAD LEVEL AND FINAL RUPTURE CYCLE

CHENEY

FABRIC 10N 35, WARP

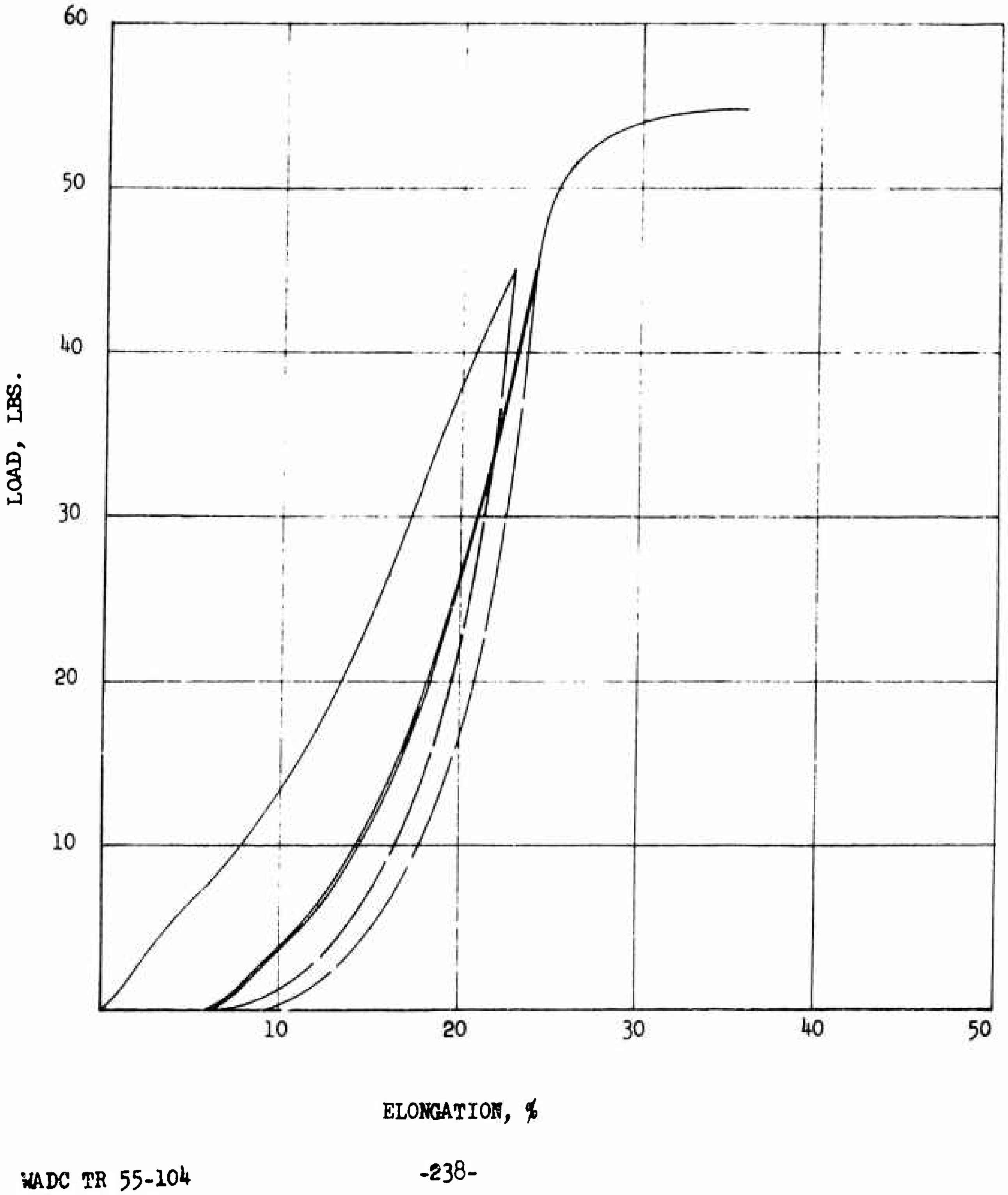

FIGURE 160

TYPICAL REPEATED STRESS-STRAIN CURVES SHOWING 1st & 5th CYCLES TO 3rd LOAD LEVEL AND FINAL RUPTURE CYCLE

CHENEY

FABRIC 10N 35, FILLING

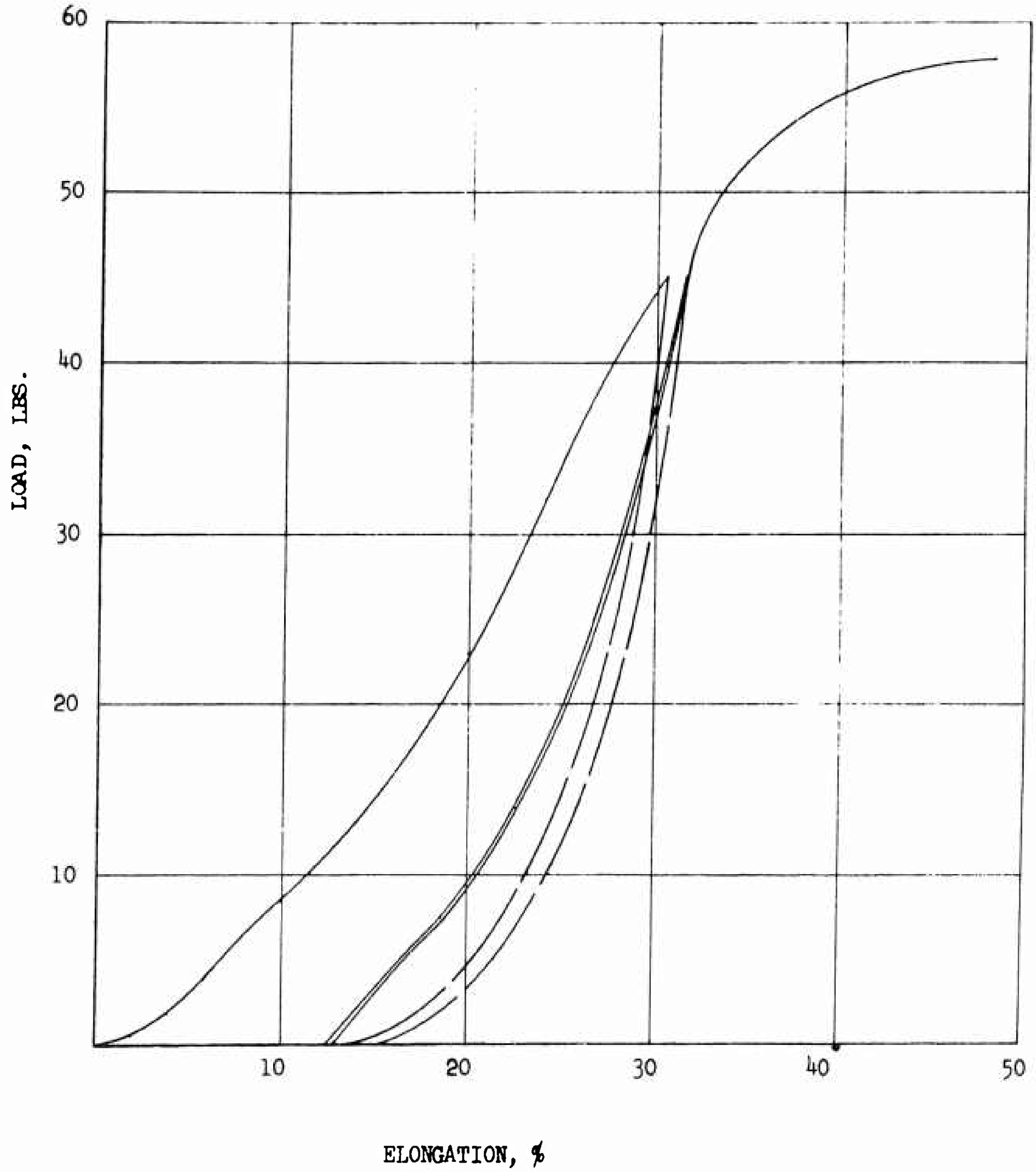

FIGURE 161

TYPICAL REPEATED STRESS-STRAIN CURVES SHOWING 1st & 5th CYCLES TO 1st LOAD LEVEL AND FINAL RUPTURE CYCLE

CHENEY

FABRIC R7N 1/2, WARP

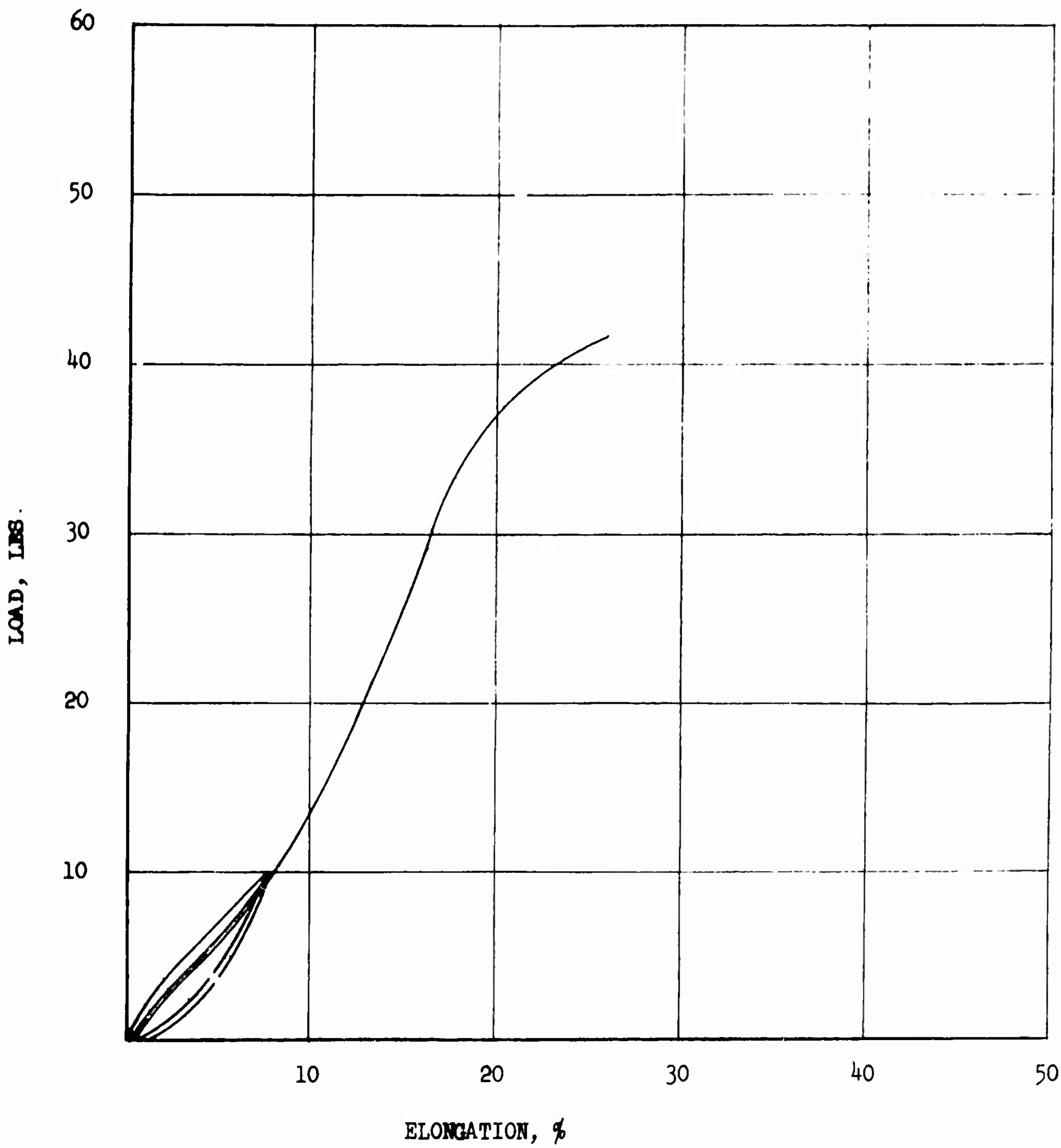

FIGURE 162

TYPICAL REPEATED STRESS-STRAIN CURVES SHOWING 1st & 5th CYCLES TO
1st LOAD LEVEL AND FINAL RUPTURE CYCLE

CHENEY

FABRIC R7N 1/2, FILLING

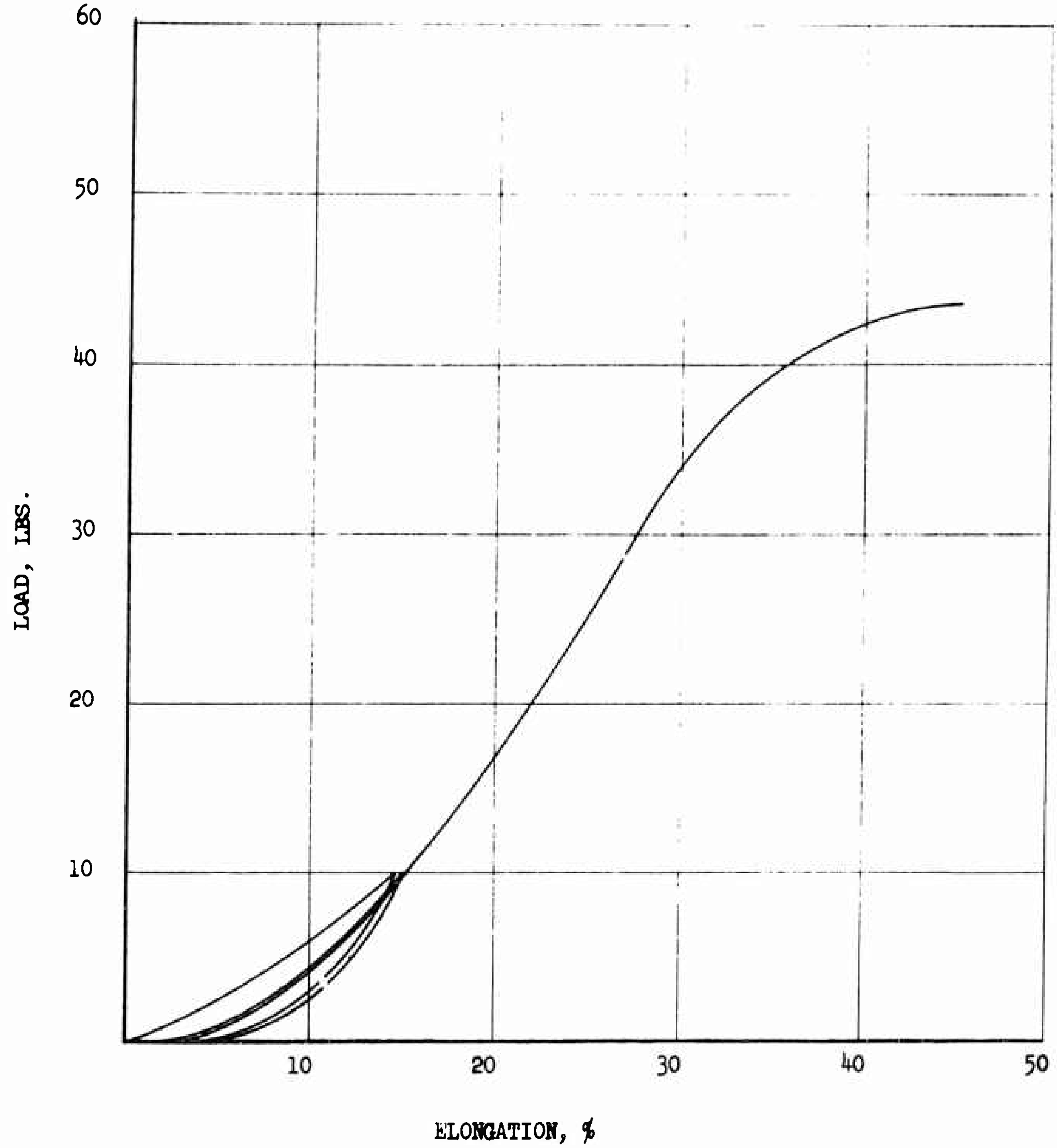

FIGURE 163

TYPICAL REPEATED STRESS-STRAIN CURVES SHOWING 1st & 5th CYCLES TO 2nd LOAD LEVEL AND FINAL RUPTURE CYCLE

CHENEY

FABRIC R7W 1/2, WARP

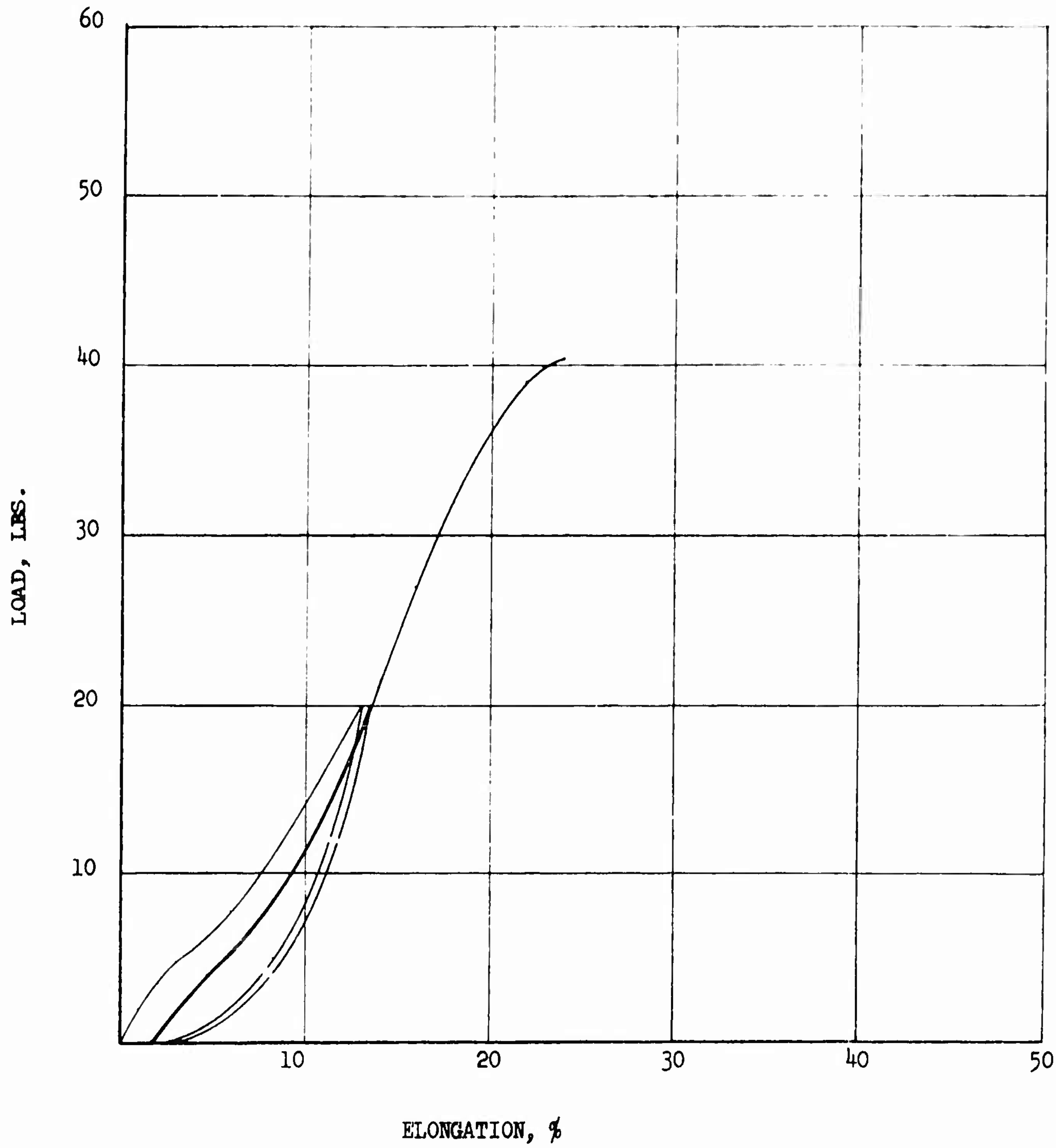

FIGURE 164

TYPICAL REPEATED STRESS-STRAIN CURVES SHOWING 1st & 5th CYCLES TO 2nd LOAD LEVEL AND FINAL RUPTURE CYCLE

CHENEY

FABRIC R7N 1/2, FILLING

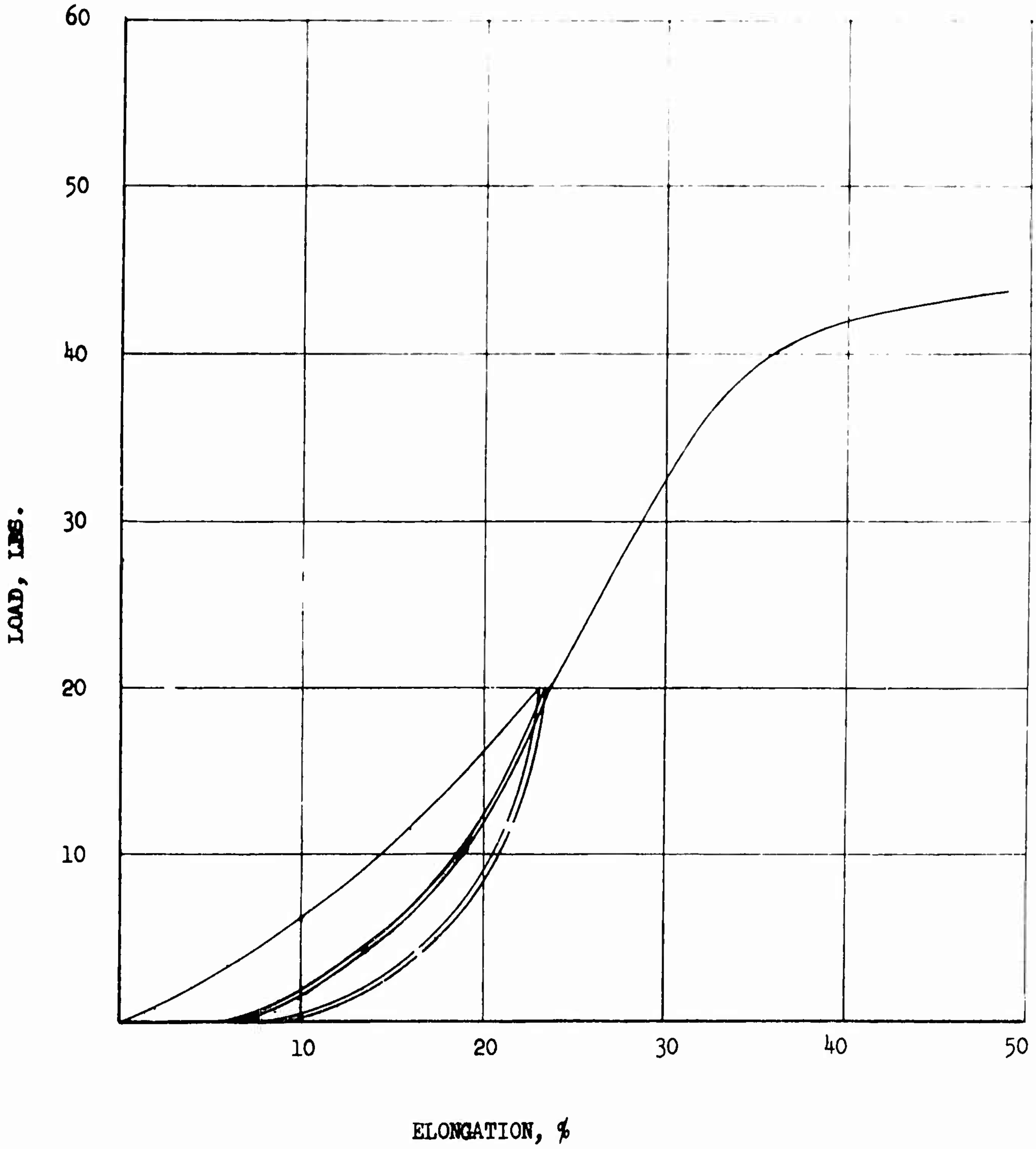

FIGURE 165

TYPICAL REPEATED STRESS-STRAIN CURVES SHOWING 1st & 5th CYCLES TO 3rd LOAD LEVEL AND FINAL RUPTURE CYCLE

CHENEY

FABRIC R7N 1/2, WARP

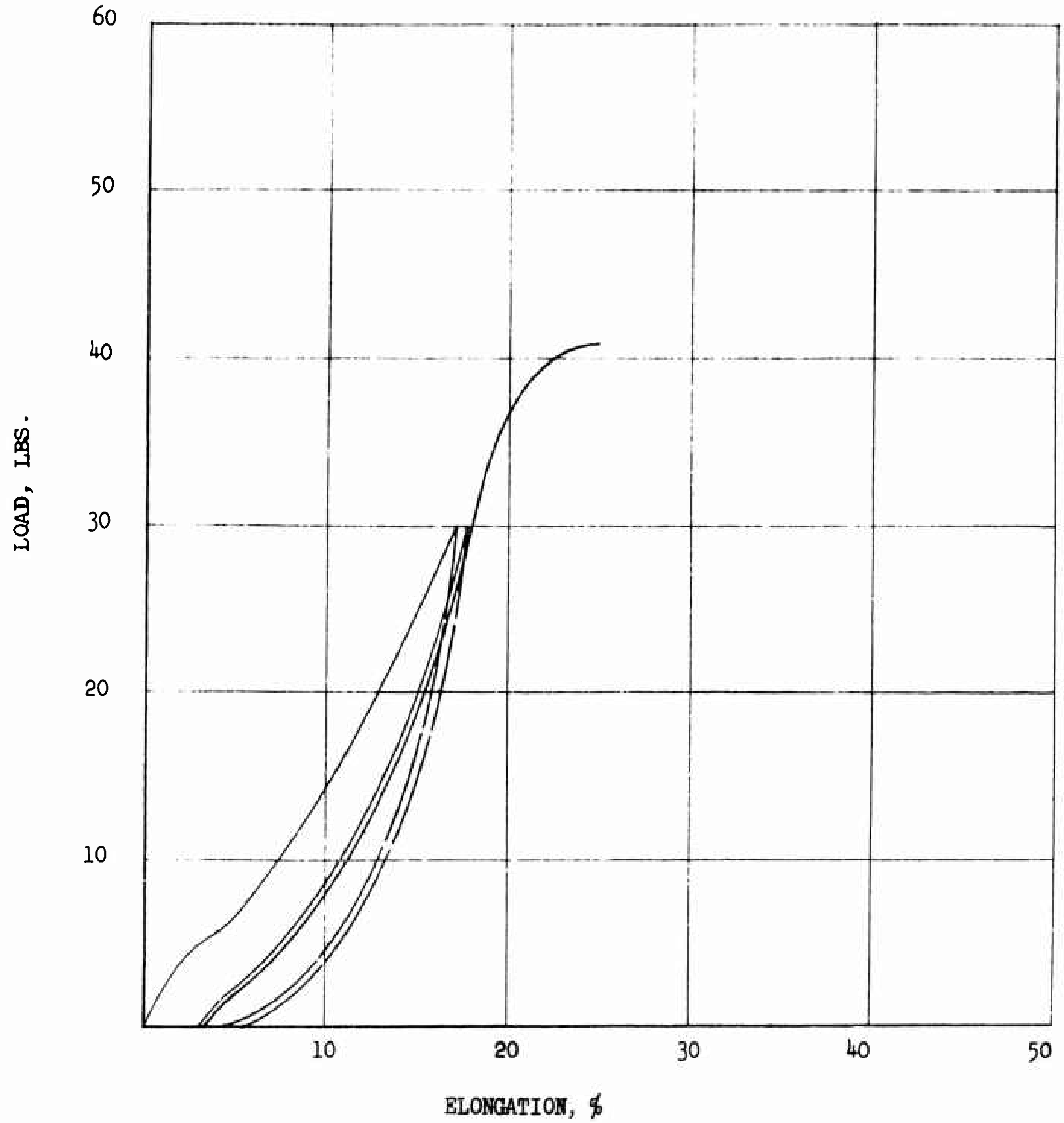

FIGURE 166

TYPICAL REPEATED STRESS-STRAIN CURVES SHOWING 1st & 5th CYCLES TO 3rd LOAD LEVEL AND FINAL RUPTURE CYCLE

CHENEY

FABRIC R7N 1/2, FILLING

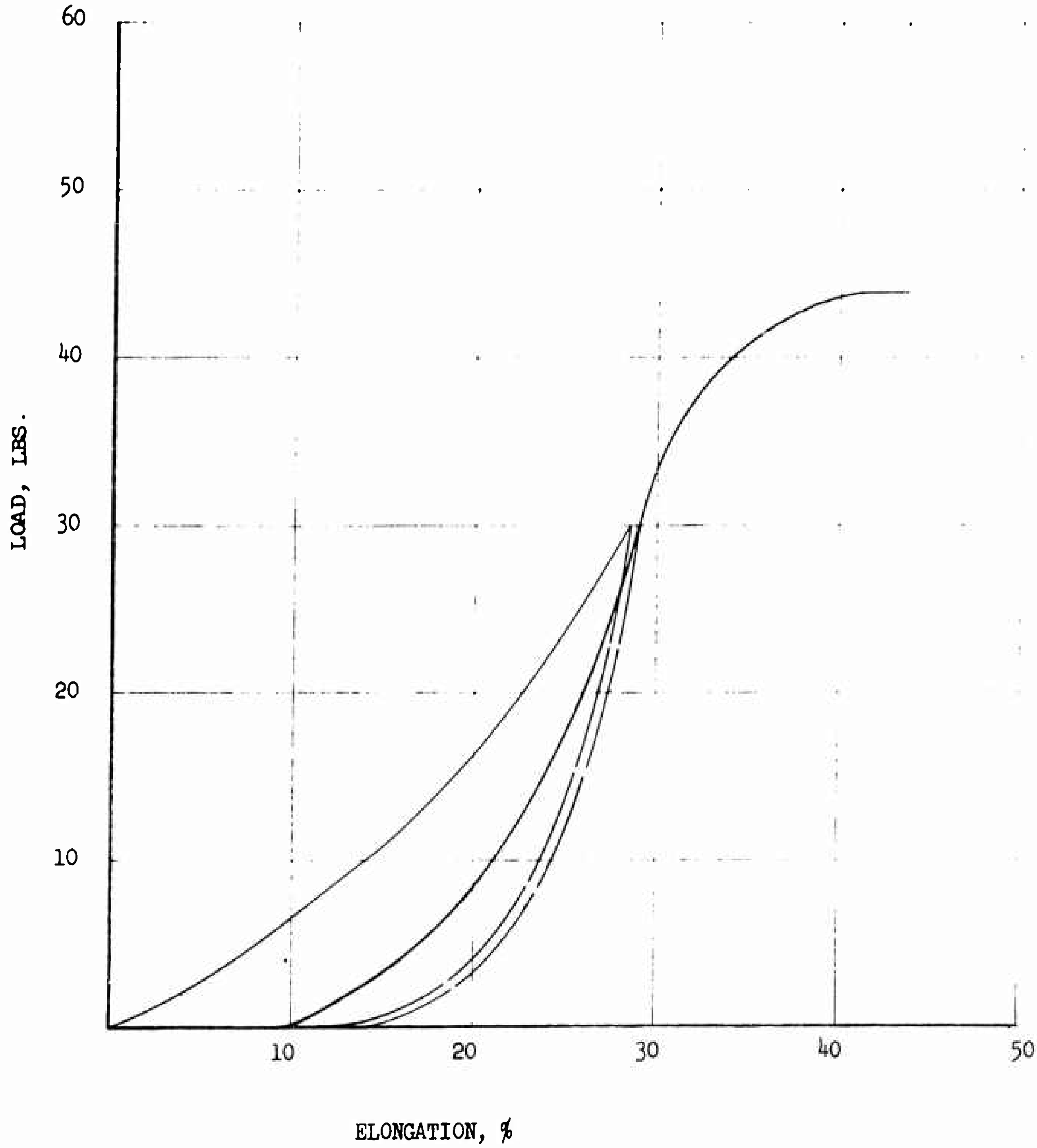

FIGURE 167

TYPICAL REPEATED STRESS-STRAIN CURVES SHOWING 1st & 5th CYCLES TO 1st LOAD LEVEL AND FINAL RUPTURE CYCLE

CHENEY

FABRIC R7N7, WARP

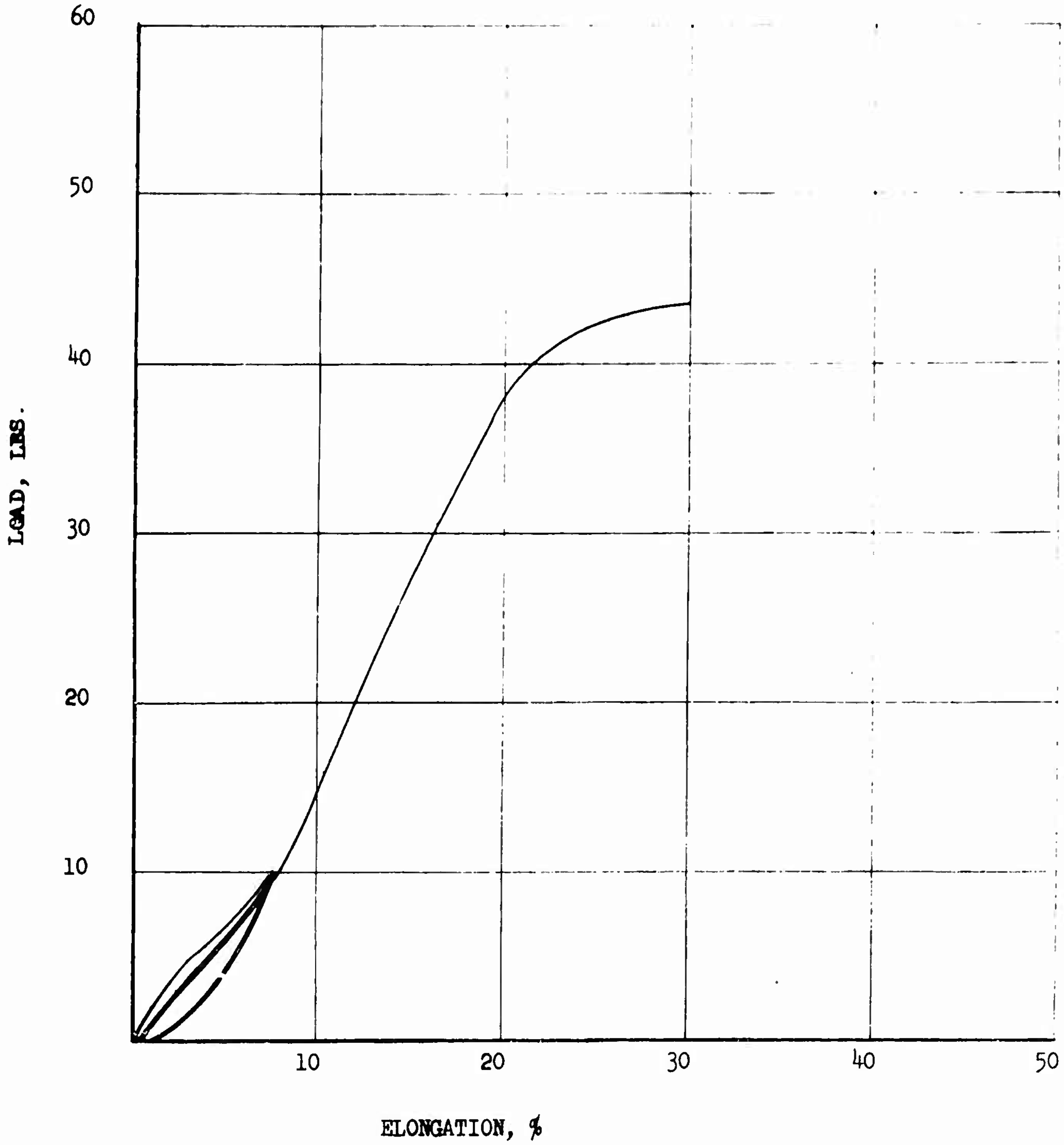

FIGURE 168

TYPICAL REPEATED STRESS STRAIN CURVES SHOWING 1st & 5th CYCLES TO 1st LOAD LEVEL AND FINAL RUPTURE CYCLE

CHENEY

FABRIC R7N7, FILLING

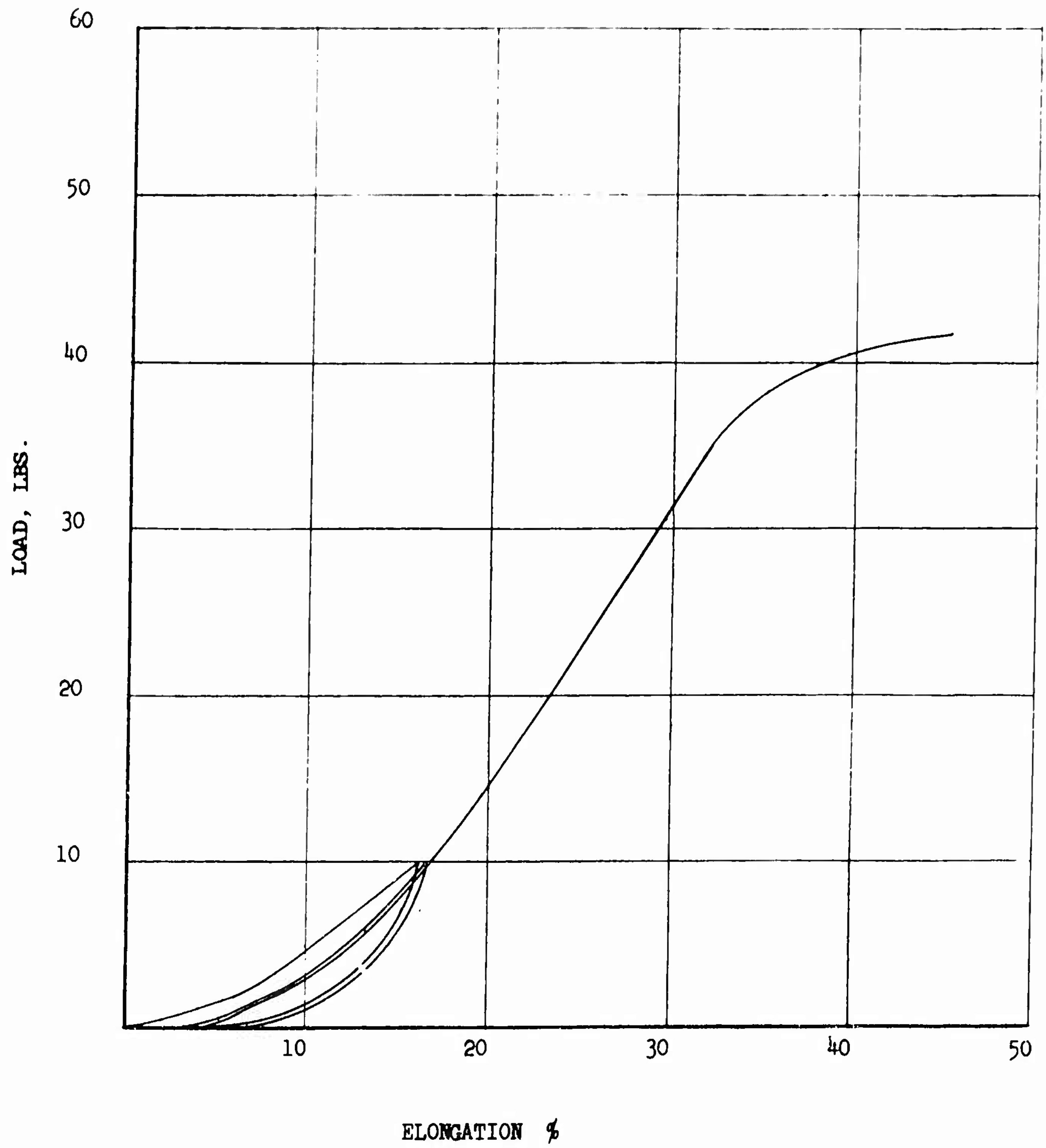

FIGURE 169

TYPICAL REPEATED STRESS-STRAIN CURVES SHOWING 1st & 5th CYCLES TO 2nd LOAD LEVEL AND FINAL RUPTURE CYCLE

CHENEY

FABRIC R7N7, WARP

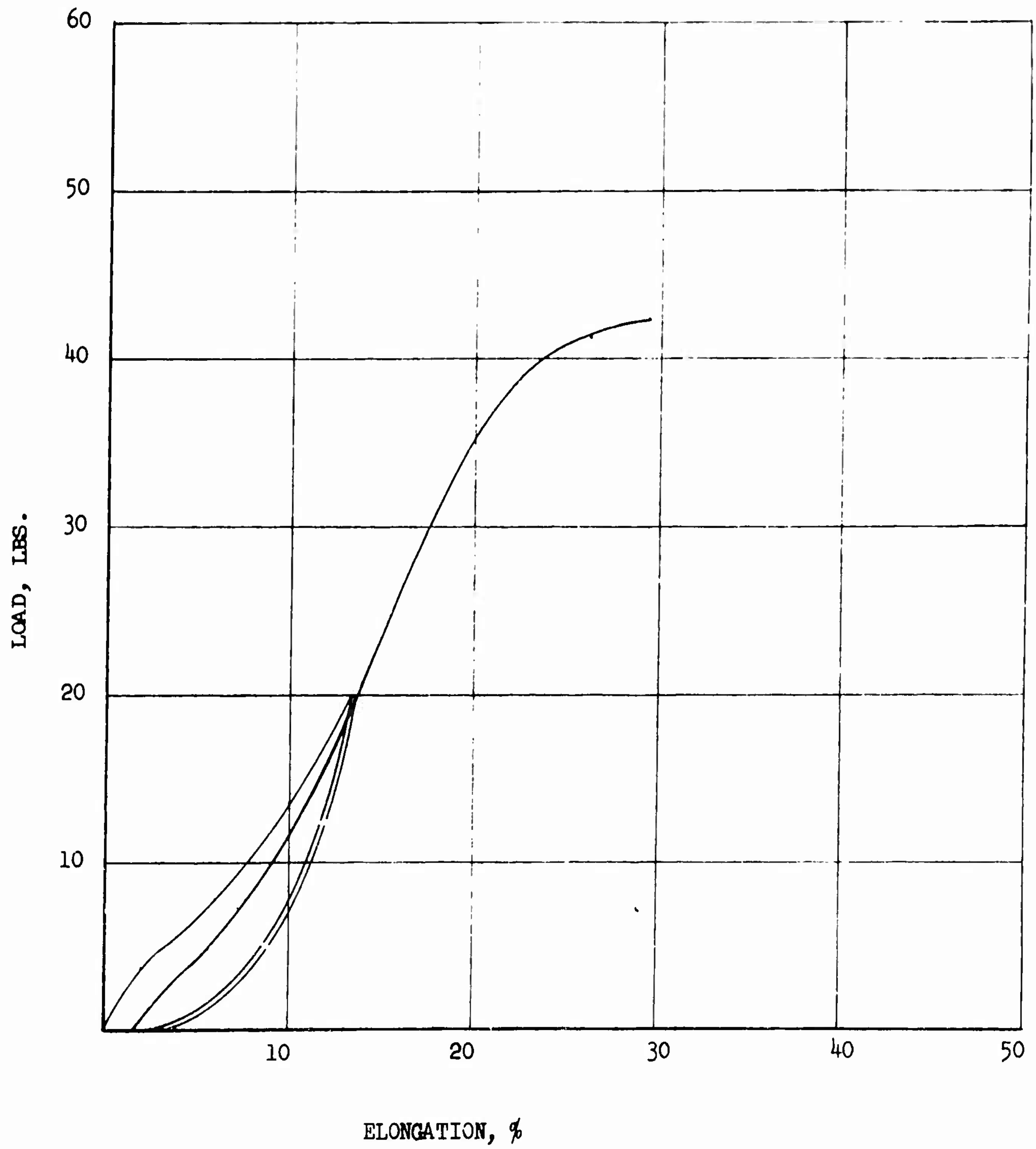

FIGURE 170

TYPICAL REPEATED STRESS-STRAIN CURVES SHOWING 1st & 5th CYCLES TO 2nd LOAD LEVEL AND FINAL RUPTURE CYCLE

CHENEY

FABRIC R7N7, FILLING

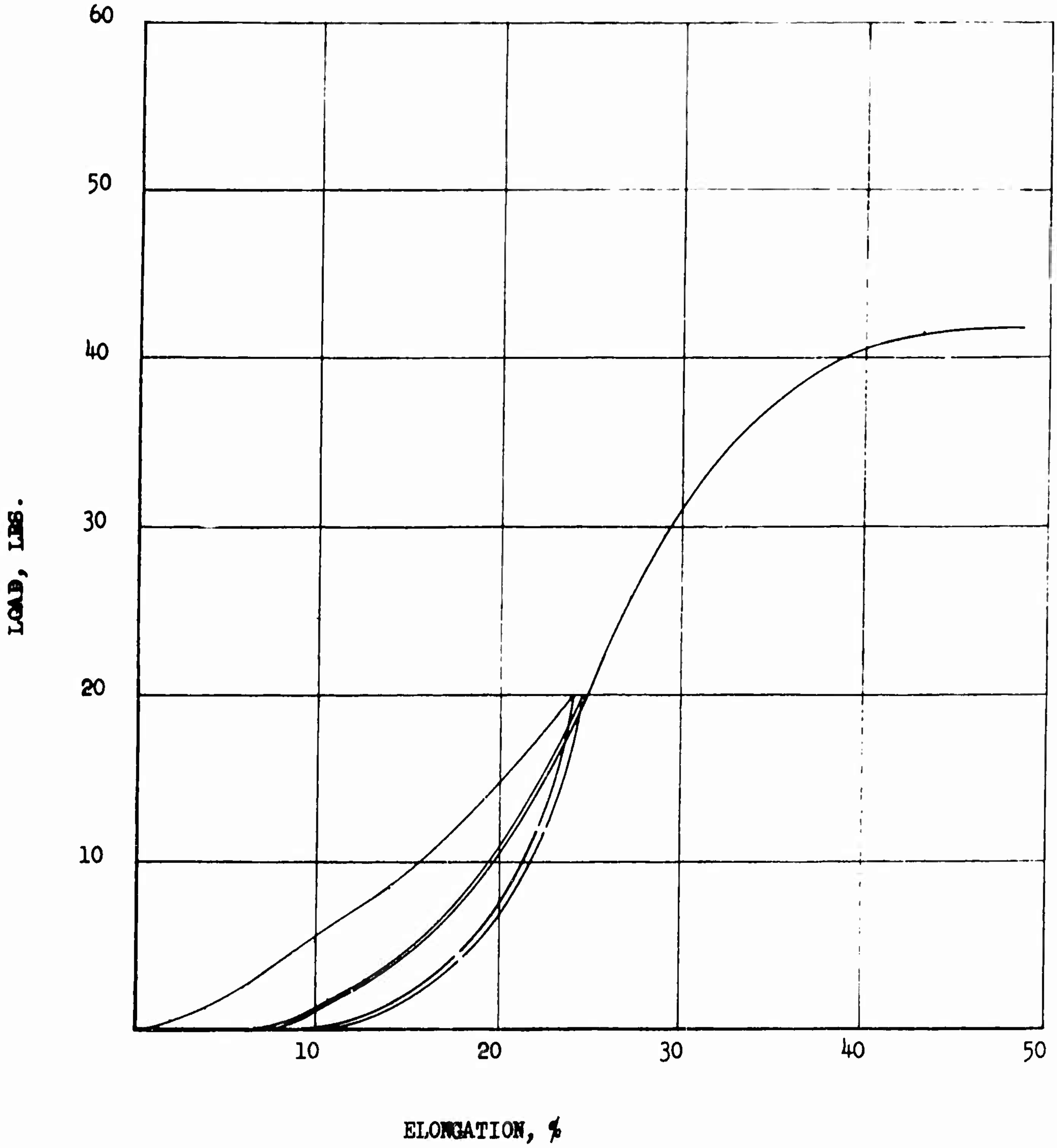

FIGURE 171

TYPICAL REPEATED STRESS-STRAIN CURVES SHOWING 1st & 5th CYCLES TO 3rd LOAD LEVEL AND FINAL RUPTURE CYCLE

CHENEY
FABRIC R7N7, WARP

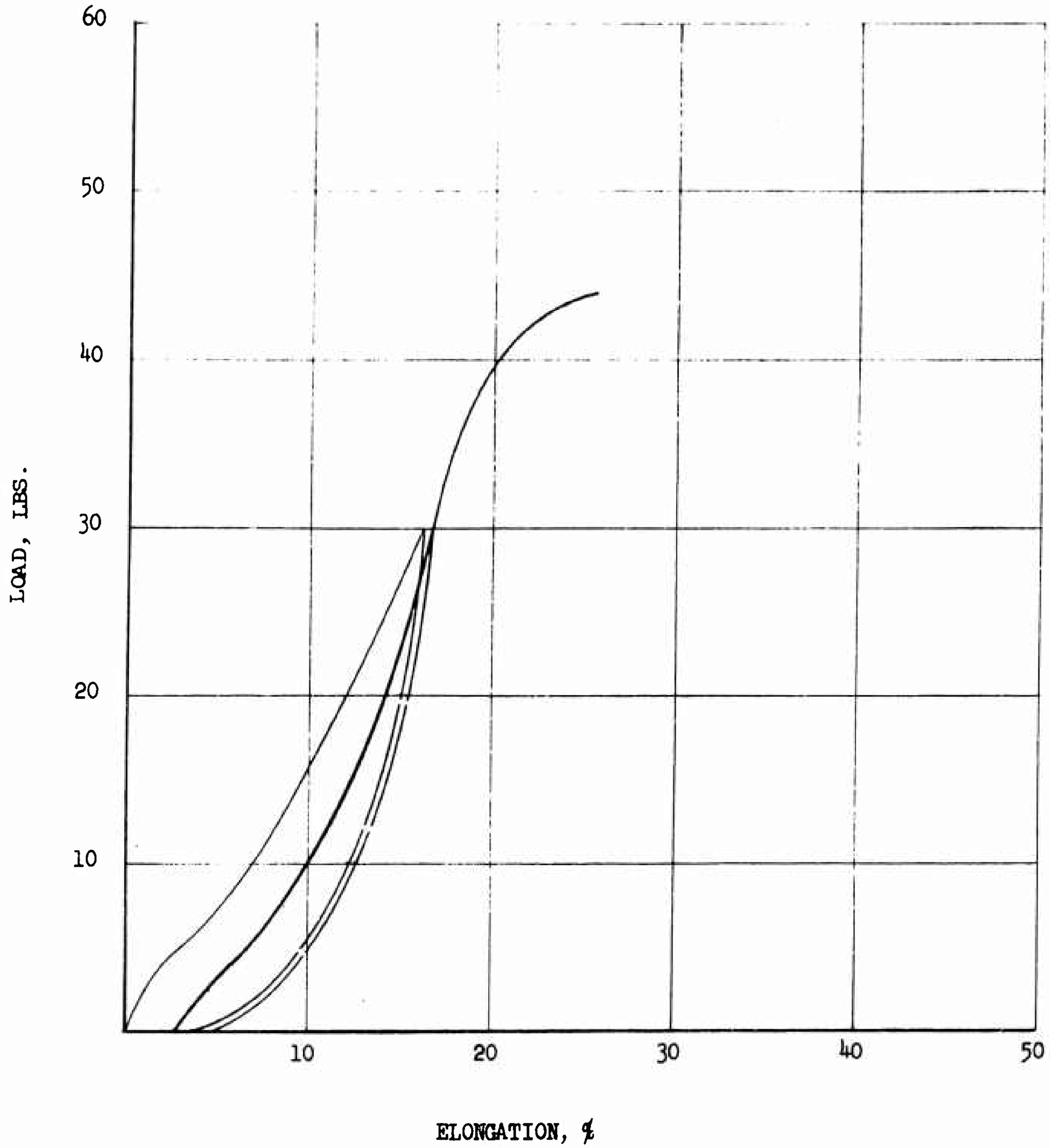

FIGURE 172

TYPICAL REPEATED STRESS-STRAIN CURVES SHOWING 1st & 5th CYCLES TO 3rd LOAD LEVEL AND FINAL RUPTURE CYCLE

CHENEY

FABRIC R7N7, FILLING

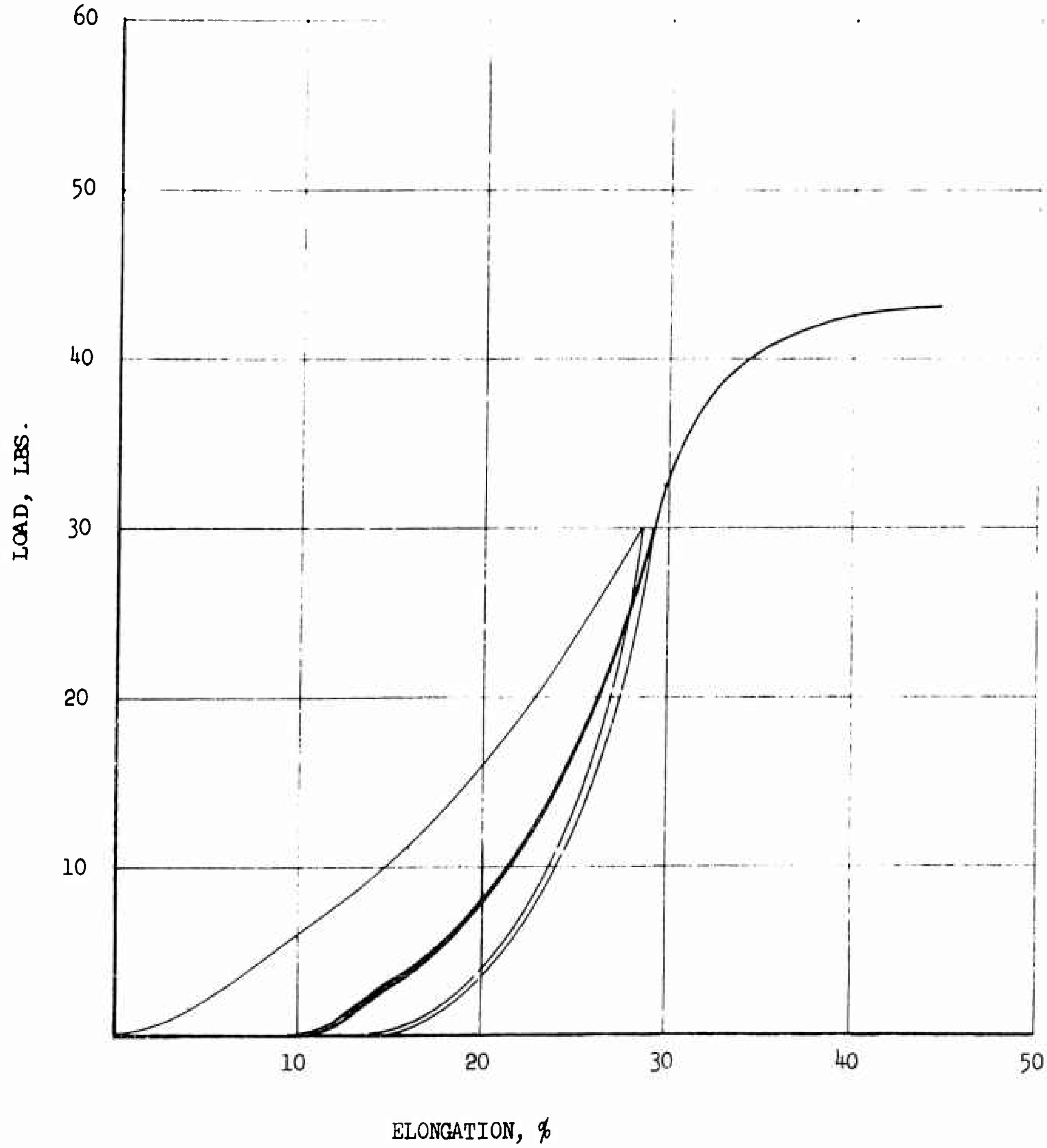

FIGURE 173

TYPICAL REPEATED STRESS-STRAIN CURVES SHOWING 1st & 5th CYCLES TO 1st LOAD LEVEL AND FINAL RUPTURE CYCLE

CHENEY

FABRIC R7N30, WARP

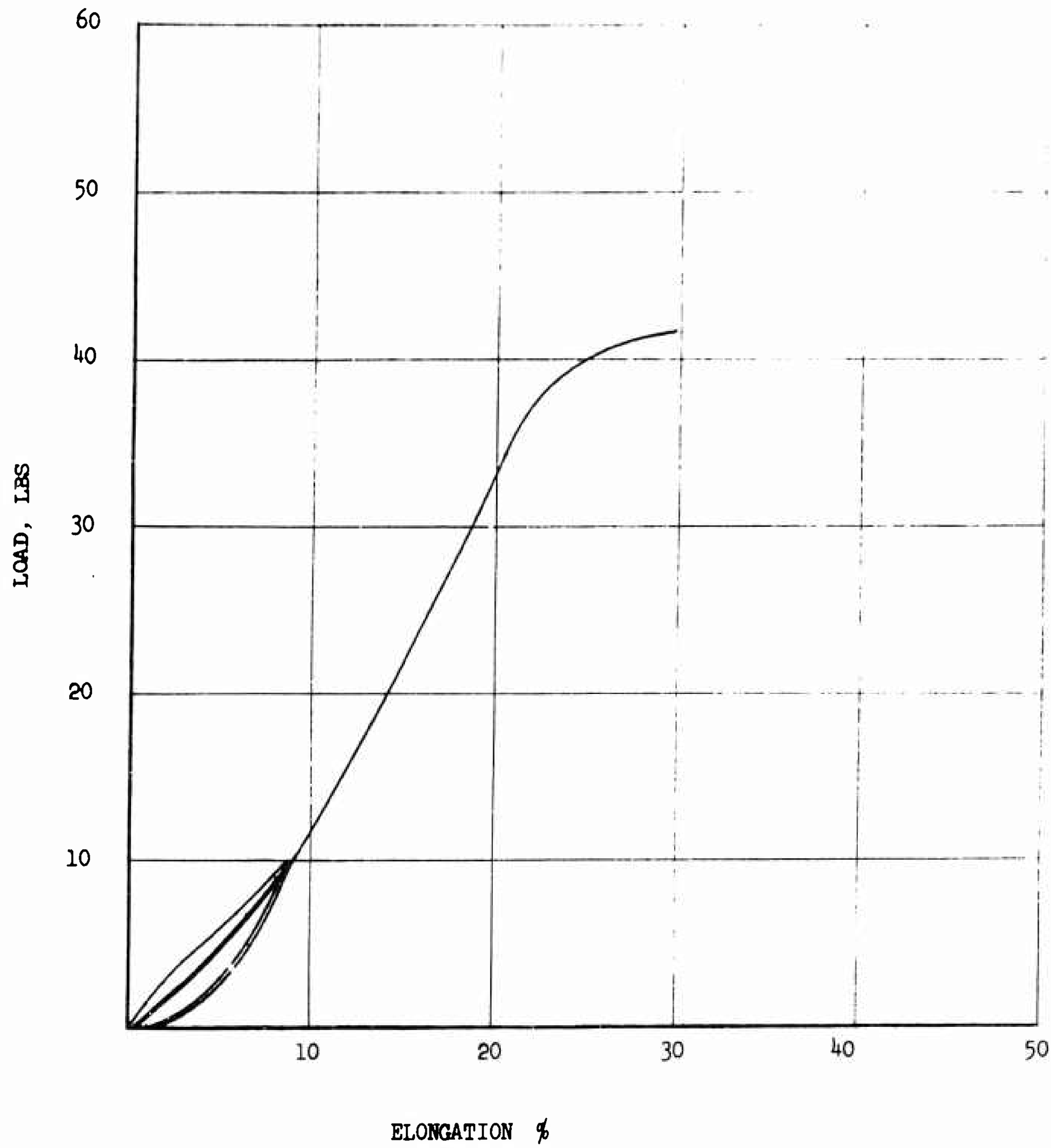

FIGURE 174

TYPICAL REPEATED STRESS-STRAIN CURVES SHOWING 1st & 5th CYCLES TO 1st LOAD LEVEL AND FINAL RUPTURE CYCLE

CHENEY

FABRIC R7N30, FILLING

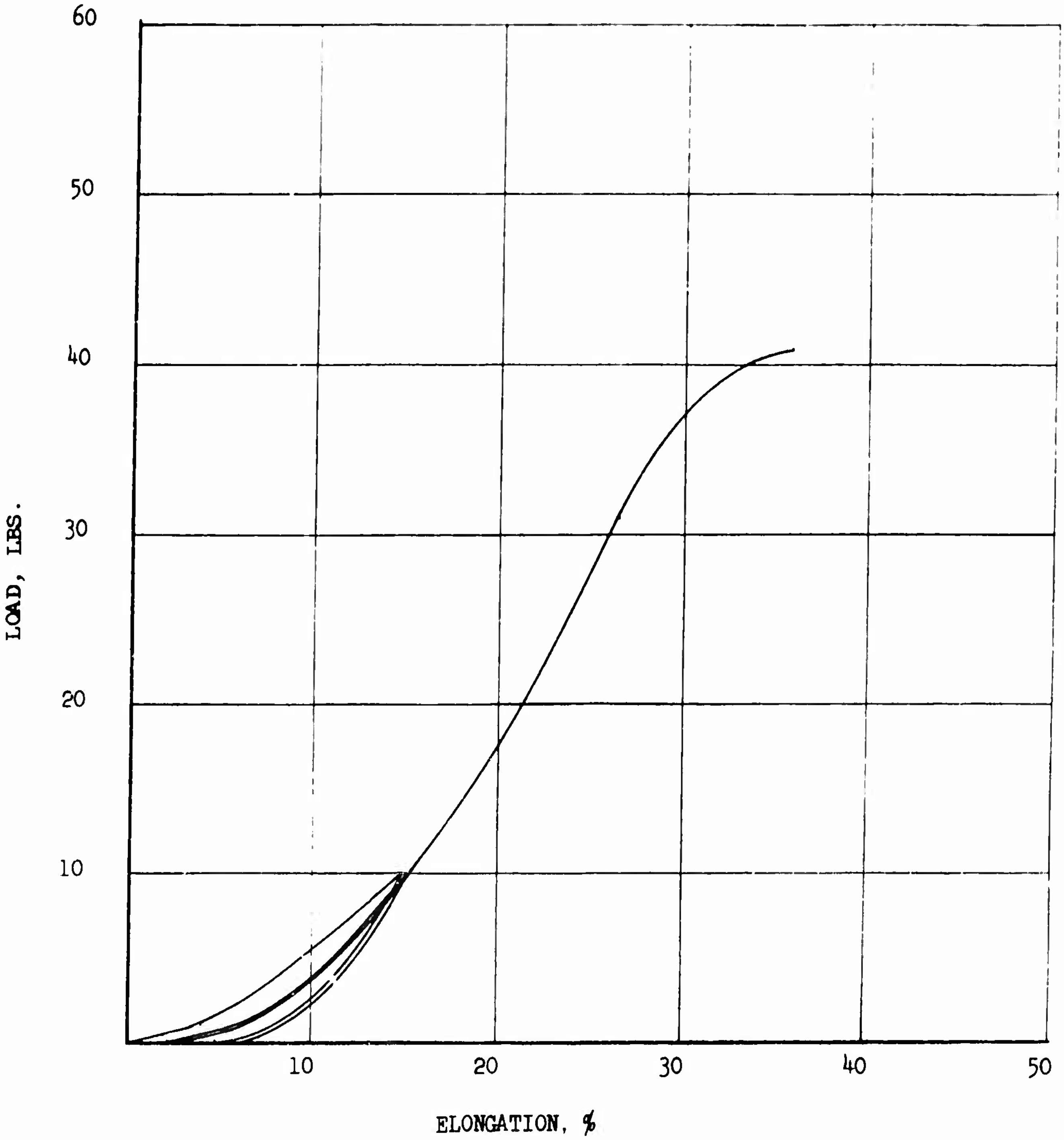

FIGURE 175

TYPICAL REPEATED STRESS-STRAIN CURVES SHOWING 1st & 5th CYCLES TO 2nd LOAD LEVEL AND FINAL RUPTURE CYCLE

CHENEY

FABRIC R7N30, WARP

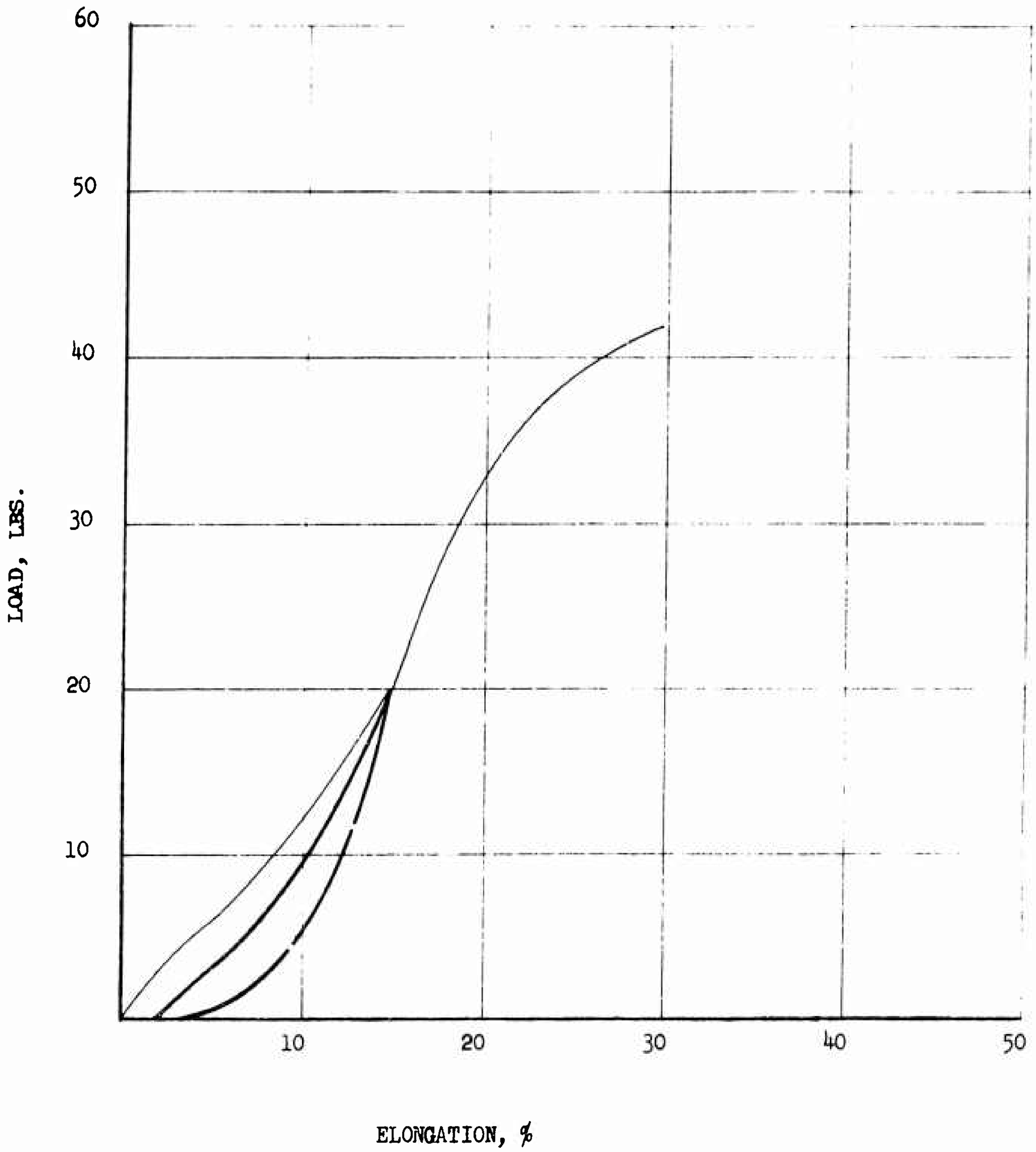

FIGURE 176

TYPICAL REPEATED STRESS-STRAIN CURVES SHOWING 1st & 5th CYCLES TO 2nd LOAD LEVEL AND FINAL RUPTURE CYCLE

CHENEY

FABRIC R7N30, FILLING

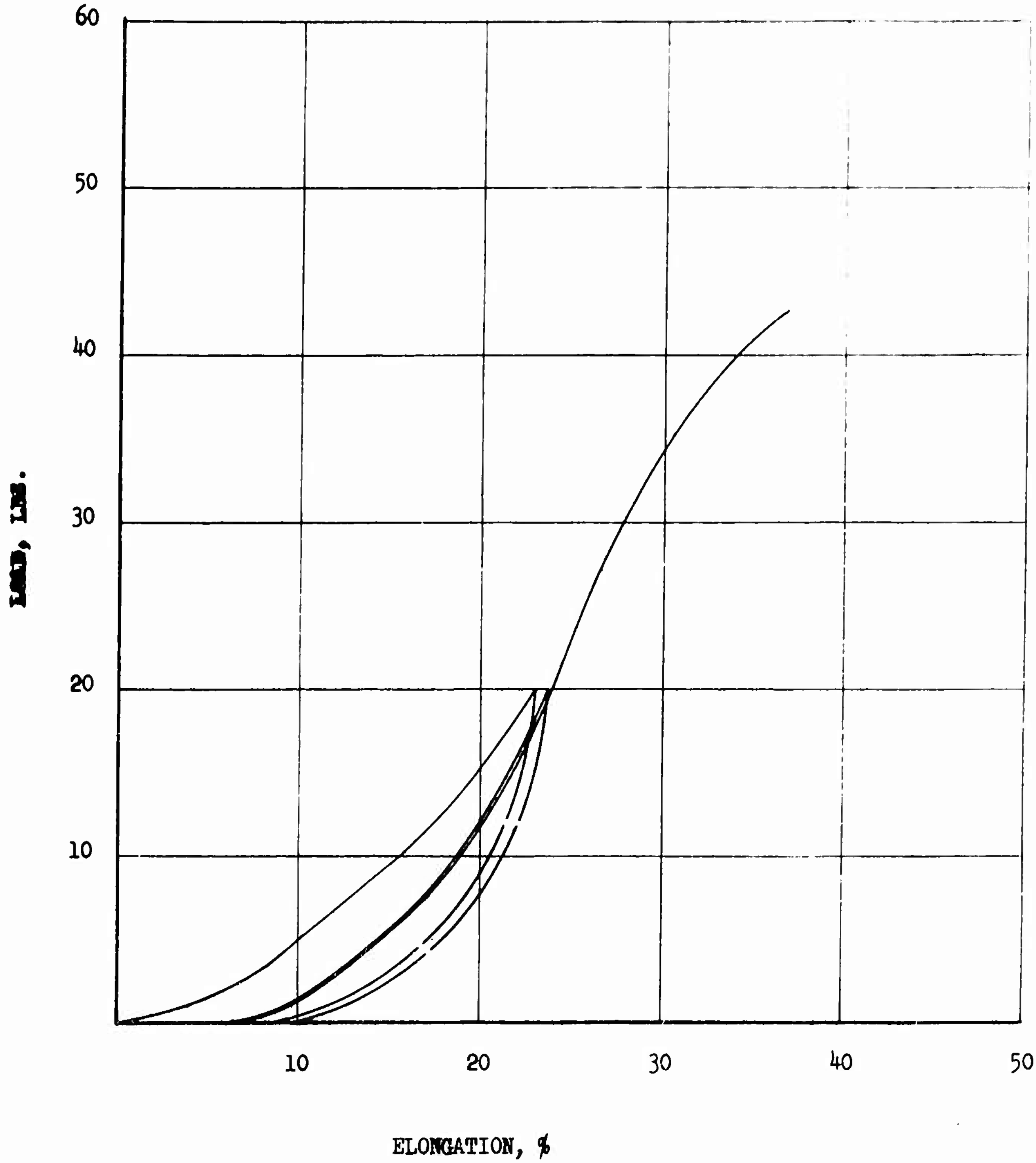

FIGURE 177

TYPICAL REPEATED STRESS-STRAIN CURVES SHOWING 1st & 5th CYCLES TO
3rd LOAD LEVEL AND FINAL RUPTURE CYCLE

CHENEY

FABRIC R7N30, WARP

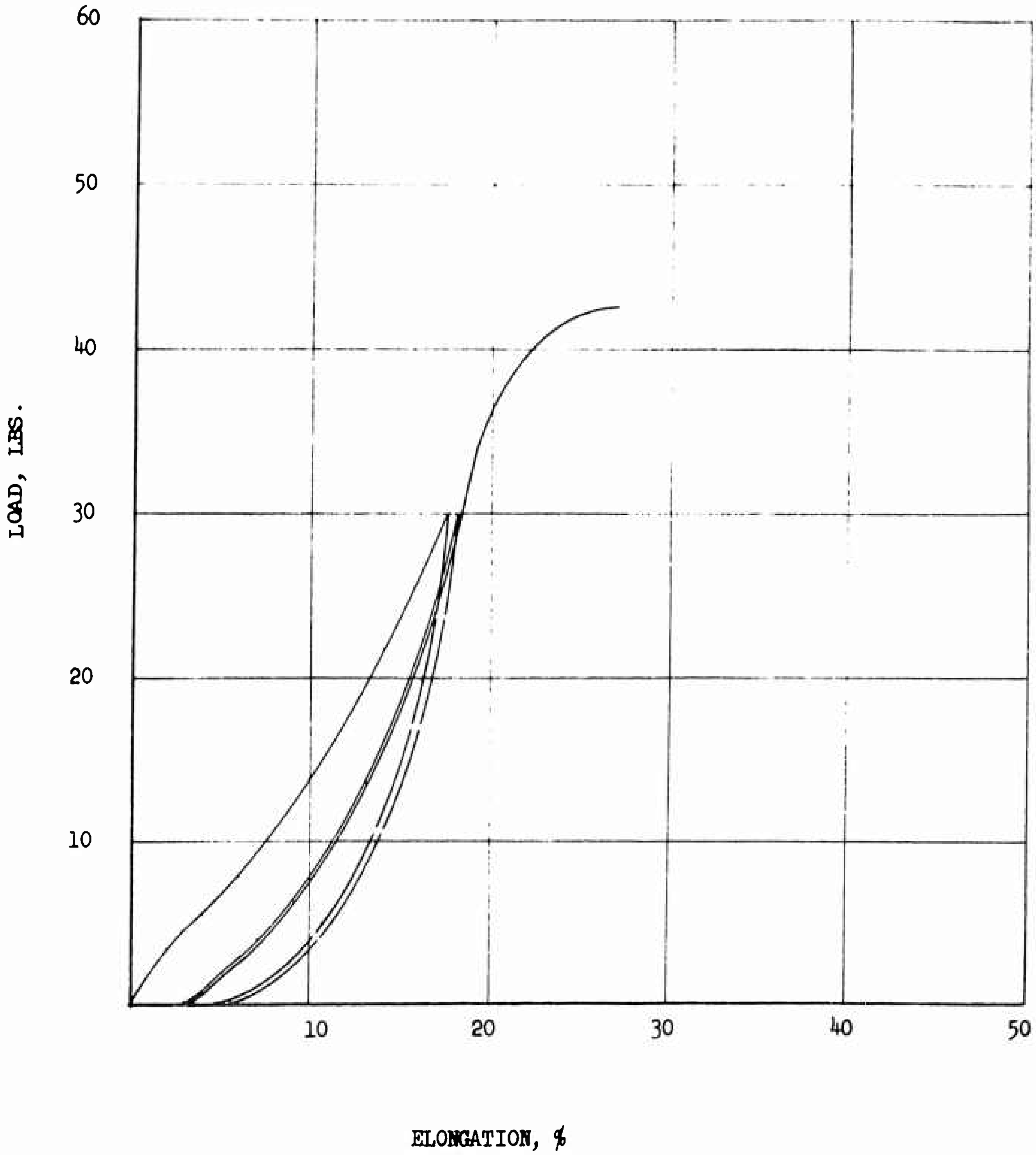

FIGURE 178

TYPICAL REPEATED STRESS-STRAIN CURVES SHOWING 1st & 5th CYCLES TO 3rd LOAD LEVEL AND FINAL RUPTURE CYCLE

CHENEY

FABRIC R7N30, FILLING

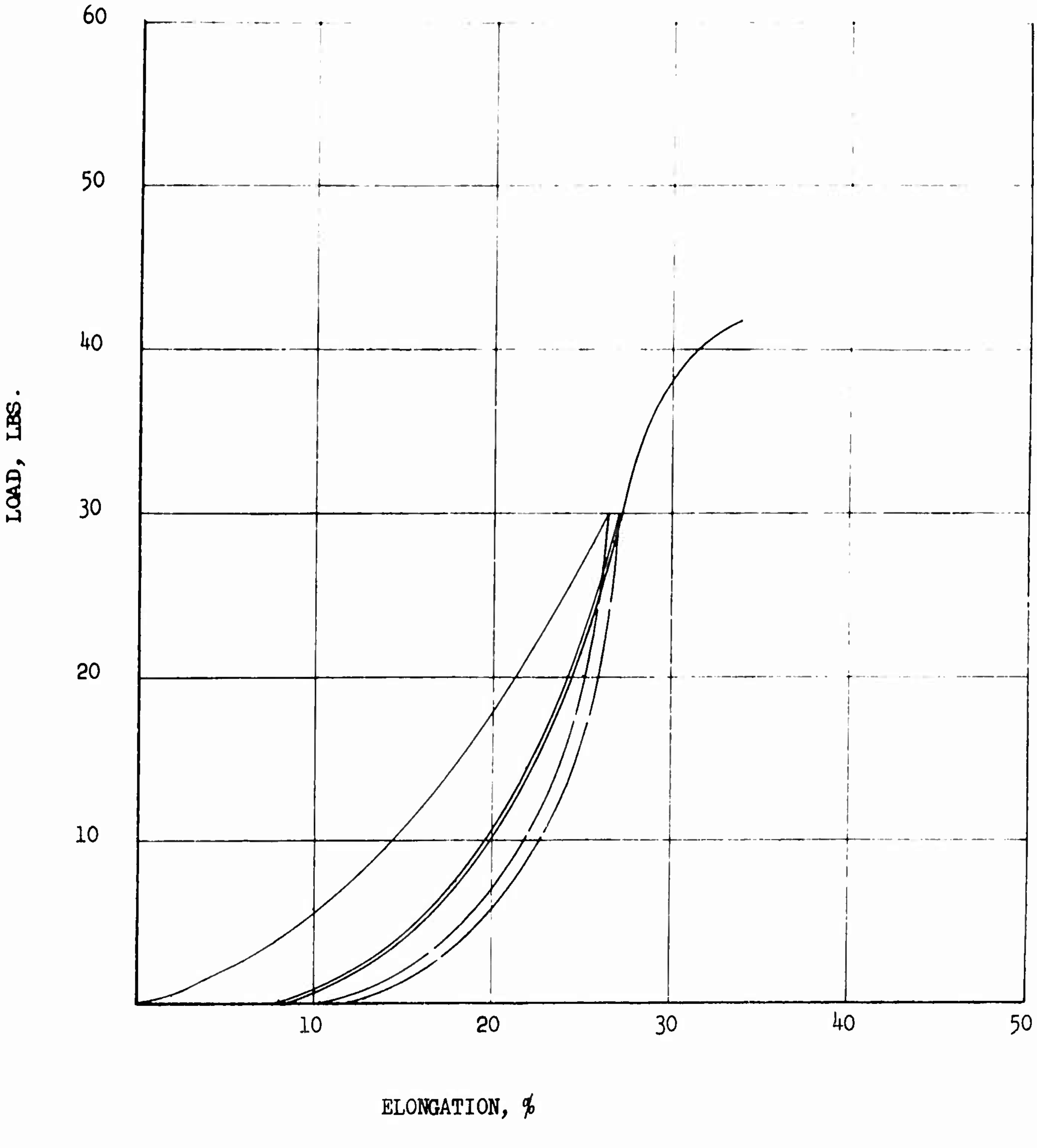

FIGURE 179

TYPICAL REPEATED STRESS-STRAIN CURVES SHOWING 1st & 5th CYCLES TO
1st LOAD LEVEL AND FINAL RUPTURE CYCLE

CHENEY

FABRIC R7C 1/2, WARP

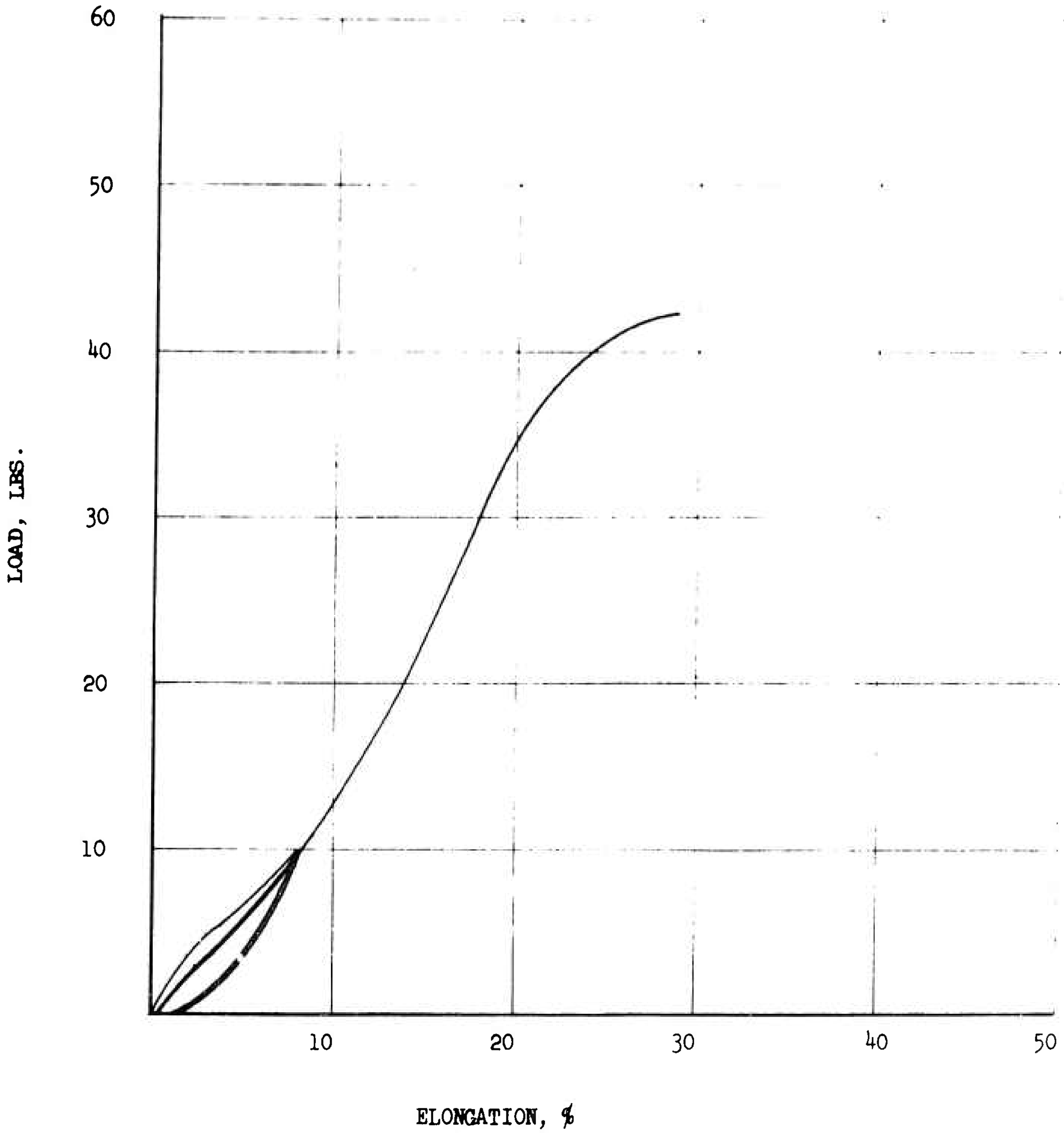

FIGURE 180

TYPICAL REPEATED STRESS-STRAIN CURVES SHOWING 1st & 5th CYCLES TO 1st LOAD LEVEL AND FINAL RUPTURE CYCLE

CHENEY

FABRIC R7C 1/2, FILLING

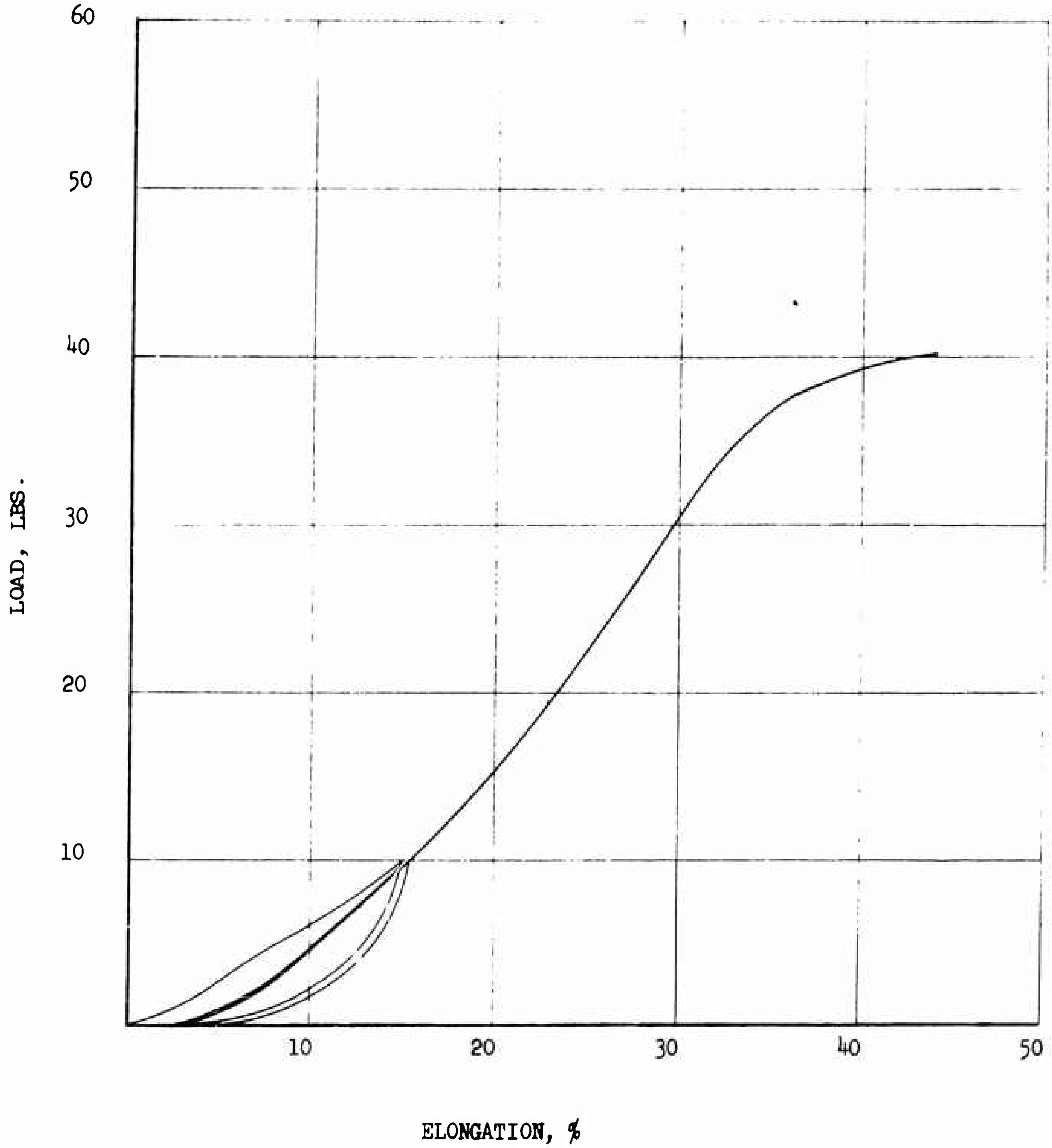

FIGURE 181

TYPICAL REPEATED STRESS-STRAIN CURVES SHOWING 1st & 5th CYCLES TO 2nd LOAD LEVEL AND FINAL RUPTURE CYCLE

CHENEY

FABRIC R7C 1/2, WARP

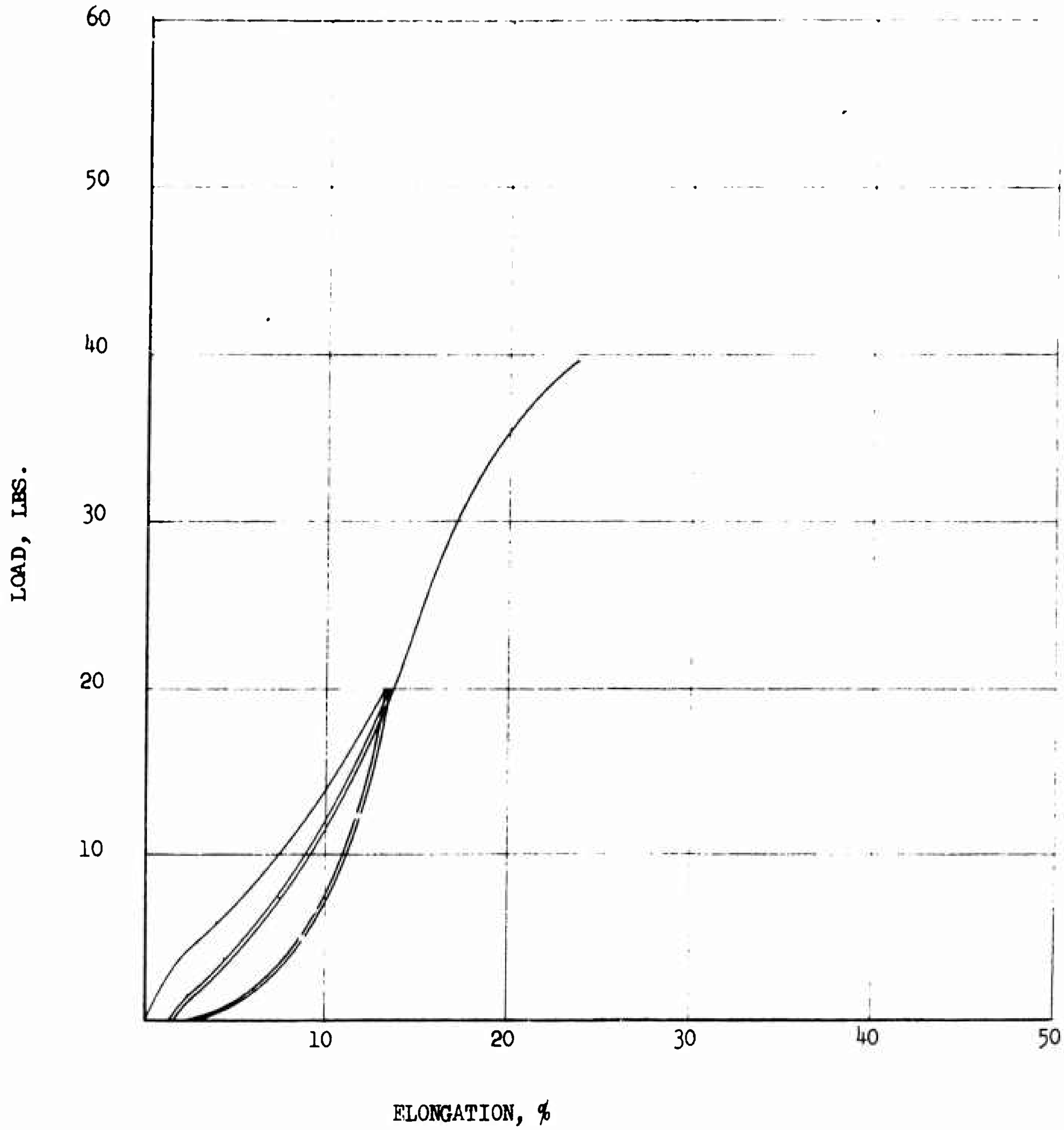

FIGURE 182

TYPICAL REPEATED STRESS-STRAIN CURVES SHOWING 1st & 5th CYCLES TO 2nd LOAD LEVEL AND FINAL RUPTURE CYCLE

CHENEY

FABRIC R7C 1/2, FILLING

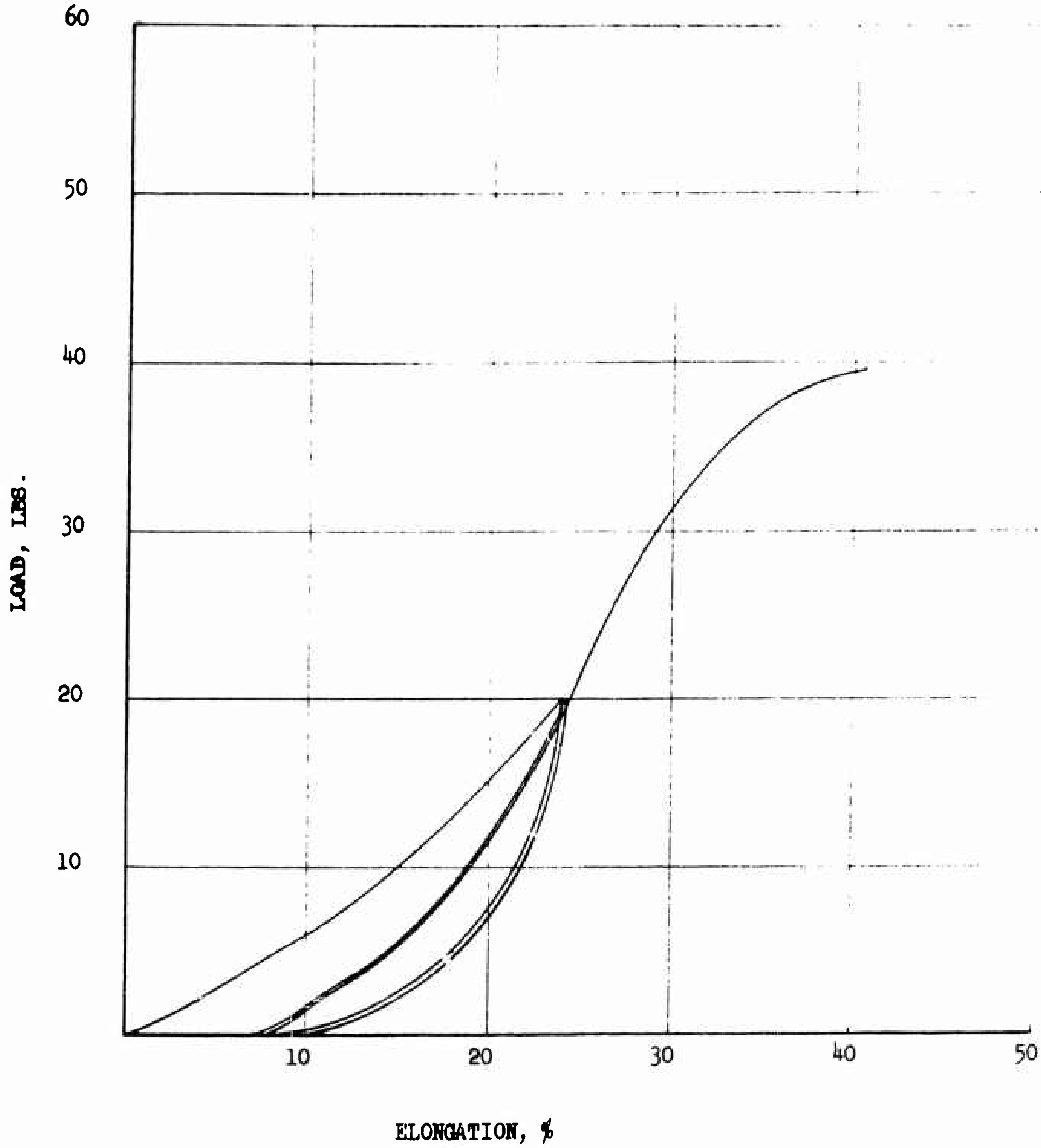

FIGURE 183

TYPICAL REPEATED STRESS-STRAIN CURVES SHOWING 1st & 5th CYCLES TO 3rd LOAD LEVEL AND FINAL RUPTURE CYCLE

CHENEY

FABRIC R7C 1/2, WARP

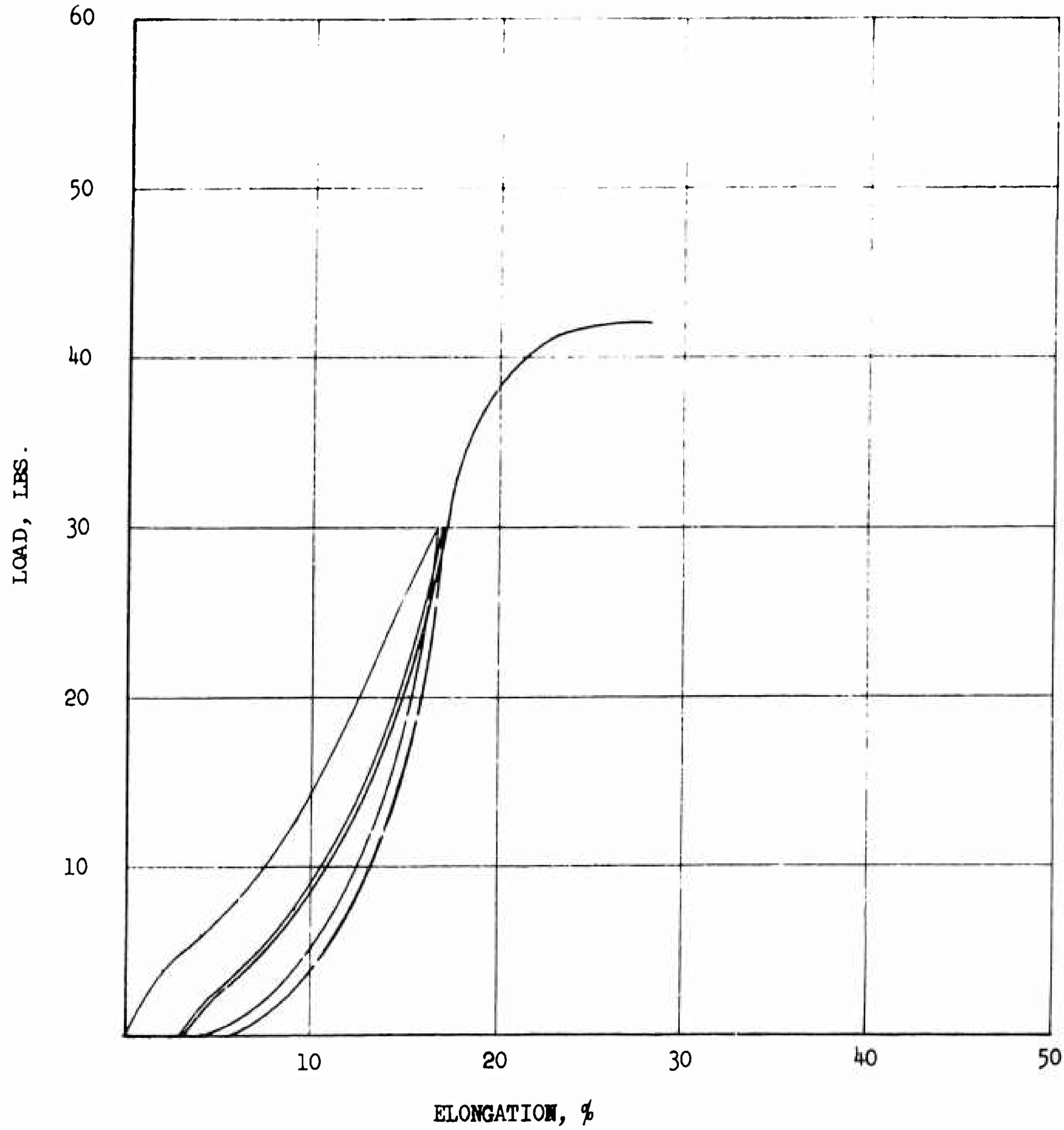

FIGURE 184

TYPICAL REPEATED STRESS-STRAIN CURVES SHOWI[illegible] 1st & 5th CYCLES TO
3rd LOAD LEVEL AND FINAL RUPTURE CYCLE

CHENEY

FABRIC R7C 1/2, FILLING

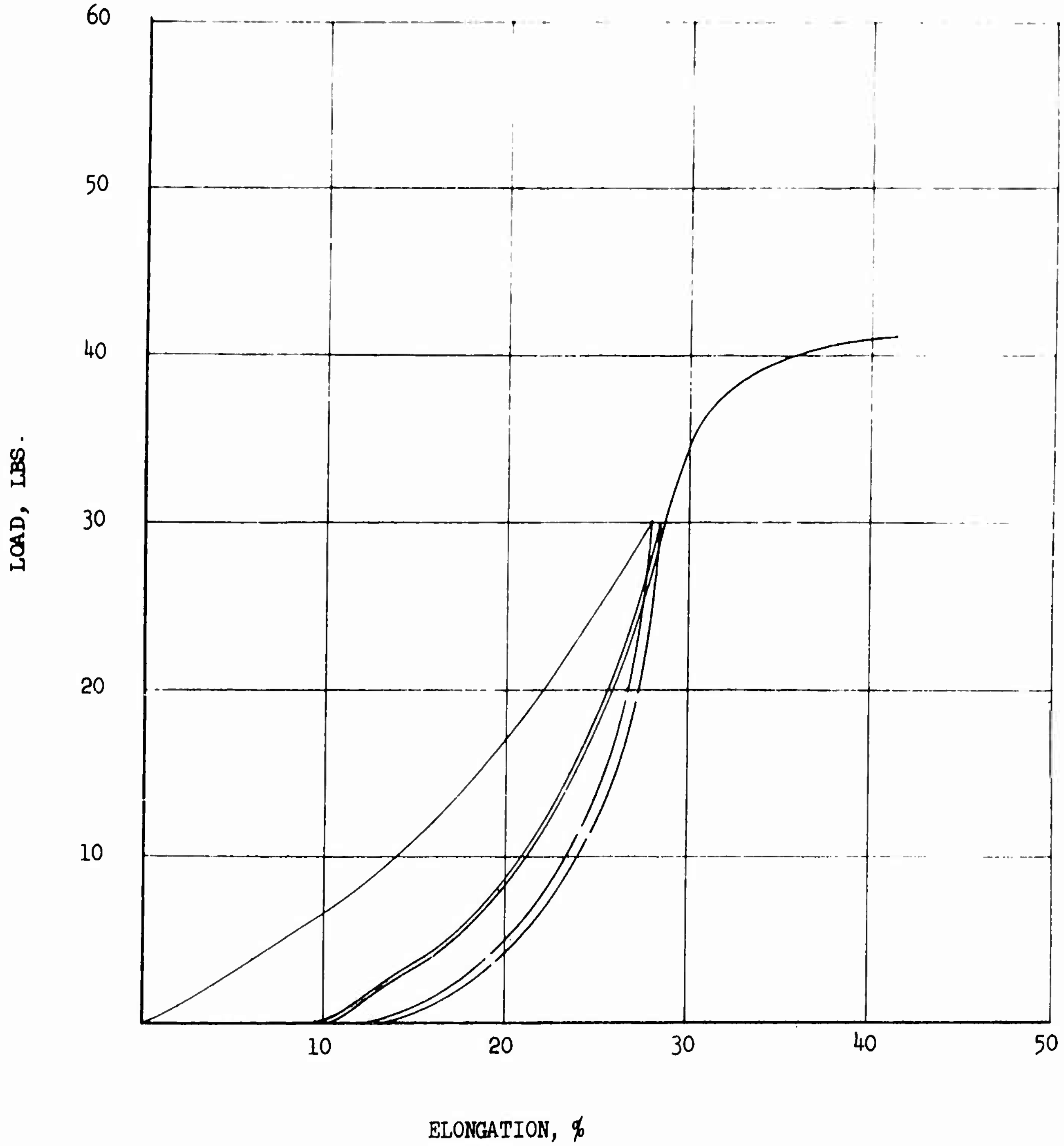

FIGURE 185

TYPICAL REPEATED STRESS-STRAIN CURVES SHOWING 1st & 5th CYCLES TO 1st LOAD LEVEL AND FINAL RUPTURE CYCLE

CHENEY

FABRIC R7C7, WARP

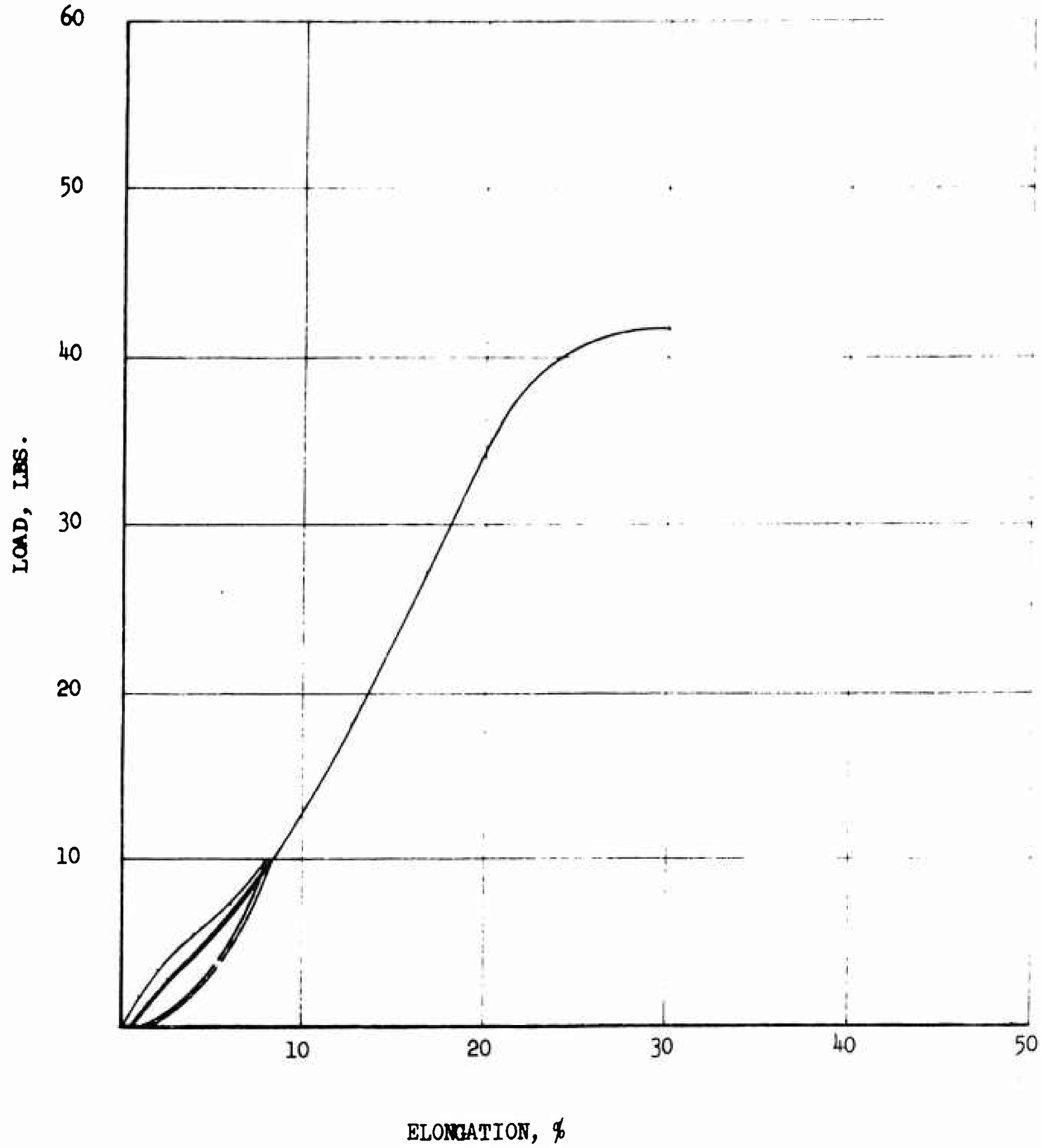

FIGURE 186

TYPICAL REPEATED STRESS-STRAIN CURVES SHOWING 1st & 5th CYCLES TO
1st LOAD LEVEL AND FINAL RUPTURE CYCLE

CHENEY
FABRIC R7C7, FILLING

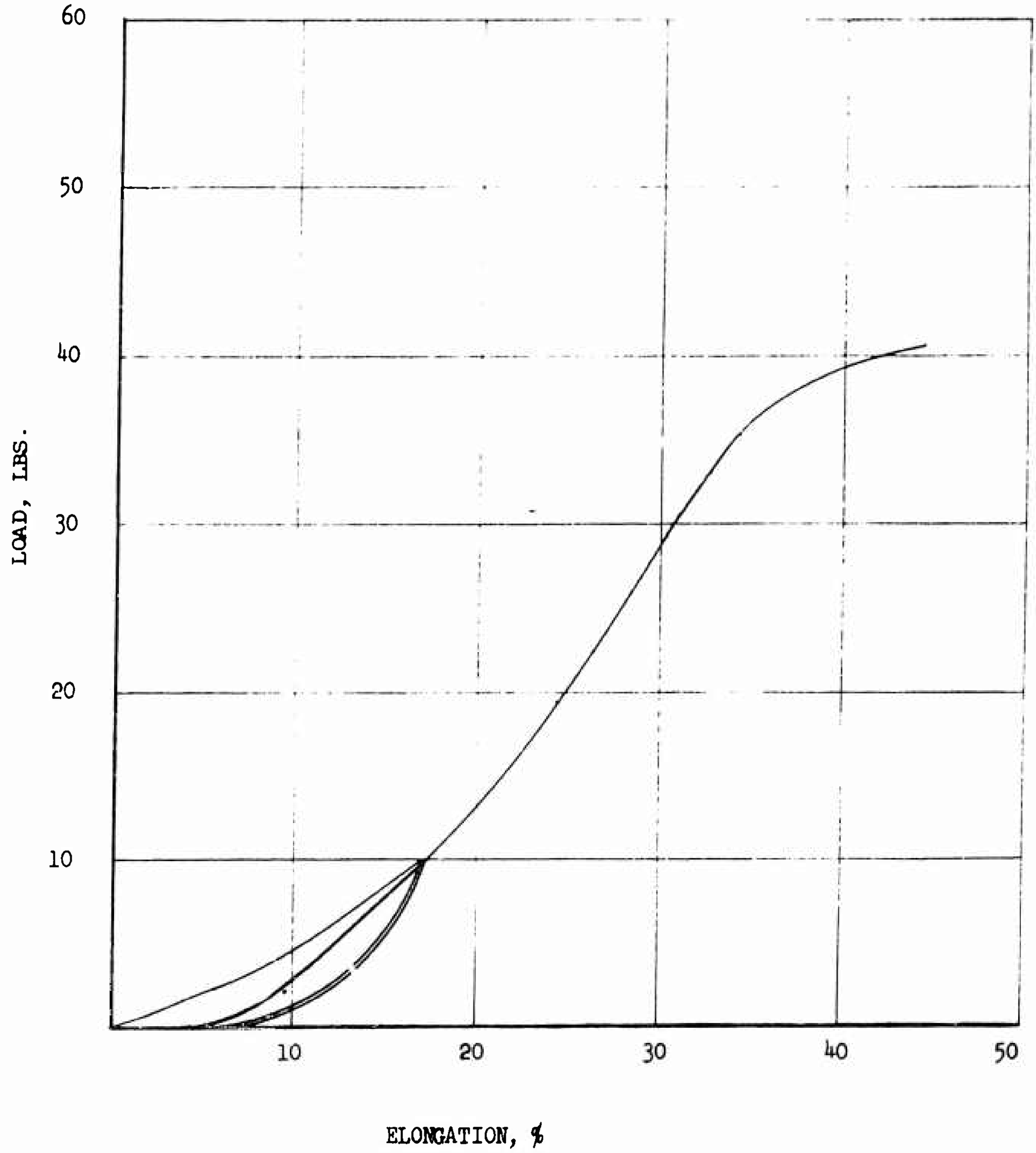

FIGURE 187

TYPICAL REPEATED STRESS-STRAIN CURVES SHOWING 1st & 5th CYCLES TO 2nd LOAD LEVEL AND FINAL RUPTURE CYCLE

CHENEY

FABRIC R7C7, WARP

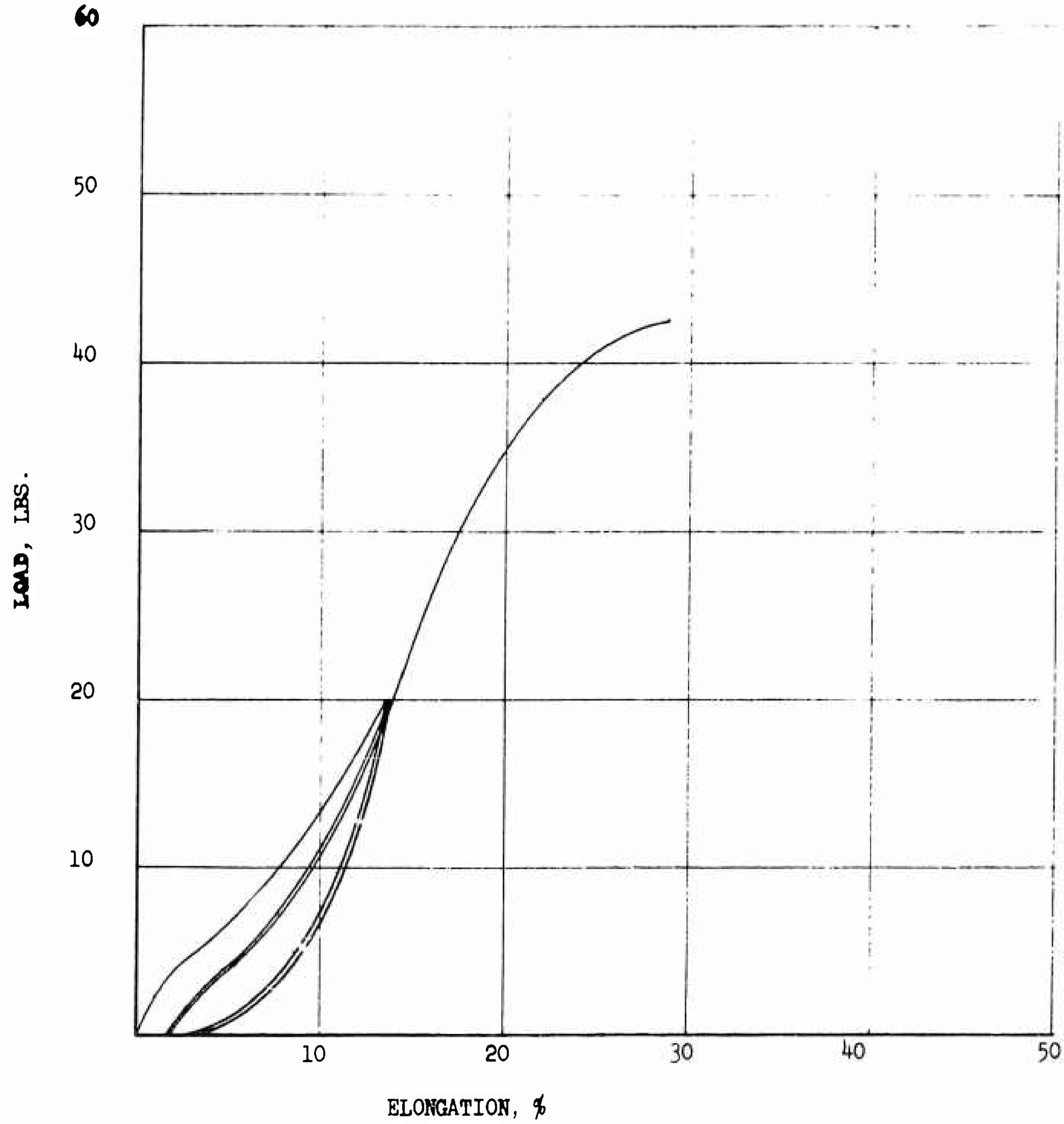

FIGURE 188

TYPICAL REPEATED STRESS-STRAIN CURVES SHOWING 1st & 5th CYCLES TO 2nd LOAD LEVEL AND FINAL RUPTURE CYCLE

CHENEY

FABRIC R7C7, FILLING

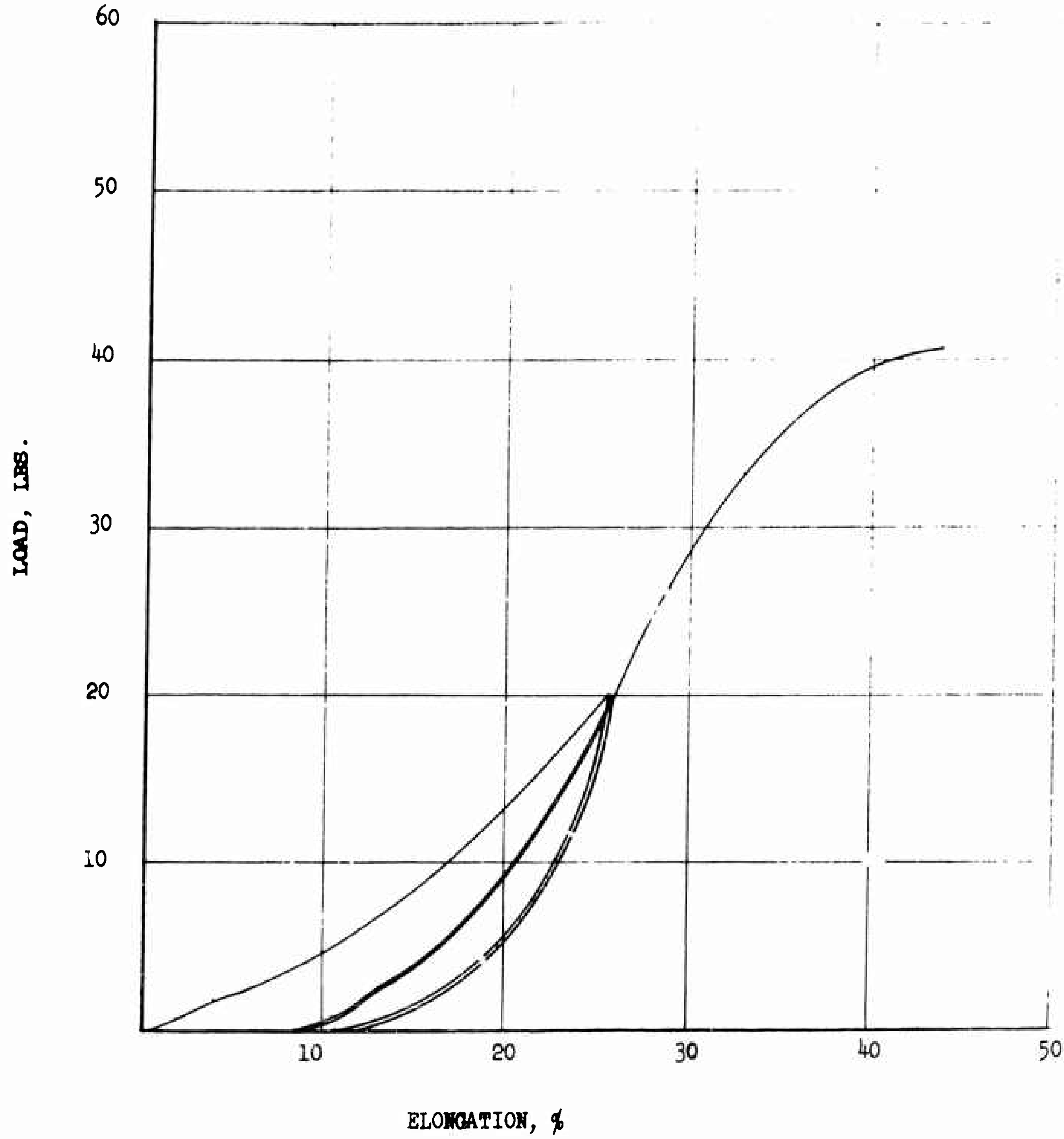

FIGURE 189

TYPICAL REPEATED STRESS-STRAIN CURVES SHOWING 1st & 5th CYCLES TO 3rd LOAD LEVEL AND FINAL RUPTURE CYCLE

CHENEY

FABRIC R7C7, WARP

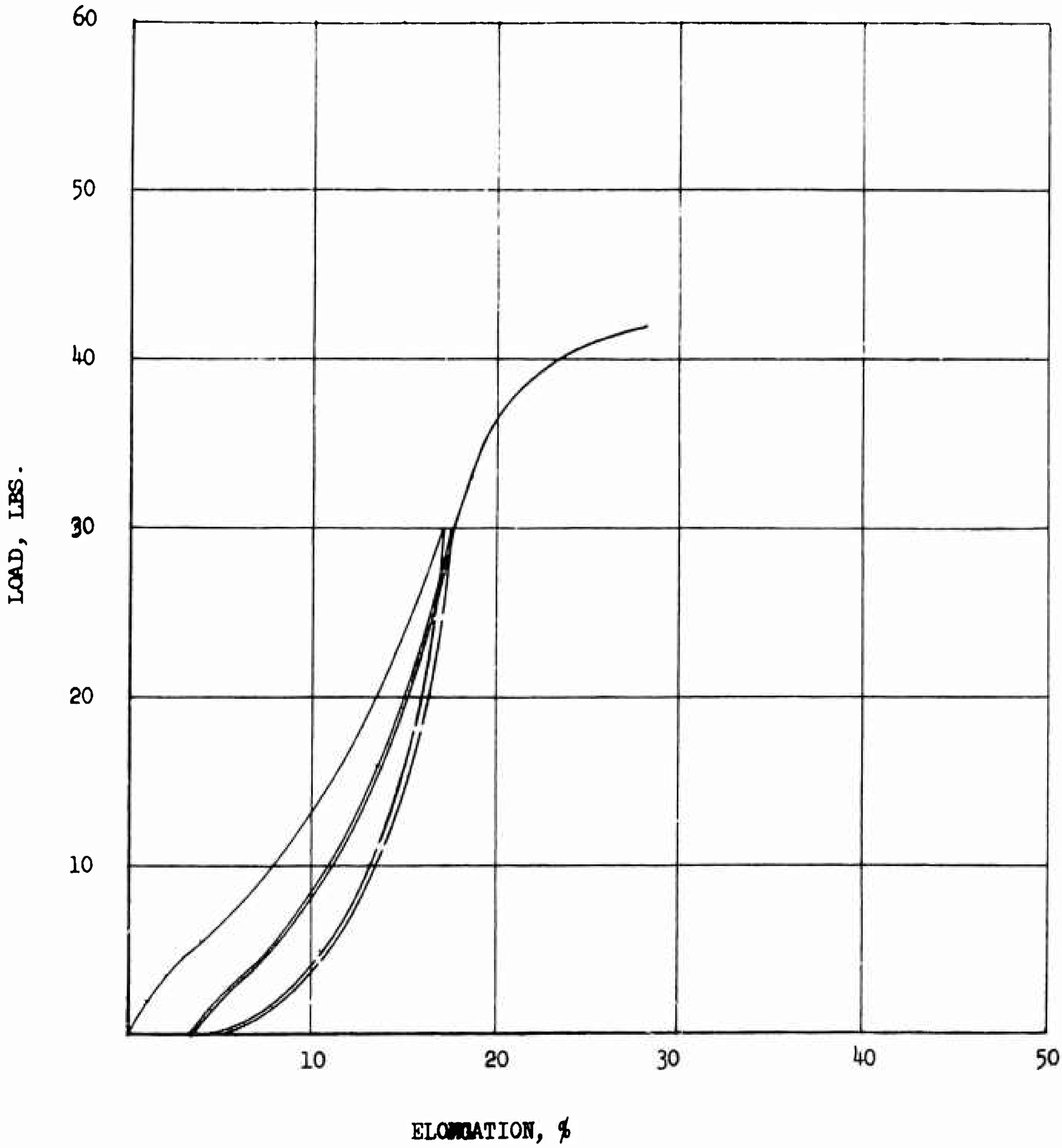

FIGURE 190

TYPICAL REPEATED STRESS-STRAIN CURVES SHOWING 1st & 5th CYCLES TO 3rd LOAD LEVEL AND FINAL RUPTURE CYCLE

CHENEY

FABRIC R7C7, FILLING

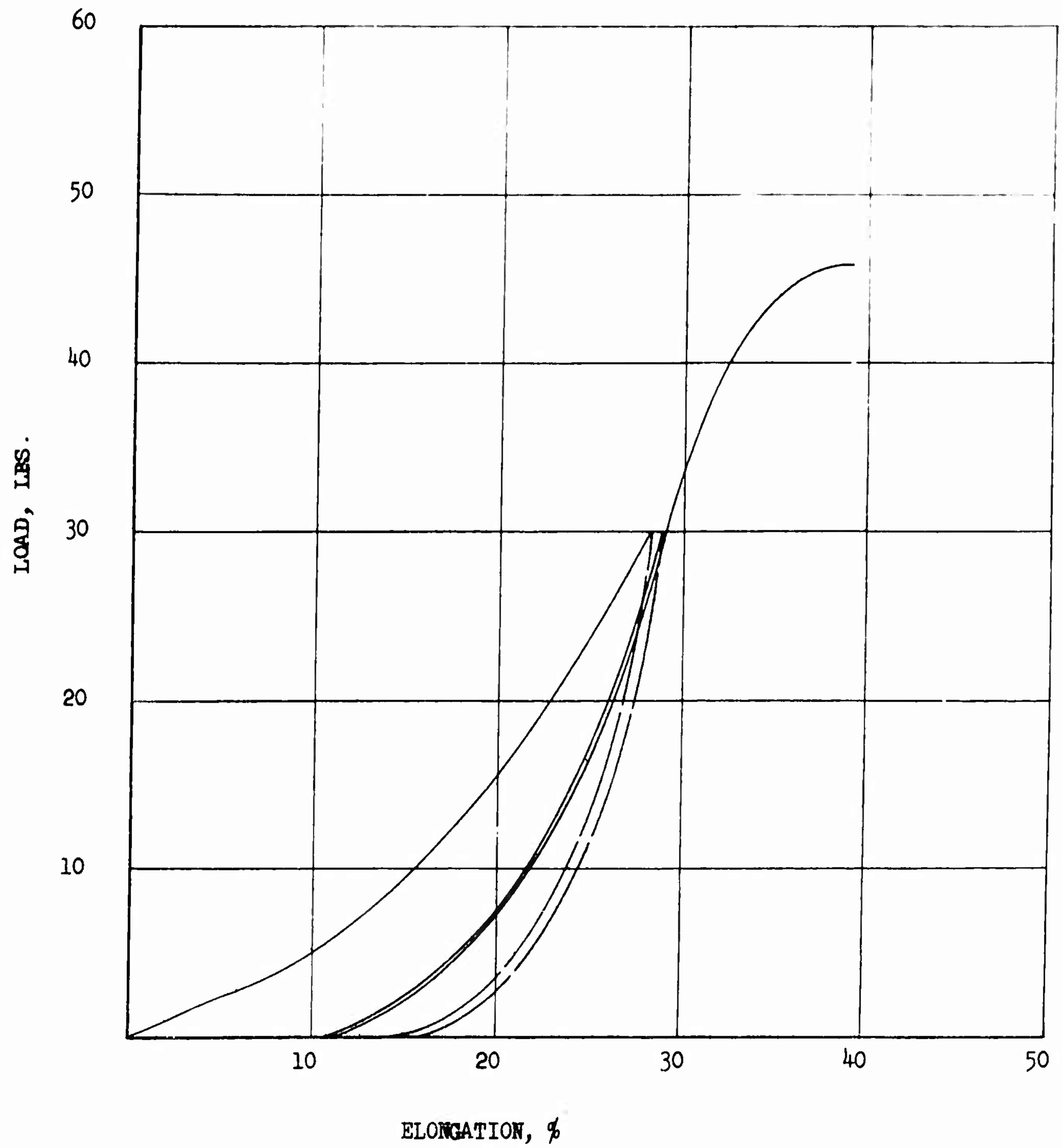

FIGURE 191

TYPICAL REPEATED STRESS-STRAIN CURVES SHOWING 1st & 5th CYCLES TO 1st LOAD LEVEL AND FINAL RUPTURE CYCLE

CHENEY

FABRIC R7C30, WARP

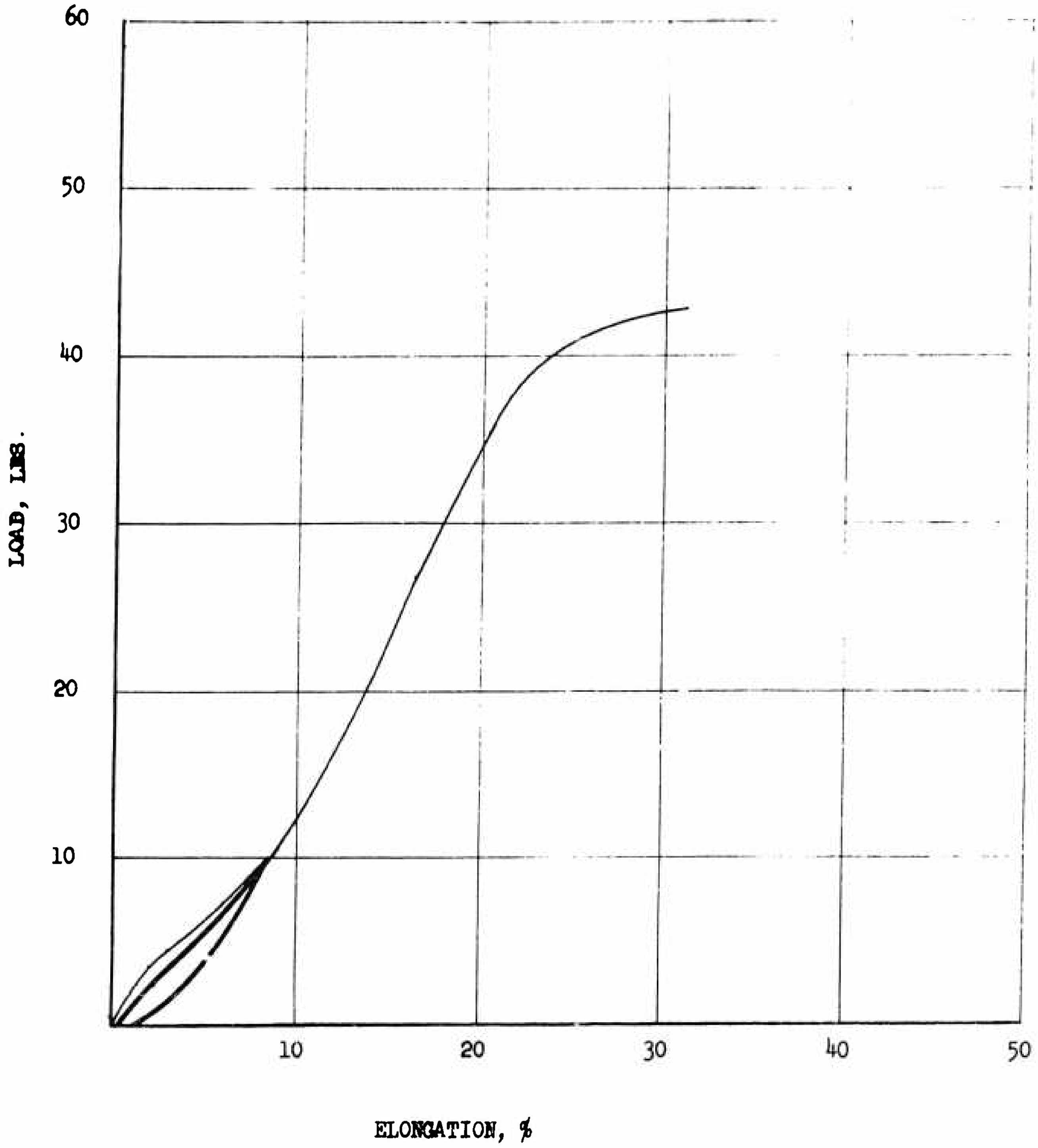

FIGURE 192

TYPICAL REPEATED STRESS-STRAIN CURVES SHOWING 1st & 5th CYCLES TO 1st LOAD LEVEL AND FINAL RUPTURE CYCLE

CHENEY

FABRIC R7C30, FILLING

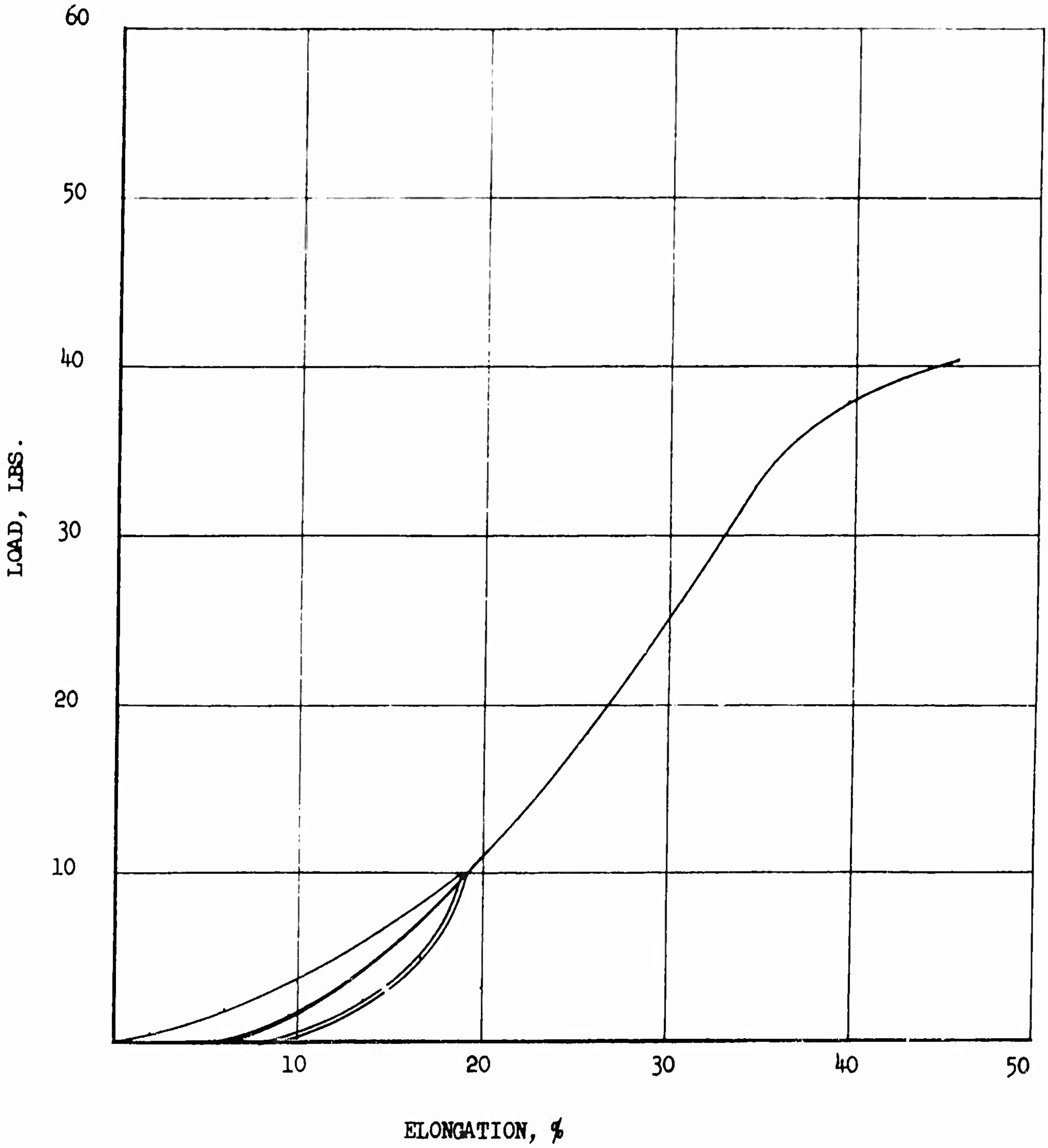

FIGURE 193

TYPICAL REPEATED STRESS-STRAIN CURVES SHOWING 1st & 5th CYCLES TO 2nd LOAD LEVEL AND FINAL RUPTURE CYCLE

CHENEY

FABRIC R7C30, WARP

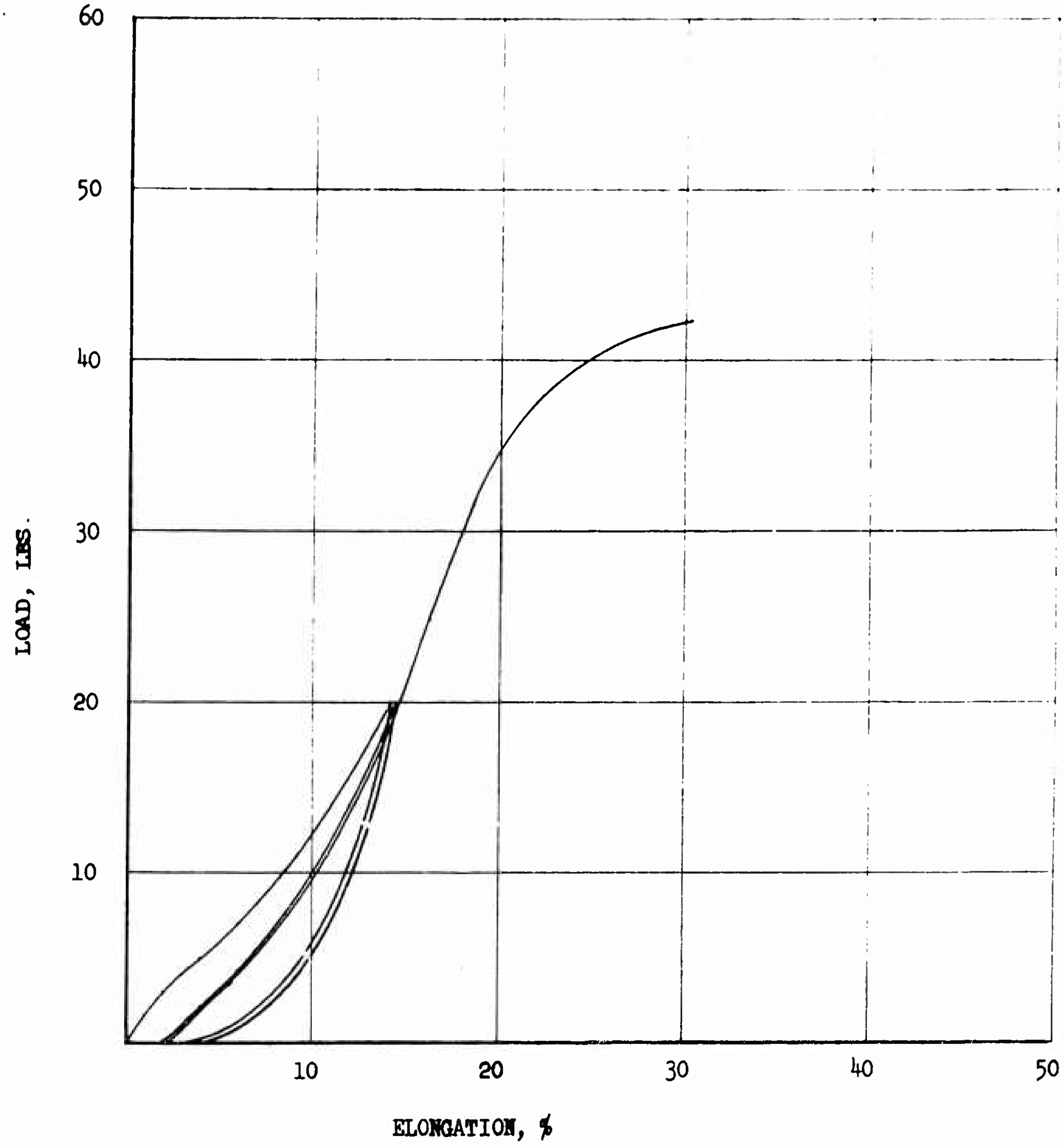

FIGURE 194

TYPICAL REPEATED STRESS-STRAIN CURVES SHOWING 1st & 5th CYCLES TO
2nd LOAD LEVEL AND FINAL RUPTURE CYCLE

CHENEY

FABRIC R7C30, FILLING

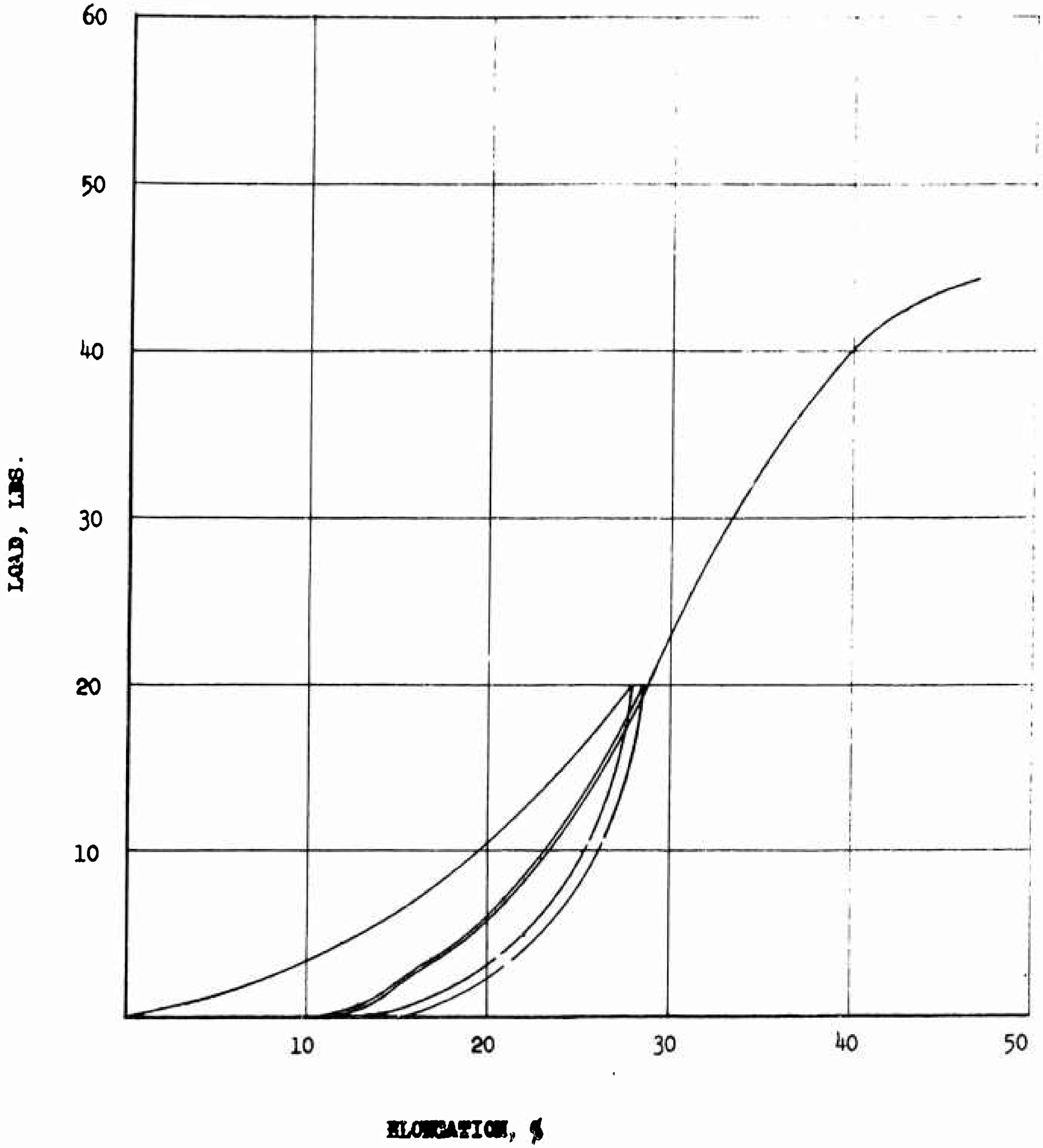

FIGURE 195

TYPICAL REPEATED STRESS-STRAIN CURVES SHOWING 1st & 5th CYCLES TO
3rd LOAD LEVEL AND FINAL RUPTURE CYCLE

CHENEY

FABRIC R7C30, WARP

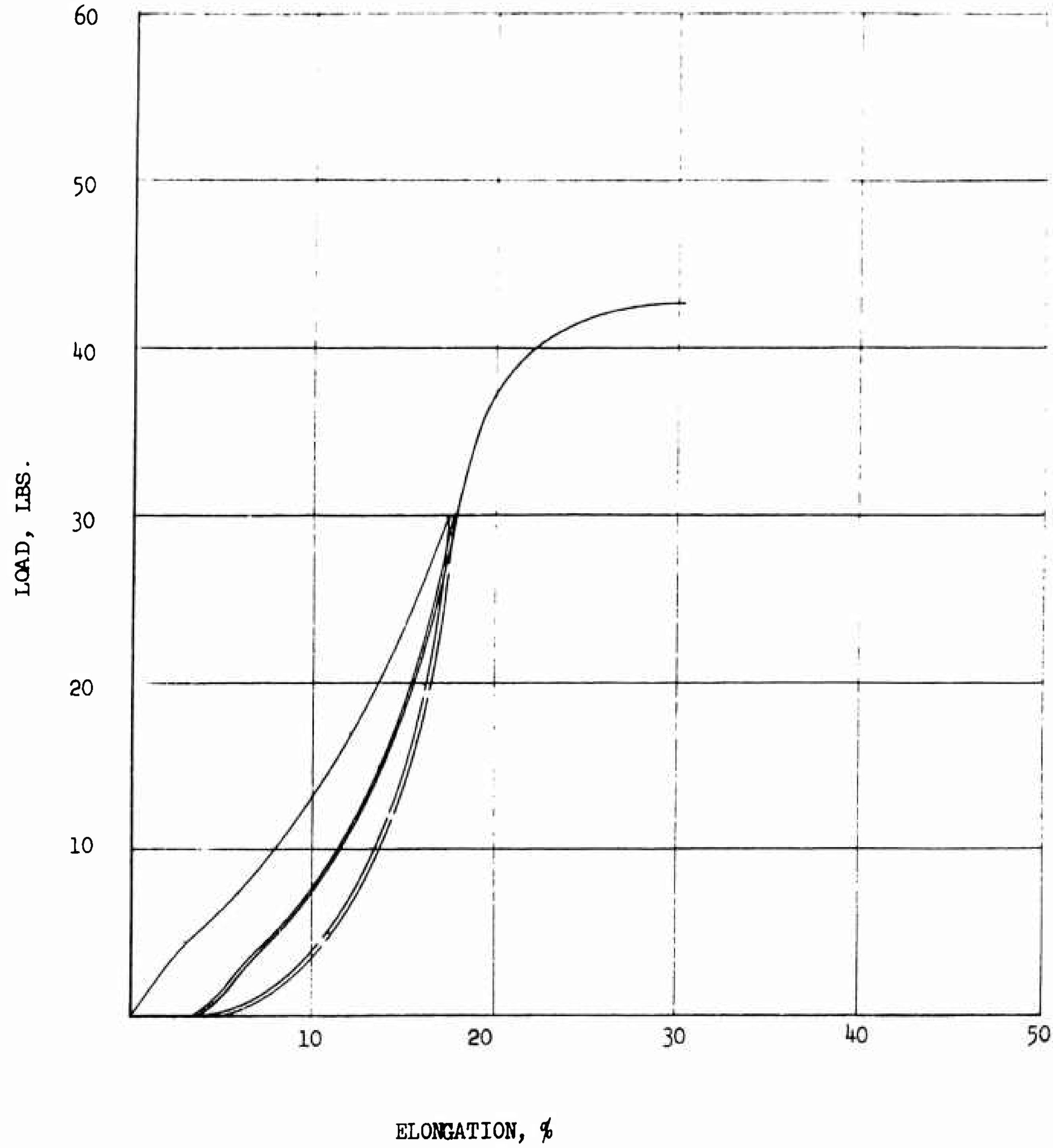

FIGURE 196

TYPICAL REPEATED STRESS-STRAIN CURVES SHOWING 1st & 5th CYCLES TO 3rd LOAD LEVEL AND FINAL RUPTURE CYCLE

CHENEY

FABRIC R7C30, FILLING

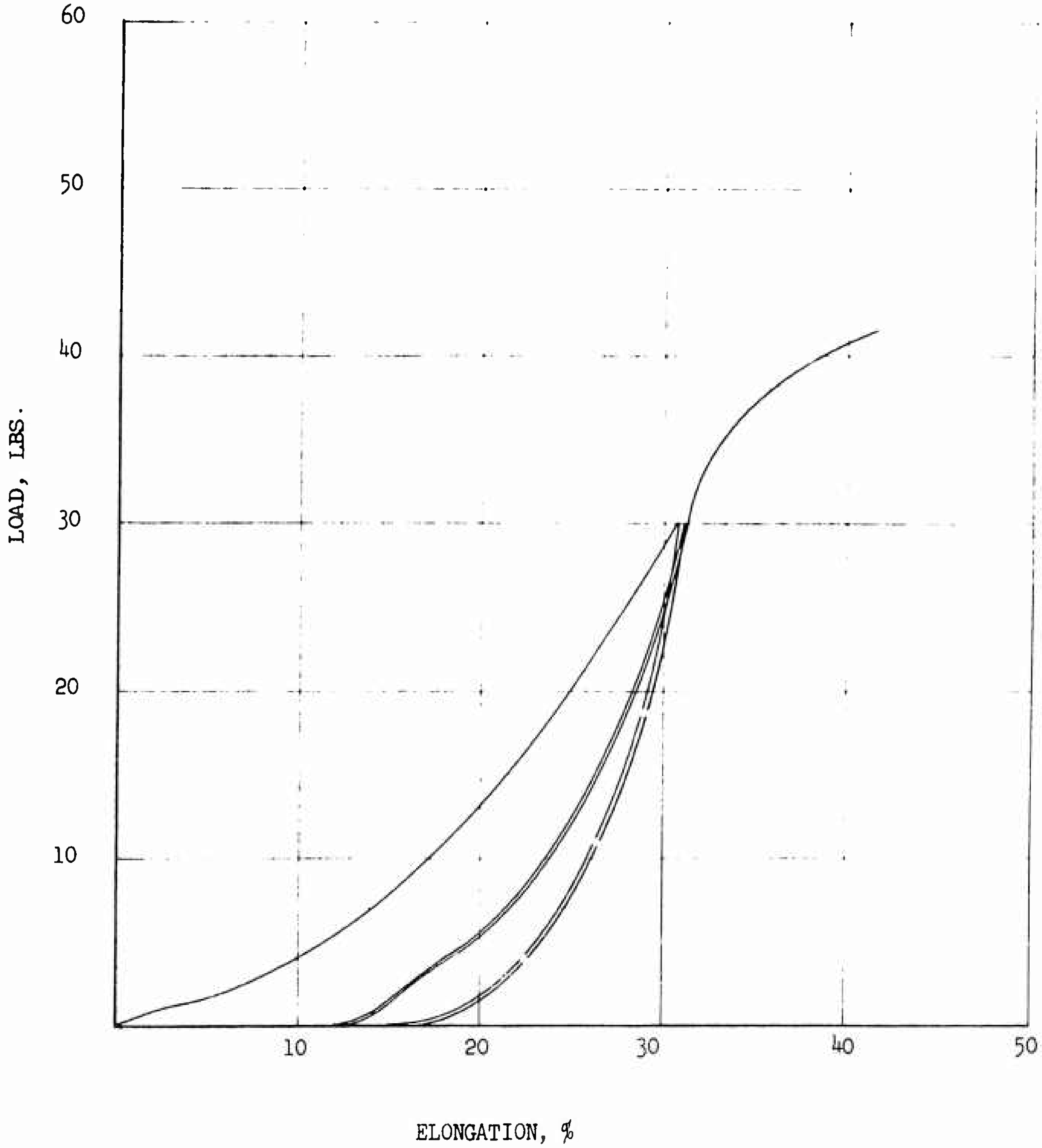

FIGURE 197
EFFECT OF CALENDERING ON
AIR PERMEABILITY

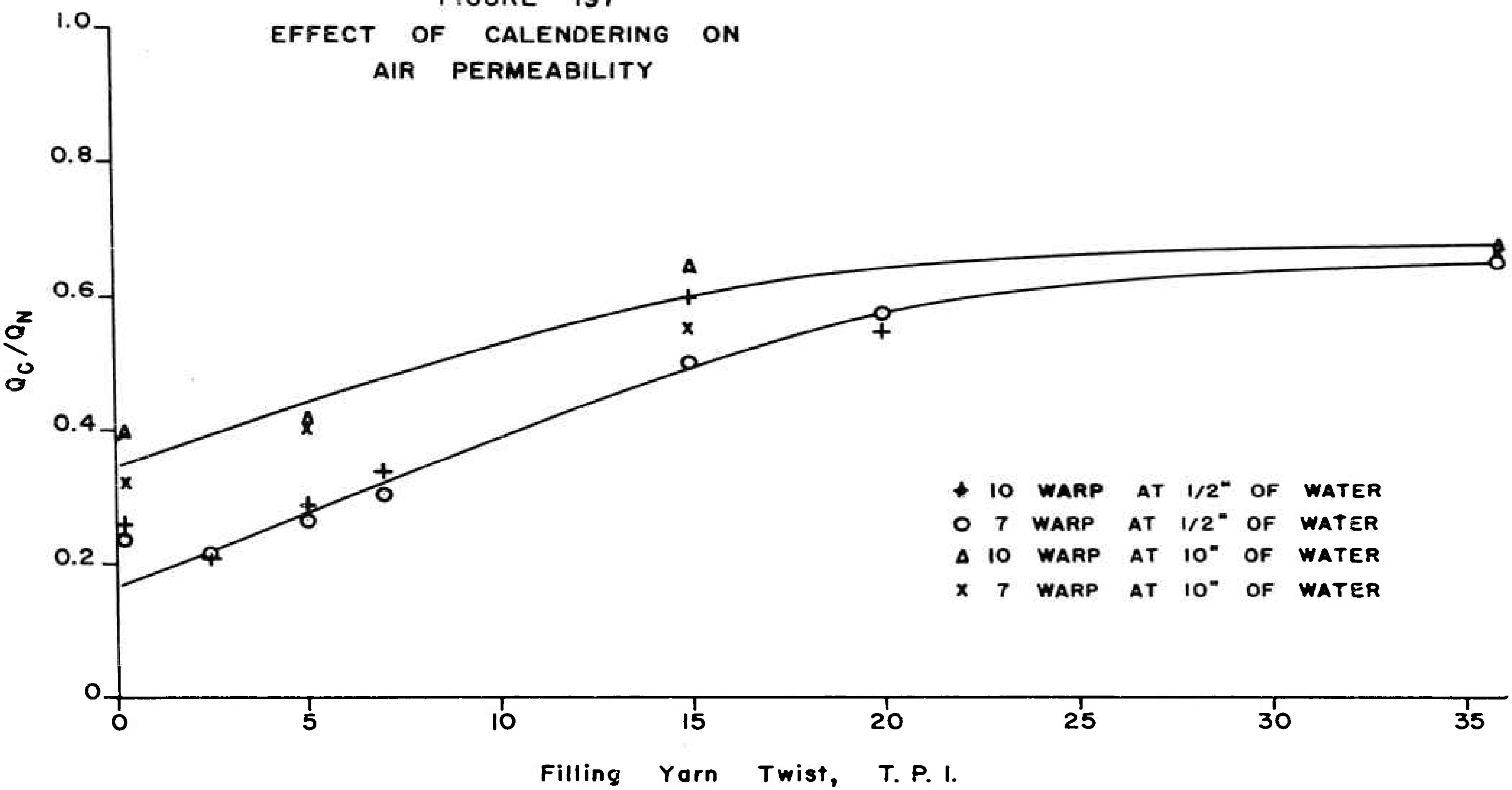

FIGURE 198
EFFECT OF CALENDERING ON AIR PERMEABILITY

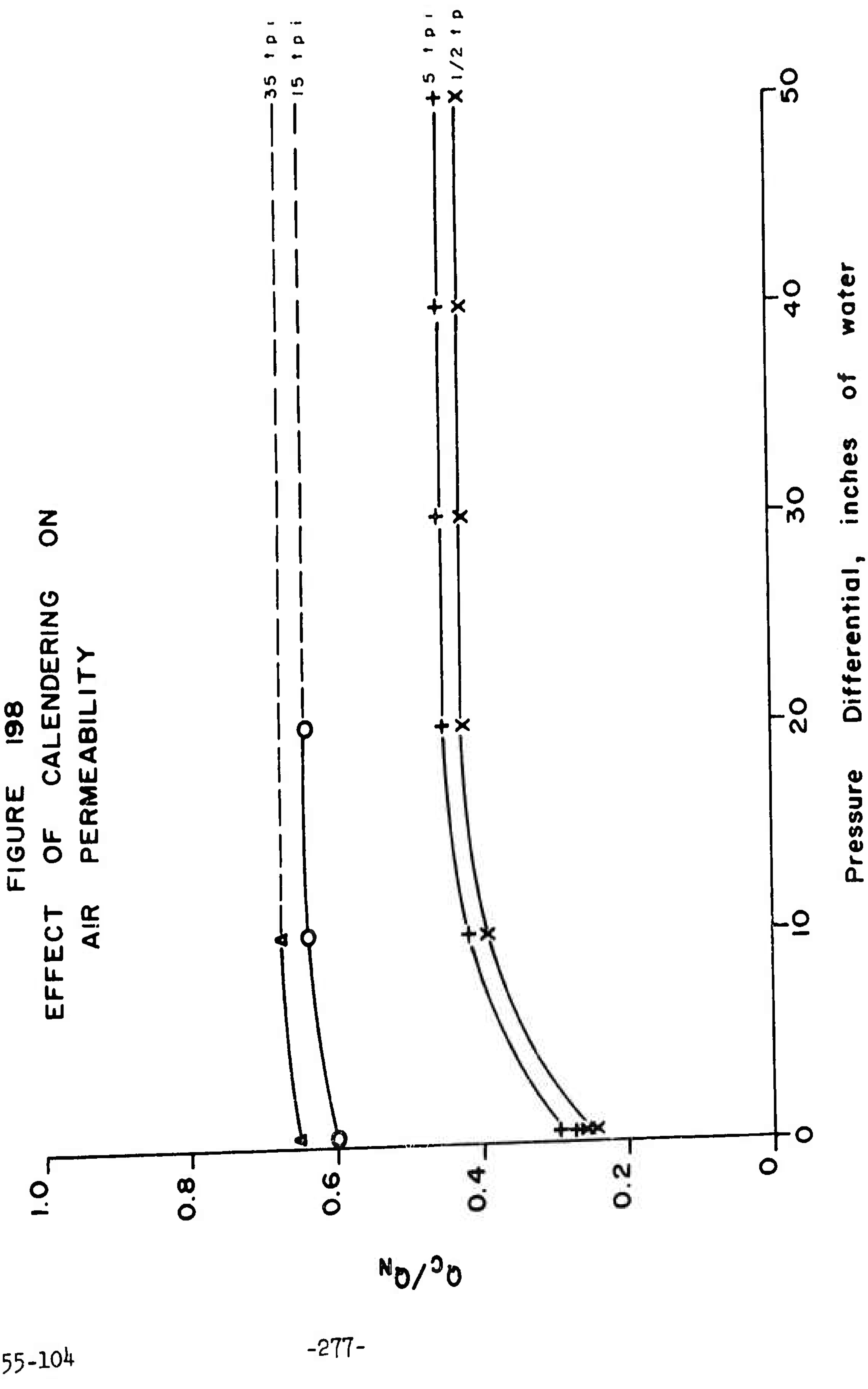

FIGURE 199

TONGUE TEAR TEST SAMPLE (WARP)

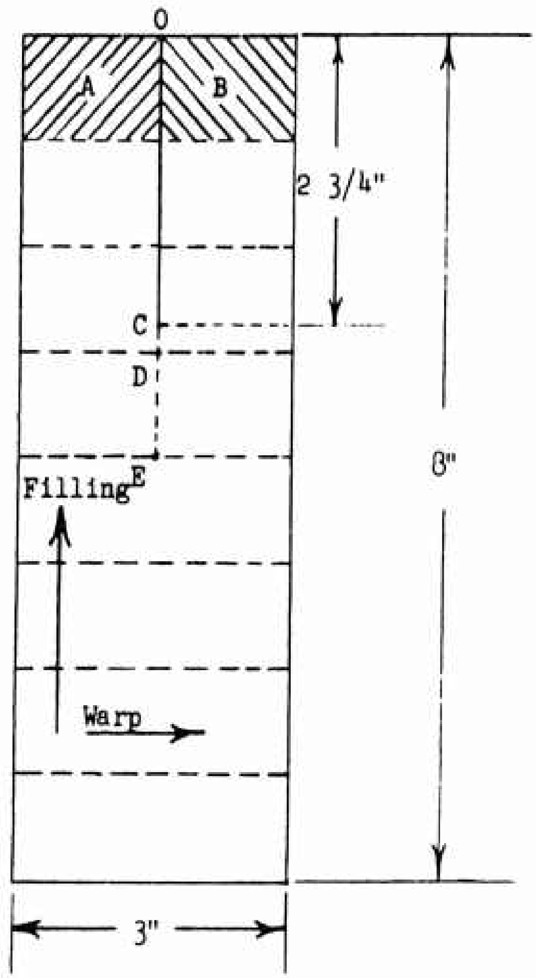

FIGURE 200

TYPICAL TEAR DIAGRAM

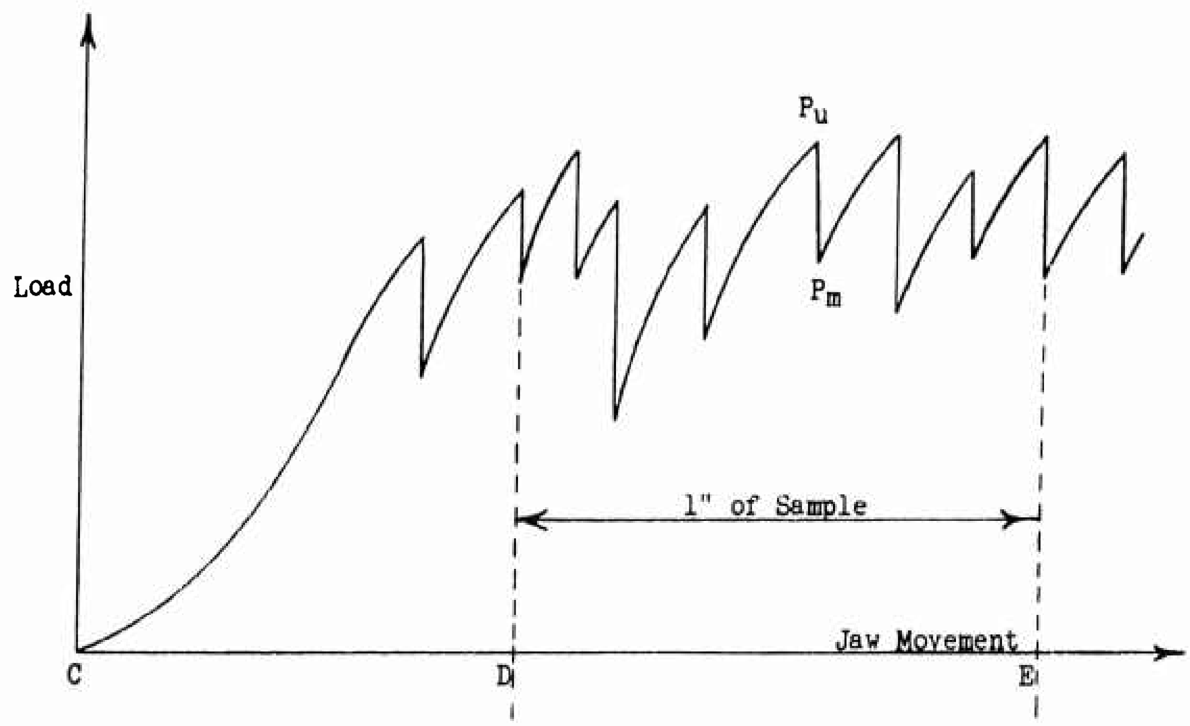

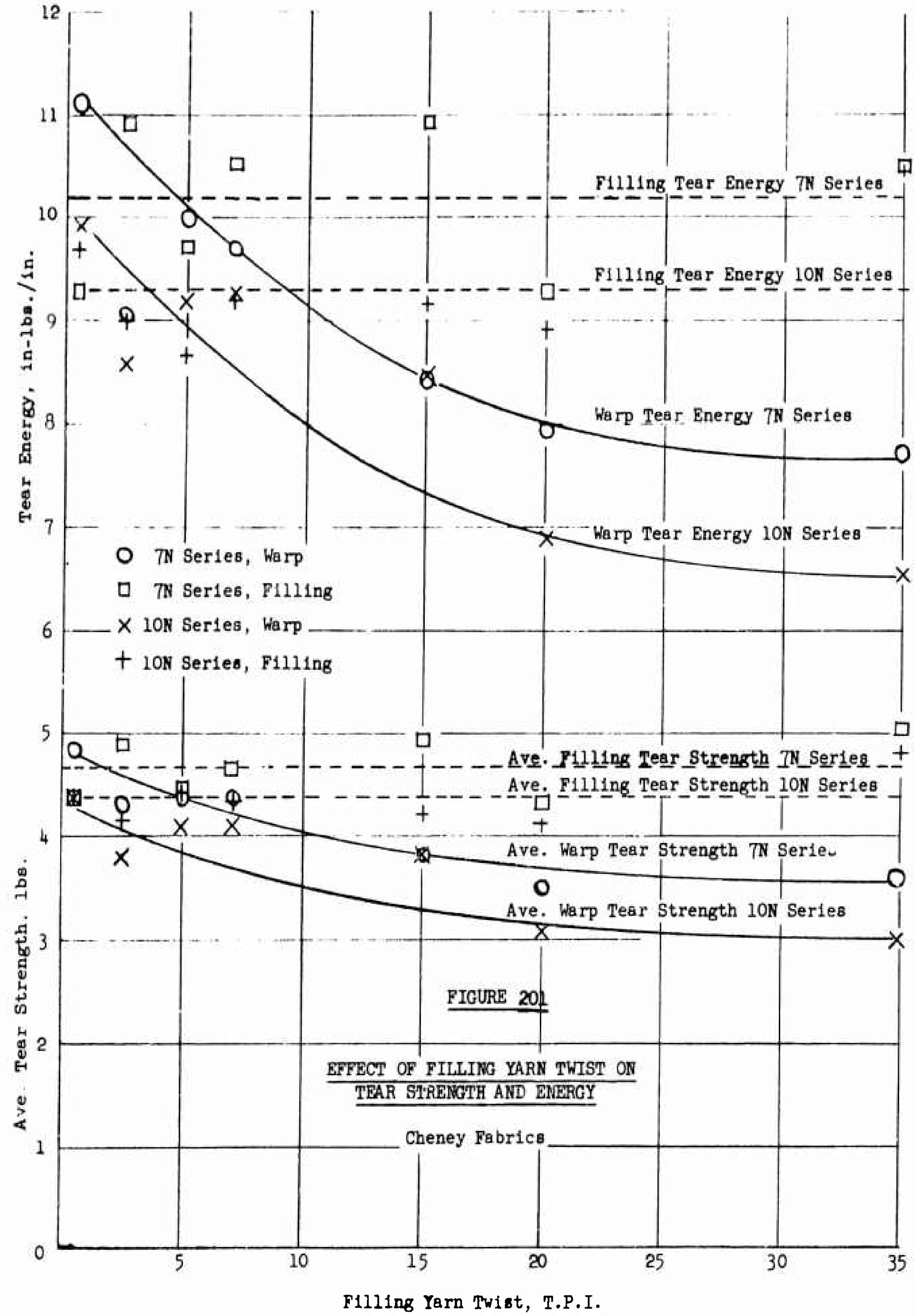

FIGURE 201

EFFECT OF FILLING YARN TWIST ON TEAR STRENGTH AND ENERGY

Cheney Fabrics

FIGURE 202

COMPARISON OF BIAXIAL AND UNIAXIAL LOAD-ELONGATION FOR R 1/2 N 1/2

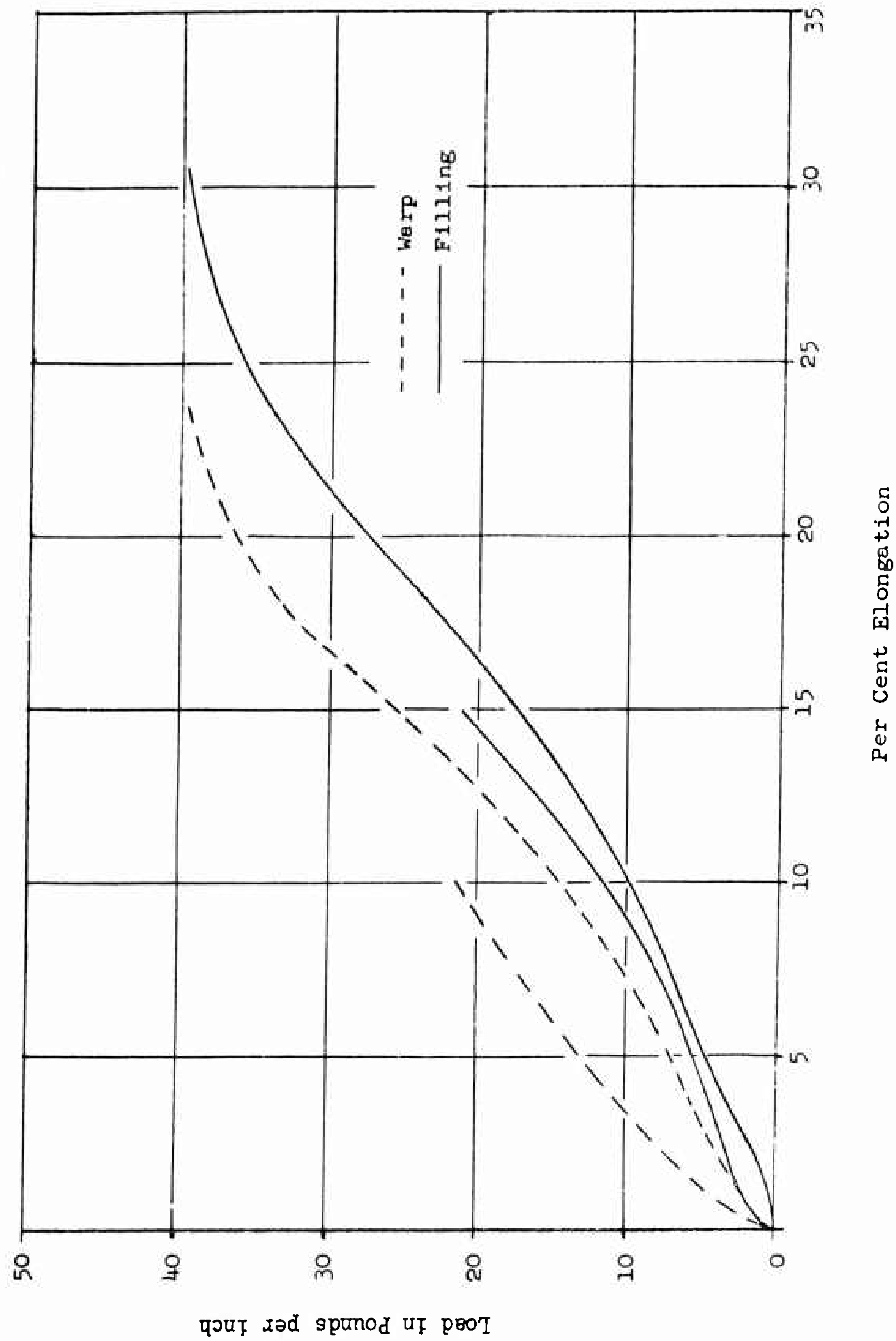

FIGURE 203

COMPARISON OF BIAXIAL AND UNIAXIAL LOAD-ELONGATION FOR R5N5

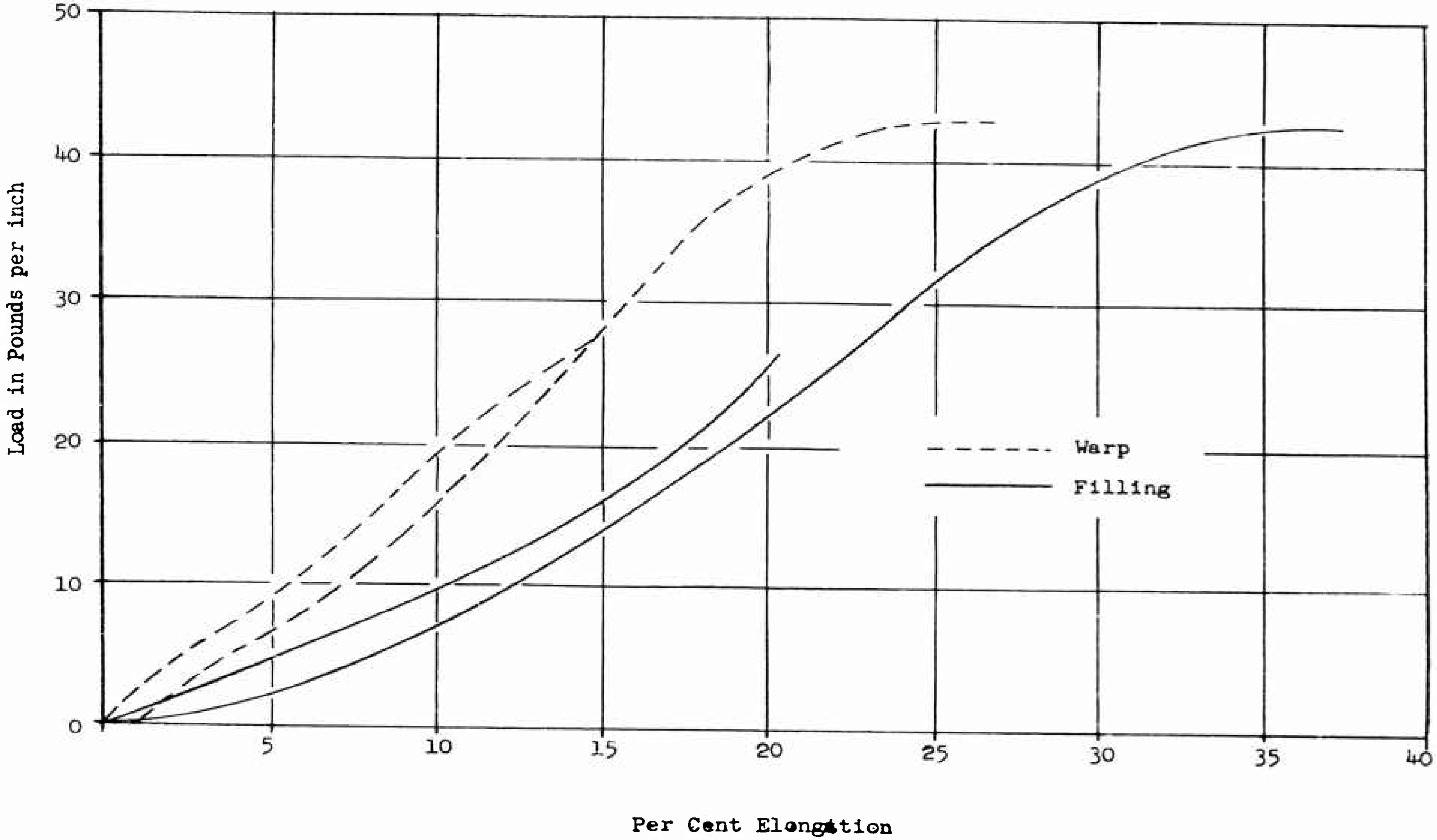

FIGURE 204

COMPARISON OF BIAXIAL AND UNIAXIAL LOAD-ELONGATION FOR R20N20

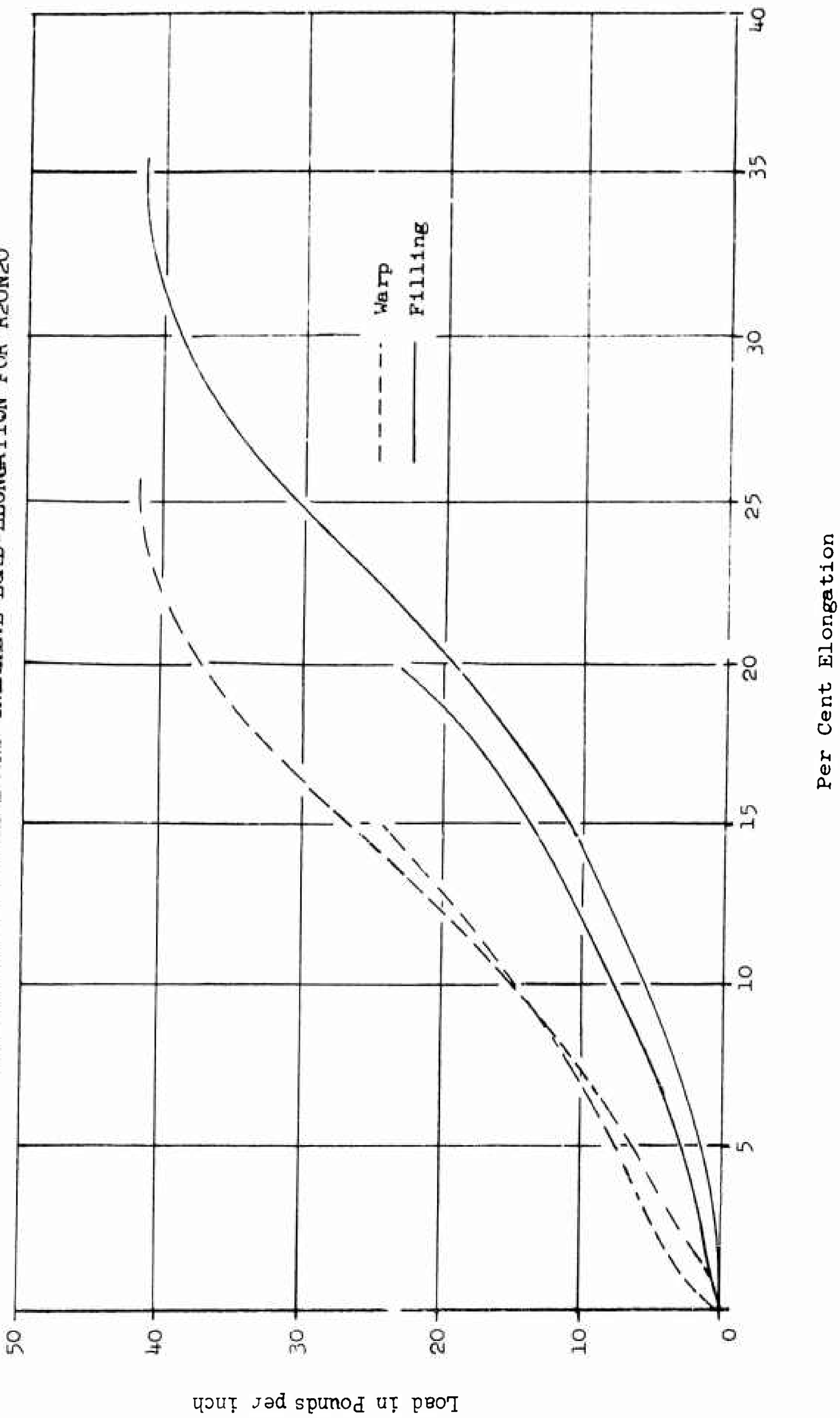

FIGURE 205

COMPARISON OF BIAXIAL AND UNIAXIAL LOAD-ELONGATION FOR R30N30

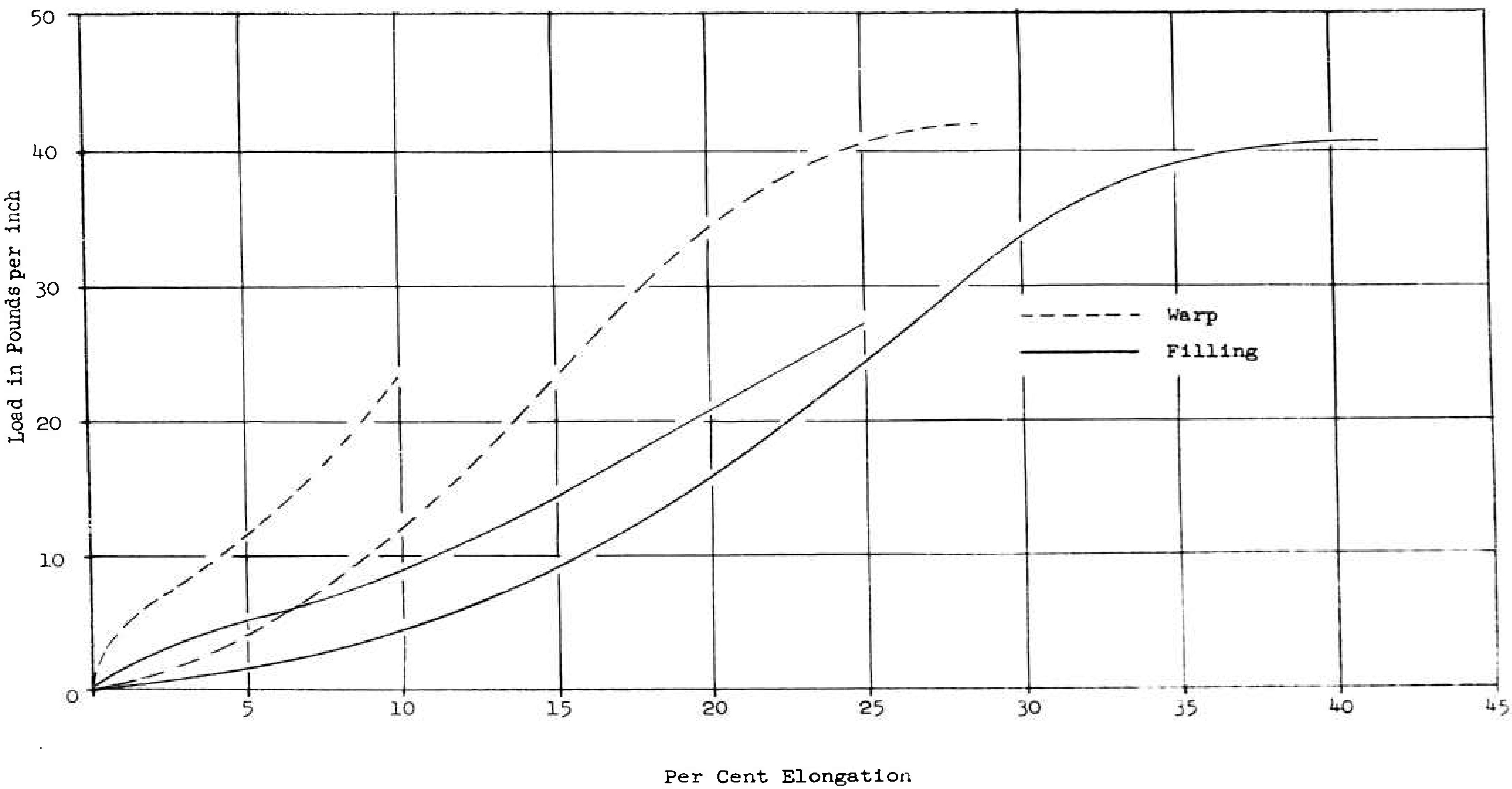

FIGURE 206

COMPARISON OF BIAXIAL FILLING LOAD-ELONGATION

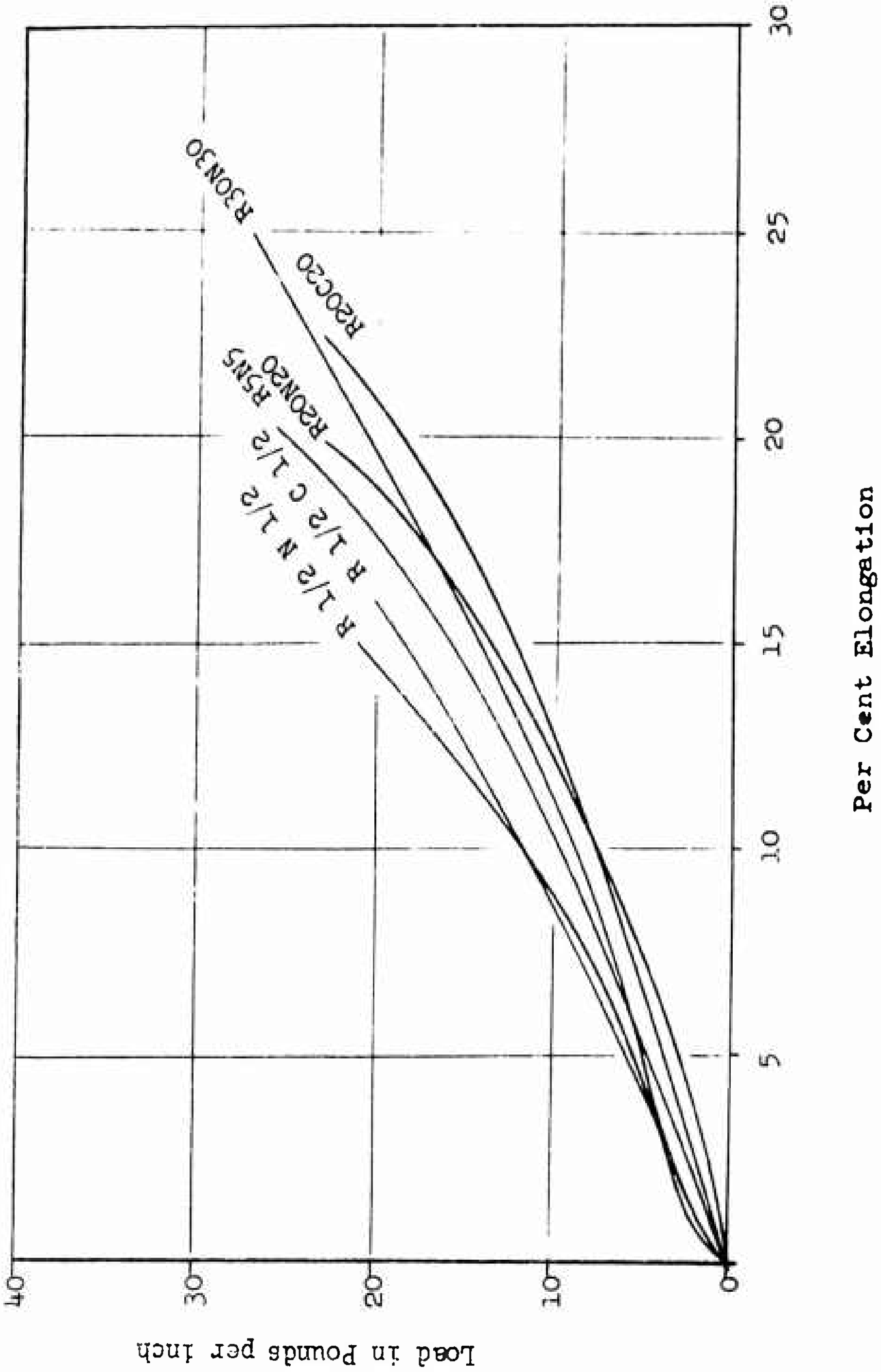

FIGURE 207

COMPARISON OF BIAXIAL WARP LOAD-ELONGATION

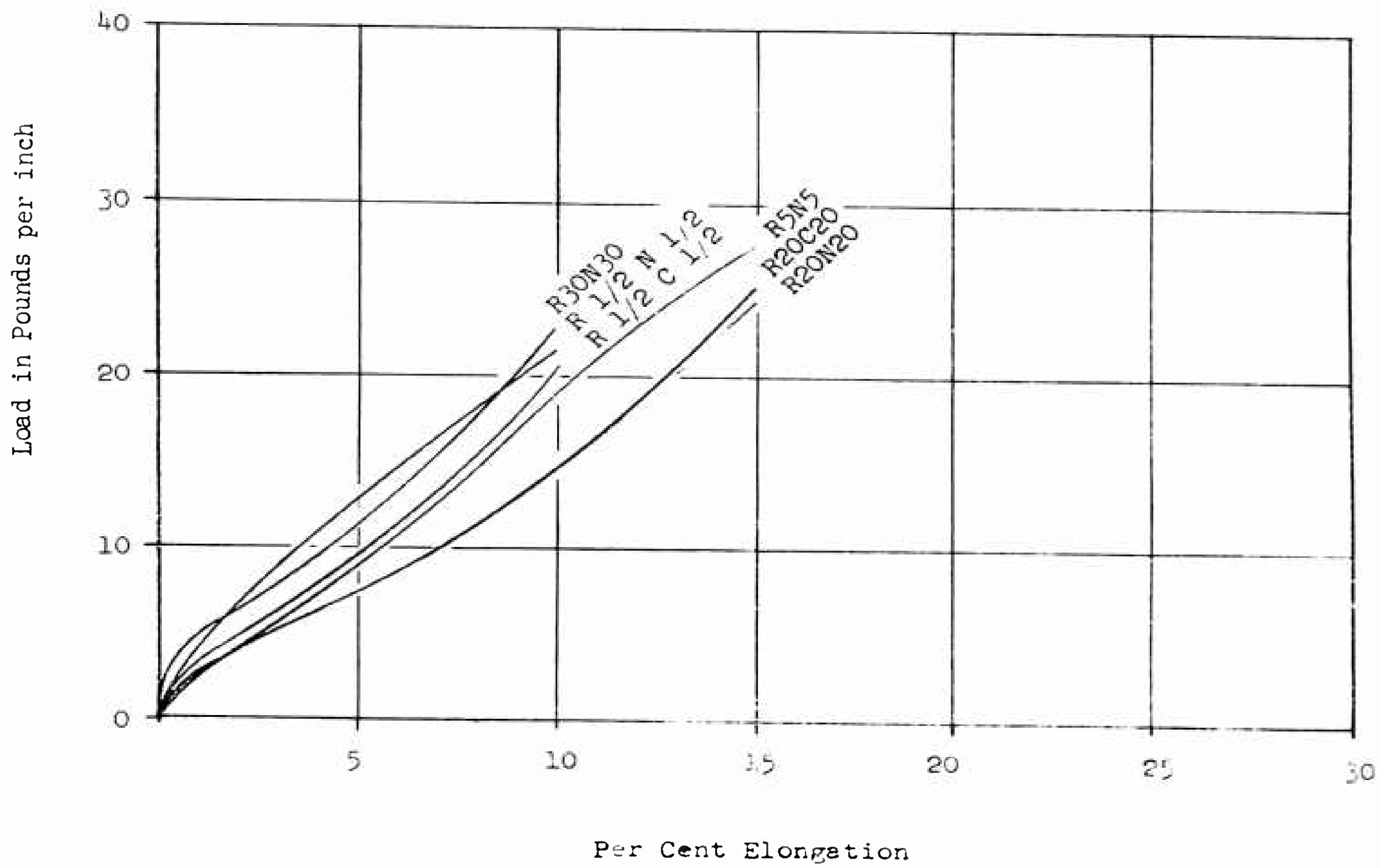

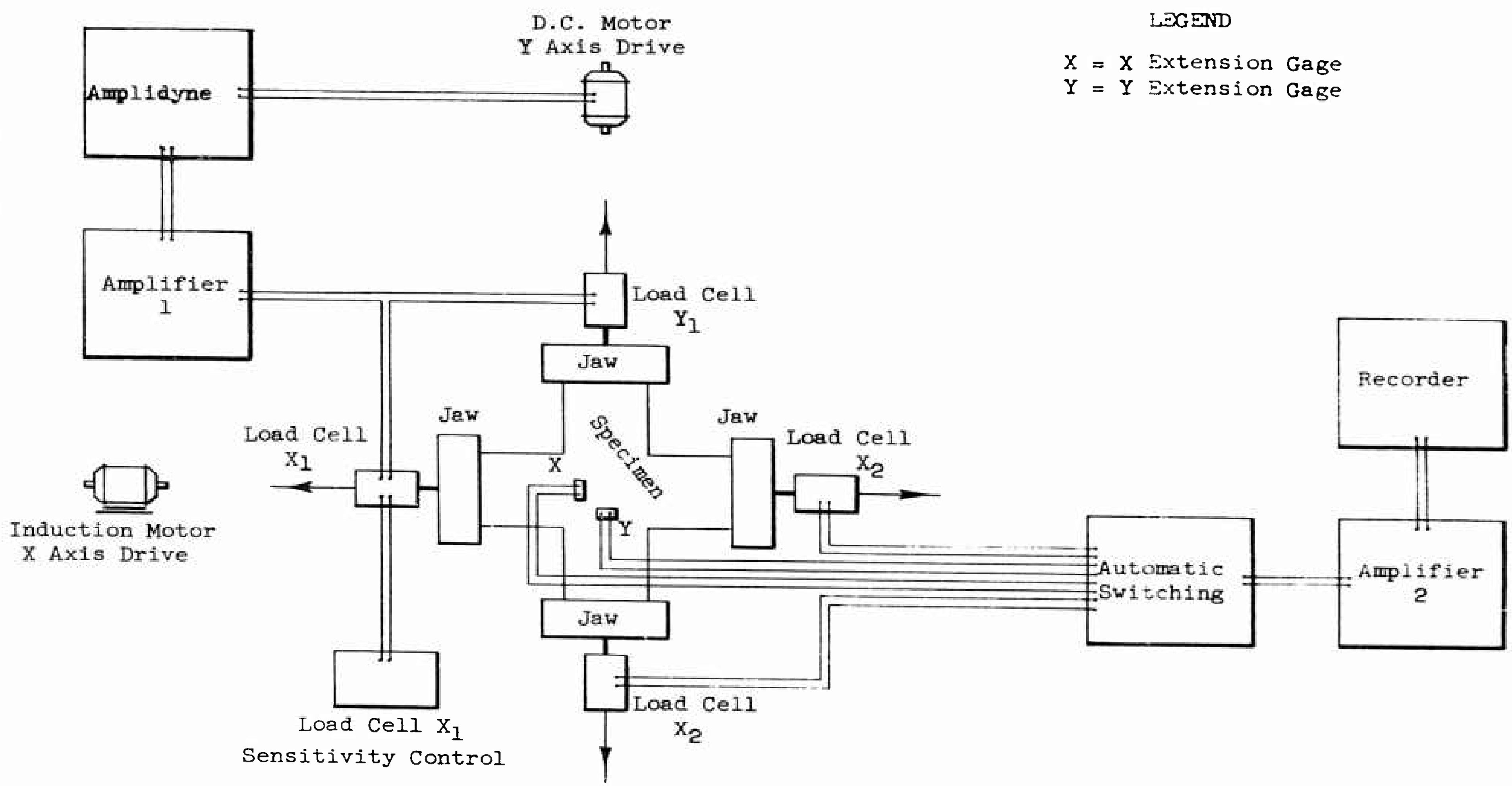

Figure 208 Schematic Diagram of Biaxial Tensile Tester

FIGURE 209

BIAXIAL TENSILE TESTER

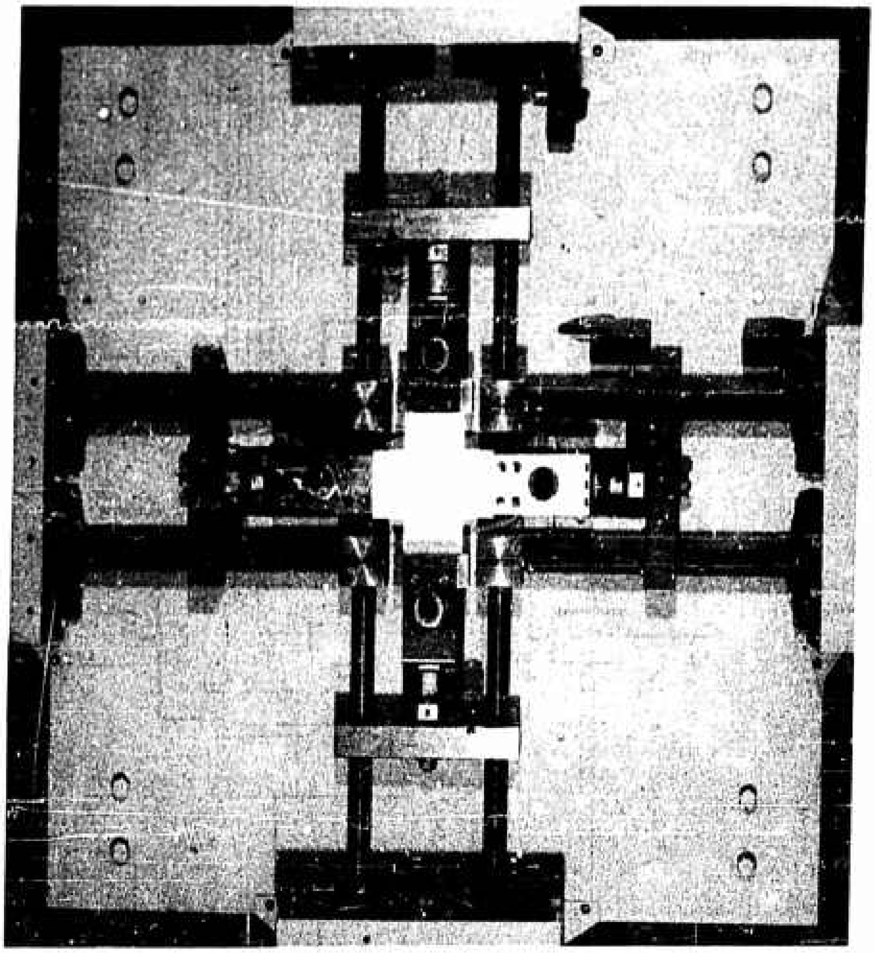

FIGURE 210

CONTROL PANEL AND RECORDER OF THE BIAXIAL TENSILE TESTER

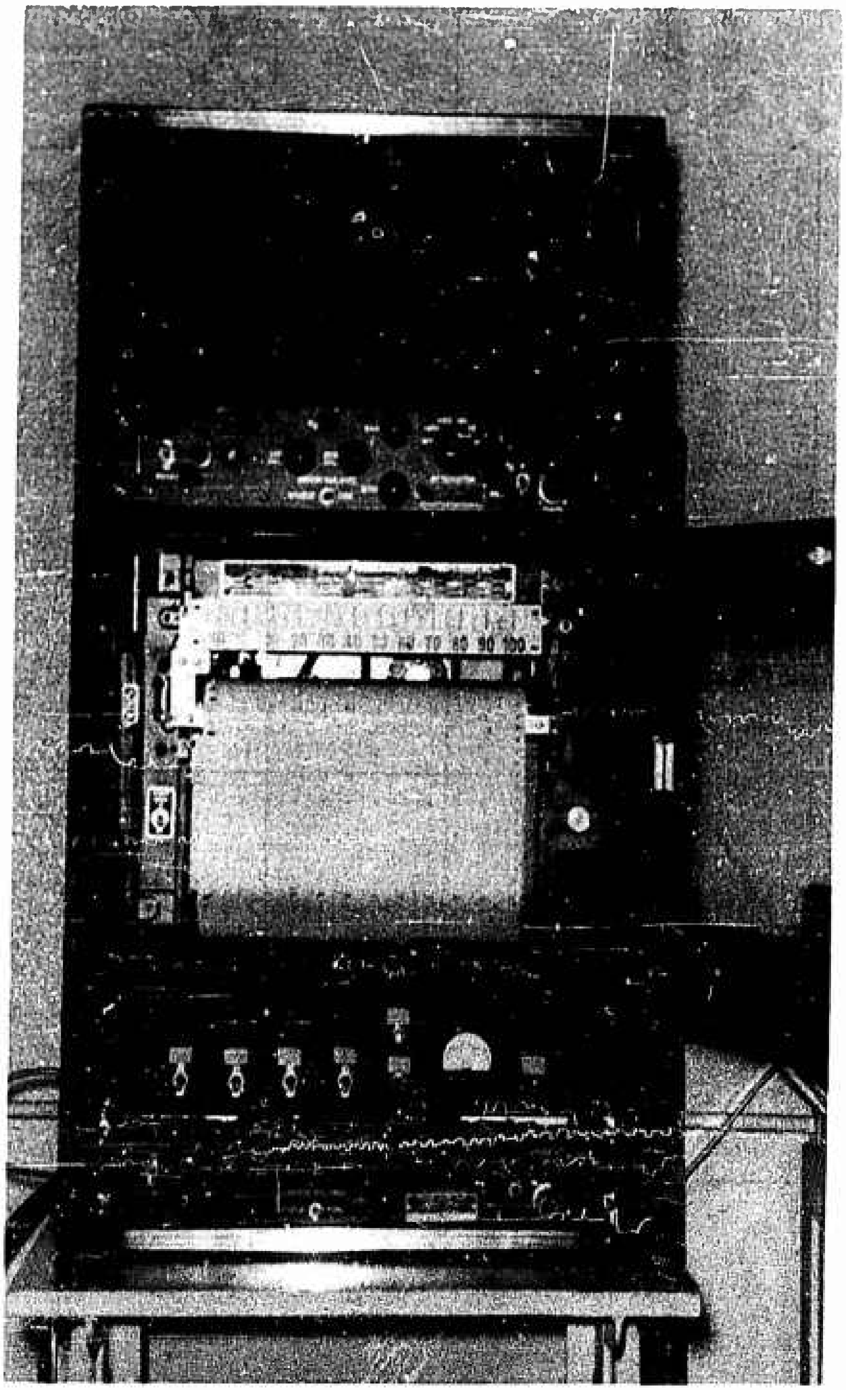

FIGURE 211

EXPONENT "n" VERSUS LIGHT PENETRABILITY

$n = 0.842 - 0.183 \log LP$

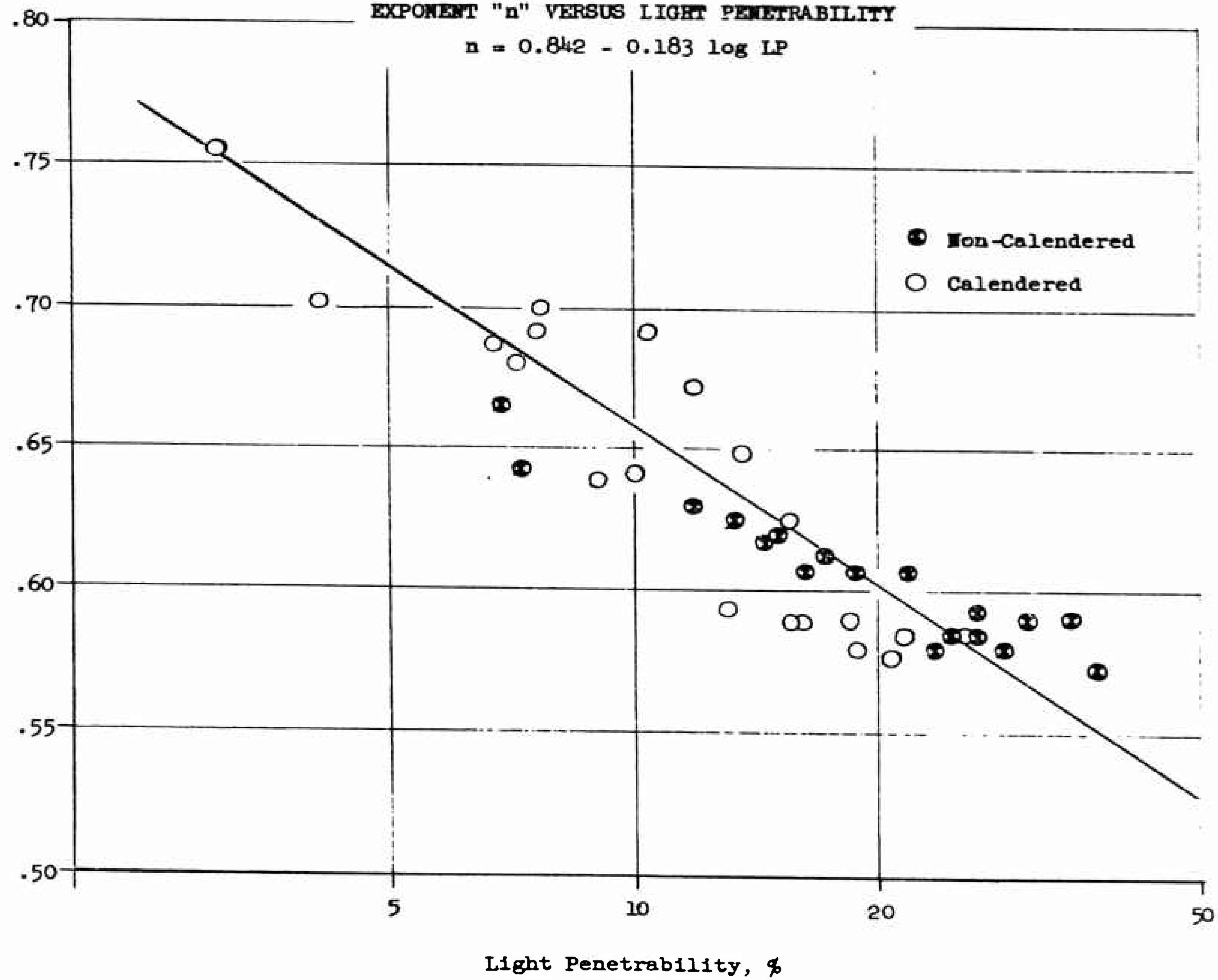

FIGURE 212

DISCHARGE COEFFICIENT VERSUS LIGHT PENETRABILITY

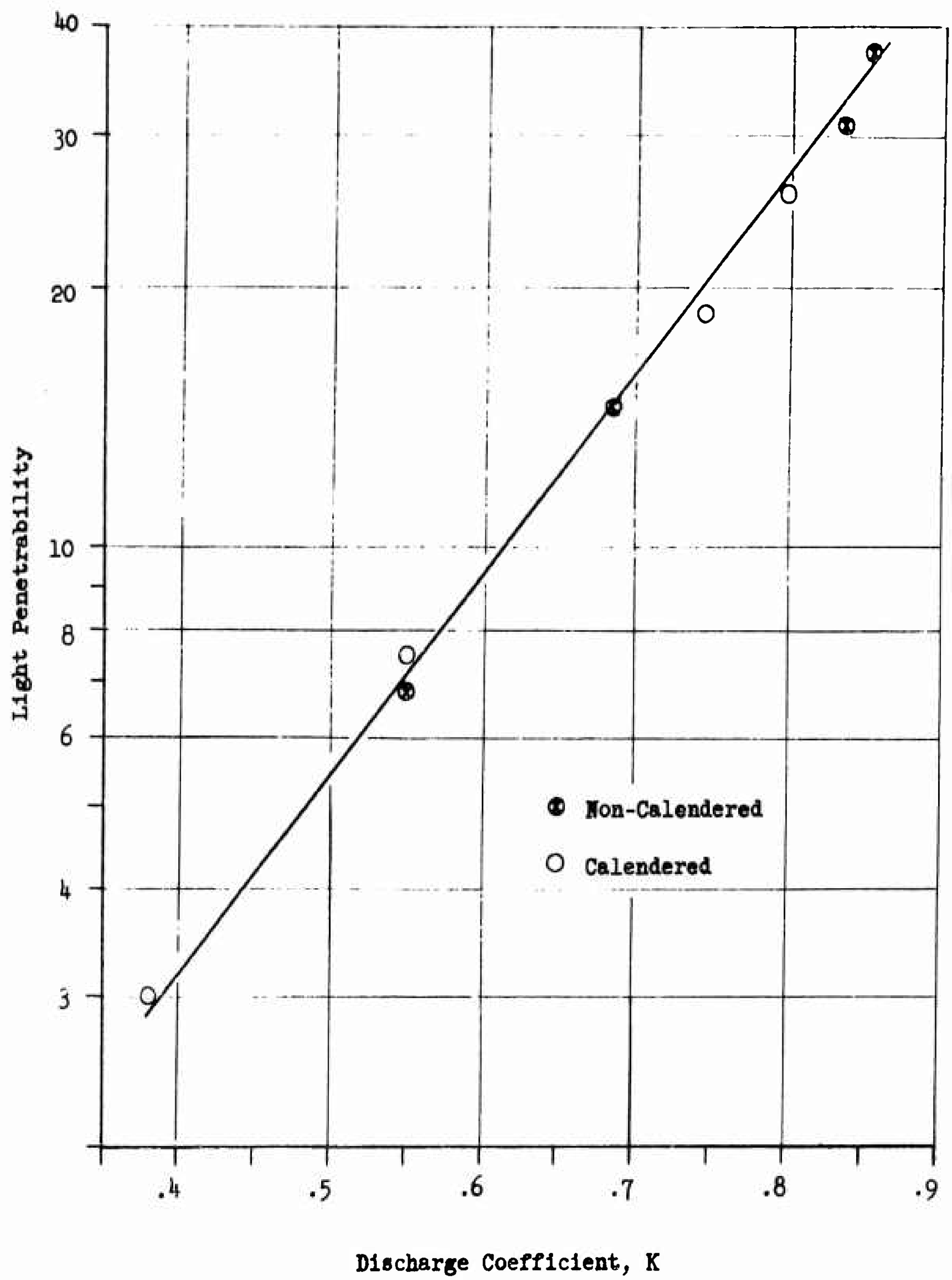

FIGURE 213

CALCULATED VERSUS MEASURED PERMEABILITIES

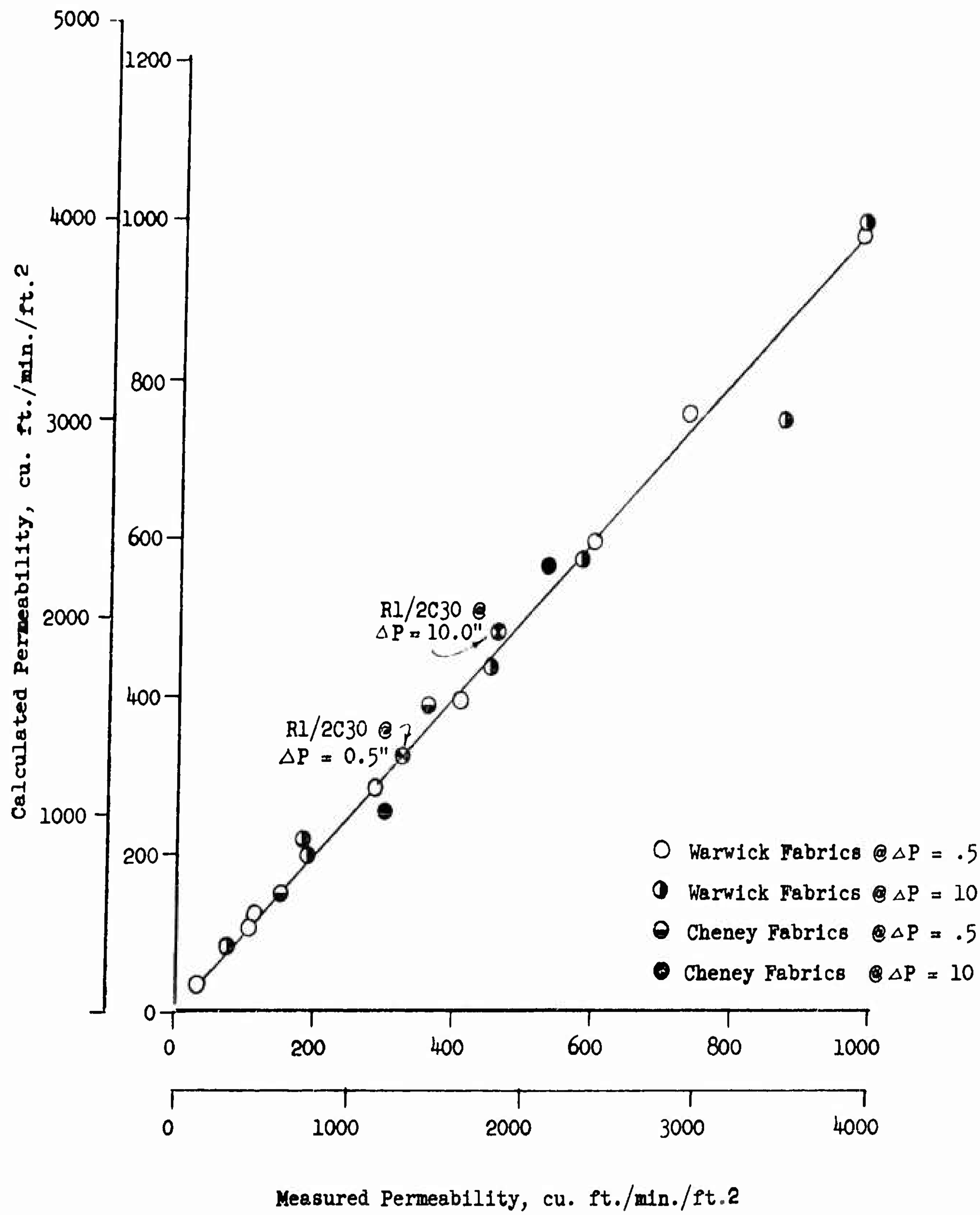

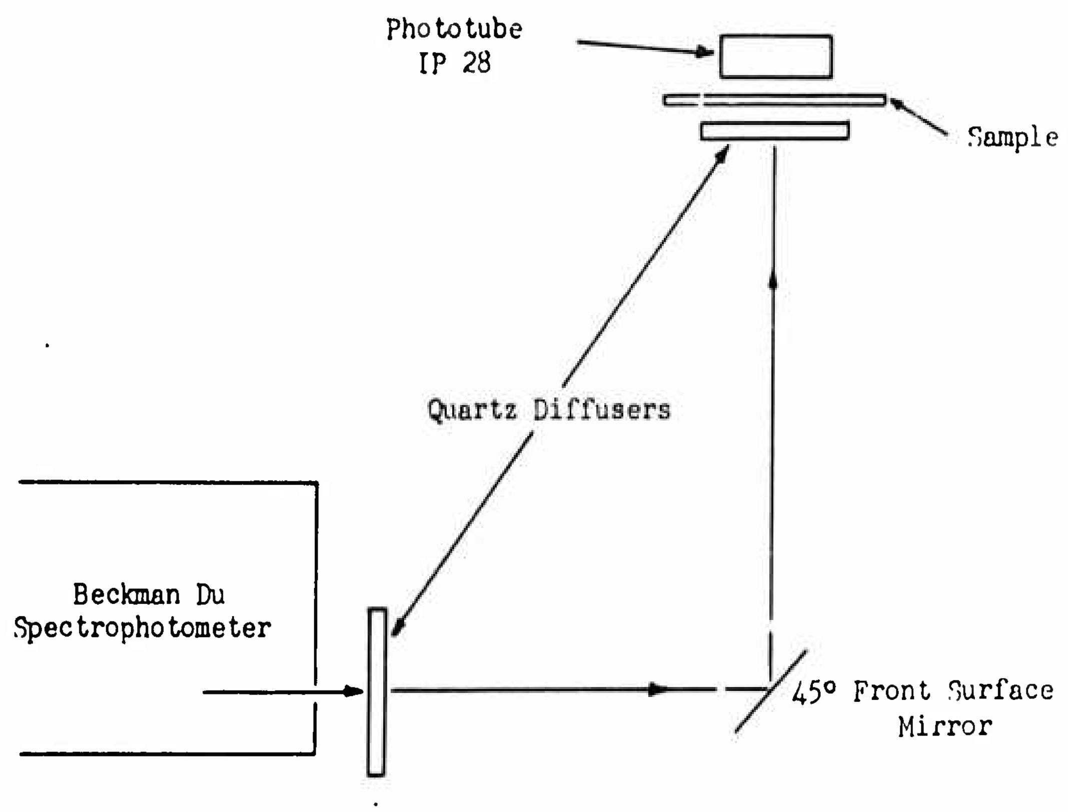

FIGURE 214

OPTICAL PATH FOR MEASURING

LIGHT PENETRABILITY ON THE BECKMAN SPECTROPHOTOMETER

FIGURE 215

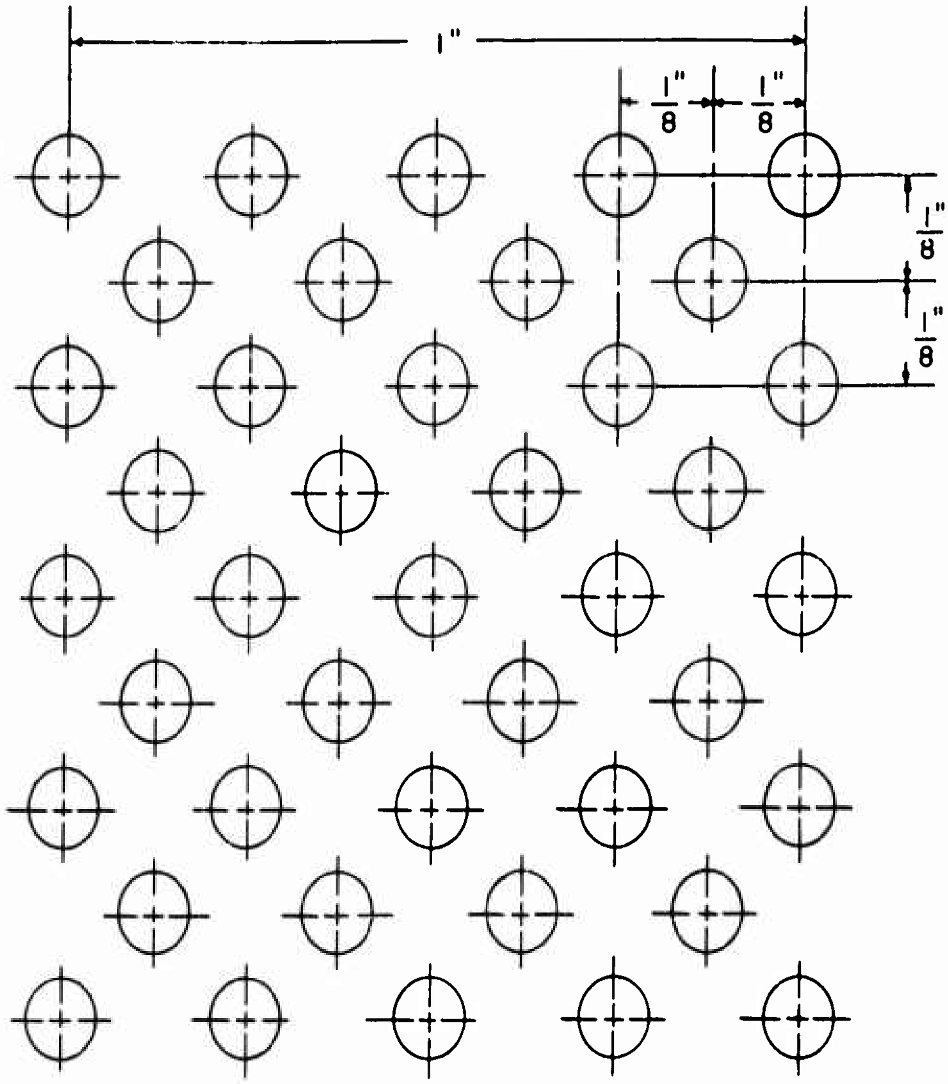

ENLARGED CROSS-SECTION

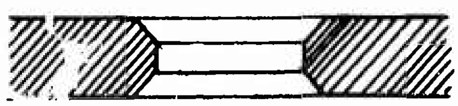

PERFORATED ALUMINUM PLATES

FIGURE 216

LIGHT PENETRABILITY VS. FREE AREA

For Perforated Plates and Metal Screens

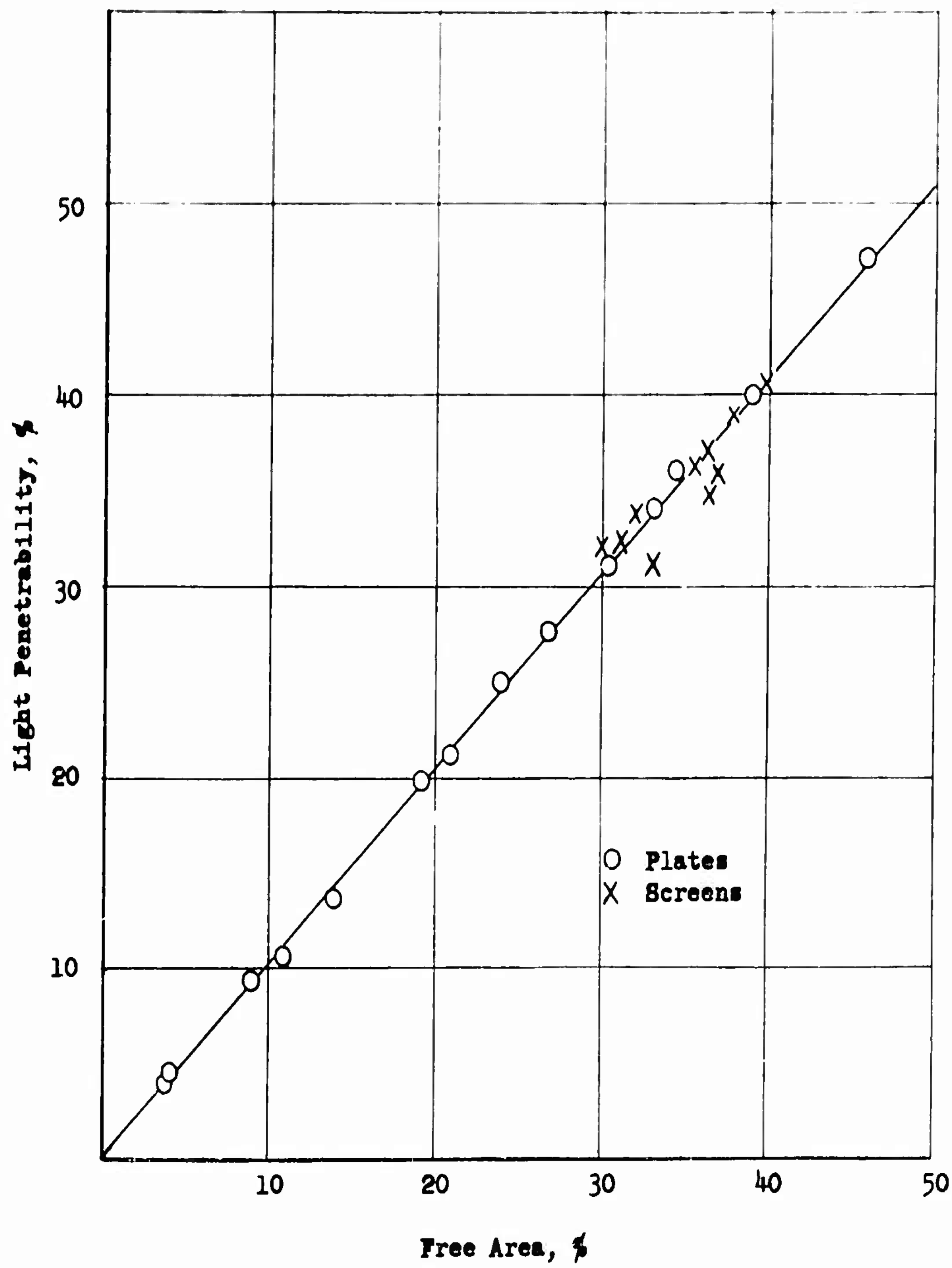

FIGURE 217

PROJECTED FREE AREA VS. LIGHT PENETRABILITY

Warwick Fabrics

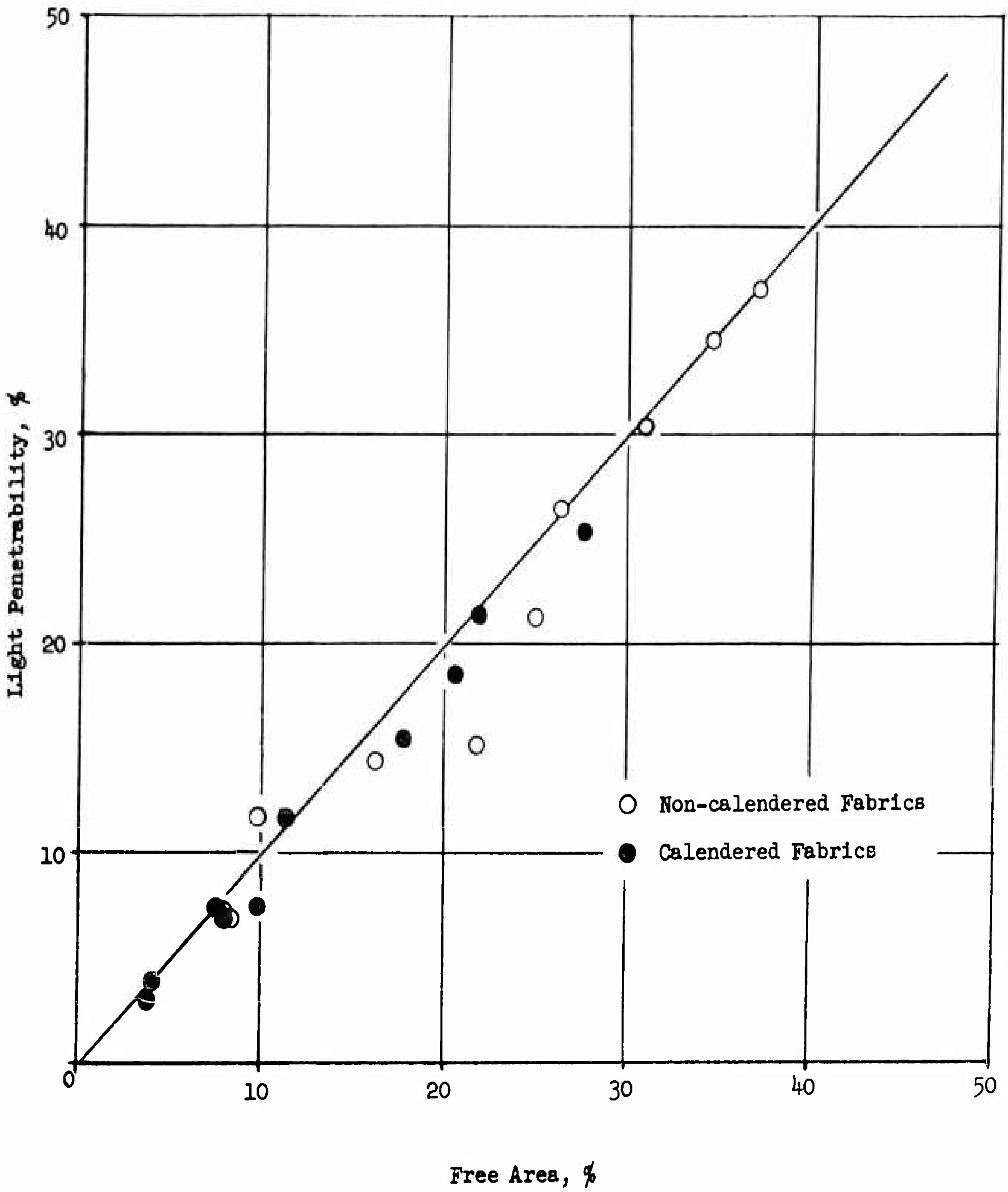

APPENDIX IV

LIGHT PENETRABILITY EXPERIMENT

<u>LIGHT PENETRABILITY TECHNIQUE AS A MEANS OF DETERMINING</u>

<u>THE PROJECTED FREE AREAS OF FABRICS</u>

Measurement of the projected free area of a fabric as calculated from measured horizontal yarn diameters and the number of yarns per inch is, at best, cumbersome because of the involved microscopy. Accuracy is also questionable unless a very large number of samples are studied to overcome the inherent variability of textile structures. As an example to illustrate the reliability, or the lack thereof, of this free area determination procedure, a check was made by taking a plan view photomicrograph of Fabric 10N35 (fabric with the highest yarn twists among the Cheney series; because of the high twist this fabric has the best definition in both cross-section and plan view) at 100X magnification. The free areas in the photomicrograph were carefully cut out from the picture and weighed. The weight of 160 such free areas amounted to 20.6% of the weight of the uncut picture. This may be compared with a 19.2% free area determined microscopically. The difference of 1.4% in free area between the two methods is actually a 7% error, assuming the photographic method to be the more precise method. However, this second method, although perhaps more accurate, is actually more laborious than the first one.

It is therefore apparent that a direct and less tedious procedure for free area determination was desired.

Both photometric measurements of light reflectance and light transmittance were considered as possible means of direct free area determination methods. This section is concerned with the description of these tests, the presentation of data and the conclusions therefrom. The findings were most encouraging in that a linear correlation between light penetrability and free area was established.

Experimental measurements of light reflectance and light penetrability (transmission) were made on a Beckman DU Spectrophotometer. Reflectance values were measured when samples dyed black were placed against white backgrounds. This procedure gave fair results on some samples, but, in general, it was not as satisfactory as the light penetrability technique.

In measuring light penetrability, a special attachment was made for the Spectrophotometer to facilitate sample handling. Figure 214 shows diagramatically the optical path of the experimental arrangement.

Light penetrability measurements were made first on perforated aluminum plates, then on wire screens, and thirdly on the nylon parachute fabrics.

It should be mentioned that not just any wavelength of light is suitable for measuring the <u>LP</u> of fabrics. All undyed fabrics transmit at least some visible light. Thus, a wavelength should be selected at which the yarns in the fabric absorb a maximum amount of the incident light. For nylon this has been found to be 230 millimicrons. The wires of the screens and the solid portions of the plates, being metallic, are impervious to light rays of wavelengths 200 - 1000 millimicrons and thus any wavelength in this range may be used for free area evaluation.

A. Perforated Aluminum Plates

A series of aluminum plates (0.02" thick) were drilled with holes equally spaced (32 holes per square inch) as shown in Figure 215. The hole diameters varied approximately from 0.041" (number 59 drill) to 0.136" (number 29 drill). The actual free areas of each plate were determined photographically; i.e., photomicrographs of the plates were taken, the holes were cut out and weighed. The free areas thus determined are given in Table 41. Both ends of holes were counter-sunk, as shown in the enlarged cross-sectional view in Figure 215.

B. Wire Screens

An assortment of wire screens whose constructions are given in Table 42 were tested as an intermediate physical structure between perforated flat plates and nylon parachute fabrics. It is evident from the results given in Table 42 that the screens gave almost as good a set of data as did the perforated plates. In both cases the average ratio of LP/FA was unity.

C. Nylon Parachute Fabrics

The relationships between free area (FA) and light penetrability (LP), having thus been established for the perforated plates and wire screens, it remained to test the applicability of findings to fabric samples. Table 43 shows the excellent agreement between the values of FA and LP for twenty Warwick fabrics. The slight disagreements between certain of these values were primarily due to the inability to ascertain free areas with reasonable precision. The free areas calculated from microscopic determination of yarn diameters were extremely sensitive to slight errors in measurement. In addition, the counting of picks and ends was equally critical. In the microscopic measurement of yarn diameters, it is not impossible to err by as much as 5%, while the counting of yarns might be off by one pick (out of 80) or one end (out of 130). The cumulative effect of these two sources of error can be great; this is particularly so for the fabrics containing low twist yarns.

The following tabulation based on data from two of the Cheney Fabrics shows the effect that slight variations in yarn count or diameter can have on the calculated free areas.

	(1) As Observed	(2) Picks & Ends off by 1	(3) Yarn Diam. erred by 5%	(4) Combination of 2 and 3
Fabric 10N 1/2				
Yarn diameter, warp, in.	0.00486	0.00486	0.00462	0.00462
Yarn diameter, filling, in.	0.01202	0.01202	0.01142	0.01142
Threads per inch, warp	130	129	130	129
Threads per inch, filling	77	76	77	76
Free area, per cent*	2.74	3.23	4.82	5.34
Per cent error**	----	17.9	75.9	94.9
Fabric 10N35				
Yarn diameter, warp, in.	0.00533	0.00533	0.00506	0.00506
Yarn diameter, filling, in.	0.00557	0.00557	0.00529	0.00529
Threads per inch, warp	124	123	124	123
Threads per inch, filling	78	77	78	77
Free area, per cent*	19.18	19.67	21.88	22.48
Per cent error**	----	2.6	14.1	16.7

*Calculated from Equation (3.2).
**Per cent error based on "As Observed" values.

Figures 216 and 217 show graphically the correlation found between the microscopic (FA) and the photometric (LP) techniques for measuring free areas of fabrics, screens and plates. In view of time saved and the amount of sample area covered, the light penetrability technique is certainly worthy of application at least for these nylon fabrics.

APPENDIX V

PHOTOMICROGRAPHS

PHOTOMICROGRAPHS OF CHENEY BROTHERS' FABRIC
Twill Series

7N 1/2 - Not Calendered

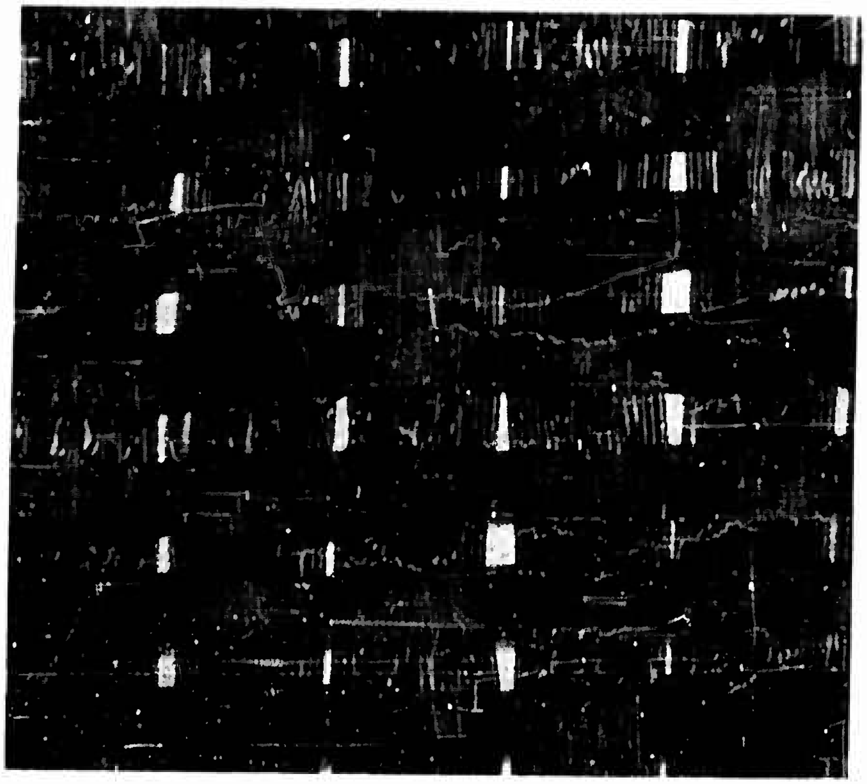

7C 1/2 Calendered

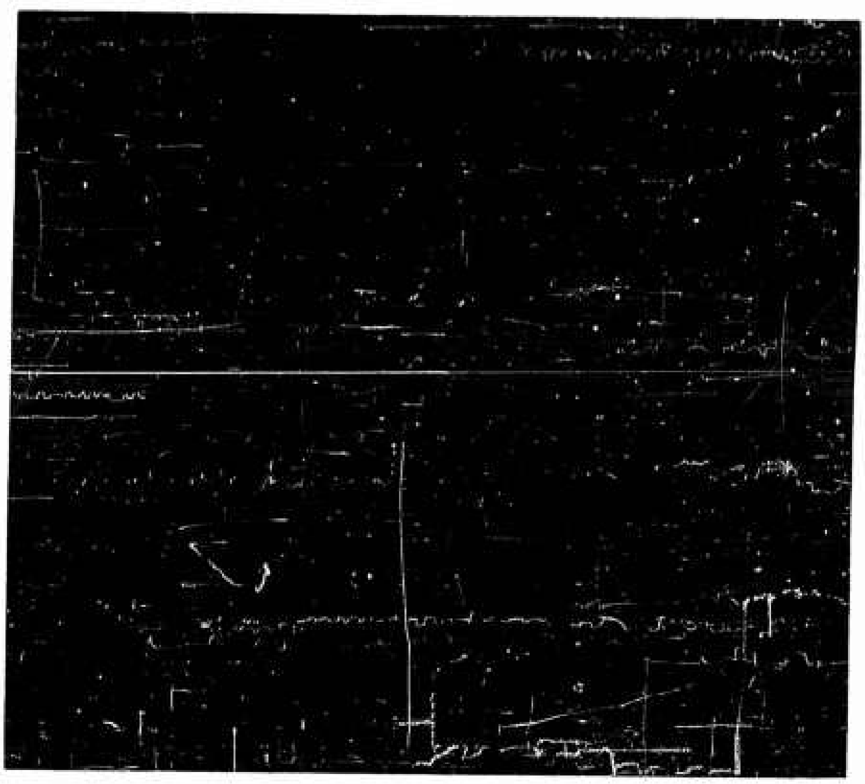

PHOTOMICROGRAPHS OF CHENEY BROTHERS' FABRIC
Twill Series

7N5 - Not Calendered

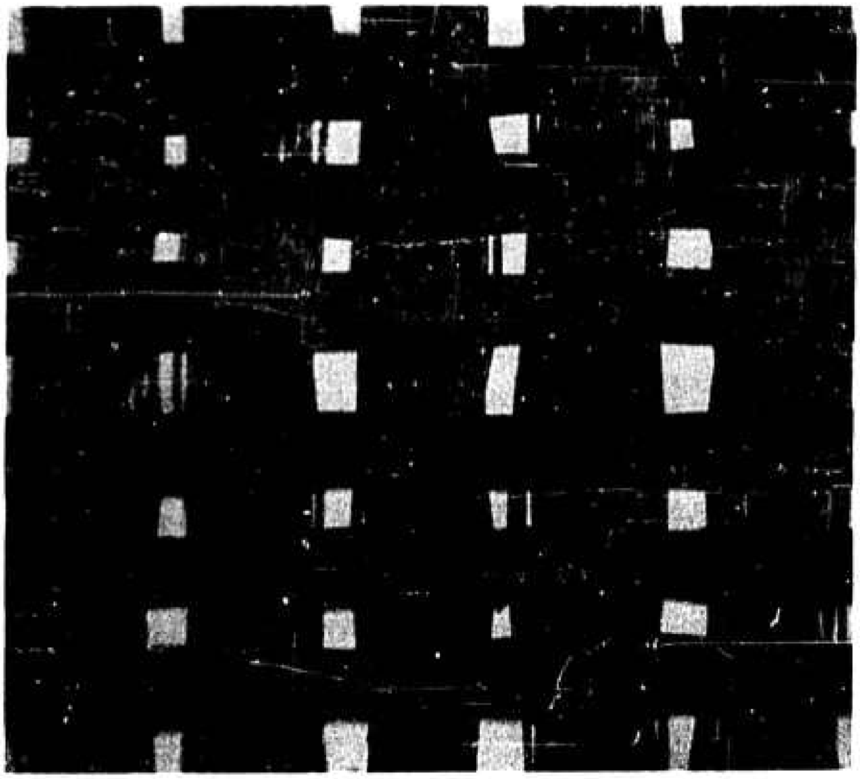

7C5 - Calendered

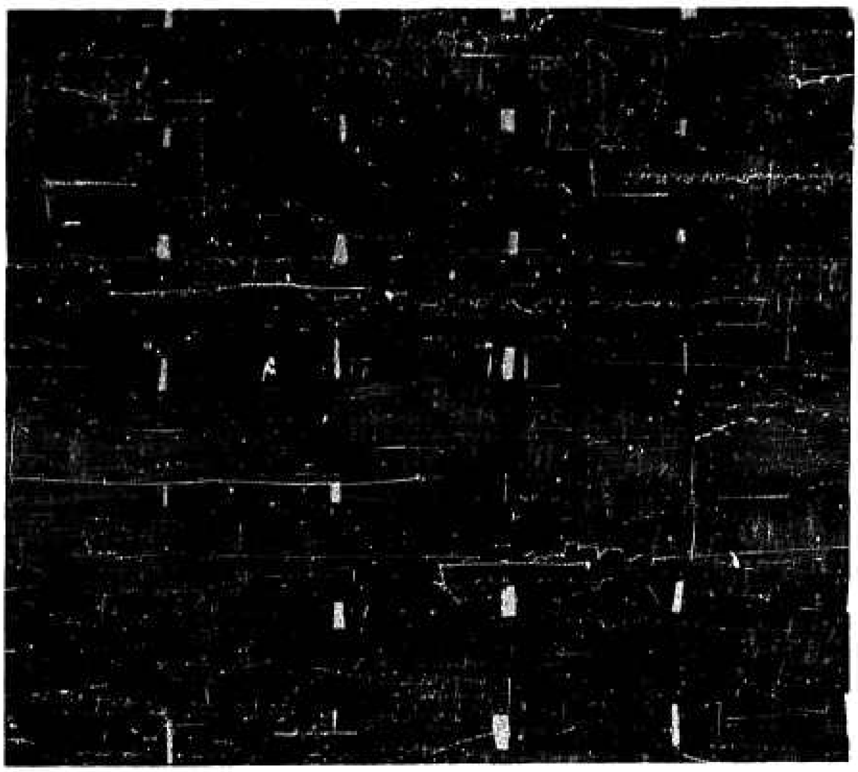

PHOTOMICROGRAPHS OF CHENEY BROTHERS' FABRIC
Twill Series

7N15 - Not Calendered

7C15 - Calendered

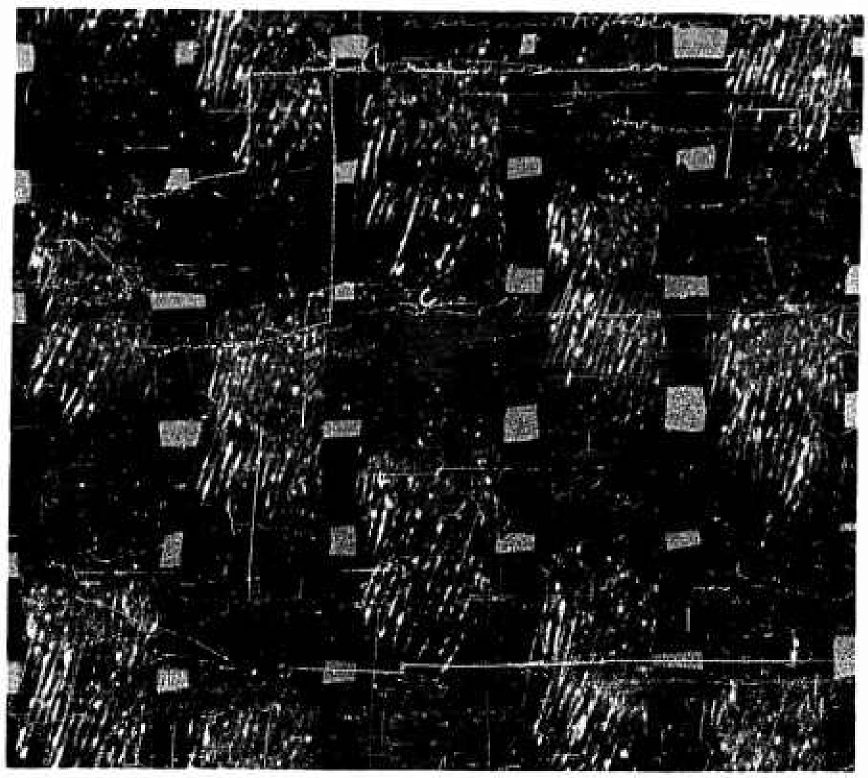

PHOTOMICROGRAPHS OF CHENEY BROTHERS' FABRICS
Twill Series

7C35 - Not Calendered

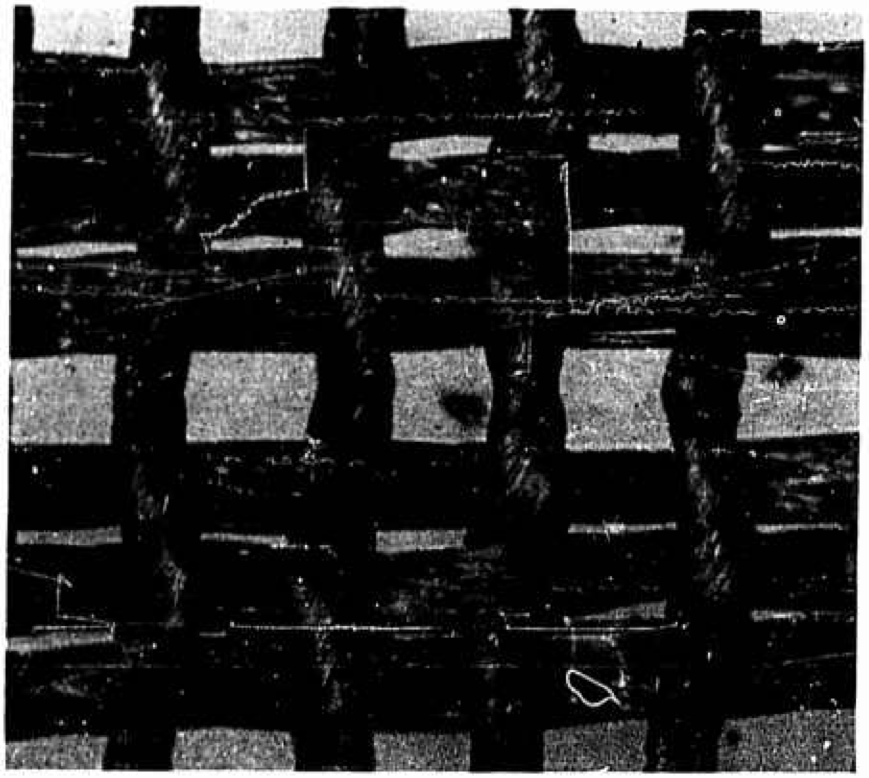

7C35 - Calendered

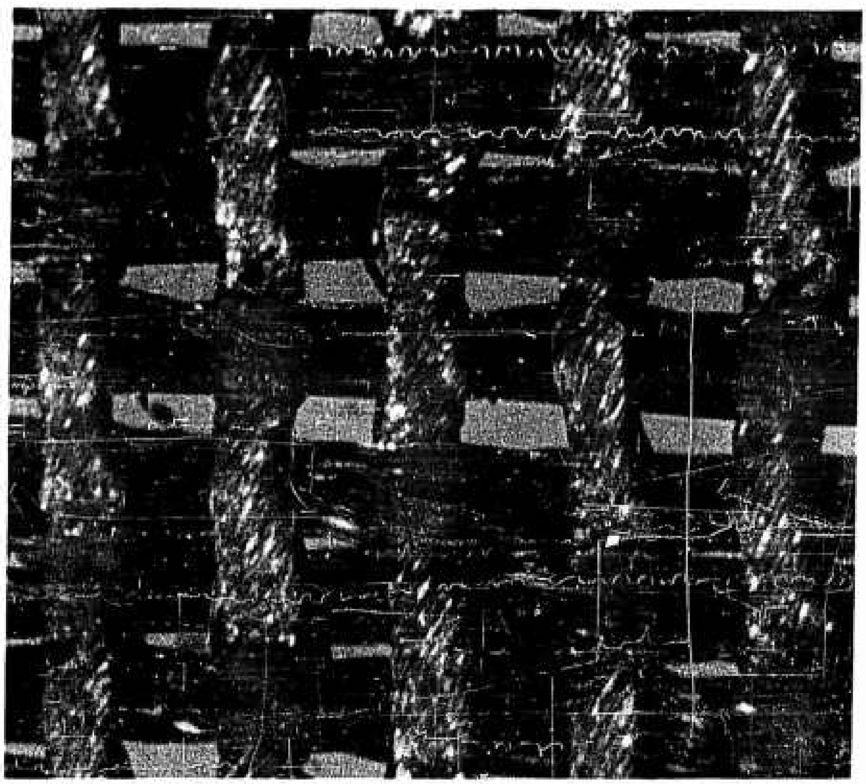

CROSS-SECTIONAL VIEWS OF CHENEY BROTHERS' FABRIC
(7N 1/2 and 7C 1/2 - Twill Series)

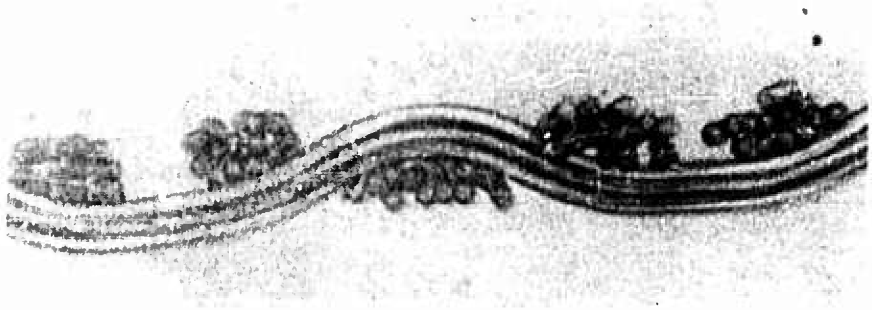

7N 1/2
Warp - Not Calendered

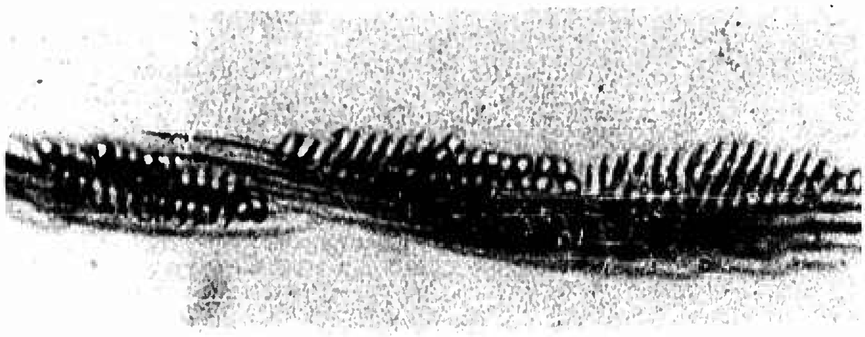

7N 1/2
Filling - Not Calendered

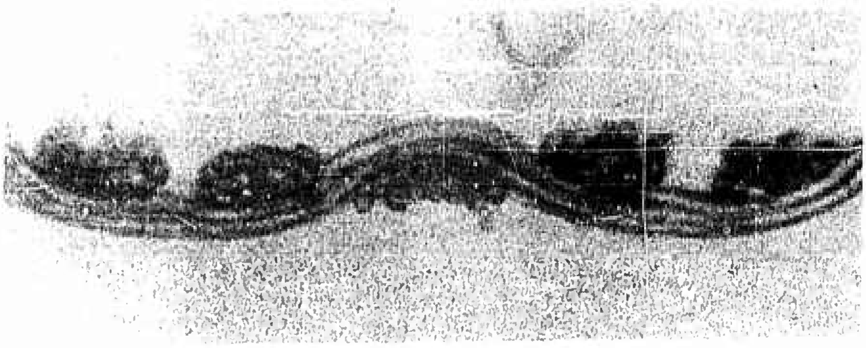

7C 1/2
Warp - Calendered

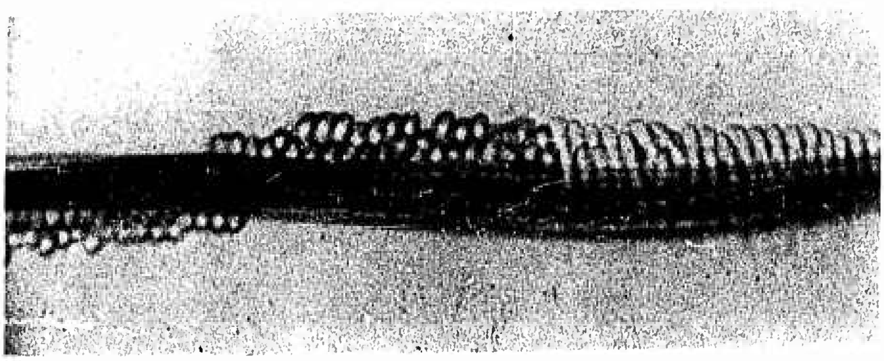

7C 1/2
Filling - Calendered

CROSS-SECTIONAL VIEWS OF CHENEY BROTHERS' FABRIC
(7N2 1/2 and 7C2 1/2 - Twill Series)

7N2 1/2
Warp - Not Calendered

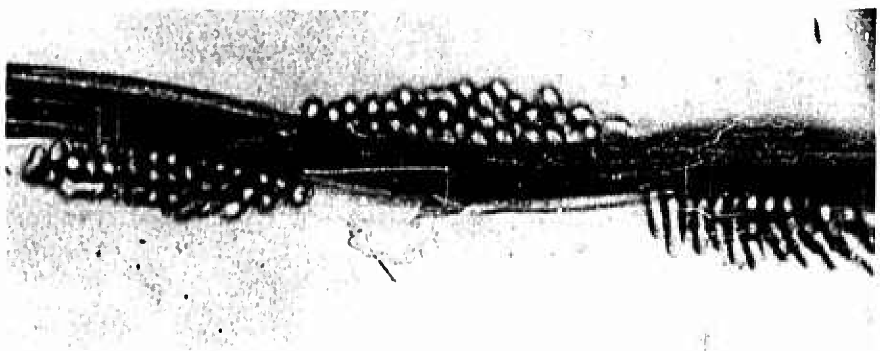

7N2 1/2
Filling - Not Calendered

7C2 1/2
Warp - Calendered

7C2 1/2
Filling - Calendered

CROSS-SECTIONAL VIEWS OF CHENEY BROTHERS' FABRIC
(7N5 and 7C5 - Twill Series)

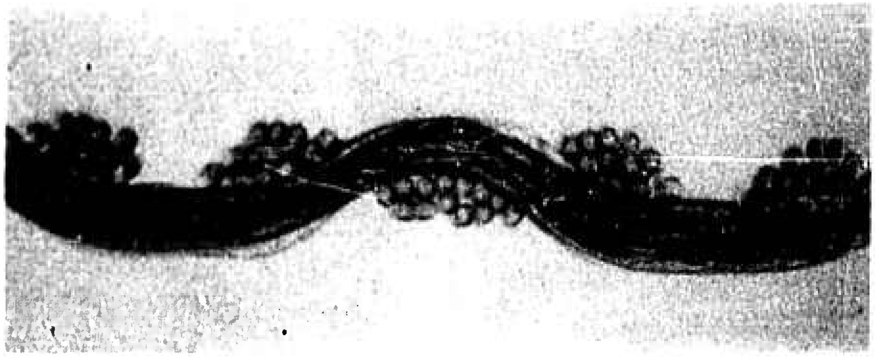

7N5
Warp - Not Calendered

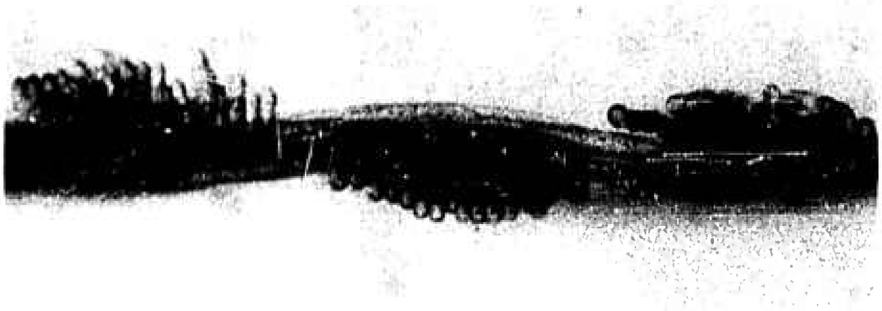

7N5
Filling - Not Calendered

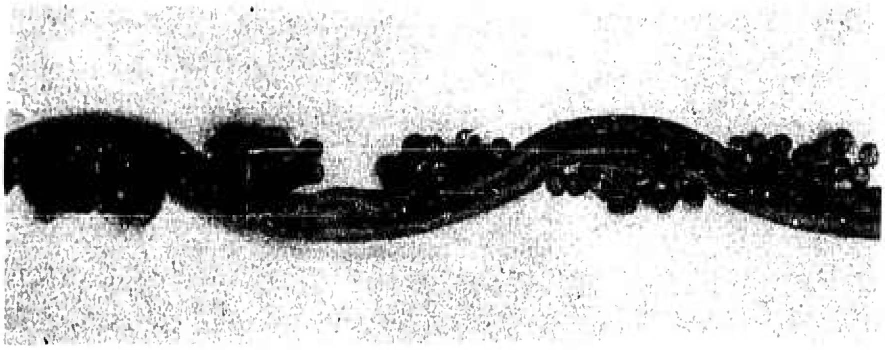

7C5
Warp - Calendered

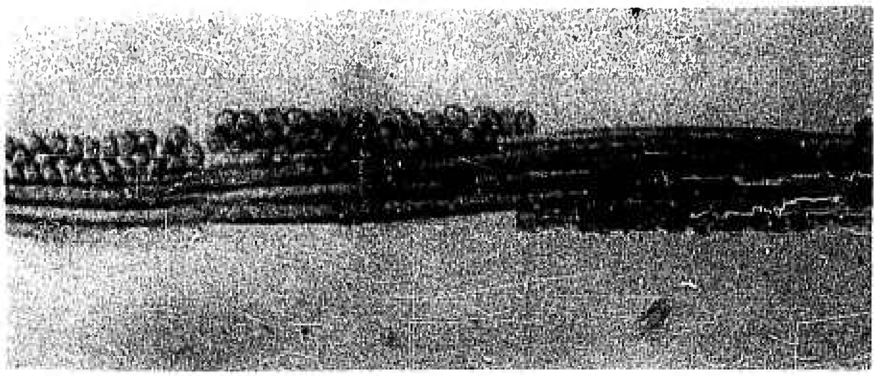

7C5
Filling - Calendered

CROSS-SECTIONAL VIEWS OF CHENEY BROTHERS' FABRIC
(7N7 and 7C7 - Twill Series)

7N7
Warp - Not Calendered

7N7
Filling - Not Calendered

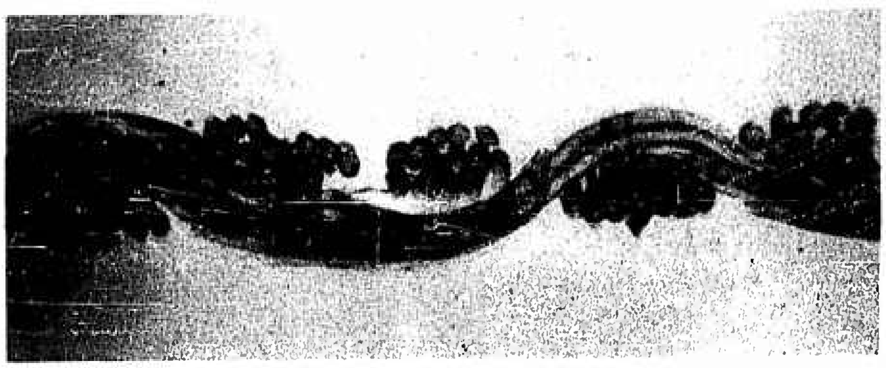

7C7
Warp - Calendered

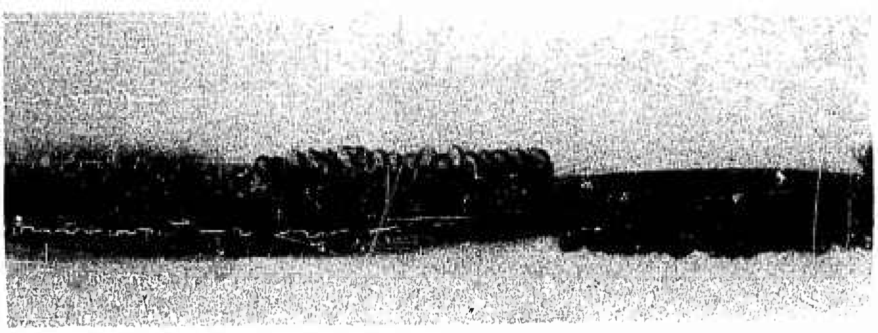

7C7
Filling - Calendered

CROSS SECTIONAL VIEWS OF CHENEY BROTHERS' FABRIC
(7N15 and 7C15 - Twill Series)

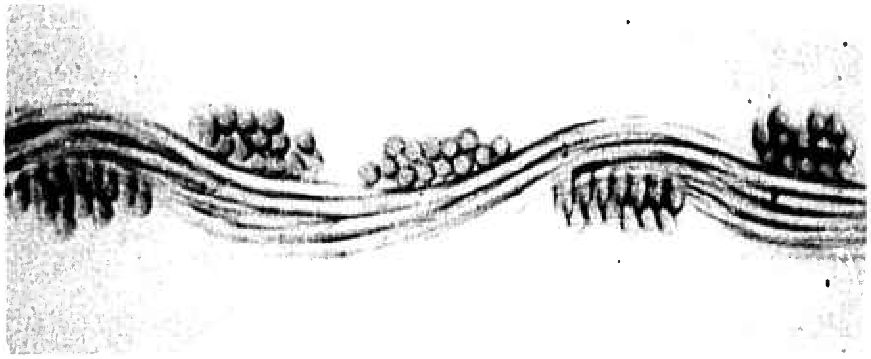

7N15
Warp - Not Calendered

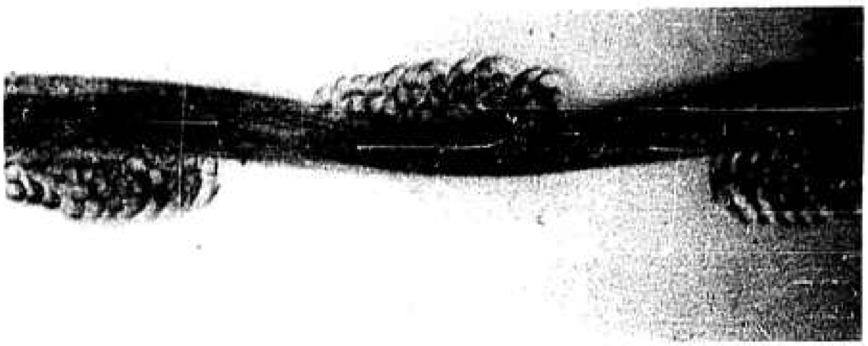

7N15
Filling - Not Calendered

7C15
Warp - Calendered

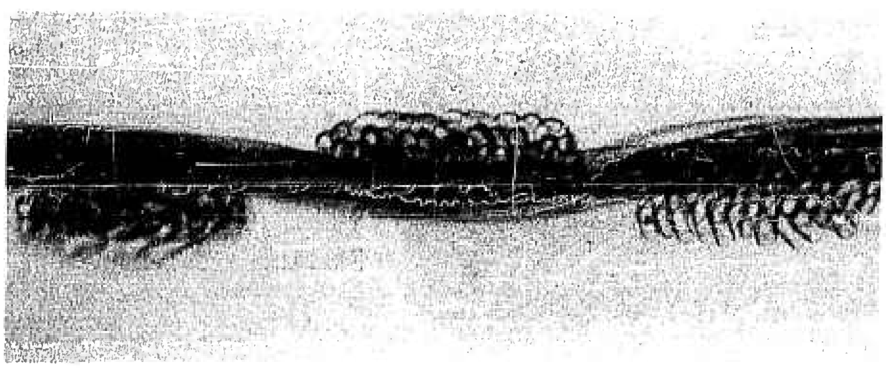

7C15
Filling - Calendered

CROSS-SECTIONAL VIEWS OF CHENEY BROTHERS' FABRIC
(7N20 and 7C20 - Twill Series)

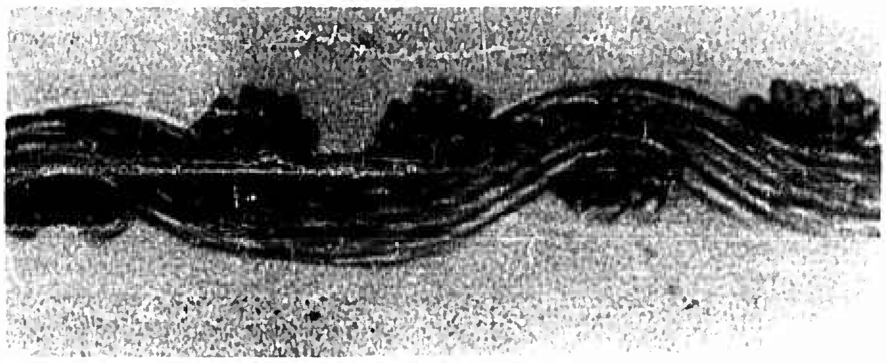

7N20
Warp - Not Calendered

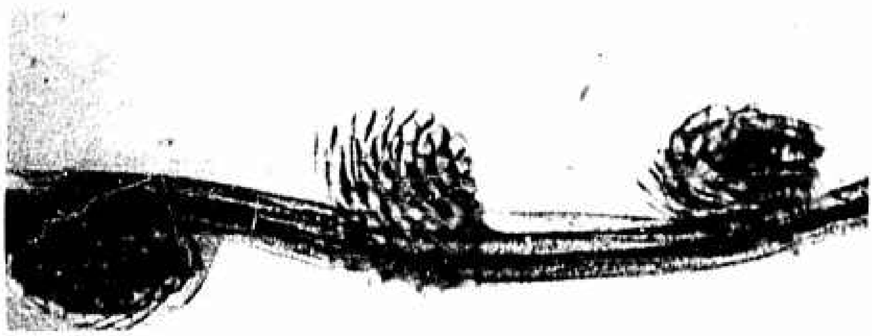

7N20
Filling - Not Calendered

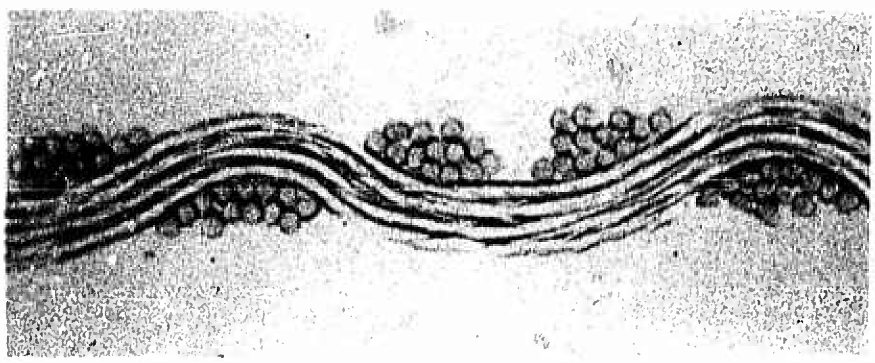

7C20
Warp - Calendered

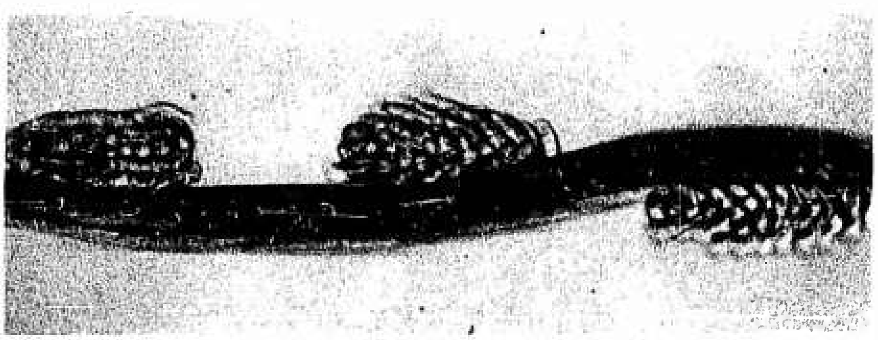

7C20
Filling - Calendered

CROSS-SECTIONAL VIEWS OF CHENEY BROTHERS' FABRIC
(7N35 and 7C35 - Twill Series)

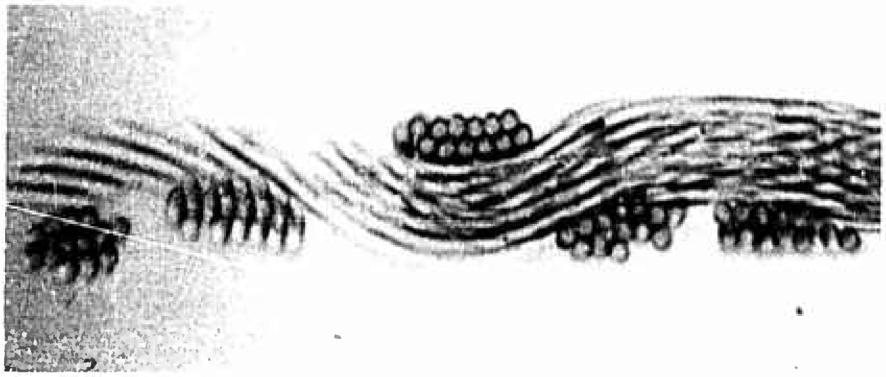

7N35
Warp - Not Calendered

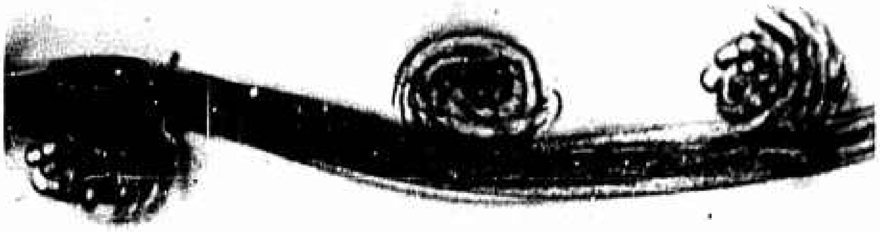

7N35
Filling - Not Calendered

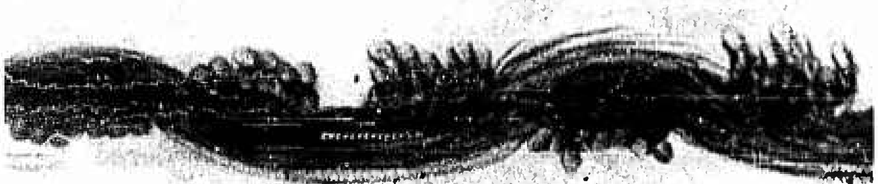

7C35
Warp - Calendered

7C35
Filling - Calendered

CROSS-SECTIONAL VIEWS OF CHENEY BROTHERS' FABRIC
(10N 1/2 and 10C 1/2 - Twill Series)

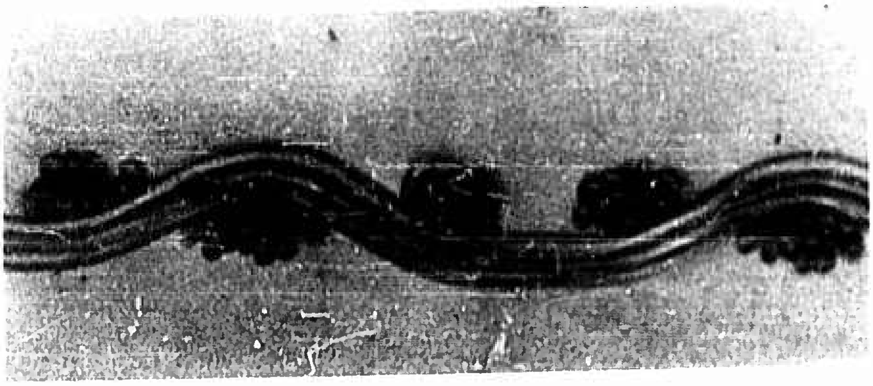

10N 1/2
Warp - Not Calendered

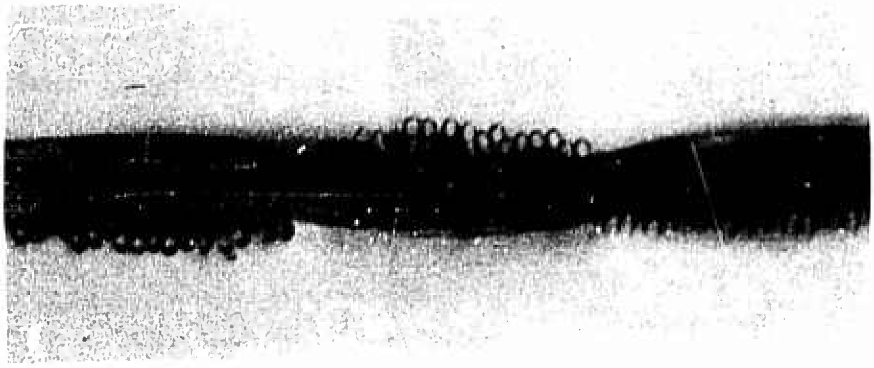

10N 1/2
Filling - Not Calendered

10C 1/2
Warp - Calendered

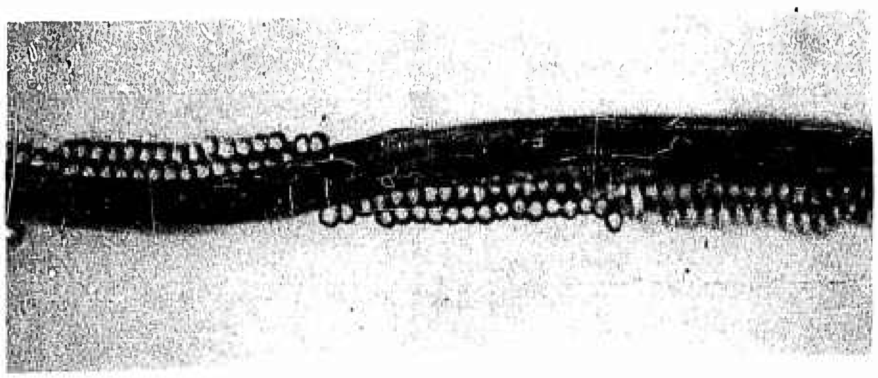

10C 1/2
Filling - Calendered

CROSS-SECTIONAL VIEWS OF CHENEY BROTHERS' FABRIC
(10N2 1/2 and 10C2 1/2 - Twill Series)

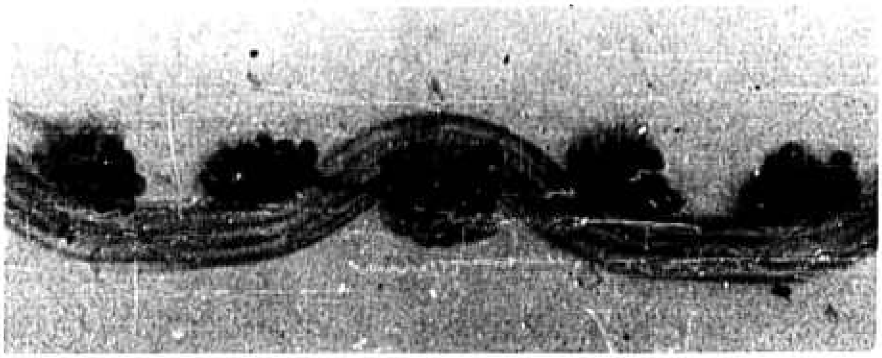

10N2 1/2
Warp - Not Calendered

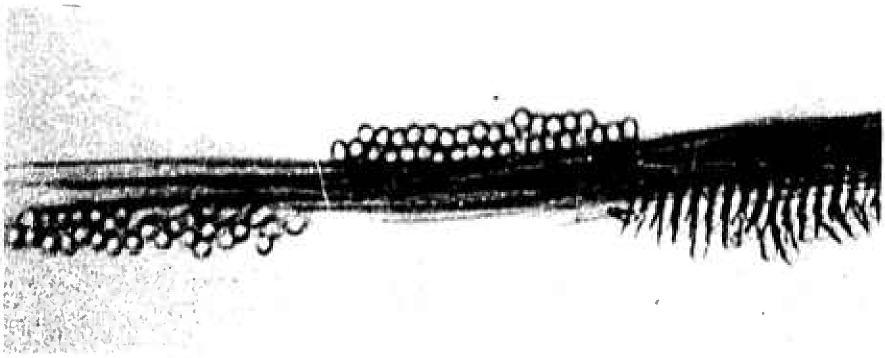

10N2 1/2
Filling - Not Calendered

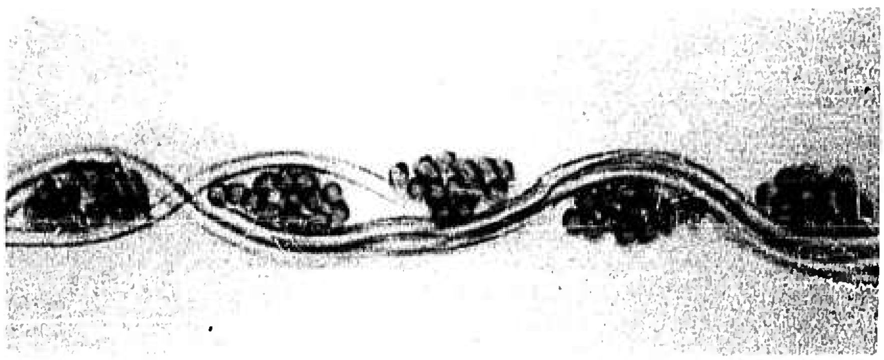

10C2 1/2
Warp - Calendered

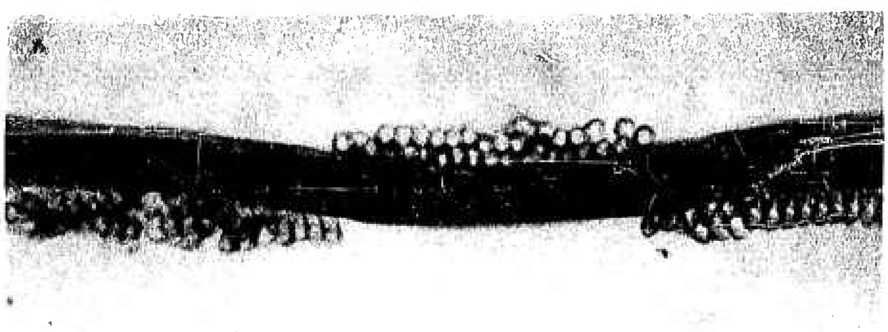

10C2 1/2
Filling - Calendered

CROSS-SECTIONAL VIEWS OF CHENEY BROTHERS' FABRIC
(10N5 and 10C5 - Twill Series)

10N5
Warp - Not Calendered

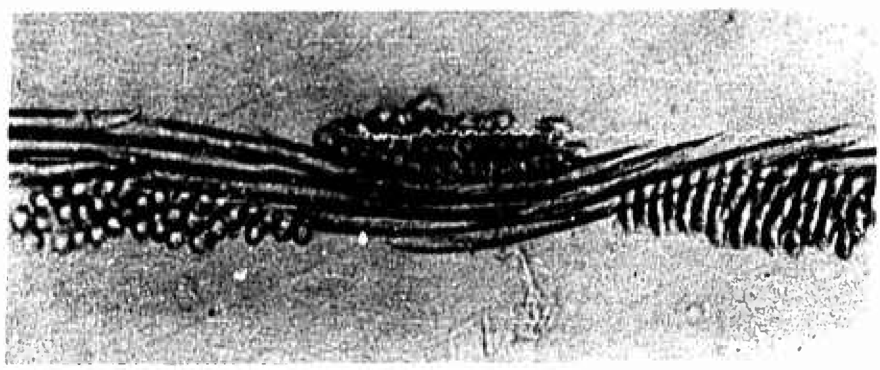

10N5
Filling - Not Calendered

10C5
Warp - Calendered

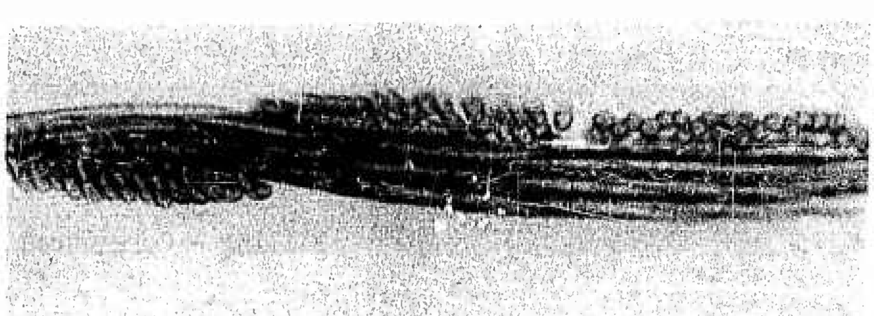

10C5
Filling - Calendered

CROSS-SECTIONAL VIEWS OF CHENEY BROTHERS' FABRIC
(10N7 and 10C7 - Twill Series)

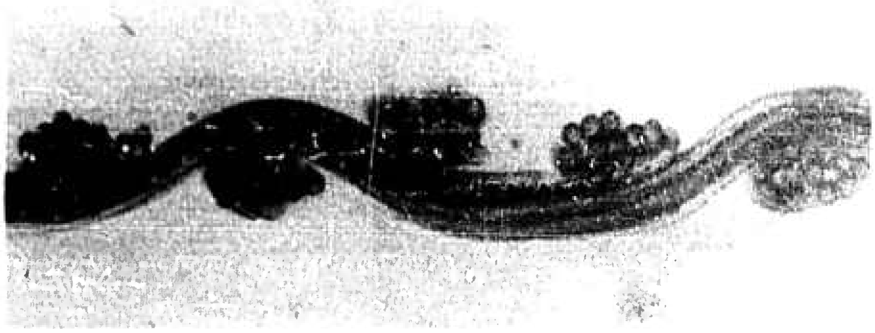

10N7
Warp - Not Calendered

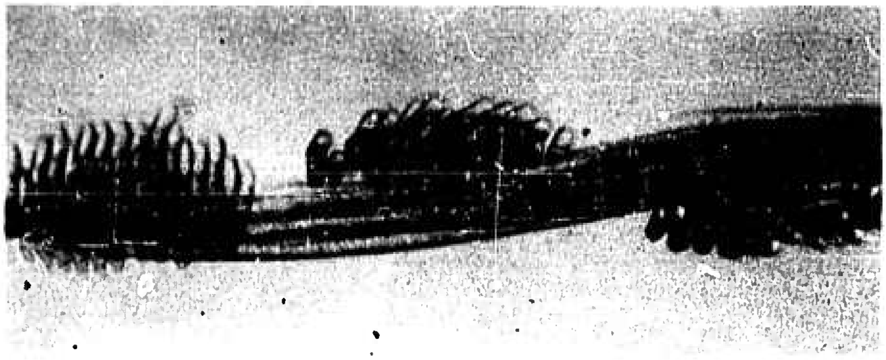

10N7
Filling - Not Calendered

10C7
Warp - Calendered

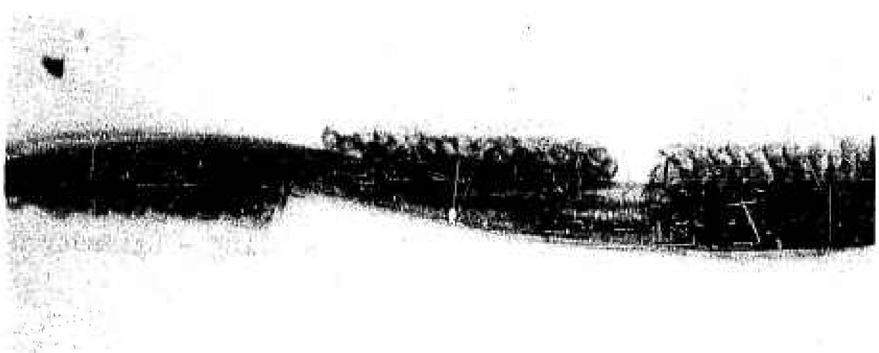

10C7
Filling - Calendered

CROSS-SECTIONAL VIEWS OF CHENEY BROTHERS' FABRIC
(10N15 and 10C15 - Twill Series

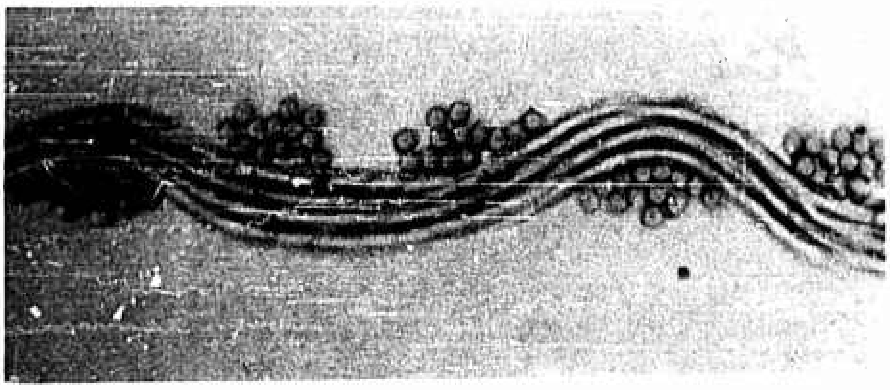

10N15
Warp - Not Calendered

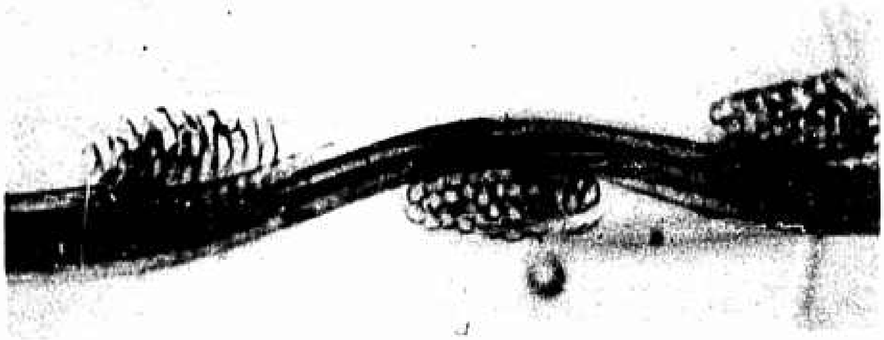

10N15
Filling - Not Calendered

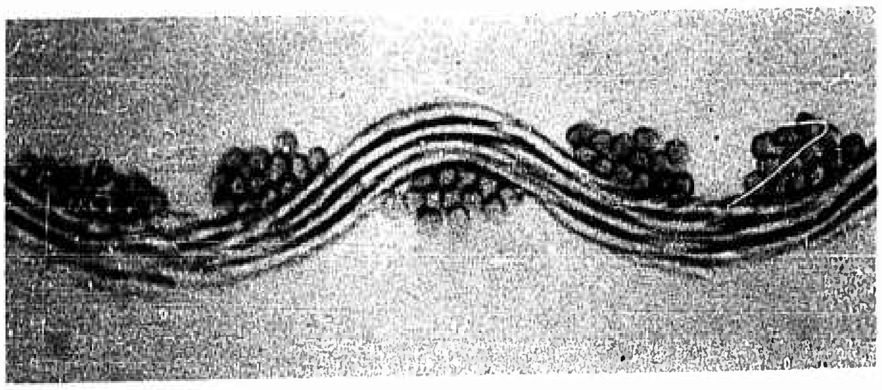

10C15
Warp - Calendered

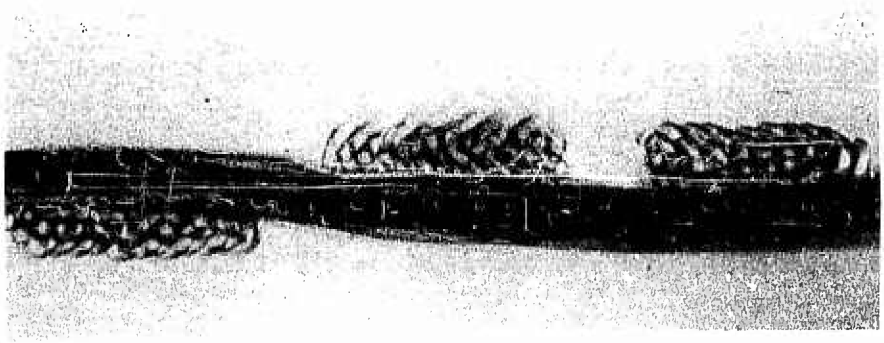

10C15
Filling - Calendered

CROSS-SECTIONAL VIEWS OF CHENEY BROTHERS' FABRIC
(10N20 and 10C20 - Twill Series)

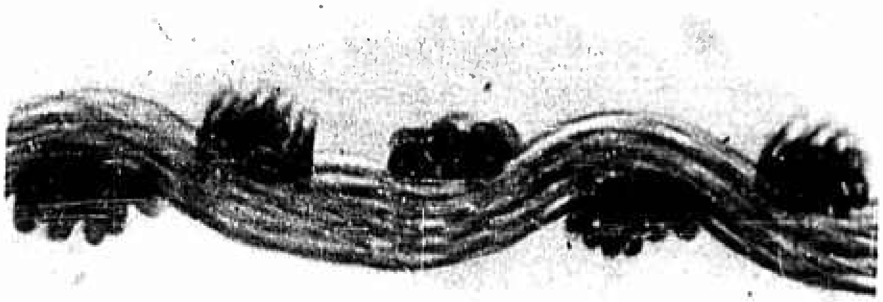

10N20
Warp - Not Calendered

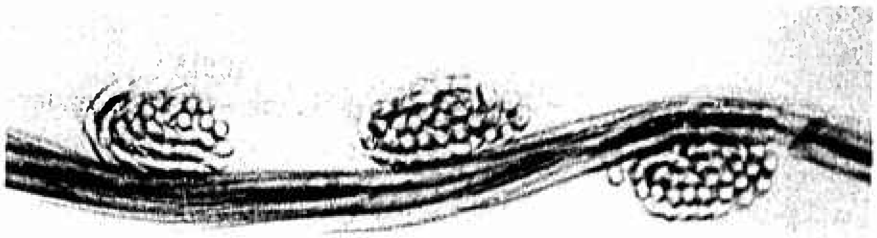

10N20
Filling - Not Calendered

10C20
Warp - Calendered

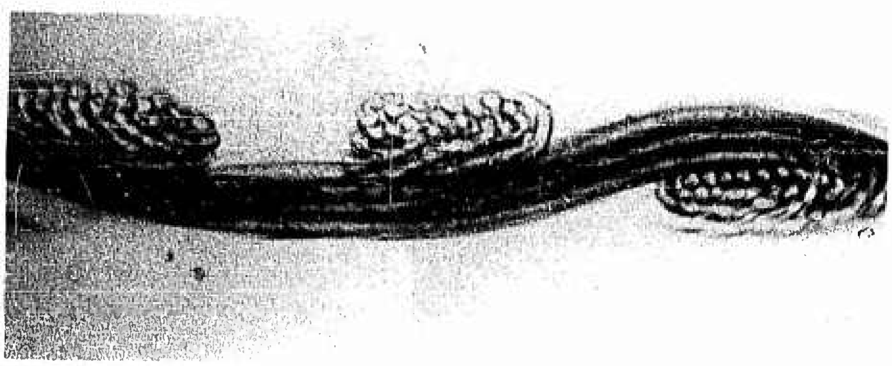

10C20
Filling - Calendered

CROSS-SECTIONAL VIEWS OF CHENEY BROTHERS' FABRIC
(10N35 and 10C35 - Twill Series)

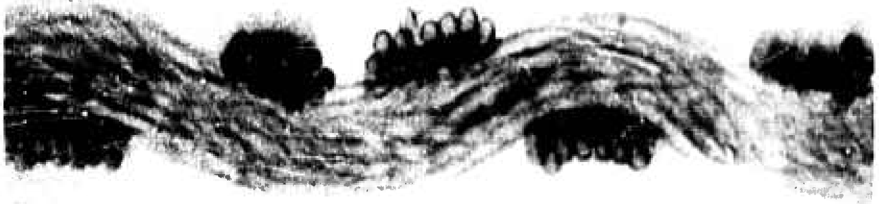

10N35
Warp - Not Calendered

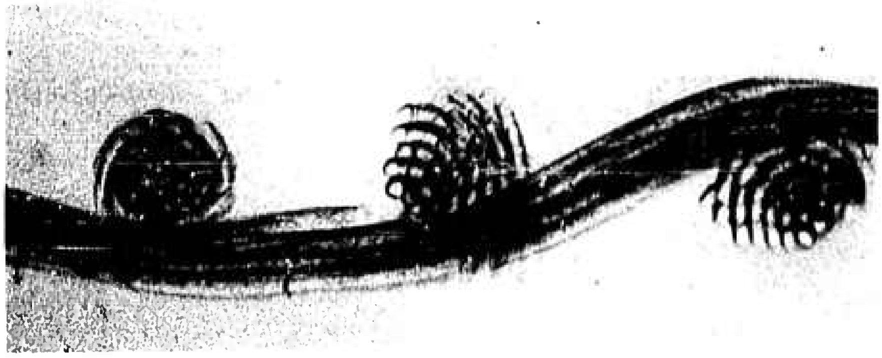

10N35
Filling - Not Calendered

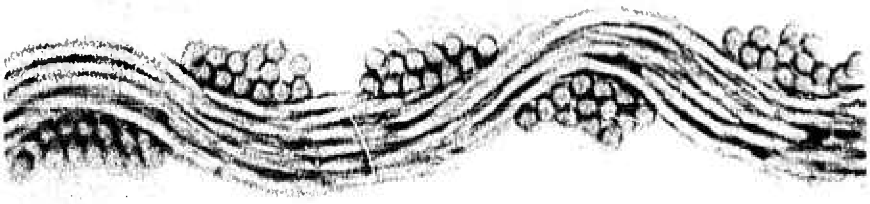

10C35
Warp - Calendered

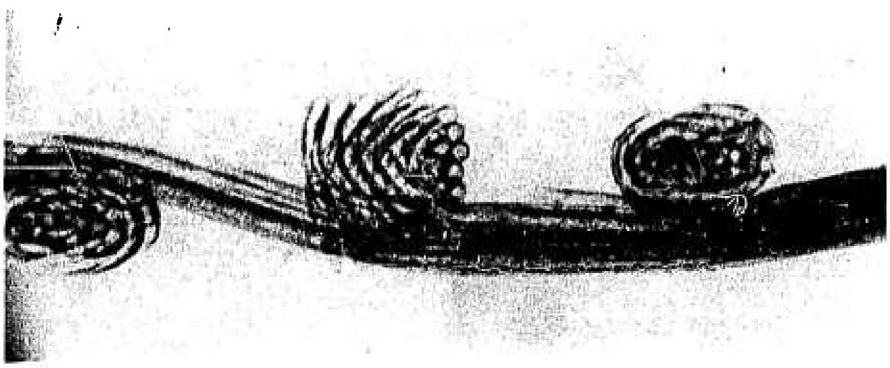

10C35
Filling - Calendered

CROSS-SECTIONAL VIEWS OF CHENEY BROTHERS' FABRIC
(R7N 1/2 and R7C 1/2 - Rip-Stop Series)

R7N 1/2
Warp - Not Calendered

R7N 1/2
Filling - Not Calendered

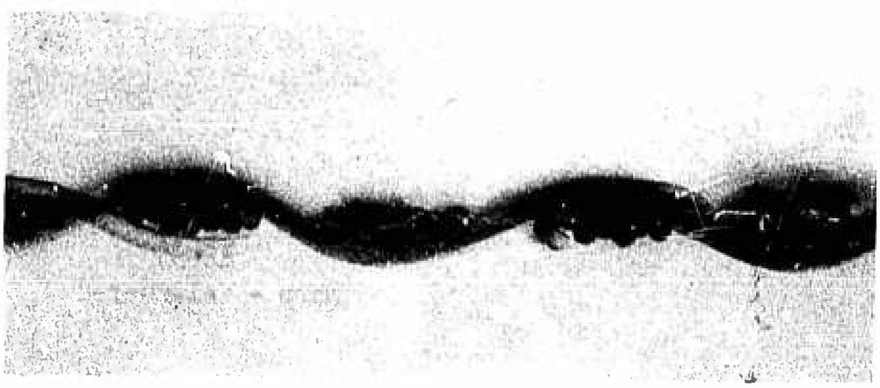

R7C 1/2
Warp - Calendered

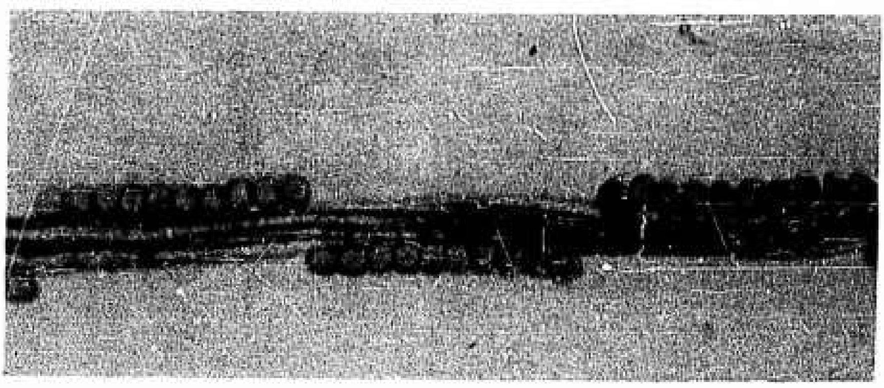

R7C 1/2
Filling - Calendered

CROSS-SECTIONAL VIEWS OF CHENEY BROTHERS' FABRIC
(R7N7 and R7C7 - Rip-Stop Series)

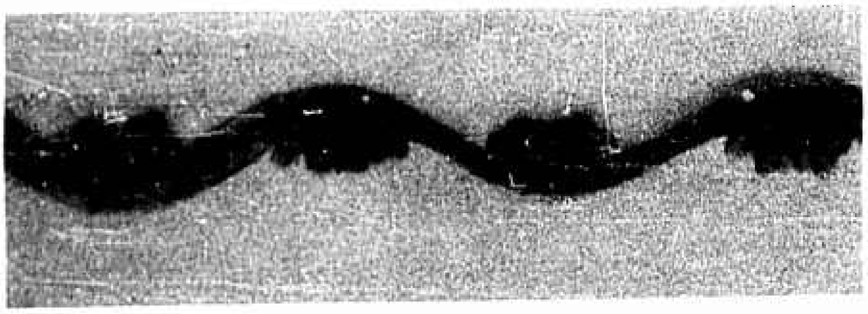

R7N7
Warp - Not Calendered

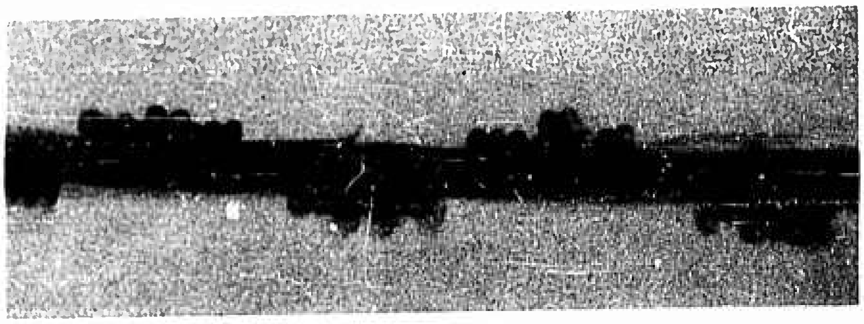

R7N7
Filling - Not Calendered

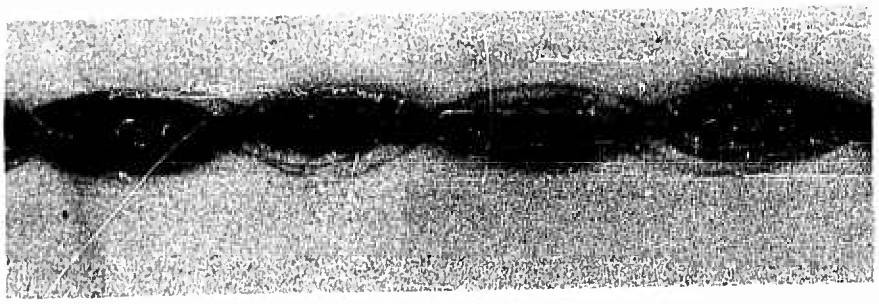

R7C7
Warp - Calendered

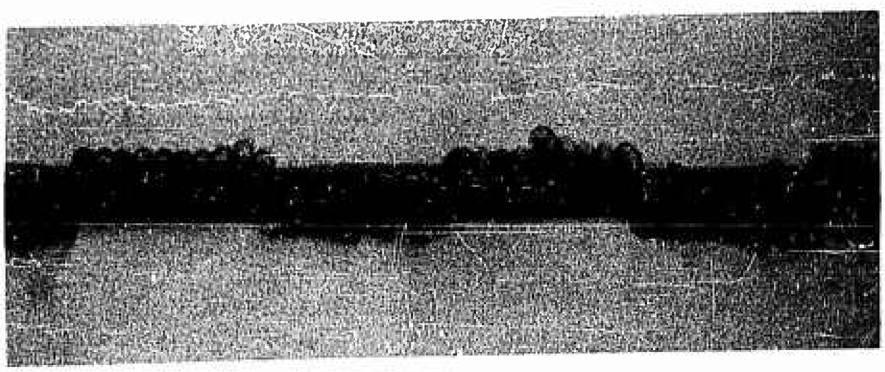

R7C7
Filling - Calendered

CROSS-SECTIONAL VIEWS OF CHENEY BROTHERS' FABRIC
(R7N30 and R7C30 - Rip-Stop Series)

R7N30
Warp - Not Calendered

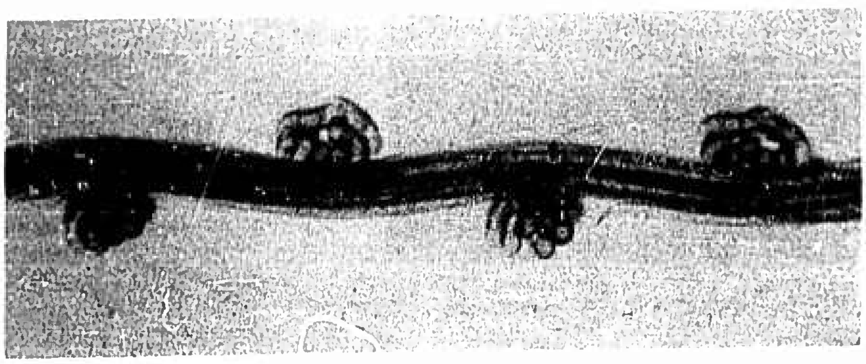

R7N30
Filling - Not Calendered

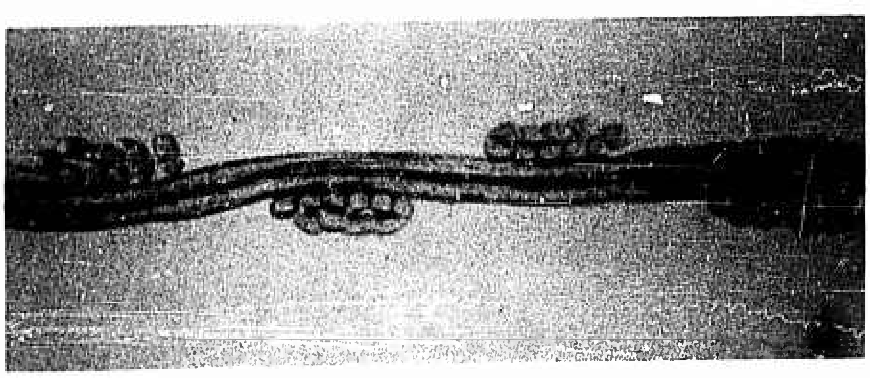

R7C30
Warp - Calendered

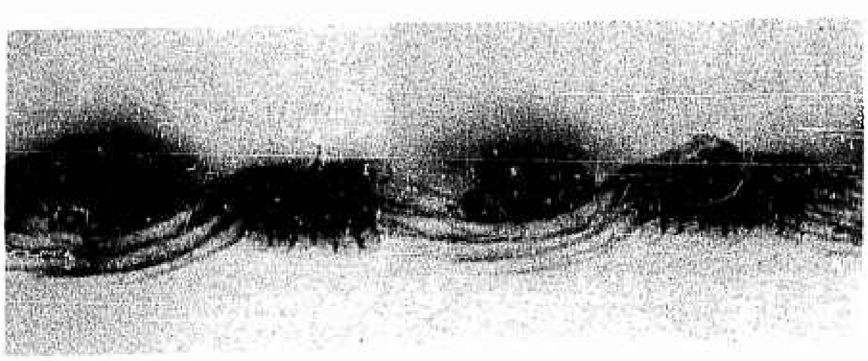

R7C30
Filling - Calendered

CROSS-SECTIONAL VIEWS OF WARWICK'S FABRICS

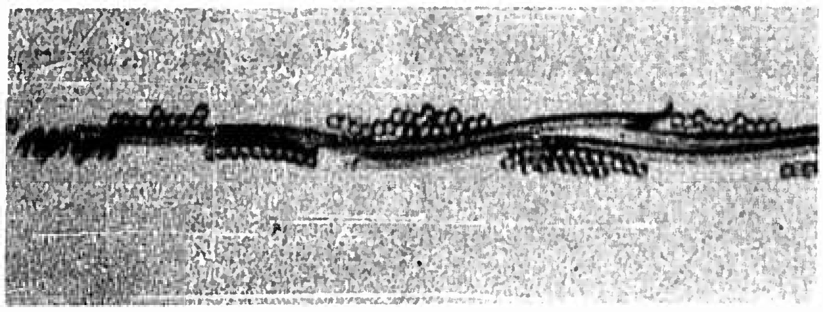

R 1/2 N 1/2
Warp - Not Calendered

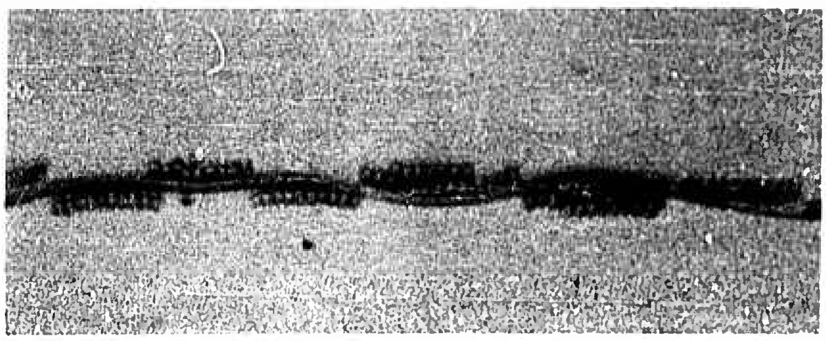

R 1/2 N 1/2
Filling - Not Calendered

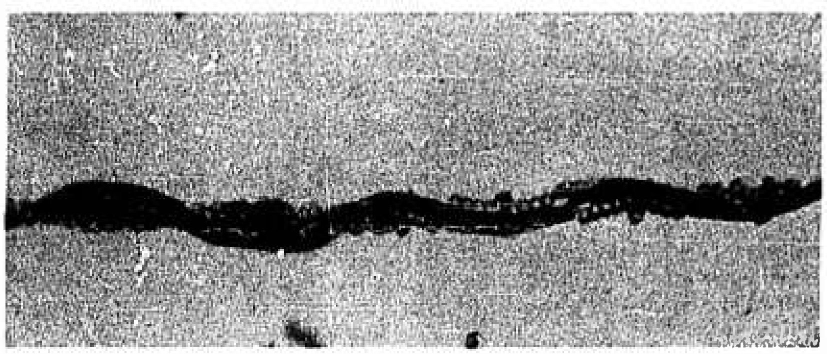

R 1/2 C 1/2
Warp - Calendered

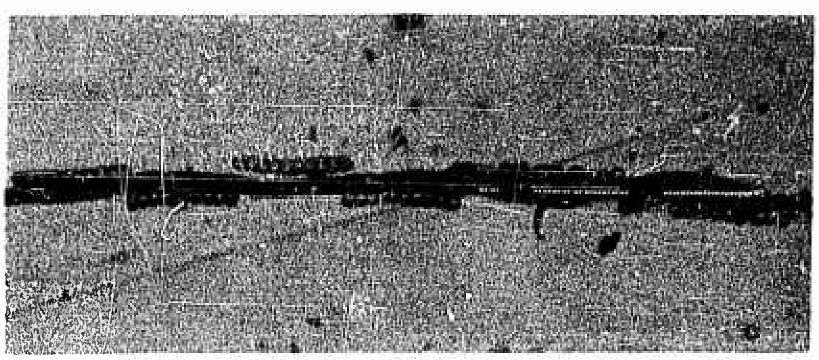

R 1/2 C 1/2
Filling - Calendered

CROSS-SECTIONAL VIEWS OF WARWICK'S FABRICS

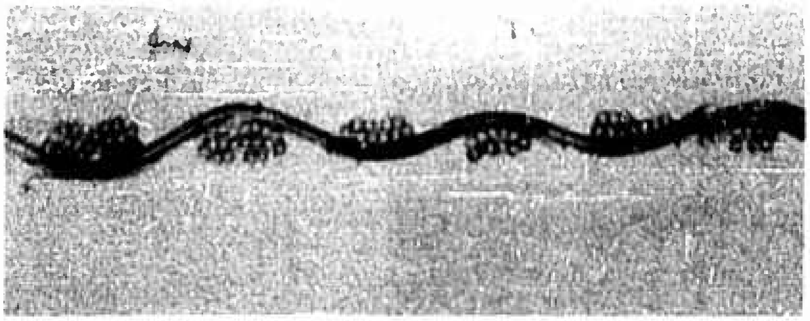

R5N 1/2
Warp - Not Calendered

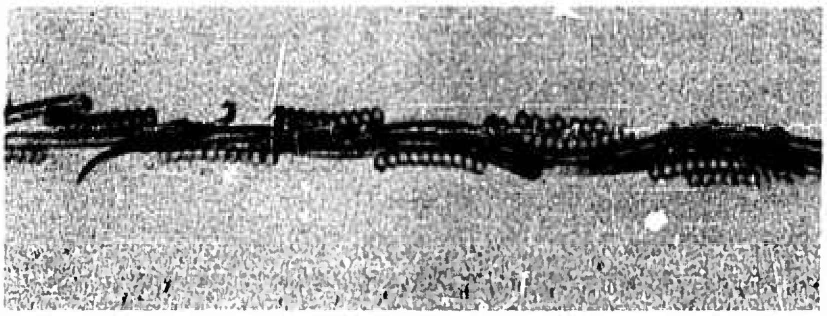

R5N 1/2
Filling - Not Calendered

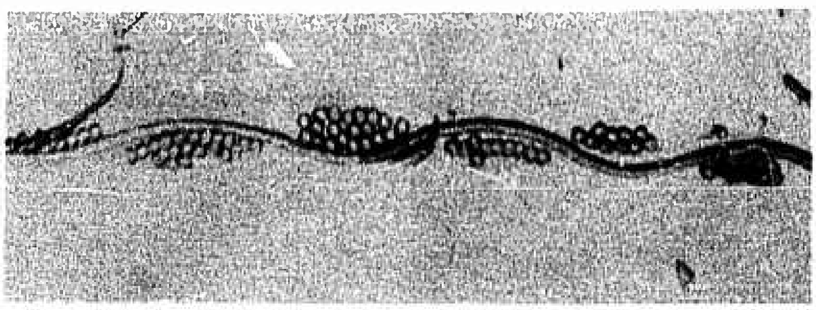

R5C 1/2
Warp - Calendered

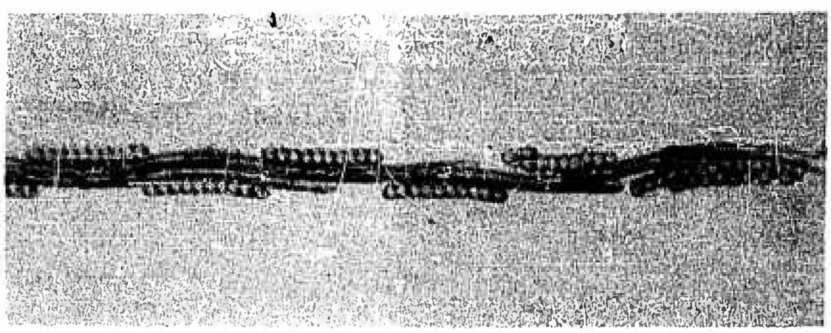

R5C 1/2
Filling - Calendered

CROSS-SECTIONAL VIEWS OF WARWICK'S FABRICS

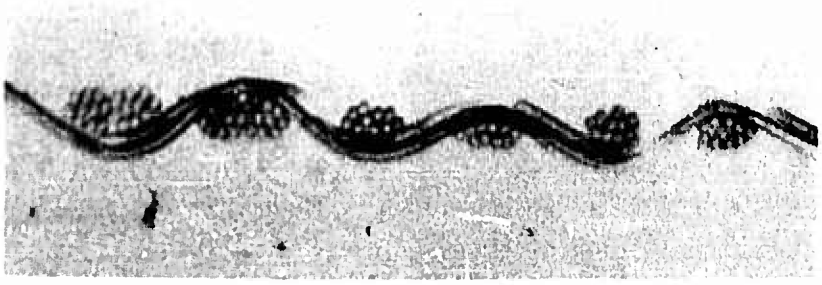

R5N5
Warp - Not Calendered

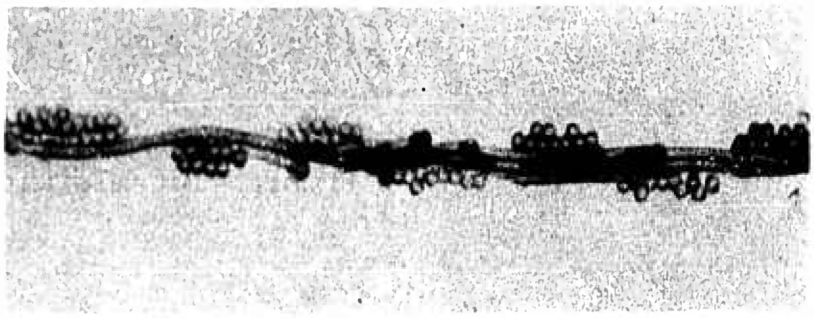

R5N5
Filling - Not Calendered

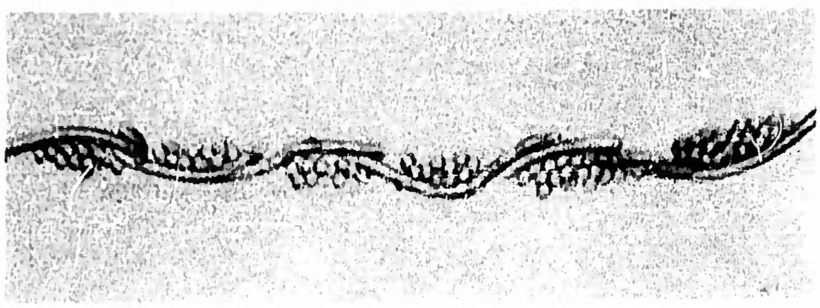

R5C5
Warp - Calendered

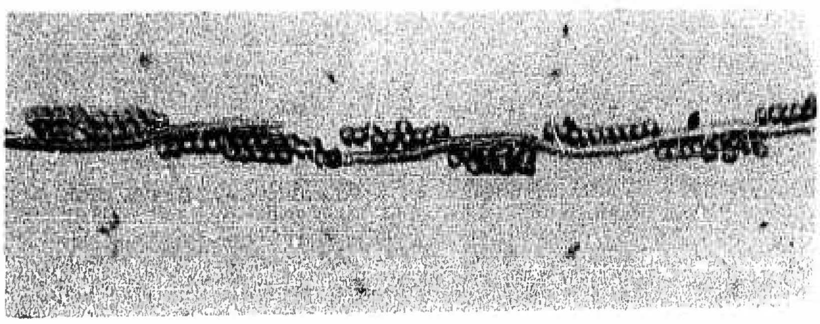

R5C5
Filling - Calendered

CROSS-SECTIONAL VIEWS OF WARWICK'S FABRICS

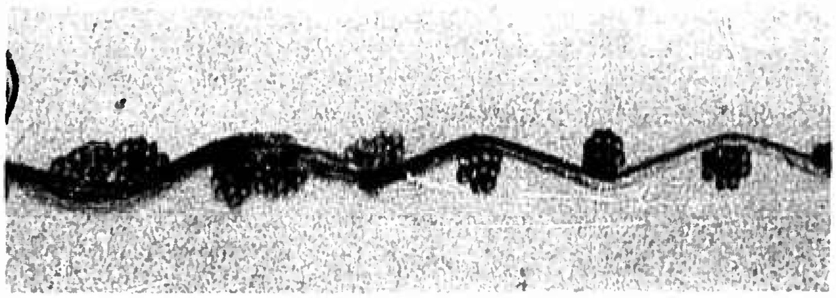

R20N 1/2
Warp - Not Calendered

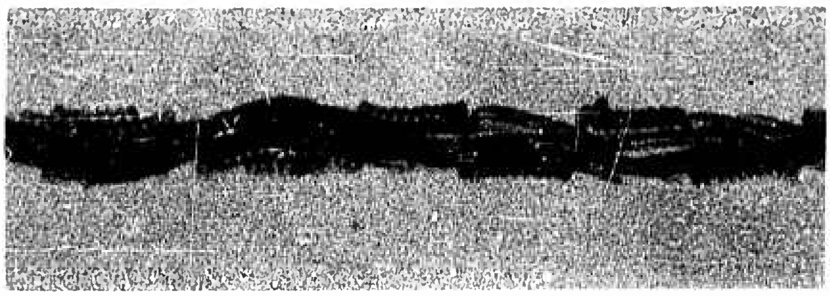

R20N 1/2
Filling - Not Calendered

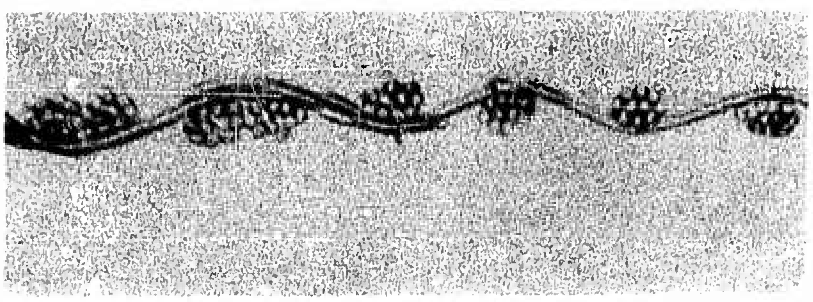

R20C 1/2
Warp - Calendered

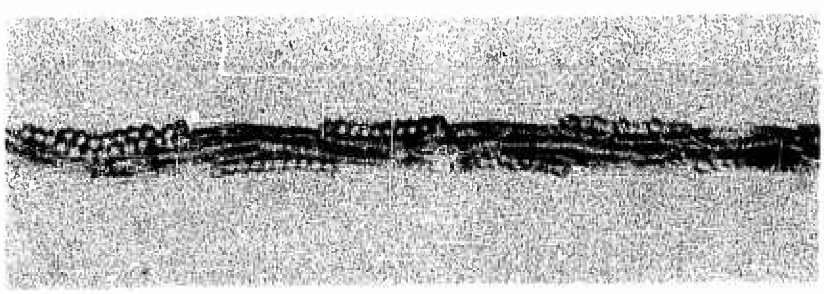

R20C 1/2
Filling - Calendered

CROSS-SECTIONAL VIEWS OF WARWICK'S FABRICS

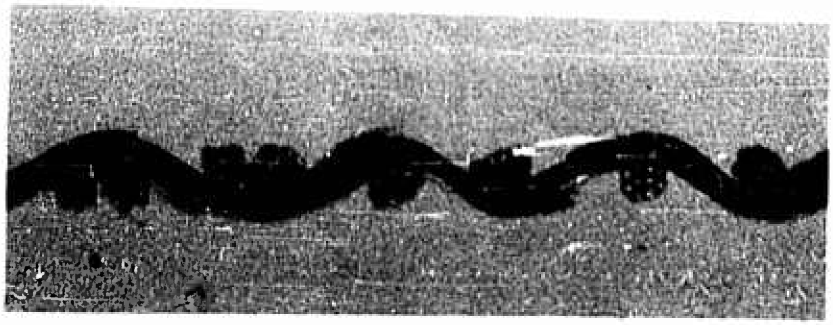

R20N20
Warp - Not Calendered

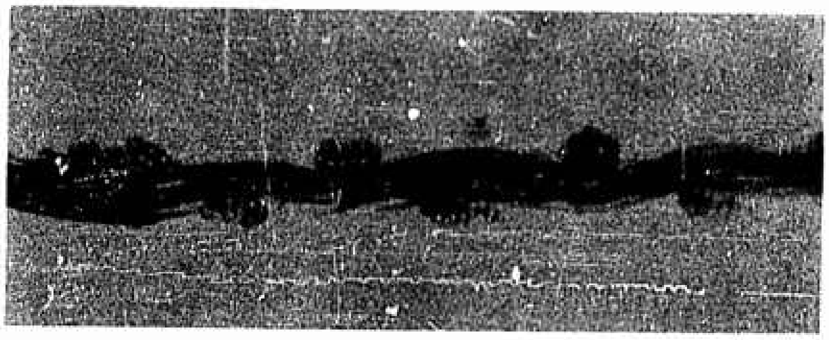

R20N20
Filling - Not Calendered

R20C20
Warp - Calendered

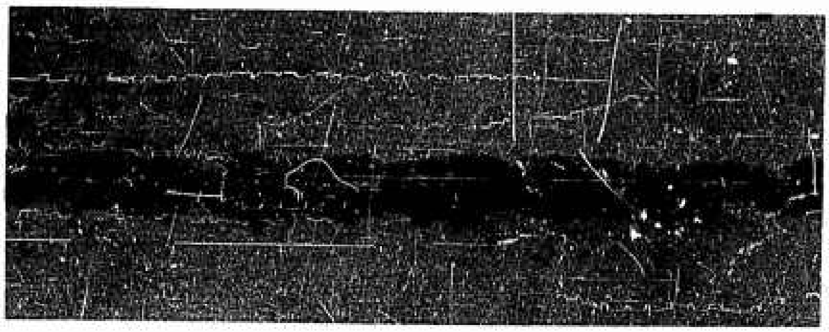

R20C20
Filling - Calendered

CROSS-SECTIONAL VIEWS OF WARWICK'S FABRICS

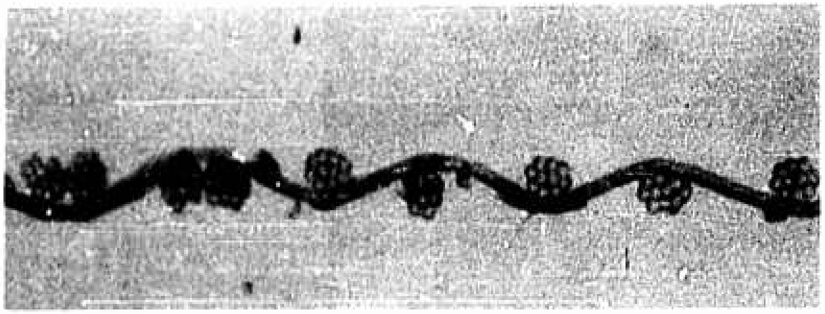

R30N 1/2
Warp - Not Calendered

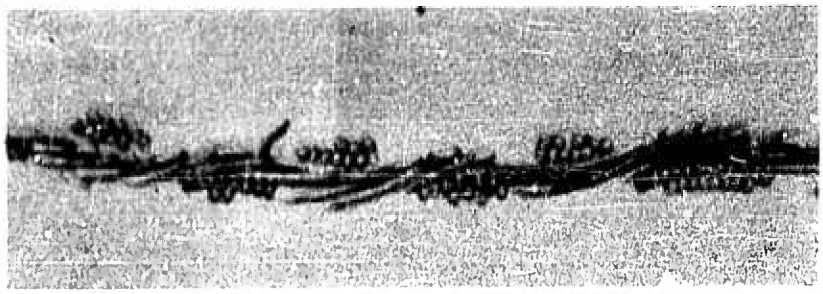

R30N 1/2
Filling - Not Calendered

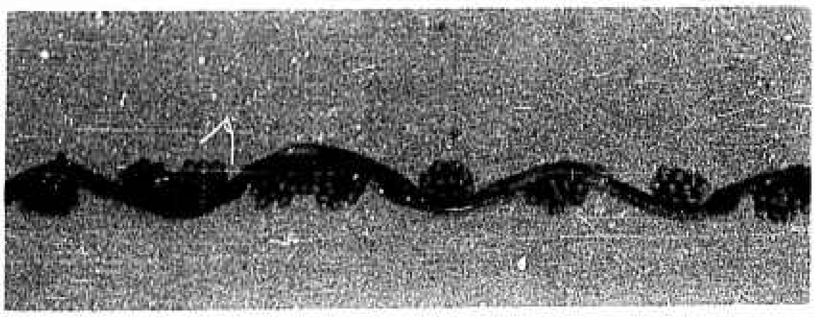

R30C 1/2
Warp - Calendered

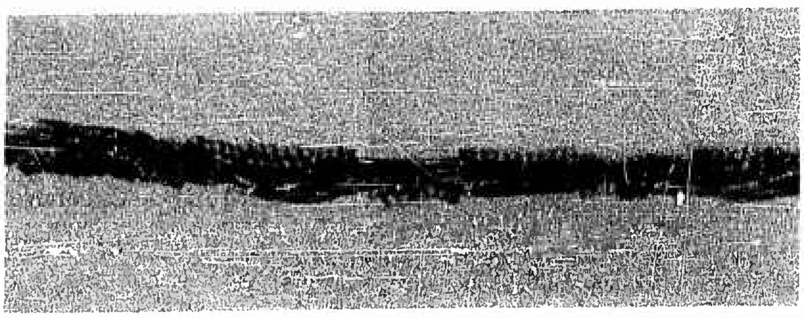

R30C 1/2
Filling - Calendered

CROSS-SECTIONAL VIEWS OF WARWICK'S FABRICS

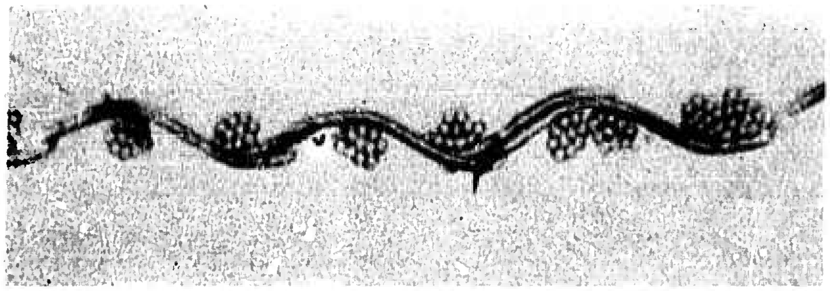

R30N5
Warp - Not Calendered

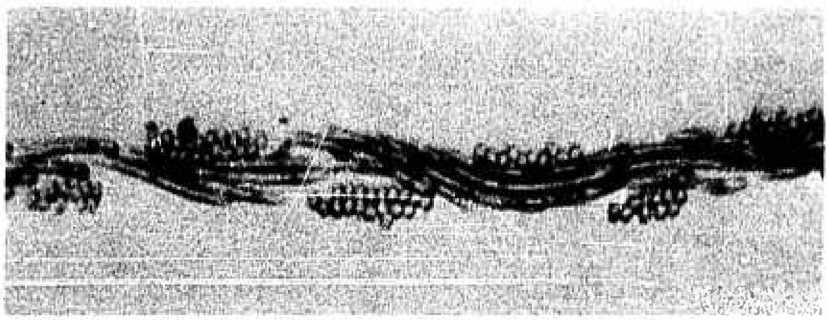

R30N5
Filling - Not Calendered

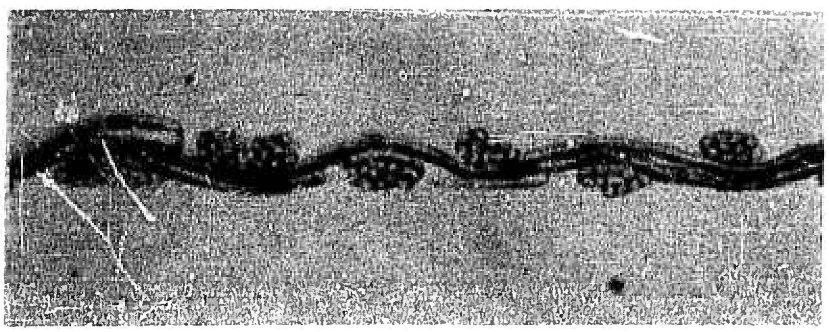

R30C5
Warp - Calendered

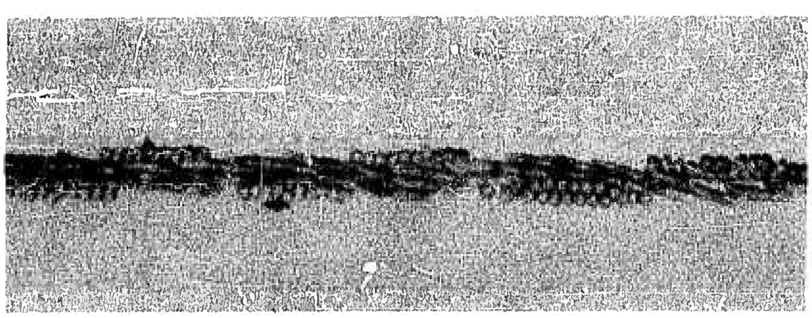

R30C5
Filling - Calendered

CROSS-SECTIONAL VIEWS OF WARWICK'S FABRICS

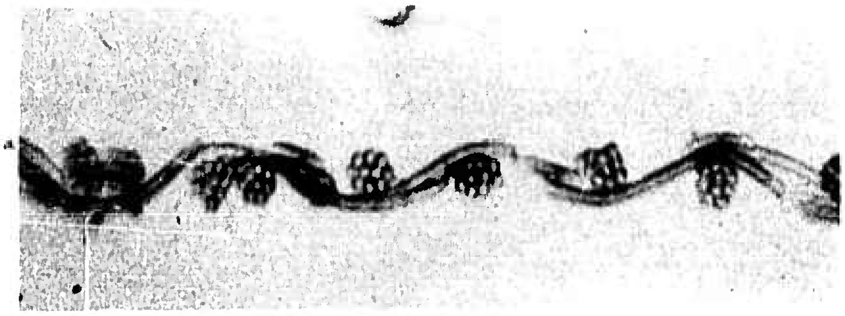

R30N10
Warp - Not Calendered

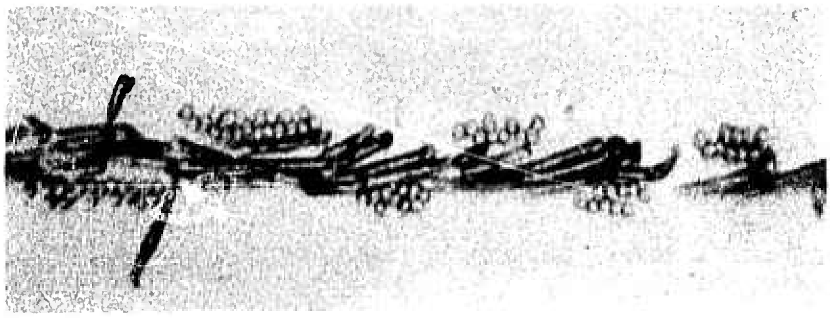

R30N10
Filling - Not Calendered

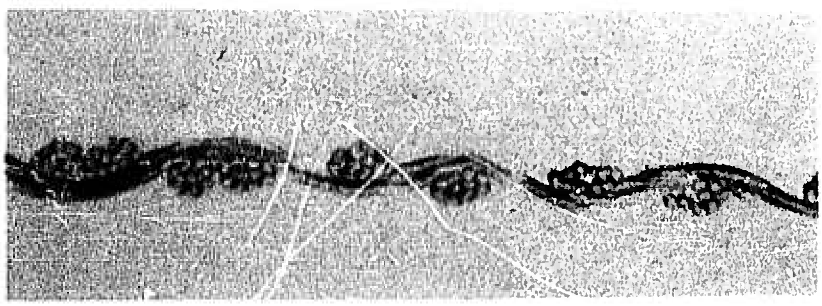

R30C10
Warp - Calendered

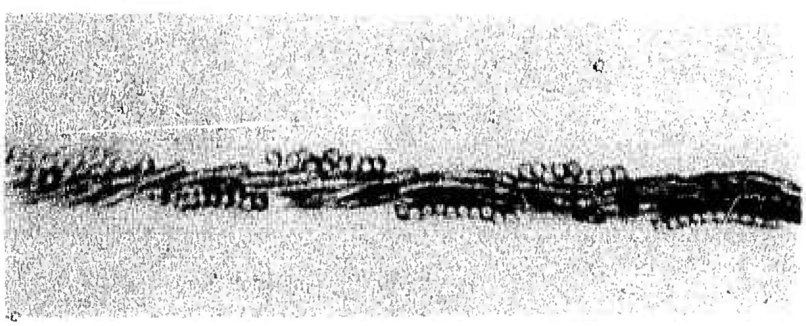

R30C10
Filling - Calendered

CROSS-SECTIONAL VIEWS OF WARWICK'S FABRICS

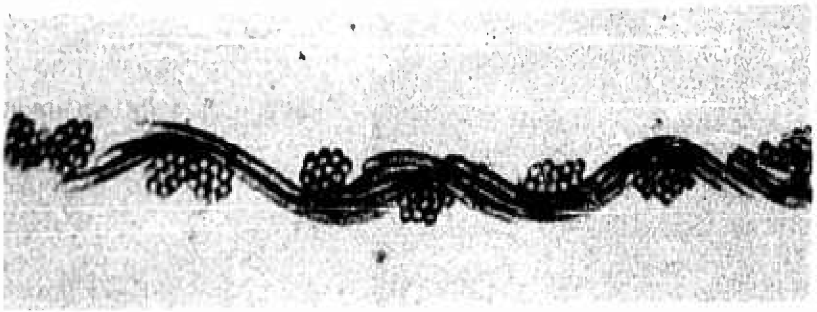

R30N20
Warp - Not Calendered

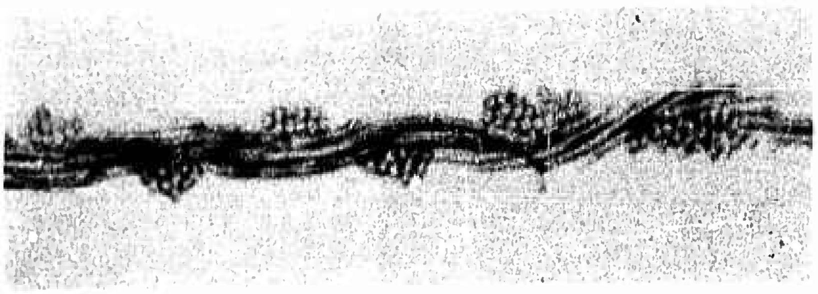

R30N20
Filling - Not Calendered

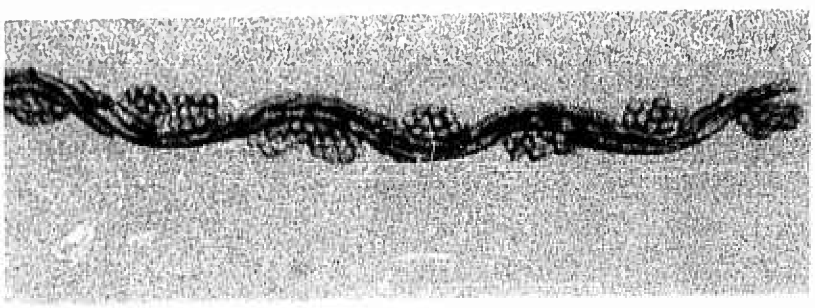

R30C20
Warp - Calendered

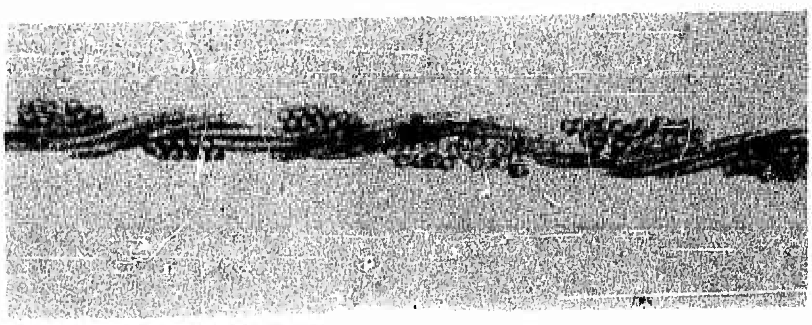

R30C20
Filling - Calendered

CROSS-SECTIONAL VIEWS OF WARWICK'S FABRICS

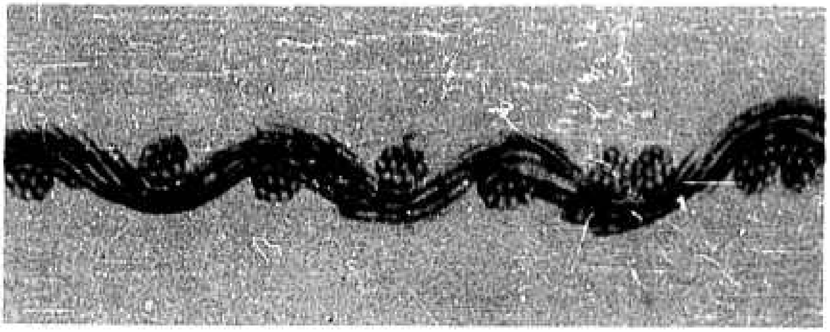

R30N30
Warp - Not Calendered

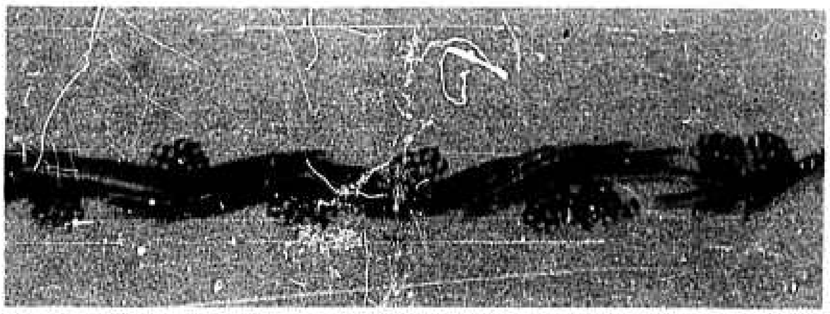

R30N30
Filling - Not Calendered

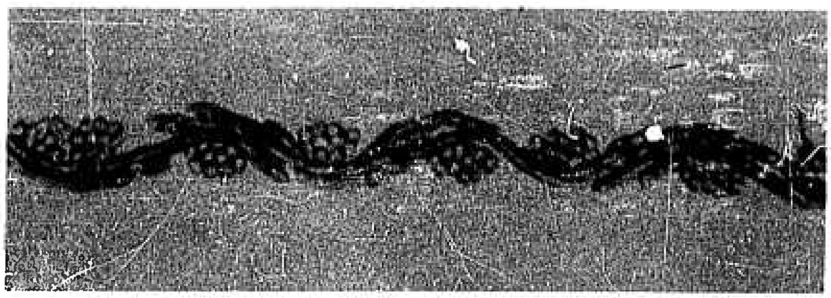

R30C30
Warp -- Calendered

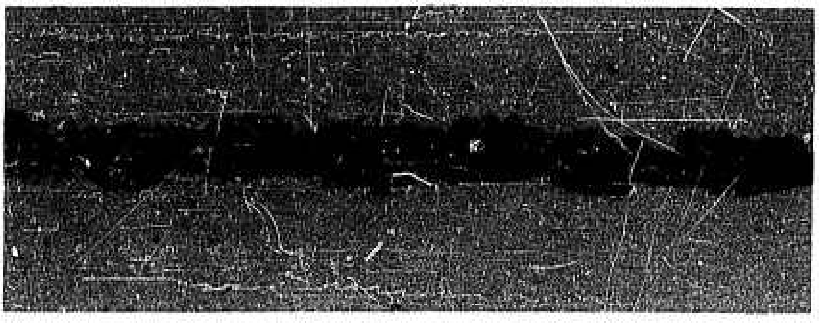

R30C30
Filling - Calendered